STUDIES IN PHOTOCATALYZED DEAROMATIVE CYCLOADDITIONS AND OTHER RADICAL CATION REACTIONS

by

AVERY KATHLEEN SMITH

(Under the Direction of Eric M. Ferreira)

ABSTRACT

Recently, there has been a resurgence of interest in the field of photocatalysis within the synthetic community. This is in part due to the development of visible light-mediated photoredox catalysis. This mild synthetic approach has allowed access to numerous novel bond-forming transformations. The most commonly employed photocatalysts to date are ruthenium and iridium-based complexes, two of the rarest metals on earth. A goal within our group has been to develop complementary photocatalysts that are based on earth-abundant metals. Namely, we have been able to exploit chromium(III) complexes as efficient photooxidants under visible light irradiation. Chapter 2 of this document will discuss our findings on the discovery of a highly reactive second-generation chromium photocatalyst that displays increased absorbance in the visible light region compared to the first-generation catalyst. Further, we have shown the utility of this photocatalyst through application in a dearomative (3 + 2) cycloaddition reaction between indoles and vinyldiazo species to synthesize densely substituted indoline substrates. In another study discussed in Chapter 3, the functional group tolerance of this dearomative cycloaddition was expounded upon. Specifically, we were able to employ valuable tryptamine and tryptophan derivatives in this cycloaddition with

vinyldiazo species to access similar indoline substrates with amine functionality. This was accomplished by utilizing a highly efficient Ru(II) photocatalyst. Finally, Chapter 4 will discuss preliminary work on a (3 + 3) cycloaddition between aminocyclopropanes and vinyldiazo species to generated functionalized aminocyclohexenes. This transformation was achieved via a visible light-mediated, photoredox-catalyzed oxidation to generate a highly reactive distonic radical cation intermediate. This dissertation will outline and described in detail these three separate studies in radical cation cycloadditions.

INDEX WORDS: Photoredox catalysis, earth-abundant metals, indoline, vinyldiazo, radical cation cycloadditions

STUDIES IN PHOTOCATALYZED DEAROMATIVE CYCLOADDITIONS AND OTHER RADICAL CATION REACTIONS

by

AVERY KATHLEEN SMITH

B.S., Mississippi State University, 2018

A Dissertation Submitted to the Graduate Faculty of The University of Georgia in Partial Fulfillment of the Requirements for the Degree

DOCTOR OF PHILOSOPHY

ATHENS, GEORGIA

2023

© 2023
Avery Kathleen Smith
All Rights Reserved

STUDIES IN PHOTOCATALYZED DEAROMATIVE CYCLOADDITIONS AND OTHER RADICAL CATION REACTIONS

by

AVERY KATHLEEN SMITH

Major Professor: Eric M. Ferreira

Committee: Steven E. Wheeler
Robert S. Phillips

Electronic Version Approved:

Ron Walcott
Vice Provost for Graduate Education and Dean of the Graduate School
The University of Georgia
December 2023

DEDICATION

For my husband and my parents. I love you.

ACKNOWLEDGMENTS

Where to begin? There are so many people whom I am deeply indebted to for their support, encouragement, wisdom, and love. All of whom and which I would not have accomplished this goal without. I will never be able to fully express how grateful I am to everyone that has contributed to my success…. but I'm gonna give it a shot.

First, I would like to thank and acknowledge my advisor, Prof. Eric Ferreira. Eric, you have been such an incredible mentor, teacher, and friend. I am extremely thankful for the opportunity to learn, grow, and freely pursue my scientific interests in your lab. I deeply admire your passion for chemistry, as well as your unfading commitment to mentoring. I have learned so much from you and I hope to make you proud in my future endeavors.

I would also like to extend my gratitude to my committee, Prof. Steven Wheeler and Prof. Robert Phillips, as well as to Prof. Chris Newton. I appreciate your continued support and guidance throughout this journey. My undergraduate research experience is also a huge reason why I am here today. Thank you, Prof. Colleen Scott, for your encouragement to continue my studies and for your belief in my abilities.

I would also like to thank all of my lab mates—past and present—who have played tremendous roles in my life. Sheneika Jackson was my first mentor in the lab, and I am so grateful for everything she has done for me. Thank you, Sheneika, for being such an amazing friend, mentor, and role model. Thanks for all the laughs, for teaching me so many things, and for making the long days fun—those first few years in the lab would have been a lot duller without you. I

would also like to extend my gratitude to Brad Gall, who I had the pleasure of working with on the Cr project. Thanks, Brad, for encouraging me to try new things and trusting my capabilities.

To my fellow cohorts, Haofan Ji and Andrew Ephron, I'm so glad to have gone through this experience together. Haofan and I managed to stay hood neighbors throughout all of grad school, even through a move to a new building. I already miss working next to you and our random late-night convos. I can't wait to see all the cool things you are going to accomplish in your postdoc and beyond. Jacob Garber and Yan-Ting (Tim) Ke have also been incredible (and interesting lol) lab mates. It has been a pleasure getting to know y'all over the past 5 years. I will truly miss you both… although I won't miss the Kid Rock. Idris, Sarah, and Vincent, I appreciate your patience with me over this past (very busy) year and I wish you all the best in the years to come.

The Newton lab has also been a substantial support system to me over the past 3 years. Thank you, Chris D., Marshall, Jess, Skylar, Jay, Geeta, Amanullah, Mary Stuart, and Audrey. Extra thanks to Jessica Budwitz for proof-reading parts of this document. And for all the snacks.

So many of my friends have helped me get to this day in ways that they probably weren't even aware of. Zach, you are my OG grad school pal and one of my very best friends. Thanks for reminding me not to take life too seriously. Lily, thank you for your constant encouragement and positivity. And for keeping me fed, you are a great friend.

My Mother- and Father-in-law have been so kind and supportive during my graduate years. Thank you both for everything. My brother, Noah, has been my life-long (built-in) best friend who I am so lucky to have. Thank you for always being there and for always being interested in whatever I am doing… or at least pretending to be. My sweet pup, Honeybun, has also been such

a blessing. She has taught me to value this short life we have above all else, and to live that life to the fullest. To all my extended family who checked in, helped with the wedding, and sent love and encouragement over the years—thank you, it did not go unnoticed.

Mom and Dad, you have always encouraged me to pursue my passions and given me the support and independence to do so. I would not be here today if it were not for your continued love and encouragement. I hope to make you proud.

Finally, and most importantly, I never could have finished this journey without my husband, Adam. I can never thank you enough for the endless love and support you have provided. The past two years have been the best of my life, and I can't wait to start our future together.

TABLE OF CONTENTS

Page

DEDICATION iv

ACKNOWLEDGMENTS v

TABLE OF CONTENTS viii

LIST OF ABBREVIATIONS xi

LIST OF TABLES xv

LIST OF FIGURES xvi

LIST OF SCHEMES xviii

CHAPTER

1 DEAROMATIVE ANNULATIONS ENABLED BY PHOTOCATALYSIS 1

1.1. Introduction: Photocatalysis 1

1.2. Dearomative Reactions via Photocatalysis 2

1.3. Dearomative Cycloadditions Enabled by EnT 4

1.4. Dearomative Cycloadditions Enabled by PET 25

1.5. Dearomative Cyclizations 33

1.6. Conclusion 42

1.7. References and Notes 44

2 A DEAROMATIVE (3 + 2) CYCLOADDITION WITH INDOLES AND VINYL DIAZOACETATES VIA CHROMIUM(III) PHOTOREDOX CATALYSIS 52

2.1. Introduction 52

2.2. Preliminary Experiments 56

2.3. Optimization of Conditions and Catalyst Development 58

2.4. Exploring Reaction Parameters 61

2.5. Scope of the Reaction 62

2.6. Accessing C2- and/or C3-Substituted Indoles 64

2.7. Scope of C2- and/or C3-Substituted Indoles 66

2.8. Mechanistic Experiments 68

2.9. Proposed Catalytic Cycle 75

2.10. Cycloaddition Product Diversification 75

2.11. Conclusion 77

2.12. Experimental Section 78

2.13. References and Notes 196

3 ACCESS TO HIGHLY FUNCTIONALIZED AMINO-INDOLINES VIA RUTHENIUM(II) PHOTOREDOX CATALYSIS: A DEAROMATIVE (3 + 2) CYCLOADDITION WITH INDOLAMINES AND VINYL DIAZOACETATES 204

3.1. Introduction 204

3.2. Preliminary Experiments 206

3.3. UV-vis Studies on Catalyst Stability 209

3.4. Scope of the Reaction 211

3.5. Product Derivatization 214

3.6. Non-amine Examples 215

3.7. Mechanistic Experiments 215

3.8. Proposed Catalytic Cycle 218

3.9. Conclusion and Project Outlook 219

3.10. Experimental Section 221

3.11. References and Notes 307

4 DISTONIC RADICAL CATIONS FROM AMINOCYCLOPROPANES AND THEIR APPLICATION IN A (3 + 3) CYCLOADDITION WITH VINYL DIAZOACETATES ... 312

4.1. Introduction: Distonic Radical Ions 312

4.2. Project Proposal 326

4.3. Preliminary Experiments 327

4.4. Preliminary Reaction Optimization 330

4.5. Scope of the Reaction 334

4.6. Proposed Catalytic Cycle 334

4.7. Conclusion and Project Outlook 335

4.8. Experimental Section 338

4.9. References and Notes 363

APPENDICES 366

A NMR SPECTRA RELEVANT TO CHAPTER 2 367

B NMR SPECTRA RELEVANT TO CHAPTER 3 474

C NMR SPECTRA RELEVANT TO CHAPTER 4 557

LIST OF ABBREVIATIONS

Å	angstrom
Ac	acetyl
Alloc	allyloxycarbonyl
app.	apparent
aq.	aqueous
Ar	aryl
Bn	benzyl
Boc	*tert*-butyloxycarbonyl
bpy	2,2'-bipyridine
bpz	2,2'-bipyrazine
br	broad
n-Bu	*normal*-butyl
t-Bu	*tert*-butyl
Bz	benzoyl
º C	degrees Celsius
Cbz	benzyloxycarbonyl
CFL	compact fluorescent light
cm	centimeters
CN	cyano
comp	complex
conv	conversion
Cz	carbazole
2-CzPN	4,5-bis(carbazol-9-yl)-1,2-dicyanobenzene
4-CzIPN	1,2,3,5-tetrakis(carbazol-9-yl)-4,6-dicyanobenzene

d	doublet
DABCO	1,4-diazabicyclo[2.2.2]octane
DCA	9,10-dicyanoanthracene
DCB	1,4-dicyanobenzene
DFT	density functional theory
DIBAL-H	diisobutylaluminum hydride
DIPA	diisopropylamine
DIPEA	*N,N*-diisopropylethylamine
DMF	dimethylformamide
DMSO	dimethylsulfoxide
dr	diastereomeric ratio
dtbbpy	4,4′-di-*tert*-butyl-2,2′-bipyridine
$E_{1/2}$	reduction potential
ee	enantiomeric excess
EnT	energy transfer
equiv	equivalents
Et	ethyl
E_T	triplet energy
Fc	ferrocene
Fmoc	9-fluorenylmethyloxycarbonyl
g	grams
HFIP	1,1,1,3,3,3-hexafluoroisopropanol
HOMO	highest occupied molecular orbital
HRMS	high resolution mass spectrometry
hν	light (Planck's constant *x* frequency)
Hz	hertz
IR	infrared
ISC	intersystem crossing

J	coupling constant
kcal	kilocalories
λ	wavelength
LEDs	light-emitting diodes
LUMO	lowest unoccupied molecular orbital
m	multiplet or milli
M	molar or mega
Me	methyl
Mes-Acr	mesityl acridinium
MLCT	metal-to-ligand charge transfer
μL	microliters
mL	milliliters
mol	moles
MS	molecular sieves
m/z	mass-to-charge ratio
nm	nanometers
NMR	nuclear magnetic resonance
NOE	nuclear Overhauser effect
ns	nanoseconds
NUV	near-UV
[O] *or* ox	oxidation
PC	photocatalyst
PCET	proton coupled electron transfer
PET	photoinduced electron transfer
Ph	phenyl
phen	phenanthroline
Phth	phthalimide
Piv	pivaloyl (trimethylacetyl)

PMP	*para*-methoxyphenyl
ppm	parts per million
ppy	2-phenylpyridine
i-Pr	*iso*-propyl
q	quartet
rr	regiomeric ratio
R_T	retention factor
s	seconds or singlet
SCE	saturated calomel electrode
SET	single electron transfer
τ	lifetime
t	triplet
TBS	*tert*-butyl(dimethyl)silyl
TEMPO	2,2,6,6-tetramethylpiperidine 1-oxyl
Tf	triflyl
TFA	trifluoroacetic acid
TFAA	trifluoroacetic anhydride
THF	tetrahydrofuran
TIPS	triisopropylsilyl
TLC	thin layer chromatography
TMS	trimethylsilyl
TPPT	2,4,6-triphenylpyrylium tetrafluoroborate
Troc	2,2,2-trichloroethoxycarbonyl
UV	ultraviolet
V	volts
VDA	ethyl vinyl diazoacetate
vis	visible
W	watt

LIST OF TABLES

Page

Table 2.2.1: Initial screening of proposed (3+2) cycloaddition 57

Table 2.3.1: Optimization of reaction conditions employing a novel, red-shifted Cr(III) photocatalyst 61

Table 2.4.1: Evaluation of photocatalyzed indole (3+2) cycloaddition conditions..... 62, 90

Table 2.6.1: Protecting groups investigated with C2/C3-substituted indoles 65

Table 2.12.1: Catalyst evaluation 84

Table 2.12.2: Solvent optimization 86

Table 2.12.3: Base optimization 87

Table 2.12.4: Acylating agent and base stoichiometry optimization 88

Table 2.12.5: Select additional experiments from Table 2.2.1 89

Table 2.12.6: Acylating agent evaluation for 2,3-disubstituted indole substrates..... 93

Table 3.2.1: Photocatalyst optimization 207, 223

Table 3.2.2: Deviations from standard conditions 208, 224

Table 4.3.1: Initial screening of Cr catalyst competency in the (3+2) cycloaddition 328, 340

Table 4.3.2: Preliminary catalyst screen in proposed (3+3) cycloaddition 328, 341

Table 4.3.3: Preliminary catalyst screen in (3+3) cycloaddition..... 329, 342

Table 4.4.1: Optimization with $[Cr(PMP_2phen)_3](BF_4)_3$..... 332, 343

Table 4.4.2: Reaction optimization 333

Table 4.8.1: Catalyst optimization 344

Table 4.8.2: Reaction optimization 345

Table 4.8.3: Further optimization studies..... 346

LIST OF FIGURES

Page

Figure 1.1.1: Photocatalysis fields and abbreviations for terminology 1

Figure 1.2.1: Select organic and transition-metal photocatalysts and their photophysical properties..... 3

Figure 1.3.1: Mechanism of Dexter EnT 4

Figure 1.4.1: Simplified molecular orbital diagram of photocatalyst $[Ru(bpy)_3]^{2+}$..... 26

Figure 1.6.1: Select indoline natural products and biologically active compounds 42

Figure 2.1.1: Select Cr(III) poly-pyridyl and poly-phenanthrolinyl complexes and their photophysical properties 53

Figure 2.3.1: (a) Ru catalyst subjected to excess BzCl and irradiation. (b) Time-lapsed UV-vis evaluation of Ru catalyst stability to BzCl and irradiation 59

Figure 2.3.2: (a) Development of a new Cr catalyst through ligand alteration. (b) UV-vis absorbance of Cr complexes. (c) Cr catalyst subjected to excess BzCl and irradiation. (d) Time-lapsed UV-vis evaluation of Cr stability to BzCl and irradiation..... 60

Figure 2.8.1: Stern-Volmer analysis. (a) Emission data at 752 nm. (b) Stern-Volmer relationship between Cr catalyst and indole or vinyl diazoacetate (VDA)..... 71

Figure 2.8.2: Stern-Volmer analysis at 464 nm..... 72

Figure 2.12.1: UV-vis absorbance measurements of $[Cr(Ph_2phen)_3](BF_4)_3$ and $[Cr(PMP_2phen)_3](BF_4)_3$..... 83

Figure 2.12.2: $[Cr(PMP_2phen)_3](BF_4)_3$ and 300 equiv of BzCl in CH_2Cl_2 irradiated with a 23 W CFL bulb over time 157

Figure 2.12.3: $[Ru(bpz)_3](PF_6)_2$ and 300 equiv of BzCl in acetonitrile irradiated with a 23 W CFL bulb over time 158

Figure 2.12.4: $[Ru(bpz)_3](PF_6)_2$ and 300 equiv of BzCl in acetonitrile over time..... 159

Figure 2.12.5: BzCl in acetonitrile irradiated with a 23 W CFL bulb over 24 h 160

Figure 2.12.6: Stern-Volmer analysis: quenching of excited state of $[Cr(PMP_2phen)_3](BF_4)_3$ by 5-bromoindole at the 752 nm emission band 167

Figure 2.12.7: Stern-Volmer analysis: quenching of the excited state of $[Cr(PMP_2phen)_3](BF_4)_3$ by ethyl vinyl diazoacetate at the 464 nm emission band 168

Figure 2.12.8: Cyclic voltammogram of indole **2-10** 183

Figure 2.12.9: Cyclic voltammogram of indole **2-55** 184

Figure 2.12.10: Cyclic voltammogram of indole **2-56** 185

Figure 3.1.1: Relevant natural products containing densely substituted tryptophan cores 205

Figure 3.3.1: UV-vis absorption of $[Ru(bpz)_3](PF_6)_2$ irradiated with (a) BzCl (300 equiv) and (b) trimethylacetic formic anhydride (**3-3**, 300 equiv) over 24 h 210

Figure 3.10.1: $[Ru(bpz)_3](PF_6)_2$ in acetonitrile irradiated with a 23 W CFL bulb over time 281

Figure 3.10.2: $[Ru(bpz)_3](PF_6)_2$ and 300 equiv of **3-3** in acetonitrile irradiated with a 23 W CFL bulb over time 282

Figure 3.10.3: $[Ru(bpz)_3](PF_6)_2$ and 300 equiv of isobutyryl chloride in acetonitrile irradiated with a 23 W CFL bulb over time 283

Figure 3.10.4: $[Ru(bpz)_3](PF_6)_2$ and 300 equiv of TrocCl in acetonitrile irradiated with a 23 W CFL bulb over time 284

Figure 3.10.5: $[Ru(bpz)_3](PF_6)_2$ and 300 equiv of benzoic pivalic anhydride in acetonitrile irradiated with a 23 W CFL bulb over time 285

Figure 3.10.6: $[Ru(bpz)_3](PF_6)_2$ and 100 equiv **3-42** in acetonitrile irradiated with a 23 W CFL bulb over time 286

Figure 3.10.7: $[Cr(PMP_2phen)_3](BF_4)_3$ and 100 equiv **3-42** in CH_2Cl_2 irradiated with a 23 W CFL bulb over time 287

Figure 4.2.1: Applicability of proposed cycloaddition with vinyl diazoacetates 327

Figure 4.7.1: Substituent effects on cyclopropylamine reactivity 336

LIST OF SCHEMES

Page

Scheme 1.3.1: UV light-promoted [2+2] cycloaddition between indoles and ketones or alkenes . 5

Scheme 1.3.2: Direct sensitization of indole by irradiation 6

Scheme 1.3.3: Regio- and stereoselectivity in the [2+2] intermolecular cycloaddition 7

Scheme 1.3.4: Mechanistic studies on [2+2] cycloaddition with indoles and alkenes 8

Scheme 1.3.5: Cis-trans isomerization of alkene tethered to acetophenone 9

Scheme 1.3.6: Dearomative [2+2] cycloaddition via direct irradiation of naphthol arenes 9

Scheme 1.3.7: Visible light-promoted enantioselective [2+2] dearomative cycloaddition 11

Scheme 1.3.8: Expansion of Bach's work to an intermolecular [2+2] cycloaddition.....11

Scheme 1.3.9: Intermolecular [2+2] cycloaddition between benzofurans and alkenes 12

Scheme 1.3.10: Proposed mechanism of enantioselective [2+2] cycloaddition with chiral Rh ... 13

Scheme 1.3.11: Glorius's expansion of Wagner's work to visible light irradiation..... 14

Scheme 1.3.12: Visible light-induced, intramolecular [2+2] cycloaddition of indoles utilizing Ir photocatalysis..... 15

Scheme 1.3.13: Koenig's complementary method to Glorius utilizing 2-CzPN 16

Scheme 1.3.14: 2-CzPN-photocatalyzed extension to indoles 17

Scheme 1.3.15: Scope and mechanism of Oderinde's [2+2] intramolecular cycloaddition 18

Scheme 1.3.16: You's 2020 divergent synthesis of functionalized indolines 19

Scheme 1.3.17: Vinylcyclopropanes in divergent cycloadditions with indoles..... 20

Scheme 1.3.18: Alkynes and arenes in intramolecular cycloadditions with indoles 20

Scheme 1.3.19: Origins of selectivity in intermolecular [2+2] cycloadditions between indoles and alkenes..... 22

Scheme 1.3.20: Select scope of intermolecular [2+2] cycloaddition..... 23

Scheme 1.3.21: Glorius's divergent cascade cycloaddition/rearrangement mechanism 24

Scheme 1.3.22: Photocatalytic isomerization of stilbene 25

Scheme 1.4.1: (4+2) cycloaddition with indoles and cyclic dienes via PET 27

Scheme 1.4.2: Mechanism of (4+2) cycloaddition with indole and 1,3-cyclohexadiene 28

Scheme 1.4.3: Select scope of (4+2) cycloaddition with indoles and cyclohexadienes 29

Scheme 1.4.4: Exocyclic dienes in (4+2) cycloaddition with indoles 30

Scheme 1.4.5: Dearomative (4+2) cycloaddition via a visible light-induced exciplex 31

Scheme 1.4.6: Facile synthesis of 3-*O*-desmethylated phomentrioloxin 32

Scheme 1.4.7: Visible light-promoted (4+2) cycloaddition with indoles and 1,3-cyclohexadienes 33

Scheme 1.5.1: Xia's divergent radical cyclization 34

Scheme 1.5.2: Cyclization and spirocyclization of tethered indoles via photoredox catalysis 35

Scheme 1.5.3: Proposed mechanism of oxidative cyclization 35

Scheme 1.5.4: Cascade spirocyclization-nucleophilic attack via PET 36

Scheme 1.5.5: Mechanism of Wang's spirocyclization of difluorinated indolamines 37

Scheme 1.5.6: Synthesis of spirocyclic oxindoles via PET 38

Scheme 1.5.7: Cyclization of indole aryloxyamide to pyrroloindoline 38

Scheme 1.5.8: Synthesis of Flustramide B 39

Scheme 1.5.9: Knowles's enantioselective synthesis of pyrroloindolines via PET 40

Scheme 1.5.10: Proposed mechanism of PCET cyclization of tryptamine derivatives 40

Scheme 1.5.11: Application of PCET cyclization towards (-)-calycanthidine 41

Scheme 2.1.1: Previous Cr(III)-photocatalyzed cycloadditions reported from our group 54

Scheme 2.1.2: Desired cycloaddition product and potential undesired rearomatization processes 55

Scheme 2.1.3: Davies's Rh(II)-catalyzed (3+2) cycloaddition 56

Scheme 2.5.1: Scope of C4, C5, C6, and C7-substituted indoles 63

Scheme 2.5.2: Scope of vinyl diazoacetates and acyl protecting groups 64

Scheme 2.6.1: Expansion of cycloaddition to C2/C3-substituted indoles. (a) Facile deprotonation of indole radical cation. (b) Base-free conditions in the cycloaddition 66

Scheme 2.7.1: Scope of C2/C3-substituted indoles 67

Scheme 2.8.1: (a) Unreactivity of *N*-substituted indoles. (b) Minimal reaction impact by triplet-quenching diene 68

Scheme 2.8.2: Competition experiments on electronically differentiated indoles 69

Scheme 2.8.3: Electronically different indoles tested in radical diazoacetate experiment 73

Scheme 2.8.4: Attempted intramolecular (3+2) cycloaddition 74

Scheme 2.9.1: Proposed catalytic cycle 75

Scheme 2.10.1: Indoline product diversification 76

Scheme 3.1.1: Indolamines performing poorly with Cr(III) photocatalyst 204

Scheme 3.4.1: Scope of (3+2) cycloaddition of indolamines and vinyl diazoacetates employing Ru photocatalysis 212

Scheme 3.4.2: Extended scope of the cycloaddition reaction 213

Scheme 3.5.1: (a) Deprotection of the Boc carbamate and conjugate addition. (b) Selective deprotection of the allyl carbamate of formamide 214

Scheme 3.6.1: Demonstrated method with non-aminated substrates 215

Scheme 3.7.1: Effect of electronic tuning of amine protecting group 216

Scheme 3.7.2: (a) Addition of external amine with Ru conditions and (b) Ru stability to amine 217

Scheme 3.7.3: (a) Addition of external amine with Cr conditions and (b) Cr stability to amine 218

Scheme 3.8.1: Proposed catalytic cycle 219

Scheme 4.1.1: Early report of the photooxidation of aminocyclopropanes 313

Scheme 4.1.2: Cha's intramolecular (3+2) annulation cascade 314

Scheme 4.1.3: Zheng's seminal report utilizing cyclopropylamine to generate highly reactive distonic radical cations via visible light-mediated photocatalysis 315

Scheme 4.1.4: Proposed catalytic cycle of (3+2) cycloaddition with aminocyclopropanes and electron-rich alkenes 316

Scheme 4.1.5: (a) Select scope of the reaction. (b) Explanation of diastereoselectivity in bicyclic examples 317

Scheme 4.1.6: Radical cycloaddition with alkyne derivatives 318

Scheme 4.1.7: Diastereoselectivity induced via substrate control 319

Scheme 4.1.8: Intermolecular (3+2) cycloaddition between *N*-sulfonyl cyclopropylamines and electron-deficient olefins 320

Scheme 4.1.9: Proposed mechanism of Aggarwal's (3+2) cycloaddition 321

Scheme 4.1.10: Direct excitation of imine-cyclopropanes and application in a (3+2) cycloaddition 322

Scheme 4.1.11: Enantioselective cycloaddition through chiral counterion association 323

Scheme 4.1.12: Enantioselective cycloaddition through chiral Brønsted acid coordination 324

Scheme 4.1.13: Enantioselective cycloaddition using a chiral photocatalyst 325

Scheme 4.2.1: Proposed complementary reaction and new methodology 326

Scheme 4.4.1: Cyclic peroxide side-product observed 330

Scheme 4.4.2: Addition of acylating agents 331

Scheme 4.5.1: Scope of the reaction 334

Scheme 4.6.1: Proposed catalytic cycle of novel (3+3) cycloaddition with photocatalyst 335

CHAPTER 1

DEAROMATIVE ANNULATIONS ENABLED BY PHOTOCATALYSIS

1.1. Introduction: Photocatalysis

Photocatalysis in chemistry refers to the process by which a reaction is accelerated through "activation" by photons (i.e., light). Two photocatalytic processes that will be discussed in this chapter are photoinduced electron transfer processes (PET)[1] and energy transfer processes (EnT)[2] (*Figure 1.1.1*). A compound acting as a photocatalyst can be excited by exposure to light, proceeding from a ground state electron configuration to a higher energy electron configuration. Depending on the photophysical properties, this excited catalyst can undergo electron or energy transfer with an organic molecule to generate other high energy intermediates *in situ*.

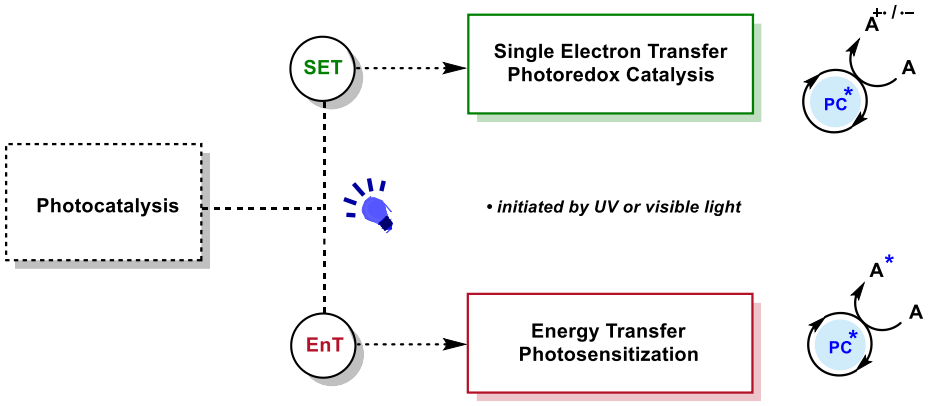

Figure 1.1.1. Photocatalysis fields and abbreviations for terminology. Recreated image from Glorius et al.[2c]

1.2. Dearomative Reactions via Photocatalysis

Dearomative reactions are inherently energetically uphill.[3] Often, harsh conditions are required to accomplish these reactions such as dissolving metal reductions,[4] oxidative dearomatizations,[5] or thermally promoted, transition-metal-mediated functionalizations.[6] As a milder approach, photocatalysis has emerged as reliable method for inducing dearomatization reactions that possess high activation barriers and unfavorable pathways. Excitation and promotion of electrons through irradiation greatly lowers the energy barrier of these reactions and often allows access to intermediates or products energetically unattainable thermally. Additionally, photochemically mediated annulations represent a practical method for constructing multiple bonds or ring systems in a single step and introducing significant complexity to molecules.[7]

Much of the early work in these photochemically-mediated dearomatization reactions employed UV light as the irradiation source by direct irradiation of substrates or irradiation of a photosensitizer (*vide infra*). A disadvantage to using UV light, especially to directly sensitize a substrate, is that numerous unwanted side reactions can occur, including dimerization, polymerization, and unproductive relaxation of substrates. Additionally, UV light fixtures can be quite expensive and operationally arduous. Recently, transition metal complexes have been found to absorb in the visible light region, inspiring a resurgence of interest in the field (*Figure 1.2.1*).[1,2] With modern visible light-mediated photochemical developments, a wider range of substrates can be employed in dearomative annulations with improved selectivity.

Chapters 2 and 3 will discuss my research efforts towards dearomative cycloadditions of indoles enabled by visible light-mediated photoredox catalysis. The purpose of this chapter is to illustrate pioneering efforts in the field of photocatalyzed dearomative annulations, with a specific focus on indole dearomative cycloadditions and cyclizations.[8,9]

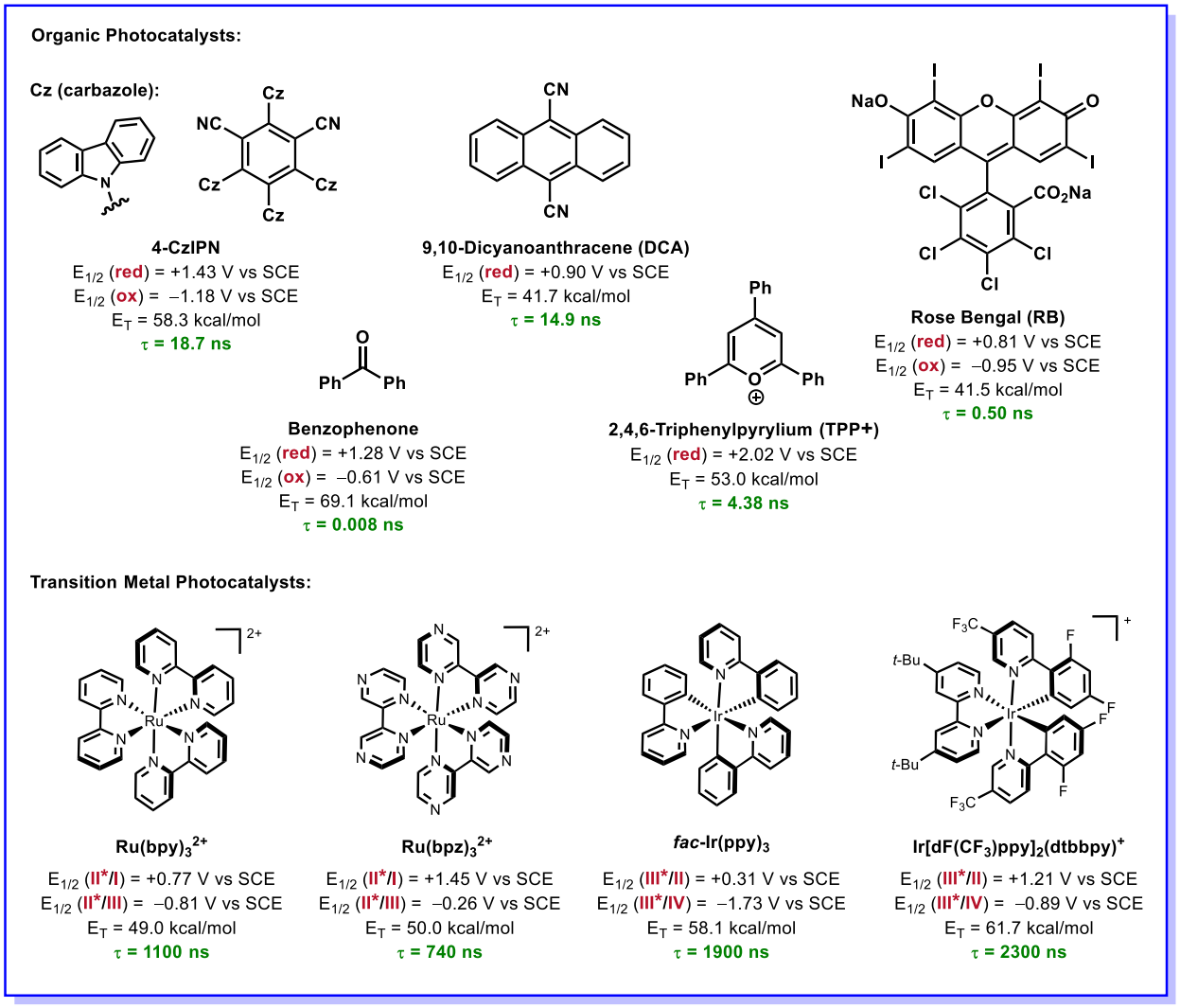

Figure 1.2.1. Select organic and transition-metal photocatalysts and their photophysical properties. Values taken from: Chem. Rev. **2016**, *116*, 10075; *Chem. Soc. Rev.*, **2018**, *47*, 7190; and *Chem. Rev.* **2013**, *113*, 5322.

1.3. Dearomative Cycloadditions Enabled by EnT

Early work in dearomative cycloaddition and cyclization reactions employed UV light to activate organic molecules or dyes acting as photosensitizers. These molecules would be excited from a ground state (S_0) to a high energy state singlet state (S_1). This higher energy state is short-lived and can undergo rapid intersystem crossing (ISC) to a triplet excited state (T_1) that has a longer lifetime. This triplet excited state complex can then simultaneously exchange its excited state electrons with nearby ground state electrons, resulting in another triplet excited state complex. This process is called Dexter energy transfer (*Figure 1.3.1*).[2,10] Due to the nature of the Dexter EnT mechanism, orbital proximity and triplet state lifetime are both important factors to consider as other processes, like phosphorescence, can be in competition with the desired reactivity. Over the past few decades several transition-metal and organic photocatalysts have been developed that possess high triplet state energy (E_T)[11] values and long triplet excited state lifetimes (*Figure 1.3.1*). A triplet energy value is the difference in Gibbs free energy between T_1 and S_0 ($E_T = \Delta G(T_1–S_0)$).[12]

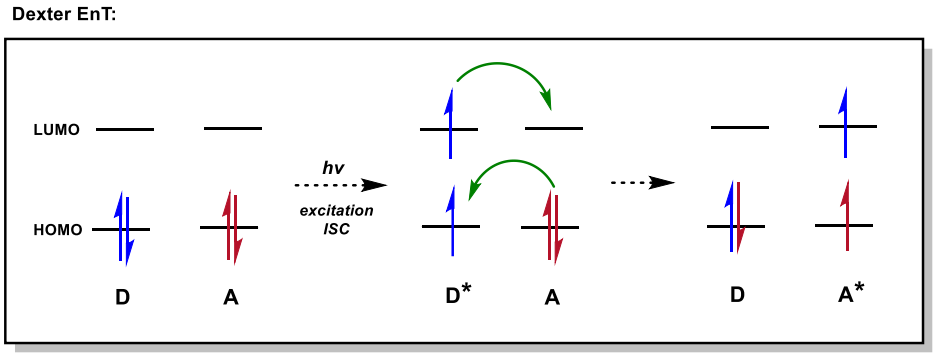

Figure 1.3.1. Mechanism of Dexter EnT.

1.3.1. UV Light-Promoted Intermolecular [2+2] Cycloadditions of Indoles

One of the more commonly explored classes of photocatalyzed dearomative reactions are [2 + 2] cycloadditions. Cyclobutanes have attracted interest from drug discovery teams due to their inherent conformational rigidity and high ring strain.[13] A [2 + 2] cycloaddition would grant access to these scaffolds, containing significant molecular complexity, in a step-conscious approach. Recently, attention in this area has exploded as interest in- and understanding of visible light-mediated photocatalysis has expanded,[1, 2] especially with respect to indoles (*vide infra*). These reactions typically proceed through EnT activation of indole, followed by radical cyclization events.

In 1973, Julian and coworkers disclosed the first [2 + 2] cycloaddition between indoles and ketones or alkenes (*Scheme 1.3.1*).[14,15] In two separate reports, *N*-acylindoles (**1-1**) could be triplet-sensitized in the presence of benzophenone (**1-2**) or acetophenone and reacted with ketone **1-2** or alkene **1-3** to form oxetanes **1-4** or cyclobutanes **1-5**, respectively. Critical to this reaction was the addition of a withdrawing group attached to the *N*-atom of indole in order to delocalize the *N*-atom lone pairs, generating a more reactive substrate once irradiated and preventing subsequent quenching of the excited ketone in the oxetane examples.

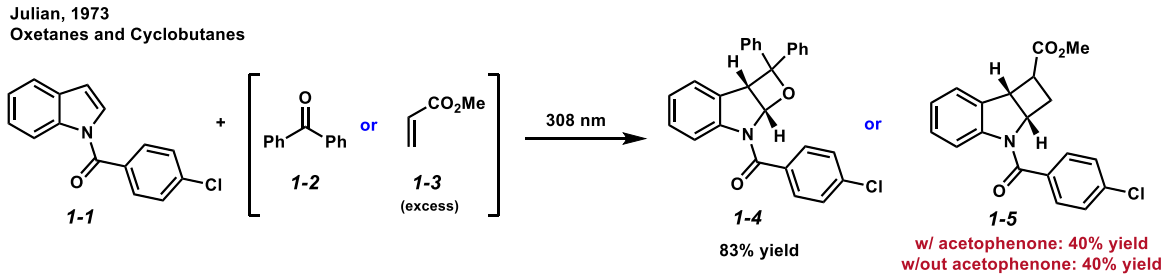

Scheme 1.3.1. UV light-promoted [2 + 2] cycloaddition between indoles and ketones or alkenes.

It was postulated that indole **1-6** could be directly sensitized by UV light to give intermediate **1-7** (*Scheme 1.3.2*). This triplet excited state could either react with another double bond in the reaction or undergo triplet energy transfer to the ketone coupling partner (**1-8**) (i.e., **1-6** acting as a sensitizer). The excited ketone could then react with indole to form oxetane products. In the second study with alkenes (*Scheme 1.3.1*), a sensitizer was not necessary for product formation (**1-5**)—further supporting the proposal of direct triplet sensitization of indole. Notably, electron-deficient alkenes were found to be more reactive. In a competition experiment between electronically different alkenes, acrylonitrile was exclusively reactive over ethyl vinyl ether.

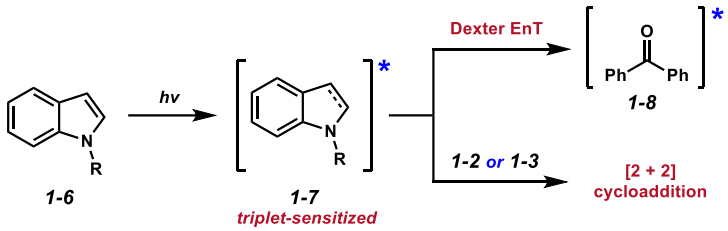

Scheme 1.3.2. Direct sensitization of indole by irradiation.

Mechanistic studies later proved the existence of the triplet diradical indole species. Ikeda and coworkers investigated stereo- and regioselectivity in this cycloaddition.[16] Using methyl acrylate (**1-3**) and *N*-benzoyl indole (**1-9**), various substitution at C2 and C3 afforded different product distribution between diastereomers **1-10** and **1-11**, and regioisomer **1-12** (*Scheme 1.3.3*). No substitution moderately favored the endo **1-11** product, although **1-10** and **1-12** were still observed. Donating groups favored the formation of the endo product (**1-11**), with no observation of regioisomer **1-12**. Withdrawing groups, however, yielded a broader distribution, slightly favoring regioisomer **1-12**. The product distribution was attributed to a stabilized triplet 1,4-diradical intermediate (**1-13**).

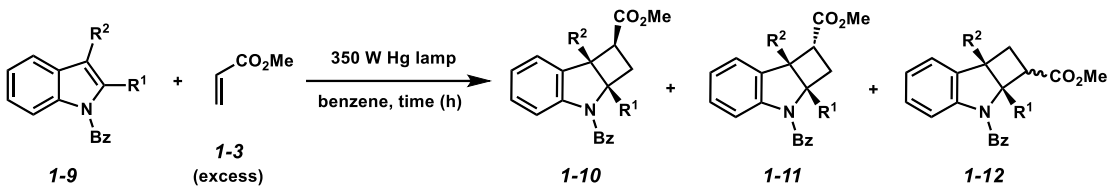

product distribution suggests:

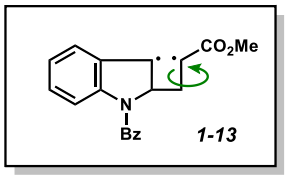

	time (h)	total yield (%)	ratio (*1-10*:*1-11*:*1-12*)
R^1 = H, R^2 = H	30	67	1 : 5 : 1.3
R^1 = Me, R^2 = H	83	51	1 : 5 : 0
R^1 = H, R^2 = Me	50	23	1 : 7 : 0
R^1 = H, R^2 = CHO	12	53	1 : 3 : 4
R^1 = H, R^2 = OAc	16	64	1 : 10 : 0

Scheme 1.3.3. Regio- and stereoselectivity in the [2 + 2] intermolecular cycloaddition.

Later, Weedon and coworkers further proved the formation of an indole triplet diradical intermediate and discovered the origins of regioselectivity in photochemical [2 + 2] cycloadditions between indoles and alkenes (*Scheme 1.3.4*).[17] Using vinyl cyclopropane (**1-14**), a "radical clock" with a known rate constant of radical ring-opening, *N*-benzoylindole (**1-13**) and **1-14** were irradiated for 5 days. Three products were observed and identified in a 5:31:64 ratio. The major product (64% yield) was identified as **1-24**, which could only result from 1,4-diradical species **1-18**. The other major product (31% yield) was identified as **1-20**. This product could be formed from 1,4-diradical species **1-17** or **1-18**; however, **1-17** would require the formation initially of a primary radical. The minor product was not fully identified and postulated to either be **1-19** or a stereoisomer of **1-20**. These products led to the identification of a tail-to-tail mechanistic proposal, specifically with the C2 position of indole reacting initially with the terminus of mono-substituted alkenes. This can be rationalized by invoking benzylic radical stability at the C3 position of indole, and secondary radical stability over primary for alkene selectivity. Using the rate of secondary cyclopropyl radical ring-opening to homoallylic radicals, the lifetime of 1,4-diradical **1-18** was

determined to be 100 ns. This lifetime is comparable to other known 1,4-diradical processes such as Norrish Type II[18] reactions and other well-studied [2 + 2] cycloadditions.[19]

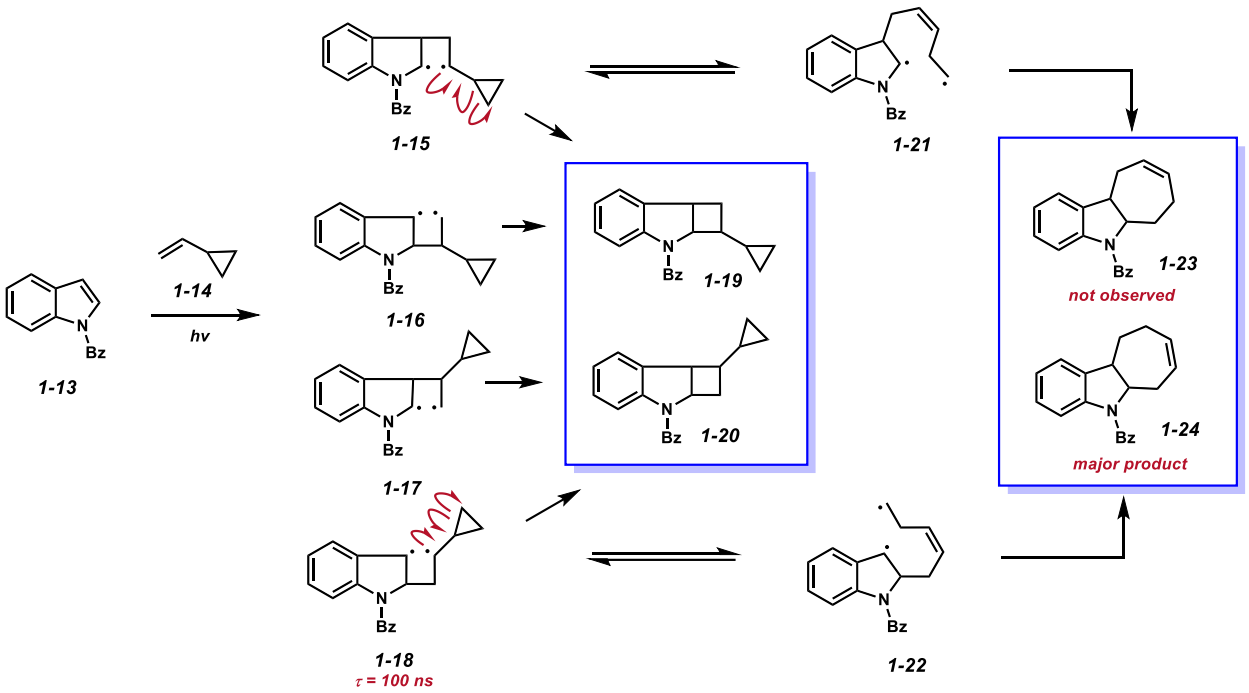

Scheme 1.3.4. Mechanistic studies on [2 + 2] cycloaddition with indoles and alkenes.

1.3.2. UV Light-Promoted Dearomatization via Triplet Arenes

Wagner and coworkers reported several dearomative intramolecular cycloadditions enabled by UV light in the mid to late 1980s.[20] It is well understood that when acetophenone is irradiated with UV light, it will be excited to a triplet state [(π, π*) or (n, π*)].[21] In their first study, Wagner and coworkers included a *p*-alkenoxy tether on acetophenone (**1-25**) and upon irradiation, witnessed a *cis-trans* isomerization of the tethered alkene (**1-27**, *Scheme 1.3.5*). It was proposed that this occurs through an intramolecular cyclized intermediate (**1-26**), because the direct energy transfer to the alkene would be energetically unfavorable.[20a]

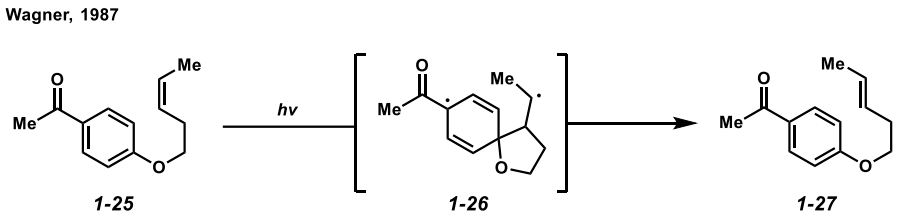

Scheme 1.3.5. Cis-trans isomerization of alkene tethered to acetophenone.

Intrigued by this proposed intermediate, the authors were inspired to pursue an intramolecular cycloaddition of butenoxyacetonaphthones (**1-28**, **1-30**) to verify the existence of the diradical intermediate **1-32** via (π, π*) triplet excited state, followed by [2 + 2] cyclization with the pendant alkene. Interestingly, **1-28** was found to cyclize much faster and more efficiently than **1-30** (*Scheme 1.3.6*). Wagner asserted that this is due to electron spin density predominantly presiding at the α-position rather than the β-position. Assuming these proceed via a stepwise mechanism, **1-28** would initially form a 5-membered ring, while **1-30** would form an unfavorable 7-membered ring, leading to slower reaction rates and lower efficiencies.

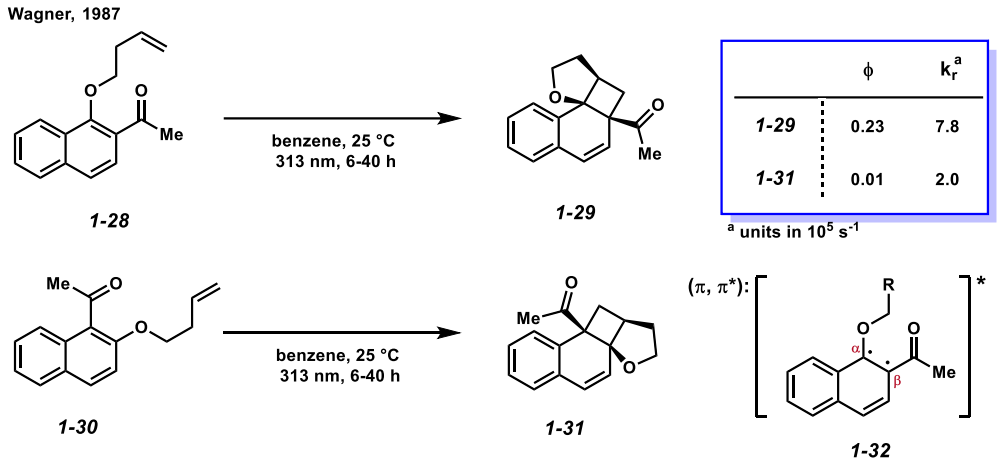

Scheme 1.3.6. Dearomative [2 + 2] cycloaddition via direct irradiation of naphthol arenes.

Yields and selectivity of desired products remained quite low throughout these seminal reports. Likewise, one of the main issues in the intermolecular cycloadditions with indoles discussed was substantial formation of indoline homodimer products. Significant advancements were not made until recently when visible light-mediated methods were applied to [2 + 2] dearomative cycloadditions (*vide infra*).

1.3.3. Early Examples of Dearomative Cycloadditions Promoted by Visible Light

While UV light is an efficient source of energy and can accomplish excitation of many organic molecules through direct irradiation, it is also considered a very harsh and high energy irradiation source.[22] Exposure of certain substrates to UV light can lead to deleterious side reactions discussed in previous sections. Significant efforts have been made to exploit triplet excited states promoted by lower-energy, cost-efficient, visible light sources.[23] In 2014 Bach and coworkers disclosed an intramolecular [2 + 2] cycloaddition of quinolones with tethered alkenes (**1-33**), initiated by visible light photocatalysis (*Scheme 1.3.7*).[24] This was realized through employing chiral thioxanthone **1-35** as an organic photosensitizer. To the authors' delight, this reaction occurred in high yield and enantioselectivity to afford tetracyclic product **1-34**. The origin of selectivity in this reaction arises from the H-bonding capacity of the photocatalyst (**1-35**). When coordinating to quinolone **1-33**, the complex (**1-36**) can be promoted to an excited triplet state (**1-37**)—in the presence of visible light—and can then undergo energy transfer with the bound quinolone. The selectivity comes from the bound planar thioxanthone steering facial attack on the excited double bond.

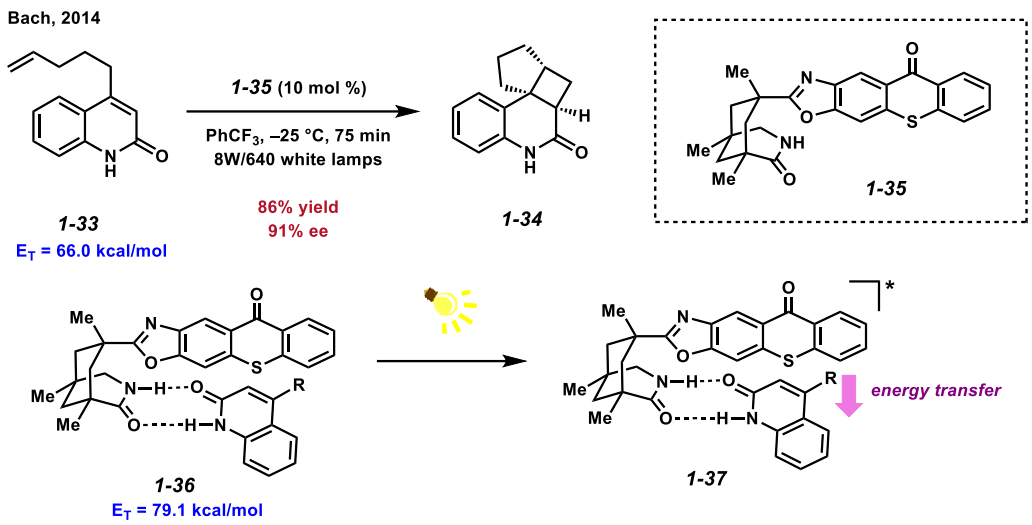

Scheme 1.3.7. Visible light-promoted enantioselective [2 + 2] dearomative cycloaddition.

This process was then translated to an intermolecular [2 + 2] cycloaddition between quinolones (**1-38**) and electron-deficient alkenes (**1-39**, *Scheme 1.3.8*).[25] High yield and enantioselectivity was observed in this reaction as well. Notably, when electron-rich dienes were employed, yield and selectivity were negatively affected. The authors propose that this is likely due to slower reaction rates, leading to irreversible dissociation of the thioxanthone complex.

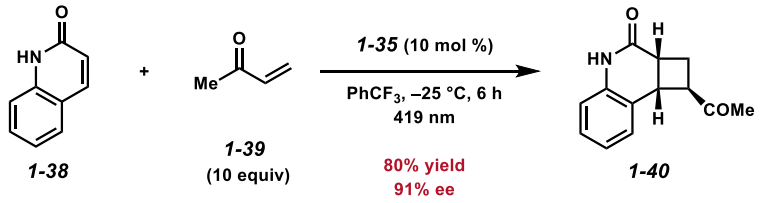

Scheme 1.3.8. Expansion of Bach's work to an intermolecular [2 + 2] cycloaddition.

Following this work, in 2018 Meggers and coworkers described an enantioselective intermolecular [2 + 2] dearomative cycloaddition between benzofurans (**1-41**) and electron-rich alkenes (**1-42**, *Scheme 1.3.9*).[26] This reaction was catalyzed by a visible light-induced chiral Rh Lewis-acid complex.[27] Under these conditions, benzofuran **1-41** and alkene **1-42** afforded cyclobutane product (**1-49**, *Scheme 1.3.10*) in high yield and enantioselectivity. Although an acyl pyrazole functional group was required for selectivity (*vide infra*), the pyrazole could be readily transformed into a methyl ester (**1-43**) which was isolated and characterized.

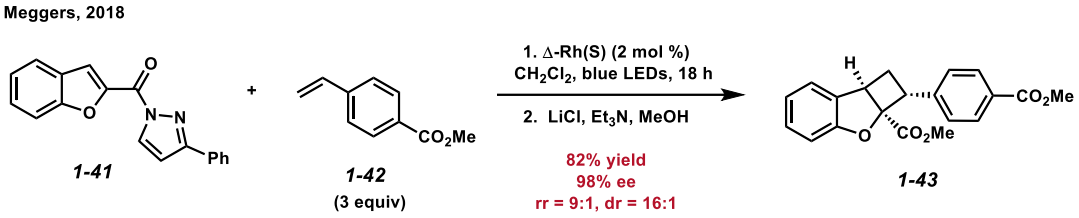

Scheme 1.3.9. Intermolecular [2 + 2] cycloaddition between benzofurans and alkenes.

The authors propose that the reaction proceeds through initial coordination of the chiral Δ-Rh(S)-complex to the acyl pyrazole moiety at C2 of benzofuran **1-41** (**1-44**, *Scheme 1.3.10*). This complex can then absorb a photon upon visible light irradiation and be excited to a triplet state (**1-44→1-46**). The triplet benzofuran can then react with alkene **1-42** to form 1,4-diradical intermediate **1-47**, followed by cyclization (**1-48**), then Rh dissociation to yield **1-49**. The authors note that while enantioselectivity is entirely controlled by the coordinating Rh complex, regioselectivity is likely controlled by the stability of the 1,4-diradical intermediate (**1-47**).

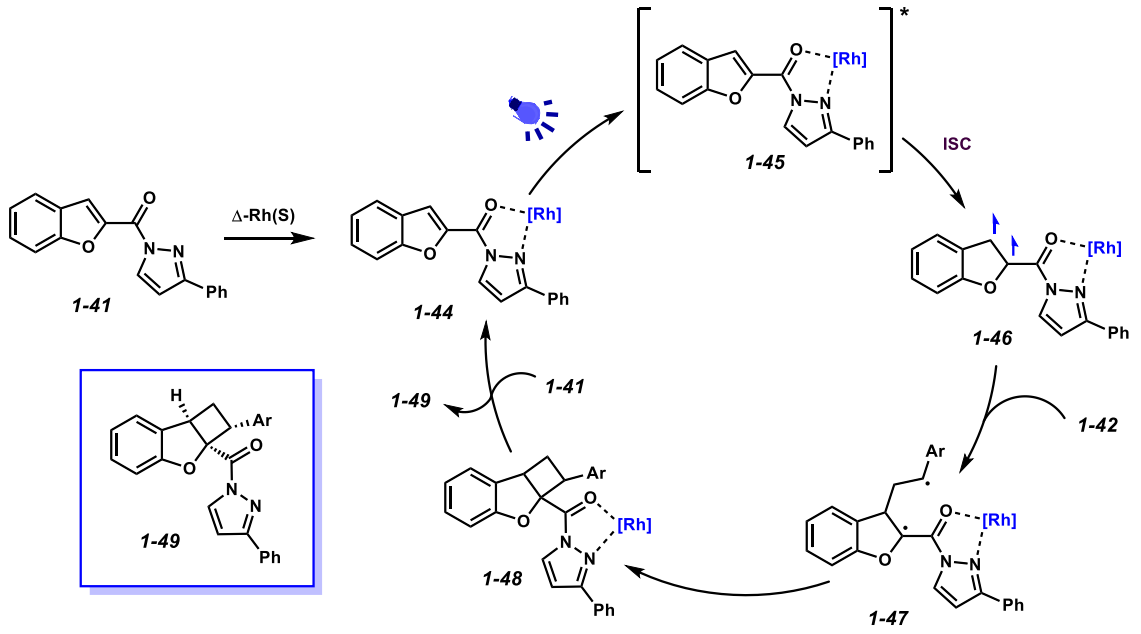

Scheme 1.3.10. Proposed mechanism of enantioselective [2 + 2] cycloaddition with chiral Rh.

This work was closely followed by Glorius and coworkers in 2018, in which they expanded on the worker of Wagner[20] to induce an intramolecular [2 + 2] cycloaddition of 1-naphthol arenes via visible light irradiation (*Scheme 1.3.11*).[28] This annulation was accomplished by applying Ir photocatalysts that absorb in the visible light region.[1,2,29] In preliminary studies, the authors found that depending on the Ir photocatalyst employed, two different products were observed (**1-29** or **1-50**). When Ir catalyst **1-51** was invoked, the Wagner product was observed as the major isomer (**1-29**, the product of triplet sensitization) followed by [2 + 2] cycloaddition. They found that this product (**1-29**) was susceptible to further triplet sensitization (**1-53**) when Ir catalyst **1-52** was employed and could undergo a vinyl cyclobutane rearrangement to generate 1,4-biradical intermediate **1-54**. Finally, radical recombination led to the other complex tetracyclic product (**1-50**). Notably, solvent was found to be an important factor in improving product distribution. An electron transfer mechanism was ruled out based on mismatched reduction potentials.

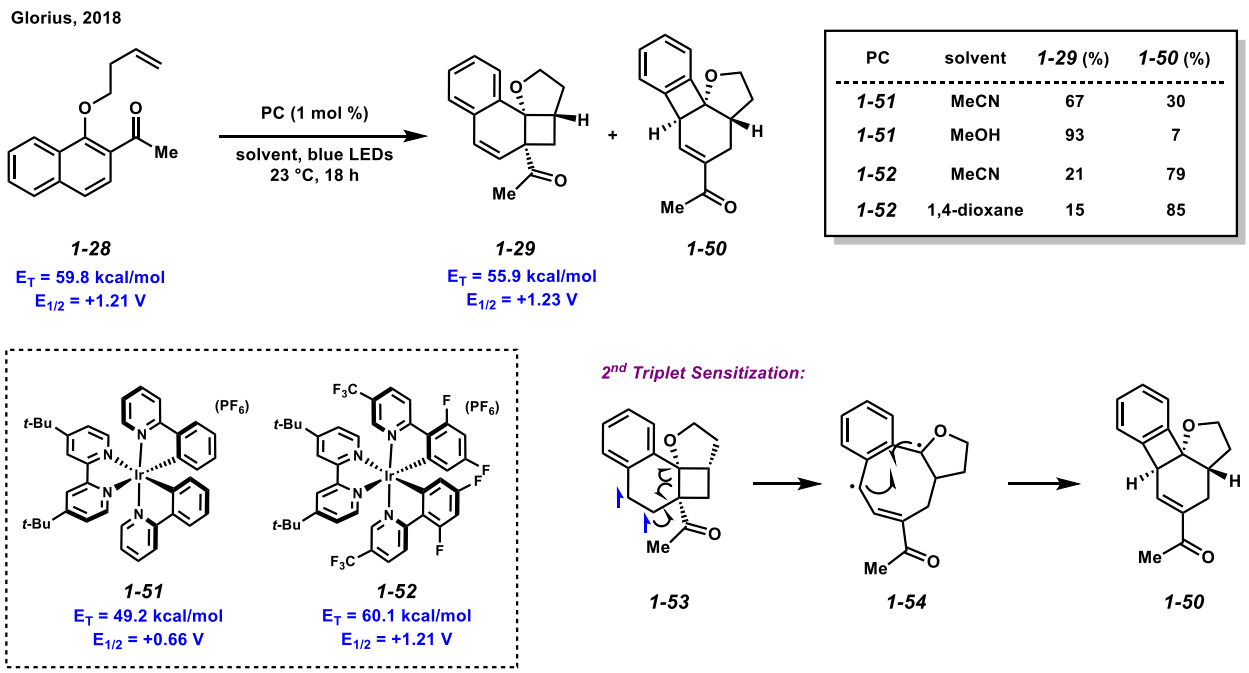

Scheme 1.3.11. Glorius's expansion of Wagner's work to visible light irradiation.

1.3.4. Visible Light-Promoted Intramolecular [2+2] Cycloadditions of Indoles

Translating work done by Bach,[30] Meggers,[26] and Glorius[31] to indoles, in 2019 You[32] and coworkers described an intramolecular [2 + 2] dearomative cycloaddition promoted by visible light (*Scheme 1.3.12*).[33] Substrate design (**1-55**) proved to be a crucial factor in designing this reaction. Initial studies with indole **1-57** were unreactive, likely because of a higher triplet energy value (E_T = 65.0 kcal/mol) than available Ir photosensitizers (E_T = 40.9–60.8 kcal/mol). Adding a phenyl group at the C2 position (**1-58**) sufficiently increased the conjugation of the indole system, thus decreasing the energy gap between T_1 and the ground state (S_0). Addition of an ester group at the C2 position (**1-59**) lowered the energy gap even more, allowing for sufficient sensitization with [Ir(dFCF$_3$ppy)$_2$(dtbbpy)](PF$_6$). Through DFT (density functional theory) calculations, the authors were able to identify a tail-to-tail cyclization as the likely mechanism for cyclobutene formation.

After sensitization with the excited Ir catalyst, intermediate **1-60** can undergo a radical *5-exo-trig* cyclization (**1-61**), followed by intersystem crossing and finally radical cyclization to generate indoline cyclobutene product **1-62**. This process was calculated to be significantly lower in energy than the ground state process (12.7 kcal/mol vs 80.7 kcal/mol).

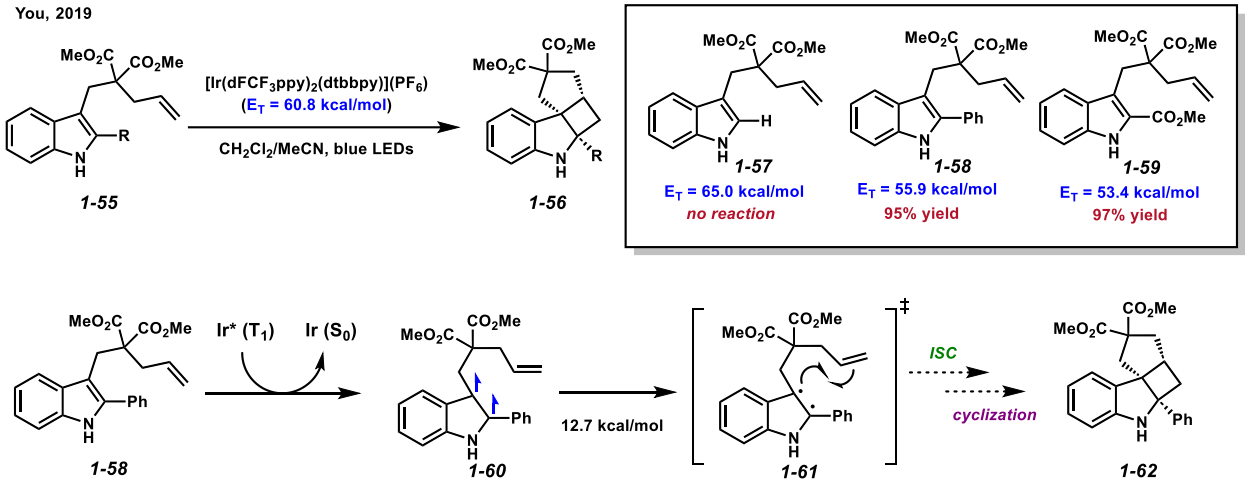

Scheme 1.3.12. Visible light-induced, intramolecular [2 + 2] cycloaddition of indoles utilizing Ir photocatalysis.

Following this report, in 2020 Koenig and coworkers disclosed a complementary visible light-promoted intramolecular [2 + 2] cycloaddition employing organic photocatalyst 2-CzPN (**1-63**, 4,5-bis(carbazol-9-yl)-1,2-dicyanobenzene), catalyzing this reaction without the use of expensive transition metals (*Scheme 1.3.13*).[34] Optimization studies were carried out on 1-naphthol derivative **1-28**.[28] Important to the success of this reaction was choice of sensitizer—one with triplet energy values corresponding to target substrates (*see Scheme 1.3.11*). Based on reports about the photophysical properties of organic dyes, 2-CzPN (E_T = 60.6 kcal/mol) was employed. The desired product **1-50**, formed via triplet sensitized [2 + 2] cycloaddition followed by another

sensitization and rearrangement (*vide supra*), was obtained in 94% yield and in a 16:1 ratio of **1-50** to mono-sensitized product **1-29**.

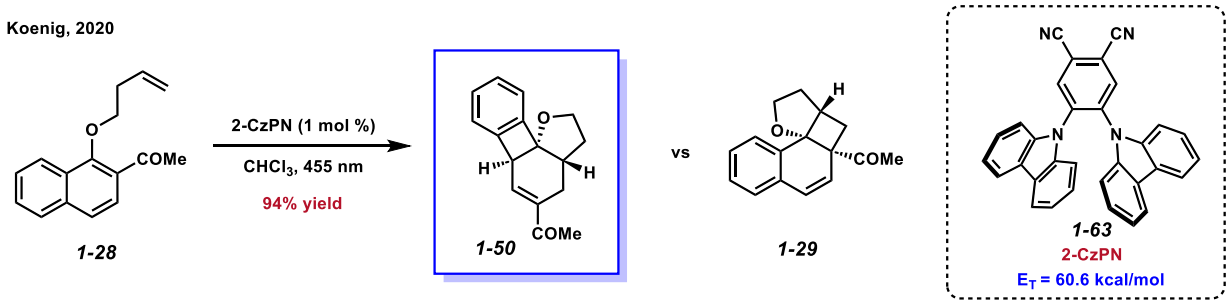

Scheme 1.3.13. Koenig's complementary method to Glorius utilizing 2-CzPN.

This strategy employing 2-CzPN was then translated to indoles with an alkene tether as a complementary method to the previously disclosed work by You[33] (*Scheme 1.3.14*). Interestingly, the authors noted that when the reaction was performed in chloroform, no dearomatized product was observed. Toluene, however, furnished product **1-64** in 95% yield. Nonpolar solvents can inhibit PET, which preferentially occurs in polar solvents in which charges can be stabilized.[35] Different substitution at C2 was tolerated, as well as free *N*-H (**1-64**, **1-67**) and *N*-acetyl (**1-65**, **1-66**). Removal of the bulky diester linker, which facilitates cyclization by the Thorpe–Ingold effect,[36] afforded dearomatized product in excellent yield (**1-66**). Another advantage of this method is that 2-CzPN was recyclable for at least one more round, adding to its sustainability.

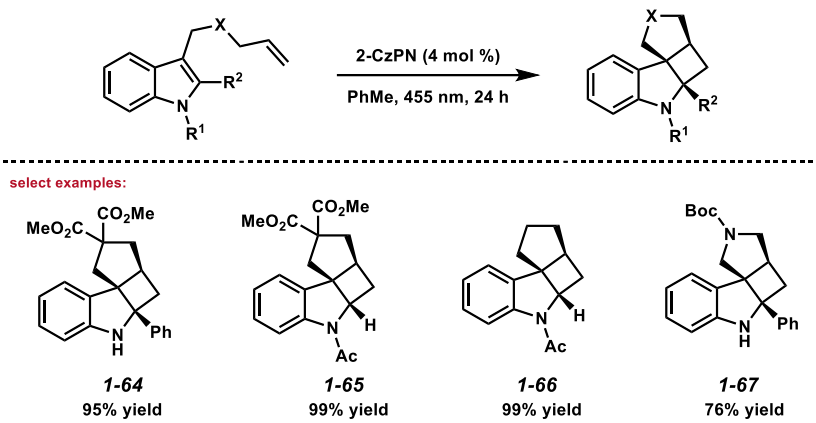

Scheme 1.3.14. 2-CzPN-photocatalyzed extension to indoles.

Shortly after this report, Oderinde and coworkers described another intramolecular [2 + 2] cycloaddition of indoles promoted by visible light (*Scheme 1.3.15*).[37] In this study, the alkene tether was attached at C2 (**1-68**) instead of C3 (*vide supra*) to synthesize highly functionalized, fused cyclobutanes (**1-69**). DFT studies suggested that this reaction proceeded through a *5-exo-trig* cyclization (**1-77**), after triplet sensitization (**1-76**). Cyclization via radical recombination then afforded the final dearomatized product **1-69**. You previously reported that the addition of a phenyl or ester group was required to lower the energy gap of the indole.[33] The authors in this study sought to lower the free energy gap through delocalization by tethering a carboxamide moiety at the C2 position. Protection of free *N*-H of the indole was tolerated in this reaction (**1-71**, **1-75**). Various functional groups on the aromatic ring were also tolerated (**1-71**, **1-75**). Interestingly, this procedure could be translated to other heterocycles such as benzofuran (**1-72**) and benzothiophene (**1-73**). Protection of the amide was found to be necessary for the reaction to proceed (**1-74**).

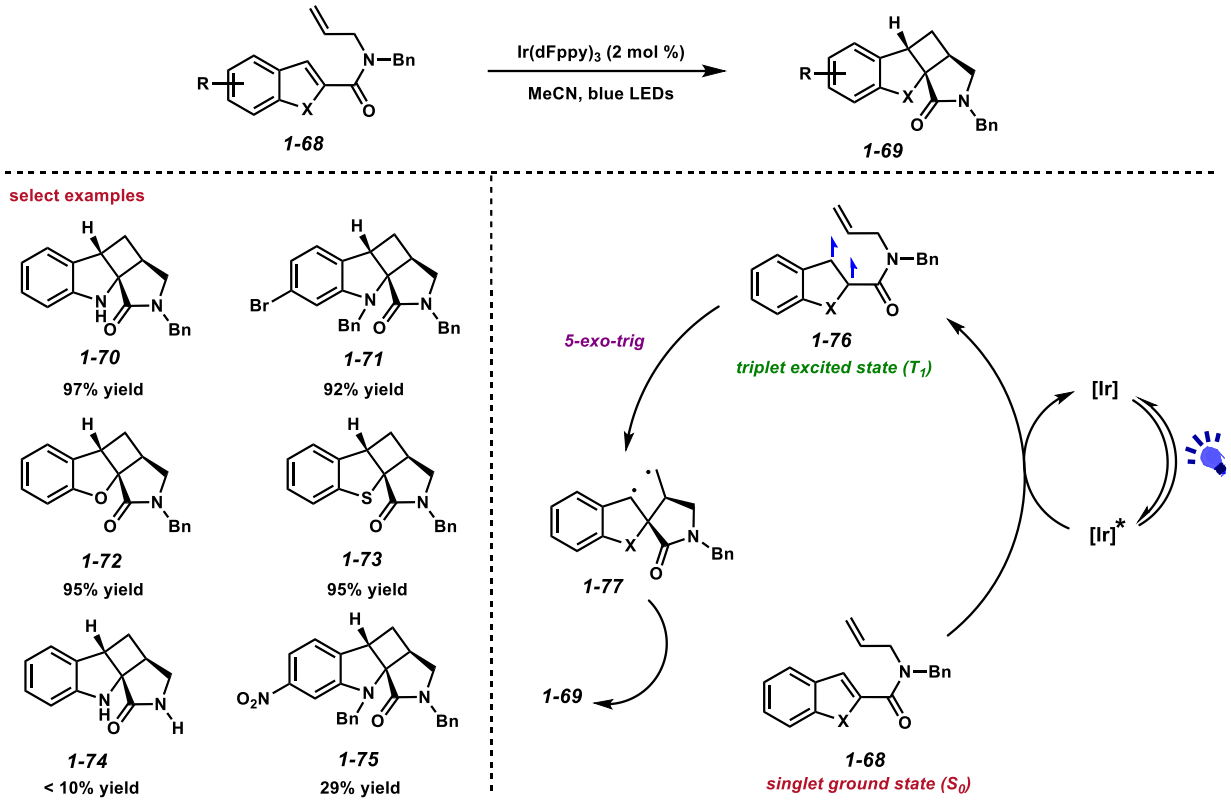

Scheme 1.3.15. Scope and mechanism of Oderinde's [2 + 2] intramolecular cycloaddition.

You and coworkers, in continuation of their previous report,[33] disclosed two additional divergent visible light-promoted intramolecular [2 + 2] reactions tethering the double bond to the *N*-atom of the indole instead of the C3 position (*Scheme 1.3.16* and *Scheme 1.3.17*). A highlight of the first work from 2020 was the divergent nature of intermediate **1-80**, where two separate products (**1-82** or **1-84**) could be obtained depending on the substitution at C3.[38] The two products are a result of either a [2 + 2] cycloaddition (**1-81**) or a 1,5-H atom transfer (**1-83**). This reaction proceeds through activation of the indole alkene in the presence of an oxime. Previously, an oxime was reported to be the excited coupling partner in an aza-Paterno-Büchi [2 + 2] cycloaddition.[39] You confirmed alkene activation over oxime through Stern-Volmer quenching studies in which the

indole substrate (**1-78**)—with the tethered oxime—quenched the excited catalyst, while an indoline-oxime derivative did not.

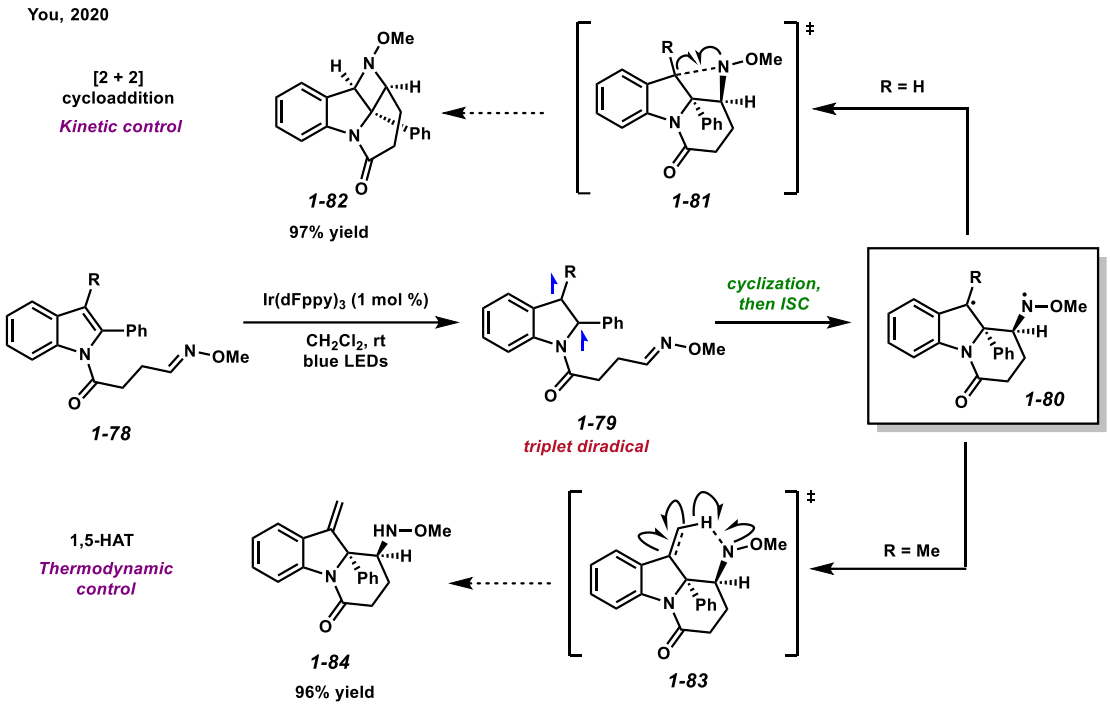

Scheme 1.3.16. You's 2020 divergent synthesis of functionalized indolines.

In a closely related study from 2021, You demonstrated that more complex products could be obtained by changing the indole coupling partner to a cyclopropane (*Scheme 1.3.17*).[40] Specifically, a vinylcyclopropane (**1-85**) was invoked, which is known to be highly reactive in the presence of radicals and is commonly employed as a radical clock (*vide supra*). When substitution was introduced at the C3 position, [2 + 2] cycloaddition products were observed with moderate diastereoselectivity (**1-86**). Interestingly, when no substitution was present at C3, a [5 + 2] thermodynamic product was exclusively obtained (**1-87**).

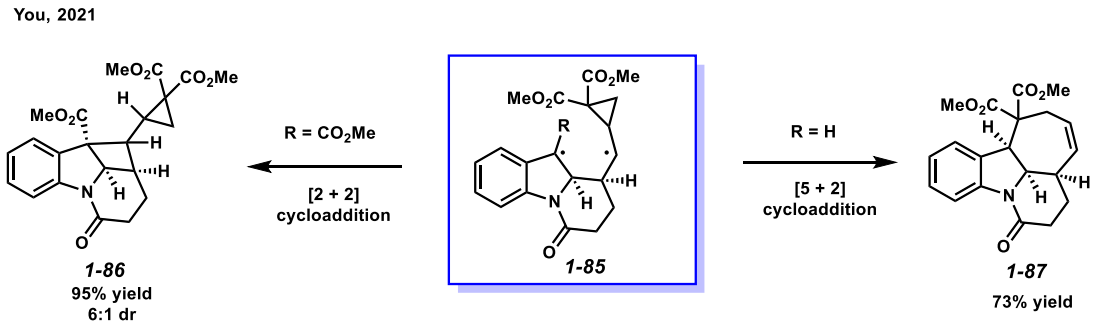

Scheme 1.3.17. Vinylcyclopropanes in divergent cycloadditions with indoles.

Other coupling partners that have proven to be compatible with this intramolecular [2 + 2] photocatalytic cycloaddition of indoles include other alkenes,[41] allenes,[34] alkynes,[42] and arenes[43] (*Scheme 1.3.18*). In concomitant reports, You demonstrated the ability to employ alkynes (**1-88**) and arenes (**1-90**) in these intramolecular cycloadditions with Ir photocatalysts. The alkyne substrates performed worse than their alkene counterparts due to the highly strained cyclobutene product formed (**1-89**).[42] Depending on the arene employed, [2 + 2] (**1-92**) or [4 + 2] (**1-91**) cycloaddition products could be obtained in excellent yields.[43] In an extension of Koenig's report (*vide supra*), allenes were also shown to be effective coupling partners.[34]

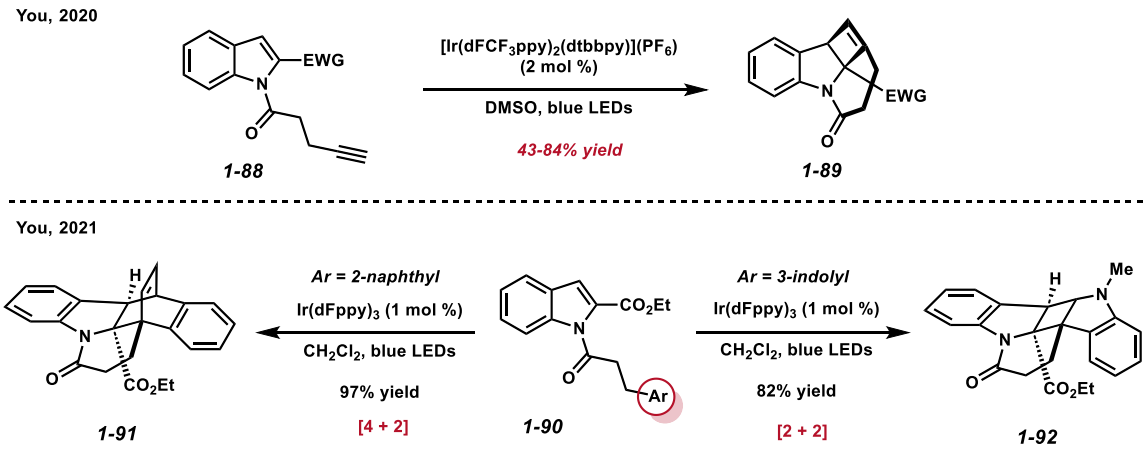

Scheme 1.3.18. Alkynes and arenes in intramolecular cycloadditions with indoles.

1.3.5. Visible Light-Promoted Intermolecular [2+2] Cycloadditions of Indoles

The first visible light-mediated intermolecular [2 + 2] cycloaddition between indoles (**1-93**) and electron-deficient alkenes (**1-94**) was disclosed by Oderinde and coworkers in 2021 (*Scheme 1.3.19*).[44] Previous UV light-promoted methods required excess alkene and encountered significant homodimerization products. An Ir photosensitizer was utilized consistent with previously reported visible light-promoted cycloadditions. A withdrawing group was required on the indole *N*-atom (**1-93**) for any reactivity to occur. Additionally, substitution of the indole C2 position proved to be important in overcoming homodimerization in this visible light-mediated process. When indole **1-96** was subjected to the reaction, the homodimer (**1-98** vs **1-97**) was the major product observed. Introducing a bulkier group at C2 (**1-99**) influenced product distribution between desired cyclobutene product (**1-100**) and the homodimer (**1-101**). The authors found that changing the group to an even bulkier methyl ester (**1-102**) had a profound effect on the reaction and was sufficient congestion to slow dimerization and extend the lifetime of the triplet diradical for the desired intermolecular [2 + 2] cycloaddition to occur (**1-103**, 95% yield). DFT calculations found that the *exo* head-to-tail addition (**1-105** from excited **1-104**) was significantly lower in energy than other addition pathways (**1-106** or **1-107**).

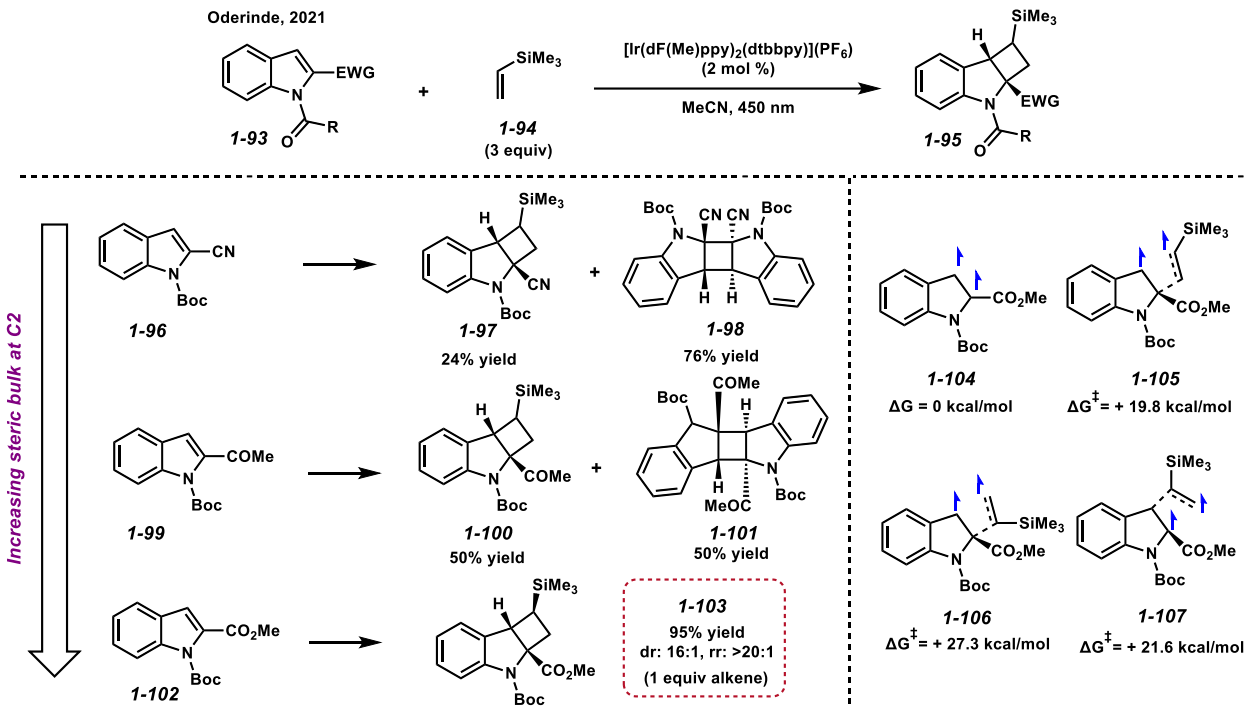

Scheme 1.3.19. Origins of selectivity in intermolecular [2 + 2] cycloadditions between indoles and alkenes.

The scope of this process was extensive (*Scheme 1.3.20*). As the first example of a visible light-promoted intermolecular [2 + 2] cycloaddition with indoles, this method possessed significant value towards the synthesis of potentially bioactive molecules. Other bulky withdrawing groups at C2, including medicinally relevant groups (**1-113**), were disclosed. Functional group tolerance of substitution on the arene of indole was broad (**1-109**, **1-110**, **1-113**). Substitution at C3 could also be incorporated (**1-111**). Mono-1,1- and 1,2-disubstituted alkenes all yielded cycloadduct. Azaindoles were incorporated (**1-112**) and two drugs in phase II/III clinical trials were synthesized using this method (**1-113**, **1-114**). Alkynes could be used as coupling partners, although lower yield was observed. Other heterocycles were also tolerated including benzofurans (**1-115**) and benzothiophenes (**1-116**).

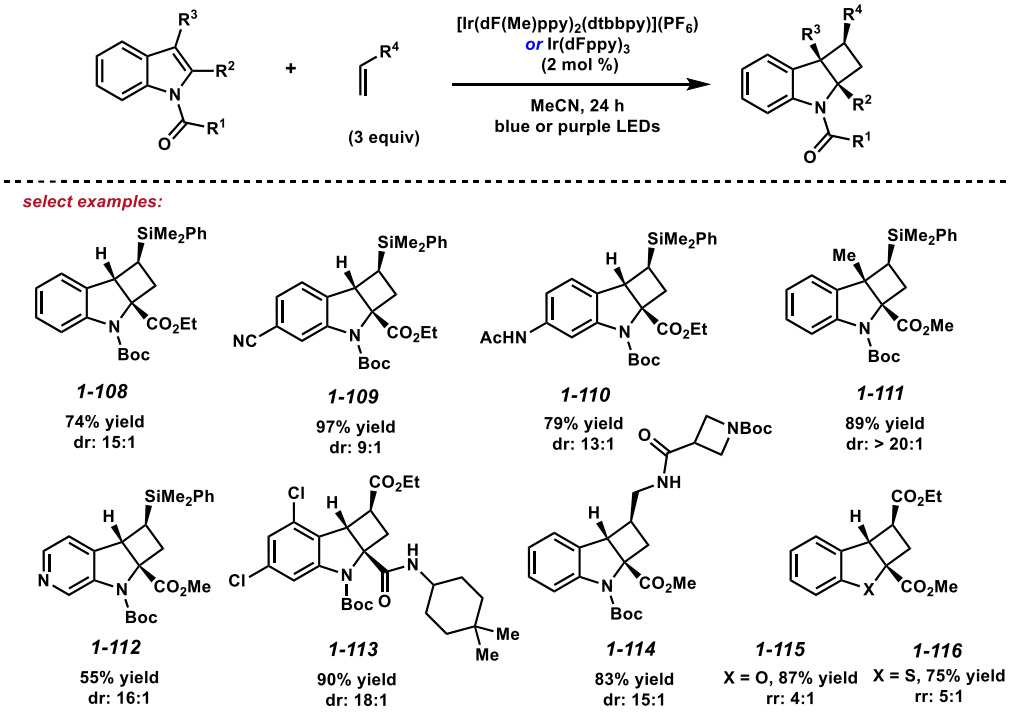

Scheme 1.3.20. Select scope of intermolecular [2 + 2] cycloaddition.

Glorius has also accomplished an intermolecular variant by combining lanthanide Lewis-acid catalysis and visible light-photosensitized energy transfer.[45] A commercially available gadolinium complex ($Gd(OTf)_3$) was found to be competent at inducing energy transfer through visible light excitation (*Scheme 1.3.21*). The desired overall transformation was a [2 + 2] cycloaddition, followed by a ring-expansion to afford cyclopentanindoline cores (**1-123**). By incorporating a pyrazole amide at C2 (**1-118**), Gd(III) can complex to the amide and under irradiation, yield long-lived triplet diradical **1-119**. This diradical can then engage in a stepwise [2 + 2] cycloaddition with present alkene (**1-120**). The authors suggest that the cyclobutene product (**1-121**) then spontaneously undergoes a semi-pinacol rearrangement to cyclopentane intermediate (**1-22** or **1-124**). Notably, when no substitution is present at C3 (**1-124**), a rearomative sequence follows this rearrangement (**1-124→1-26**). However, when an alkyl group is present at

C3 (**1-122**), the pyrazole group can migrate to C2 to furnish product **1-123** in excellent yields and regioselectivity. Other lanthanide complexes, photosensitizers, and even dual Lewis-acid–photocatalyst systems were unsuccessful in catalyzing this reaction.

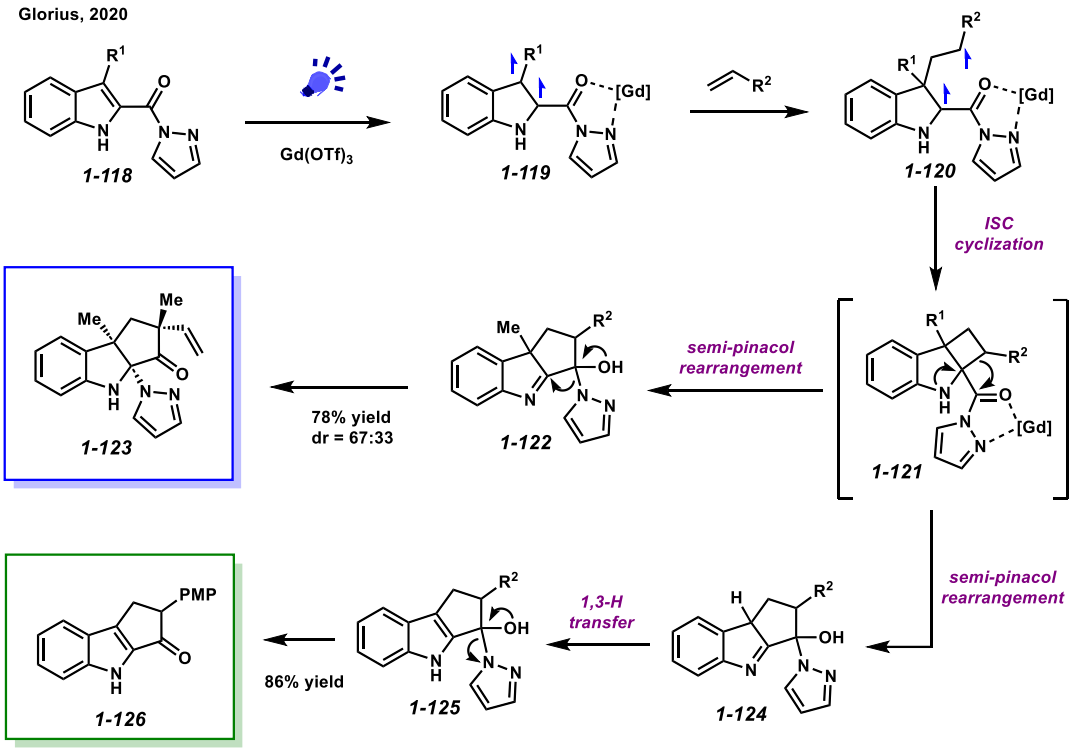

Scheme 1.3.21. Glorius's divergent cascade cycloaddition/rearrangement mechanism.

Experiments were performed to support this proposed energy transfer pathway. Separately, indole **1-118** or $Gd(OTf)_3$ showed no absorbance in the visible light region; however, when mixed together a significant bathochromic shift was observed in the UV-vis absorbance spectrum. Additionally, alkene dimerization was observed as a background reaction, purportedly through triplet energy transfer to the alkene, followed by [2 + 2] cycloaddition. When *(E)*-stilbene (**1-127**) was irradiated with catalytic indole, minimal isomerization product was detected (**1-128**) ((*E*) to (*Z*) stilbene isomerization is a known photocatalytic process)[46] (*Scheme 1.3.22*). A similar result

was observed when catalytic $Gd(OTf)_3$ was employed. When indole **1-118** (5 mol %) and $Gd(OTf)_3$ (1 mol %) were irradiated together with alkene **1-127**, significant isomerization was observed. These results support a triplet excitation of an indole-Gd complex.

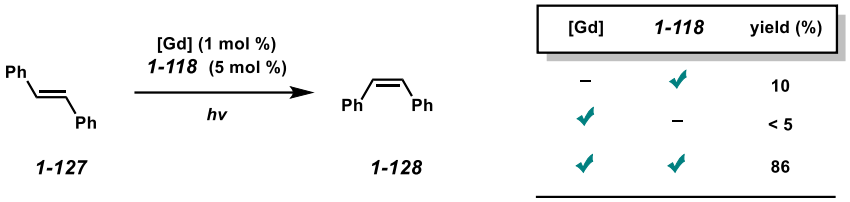

Scheme 1.3.22. Photocatalytic isomerization of stilbene.

1.4. Dearomative Cycloadditions Enabled by PET

Upon excitation with a photon, certain compounds have the capacity to engage in electron transfer, known as photoredox catalysis.[1] Photoredox catalysis details the process by which metal complexes or organic dyes engage in single electron transfer (SET) with organic molecules upon excitation with UV or visible light (i.e., PET). Early photocatalysts were typically organic dyes, most of which require high energy UV light to be excited. Many recently reported transition-metal based photocatalysts, however, can be activated by lower-energy visible light. Commonly employed metal-based photocatalysts are ruthenium- or iridium-based, with highly conjugated ligand frameworks that can be tuned to reflect desired reactivity (i.e., either making them more oxidizing or more reducing). To explain how these electron transfers occur with transition-metal complexes, $Ru(bpy)_3^{2+}$ will be used as a representative example (*Figure 1.4.1*). When this complex, with a λ_{max} in the visible light region (451 nm), is irradiated with a compatible light source, it will absorb a photon and become excited. An electron from the metal-centered t_{2g} orbital

is promoted to a ligand-centered π* orbital. This process is known as metal-to-ligand charge transfer (MLCT). This high energy singlet excited state then undergos rapid ISC to afford the lowest energy triplet excited state, in which the Ru metal center has been oxidized (hole in t_{2g}) and the ligand has been reduced (unpaired electron in π*). Organic sensitizers undergo a similar process, excluding the MLCT event. These catalysts typically have very long excited state lifetimes and can engage in EnT (*vide supra*) or PET processes. Notably, it has been found that many transition-metal photocatalysts have extremely long excited state lifetimes, especially compared to their organic counterparts (*Figure 1.2.1*). This excited state catalyst ($[Ru(bpy)]^{2+*}$) is highly reactive and can react as either a single electron oxidant (hole in t_{2g} is filled) or a single electron reductant (unpaired electron in π* is donated). Similar to E_T values previously discussed, each photocatalyst has potentials associated with their capacity to oxidize or reduce other molecules through SET called reduction potentials ($E_{1/2}$).

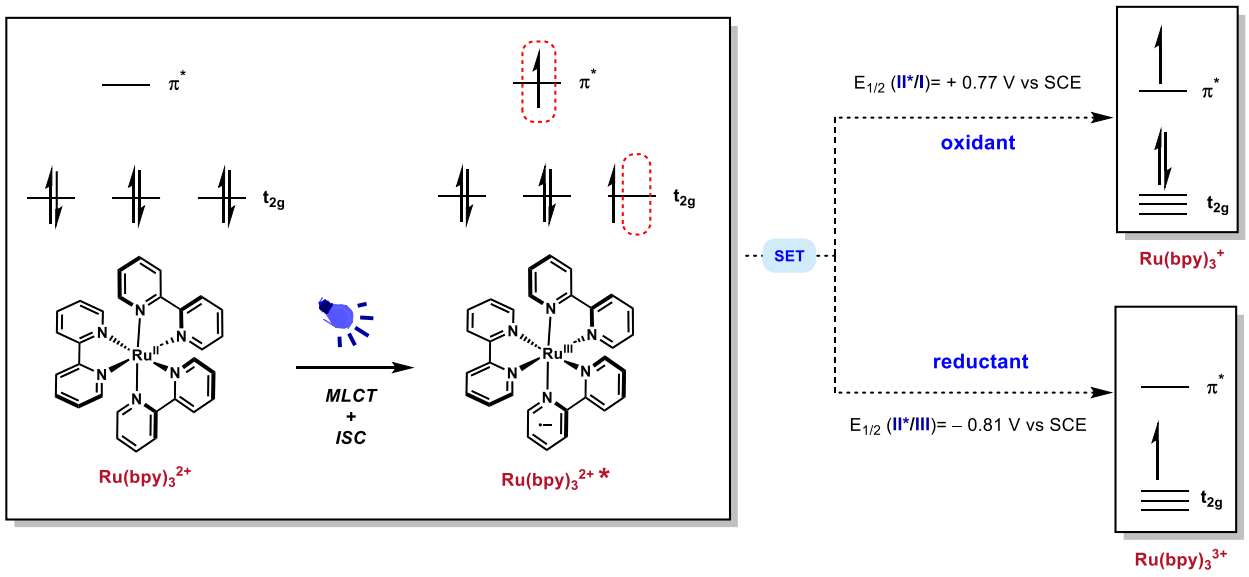

Figure 1.4.1. Simplified molecular orbital diagram of photocatalyst $[Ru(bpy)_3]^{2+}$. Recreated image from MacMillan et al.[1a]

1.4.1. UV Light-Promoted (4+2) Cycloadditions of Indoles

In 1990, Steckhan and coworkers reported a radical cation Diels–Alder cycloaddition between indole (**1-129**) and 1,3-cyclohexadiene (**1-130**) to generate dearomatized, highly functionalized indolines (**1-132**) (*Scheme 1.4.1*).[47] This was accomplished through irradiation with TPPT (triphenylpyrylium tetrafluoroborate), an organic photosensitizer ($E_{1/2}$ = +2.02 V).[48] The authors accomplished this cycloaddition, otherwise not attainable by thermal means, through a single electron oxidation of the indole substrate. The subsequent radical cation generated could react with present electron rich diene in a formal (4 + 2) cycloaddition, followed by acylation of the cycloadduct (**1-131**). Notably, the authors found that when indole was subjected to reaction conditions with no acetyl chloride present, only trace amounts of cycloaddition product (**1-131**) were observed. This is because the indoline product of cycloaddition (**1-131**) would be in competition with starting indole to quench the excited photocatalyst ($E_{1/2}$ = +0.46 V, **1-131** vs. $E_{1/2}$ = +1.16 V, **1-129**), leading to product inhibition.[49] Acylation of the indoline product (**1-131**) would raise the oxidation potential of the cycloadduct (**1-132**, $E_{1/2}$ = +1.30 V) above indole **1-129**, thus allowing the reaction to proceed.

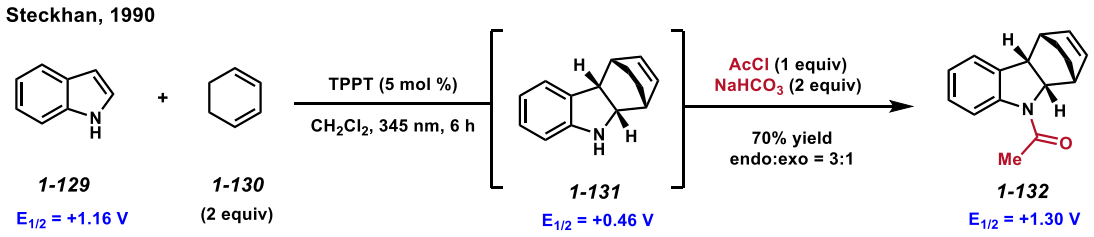

Scheme 1.4.1. (4 + 2) cycloaddition with indoles and cyclic dienes via PET.

The reaction proceeds via excitation of TPPT, followed by quenching of this excited state with indole to generate radical cation **1-133** and reduced TPPT (*Scheme 1.4.2*). This reaction was found to be highly regioselective when substitution was present on the diene, with the *endo* adduct being favored. After nucleophilic attack of indole radical cation **1-133** by 1,3-cyclohexadiene (**1-130**) a highly stabilized radical cation intermediate (**1-134**) is formed. Back reduction, or propagation, can afford cycloadduct **1-131**. As previously mentioned, without acetyl chloride, **1-131** can be preferentially oxidized (**1-135**), halting reactivity. The authors noted that when acetylated indole was subjected to the reaction, no product was observed, leading them to assume acylation (**1-131**→**1-132**) occurs as the ultimate step. Calculations indicated that this pathway proceeds through an asynchronous mechanism and that nucleophilic attack at C3 leads to a lower energy transition state and intermediate than nucleophilic attack at C2, justifying selectivity.[50] Semiempirical evidence of a long-bond intermediate stabilized as a distonic radical cation (**1-134**) further supported the mechanistic proposal.

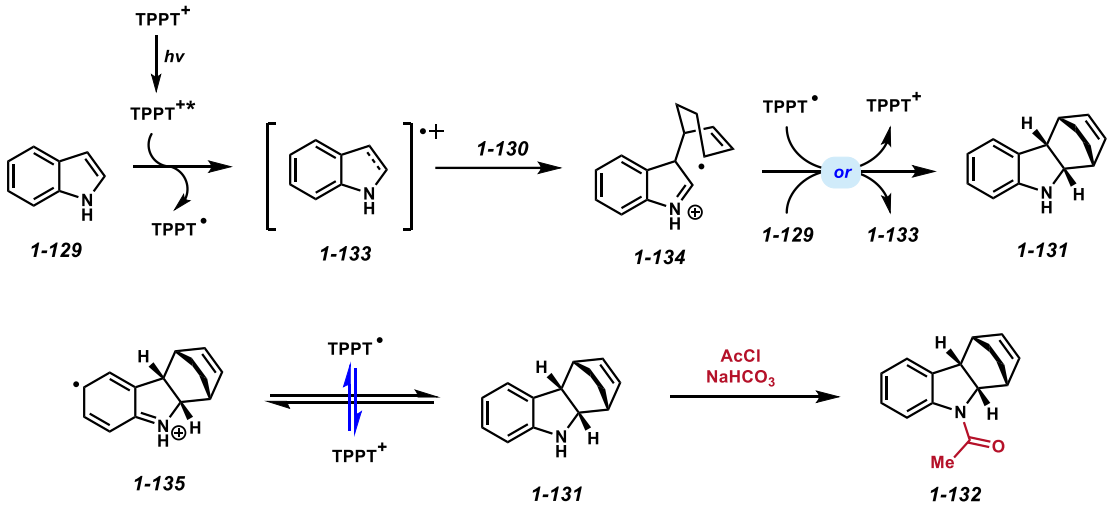

Scheme 1.4.2. Mechanism of (4 + 2) cycloaddition with indole and 1,3-cyclohexadiene.

The scope of 1,3-cyclohexadienes (**1-136**) that were tolerated in the reaction are shown in *Scheme 1.4.3*. A number of different cyclic dienes with alkyl (**1-138**–**1-140**) and acetoxy (**1-141**, **1-142**) substitution led to moderate yields of cycloaddition product, with only minimal dimerization observed (< 10%). When indoles with C2 or C3 substitution were tested, they yielded no (C2) or trace (C3) cycloaddition product, likely due to steric constraints.

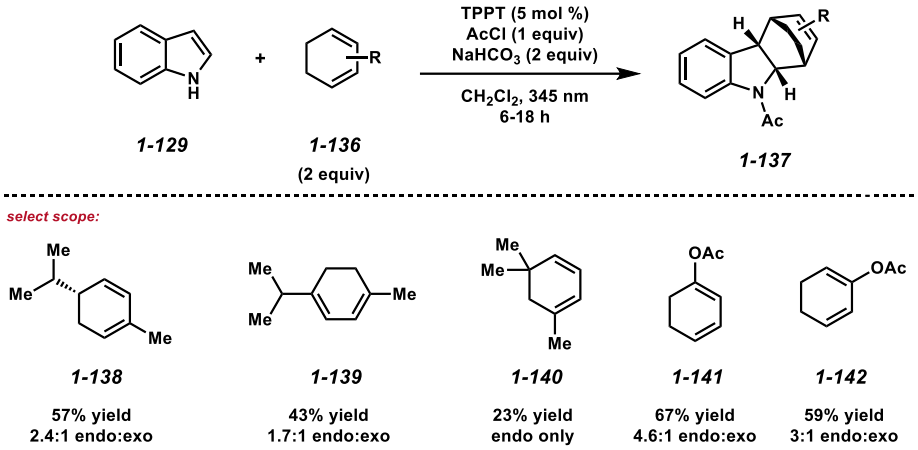

Scheme 1.4.3. Select scope of (4 + 2) cycloaddition with indoles and cyclohexadienes.

Steckhan and coworkers reported several follow-up studies to this in which other dienes were explored. In 1993, they reported a (4 + 2) cycloaddition with indole (**1-129**) and exocyclic dienes (**1-143**, *Scheme 1.4.4*).[51] Cis dienes were required for reactivity to occur; however, the product was observed as a 1:1 mixture of diastereoisomers (**1-45**). The authors used this mixture as further corroborating evidence of the existence of stabilized intermediate **1-144**, as this is the most likely point of isomerization.[52] Since cis dienes were required for reactivity, a diene with intentional cleavage points was next pursued.[53] Diene **1-147** was found to successfully afford highly functionalized tetrahydrocarbazoles (**1-148**). The N-O bond could be readily cleaved using reductive sodium amalgam conditions to furnish tetrahydrocarbazole **1-149**.

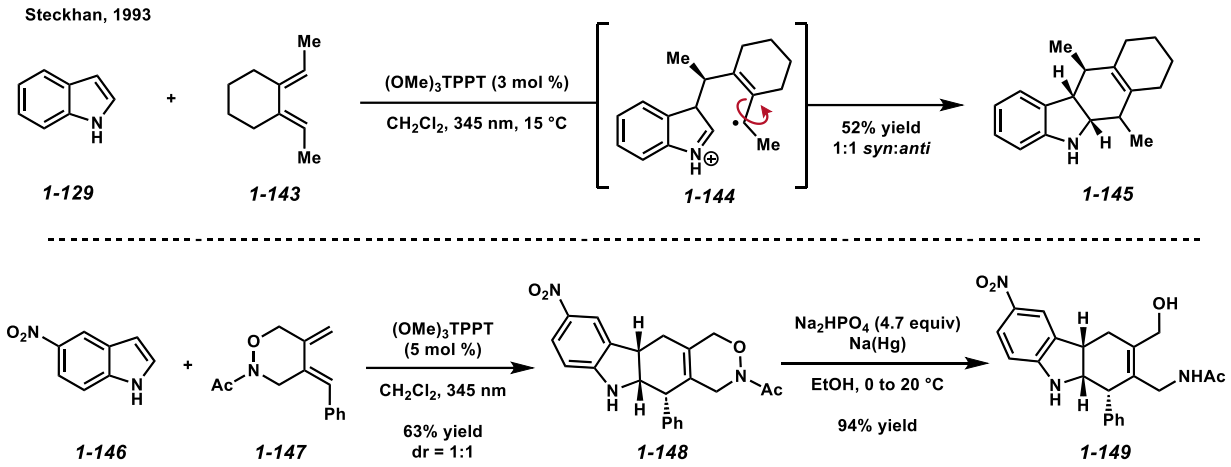

Scheme 1.4.4. Exocyclic dienes in (4 + 2) cycloadditions with indoles.

1.4.2. Visible Light-Promoted (4 + 2) Cycloadditions of Arenes

Sarlah and coworkers have reported several examples of dearomative cycloadditions using a visible light-promoted exciplex system.[54] In 2016, his group disclosed a dearomative cycloaddition between arenes (**1-150**) and MTAD (*N*-methyl-1,2,4-triazole-3,5-dione, **1-151**, *Scheme 1.4.5*).[55] MTAD was chosen as an "areneophile" because of its low lying and narrow HOMO-LUMO gap, which allows for excitation when irradiated with visible light. After excitation (**1-152**), MTAD can form an exciplex with present arene either through electron transfer (**1-153**) or a charge transfer (*not pictured*). The product of subsequent cycloaddition (**1-154**) is poised for a number of further modifications. The authors were able to perform an *in situ* dihydroxylation with OsO_4 to afford relevant diols.

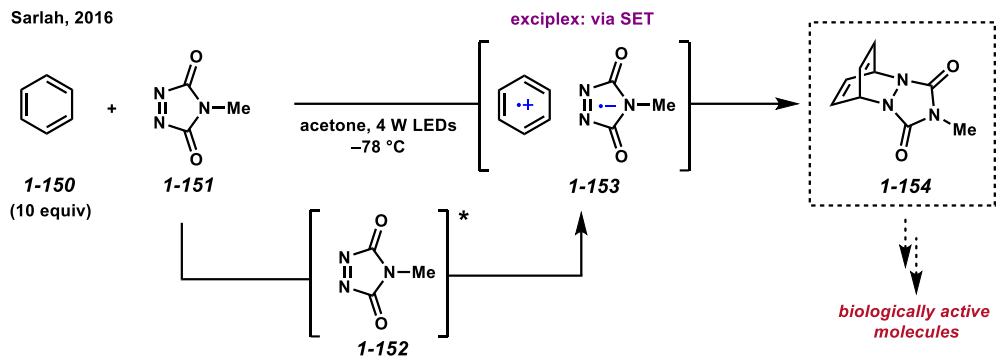

Scheme 1.4.5. Dearomative (4 + 2) cycloaddition via a visible light induced exciplex.

This article represented one of the first examples of a mild, photochemical dearomative approach that did not require excessive post-transformation steps to access biologically relevant compounds. The synthesis of **1-159**, an analogue of a known potent herbicide, was accomplished through the route shown in *Scheme 1.4.6*. After the key formal (4 + 2) transformation and *in situ* dihydroxylation (**1-156**), the resulting diol could be protected as an acetal. The "arenophile" was then fragmented via urazole hydrolysis, followed by subsequent hydrazine oxidation to afford **1-157**. Next, dihydroxylation of **1-157** yielded **1-158** stereoselectively. Lastly, a Sonogashira coupling and acetal deprotection furnished the highly oxygenated compound **1-159** in excellent yield.

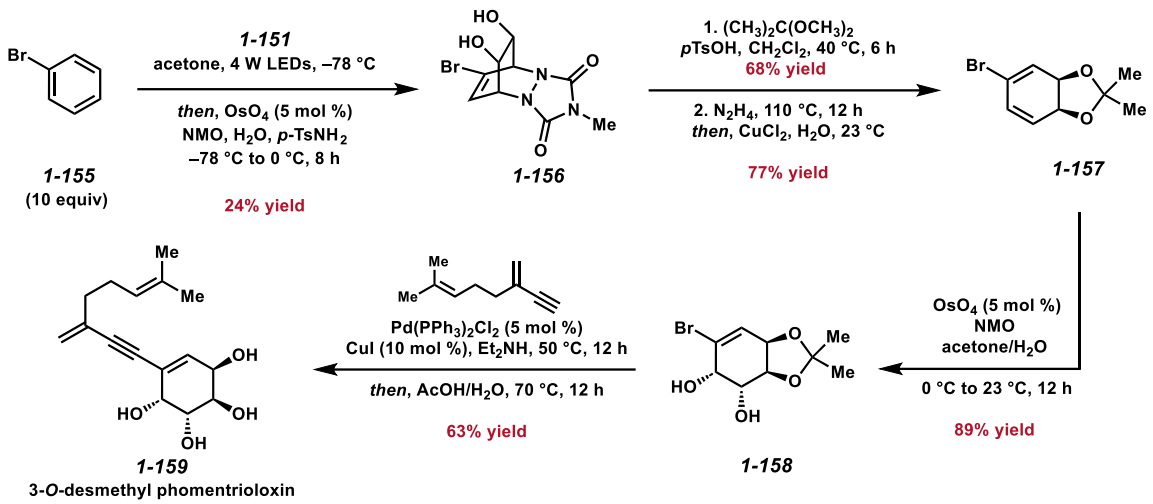

Scheme 1.4.6. Facile synthesis of 3-O-desmethylated phomentrioloxin.

1.4.3. Visible Light-Promoted (4 + 2) Cycloadditions of Indoles

Inspired by the work of Steckhan and coworkers,[47] in 2017 the Yoon group[56] reported a similar (4 + 2) cycloaddition between indole (**1-129**) and 1,3-cyclohexadienes (**1-136**), catalyzed by platinum nanoparticles supported on titanium dioxide semiconductor particles (Pt(0.2%)@TiO_2) that could be excited by visible light irradiation (*Scheme 1.4.7*).[57] As a highlight of this work, the heterogeneous catalyst utilized is recyclable with no loss in efficiency after two uses. After the fourth use, reactivity dropped dramatically, possibly due to surface poisoning by present organics. The scope was more extensive than the TPPT-catalyzed system, although selectivity remained similar (i.e., *endo* vs *exo*). Various functional groups on indole were tolerated (**1-160**), as well as substitution of the cyclohexadiene (**1-162**). While C2-methyl indole afforded no product, C3-substituted indole yielded **1-161**, albeit in low yields. Other protecting groups were also compatible, such as Troc (**1-163**), albeit in reduced yields. The authors suggested that this reaction likely proceeds through initial surface binding of indole to TiO_2, and the subsequent

complex can absorb a photon and become excited. This excited complex can be quenched by O_2 or $MeNO_2$ to form the reactive indole radical cation that can be intercepted by cyclohexadiene and proceed to **1-137**.

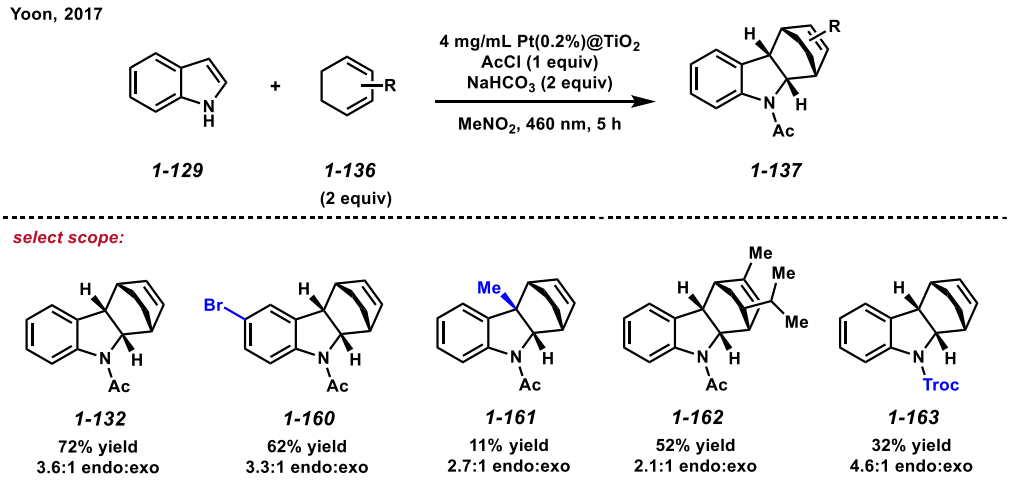

Scheme 1.4.7. Visible light-promoted (4 + 2) cycloaddition with indoles and 1,3-cyclohexadienes.

1.5. Dearomative Cyclizations

1.5.1. Visible Light-Promoted Intramolecular Dearomative Cyclizations of Arenes

Cycloadditions of aromatic compounds induced by PET have been extremely limited in the literature. While still underreported, radical *cyclizations* via PET have been more explored.[58] The majority of methods that invoke UV light-promoted radical additions into aromatic systems has led to rearomatized products.[59] With the advent of modern photochemistry, new methods have allowed for more careful design of reaction methodology. Specifically, reductive dehalogenation[60] has opened the door for many dearomative radical cyclizations to successfully operate under mild conditions. In 2015, Xia and authors disclosed a trifluoromethylation–spirocyclization sequence

initiated by visible light-mediated PET (*Scheme 1.5.1*).[61] The researchers were inspired to generate a trifluormethyl radical interemediate via oxidative quenching of an excited Ir(III) photocatalyst by Togni's reagent (**1-167**). They chose *N*-arylcinnamamide (**1-164**) as the coupling partner with the intent of synthesizing trifluoromethylated dihydroquinolin-2(1*H*)-one derivatives (**1-165**). Interestingly, the authors observed that when **1-164** was *para*-substituted with a hydroxyl or OTBS functional group, dearomatized, spirocyclic compound **1-166** was formed in 70% yield. This report represented one of the first examples of a visible light-promoted aza-spirocyclization.

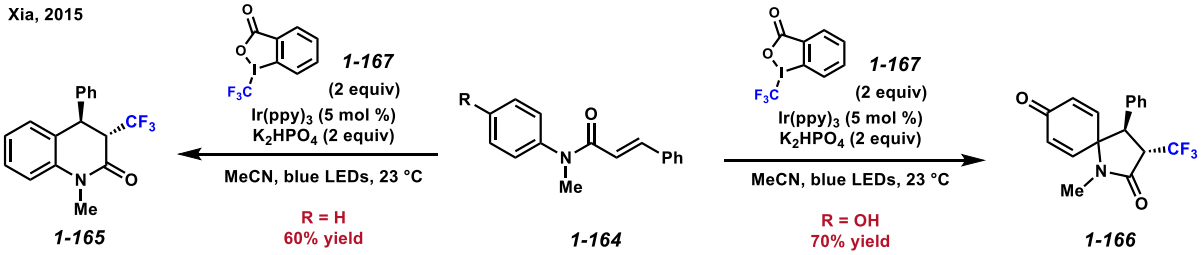

Scheme 1.5.1. Xia's divergent radical cyclization.

1.5.2. Visible Light-Promoted Intramolecular Dearomative Cyclizations of Indoles

In 2016, Zhu and coworkers were inspired to synthesize fused or spirocyclic indolinones because of their structural abundance in alkaloid natural products.[62] The authors envisioned accomplishing this through an oxidative photochemical process. It was found that when indole **1-168**, containing an *N*-tethered alcohol functional group, was irradiated with visible light in the presence of $[Ru(bpy)_3]Cl_2$, O_2, and CsOAc—oxindoline **1-169** was afforded in 68% yield (*Scheme 1.5.2*). While substitution at C3 was not tolerated, alkyl groups could be incorporated at C2 with little impact on indolone yield (**1-170**). Interestingly, when the alcohol tether was changed to the C2 position (**1-171**), spirocyclic indoline **1-172** could also be obtained in good yield.

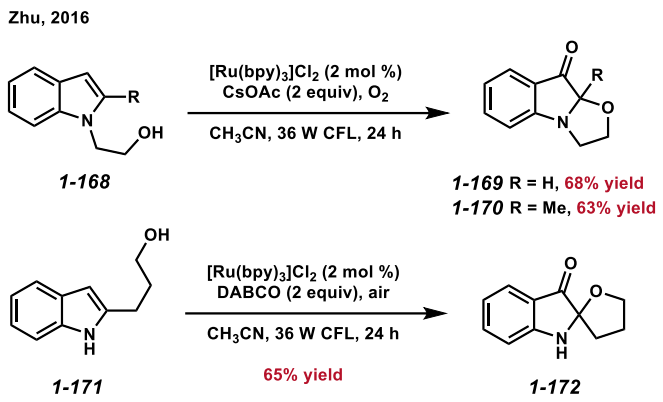

Scheme 1.5.2. Cyclization and spirocyclization of tethered indoles via photoredox catalysis.

This reaction was thought to proceed through an initial photooxidation of indole **1-168** by Ru(II) to generate indole radical cation **1-173** (*Scheme 1.5.3*). The reduced Ru(I) species could then be oxidized back to ground state Ru(II) by molecular oxygen. The generated superoxide radical anion could then react with radical cation **1-173** to afford peroxy intermediate **1-174**. **1-174** could then cyclize via an intramolecular, base-promoted, nucleophilic attack to yield peroxide **1-175**. The formation of indolinone **1-169** occurs by cleavage of the O-O peroxide bond and loss of water, presumably during the aqueous workup.

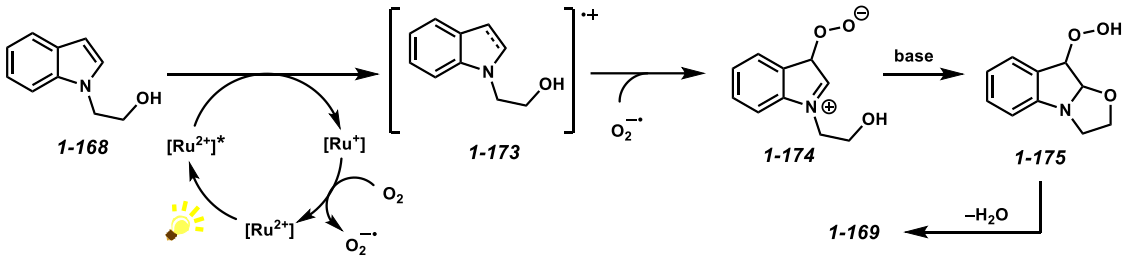

Scheme 1.5.3. Proposed mechanism of oxidative cyclization.

In 2018, Wang and coworkers disclosed another dearomative cyclization.[63] They were enticed by the idea of introducing a difluoromethylene (CF_2) group to 3,3-spirocyclic indolines, both of which have extensive foundations in biologically active molecules.[64] Previous methods to synthesize these compounds invoked a thermally promoted dearomative cyclization–nucleophilic attack sequence. Wang and coworkers sought to develop a complementary approach to these methods that proceed through PET (*Scheme 1.5.4*). Indoline **1-177** was formed upon irradiation with visible light, in the presence of **1-176**, TMSCN, Ir photocatalyst, and base. HFIP was also found to be an important additive, stabilizing the charged intermediate produced after radical cyclization and oxidation (**1-184**, *Scheme 1.5.5*, *vide infra*). The authors found that electron-donating (**1-178**) and withdrawing (**1-179**) groups were tolerated at C2, with only one diastereomer observed. Other groups such as *N*-allyl (**1-180**) or benzyl (*not pictured*) were also tolerated with moderate diastereoselectivity. Interestingly, when the indole *N*-substituent was replaced with Boc (*tert*-butyloxycarbonyl), only the β-H elimination product was observed (**1-181**).

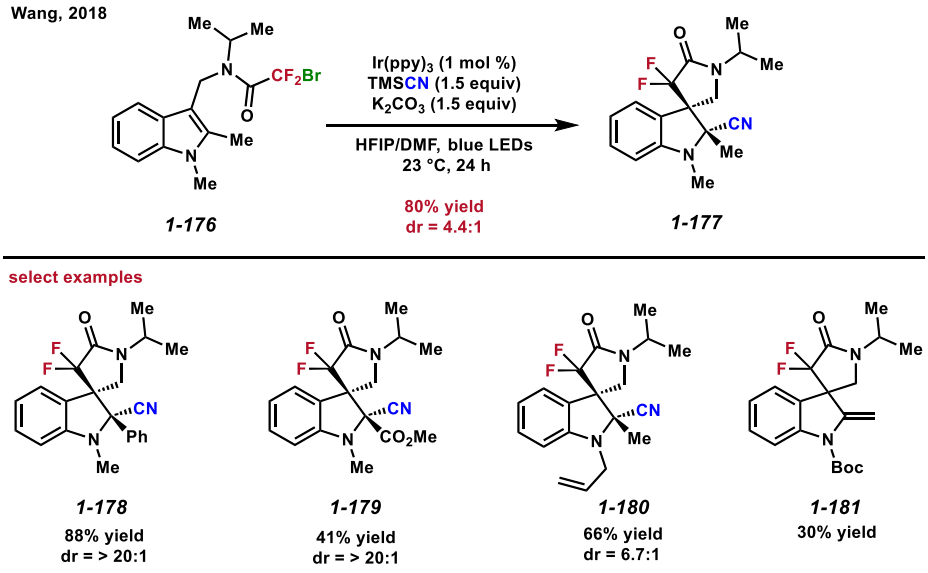

Scheme 1.5.4. Cascade spirocyclization-nucleophilic attack via PET.

The mechanism of this reaction is depicted in *Scheme 1.5.5*. The PET catalytic cycles described thus far have been reductive quenching cycles, whereas this process occurs through an oxidative quenching cycle. **1-176** is reduced by excited Ir(III) photocatalyst and will spontaneously extrude Br anion (Br^-) to form radical intermediate **1-182** and oxidized Ir(IV). **1-182** could then cyclize to generate a new radical intermediate (**1-183**), which in turn can be oxidized by Ir(IV) to generate cation **1-184** and ground state Ir(III). Finally, nucleophilic attack by TMSCN will afford product **1-177**.

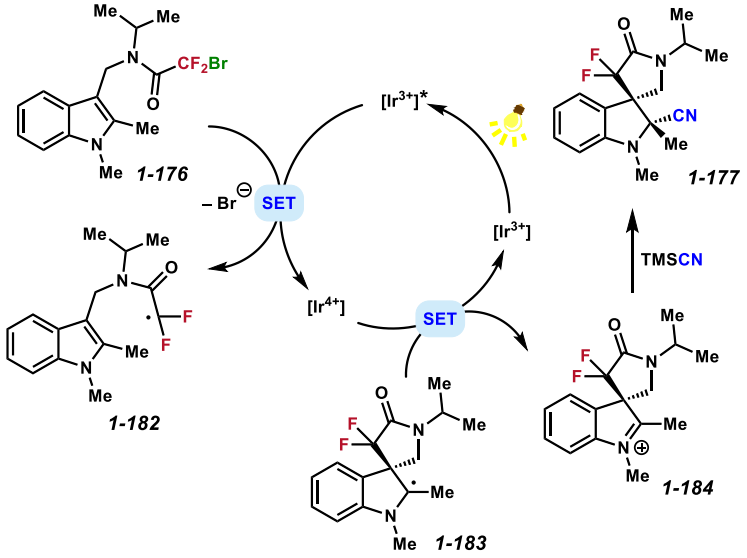

Scheme 1.5.5. Mechanism of Wang's spirocyclization of difluorinated indolamines.

Wang followed this study with a closely related method in which cation generated from **1-185** was trapped by water to generate hydroxyl indoline spirocycles that could be readily oxidized to oxindoles (**1-186**, *Scheme 1.5.6*).[65] The authors found that PCC (pyridinium chlorochromate) was sufficient to oxidize the hydroxy-spirocycles to oxindoles.

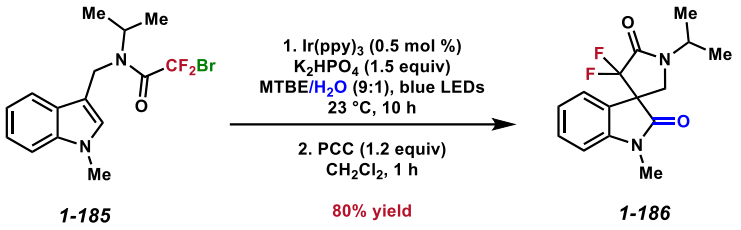

Scheme 1.5.6. Synthesis of spirocyclic oxindoles via PET.

In 2017, Wang and coworkers pursued a PET-mediated cyclization of indole aryloxyamide derivatives (**1-187**) to synthesize pyrroloindolines (**1-189**, *Scheme 1.5.7*).[66] By employing an amidyl radical (**1-191**) as the reactive intermediate that can be generated through photoreduction (**1-190**),[67] cyclization (**1-192**) and intermolecular radical addition will transpire to afford pyrroloindoline **1-189**.

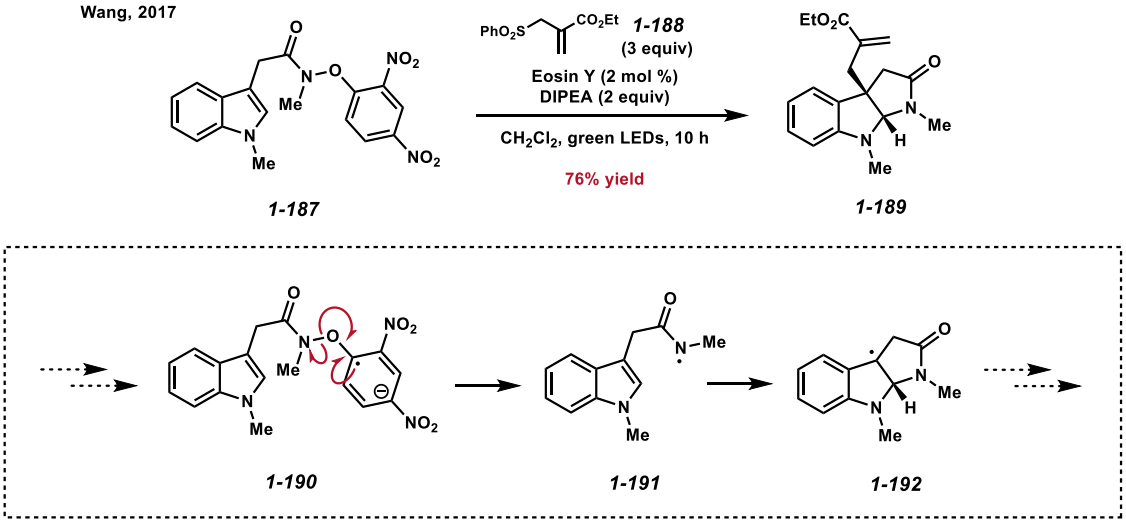

Scheme 1.5.7. Cyclization of indole aryloxyamide to pyrroloindoline.

The authors applied this method toward the synthesis of natural product (±)-Flustramide B (*Scheme 1.5.8*). Employing the *N*-prenylated indole aryloxyamide **1-194** and alkene **1-195** in the key cyclization reaction afforded **1-196** in 76% yield. Reduction of sulfone **1-196**, followed by cross metathesis, furnished Flustramide B (**1-198**) in five total steps from 6-bromoindole acetic acid (**1-193**).

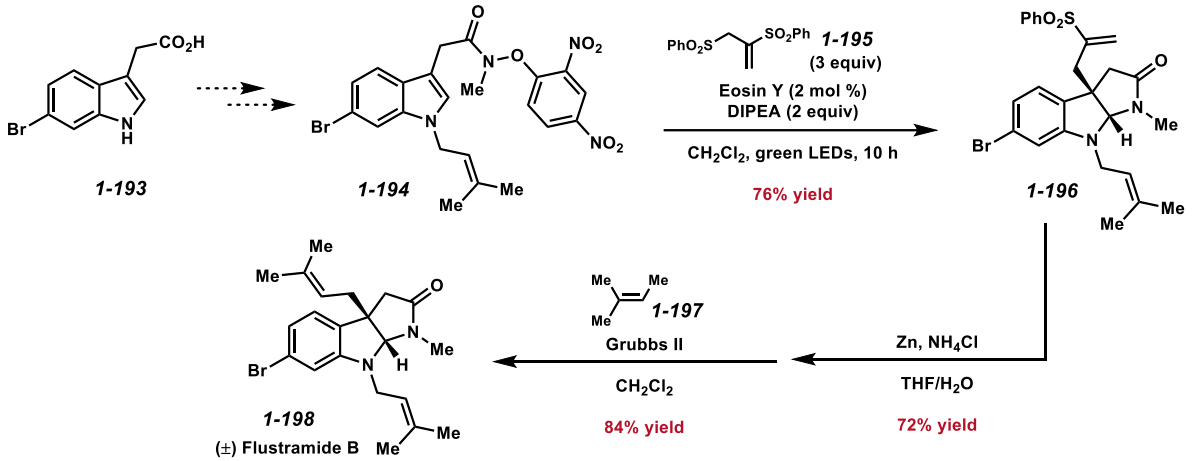

Scheme 1.5.8. Synthesis of Flustramide B.

Expanding on this work and inspired by known enzymatic processes,[68] in 2018 Knowles and coworkers described an enantioselective cyclization and nucleophilic trapping of tryptamine derivatives (**1-199**) initiated by visible light-promoted PCET (proton-coupled electron transfer) (*Scheme 1.5.9*).[69] A key aspect of this study was employing a chiral Brønsted base that could participate in H-bonding to the indole *N*-H. By careful selection of catalyst, indole, and Brønsted base, this association could lower the oxidation potential of indole within the range of the photocatalyst, thus ensuring pre-complexation before oxidation. This association would also provide a means of guiding enantioselectivity. Indeed, the authors found that when chiral phosphate **1-201** was employed in an oxidative PCET cycle with $Ir(ppy)_3$ photocatalyst, followed

by trapping with TEMPO, alkoxyamine-pyrroloindoline **1-200** was furnished in excellent yield and ee.

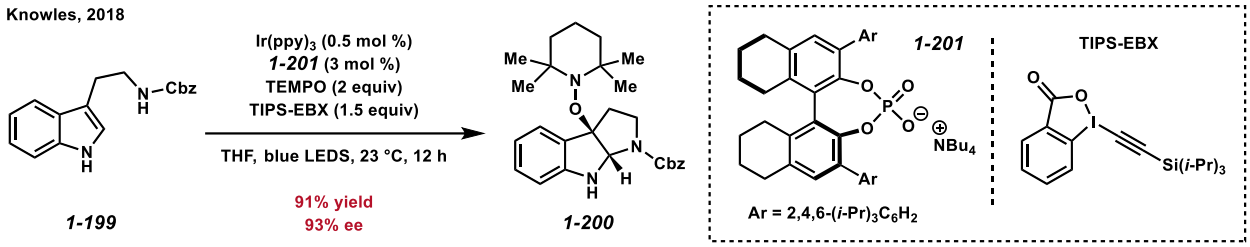

Scheme 1.5.9. Knowles's enantioselective synthesis of pyrroloindolines via PCET.

The mechanism of this reaction is depicted in *Scheme 1.5.10*. Excited Ir(III) ($E_{1/2}$ = –1.73 V) can be oxidized to Ir(IV) by TIPS-EBX (1-([tris-(1-methylethyl)silyl]ethynyl])-1,2-benziodoxol-3(1*H*)-one). The oxidized ground state Ir(IV) ($E_{1/2}$ = +0.80 V) could then serve as a mild photooxidant and generate radical cation **1-203** after complexation of chiral phosphate (**1-202**) in a PCET event. The authors then proposed that radical C-O bond formation would occur (**1-204**) first, followed by C-N bond formation by nucleophilic attack of the *N*-tether. Lastly, dissociation of the phosphate would furnish cyclized product **1-204**, formed with complete enantiocontrol throughout the cycle.

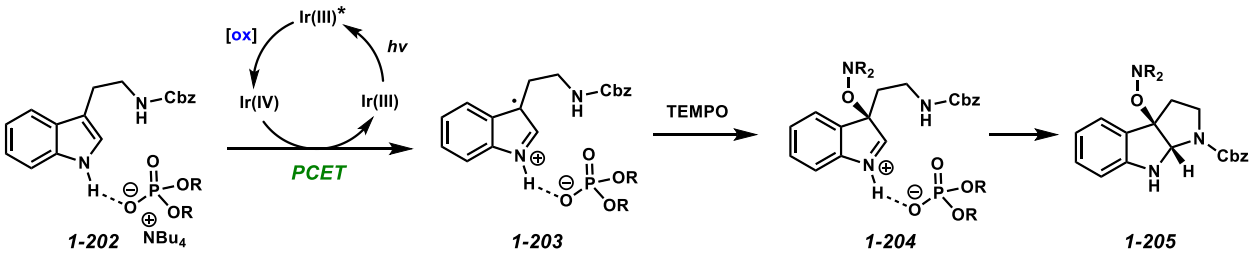

Figure 1.5.10. Proposed mechanism of PCET cyclization of tryptamine derivatives.

Next, Knowles and coworkers were intrigued by the potential application this method possessed towards synthesizing unsymmetrical pyrroloindoline natural products. They set their sights initially on the unsymmetrical dimer (-)-calycanthidine (**1-208**), with local C_2-symmetry at the C3 quaternary centers (*Scheme 1.5.11*). It was proposed that the enantioselective synthesis of calycanthidine could be accomplished by a mesolytic cleavage of methylated cyclization product **1-206**, followed by nucleophilic capture by indole **1-199**. Indeed, when indoline **1-206** ($E_{p/2}$ = +0.82 V) was irradiated in the presence of [Ir(dCF$_3$Me-ppy$_3$)$_2$(dtbbbpy)](PF$_6$) ($E_{1/2}$ = +1.22 V), mesolytic cleavage occurred to afford a tertiary carbocation at the C3 position. A subsequent Friedel–Crafts type process by nucleophilic attack with **1-199**, furnished **1-207** with excellent diastereoselectivity. They found that the addition of TFA (trifluoroacetic acid) and low temperatures were extremely beneficial to the overall yield and selectivity. Lastly, reduction of the benzyl carbamate groups with excess Red-Al afforded the natural product (**1-208**) cleanly. The full sequence was quite succinct (i.e., only 4 total steps) and high yielding with excellent selectivity.

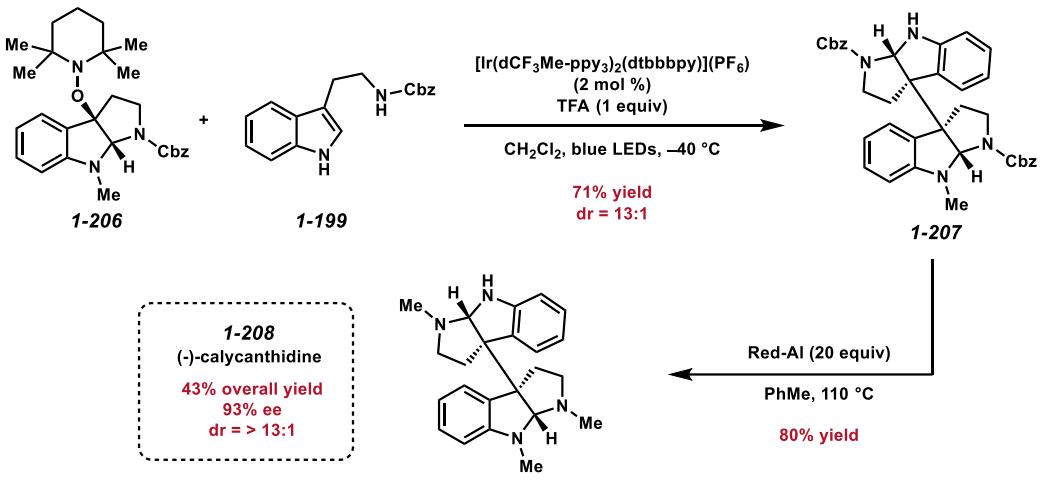

Scheme 1.5.11. Application of PCET cyclization towards (-)-calycanthidine.

1.6. Conclusion

Efforts toward synthesizing functionalized indoline cores has been a long sought after goal within the synthetic community. This core is present in hundreds of alkaloid natural products and biologically active molecules (*Figure 1.6.1*).[32b,70] Methods for their mild synthesis and/or modification for future biological screening are of utmost importance.[71]

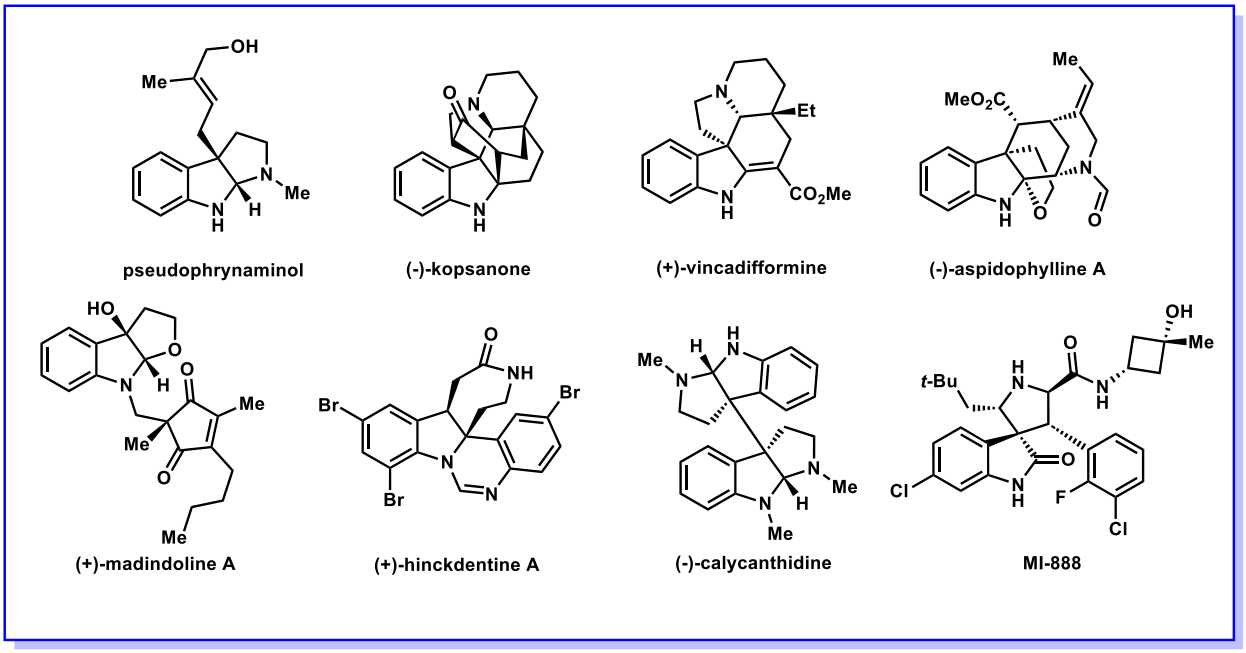

Figure 1.6.1. Select indoline natural products and biologically active compounds.

There have been a number of exploits in dearomative annulations employing EnT mechanisms to access relevant indoline cores. Traditionally, these transformations invoked direct sensitization of arenes and indoles or used inexpensive organic photocatalysts. However, as alluded to in previous sections, UV light sources can be quite large and expensive apparatuses. UV light also is an extremely high energy light source which sometimes leads to other undesired

reactions occurring. Modern photochemical methods have incorporated the discovery of many transition metal, and even some organic photosensitizers, that can be activated by a simple household light bulb. Due to the nature of activation, the majority of these EnT processes have been limited to fused cyclobutane products formed via [2 + 2] cycloadditions.

Other desirable indoline motifs have been accessed through SET pathways, but this area of study remains drastically underdeveloped. Only a few examples of dearomative annulations have been reported that employ PET. Within these reports, the standard is to use harsh UV light or expensive photocatalysts such as Ir or Ru-based catalysts. In conclusion, there remains an urgent need to synthesize functionalized indoline cores using mild photocatalytic conditions.

1.7. References and Notes

[1] For select reviews on photoredox catalysis, see: (a) Prier, C. K.; Rankic, D. A.; MacMillan, D. W. C. *Chem. Rev.* **2013**, *113*, 5322-5363. (b) Shaw, M. H.; Twilton, J.; MacMillan, D, W. C. *J. Org. Chem.* **2016**, *81*, 6898-6926. (c) Romero, N. A.; Nicewicz, D. A. *Chem. Rev.* **2016**, *116*, 10075-10166. (d) Narayanam, J. M. R.; Stephenson, C. R. J. *Chem. Soc. Rev.* **2011**, *40*, 102-113. (e) Bell, J. D.; Murphy, J. A. *Chem. Soc. Rev*. **2021**, *50*, 9540-9685. (f) Yoon, T. P. *ACS Catal*. **2013**, *3*, 895-902.

[2] For select reviews on energy transfer, see: (a) Hammond, G. S.; Turro, N. J. *Science* **1963**, *142*, 1541-1553. (b) Hoffmann, N. *Chem. Rev.* **2008**, *108*, 1052-1103. (c) Strieth-Kalthoff, F.; James, M. J.; Teders, M.; Pitzera, L.; Glorius, F. *Chem. Soc. Rev.* **2018**, *47*, 7190-7202. (d) Strieth-Kalthoff, F.; Glorius, F. *Chem.* **2020**, *6*, 1888-1903. (e) Großkopf, J.; Kratz, T.; Rigotti, T.; Bach, T. *Chem. Rev.* **2022**, *122*, 1626-1653.

[3] (a) Pigge, F. C. Dearomatization Reactions. In *Arene Chemistry*, 1st ed.; Mortier, J. Ed.; John Wiley & Sons, Inc., 2016, pp 399-423. (b) Huck, C. J.; Sarlah, D. *Chem.* **2020**, *6*, 1589-1603. (c) Zheng, C.; You, S.-L. *ACS Cent. Sci.* **2021**, *7*, 432-444.

[4] (a) Birch, A. J. *J. Chem. Soc.* **1944**, 430-436. (b) Rabideau, P. W.; Marcinow, Z. *Org. React.* **1992**, *42*, 1-334.

[5] (a) Magdziak, D.; Meek, S. J.; Pettus, T. R. R. *Chem. Rev.* **2004**, *104*, 1383-1430. (b) Cook, S. P.; Polara, A.; Danishefsky, S. J. *J. Am. Chem. Soc.* **2006**, *128*, 16440-16441. (c) Vo, N. T.; Pace, R. D. M.; O'Har, F.; Gaunt, M. J. *J. Am. Chem. Soc.* **2008**, *130*, 404-405. (d) Wu, W.-T.; Zhang, L.; You, S.-L. *Chem. Soc. Rev.* **2016**, *45*, 1570-1580.

[6] (a) Pape, A. R.; Kaliappan, K. P.; Kündig, E. P. *Chem. Rev.* **2000**, *100*, 2917-2940. (b) Rosillo, M.; Domíngueza, G.; Pérez-Castells, J. *Chem. Soc. Rev.* **2007**, *36*, 1589-1604. (c) Liebov, B. K.; Harman, W. D. *Chem. Rev.* **2017**, *117*, 13721-13755.

[7] (a) Bach, T.; Hehn, J. P. *Angew. Chem. Int. Ed.* **2011**, *50*, 1000-1045. (b) Kärkäs, M. D.; Porco, J. A., Jr.; Stephenson, C. R. J. *Chem. Rev.* **2016**, *116*, 9683-9747. (c) Pitre, S. P.; Overman, L. E. *Chem. Rev.* **2022**, *122*, 1717-1751.

[8] For select reviews on indole dearomatization and applications in synthesis, see: (a) Roche, S. P.; Youte Tendoung, J.-J.; Tréguier, B. *Tetrahedron* **2015**, *71*, 3549-3591. (b) Huang, G.; Yin, B. *Adv. Synth. Catal*. **2019**, *361*, 405-425. (c) Zheng, C.; You, S.-L. *Nat. Prod. Rep.* **2019**, *36*, 1589-1605. (d) Abou-Hamdan, H.; Kouklovsky, C.; Vincent, G. *Synlett* **2020**, *31*, 1775-1788.

[9] Zhu, M.; Zhang, X.; Zheng, C.; You, S.-L. *Acc. Chem. Res.* **2022**, *55*, 2510-2525.

[10] Skourtisa, S. S.; Liub, C.; Antonioua, P.; Virshup, A. M.; Beratan, D. N. *Proc. Natl. Acad. Sci. U.S.A.* **2016**, *113*, 8115-8120.

[11] All E_T values are reported in kcal/mol unless otherwise noted.

[12] (a) Coxon, J. M.; Halton, B. *Organic photochemistry*. Cambridge University Press: London, 1974. (b) Murov, S. L.; Charmichael, I.; Hug, G. L. *Handbook of Photochemistry*. Marcel Dekker Inc: New York, 1993. (c) Peach, M. J. G.; Benfield, P.; Helgaker, T.; Tozer, D. J. *J. Chem. Phys.* **2008**, *128*, 044118.

[13] van der Kolk, M. R.; Janssen, M. A. C. H.; Rutjes, F. P. J. T.; Blanco-Ania, D. *ChemMedChem* **2022**, *17*, e202200020.

[14] Julian, D. R.; Tringham, G. D. *J. Chem. Soc., Chem. Commun*. **1973**, 13b-14.

[15] Julian, D. R.; Foster, R. *J. Chem. Soc., Chem. Commun*. **1973**, 311-312.

[16] (a) Ikeda, M.; Ohno, K.; Takahashi, M.; Uno, T.; Tamura, Y.; Kido, M. *J. Chem. Soc., Perkin Trans. 1* **1982**, 741-748. (b) Ikeda, M.; Ohno, K.; Mohri, S.-i.; Takahashi, M.; Tamura, Y. *J. Chem. Soc., Perkin Trans. 1* **1984**, 405-412.

[17] Hastings, D. J.; Weedon, A. C. *J. Org. Chem.* **1991**, *56*, 6326-6331.

[18] (a) Norrish, R. G. W.; Bamford, C. H. *Nature* **1937**, *140*, 195-196. (b) Caldwell, R. A.; Majima, T.; Pac, C. *J. Am. Chem. Soc.* **1982**, *104*, 629-630.

[19] Becker, D.; Haddad, N.; Sahali, Y. *Tetrahedron Lett.* **1989**, *30*, 2661-2664.

[20] (a) Wagner, P. J.; Nahm, K. *J. Am. Chem. Soc*. **1987**, *109*, 4404-4405. (b) Wagner, P. J.; Nahm, K. *J. Am. Chem. Soc.* **1987**, *109*, 6528-6530. (c) Wagner, P. J.; Sakamoto, M. *J. Am. Chem. Soc.* **1989**, *111*, 9254-9256. (d) Wagner, P. J. *Acc. Chem. Res*. **2001**, *34*, 1-8.

[21] (a) Lamola, A. A. *J. Chem. Phys*. **1967**, *47*, 4810-4816. (b) Huix-Rotllant, M.; Siria, D.; Ferré, N. *Phys. Chem. Chem. Phys.,* **2013**, *15*, 19293-19300.

[22] (a) Yoon, T. P.; Ischay, M. A.; Du, J. *Nature Chem.* **2010**, *2*, 527-532. (b) Laboratory Safety Library, University of Georgia, 2022.

[23] For select early examples of [2 + 2] cycloadditions enabled by visible light, see: (a) Ikezawa, H.; Kutal, C.; Yasufuku, K.; Yamazaki, H. *J. Am. Chem. Soc.* **1986**, *108*, 1589-1594. (b) Lu, Z.; Yoon, T. P. *Angew. Chem. Int. Ed*. **2012**, *51*, 10329-10332. (c) Poplata, S.; Tröster, A.; Zou, Y.-Q.; Bach, T. *Chem. Rev.* **2016**, *116*, 9748-9815.

[24] Alonso, R.; Bach, T. *Angew. Chem. Int. Ed.* **2014**, *53*, 4368-4371.

[25] Tröster, A.; Alonso, R.; Bauer, A.; Bach, T. *J. Am. Chem. Soc.* **2016**, *138*, 7808-7811.

[26] Hu, N.; Jung, H.; Zheng, Y.; Lee, J.; Zhang, L.; Ullah, Z.; Xie, X.; Harms, K.; Baik, M.-H.; Meggers, E. *Angew. Chem. Int. Ed*. **2018**, *57*, 6242-6246.

[27] The Meggers group has developed several Rh and Ir chiral photoactive complexes. For more information, see: (a) Huang, X.; Quinn, T. R.; Harms, K.; Webster, R. D.; Zhang, L.; Wiest, O.; Meggers, E. *J. Am. Chem. Soc.* **2017**, *139*, 9120-9123. (b) Zhang, L.; Meggers, E. *Chem. Asian J.* **2017**, *12*, 2335-2342. (c) Jung, H.; Hong, M.; Marchini, M.; Villa, M.; Steinlandt, P. S.; Huang, X.; Hemming, M.; Meggers, E.; Ceroni, P.; Park, J.; Baik, M.-H. *Chem. Sci.* **2021**, *12*, 9673-9681. (d) Steinlandt, P. S.; Zhang, L.; Meggers, E. *Chem. Rev.* **2023**, *123*, 4764-4794.

[28] James, M. J.; Schwarz, J. L.; Strieth-Kalthoff, F.; Wibbeling, B.; Glorius, F. *J. Am. Chem. Soc.* **2018**, *140*, 8624-8628.

[29] Teegardin, K.; Day, J. I.; Chan, J.; Weaver, J. *Org. Process Res. Dev*. **2016**, *20*, 1156-1163.

[30] For other select dearomative annulations reported by Bach, see: (a) Li, X.; Großkopf, J.; Jandl, C.; Bach, T. *Angew. Chem. Int. Ed.* **2021**, *60*, 2684-2688. (b) Xiong, Y.; Großkopf, J.; Jandl, C.; Bach, T. *Angew. Chem. Int. Ed.* **2022**, *61*, e202200555. (c) Stegbauer, S.; Jandl, C.; Bach, T. *Chem. Sci.* **2022**, *13*, 11856-11862.

[31] For other select dearomative annulations reported by Glorius, see: (a) Ma, J.; Strieth-Kalthoff, F.; Dalton, T.; Freitag, M.; Schwarz, L.; Bergander, K.; Daniliuc, C.; Glorius, F. *Chem* **2019**, *5*, 2854-2864. (b) Ma, J.; Chen, S.; Bellotti, P.; Guo, R.; Schäfer, F.; Heusler, A.; Zhang, X.; Daniliuc, C.; Brown, M. K.; Houk, K. N.; Glorius, F. *Science* **2021**, *371*, 1338-1345. (c) Guo, R.; Adak, S.; Bellotti, P.; Gao, X.; Smith, W. W.; Ngan Le, S.; Ma, J.; Houk, K. N.; Glorius, F.; Chen, S.; Brown, M. K. *J. Am. Chem. Soc.* **2022**, *144*, 17680-17691.

[32] For select reviews on cascade asymmetric dearomatization (CADA) reactions, see: (a) Zhuo, C.-X.; Zhang, W.; You, S.-L. *Angew. Chem. Int. Ed.* **2012**, *51*, 12662-12686. (b) Zheng, C.; You, S.-L. *Nat. Prod. Rep.* **2019**, *36*, 1589-1605. (c) Zheng, C.; You, S.-L. *ACS Cent. Sci.* **2021**, *7*, 432-444.

[33] Zhu, M.; Zheng, C.; Zhang, X.; You, S.-L. *J. Am. Chem. Soc.* **2019**, *141*, 2636-2644.

[34] Rolka, A. B.; Koenig, B. *Org. Lett.* **2020**, *22*, 5035-5040.

[35] (a) Marcus, R. A. *J. Chem. Phys.* **1956**, *24*, 966-978. (b) Maroncelli, M.; Macinnis, J.; Flemming, G. R. *Science* **1989**, *243*, 1674-1681. (c) Leo, A.; Peluso, A. *J. Phys. Chem. Lett.* **2022**, *13*, 9148-9155.

[36] (a) Beesley, R. M.; Ingold, C. K.; Thorpe, J. F. *J. Chem. Soc., Trans.* **1915**, *107*, 1080-1106. (b) Bachrach, S. M. *J. Org. Chem.* **2008**, *73*, 2466-2468.

[37] Oderinde, M. S.; Mao, E.; Ramirez, A.; Pawluczyk, J.; Jorge, C.; Cornelius, L. A. M.; Kempson, J.; Vetrichelvan, M.; Pitchai, M.; Gupta, A.; Gupta, A. K.; Meanwell, N. A.; Mathur, A.; Dhar, T. G. M. *J. Am. Chem. Soc.* **2020**, *142*, 3094-3103.

[38] Zhu, M.; Zhang, X.; Zheng, C.; You, S.-L. *ACS Catal.* **2020**, *10*, 12618-12626.

[39] Becker, M. R.; Wearing, E. R.; Schindler, C. S. *Nat. Chem.* **2020**, *12*, 898-905.

[40] Zhu, M.; Huang, X.-L.; Sun, S.; Zheng, C.; You, S.-L. *J. Am. Chem. Soc.* **2021**, *143*, 13441-13449.

[41] Zhang, Z.; Yi, D.; Zhang, M.; Wei, J.; Lu, J.; Yang, L.; Wang, J.; Hao, N.; Pan, X.; Zhang, S.; Wei, S.; Fu, Q. *ACS Catal.* **2020**, *10*, 10149-10156.

[42] Zhu, M.; Huang, X.-L.; Xu, H.; Zhang, X.; Zheng, C.; You, S.-L. *CCS Chem.* **2020**, *2*, 652-664.

[43] Zhu, M.; Xu, H.; Zhang, X.; Zheng, C.; You, S.-L. *Angew. Chem. Int. Ed.* **2021**, *60*, 7036-7040.

[44] Oderinde, M. S.; Ramirez, A.; Murali Dhar, T. G.; Cornelius, L. A. M.; Jorge, C.; Aulakh, D.; Sandhu, B.; Pawluczyk, J.; Sarjeant, A. A.; Meanwell, N. A.; Mathur, A.; Kempson, J. *J. Org. Chem.* **2021**, *86*, 1730-1747.

[45] Ma, J.; Schäfers, F.; Daniliuc, C.; Bergander, K.; Strassert, C. A.; Glorius, F. *Angew. Chem. Int. Ed*. **2020**, *59*, 9639-9645.

[46] (a) Hammond, G. S.; Saltiel, J. *J. Am. Chem. Soc.* **1962**, *84*, 4983-4984. (b) Singh, K.; Staig, S. J.; Weaver, J. D. *J. Am. Chem. Soc.* **2014**, *136*, 5275-5278. (c) Molloy, J. J.; Morack, T.; Gilmour, R. *Angew. Chem. Int. Ed.* **2019**, *58*, 13654-13664.

[47] Gieseler, A.; Steckhan, E.; Wiest, O. *Synlett* **1990**, 275-277.

[48] All potentials are reported in V vs SCE unless otherwise noted.

[49] Gieseler, A.; Steckhan, E.; Wiest, O.; Knoch, F. *J. Org. Chem.* **1991**, *56*, 1405-1411.

[50] Wiest, O.; Steckhan, E.; Grein, F. *J. Org. Chem*. **1992**, *57*, 4034-4037.

[51] Wiest, O.; Steckhan, E. *Tetrahedron Lett.* **1993**, *34*, 6391-6394.

[52] Haberl, U.; Steckhan, E.; Blechert, S.; Wiest, O. *Chem. Eur. J.* **1999**, *5*, 2859-2865.

[53] Peglow, T.; Blechert, S.; Steckhan, E. *Chem. Commun*. **1999**, 433-434.

[54] Okumura, M.; Sarlah, D. *Synlett* **2018**, *29*, 845-855.

[55] Southgate, E. H.; Pospech, J.; Fu, J.; Holycross, D. R.; Sarlah, D. *Nat. Chem.* **2016**, *8*, 922-928.

[56] For important precedent work by Yoon regarding photocatalytic radical cation cycloadditions, see: (a) Lin, S.; Ischay, M. A.; Fry, C. G.; Yoon, T. P. *J. Am. Chem. Soc.* **2011**, *133*, 19350-19353. (b) Ischay, M. A.; Ament, M. S.; Yoon, T. P. *Chem. Sci.* **2012**, *3*, 2807-2811. (c) Blum, T. R.; Zhu, Y.; Nordeen, S. A.; Yoon, T. P. *Angew. Chem. Int. Ed.* **2014**, *53*, 11056-11059. (d) Lin, S. S.; Lies, S. D.; Gravatt, C. S.; Yoon, T. P. *Org. Lett.* **2017**, *19*, 368-371.

[57] Pitre, S. P.; Scaiano, J. C.; Yoon, T. P. *ACS Catal*. **2017**, *7*, 6440-6444.

[58] For a review on visible light mediated reactions of indoles, see: Festa, A. A.; Voskressensky, L. G.; Van der Eycken, E. V. *Chem. Soc. Rev*. **2019**, *48*, 4401-4423.

[59] For select examples and reviews, see: (a) Portela-Cubillo, F.; Lymer, J.; Scanlan, E. M.; Scott, J. S.; Walton, J. C. *Tetrahedron* **2008**, *64*, 11908-11916. (b) Jiang, H.; An, X.; Tong, K.; Zheng,

T.; Zhang, Y.; Yu, S. *Angew. Chem. Int. Ed*. **2015**, *54*, 4055-4059. (c) Del Tito, A.; Abdulla, H. O.; Ravelli, D.; Protti, S.; Fagnoni, M. *Beilstein J Org Chem.* **2020**, *16*, 1476-1488.

[60] Narayanam, J. M. R.; Tucker, J. W.; Stephenson, C. R. J. *J. Am. Chem. Soc.* **2009**, *131*, 8756-8757.

[61] Gao, F.; Yang, C.; Gao, G.-L.; Zheng, L.; Xia, W. *Org. Lett.* **2015**, *17*, 3478-3481.

[62] Zhang, M.; Duan, Y.; Li, W.; Cheng, Y.; Zhu, C. *Chem. Commun.* **2016**, *52*, 4761-4763.

[63] Wang, Q.; Qu, Y.; Xia, Q.; Song, H.; Song, H.; Liu, Y.; Wang, Q. *Adv. Synth. Catal.* **2018**, *360*, 2879-2884.

[64] (a) Wang, J.; Sánchez-Roselló, M.; Aceña, J. L.; del Pozo, C.; Sorochinsky, A. E.; Fustero, S.; Soloshonok, V. A.; Liu, H. *Chem. Rev.* **2014**, *114*, 2432-2506. (b) Qiao, J. X.; Wang, T. C.; Ruel, R.; Thibeault, C.; L'Heureux, A.; Schumacher, W. A.; Spronk, S. A.; Hiebert, S.; Bouthillier, G.; Lloyd, J.; Pi, Z.; Schnur, D. M.; Abell, L. M.; Hua, J.; Price, L. A.; Liu, E.; Wu, Q.; Steinbacher, T. E.; Bostwick, J. S.; Chang, M.; Zheng, J.; Gao, Q.; Ma, B.; McDonnell, P. A.; Huang, C. S.; Rehfuss, R.; Wexler, R. R.; Lam, P. Y. S. *J. Med. Chem.* **2013**, *56*, 9275-9295.

[65] Wang, Q.; Qu, Y.; Xia, Q.; Song, H.; Song, H.; Liu, Y.; Wang, Q. *Chem. Eur. J.* **2018**, *24*,11283-11287.

[66] Wu, K.; Du, Y.; Wang, T. *Org. Lett.* **2017**, *19*, 5669-5672.

[67] Davies, J.; Svejstrup, T. D.; Fernandez Reina, D.; Sheikh, N. S.; Leonori, D. *J. Am. Chem. Soc* **2016**, *138*, 8092-8095.

[68] Migliore, A.; Polizzi, N. F.; Therien, M. J.; Beratan, D. N. *Chem. Rev.* **2014**, *114*, 3381-3465.

[69] Gentry, E. C.; Rono, L. J.; Hale, M. E.; Matsuura, R.; Knowles, R. R. *J. Am. Chem. Soc.* **2018**, *140*, 3394-3402.

[70] (a) Saxtonin, J. E. *The Alkaloids: Chemistry and Biology*, Vol. 51(Ed.: G. A. Cordell), Academic Press: San Diego, 1998, Ch. 1. (b) Kam, T.-S.; Lim, K.-H. in *The Alkaloids: Chemistry and Biology,* Vol. 66 (Ed.: Cordell, G. A.), Elsevier: Amsterdam, 2008, Ch. 1. (c) Cuendet, M.; Pezzutoin, J. M. *Modern Alkaloids: Structure, Isolation, Biology* (Ed.: Fattorusso, E.; Taglialatela-Scafati, O.), Wiley-VCH: Weinheim, 2008, Ch. 2. (d) Liu, X.-Y.; Qin, Y. *Acc. Chem. Res.* **2019**, *52*, 1877-1891. (e) Ishikawa, H.; Elliott, G. I.; Velcicky, J.; Choi, Y.; Boger, D. L. *J. Am. Chem. Soc.* **2006**, *128*, 10596-10612. (f) Martin, G.; Angyal, P.; Egyed, O.; Varga, S.; Soós. T. *Org. Lett.* **2020**, *22*, 4675-4679. (g) Qin, B.; Wang, Y.; Wang, X.; Jia, Y. *Org. Chem. Front.* **2021**, *8*, 369-383.

[71] For select electrochemical dearomative annulations, see: (a) Liu, K.; Tang, S.; Huang, P.; Lei, A. *Nat. Commun.* **2017**, *8*, 775. (b) Wu, J.; Dou, Y.; Guillot, R.; Kouklovsky, C.; Vincent, G. *J. Am. Chem. Soc*. **2019**, *141*, 2832-2837. (c) Song, C.; Liu, K.; Jiang, X.; Dong, X.; Weng, Y.; Chiang, C.-W.; Lei, A. *Angew. Chem. Int. Ed.* **2020**, *59*, 7193-7197. (d) Liu, K.; Song, W.; Deng, Y.; Yang, H.; Song, C.; Abdelilah, T.; Wang, S.; Cong, H.; Tang, S.; Lei, A. *Nat. Commun*. **2020**, *11*, 3.

CHAPTER 2

A DEAROMATIVE (3 + 2) CYCLOADDITION WITH INDOLES AND VINYL DIAZOACETATES VIA CHROMIUM(III) PHOTOREDOX CATALYSIS

2.1. Introduction

Disclaimer: the work discussed in this chapter was previously published in *Angewandte Chemie International Edition*.[1] Recently, photoredox catalysis has emerged as a powerful method for novel bond-forming transformations.[2] Reactions in this class, originating from an excited-state species generated by light initiation, involve highly active intermediates that are produced via single electron transfer. Chemists now have an arsenal of metal- and nonmetal-based photocatalysts that display ranges of reactivity owing to their respective excited state reduction potentials. Multiple classes of reaction types proceeding by electron transfer can be catalyzed by these species, such as atom-transfer processes, cross-couplings, and cycloadditions. Despite numerous catalysts at our disposal, advancements remain necessary when limitations are encountered in reaction manifolds. Commonly used transition-metal photocatalysts employ iridium and ruthenium, two of the rarest and most expensive metals on earth. Expanding the field of photoredox-catalysis to include complementary methods utilizing *earth-abundant*, or first-row, transition-metal photocatalysts has been a goal within our research group. Known photocatalysts employing first-row transition metals include chromium, cobalt, copper, iron, zinc, and nickel.[3] In

2010, our collaborators at Colorado State University and the University of Colorado Boulder, the Shores and Damrauer groups, performed seminal photophysical studies on chromium(III) poly-pyridyl and poly-phenanthrolinyl complexes.[4] It was discovered that these complexes absorbed in the near-UV to visible light region, featured long excited state lifetimes (~8-425 μs), and possessed relatively high excited state reduction potentials (+1.40–1.84 V vs SCE) (*Figure 2.1.1*).

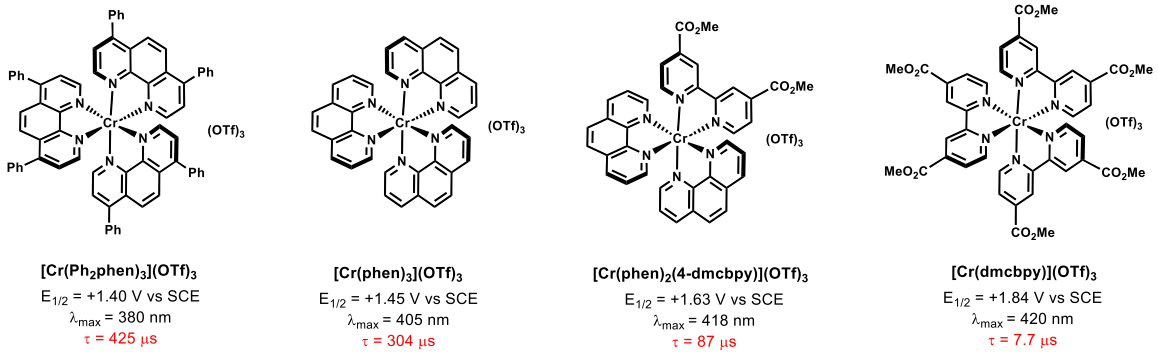

Figure 2.1.1. Select Cr(III) poly-pyridyl and poly-phenanthrolinyl complexes and their photophysical properties.

Following this report, we sought to explore the synthetic utility of these potential photooxidants. In 2015 our group reported a Cr(III)-photocatalyzed (4 + 2) cycloaddition between electron-rich styrenyl dienophiles (**2-1**) and butadiene derivatives (**2-2**) in the presence of near-UV light (*Scheme 2.1.1*).[5] This was accomplished through a photooxidation of the dienophile to generate a reactive radical cation intermediate that could undergo a cycloaddition with isoprene. Notably, the product (**2-3**) was obtained with exclusive diastereoselectivity, regardless of the stereochemistry of the starting electron-rich alkene. This study was the first complementary example of Cr photocatalysis to other known photooxidants; in 2011, Yoon reported this (4 + 2) cycloaddition catalyzed by $[Ru(bpz)_3](PF_6)_2$. We were able to expand the scope of this Cr(III) (4+2) cycloaddition in 2017 to include electron-deficient alkenes (**2-4**).[6] Several mechanistic

pathways were identified, including an energy transfer process. After photosensitization, a [2 + 2] cycloaddition occurs, followed by vinyl-cyclobutene rearrangement to generate the formal (4 + 2) cycloadduct (**2-5**). A subsequent study by our group in 2017 disclosed a (2 + 1) cyclopropanation with electron-rich alkenes (**2-1**) and diazoacetates (**2-6**).[7] Diazoacetates were found to be sufficiently nucleophilic and reacted with radical cation intermediates. Most recently, we reported a (3 + 2) cycloaddition between electron-rich alkenes (**2-1**) and vinyl diazoacetates (**2-8**).[8] This transformation initiates via oxidation of the alkene using either chromium or ruthenium catalysis. Both diazo nucleophiles yielded products (**2-7** and **2-9**) with exclusive diastereoselectivity.

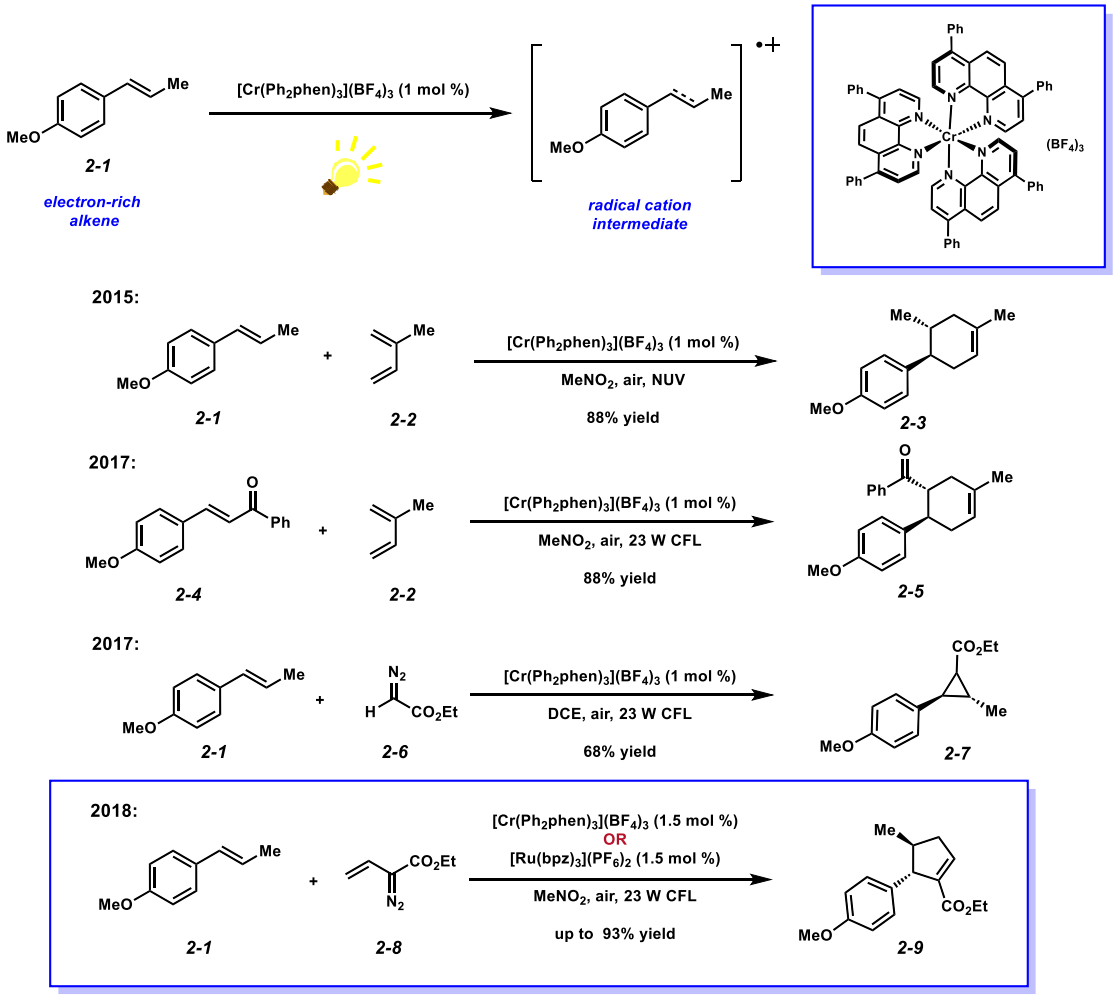

Scheme 2.1.1. Previous Cr(III)-photocatalyzed cycloadditions reported from our group.

In continuation of our goal to access complex organic molecules using metals based on the first row, we were enticed by the prospect that this photocatalyzed (3 + 2) cycloaddition may translate to heterocycles such as indoles. The densely-substituted fused indoline structure that would result from a cycloaddition is a prevalent structural motif in a variety of natural products and bioactive molecules (*Scheme 2.1.2*).[9] A differentiating challenge of this proposed process is that it would necessitate a *dearomatization*. A potentially competing nucleophile addition pathway would involve substitution with rapid rearomatization (*Scheme 2.1.2*). In seminal reports, Nicewicz and coworkers showed downhill rearomatization after diazoacetate addition to arene radical cations (*Scheme 2.1.2*).[10] Similarly, Gryko and coworkers described the photoredox C2 alkylation of indoles with α-diazoesters to yield rearomatized substituted products.[11]

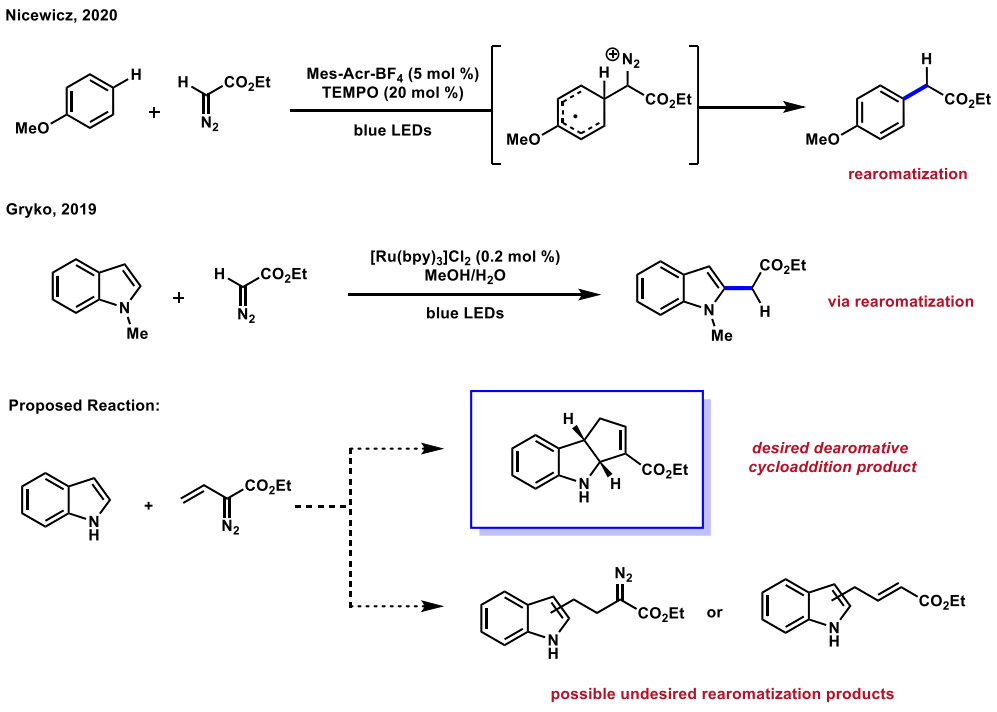

Scheme 2.1.2. Desired cycloaddition product and potential undesired rearomatization processes.

Photocatalytic intra- and intermolecular dearomative cycloadditions proceeding by energy transfer have been described, as have photoredox dearomative additions featuring intramolecular nucleophiles (*see Chapter 1*).[12] Metal-photocatalyzed dearomative cycloadditions *proceeding by electron transfer*, however, are quite rare. Photocatalyzed (4 + 2) cycloadditions between indoles and dienes have been achieved using either oxidizing triarylpyryliums or heterogeneous metal compositions (*see Chapter 1*),[13] which offered promise that extrapolating to this type of (3 + 2) cycloaddition was conceivable and would represent a mechanistic complement to rhodium carbene-mediated processes by Davies and Doyle (*Scheme 2.1.3*).[14,15] This chapter catalogues the successful realization of this photoredox-catalyzed transformation, specifically enabled by the development of a novel chromium(III) photocatalyst with increased activity.

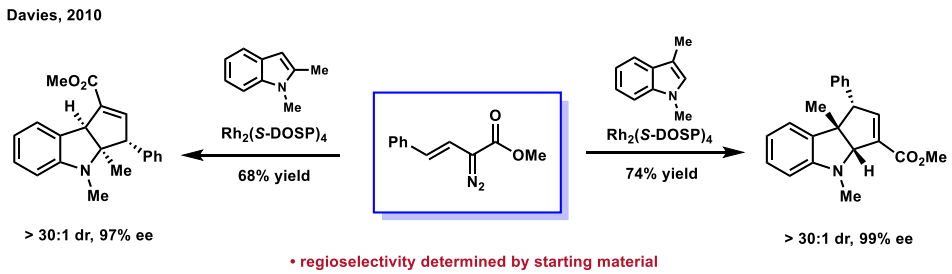

Scheme 2.1.3. Davies's Rh(II)-catalyzed (3 + 2) cycloaddition.

2.2. Preliminary Experiments

In our previously reported radical cation (3 + 2) cycloaddition between alkenes and vinyldiazo species (*Scheme 2.1.1*),[8] both $[Cr(Ph_2phen)_3](BF_4)_3$ ($E_{1/2}$ = +1.40 V in CH_3NO_2)[16] and $[Ru(bpz)_3](PF_6)_2$ ($E_{1/2}$ = +1.45 V in CH_3CN) were active photocatalysts; the Ru catalyst generally afforded faster reactivity, but in select cases Cr was uniquely operative. The reduction potential of N-H indole ($E_{1/2}$ = +1.16 V in CH_3CN)[17] suggested that this oxidative process could be

transferable to these heterocycles; a heteroarene oxidation leading to its radical cation would initiate the cycloaddition mechanism. A key aspect in the design of this process is that *in situ N*-substitution would likely be necessary; the indoline product would otherwise be more susceptible to oxidation than the indole itself, thus suppressing propagation. This principle is consistent with earlier examples of photosensitized dearomative (4 + 2) cycloadditions between indoles and dienes (*see Giesler and Yoon examples, Chapter 1*).[13] Without substitution, the lone pair of electrons on the indoline *N*-atom could be competitively oxidized over the starting alkene. To that end, our initial screening of reactivity is shown in *Table 2.2.1*. We treated 5-bromoindole (**2-10**), which was used in most of our probing experiments for spectroscopic clarity, with ethyl vinyldiazoacetate (**2-8**)—using both $[Cr(Ph_2phen)_3](BF_4)_3$ and $[Ru(bpz)_3](PF_6)_2$ as photocatalysts (*entries 1, 2*)—and adding an acid chloride and $NaHCO_3$ for post-cycloaddition acylation. AcCl afforded modest yields, but more encouraging results were obtained using BzCl. We were delighted to observe the formation of product **2-11**—with exclusive regio- and diastereoselectivity—but in somewhat modest yield compared to the previous cycloaddition yields using electron rich alkenes.

Table 2.2.1. Initial screening of proposed (3 + 2) cycloaddition.

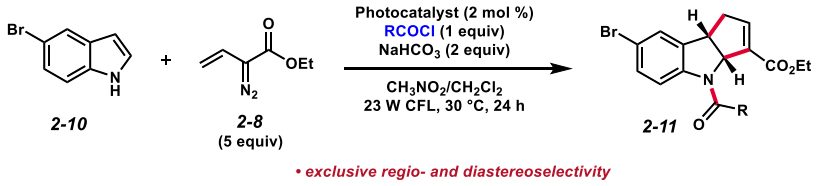

entry	photocatalyst	RCOCl	yield (%)
1	$[Cr(Ph_2phen)_3](BF_4)_3$	AcCl	8
2	$[Ru(bpz)_3](PF_6)_2$	AcCl	31
3	$[Cr(Ph_2phen)_3](BF_4)_3$	BzCl	26
4	$[Ru(bpz)_3](PF_6)_2$	BzCl	44

2.3. Optimization of Conditions and Catalyst Development

Other oxidizing photocatalyst systems were examined, both organic and inorganic, but were met with limited success (*see Experimental Section, Table 2.12.1*).[18] $[Ru(bpz)_3](PF_6)_2$ has been the most broadly successful photocatalyst in inducing radical cation cycloadditions[8,19]—and has performed well in our previous cycloadditions as well; thus its unexceptional activity here prompted us to probe deeper. The exceptional reactivity as a photooxidant can be attributed to the bipyrazine ligands imparting improved oxidation capacity over bipyridine ligands (i.e., as in $[Ru(bpy)_3]^{2+}$) by decreasing electron density on the ligand framework.[20] We hypothesized, though, that these ligands may also be reactive with the acylating agent necessary in our proposed reaction. Indeed, when we subjected $[Ru(bpz)_3](PF_6)_2$ to excess BzCl and irradiation, a marked change in UV-vis absorption was observed (*Figure 2.3.1*), suggesting the catalyst composition had drastically transformed during the reaction. Likely, acylation of the bipyrazine ligand led to a complex mixture of acylated species. Because the required acylation seemed to cause catalyst decomposition of $[Ru(bpz)_3](PF_6)_2$, we were inclined to search elsewhere for a highly reactive photooxidant.

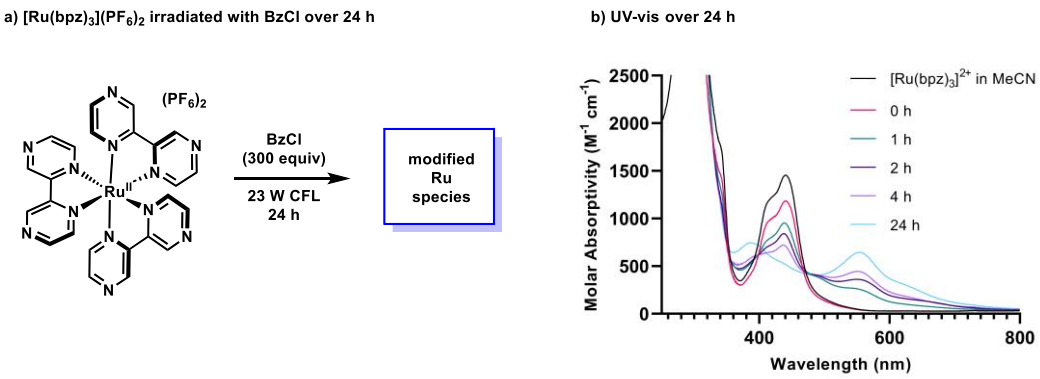

Figure 2.3.1. (a) Ru catalyst subjected to excess BzCl and irradiation. (b) Time-lapsed UV-vis evaluation of Ru catalyst stability to BzCl and irradiation.

$[Cr(Ph_2phen)_3](BF_4)_3$ was generally less reactive than $[Ru(bpz)_3](PF_6)_2$ in radical cation cycloadditions, but we thought this catalyst system framework may offer a path forward. The bathophenanthroline ligand framework should not have acylation issues like bipyrazine. One reason for the lesser reactivity of the Cr complex is its weaker absorption properties; if absorbance could be increased in the visible light region, then it could possibly translate to a more reactive catalyst. Electron-rich substituents are known to have measurable effects on bathochromic shifts in absorbance, and we hypothesized this principle may be applicable to the chromium trisphenanthrolinyl complexes.[21] We found that introducing *p*-OMe substituents on the phenyls of the bathophenanthroline ($[Cr(PMP_2phen)_3](BF_4)_3$) led to a complex with a red-shifted and increased absorbance (*Figure 2.3.2a-b*). $[Cr(PMP_2phen)_3](BF_4)_3$ was also subjected to excess BzCl and irradiation to investigated catalyst stability. This catalyst showed little change in absorbance over 24 h, indicating stability to acylating conditions and irradiation (*Figure 2.3.2c-d*). $[Cr(PMP_2phen)_3](BF_4)_3$ was also found to have a reduction potential of $E_{1/2}$ = +1.43 V vs SCE in CH_3CN.

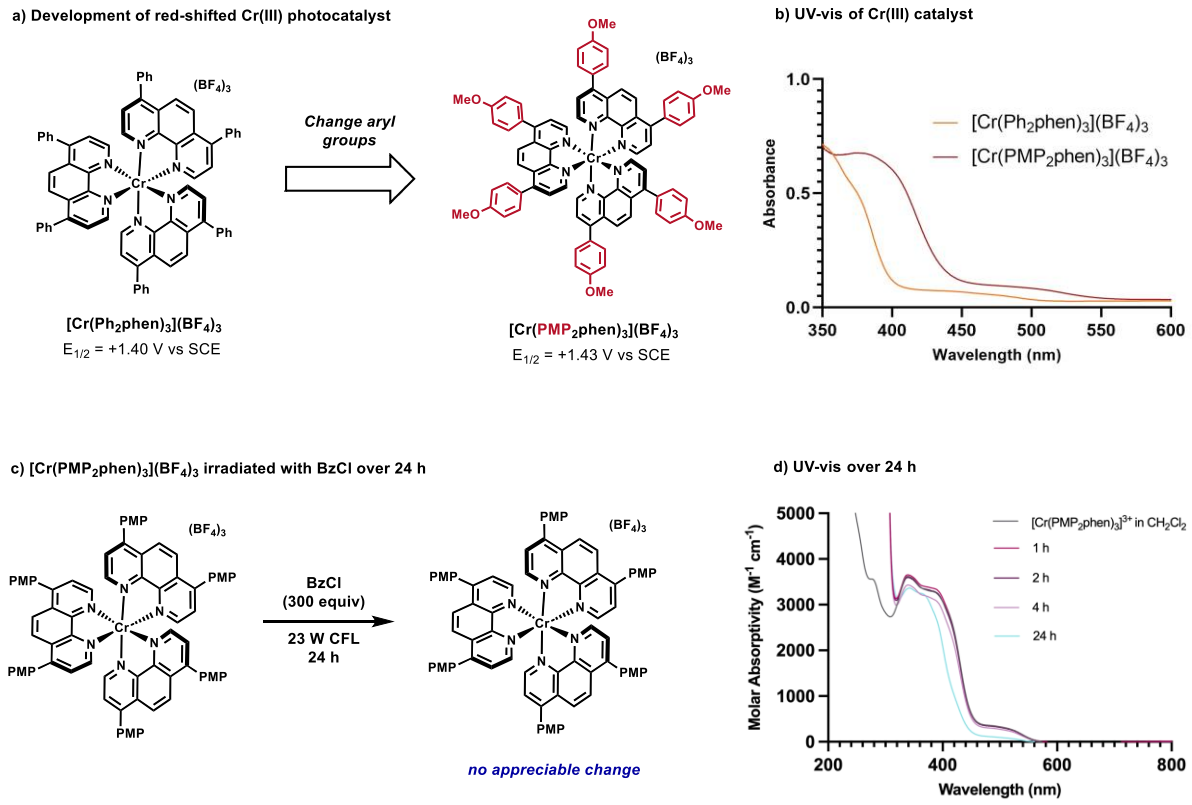

Figure 2.3.2. (a) Development of a new Cr catalyst through ligand alteration. (b) UV-vis absorbance of Cr complexes. (c) Cr catalyst subjected to excess BzCl and irradiation. (d) Time-lapsed UV-vis evaluation of Cr stability to BzCl and irradiation.

The newly developed catalyst was then tested in the proposed reaction. To our delight, this complex led to a significant increase in yield in the (3 + 2) cycloaddition, affording an improvement to 75% yield of the desired acylated cycloadduct (**2-11**, *Table 2.3.1*). Excess vinyl diazoacetate is required in this reaction due to unproductive pyrazole formation that occurs when it is exposed to light or heated. Acylated pyrazole was observed in the reaction (i.e., pyrazole by-product was consuming acylation reagents leading to lower yield of the desired product). Further increasing the amount of BzCl and $NaHCO_3$ to 3 and 5 equivalents respectively was highly beneficial, yielding 94% of cycloadduct **2-11**. Chloroformates were equally effective as acylating agents in the transformation; using TrocCl we obtained an excellent 95% yield of the cycloadduct (**2-11**). Other solvents and protecting groups were also examined in this reaction with the

optimized reaction parameters shown in red in *Table 2.3.1* (further optimization: *see Experimental Section, Tables 2.12.2-2.12.5*).

Table 2.3.1. Optimization of reaction conditions employing a novel, red-shifted Cr(III) photocatalyst.

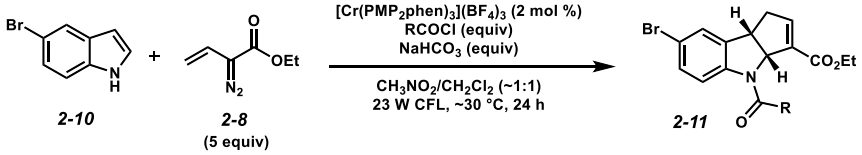

RCOCl	RCOCl (equiv)	$NaHCO_3$ (equiv)	NMR yield (%)
BzCl	1	2	75
BzCl	3	5	94
TrocCl	3	5	95

2.4. Exploring Reaction Parameters

Table 2.4.1 highlights the importance of various parameters in this cycloaddition. The choice of base was important; other inorganic and organic bases were not as successful (*entries 2-4*), sometimes shutting down the cycloaddition altogether. White light (23 W CFL) was the optimal light source, although other light sources still promoted reactivity (*entries 6, 7*). Fewer equivalents of the vinyl diazoacetate reagent were tolerated, albeit in modestly diminished yield (*entry 8*). This reaction can be conveniently set up open to air, although we found the reaction performed equally well in an oxygen or inert atmosphere (*entries 9, 10*), suggesting little to no role for O_2. Lower catalyst loading led to a marginal decrease in yield (*entry 11*). Catalyst and light were essential for cycloaddition to occur (*entries 12, 13*), while acylating agent was critical for the reaction to progress (*entry 14*). Added TEMPO significantly hampered reactivity, suggesting radical intermediacy in the mechanism (*entry 16*).

Table 2.4.1. Evaluation of photocatalyzed indole (3 + 2) cycloaddition conditions.

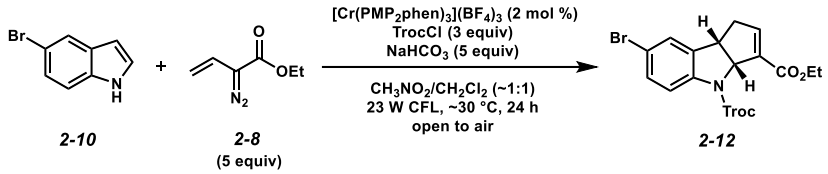

2-10 + *2-8* (5 equiv) → *2-12*

entry	deviation from standard conditions	yield (%)
1	none	95
2	$KHCO_3$	51
3	NaH_2PO_4	52
4	Et_3N	0
5	CH_2Cl_2 only	86
6	blue LED (390 nm)	28
7	near UV irradiation	39
8	2 equiv *2-8*	73
9	inert atmosphere	88
10	O_2 atmosphere	91
11	0.5 mol % catalyst	76
12	No catalyst	0
13	No light	0
14	No TrocCl	0[a]
15	No $NaHCO_3$	45
16	1 equiv TEMPO added	19

[a] <20% unprotected cycloaddition product observed.

2.5. Scope of the Reaction

The scope of this dearomative cycloaddition is depicted in *Scheme 2.5.1*. The reaction tolerated a number of C5-functional groups on the heterocycle, including halides (**2-12**, **2-13**), silyl ethers (**2-17**), esters (**2-18**), nitriles (**2-19**), boronates (**2-20**), and nitro groups (**2-21**). Silyl ether **2-17** and nitro **2-21** were afforded in moderate yields, implicating a window of optimal reactivity based on the electronic nature of the indole starting material. Interestingly, when 5-OMe indole was tested in the reaction, a very low yield was observed (**2-22**). This is likely due to a stabilizing effect the methoxy group has on the radical cation—making it significantly less reactive. Substitutions at C4, C6, and C7 (**2-23**–**2-25**) were all accommodated.

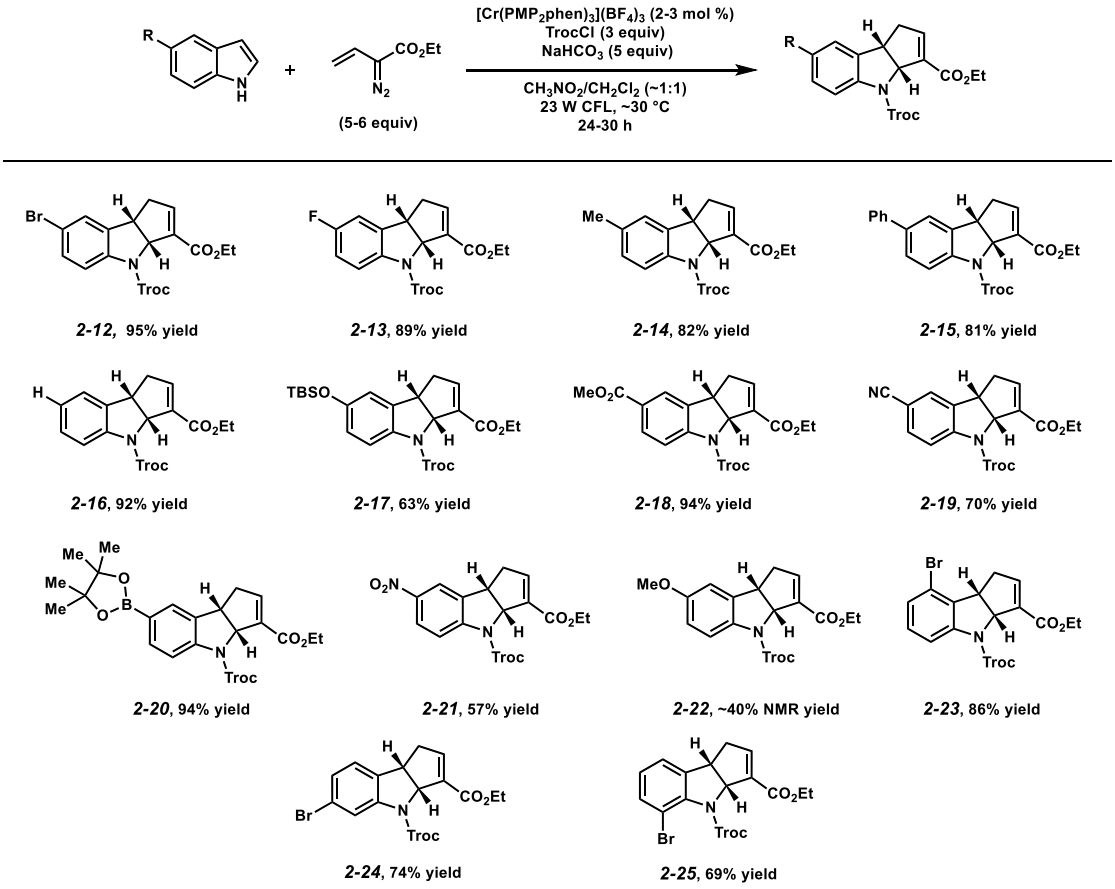

Scheme 2.5.1. Scope of C4, C5, C6, and C7-substituted indoles.

In addition to ethyl vinyldiazoacetate, the *tert*-butyl, benzyl, and phenyl esters were effectively reactive (**2-26**–**2-28**). A diazoacetate with β-substitution could also participate in the cycloaddition (**2-29**), although γ-substitution was not tolerated—this diazo is susceptible to rapid pyrazole formation. Several acid chlorides and chloroformates could be utilized (**2-30**–**2-35**), generally with the stipulation that there was no α-C–H on the acylating agent—enolizable acyl species led to rapid decomposition of vinyl diazoacetate. Finally, the reaction was also not limited to diazoesters; the (3 + 2) cycloaddition was effective using an acylpyrazole-based vinyldiazo species (**2-36**, 64% yield).

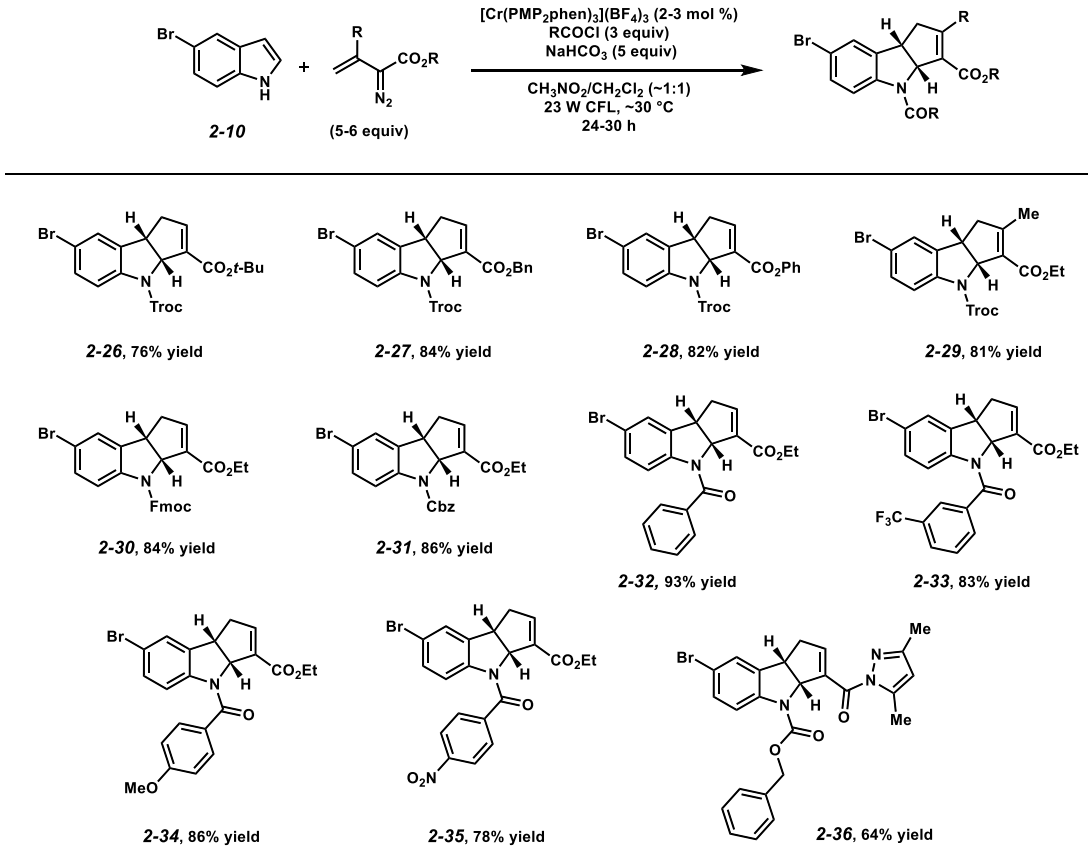

Scheme 2.5.2. Scope of vinyl diazoacetates and acyl protecting groups.

2.6. Accessing C2- and/or C3-Substituted Indoles

Indoles with C2- and/or C3-substitution proved to be uniquely challenging. Several acylating agents were investigated with indole **2-37** (*Table 2.6.1*). Standard conditions utilizing TrocCl with $NaHCO_3$ for acylation proved to be incompatible (*entry 1*), as were most other acylating reagents examined. More activated electron deficient benzoyl chlorides exhibited moderate reactivity (*entries 3–5*). Other activated benzoyl groups were tested and did not yield any desired reactivity (*entries 6, 7*). We believed a different reagent could be fruitful. Specifically, we were looking for a reagent that was "compact" or "smaller" and would also avoid HCl byproduct generation. TrocCl

or BzCl could also pose a steric issue with the additional substitution close to the site of acylation. TFAA and Boc_2O were ineffective (*entries 8, 9*), but encouragingly, the infrequently used trimethylacetic formic anhydride (**2-39**)[22,23] showed measurable activity (*entry 10*).

Table 2.6.1. Protecting groups investigated with C2/C3-substituted indoles.

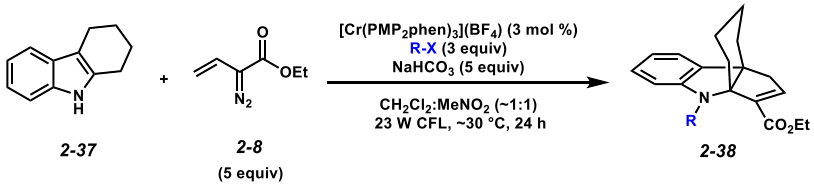

entry	R-X	yield (%)
1	TrocCl	0
2	TsCl	0
3[a]	BzCl	0
4	(*p*-NO_2)BzCl	40
5	(3,5-(NO_2)$_2$)BzCl	55
6	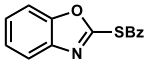	0
7	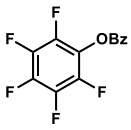	0
8	TFAA	0
9	Boc_2O	0
10	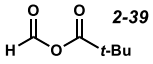 *2-39*	25

[a] <20% yield of unprotected product was detected.

Although the modest reactivity across these acylating agents was perhaps predictable due to the increased substitution around the indoline nitrogen, we did not believe that sterics alone could fully explain the reaction failure. We hypothesized that in the presence of the base necessary for *N*-acylation, the radical cation intermediate could be competitively deprotonated, leading to a radical species that complicates reactivity (*Scheme 2.6.1a*). Deprotonation could lead to re-aromatization and regeneration of starting indole. A *base-free* acylation may circumvent this

problem. We thus examined several potential acylation agents *without* the addition of base on indole **2-37** (*Scheme 2.6.1b*). Trimethylacetic formic anhydride (**2-39**) was singularly effective, generating *N*-formyl cycloadduct **2-38** in excellent yield.

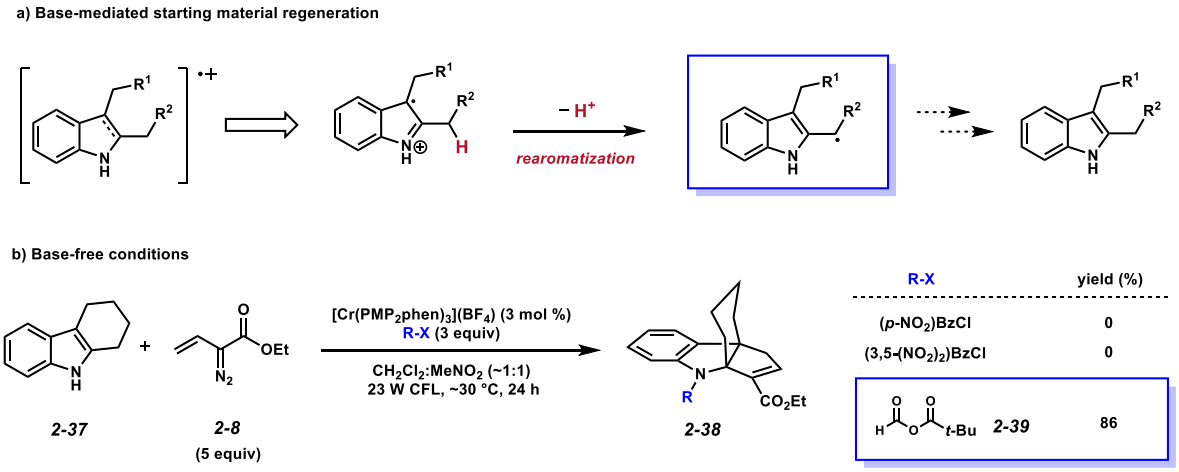

Scheme 2.6.1. Expansion of cycloaddition to C2/C3-substituted indoles. (a) Facile deprotonation of indole radical cation. (b) Base-free conditions in the cycloaddition.

2.7. Scope of C2- and/or C3-Substituted Indoles

A range of C2/C3 mono- and di-substituted indoles could engage in the cycloaddition using this unique anhydride reagent (*Scheme 2.7.1*). Methyl substitution at both C2/C3 (**2-40**), as well as substitution only at C2 (**2-43**) or C3 (**2-42**) worked well in this reaction. A β-substituted vinyl diazoacetate was also tolerated (**2-41**). Indoles with fused rings were notably effective (**2-44**–**2-47**). A substituent on the fused ring induces high diastereoselectivity in the facial addition (**2-47**). Nitrogen substituents have been routinely challenging in this class of cycloadditions, but in this case a phthalimide-based tryptamine derivative was tolerated (**2-48**), albeit in low yield. A comparison of products **2-49** and **2-50** is also informative. Based on our previous understanding

of this class of reactions, the vinyl diazoacetate acts as a nucleophile to attack the C3 position of the radical cation intermediate. The yields of adducts **2-49** (31%) and **2-50** (0%) are consistent with this mechanistic picture, implicating a responsiveness to the steric environment in this nucleophilic attack. Radical stability may also contribute to the lack of **2-50** observed.

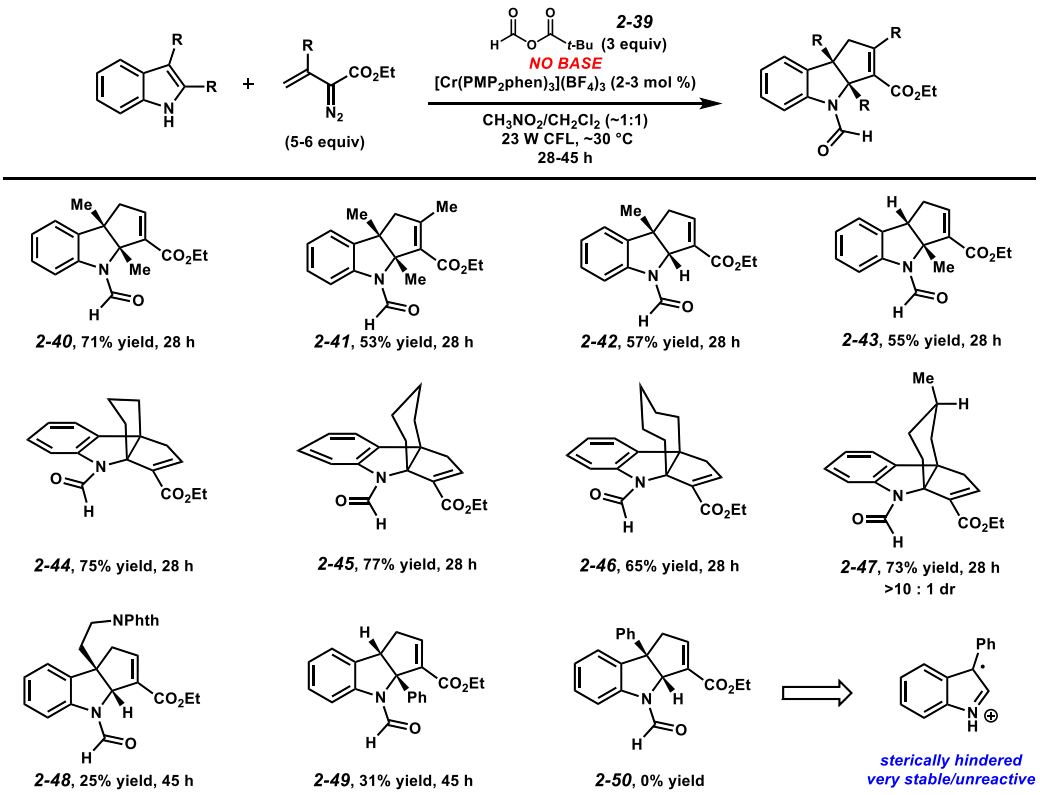

Scheme 2.7.1. Scope of C2/C3-substituted indoles.

2.8. Mechanistic Experiments

To shed insight on the mechanistic pathway, several experiments were conducted. First, both *N*-Troc indole **2-51** and *N*-Me indole **2-52** were investigated in the reaction and were found to not be viable substrates (*Scheme 2.8.1a*). Additionally, we demonstrated that acylation with TrocCl and $NaHCO_3$ (with and without photoredox conditions) leads to only trace yields of **2-51** (*see Experimental Section 2.12.7*). This established that the N-H indole species is required for the cycloaddition to proceed, and the acylation occurs later in the cycle—acylated indole is likely outside the oxidation window of the photocatalyst. Next, the (3 + 2) cycloaddition was performed in the presence of 2,5-dimethyl-2,4-hexadiene (**2-54**, *Scheme 2.8.1b*). This triplet-quenching additive has been shown to inhibit reactivity in photocatalytic intramolecular [2 + 2] cycloadditions between indoles and alkenes.[24] The (3 + 2) cycloaddition between indole **2-10** and vinyl diazoacetate **2-8** is virtually unaffected by this diene; this outcome implicates the lack of an energy transfer pathway leading to desired cycloadduct **2-12**.

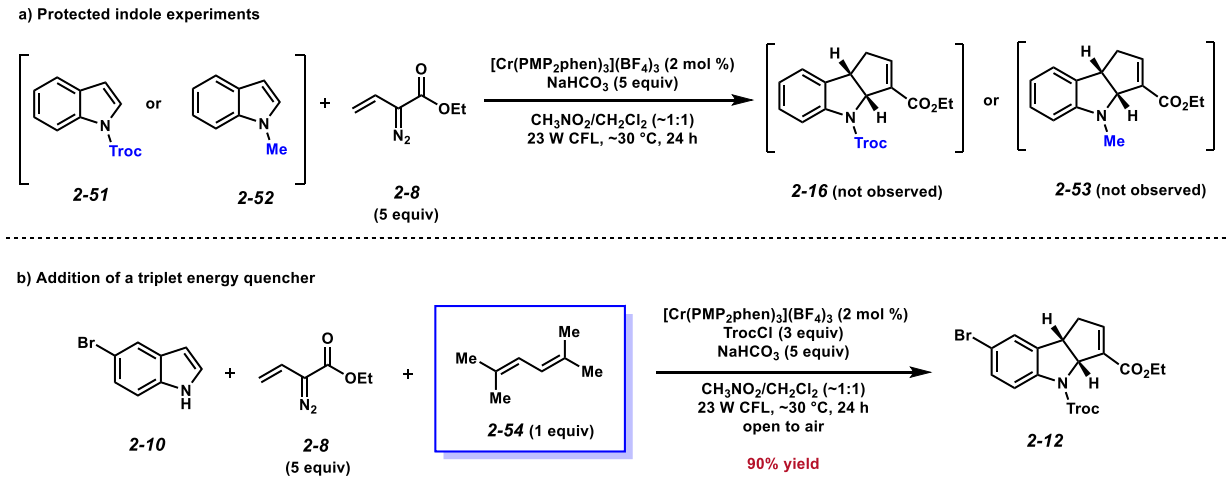

Scheme 2.8.1. (a) Unreactivity of N-substituted indoles. (b) Minimal reaction impact by triplet-quenching diene.

We next were interested in exploring a competitive experiment between indoles with varying reduction potentials. Indole competitions are depicted in *Scheme 2.8.2*. 5-Bromoindole (**2-10**, $E_{1/2}$ = +1.30 V vs SCE in CH_3CN) was subjected to the cycloaddition in the presence of an equivalent of either 5-methoxycarbonylindole (**2-55**, $E_{1/2}$ = +1.33 V vs SCE in CH_3CN) or 5-methylindole (**2-56**, $E_{1/2}$ = +1.18 V vs SCE in CH_3CN). In the former case the cycloaddition preferences are about the same, while in the latter there is a near-exclusive selectivity for cycloaddition with the 5-methylindole (**2-56**). This reaction profile is consistent with reactivity being governed by the indole's electronic properties; the more oxidizable indole preferentially engages. The reduction potential of vinyl diazoacetate **2-8** is +1.57 V vs. SCE,[8] higher than the indoles used in this experiment. This difference suggests photocatalyzed oxidation of the vinyl diazoacetate species—while not impossible—is not as likely or favorable.

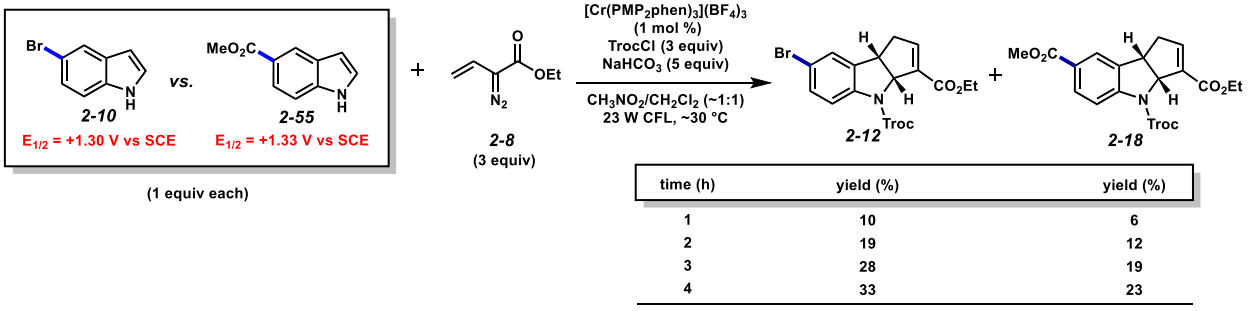

Scheme 2.8.2. Competition experiments on electronically differentiated indoles.

A couple of additional pieces of evidence are also consistent with the proposed single electron transfer mechanism. The suppressed reactivity by TEMPO (*vide supra, Table 2.4.1, entry 16*) implicates the intermediacy of a radical species. Stern-Volmer quenching studies were also performed to establish radical cation quenching. The purpose of this study is to monitor the emission band (relaxation) of an excited species and look for any observed "quenching" or diminishing of that band after increasing concentrations of an additive—this could indicate an energy transfer or single electron transfer between the excited species and the additive. Two main emission bands are observed with the $[Cr(PMP_2phen)_3](BF_4)_3$ excited catalyst at 464 nm and 752 nm.[6,25]

The emission band at 752 nm is much lower in energy and can be attributed to single electron transfer. The Stern-Volmer studies at this wavelength revealed a strong linear relationship between the concentration of indole **2-10** and the emission signal from the Cr complex excited state related to electron transfer (*Figure 2.8.1a-b*). Meanwhile, varying concentrations of vinyl diazoacetate **2-8** did not impact the same Cr emission signal whatsoever (*Figure 2.8.1a-b*). These photophysical experiments further point to a reaction mechanism involving initiation by electron transfer.

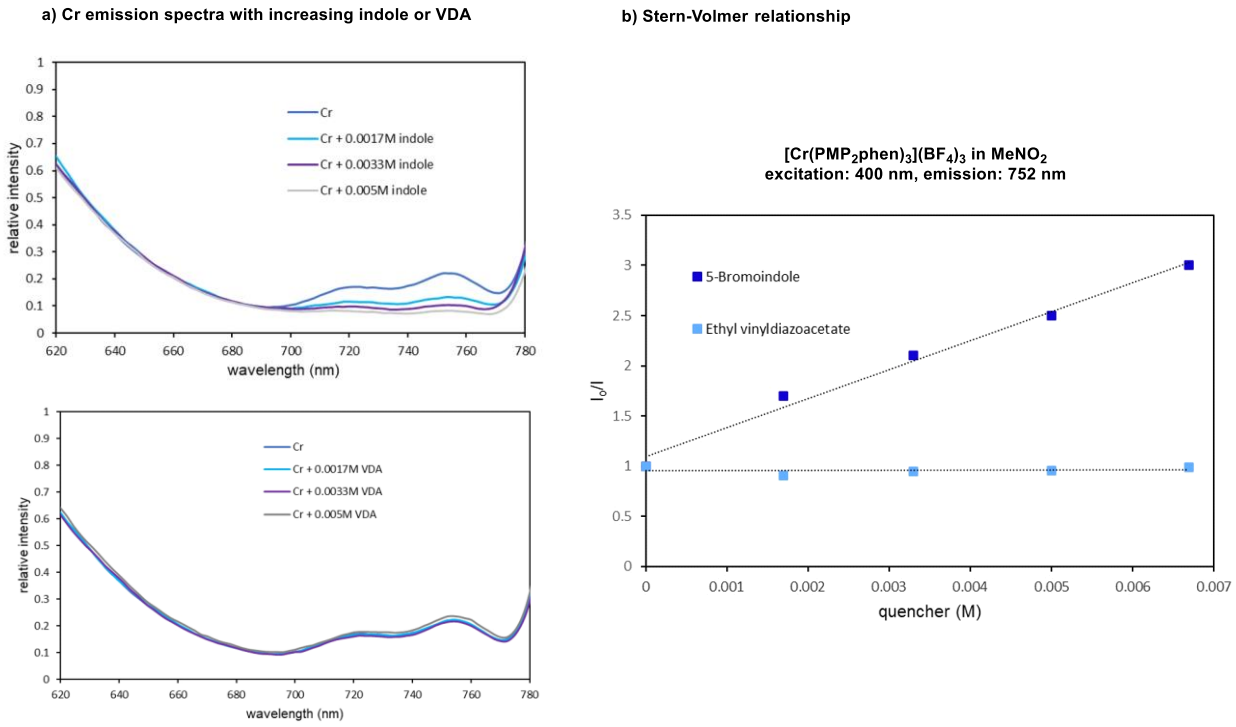

Figure 2.8.1. Stern-Volmer analysis. (a) Emission data at 752 nm. (b) Stern-Volmer relationship between Cr catalyst and indole or vinyl diazoacetate (VDA).

The other emission band at 464 nm is much higher in energy and can be attributed to energy transfer processes. We observed less pronounced linear Stern–Volmer quenching at this band by both the indole (**2-10**) and the vinyl diazoacetate (**2-8**) evaluated (*Figure 2.8.2*).[26] These Cr(III)-polypyridyl species are capable of energy transfer; we attribute this type of quenching to non-productive outcomes such as pyrazole formation or non-productive relaxation. This unproductive decomposition pathway of vinyl diazoacetate helps to explain the need for excess reagent in the reaction as well.

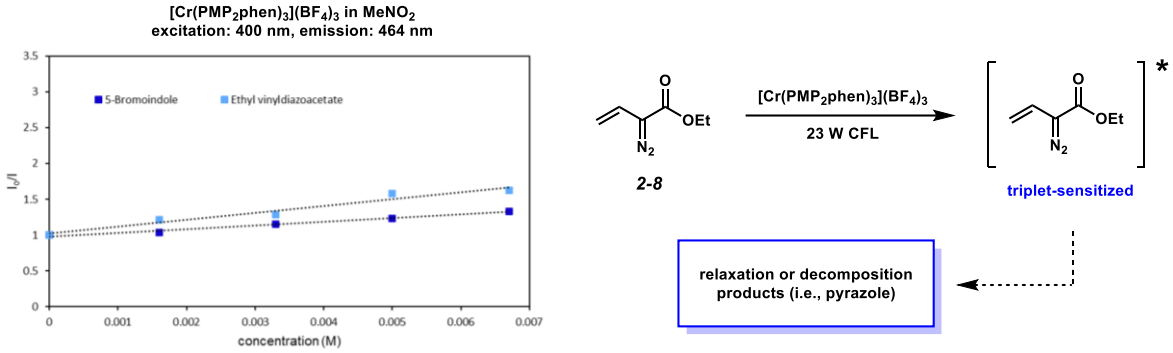

Figure 2.8.2. Stern-Volmer analysis at 464 nm.

Electron transfer processes with vinyl diazoacetate **2-8**, while not impossible, should not be favorable; the reduction potential of vinyl diazoacetate **2-8** is +1.57 V vs. SCE (measured in CH_3NO_2), significantly higher than the indoles used in these experiments (approx. +1.10–1.40 V vs. SCE).[8] The competency of the cycloaddition in the presence of rapid triplet quencher 2,5-dimethyl-2,4-hexadiene (**2-54**) is also consistent with product formation occurring via a non-energy transfer pathway; related photocatalytic dearomative [2 + 2] cycloadditions that proceed by energy transfer were considerably suppressed when this diene was added.[12,24]

In a separate experiment modeled after the work of Gryko and coworkers,[11] a reactivity competition was performed between 5-bromoindole (**2-10**) and 5-methylindole (**2-56**). In the Gryko report, the α-carbonyl radical derived photocatalytically from ethyl diazoacetate (**2-57**) adds to N-H indoles at C2. In this competition experiment, there are similar rates of reactivity between the two tested indoles (**2-58**, **2-59**), starkly different from our cycloaddition, where we observed near exclusive preference for reaction with 5-methylindole. If the vinyl diazoacetate (**2-8**) were undergoing energy transfer followed by addition to indole, it is anticipated the addition would be radical in nature, much like the Gryko reactivity. Both the regioselectivity observed (addition at

C3) and the electronically-differentiated reactivity in our (3 + 2) cycloaddition are inconsistent with this putative energy transfer pathway.

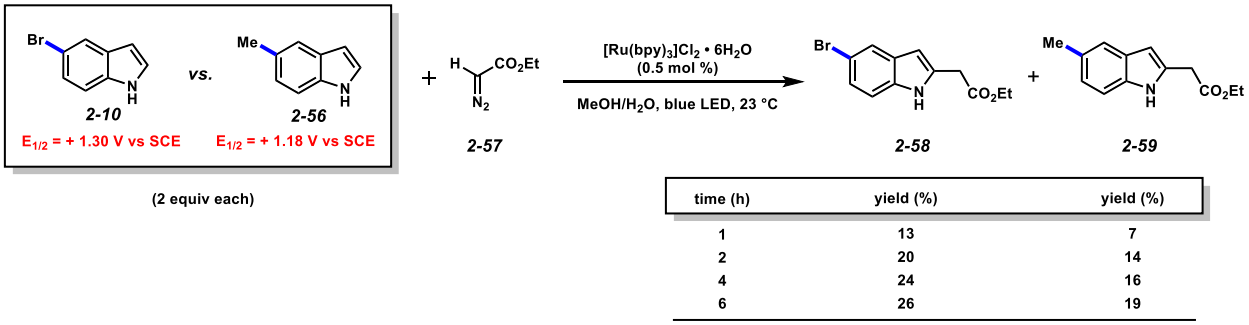

time (h)	yield (%)	yield (%)
1	13	7
2	20	14
4	24	16
6	26	19

Scheme 2.8.3. Electronically different indoles tested in radical diazoacetate experiment.

Additional experiments were performed to examine the exclusive regioselectivity observed in this reaction. Our intention was to show two *intramolecular* examples, with vinyldiazo attached at either the C2 or C3 position. Employing our C2/C3 conditions with trimethylacetic formic anhydride (**2-39**) and no base, we tested indole **2-60** and indole **2-62** under standard conditions (*Scheme 2.8.4*). Unsurprisingly, the C3-substituted intramolecular cycloadduct (**2-61**) was not observed—this product would be highly strained and would invoke an even more strained intermediate after nucleophile addition (*Scheme 2.8.4a*). Interestingly, when the C2-substituted indole (**2-62**) was subjected to the reaction conditions, a mixture of products was observed (**2-63**, **2-64**, *Scheme 2.8.4b*). Compound **2-64** is a result of intramolecular pyrazole formation, while compound **2-63** is the product of a (3 + 2) cycloaddition reaction between **2-64** and **2-62**, followed by formylation. Although desired intramolecular cycloaddition was not observed, the experiment

was still insightful. Steric hindrance at the C3 position has an immense effect on reaction outcomes, this is possibly why a similar intermolecular process is not observed in *Scheme 2.8.4a*.

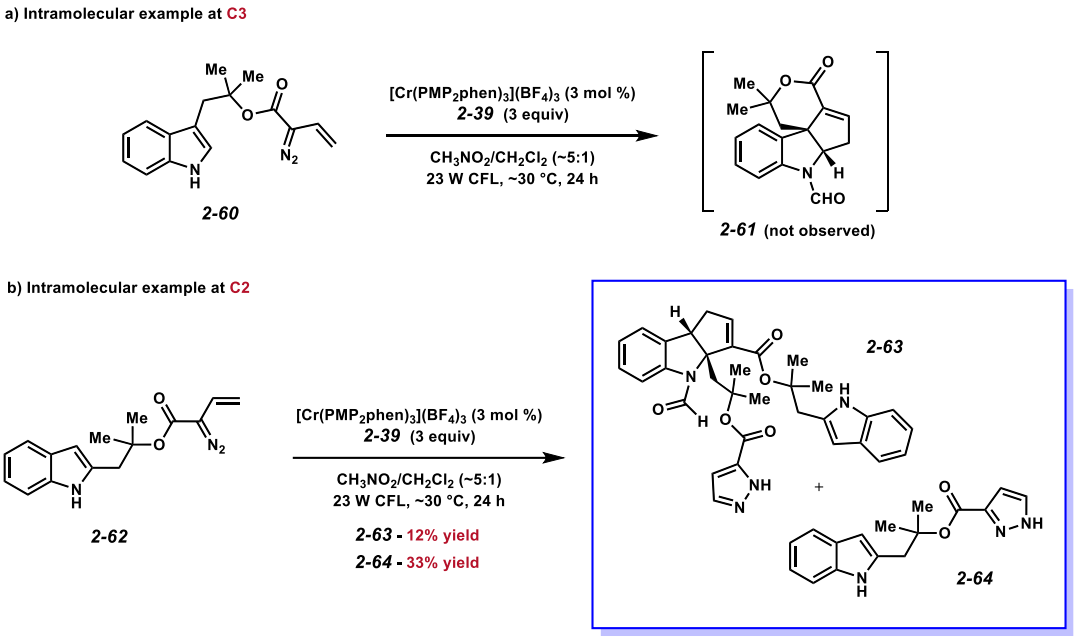

Scheme 2.8.4. Attempted intramolecular (3 + 2) cycloaddition.

2.9. Proposed Catalytic Cycle

Based on these experiments and the aforementioned indole-diene (4 + 2) cycloadditions,[8,13] we propose the transformation occurs as depicted in *Scheme 2.9.1*. Oxidation of the indole (**2-65**) by the Cr(III) excited state generates radical cation **2-66**$^{+\bullet}$. There is significant radical character at C3 in this species, which then combines with the vinyl diazoacetate to yield intermediate **2-67**, after loss of N_2. Ring closure (**2-68**) and subsequent reduction with either reduced Cr(II) or indole (**2-65**) affords fused indoline **2-69**. The transformation culminates with an acylation to drive the product (**2-70**) outside the oxidation window of the catalyst. In Davies's analogous Rh-catalyzed (3 + 2) cycloaddition via a carbenoid species, the regioselectivity of the addition was dictated by

C2/C3-substitution on the indole.[14] In this particular photocatalyzed cycloaddition, regioselectivity is exclusive and distinct, governed entirely by the selectivity induced from the indole radical cation intermediate (**2-66**$^{+\bullet}$).

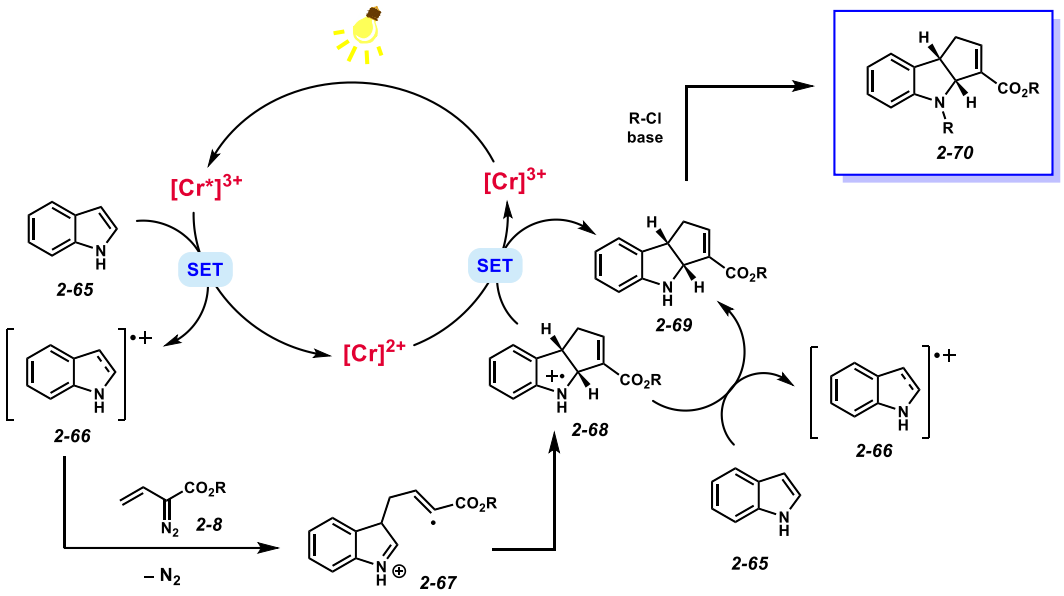

Scheme 2.9.1. Proposed catalytic cycle.

2.10. Cycloaddition Product Diversification

The indoline cycloadducts can be readily diversified, as shown by the transformations of indoline **2-12** (*Scheme 2.10.1*). Removal of the trichloroethoxycarbonyl proceeds in excellent yield (**2-78**). Cross couplings with the aryl bromide moiety can be achieved with aryl or heteroaryl boron reagents (**2-71**, **2-72**). Allylic oxidation affords enone **2-77**,[27] while DIBAL reduction generates hemiaminal ether **2-76**.[28] The fused 5,5-ring system also allows for diastereoselective transformations. Conjugate reduction using $NaBH_4$/Fe(tpp)Cl generates the exclusive saturated ester diastereomer (**2-75**).[29] Similarly, the enoate is also poised for subsequent cycloadditions.

Nitrile oxide (**2-80**) addition affords isoxazoline **2-73** with excellent regioselectivity and moderate dr, while Ag-catalyzed glycine-imine (**2-81**) (3 + 2) cycloaddition yields pyrrolidine **2-74**, featuring six stereogenic centers.[30] For formylated derivatives, the removal of the *N*-protecting group is also straightforward under acidic conditions (**2-79**). The synthetic handles generated via this cycloaddition presents a breadth of options for subsequent manipulations, offering promise for wider applications.

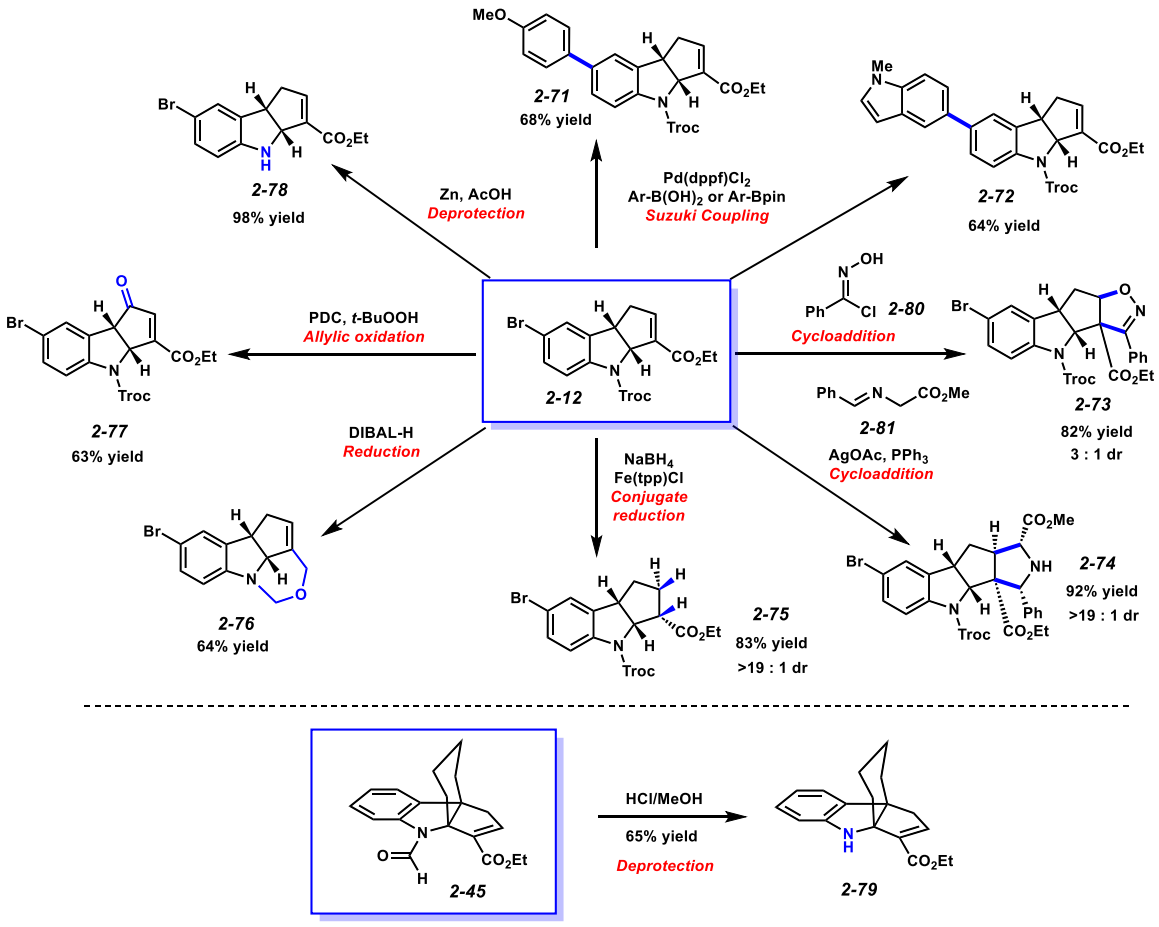

Scheme 2.10.1. Indoline product diversification.

2.11. Conclusion

The development of catalysts based on earth-abundant metals is an important endeavor toward sustainable chemistry. These catalysts also present the possibility of discovering unique transformations altogether that are not achievable by previously established photocatalysts. We have described the development of an increased-activity first row metal photocatalyst, $[Cr(PMP_2phen)_3](BF_4)_3$, and demonstrated its efficacy in dearomative (3 + 2) cycloaddition with indoles and vinyl diazoacetates. Densely functionalized indolines are accessible via this extremely mild transformation, with synthetic handles poised for further manipulation.

Further characterization of this new catalyst and derivatives, mechanistic studies, and applications in additional transformations are underway within our group. A follow-up study describing access to products containing functional groups not typically tolerated via a similar (3 + 2) cycloaddition is featured in Chapter 3.

2.12. Experimental Section

2.12.1. Materials and Methods

$[Ru(bpz)_3](PF_6)_2$ was prepared according to the procedure by Yoon and coworkers.[20] Reactions were performed under argon atmosphere unless otherwise noted. Dichloromethane, tetrahydrofuran, dimethylformamide, and toluene were purified by passing through activated alumina columns. Nitromethane (99%) and 1,4-dioxane were used as received. Commercially available chemicals were purchased from Alfa Aesar (Ward Hill, MA), Sigma-Aldrich (St. Louis, MO), Oakwood Products, (West Columbia, SC), Strem (Newburport, MA), and TCI America (Portland, OR). Qualitative TLC analysis was performed on 250 mm thick, 60 Å, glass backed, F254 silica (SiliCycle, Quebec City, Canada). Visualization was accomplished with UV light and/or exposure to cerium ammonium molybdate (Hanessian's Stain), $KMnO_4$, or *p*-anisaldehyde stain solutions followed by heating. Flash chromatography was performed using SiliCycle silica gel (230-400 mesh). ^1H NMR spectra were acquired on a Bruker AVANCE III HD NMR (at 400 MHz) and are reported relative to $SiMe_4$ (δ 0.00). ^{13}C NMR spectra were acquired on a Bruker AVANCE III HD NMR (at 100 MHz) and are reported relative to $SiMe_4$ (δ 0.0). ^{19}F NMR spectra were acquired on a Bruker AVANCE III HD NMR (at 376 MHz) and are reported relative to $CFCl_3$ (δ 0.0). Variable Temperature (VT) ^1H NMR was acquired on a Varian INOVA (at 500 MHz) and are reported relative to $SiMe_4$ (δ 0.00). Variable Temperature (VT) ^{13}C NMR was acquired on a Varian INOVA (at 125 MHz) and are reported relative to $SiMe_4$ (δ 0.00). All IR spectra were obtained Thermo Nicolet iS10 spectrometer and are reported in wavenumbers (ν). High resolution mass spectrometry (HRMS) data were acquired via electrospray ionization (ESI) using a ThermoFisher Orbitrap Q-Exactive. Cyclic voltammetry (CV) measurements were performed with a WaveDriver 40 Bipotentiostat/Galvanostat from the Pine Research Instrument

Company using non-aqueous Ag/Ag^+ reference electrode (Ag wire immersed in CH_3CN containing 0.25 M Bu_4NPF_6), Pt wire counter electrode, and a stationary glassy-carbon working milli-electrode (3 mm diameter). Measurements were performed at ambient temperature under argon atmosphere using 5 mM analyte in CH_3CN containing 0.25 M Bu_4NPF_6 as the supporting analyte. Analyte potentials were referenced against 5 mM ferrocene internal standard under identical conditions, where $E_{1/2}$ = 0.275 V in CH_3CN vs the reported non-aqueous Ag/Ag^+ electrode. Potential is referenced to Fc^+/Fc. Scans were performed at 100 mV/s scan rate in 0.25 M Bu_4NPF_6. To convert potentials from V vs. Fc^+/Fc to V vs. SCE, 0.400 was added to the potentials taken in CH_3CN.[31] Reactions under near-UV irradiation (NUV) were performed in a Luzchem photoreactor (LZC-ORG) equipped with 10 lamps of wavelengths 419, 350, and 300 nm. Catalyst absorbance measurements were taken on either a Varian Cary 300 Bio UV-Visible spectrophotometer or a Varian Cary 5000 UV-Visible-NIR spectrophotometer. Reactions under blue LED irradiation were performed using a 390 nm Kessil PR160L LED PhotoReaction light. Irradiation with visible light was performed with one 23 W compact fluorescent light bulb (EcoSmart 23 W bright white CFL spiral bulb, 1600 lumens). Luminescence quenching data were collected on a Hitachi F-7000 fluorescence spectrophotometer with a 150 W Xe lamp as the light source. Cycloadditions using all modes of irradiation were performed using flame-dried borosilicate vials. The internal temperature of the photobox was maintained at 30 °C.

2.12.2. Synthesis of $[Cr(PMP_2phen)_3](BF_4)_3$:[32]

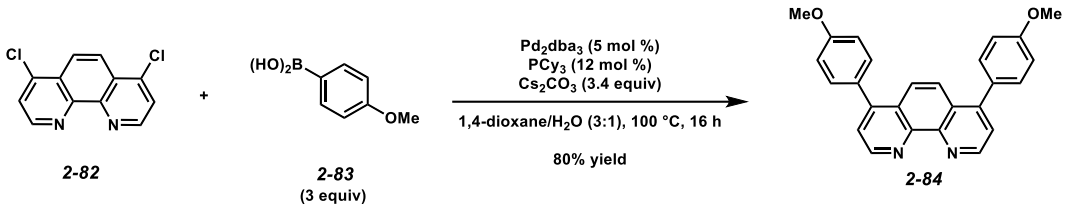

4,7-Bis(4-methoxyphenyl)-1,10-phenanthroline (**2-84**). A flame-dried flask charged with 4,7-dichloro-1,10-phenanthroline (**2-82**, 0.500 g, 2.01 mmol), 4-methoxyphenylboronic acid (**2-83**, 0.916 g, 6.03 mmol), Cs_2CO_3 (2.22 g, 6.82 mmol), $Pd_2(dba)_3$ (91.9 mg, 0.100 mmol), and PCy_3 (67.5 mg, 0.241 mmol) in 3:1 1,4-dioxane/H_2O (10 mL) was degassed with argon for 15 min at 23 °C. The reaction mixture was then heated to 100 °C and stirred for 16 h. Upon completion, the reaction mixture was cooled to room temperature, diluted with $CHCl_3$, (50 mL), and poured into H_2O (25 mL). The layers were separated, and the aqueous layer was extracted with $CHCl_3$ (3 x 50 mL). The combined organic layers were washed sequentially with H_2O (200 mL), sat. aq. Na_2CO_3 (200 mL), 10% aq. NaOH (200 mL), H_2O (200 mL), and brine (200 mL), and then dried over Na_2SO_4 and concentrated in vacuo. The crude residue was triturated with hexanes (50 mL), and the solid was collected and rinsed with hexanes to afford phenanthroline **2-84** (630 mg, 80% yield) as an off-white solid.

TLC: R_f = 0.15 in 3:1 EtOAc/hexanes.

^{1}H NMR (400 MHz, $CDCl_3$): δ 9.19 (d, *J* = 4.5 Hz, 2H), 7.88 (s, 2H), 7.54 (d, *J* = 4.5 Hz, 2H), 7.46 (d, *J* = 8.6 Hz, 4H), 7.05 (d, *J* = 8.6 Hz, 4H), 3.88 (s, 6H).

^{13}C NMR (100 MHz, $CDCl_3$): δ 160.0, 149.8, 148.2, 147.0, 131.1, 130.3, 126.6, 124.0, 123.6, 114.2, 55.5.

IR (ATR, neat): 2935, 1605, 1502, 1246, 1175, 815 cm^{-1}.

HRMS (ESI+): *m/z* calc'd for $(M + H)^+$ $[C_{26}H_{20}N_2O_2 + H]^+$: 393.1598 found 393.1600

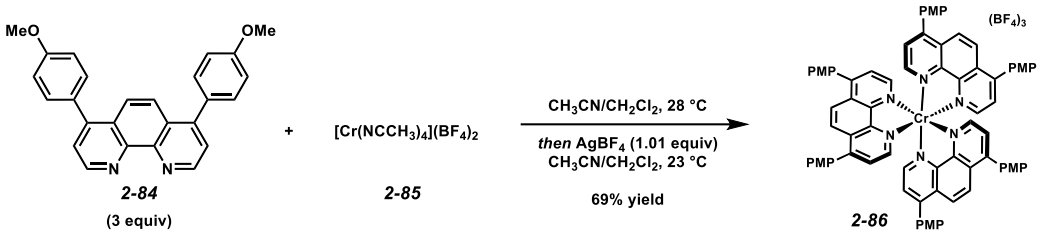

[Cr(PMP$_2$phen)$_3$](BF$_4$)$_3$ (2-86): In an argon-filled glove box at 28 °C, a solution of [Cr(NCCH$_3$)$_4$](BF$_4$)$_2$ (**2-85**, 0.218 g, 0.559 mmol) in CH$_3$CN (4.60 mL) was added to a solution of phenanthroline **2-84** (0.650 g, 1.66 mmol) in CH$_3$CN (2.70 mL) and CH$_2$Cl$_2$ (1.85 mL). The reaction mixture was stirred for 2 h, and then AgBF$_4$ (0.110 g, 0.565 mmol) was added, resulting in a brownish-colored mixture. The reaction vessel was then sealed and removed from the glove box, and the reaction mixture was stirred in the hood under an argon atmosphere overnight at 23 °C. The mixture was then filtered over celite by vacuum filtration, washing with the minimal amount of CH$_3$CN (15 mL). Et$_2$O (300 mL) was added to the filtrate while stirring, causing an orange solid to precipitate. After 10 min stirring, the solid was collected by vacuum filtration, rinsed with Et$_2$O, and then dried under vacuum overnight, yielding the [Cr(PMP$_2$phen)$_3$](BF$_4$)$_3$ complex as an orange solid. The crude material was purified by recrystallization using vapor diffusion. In a scintillation vial, crude catalyst (~100 mg) was completely dissolved in CH$_3$CN (~5 mL). The vial was placed in a 150 mL beaker filled with Et$_2$O (30 mL). A watchglass was placed on top of the beaker, and the system was only disturbed to replenish Et$_2$O each day, maintaining approximately 30 mL in volume. After 7 d, the vial was decanted and the solid was washed with excess Et$_2$O. The solid was then collected and dried under vacuum to afford pure [Cr(PMP$_2$phen)$_3$](BF$_4$)$_3$ (**2-86**, 0.571 g, 69% yield) as a red solid.

HRMS (ESI+): *m/z* calc'd for $(M - 3BF_4)^{3+}$: $[C_{78}H_{60}CrN_6O_6]^{3+}$: 409.4654, found 409.4673.

Cr(III) Catalyst UV-Vis Analysis

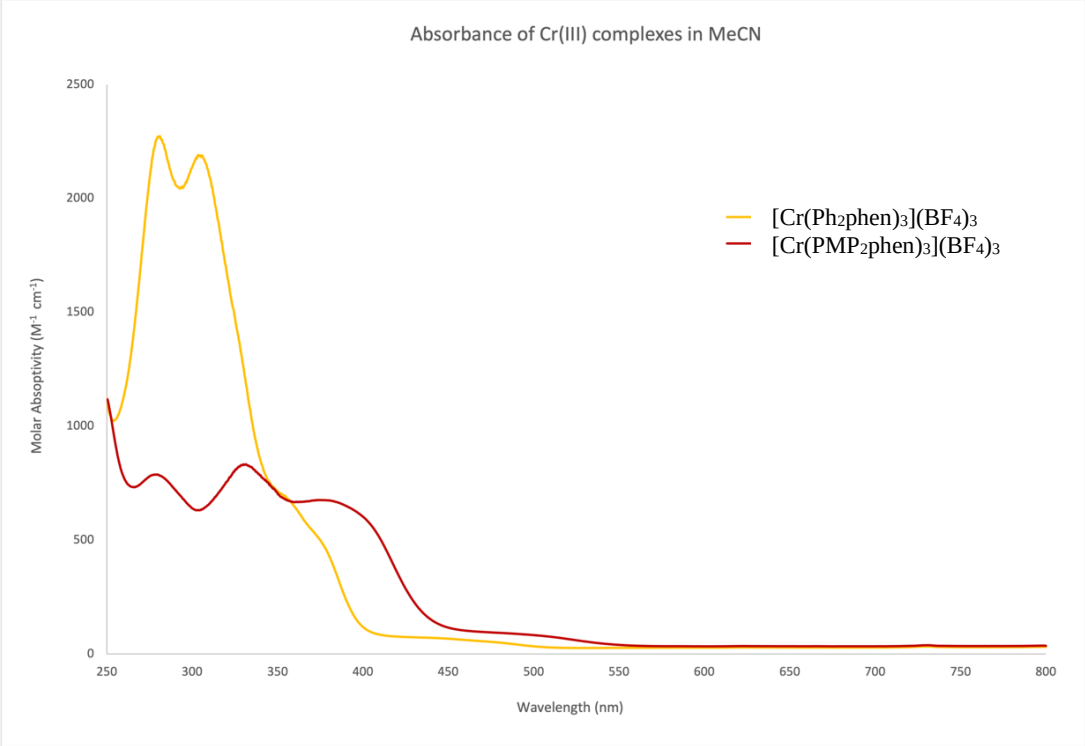

Figure 2.12.1. UV-Vis absorbance measurements of [Cr(Ph$_2$phen)$_3$](BF$_4$)$_3$ and [Cr(PMP$_2$phen)$_3$](BF$_4$)$_3$.

General procedure for absorbance analysis: Each catalyst was dissolved in CH_3CN at a concentration of 0.001 M and analyzed by UV/vis spectroscopy.

2.12.3. Optimization Experiments

Table 2.12.1. Catalyst evaluation.

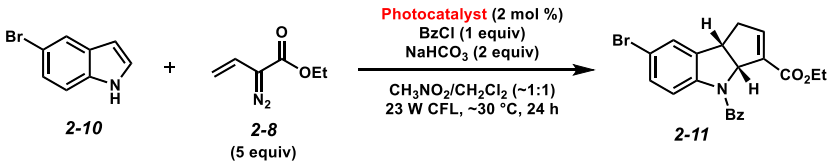

Entry	Photocatalyst	NMR yield (%)
1	$[Cr(Ph_2phen)_3](BF_4)_3$	26
2	TPPT	41
3	$(OMe)_3$TPPT	43
4	DCB	0
5	DCA	23
6	Mes-Acr(BF_4)	46
7	4-CzIPN	trace
8	$[Ru(bpy)_3]Cl_2$	10
9	$[Ru(bpy)_3]Cl_2$ + MV	trace
10	$[Ru(bpz)_3](PF_6)_2$	44
11	$[Ir(dFCF_3ppy)_2(bpy)](PF_6)$	0
12	$[Ir(dFCF_3ppy)_2(5,5'\text{-}dCF_3bpy)](PF_6)$	62
13	$[Cr(PMP_2phen)_3](BF_4)_3$	75
14	$[Cr(PMP_2phen)_3](BF_4)_3$ (no light)	0
15	none	0

Catalysts:

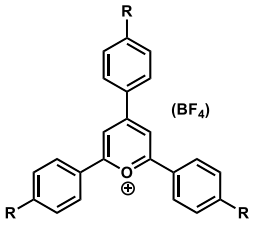

R = H, TPPT
R = OMe, $(OMe)_3$TPPT

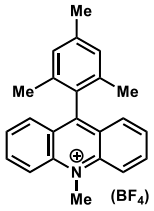

Mes-Acr(BF_4)

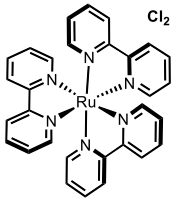

$[Ru(bpy)_3]Cl_2$

MV = methyl viologen dichloride hydrate

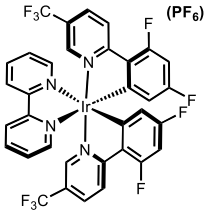

$[Ir(dFCF_3ppy)_2(bpy)](PF_6)$

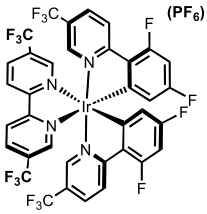

$[Ir(dFCF_3ppy)_2(5,5'\text{-}dCF_3bpy)](PF_6)$

DCB = 1,4-dicyanobenzene
DCA = 9,10-dicyanoanthrancene

General procedure for CATALYST optimization: 5-Bromoindole (**2-10**, 0.100 mmol), $NaHCO_3$ (0.200 mmol), and photocatalyst (half of indicated amount in table) were added to a flame-dried 1-dram borosilicate vial open to air. The reagents were suspended in nitromethane (0.500 mL), and then benzoyl chloride (0.100 mmol) and vinyl diazoacetate reagent **2-8** (0.300 mmol, 1.0 M solution in CH_2Cl_2) were added. The vial was then capped, and the reaction mixture was irradiated with a 23 W CFL bulb while stirring. After 8 h, second charges of vinyl diazoacetate **2-8** (0.200 mmol, 1.0 M solution in CH_2Cl_2) and photocatalyst (half of indicated amount in table) were added, and the reaction mixture was irradiated for another 16 h. At the 24 h timepoint, the solvent was removed by rotary evaporation. The crude residue was then dissolved in CH_2Cl_2 (~1 mL), and the solution was passed through a SiO_2 plug (0.5 x 3 cm), using CH_2Cl_2 as eluent (~8 mL). The filtrate was concentrated in vacuo, and the crude residue was analyzed by ^1H NMR using CH_2Br_2 as an internal standard.

Table 2.12.2. Solvent optimization.

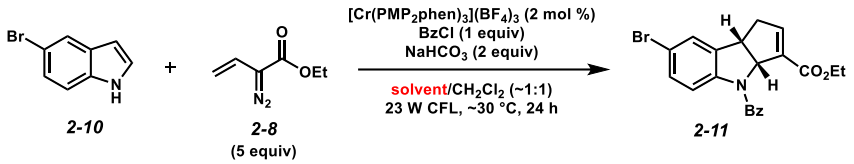

Entry	Solvent	NMR yield (%)
1	CH_3NO_2	75
2	CH_3CN	54
3	acetone	51
4	CH_2Cl_2 only	62

General procedure for SOLVENT optimization: 5-Bromoindole (**2-10**, 0.100 mmol), $NaHCO_3$ (0.200 mmol), and $[Cr(PMP_2phen)_3](BF_4)_3$ (0.00100 mmol) were added to a flame-dried 1-dram borosilicate vial open to air. The reagents were suspended in solvent (0.500 mL), and then benzoyl chloride (0.100 mmol) and vinyl diazoacetate reagent **2-8** (0.300 mmol, 1.0 M solution in CH_2Cl_2) were added. The vial was then capped, and the reaction mixture was irradiated with a 23 W CFL bulb while stirring. After 8 h, second charges of vinyl diazoacetate **2-8** (0.200 mmol, 1.0 M solution in CH_2Cl_2) and $[Cr(PMP_2phen)_3](BF_4)_3$ (0.00100 mmol) were added, and the reaction mixture was irradiated for another 16 h. At the 24 h timepoint, the solvent was removed by rotary evaporation. The crude residue was then dissolved in CH_2Cl_2 (~1 mL), and the solution was passed through a SiO_2 plug (0.5 x 3 cm), using CH_2Cl_2 as eluent (~8 mL). The filtrate was concentrated in vacuo, and the crude residue was analyzed by ^1H NMR using CH_2Br_2 as an internal standard.

Table 2.12.3. Base optimization.

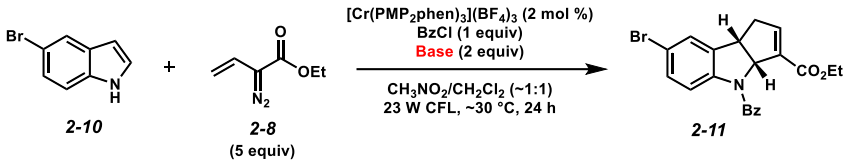

Entry	Base	NMR yield (%)
1	$NaHCO_3$	75
2	$KHCO_3$	51
3	NaH_2PO_4	18
4	Na_2HPO_4	32
5	pyridine	0
6	Et_3N	0

General procedure for BASE optimization: 5-Bromoindole (**2-10**, 0.100 mmol), base (for entries 1-4, 0.200 mmol), and $[Cr(PMP_2phen)_3](BF_4)_3$ (0.00100 mmol) were added to a flame-dried 1-dram borosilicate vial open to air. The reagents were suspended in nitromethane (0.500 mL), and then benzoyl chloride (0.100 mmol), base (for entries 5-6, 0.200 mmol) and vinyl diazoacetate reagent **2-8** (0.300 mmol, 1.0 M solution in CH_2Cl_2) were added. The vial was then capped, and the reaction mixture was irradiated with a 23 W CFL bulb while stirring. After 8 h, second charges of vinyl diazoacetate **2-8** (0.200 mmol, 1.0 M solution in CH_2Cl_2) and $[Cr(PMP_2phen)_3](BF_4)_3$ (0.00100 mmol) were added, and the reaction mixture was irradiated for another 16 h. At the 24 h timepoint, the solvent was removed by rotary evaporation. The crude residue was then dissolved in CH_2Cl_2 (~1 mL), and the solution was passed through a SiO_2 plug (0.5 x 3 cm), using CH_2Cl_2 as eluent (~8 mL). The filtrate was concentrated in vacuo, and the crude residue was analyzed by ^1H NMR using CH_2Br_2 as an internal standard.

Table 2.12.4. Acylating agent and base stoichiometry optimization.

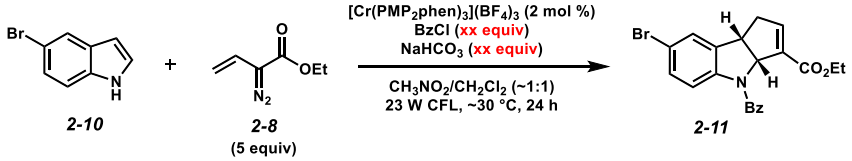

Entry	BzCl equiv	$NaHCO_3$ equiv	NMR yield (%)
1	1.0	2.0	75
2	2.0	4.0	79
3	3.0	5.0	94
4	5.0	5.0	95

General procedure for STOICHIOMETRY optimization: 5-Bromoindole (**2-10**, 0.100 mmol), base (see table for equivalents), and $[Cr(PMP_2phen)_3](BF_4)_3$ (0.00100 mmol) were added to a flame-dried 1-dram borosilicate vial open to air. The reagents were suspended in nitromethane (0.500 mL), and then benzoyl chloride (see table for equivalents) and vinyl diazoacetate reagent **2-8** (0.300 mmol, 1.0 M solution in CH_2Cl_2) were added. The vial was then capped, and the reaction mixture was irradiated with a 23 W CFL bulb while stirring. After 8 h, second charges of vinyl diazoacetate **2-8** (0.200 mmol, 1.0 M solution in CH_2Cl_2) and $[Cr(PMP_2phen)_3](BF_4)_3$ (0.00100 mmol) were added, and the reaction mixture was irradiated for another 16 h. At the 24 h timepoint, the solvent was removed by rotary evaporation. The crude residue was then dissolved in CH_2Cl_2 (~1 mL), and the solution was passed through a SiO_2 plug (0.5 x 3 cm), using CH_2Cl_2 as eluent (~8 mL). The filtrate was concentrated in vacuo, and the crude residue was analyzed by ^1H NMR using CH_2Br_2 as an internal standard.

Table 2.12.5. Select additional experiments from Table 2.2.1.

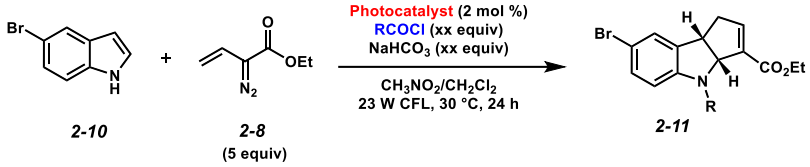

entry	Photocatalyst	RCOCl (equiv)	$NaHCO_3$ equiv	NMR yield (%)
1	$[Cr(Ph_2phen)_3](BF_4)_3$	AcCl (1)	2	8
2	$[Ru(bpz)_3](PF_6)_2$	AcCl (1)	2	31
3	$[Cr(PMP_2phen)_3](BF_4)_3$	BzCl (1)	2	75
4	$[Cr(PMP_2phen)_3](BF_4)_3$	BzCl (3)	5	94
5	$[Cr(PMP_2phen)_3](BF_4)_3$	TrocCl (3)	5	95

General procedure for select additional experiments: 5-Bromoindole (**2-10**, 0.100 mmol), $NaHCO_3$ (see table for equivalents), and photocatalyst (0.00100 mmol) were added to a flame-dried 1-dram borosilicate vial open to air. The reagents were suspended in nitromethane (0.500 mL), and then acylating agent (see table for equivalents) and vinyl diazoacetate reagent **2-8** (0.300 mmol, 1.0 M solution in CH_2Cl_2) were added. The vial was then capped, and the reaction mixture was irradiated with a 23 W CFL bulb while stirring. After 8 h, second charges of vinyl diazoacetate **2-8** (0.200 mmol, 1.0 M solution in CH_2Cl_2) and photocatalyst (0.00100 mmol) were added, and the reaction mixture was irradiated for another 16 h. At the 24 h timepoint, the solvent was removed by rotary evaporation. The crude residue was then dissolved in CH_2Cl_2 (~1 mL), and the solution was passed through a SiO_2 plug (0.5 x 3 cm), using CH_2Cl_2 as eluent (~8 mL). The filtrate was concentrated in vacuo, and the crude residue was analyzed by ^1H NMR using CH_2Br_2 as an internal standard.

Table 2.4.1 (recreated). Deviations from standard conditions.

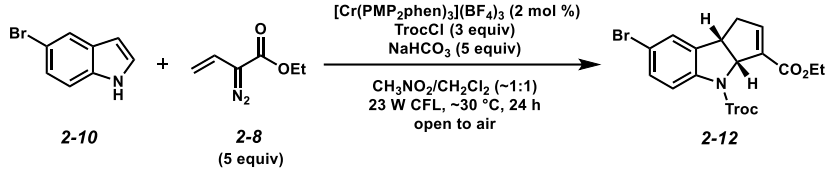

entry	deviation from standard conditions	yield (%)
1	none	95
2	$KHCO_3$	51
3	NaH_2PO_4	52
4	Et_3N	0
5	CH_2Cl_2 only	86
6	blue LED (390 nm)	28
7	near UV irradiation	39
8	2 equiv ***2-8***	73
9	inert atmosphere	88
10	O_2 atmosphere	91
11	0.5 mol % catalyst	76
12	No catalyst	0
13	No light	0
14	No TrocCl	0[a]
15	No $NaHCO_3$	45
16	1 equiv TEMPO added	19

[a] <20% unprotected cycloaddition product observed.

Standard procedure for the analysis of conditions deviations: 5-Bromoindole (**2-10**, 0.100 mmol), $NaHCO_3$ (0.500 mmol), and $[Cr(PMP_2phen)_3](BF_4)_3$ (0.00100 mmol) were added to a flame-dried 1- dram borosilicate vial open to air. The reagents were suspended in nitromethane (0.500 mL), and then TrocCl (0.300 mmol) and vinyl diazoacetate **2-8** (0.300 mmol, 1.0 M solution in CH_2Cl_2) were added. The vial was then capped, and the reaction mixture was irradiated with a 23 W CFL bulb while stirring. After 8 h, second charges of vinyl diazoacetate **2-8** (0.200 mmol, 1.0 M solution in CH_2Cl_2) and $[Cr(PMP_2phen)_3](BF_4)_3$ (0.00100 mmol) were added, and the reaction mixture was irradiated for another 16 h. At the 24 h timepoint, the solvent was removed by rotary evaporation. The crude residue was then dissolved in CH_2Cl_2 (~1 mL), and the solution was passed through a SiO_2 plug (0.5 x 3 cm), using CH_2Cl_2 as eluent (~8 mL). The filtrate was

concentrated in vacuo, and the crude residue was analyzed by ^{1}H NMR using CH_2Br_2 as an internal standard.

Deviation:

Entries 2-4: Instead of $NaHCO_3$, the listed base (0.500 mmol) was added. $KHCO_3$ and NaH_2PO_4 were added with the other solids, while Et_3N was added after suspension in nitromethane.

Entry 5: Instead of 0.500 mL nitromethane, the initially added reagents were suspended in 0.500 mL CH_2Cl_2.

Entries 6 and 7: Instead of irradiation with the 23 W CFL bulb, the reaction mixture was irradiated with either blue LEDs or NUV, as described in the Materials and Methods section.

Entry 8: Instead of 0.500 mmol vinyl diazoacetate **2-8**, 0.200 mmol vinyl diazoacetate **2-8** was added in two charges (0.100 mmol + 0.100 mmol) at the 0 and 8 h timepoints.

Entry 9: The experiment was set up under Ar via manifold. After all reagents were added, the vial was capped and sealed with electrical tape. The mixture was placed under Ar for the second charges of vinyldiazo **2-8** and catalyst.

Entry 10: After adding the solid reagents, the vial was quickly evacuated and backfilled three times with O_2 via balloon and kept under the O_2 atmosphere for the addition of the liquid reagents. After all reagents were added, the vial was capped and sealed with electrical tape. The mixture was placed under O_2 for the second charges of vinyldiazo **2-8** and catalyst.

Entry 11: Only 0.000500 mmol $[Cr(PMP_2phen)_3](BF_4)_3$ was added at the beginning, with no second charge added.

Entry 12: No $[Cr(PMP_2phen)_3](BF_4)_3$ was added at either timepoint.

Entry 13: Instead of irradiation, the reaction mixture was placed in a sealed box and stirred.

Entries 14 and 15: TrocCl or $NaHCO_3$ were not added.

Entry 16: 0.100 mmol of TEMPO (15.6 mg) was added with all other solid reagents.

Table 2.12.6. Acylating agent evaluation for 2,3-disubstituted indole substrates.

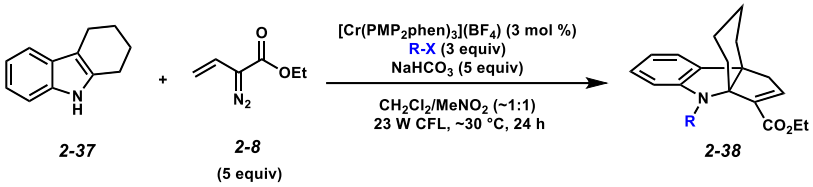

Entry	R-X	$NaHCO_3$ (Y/N)	yield (%)
1	TrocCl	Y	0
2	TsCl	Y	0
3[a]	BzCl	Y	0
4	(*p*-NO_2)BzCl	Y	40
5	(*p*-NO_2)BzCl	N	0
6	(3,5-(NO_2)$_2$)BzCl	Y	55
7	(3,5-(NO_2)$_2$)BzCl	N	0
8	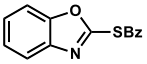	Y	0
9	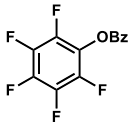	Y	0
10	TFAA	Y	0
11	Boc_2O	Y	0
12	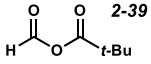 *2-39*	Y	30
13	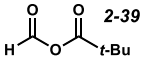 *2-39*	N	86

[a] < 20% yield of unprotected product was detected.

General Procedure for acylating agent optimization with 2,3-disubstituted indole substrates: Indole **2-37** (0.0600 mmol), $NaHCO_3$ (0.300 mmol, if added), and $[Cr(PMP_2phen)_3](BF_4)_3$ (0.000900 mmol) were added to a flame-dried 1-dram borosilicate vial open to air. The reagents were suspended in nitromethane (0.300 mL), and then acylating agent/electrophile (0.180 mmol) and vinyl diazoacetate reagent **2-8** (0.180 mmol, 1.0 M solution in CH_2Cl_2) were added. The vial was then capped, and the reaction mixture was irradiated with a 23 W CFL bulb while stirring.

After 8 h, second charges of vinyl diazoacetate **2-8** (0.120 mmol, 1.0 M solution in CH_2Cl_2) and $[Cr(PMP_2phen)_3](BF_4)_3$ (0.000900 mmol) were added, and the reaction mixture was irradiated for another 16 h. At the 24 h timepoint, the solvent was removed by rotary evaporation. The crude residue was then dissolved in CH_2Cl_2 (~1 mL), and the solution was passed through a SiO_2 plug (0.5 x 3 cm), using CH_2Cl_2 as eluent (~8 mL). The filtrate was concentrated in vacuo, and the crude residue was analyzed by ^1H NMR using CH_2Br_2 as an internal standard.

2.12.4. Photocatalyzed Cycloaddition Reactions

General Procedure A:

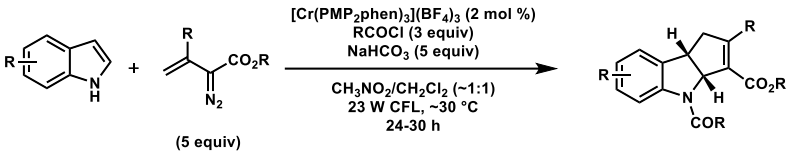

Indole (1.0 equiv), $NaHCO_3$ (5.0 equiv), and $[Cr(PMP_2phen)_3](BF_4)_3$ (1.0 mol %) were added to a flame-dried 1-dram borosilicate vial open to air. The reagents were suspended in CH_3NO_2 (0.20 M), and to this suspension were added acylating agent (3.0 equiv) and vinyl diazoacetate reagent (3.0 equiv, 1.0 M solution in CH_2Cl_2). The vial was then capped, and the reaction mixture was irradiated with a 23 W CFL bulb while stirring. After 8 h, second charges of vinyl diazoacetate reagent (2.0 equiv, 1.0 M solution in CH_2Cl_2) and $[Cr(PMP_2phen)_3](BF_4)_3$ (1.0 mol %) were added, and irradiation was continued. Reaction progress was monitored by TLC. When determined complete, the solvent was removed by rotary evaporation. The crude residue was then dissolved in CH_2Cl_2 (~1 mL), and the solution was passed through a SiO_2 plug (0.5 x 3 cm), using CH_2Cl_2 as eluent (~8 mL). The filtrate was concentrated in vacuo, and the crude residue was purified by silica gel flash chromatography to afford pure indoline product.

General Procedure B:

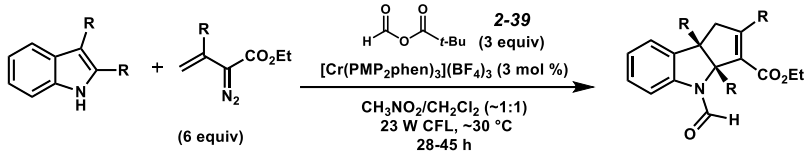

In a flame-dried 1-dram borosilicate vial open to air, trimethylacetic formic anhydride (**2-39**, 3.0 equiv) was dissolved in CH_3NO_2 (0.20 M). To this solution were added indole (1.0 equiv), $[Cr(PMP_2phen)_3](BF_4)_3$ (1.0 mol %), and vinyl diazoacetate reagent (3.0 equiv, 1.0 M solution in CH_2Cl_2). The vial was then capped, and the reaction mixture was irradiated with a 23 W CFL bulb while stirring. After 8 h, second charges of vinyl diazoacetate reagent (2.0 equiv) and $[Cr(PMP_2phen)_3](BF_4)_3$ (1.0 mol %) were added, and irradiation was continued. At the 24 h timepoint, third charges of vinyl diazoacetate reagent (1.0 equiv) and $[Cr(PMP_2phen)_3](BF_4)_3$ (1.0 mol %) were added, and irradiation was continued. Reaction progress was monitored by TLC. When determined complete, the solvent was removed by rotary evaporation. The crude residue was then dissolved in CH_2Cl_2 (~1 mL), and the solution was passed through a SiO_2 plug (0.5 x 3 cm), using CH_2Cl_2 as eluent (~8 mL). The filtrate was concentrated in vacuo, and the crude residue was purified by silica gel flash chromatography to afford pure indoline product.

Note about characterization: Several compounds, particularly the Troc-protected indolines, required high temperature NMR for ^{13}C characterization due to rotameric complications. Even with this extra measure, 1-2 carbons were not detected in some cases.

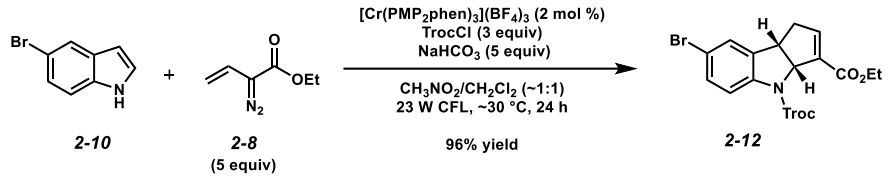

Indoline 2-12. According to General Procedure A, 5-bromoindole (**2-10**, 29.0 mg, 0.148 mmol), $NaHCO_3$ (62.1 mg, 0.740 mmol), and $[Cr(PMP_2phen)_3](BF_4)_3$ (2.2 mg, 0.00148 mmol) were added to a flame-dried 1-dram borosilicate vial. The reagents were suspended in CH_3NO_2 (0.74 mL), and to this suspension were added 2,2,2-trichloroethoxycarbonyl chloride (61.1 µL, 0.444 mmol) and vinyl diazoacetate **2-8** (0.444 mL, 1.0 M in CH_2Cl_2, 0.444 mmol). The reaction mixture was irradiated with a 23 W CFL bulb while stirring. After 8 h, second charges of vinyl diazoacetate **2-8** (0.296 mL, 1.0 M in CH_2Cl_2, 0.296 mmol) and $[Cr(PMP_2phen)_3](BF_4)_3$ (2.2 mg, 0.00148 mmol) were added, and irradiation was continued. At the 24 h timepoint, the solvent was removed via rotary evaporation. The crude residue was dissolved in CH_2Cl_2 (~1 mL), and the solution was passed through a SiO_2 plug (0.5 x 3 cm), using CH_2Cl_2 as eluent (~8 mL). The filtrate was concentrated in vacuo, and the residue was purified by silica gel flash chromatography (2:1 hexanes/Et_2O eluent) to afford indoline **2-12** (68.7 mg, 96% yield) as a white solid.

TLC R_f: 0.50 in 1:1 hexanes/Et_2O, visualized by UV, stained blue in Hanessian's stain.

^{1}H NMR (400 MHz, $CDCl_3$): δ 7.72-7.48 (br. m, 1H), 7.33 (d, *J* = 8.4 Hz, 1H), 7.30 (s, 1H), 6.86 (app. s, 1H), 5.87 (app. d, *J* = 6.7 Hz, 1H), 5.35-4.50 (br. m, 2H), 4.25-4.08 (comp. m, 3H), 3.03 (app. ddt, *J* = 18.4, 7.7, 2.0 Hz, 1H), 2.75 (app. d, *J* = 18.4 Hz, 1H), 1.26 (t, *J* = 7.2 Hz).

^{13}C NMR (125 MHz, 50 °C, $CDCl_3$): δ 163.7, 151.7, 144.6, 140.0, 137.7, 135.1, 131.5, 127.5, 118.6, 116.7, 95.4, 75.8, 69.2, 60.6, 43.8, 37.7, 14.3.

IR (ATR, neat): 2980, 1720, 1630, 1478, 1102, 746 cm^{-1}.

HRMS (ESI+): *m/z* calc'd for $(M + H)^+$ $[C_{17}H_{15}BrCl_3NO_4 + H]^+$: 481.9323 found 481.9313.

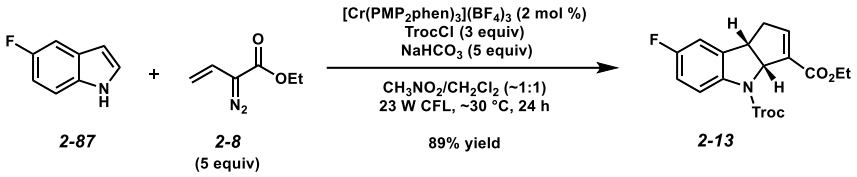

Indoline 2-13. According to General Procedure A, 5-fluoroindole (**2-87**, 27.5 mg, 0.203 mmol), $NaHCO_3$ (85.5 mg, 1.02 mmol), and $[Cr(PMP_2phen)_3](BF_4)_3$ (3.0 mg, 0.00203 mmol) were added to a flame-dried 1-dram borosilicate vial. The reagents were suspended in CH_3NO_2 (1.02 mL), and to this suspension were added 2,2,2-trichloroethoxycarbonyl chloride (84.0 µL, 0.610 mmol) and vinyl diazoacetate **2-8** (0.610 mL, 1.0 M in CH_2Cl_2, 0.610 mmol). The reaction mixture was irradiated with a 23 W CFL bulb while stirring. After 8 h, second charges of vinyl diazoacetate **2-8** (0.406 mL, 1.0 M in CH_2Cl_2, 0.406 mmol) and $[Cr(PMP_2phen)_3](BF_4)_3$ (3.0 mg, 0.00203 mmol) were added, and irradiation was continued. At the 24 h timepoint, the solvent was removed via rotary evaporation. The crude residue was dissolved in CH_2Cl_2 (~1 mL), and the solution was passed through a SiO_2 plug (0.5 x 3 cm), using CH_2Cl_2 as eluent (~8 mL). The filtrate was concentrated in vacuo, and the residue was purified by silica gel flash chromatography (4:1 hexanes/Et_2O eluent) to afford indoline **2-13** (76.5 mg, 89% yield) as a white solid.

TLC R_f: 0.43 in 1:1 hexanes/Et_2O, visualized by UV, stained blue in Hanessian's stain.

^{1}H NMR (400 MHz, $CDCl_3$): δ 7.80-7.50 (br. m, 1H), 6.96-6.82 (comp. m, 3H), 5.90 (app. d, *J* = 6.6 Hz, 1H), 5.30-4.50 (br. m, 2H), 4.26-4.05 (comp. m, 3H), 3.03 (app. ddt, *J* = 18.4, 7.8, 2.0 Hz, 1H), 2.74 (app. d, *J* = 18.4 Hz, 1H), 1.26 (t, *J* = 7.2 Hz, 3H).

^{13}C NMR (125 MHz, 50 °C, $CDCl_3$): δ 163.7, 160.9, 159.0, 151.8, 144.5, 136.7, 136.3 (d, *J* = 268 Hz), 135.2, 118.1, 114.9 (d, *J* = 23.0 Hz), 111.4 (d, *J* = 23.9 Hz), 95.5, 75.7, 69.3, 60.6, 43.9, 37.7, 14.3.

^{19}F NMR (376 MHz, $CDCl_3$): δ -119.0.

IR (ATR, neat): 2981, 1720, 1630, 1487, 1103, 747 cm^{-1}.

HRMS (ESI+): *m/z* calc'd for $(M + H)^+$ $[C_{17}H_{15}Cl_3FNO_4 + H]^+$: 422.0123, found 422.0113.

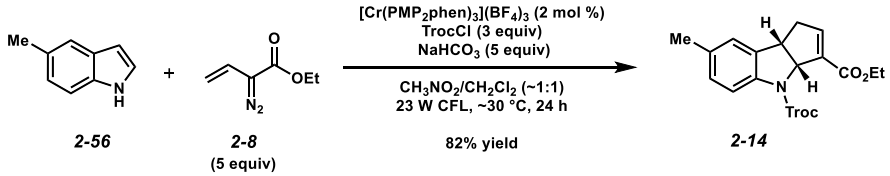

2-56 *2-8* (5 equiv) *2-14*

Indoline 2-14. According to General Procedure A, 5-methylindole (**2-56**, 25.0 mg, 0.191 mmol), $NaHCO_3$ (80.0 mg, 0.953 mmol), and $[Cr(PMP_2phen)_3](BF_4)_3$ (2.8 mg, 0.00191 mmol) were added to a flame-dried 1-dram borosilicate vial. The reagents were suspended in CH_3NO_2 (0.953 mL), and to this suspension were added 2,2,2-trichloroethoxycarbonyl chloride (78.9 μL, 0.573 mmol) and vinyl diazoacetate **2-8** (0.573 mL, 1.0 M in CH_2Cl_2, 0.573 mmol). The reaction mixture was irradiated with a 23 W CFL bulb while stirring. After 8 h, second charges of vinyl diazoacetate **2-8** (0.381 mL, 1.0 M in CH_2Cl_2, 0.381 mmol) and $[Cr(PMP_2phen)_3](BF_4)_3$ (2.8 mg, 0.00191 mmol) were added, and irradiation was continued. At the 24 h timepoint, the solvent was removed via rotary evaporation. The crude residue was dissolved in CH_2Cl_2 (~1 mL), and the solution was passed through a SiO_2 plug (0.5 x 3 cm), using CH_2Cl_2 as eluent (~8 mL). The filtrate was concentrated in vacuo, and the residue was purified by silica gel flash chromatography (4:1 hexanes/Et_2O eluent) to afford indoline **2-14** (65.4 mg, 82% yield) as a white solid.

TLC R_f: 0.46 in 1:1 hexanes/Et_2O, visualized by UV, stained blue in Hanessian's stain.

^{1}H NMR (400 MHz, $CDCl_3$): δ 7.75-7.50 (br. m, 1H), 7.05 (d, *J* = 8.2 Hz, 1H), 7.00 (s, 1H), 6.85 (app. s, 1H), 5.87 (app. d, *J* = 6.0 Hz, 1H), 5.30-4.50 (comp. m, 2H), 4.23-4.10 (comp. m, 2H), 4.09 (app. t, *J* = 7.2 Hz, 1H), 3.00 (app. ddt, *J* = 18.4, 7.8, 2.0 Hz, 1H), 2.77 (app. d, *J* = 18.4 Hz, 1H), 2.31 (s, 3H), 1.26 (t, *J* = 7.1 Hz, 3H).

^{13}C NMR (125 MHz, 50 °C, $CDCl_3$): δ 164.0, 151.9, 144.7, 138.4, 135.3, 133.8, 129.0, 124.8, 117.0, 95.6, 75.7, 69.0, 60.5, 43.9, 37.8, 21.1, 14.3 (*1 carbon not detected*).

IR (ATR, neat): 2980, 1720, 1626, 1491, 1102, 817 cm^{-1}.

HRMS (ESI+): *m/z* calc'd for $(M + H)^+$ $[C_{18}H_{18}Cl_3NO_4 + H]^+$: 418.0374, found 418.0362.

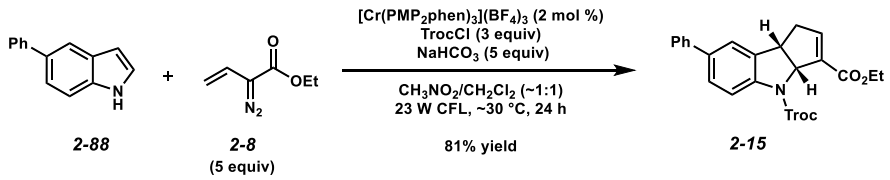

Indoline 2-15. According to General Procedure A, 5-phenylindole (**2-88**, 28.0 mg, 0.145 mmol), $NaHCO_3$ (60.8 mg, 0.724 mmol), and $[Cr(PMP_2phen)_3](BF_4)_3$ (2.2 mg, 0.00145 mmol) were added to a flame-dried 1-dram borosilicate vial. The reagents were suspended in CH_3NO_2 (0.725 mL), and to this suspension were added 2,2,2-trichloroethoxycarbonyl chloride (59.8 µL, 0.435 mmol) and vinyl diazoacetate **2-8** (0.435 mL, 1.0 M in CH_2Cl_2, 0.435 mmol). The reaction mixture was irradiated with a 23 W CFL bulb while stirring. After 8 h, second charges of vinyl diazoacetate **2-8** (0.290 mL, 1.0 M in CH_2Cl_2, 0.290 mmol) and $[Cr(PMP_2phen)_3](BF_4)_3$ (2.2 mg, 0.00145 mmol) were added, and irradiation was continued. At the 24 h timepoint, the solvent was removed via rotary evaporation. The crude residue was dissolved in CH_2Cl_2 (~1 mL), and the solution was

passed through a SiO_2 plug (0.5 x 3 cm), using CH_2Cl_2 as eluent (~8 mL). The filtrate was concentrated in vacuo, and the residue was purified by silica gel flash chromatography (4:1 hexanes/Et_2O eluent) to afford indoline **2-15** (56.4 mg, 81% yield) as a white solid.

TLC R_f: 0.43 in 1:1 hexanes/Et_2O, visualized by UV, stained blue in Hanessian's stain.

^{1}H NMR (400 MHz, $CDCl_3$): δ 7.93-7.67 (br. m, 1H), 7.55 (d, *J* = 7.2 Hz, 2H), 7.49 (d, *J* = 8.4 Hz, 1H), 7.44-7.41 (comp. m, 3H), 7.33 (t, *J* = 7.3 Hz, 1H), 6.90 (app. s, 1H), 5.94 (app. d, *J* = 6.2 Hz, 1H), 5.40-4.47 (br. m, 2H), 4.26-4.13 (comp m, 3H), 3.07 (app. ddt, *J* = 18.4, 7.7, 1.9 Hz, 1H), 2.86 (app. d, *J* = 18.4 Hz, 1H), 1.28 (t, *J* = 7.1 Hz, 3H).

^{13}C NMR (125 MHz, 50 °C, $CDCl_3$): δ 163.9, 151.9, 144.8, 141.0, 140.1, 137.7, 136.0, 135.3, 128.9, 127.6, 127.2, 127.1, 123.0, 117.4, 95.6, 75.8, 69.2, 60.6, 44.0, 37.9, 14.4.

IR (ATR, neat): 2980, 1720, 1628, 1102, 833 cm^{-1}.

HRMS (ESI+): *m/z* calc'd for $(M + H)^+$ $[C_{23}H_{20}Cl_3NO_4 + H]^+$: 480.0531, found 480.0520.

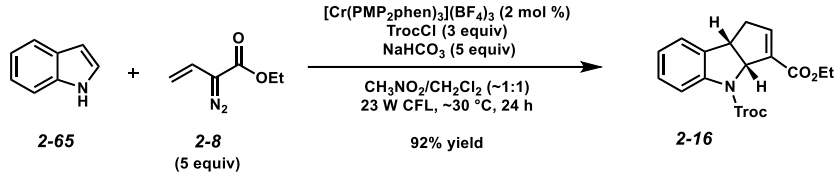

Indoline 2-16. According to General Procedure A, indole (**2-65**, 25.0 mg, 0.213 mmol), $NaHCO_3$ (89.5 mg, 1.07 mmol), and $[Cr(PMP_2phen)_3](BF_4)_3$ (3.2 mg, 0.00213 mmol) were added to a flame-dried 1-dram borosilicate vial. The reagents were suspended in CH_3NO_2 (1.07 mL), and to this suspension were added 2,2,2-trichloroethoxycarbonyl chloride (88.1 µL, 0.640 mmol) and vinyl diazoacetate **2-8** (0.640 mL, 1.0 M in CH_2Cl_2, 0.640 mmol). The reaction mixture was irradiated with a 23 W CFL bulb while stirring. After 8 h, second charges of vinyl diazoacetate **2-**

8 (0.426 mL, 1.0 M in CH_2Cl_2, 0.426 mmol) and $[Cr(PMP_2phen)_3](BF_4)_3$ (3.2 mg, 0.00213 mmol) were added, and irradiation was continued. At the 24 h timepoint, the solvent was removed via rotary evaporation. The crude residue was dissolved in CH_2Cl_2 (~1 mL), and the solution was passed through a SiO_2 plug (0.5 x 3 cm), using CH_2Cl_2 as eluent (~8 mL). The filtrate was concentrated in vacuo, and the residue was purified by silica gel flash chromatography (4:1 hexanes/Et_2O eluent) to afford indoline **2-16** (79.4 mg, 92% yield) as a white solid.

TLC R_f: 0.50 in 1:1 hexanes/Et_2O, visualized by UV, stained blue in Hanessian's stain.

^{1}H NMR (400 MHz, $CDCl_3$): δ 7.90-7.60 (br. m, 1H), 7.24 (app. t, *J* = 7.8 Hz, 1H), 7.19 (d, *J* = 7.5 Hz, 1H), 7.07 (app. t, *J* = 7.4 Hz, 1H), 6.86 (app. s, 1H), 5.89 (app. d, *J* = 6.1 Hz, 1H), 5.40-4.50 (br. m, 2H), 4.24-4.11 (comp. m, 3H), 3.03 (app. ddt, *J* = 18.4, 7.7, 2.0 Hz, 1H), 2.79 (app. d, *J* = 18.4 Hz, 1H), 1.26 (t, *J* = 7.1 Hz, 3H).

^{13}C NMR (125 MHz, 50 °C, $CDCl_3$): δ 163.9, 151.8, 144.7, 140.7, 135.3, 128.5, 124.2, 117.2, 95.6, 75.7, 68.9, 60.5, 43.9, 37.8, 14.3 (*2 carbons not detected*).

IR (ATR, neat): 2981, 1723, 1628, 1198, 755 cm^{-1}.

HRMS (ESI+): *m/z* calc'd for $(M + H)^+$ $[C_{17}H_{16}Cl_3NO_4 + H]^+$: 404.0218, found 404.0199.

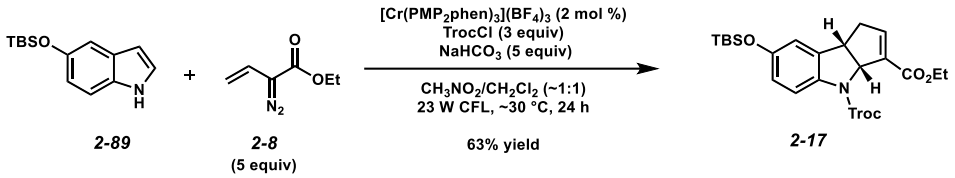

Indoline 2-17. According to General Procedure A, 5-(*tert*-butyl-dimethyl-silanyloxy)-1*H*-indole (**2-89**, 31.3 mg, 0.127 mmol), $NaHCO_3$ (53.1 mg, 0.633 mmol), and $[Cr(PMP_2phen)_3](BF_4)_3$ (1.9 mg, 0.00127 mmol) were added to a flame-dried 1-dram borosilicate vial. The reagents were suspended in CH_3NO_2 (0.633 mL), and to this suspension were added 2,2,2-trichloroethoxycarbonyl chloride (52.2 µL, 0.380 mmol) and vinyl diazoacetate **2-8** (0.380 mL, 1.0 M in CH_2Cl_2, 0.380 mmol). The reaction mixture was irradiated with a 23 W CFL bulb while stirring. After 8 h, second charges of vinyl diazoacetate **2-8** (0.253 mL, 1.0 M in CH_2Cl_2, 0.253 mmol) and $[Cr(PMP_2phen)_3](BF_4)_3$ (1.9 mg, 0.00127 mmol) were added, and irradiation was continued. At the 24 h timepoint, the solvent was removed via rotary evaporation. The crude residue was dissolved in CH_2Cl_2 (~1 mL), and the solution was passed through a SiO_2 plug (0.5 x 3 cm), using CH_2Cl_2 as eluent (~8 mL). The filtrate was concentrated in vacuo, and the residue was purified by silica gel flash chromatography (9:1 → 4:1 hexanes/Et_2O eluent) to afford indoline **2-17** (42.6 mg, 63% yield) as a yellow solid.

TLC R_f: 0.64 in 2:1 hexanes/Et_2O, visualized by UV, stained blue in Hanessian's stain.

^{1}H NMR (400 MHz, $CDCl_3$): δ 7.70-7.40 (br. m, 1H), 6.84 (s, 1H), 6.69 (d, *J* = 8.6 Hz, 1H), 6.65 (app. s, 1H), 5.87 (app. d, *J* = 6.3 Hz, 1H), 5.35-4.45 (br. m, 2H), 4.24-4.12 (comp. m, 2H), 4.07 (app. t, *J* = 7.3 Hz, 1H), 2.99 (app. dd, *J* = 18.4, 6.1 Hz, 1H), 2.72 (app. d, *J* = 18.4 Hz, 1H), 1.26 (t, *J* = 7.2 Hz, 3H), 0.97 (s, 9H), 0.17 (s, 6H).

^{13}C NMR (125 MHz, 50 °C, $CDCl_3$): δ 164.0, 152.7, 151.9, 144.6, 136.7, 135.4, 134.6, 119.6, 117.9, 115.9, 95.7, 75.7, 69.2, 60.6, 43.9, 37.9, 25.9, 18.3, 14.4, -4.26, -4.28.

IR (ATR, neat): 2955, 2929, 1721, 1635, 1266, 839 cm^{-1}.

HRMS (ESI+): *m/z* calc'd for $(M + H)^+$ $[C_{23}H_{30}Cl_3NO_5Si + H]^+$: 534.1032, found 534.1019.

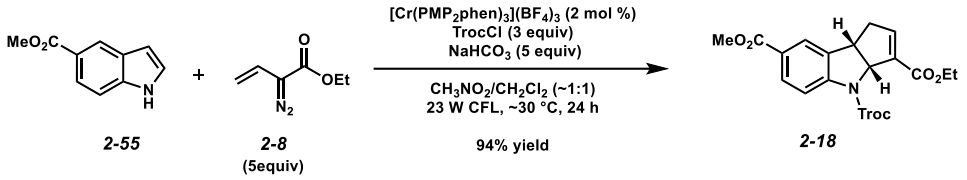

Indoline 2-18. According to General Procedure A, methyl 1*H*-indole-5-carboxylate (**2-55**, 28.0 mg, 0.160 mmol), $NaHCO_3$ (67.1 mg, 0.799 mmol), and $[Cr(PMP_2phen)_3](BF_4)_3$ (2.4 mg, 0.00160 mmol) were added to a flame-dried 1-dram borosilicate vial. The reagents were suspended in CH_3NO_2 (0.800 mL), and to this suspension were added 2,2,2-trichloroethoxycarbonyl chloride (66.0 µL, 0.479 mmol) and vinyl diazoacetate **2-8** (0.479 mL, 1.0 M in CH_2Cl_2, 0.479 mmol). The reaction mixture was irradiated with a 23 W CFL bulb while stirring. After 8 h, second charges of vinyl diazoacetate **2-8** (0.320 mL, 1.0 M in CH_2Cl_2, 0.320 mmol) and $[Cr(PMP_2phen)_3](BF_4)_3$ (2.4 mg, 0.00160 mmol) were added, and irradiation was continued. At the 24 h timepoint, the solvent was removed via rotary evaporation. The crude residue was dissolved in CH_2Cl_2 (~1 mL), and the solution was passed through a SiO_2 plug (0.5 x 3 cm), using CH_2Cl_2 as eluent (~8 mL). The filtrate was concentrated in vacuo, and the residue was purified by silica gel flash chromatography (4:1 hexanes/Et_2O eluent) to afford indoline **2-18** (69.4 mg, 94% yield) as a white solid. (73.8 mg total mass was isolated. This included 4.4 mg Troc-protected pyrazole **2-127**, which was chromatographically inseparable from the product.)

TLC R_f: 0.40 in 2:1 hexanes/Et_2O, visualized by UV, stained blue in Hanessian's stain.

^{1}H NMR (400 MHz, $CDCl_3$): δ 7.95 (d, *J* = 8.5 Hz, 1H), 7.87 (s, 1H), 7.78 (br. s, 1H), 6.86 (app. s, 1H), 5.92 (d, *J* = 6.0 Hz, 1H), 5.20-4.60 (br. m, 2H), 4.20-4.10 (comp. m, 3H), 3.88 (s, 3H), 3.04 (app. dd, *J* = 18.5, 6.2 Hz, 1H), 2.84 (app. d, *J* = 18.5 Hz, 1H), 1.25 (t, *J* = 7.2 Hz, 1H).

^{13}C NMR (125 MHz, 50 °C, $CDCl_3$): δ 166.7, 163.8, 151.7, 144.9, 135.6, 135.0, 132.6, 130.9, 126.1, 125.9, 116.5, 95.3, 75.9, 69.5, 60.7, 52.1, 43.6, 37.8, 14.3.

IR (ATR, neat): 2982, 1717, 1610, 1276, 1187 cm^{-1}.

HRMS (ESI+): *m/z* calc'd for $(M + H)^+$ $[C_{19}H_{18}Cl_3NO_6 + H]^+$: 462.0272, found 462.0257.

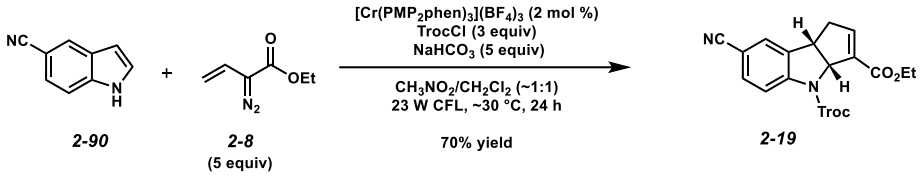

Indoline 2-19. According to General Procedure A, 5-cyanoindole (**2-90**, 29.2 mg, 0.205 mmol), $NaHCO_3$ (86.3 mg, 1.03 mmol), and $[Cr(PMP_2phen)_3](BF_4)_3$ (3.1 mg, 0.00205 mmol) were added to a flame-dried 1-dram borosilicate vial. The reagents were suspended in CH_3NO_2 (1.03 mL), and to this suspension were added 2,2,2-trichloroethoxycarbonyl chloride (84.8 µL, 0.616 mmol) and vinyl diazoacetate **2-8** (0.616 mL, 1.0 M in CH_2Cl_2, 0.616 mmol). The reaction mixture was irradiated with a 23 W CFL bulb while stirring. After 8 h, second charges of vinyl diazoacetate **2-8** (0.411 mL, 1.0 M in CH_2Cl_2, 0.411 mmol) and $[Cr(PMP_2phen)_3](BF_4)_3$ (3.1 mg, 0.00205 mmol) were added, and irradiation was continued. At the 24 h timepoint, the solvent was removed via rotary evaporation. The crude residue was dissolved in CH_2Cl_2 (~1 mL), and the solution was

passed through a SiO_2 plug (0.5 x 3 cm), using CH_2Cl_2 as eluent (~8 mL). The filtrate was concentrated in vacuo, and the residue was purified by silica gel flash chromatography (2:1 hexanes/Et_2O eluent) to afford indoline **2-19** (61.7 mg, 70% yield) as a yellow oil.

TLC R_f: 0.32 in 2:1 hexanes/Et_2O, visualized by UV, stained blue in Hanessian's stain.

^{1}H NMR (400 MHz, $CDCl_3$): δ 7.88-7.78 (br. m, 1H), 7.55 (d, *J* = 8.4 Hz, 1H), 7.46 (s, 1H), 6.87 (app. s, 1H), 5.92 (d, *J* = 6.0 Hz, 1H), 5.20-4.60 (br. m, 2H), 4.23-4.11 (comp. m, 3H), 3.08 (app. dd, *J* = 18.3, 6.2 Hz, 1H), 2.78 (app. d, *J* = 18.3 Hz, 1H), 1.26 (t, *J* = 7.2 Hz, 1H).

^{13}C NMR (125 MHz, 50 °C, $CDCl_3$): δ 163.6, 151.4, 144.7, 136.6, 134.8, 133.4, 128.1, 119.0, 117.3, 107.4, 95.2, 75.9, 69.3, 60.8, 43.6, 37.7, 14.3 (*1 carbon not detected*).

IR (ATR, neat): 2982, 2224, 1720, 1628, 1484, 832 cm^{-1}.

HRMS (ESI+): *m/z* calc'd for $(M + H)^+$ $[C_{18}H_{15}Cl_3N_2O_4 + H]^+$: 429.0170, found 429.0160.

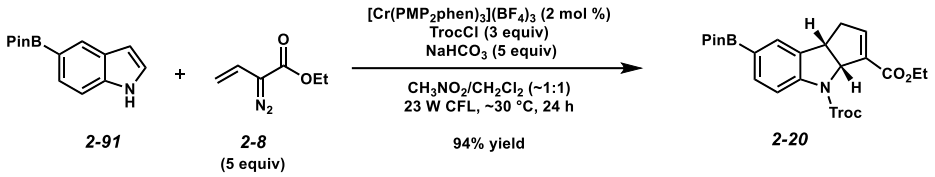

Indoline 2-20. According to General Procedure A, indole **2-91** (30.2 mg, 0.124 mmol), $NaHCO_3$ (52.2 mg, 0.621 mmol), and $[Cr(PMP_2phen)_3](BF_4)_3$ (1.9 mg, 0.00124 mmol) were added to a flame-dried 1-dram borosilicate vial. The reagents were suspended in CH_3NO_2 (0.621 mL), and to this suspension were added 2,2,2-trichloroethoxycarbonyl chloride (51.3 µL, 0.373 mmol) and vinyl diazoacetate **2-8** (0.373 mL, 1.0 M in CH_2Cl_2, 0.373 mmol). The reaction mixture was irradiated with a 23 W CFL bulb while stirring. After 8 h, second charges of vinyl diazoacetate **2-8** (0.248 mL, 1.0 M in CH_2Cl_2, 0.248 mmol) and $[Cr(PMP_2phen)_3](BF_4)_3$ (1.9 mg, 0.00124 mmol) were added, and irradiation was continued. At the 24 h timepoint, the solvent was removed via rotary evaporation. The crude residue was dissolved in CH_2Cl_2 (~1 mL), and the solution was passed through a SiO_2 plug (0.5 x 3 cm), using CH_2Cl_2 as eluent (~8 mL). The filtrate was concentrated in vacuo, and the residue was purified by silica gel flash chromatography (4:1 hexanes/Et_2O eluent) to afford indoline **2-20** (62.0 mg, 94% yield) as a white solid.

TLC R_f: 0.48 in 2:1 hexanes/Et_2O, visualized by UV, stained blue in Hanessian's stain.

^{1}H NMR (400 MHz, $CDCl_3$): δ 7.80-7.71 (comp. m, 2H), 7.64 (s, 1H), 6.84 (app. s, 1H), 5.88 (app. d, *J* = 6.0 Hz, 1H), 5.30-4.50 (br. m, 2H), 4.23-4.09 (comp. m, 3H), 3.01 (app. ddt, *J* = 18.4, 6.1, 2.0 Hz, 1H), 2.87 (app. d, *J* = 18.4 Hz, 1H), 1.33 (s, 6H), 1.32 (s, 6H), 1.25 (t, *J* = 7.1 Hz, 1H).

^{13}C NMR (125 MHz, 50 °C, $CDCl_3$): δ 164.0, 151.8, 145.0, 143.3, 135.8, 135.2, 134.7, 130.6, 124.7 (br, *C*-BPin), 116.5, 95.5, 83.9, 75.8, 69.1, 60.5, 43.7, 37.8, 25.1, 25.0, 14.4.

IR (ATR, neat): 2978, 1724, 1607, 1433, 856 cm^{-1}.

HRMS (ESI+): *m/z* calc'd for $(M + H)^+$ $[C_{23}H_{27}BCl_3NO_6 + H]^+$: 530.1070, found 530.1071.

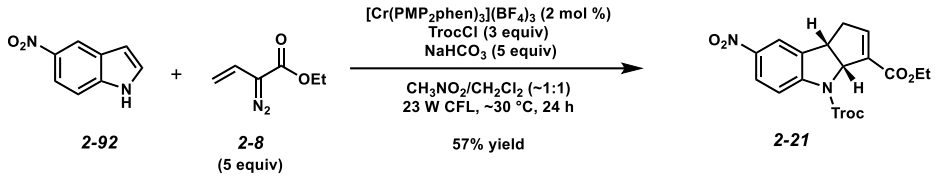

Indoline 2-21. According to General Procedure A, 5-nitroindole (**2-92**, 22.5 mg, 0.139 mmol), $NaHCO_3$ (58.3 mg, 0.694 mmol), and $[Cr(PMP_2phen)_3](BF_4)_3$ (2.1 mg, 0.00139 mmol) were added to a flame-dried 1-dram borosilicate vial. The reagents were suspended in CH_3NO_2 (0.694 mL), and to this suspension were added 2,2,2-trichloroethoxycarbonyl chloride (57.3 µL, 0.416 mmol) and vinyl diazoacetate **2-8** (0.416 mL, 1.0 M in CH_2Cl_2, 0.416 mmol). The reaction mixture was irradiated with a 23 W CFL bulb while stirring. After 8 h, second charges of vinyl diazoacetate **2-8** (0.278 mL, 1.0 M in CH_2Cl_2, 0.278 mmol) and $[Cr(PMP_2phen)_3](BF_4)_3$ (2.1 mg, 0.00139 mmol) were added, and irradiation was continued. At the 24 h timepoint, the solvent was removed via rotary evaporation. The crude residue was dissolved in CH_2Cl_2 (~1 mL), and the solution was passed through a SiO_2 plug (0.5 x 3 cm), using CH_2Cl_2 as eluent (~8 mL). The filtrate was concentrated in vacuo, and the residue was purified by silica gel flash chromatography (9:1:1 hexanes/Et_2O/CH_2Cl_2 eluent) to afford indoline **2-21** (35.6 mg, 57% yield) as a white solid.

TLC R_f: 0.42 in 1:1 hexanes/Et_2O, visualized by UV, stained blue in Hanessian's stain.

^{1}H NMR (400 MHz, $CDCl_3$): δ 8.18 (d, *J* = 8.7 Hz, 1H), 8.07 (s, 1H), 7.94-7.82 (br. m, 1H), 6.90 (app. s, 1H), 5.97 (d, *J* = 7.0 Hz, 1H), 5.20-4.60 (br. m, 2H), 4.27-4.13 (comp. m, 3H), 3.12 (app. dd, *J* = 18.5, 7.6 Hz, 1H), 2.87 (app. d, *J* = 18.5 Hz, 1H), 1.27 (t, *J* = 7.1 Hz, 1H).

^{13}C NMR (125 MHz, 50 °C, $CDCl_3$): δ 163.6, 151.5, 144.8, 144.5, 136.7, 134.8, 125.4, 120.3, 116.5, 95.1, 76.0, 69.9, 60.8, 43.6, 37.7, 14.4 (*1 carbon not detected*).

IR (ATR, neat): 2925, 1720, 1518, 1479, 832 cm^{-1}.

HRMS (ESI+): *m/z* calc'd for $(M + H)^+$ $[C_{17}H_{15}Cl_3N_2O_6 + H]^+$: 449.0068, found 449.0062.

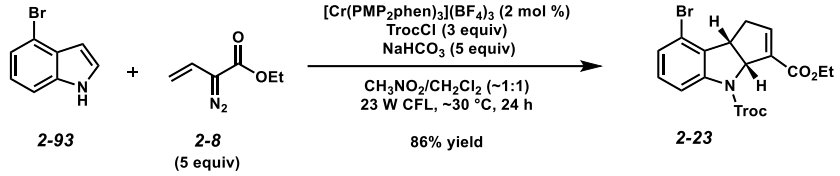

Indoline 2-23. According to General Procedure A, 4-bromoindole (**2-93**, 25.5 mg, 0.130 mmol), $NaHCO_3$ (54.6 mg, 0.650 mmol), and $[Cr(PMP_2phen)_3](BF_4)_3$ (2.0 mg, 0.00130 mmol) were added to a flame-dried 1-dram borosilicate vial. The reagents were suspended in CH_3NO_2 (0.650 mL), and to this suspension were added 2,2,2-trichloroethoxycarbonyl chloride (53.7 µL, 0.390 mmol) and vinyl diazoacetate **2-8** (0.390 mL, 1.0 M in CH_2Cl_2, 0.390 mmol). The reaction mixture was irradiated with a 23 W CFL bulb while stirring. After 8 h, second charges of vinyl diazoacetate **2-8** (0.260 mL, 1.0 M in CH_2Cl_2, 0.260 mmol) and $[Cr(PMP_2phen)_3](BF_4)_3$ (2.0 mg, 0.00130 mmol) were added, and irradiation was continued. At the 24 h timepoint, the solvent was removed via rotary evaporation. The crude residue was dissolved in CH_2Cl_2 (~1 mL), and the solution was passed through a SiO_2 plug (0.5 x 3 cm), using CH_2Cl_2 as eluent (~8 mL). The filtrate was concentrated in vacuo, and the residue was purified by silica gel flash chromatography (2:1 hexanes/Et_2O eluent) to afford indoline **2-23** (54.1 mg, 86% yield) as a white solid.

TLC R_f: 0.67 in 1:1 hexanes/Et_2O, visualized by UV, stained blue in Hanessian's stain.

^{1}H NMR (400 MHz, $CDCl_3$): δ 7.71 (br. d, *J* = 7.6 Hz, 1H), 7.19 (d, *J* = 8.0 Hz, 1H), 7.10 (app. t, *J* = 8.0 Hz, 1H), 6.84 (app. d, *J* = 1.5 Hz, 1H), 5.90 (dd, *J* = 8.3, 1.5 Hz, 1H), 5.23-4.60 (br. m, 2H), 4.31-4.10 (comp. m, 3H), 3.13 (app. d, *J* = 17.4 Hz, 1H), 3.04 (app. dd, *J* = 17.4, 8.0 Hz, 1H), 1.28 (t, *J* = 7.1 Hz, 3H).

^{13}C NMR (125 MHz, 50 °C, $CDCl_3$): δ 164.1, 151.8, 144.8, 142.5, 135.1, 134.3, 129.9, 127.6, 119.6, 116.0, 95.4, 75.8, 68.4, 60.6, 45.4, 37.5, 14.4.

IR (ATR, neat): 2980, 1723, 1633, 1453, 848 cm^{-1}.

HRMS (ESI+): *m/z* calc'd for $(M + Na)^+$ $[C_{17}H_{15}BrCl_3NO_4 + Na]^+$: 503.9142, found 503.9125.

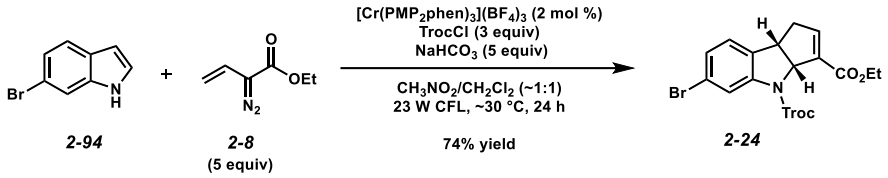

Indoline 2-24. According to General Procedure A, 6-bromoindole (**2-94**, 27.9 mg, 0.142 mmol), $NaHCO_3$ (59.8 mg, 0.712 mmol), and $[Cr(PMP_2phen)_3](BF_4)_3$ (2.1 mg, 0.00142 mmol) were added to a flame-dried 1-dram borosilicate vial. The reagents were suspended in CH_3NO_2 (0.712 mL), and to this suspension were added 2,2,2-trichloroethoxycarbonyl chloride (58.8 µL, 0.427 mmol) and vinyl diazoacetate **2-8** (0.427 mL, 1.0 M in CH_2Cl_2, 0.427 mmol). The reaction mixture was irradiated with a 23 W CFL bulb while stirring. After 8 h, second charges of vinyl diazoacetate **2-8** (0.285 mL, 1.0 M in CH_2Cl_2, 0.285 mmol) and $[Cr(PMP_2phen)_3](BF_4)_3$ (2.1 mg, 0.00142 mmol) were added, and irradiation was continued. At the 24 h timepoint, the solvent was removed via rotary evaporation. The crude residue was dissolved in CH_2Cl_2 (~1 mL), and the solution was passed through a SiO_2 plug (0.5 x 3 cm), using CH_2Cl_2 as eluent (~8 mL). The filtrate was

concentrated in vacuo, and the residue was purified by silica gel flash chromatography (2:1 hexanes/Et_2O eluent) to afford indoline **2-24** (50.9 mg, 74% yield) as a white solid.

TLC R_f: 0.40 in 1:1 hexanes/Et_2O, visualized by UV, stained blue in Hanessian's stain.

^{1}H NMR (400 MHz, $CDCl_3$): δ 8.05-7.83 (br. m, 1H), 7.18 (dd, *J* = 8.0, 1.7 Hz, 1H), 7.04 (d, *J* = 8.0 Hz, 1H), 6.85 (app. s, 1H), 5.88 (app. d, *J* = 6.3 Hz, 1H), 5.35-4.45 (br. m, 2H), 4.23-4.12 (comp. m, 2H), 4.06 (app. t, *J* = 7.5 Hz, 1H), 3.02 (app. ddt, *J* = 18.4, 6.2, 2.0 Hz, 1H), 2.74 (app. d, *J* = 18.4 Hz, 1H), 1.26 (t, *J* = 7.2 Hz, 1H).

^{13}C NMR (125 MHz, 50 °C, $CDCl_3$): δ 163.8, 151.6, 144.7, 142.1, 135.1, 134.4, 127.1, 125.3, 121.9, 120.5, 95.4, 75.8, 69.3, 60.7, 43.6, 37.7, 14.4.

IR (ATR, neat): 2981, 1720, 1630, 1479, 778 cm^{-1}.

HRMS (ESI+): *m/z* calc'd for $(M + H)^+$ $[C_{17}H_{15}BrCl_3NO_4 + H]^+$: 481.9323, found 481.9312.

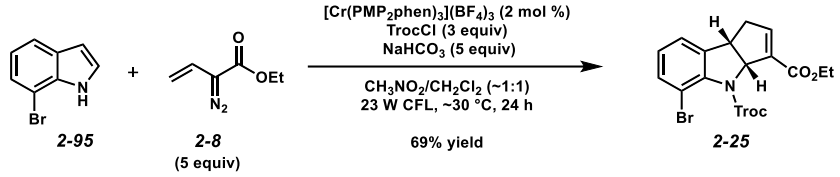

Indoline 2-25. According to General Procedure A, 7-bromoindole (**2-95**, 28.3 mg, 0.144 mmol), $NaHCO_3$ (60.6 mg, 0.722 mmol), and $[Cr(PMP_2phen)_3](BF_4)_3$ (2.2 mg, 0.00144 mmol) were added to a flame-dried 1-dram borosilicate vial. The reagents were suspended in CH_3NO_2 (0.722 mL), and to this suspension were added 2,2,2-trichloroethoxycarbonyl chloride (59.6 µL, 0.433 mmol) and vinyl diazoacetate **2-8** (0.433 mL, 1.0 M in CH_2Cl_2, 0.433 mmol). The reaction mixture was irradiated with a 23 W CFL bulb while stirring. After 8 h, second charges of vinyl diazoacetate **2-**

8 (0.288 mL, 1.0 M in CH_2Cl_2, 0.288 mmol) and $[Cr(PMP_2phen)_3](BF_4)_3$ (2.2 mg, 0.00144 mmol) were added, and irradiation was continued. At the 24 h timepoint, the solvent was removed via rotary evaporation. The crude residue was dissolved in CH_2Cl_2 (~1 mL), and the solution was passed through a SiO_2 plug (0.5 x 3 cm), using CH_2Cl_2 as eluent (~8 mL). The filtrate was concentrated in vacuo, and the residue was purified by silica gel flash chromatography (2:1 hexanes/Et_2O eluent) to afford indoline **2-25** (47.7 mg, 69% yield) as a white solid. (49.3 mg total mass was isolated. This included 1.6 mg Troc-protected pyrazole **2-127**, which was chromatographically inseparable from the product.)

TLC R_f: 0.35 in 1:1 hexanes/Et_2O, visualized by UV, stained blue in Hanessian's stain.

^{1}H NMR (400 MHz, $CDCl_3$): δ 7.42 (d, *J* = 8.0 Hz, 1H), 7.14 (d, *J* = 7.5 Hz, 1H), 7.01 (app. t, *J* = 7.8 Hz, 1H) 6.88-6.80 (m, 1H), 6.00-5.90 (m, 1H), 5.10 (d, *J* = 12.0 Hz, 1H), 4.79 (d, *J* = 12.0 Hz, 1H), 4.29 (dq, *J* = 14.2, 7.1 Hz, 1H), 4.23-4.12 (comp. m, 2H), 2.97 (app. ddt, *J* = 18.4, 7.6, 2.2 Hz, 1H), 2.69 (app. d, *J* = 18.4 Hz, 1H), 1.29 (t, *J* = 7.1 Hz, 3H).

^{13}C NMR (125 MHz, 50 °C, $CDCl_3$): δ 163.6, 152.7, 144.7, 140.8, 140.4, 135.5, 133.1, 127.1, 123.0, 114.2, 95.6, 75.7, 71.5, 60.6, 45.2, 37.7, 14.4.

IR (ATR, neat): 2981, 1724, 1636, 1478, 794 cm^{-1}.

HRMS (ESI+): *m/z* calc'd for $(M + H)^+$ $[C_{17}H_{15}BrCl_3NO_4 + H]^+$: 481.9323, found 481.9316.

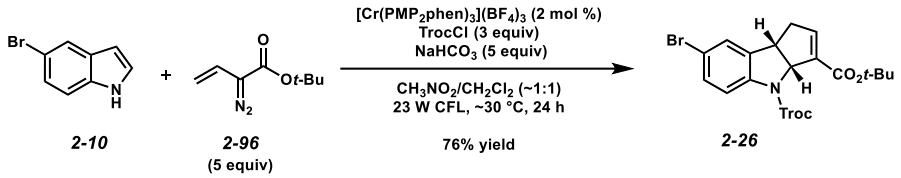

Indoline 2-26. According to General Procedure A, 5-bromoindole (**2-10**, 28.0 mg, 0.143 mmol), $NaHCO_3$ (60.0 mg, 0.714 mmol), and $[Cr(PMP_2phen)_3](BF_4)_3$ (2.1 mg, 0.00143 mmol) were added to a flame-dried 1-dram borosilicate vial. The reagents were suspended in CH_3NO_2 (0.714 mL), and to this suspension were added 2,2,2-trichloroethoxycarbonyl chloride (59.0 µL, 0.428 mmol) and vinyl diazoacetate **2-96** (0.428 mL, 1.0 M in CH_2Cl_2, 0.428 mmol). The reaction mixture was irradiated with a 23 W CFL bulb while stirring. After 8 h, second charges of vinyl diazoacetate **2-96** (0.286 mL, 1.0 M in CH_2Cl_2, 0.286 mmol) and $[Cr(PMP_2phen)_3](BF_4)_3$ (2.1 mg, 0.00143 mmol) were added, and irradiation was continued. At the 24 h timepoint, the solvent was removed via rotary evaporation. The crude residue was dissolved in CH_2Cl_2 (~1 mL), and the solution was passed through a SiO_2 plug (0.5 x 3 cm), using CH_2Cl_2 as eluent (~8 mL). The filtrate was concentrated in vacuo, and the residue was purified by silica gel flash chromatography (4:1 hexanes/Et_2O eluent) to afford indoline **2-26** (55.5 mg, 76% yield) as a yellow oil.

TLC R_f: 0.72 in 1:1 hexanes/Et_2O, visualized by UV, stained blue in Hanessian's stain.

^{1}H NMR (400 MHz, $CDCl_3$): δ 7.75-7.43 (br. m, 1H), 7.34 (d, *J* = 8.6 Hz, 1H), 7.29 (s, 1H), 6.73 (app. s, 1H), 5.84 (app. d, *J* = 6.8 Hz, 1H), 5.31-4.40 (br. m, 2H), 4.09 (app. t, *J* = 7.5 Hz, 1H), 2.98 (app. ddt, *J* = 18.3, 7.7, 2.0 Hz, 1H), 2.72 (app. d, *J* = 18.3 Hz, 1H), 1.45 (s, 9H).

^{13}C NMR (125 MHz, 50 °C, $CDCl_3$): δ 163.1, 151.7, 143.4, 140.0, 137.9, 136.5, 131.4, 127.4, 118.7, 116.7, 95.4, 81.2, 75.8, 69.2. 43.8, 37.5, 28.3.

IR (ATR, neat): 2978, 1716, 1629, 1478, 1161 cm^{-1}.

HRMS (ESI+): *m/z* calc'd for $(M + Na)^+$ $[C_{19}H_{19}BrCl_3NO_4 + Na]^+$: 531.9455, found 531.9443.

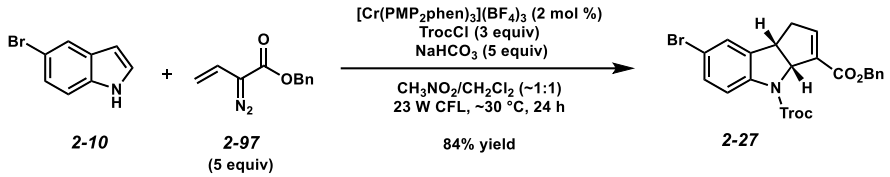

Indoline 2-27. According to General Procedure A, 5-bromoindole (**2-10**, 27.9 mg, 0.142 mmol), $NaHCO_3$ (59.8 mg, 0.712 mmol), and $[Cr(PMP_2phen)_3](BF_4)_3$ (2.1 mg, 0.00142 mmol) were added to a flame-dried 1-dram borosilicate vial. The reagents were suspended in CH_3NO_2 (0.712 mL), and to this suspension were added 2,2,2-trichloroethoxycarbonyl chloride (58.8 µL, 0.427 mmol) and vinyl diazoacetate **2-97** (0.427 mL, 1.0 M in CH_2Cl_2, 0.427 mmol). The reaction mixture was irradiated with a 23 W CFL bulb while stirring. After 8 h, second charges of vinyl diazoacetate **2-97** (0.284 mL, 1.0 M in CH_2Cl_2, 0.284 mmol) and $[Cr(PMP_2phen)_3](BF_4)_3$ (2.1 mg, 0.00142 mmol) were added, and irradiation was continued. At the 24 h timepoint, the solvent was removed via rotary evaporation. The crude residue was dissolved in CH_2Cl_2 (~1 mL), and the solution was passed through a SiO_2 plug (0.5 x 3 cm), using CH_2Cl_2 as eluent (~8 mL). The filtrate was concentrated in vacuo, and the residue was purified by silica gel flash chromatography (4:1 hexanes/Et_2O eluent) to afford indoline **2-27** (65.2 mg, 84% yield) as a white solid.

TLC R_f: 0.53 in 1:1 hexanes/Et_2O, visualized by UV, stained blue in Hanessian's stain.

^{1}H NMR (400 MHz, $CDCl_3$): δ 7.78-7.44 (br. m, 1H), 7.44-7.27 (comp. m, 7H), 6.94 (app. s, 1H), 5.89 (d, *J* = 6.7 Hz, 1H), 5.20-4.60 (br. m, 2H), 5.15 (ABq, *J* = 12.3 Hz, Δν = 35.1 Hz, 2H), 4.13 (app. t, *J* = 7.6 Hz, 1H), 3.03 (app. dd, *J* = 18.5, 7.7 Hz, 1H), 2.76 (app. d, *J* = 18.5 Hz, 1H).

^{13}C NMR (125 MHz, 50 °C, $CDCl_3$): δ 163.6, 151.6, 145.5, 140.0, 137.6, 136.0, 134.8, 131.5, 128.8, 128.6, 128.5, 127.5, 118.6, 116.7, 95.4, 75.5, 69.1, 66.6, 43.9, 37.7.

IR (ATR, neat): 2951, 1720, 1629, 1477, 819 cm^{-1}.

HRMS (ESI+): *m/z* calc'd for $(M + H)^+$ $[C_{22}H_{17}BrCl_3NO_4 + H]^+$: 543.9479, found 543.9471.

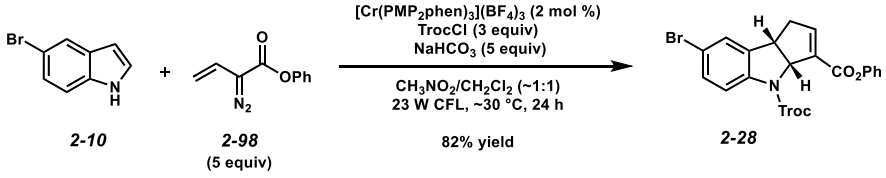

2-10 *2-98* (5 equiv) *2-28*

Indoline 2-28. According to General Procedure A, 5-bromoindole (**2-10**, 28.1 mg, 0.143 mmol), $NaHCO_3$ (60.2 mg, 0.717 mmol), and $[Cr(PMP_2phen)_3](BF_4)_3$ (2.2 mg, 0.00143 mmol) were added to a flame-dried 1-dram borosilicate vial. The reagents were suspended in CH_3NO_2 (0.717 mL), and to this suspension were added 2,2,2-trichloroethoxycarbonyl chloride (59.2 µL, 0.430 mmol) and vinyl diazoacetate **2-98** (0.430 mL, 1.0 M in CH_2Cl_2, 0.430 mmol). The reaction mixture was irradiated with a 23 W CFL bulb while stirring. After 8 h, second charges of vinyl diazoacetate **2-98** (0.287 mL, 1.0 M in CH_2Cl_2, 0.287 mmol) and $[Cr(PMP_2phen)_3](BF_4)_3$ (2.2 mg, 0.00143 mmol) were added, and irradiation was continued. At the 24 h timepoint, the solvent was removed via rotary evaporation. The crude residue was dissolved in CH_2Cl_2 (~1 mL), and the solution was passed through a SiO_2 plug (0.5 x 3 cm), using CH_2Cl_2 as eluent (~8 mL). The filtrate was concentrated in vacuo, and the residue was purified by silica gel flash chromatography (4:1 hexanes/Et_2O eluent) to afford indoline **2-28** (62.5 mg, 82% yield) as a white solid.

TLC R_f: 0.53 in 1:1 hexanes/Et_2O, visualized by UV, stained blue in Hanessian's stain.

^{1}H NMR (400 MHz, $CDCl_3$): δ 7.80-7.45 (br. m, 1H), 7.44-7.30 (comp. m, 4H), 7.22 (t, *J* = 7.4 Hz, 1H), 7.17-7.02 (comp. m, 3H), 6.00 (d, *J* = 6.7 Hz, 1H), 5.25-4.35 (br. m, 2H), 4.21 (app. t, *J* = 7.5 Hz, 1H), 3.13 (app. dd, *J* = 18.7, 7.8 Hz, 1H), 2.86 (app. d, *J* = 18.7 Hz, 1H).

^{13}C NMR (125 MHz, 50 °C, $CDCl_3$): δ 161.8, 151.7, 150.8, 147.1, 140.0, 137.5, 134.5, 131.6, 129.6, 127.5, 126.0, 121.7, 118.7, 116.9, 95.4, 75.7, 69.1, 44.0, 38.0.

IR (ATR, neat): 2924, 1724, 1628, 1478, 1190, 817 cm^{-1}.

HRMS (ESI+): *m/z* calc'd for $(M + H)^+$ $[C_{21}H_{15}BrCl_3NO_4 + H]^+$: 529.9323, found 529.9315.

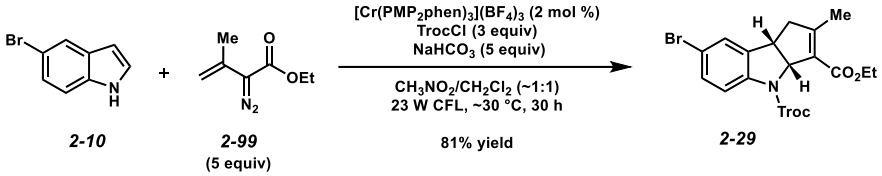

Indoline 2-29. According to General Procedure A, 5-bromoindole (**2-10**, 28.5 mg, 0.145 mmol), $NaHCO_3$ (61.1 mg, 0.727 mmol), and $[Cr(PMP_2phen)_3](BF_4)_3$ (2.2 mg, 0.00145 mmol) were added to a flame-dried 1-dram borosilicate vial. The reagents were suspended in CH_3NO_2 (0.727 mL), and to this suspension were added 2,2,2-trichloroethoxycarbonyl chloride (60.0 µL, 0.436 mmol) and vinyl diazoacetate **2-99** (0.436 mL, 1.0 M in CH_2Cl_2, 0.436 mmol). The reaction mixture was irradiated with a 23 W CFL bulb while stirring. After 8 h, second charges of vinyl diazoacetate **2-99** (0.291 mL, 1.0 M in CH_2Cl_2, 0.291 mmol) and $[Cr(PMP_2phen)_3](BF_4)_3$ (2.2 mg, 0.00145 mmol) were added, and irradiation was continued. At the 30 h timepoint, the solvent was removed via rotary evaporation. The crude residue was dissolved in CH_2Cl_2 (~1 mL), and the solution was passed through a SiO_2 plug (0.5 x 3 cm), using CH_2Cl_2 as eluent (~8 mL). The filtrate was

concentrated in vacuo, and the residue was purified by silica gel flash chromatography (2:1 hexanes/Et_2O eluent) to afford indoline **2-29** (58.6 mg, 81% yield) as a colorless oil.

TLC R_f: 0.61 in 1:1 hexanes/Et_2O, visualized by UV, stained blue in Hanessian's stain.

^{1}H NMR (400 MHz, $CDCl_3$): δ 7.68-7.47 (br. m, 1H), 7.34 (d, *J* = 8.6 Hz, 1H), 7.29 (s, 1H), 5.88 (d, *J* = 6.4 Hz, 1H), 5.30-4.40 (br. m, 2H), 4.24-4.15 (comp. m, 2H), 3.97 (app. t, *J* = 7.6 Hz, 1H), 3.01 (dd, *J* = 17.7, 8.0 Hz, 1H), 2.66 (app. d, *J* = 17.7 Hz, 1H), 2.01 (s, 3H), 1.28 (t, *J* = 7.1 Hz, 1H).

^{13}C NMR (125 MHz, 50 °C, $CDCl_3$): δ 165.4, 153.9, 151.6, 140.0, 138.1, 131.3, 127.5, 127.3, 118.8, 116.7, 111.9, 95.4, 75.7, 71.3, 60.4, 44.3, 42.0, 16.5, 14.4.

IR (ATR, neat): 2975, 1723, 1643, 1478, 1104, 821 cm^{-1}.

HRMS (ESI+): *m/z* calc'd for $(M + H)^+$ $[C_{18}H_{17}BrCl_3NO_4 + H]^+$: 495.9479, found 495.9467.

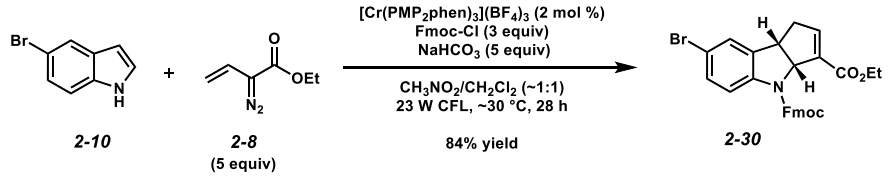

Indoline 2-30. According to a modified General Procedure A, 5-bromoindole (**2-10**, 25.5 mg, 0.130 mmol), $NaHCO_3$ (54.6 mg, 0.650 mmol), and $[Cr(PMP_2phen)_3](BF_4)_3$ (2.0 mg, 0.00130 mmol) were added to a flame-dried 1-dram borosilicate vial. The reagents were suspended in CH_3NO_2 (0.650 mL), and to this suspension were added 9-fluorenylmethyl chloroformate (101 mg, 0.390 mmol) and vinyl diazoacetate **2-8** (0.390 mL, 1.0 M in CH_2Cl_2, 0.390 mmol). The reaction mixture was irradiated with a 23 W CFL bulb while stirring. After 8 h, second charges of vinyl diazoacetate **2-8** (0.260 mL, 1.0 M in CH_2Cl_2, 0.260 mmol) and $[Cr(PMP_2phen)_3](BF_4)_3$

(2.0 mg, 0.00130 mmol) were added, and irradiation was continued. At the 20 h timepoint, third charges of vinyl diazoacetate **2-8** (0.130 mL, 1.0 M in CH_2Cl_2, 0.130 mmol) and $[Cr(PMP_2phen)_3](BF_4)_3$ (2.0 mg, 0.00130 mmol) were added, and irradiation was continued. At the 28 h timepoint, the solvent was removed via rotary evaporation. The crude residue was then dissolved in CH_2Cl_2 (~1 mL), and the solution was passed through a SiO_2 plug (0.5 x 3 cm), using CH_2Cl_2 as eluent (~8 mL). The filtrate was concentrated in vacuo, and the crude residue was purified by silica gel flash chromatography (6:1 hexanes/EtOAc eluent) to afford indoline **2-30** (58.1 mg, 84% yield) as a white solid.

TLC: R_f = 0.36 in 4:1 hexanes/EtOAc, visualized by UV.

^{1}H NMR (400 MHz, $CDCl_3$): δ 7.78 (app. t, *J* = 6.6 Hz, 2H), 7.65-7.57 (comp. m, 2H), 7.41 (app. q, *J* = 6.6 Hz, 2H), 7.35-7.27 (comp. m, 3H), 7.27-7.08 (br. m, 1H), 7.24 (s, 1H), 6.83 (app. s, 1H), 5.82 (dd, *J* = 7.6, 1.6 Hz, 1H), 4.80-4.50 (br. m, 2H), 4.36 (app. t, *J* = 6.1 Hz, 1H), 4.26-3.98 (comp. m, 3H), 3.00 (app. dd, *J* = 18.0, 7.9 Hz, 1H), 2.72 (app. d, *J* = 18.0 Hz, 1H), 1.20 (t, *J* = 7.1 Hz, 3H).

^{13}C NMR (100 MHz, $CDCl_3$): δ 163.9, 153.5, 144.8, 144.1, 141.5, 131.1, 127.9, 127.7, 127.3, 127.24, 127.20, 125.1, 120.21, 120.17, 120.1, 115.9, 68.7, 67.8, 60.6, 50.5, 47.3, 37.7, 14.3.

IR (ATR, neat): 2955, 1713, 1635, 1477, 757 cm^{-1}.

HRMS (ESI+): *m/z* calc'd for $(M + Na)^+$ $[C_{29}H_{24}BrNO_4 + Na]^+$: 552.0781, found 552.0784.

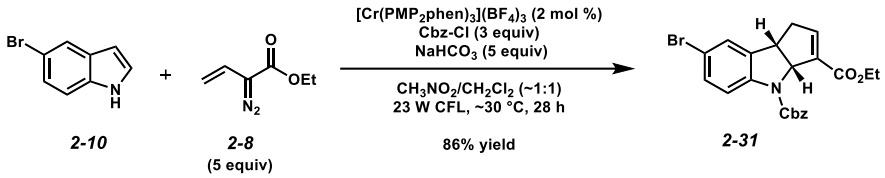

Indoline 2-31. According to a modified General Procedure A, 5-bromoindole (**2-10**, 25.3 mg, 0.129 mmol), $NaHCO_3$ (54.2 mg, 0.645 mmol), and $[Cr(PMP_2phen)_3](BF_4)_3$ (2.0 mg, 0.00129 mmol) were added to a flame-dried 1-dram borosilicate vial. The reagents were suspended in CH_3NO_2 (0.645 mL), and to this suspension were added benzyl chloroformate (55.3 µL, 0.387 mmol) and vinyl diazoacetate **2-8** (0.387 mL, 1.0 M in CH_2Cl_2, 0.387 mmol). The reaction mixture was irradiated with a 23 W CFL bulb while stirring. After 8 h, second charges of vinyl diazoacetate **2-8** (0.258 mL, 1.0 M in CH_2Cl_2, 0.258 mmol) and $[Cr(PMP_2phen)_3](BF_4)_3$ (2.0 mg, 0.00129 mmol) were added, and irradiation was continued. At the 20 h timepoint, third charges of vinyl diazoacetate **2-8** (0.129 mL, 1.0 M in CH_2Cl_2, 0.129 mmol) and $[Cr(PMP_2phen)_3](BF_4)_3$ (2.0 mg, 0.00129 mmol) were added, and irradiation was continued. At the 28 h timepoint, the solvent was removed via rotary evaporation. The crude residue was dissolved in CH_2Cl_2 (~1 mL), and the solution was passed through a SiO_2 plug (0.5 x 3 cm), using CH_2Cl_2 as eluent (~8 mL). The filtrate was concentrated in vacuo, and the residue was purified by silica gel flash chromatography (6:1 hexanes/EtOAc eluent) to afford indoline **2-31** (49.0 mg, 86% yield) as a yellow oil.

TLC: R_f = 0.45 in 4:1 hexanes/EtOAc, visualized by UV.

^{1}H NMR (400 MHz, $CDCl_3$): δ 7.69-7.38 (br. m, 1H), 7.45 (d, *J* = 6.9 Hz, 2H), 7.41-7.23 (comp. m, 5H), 6.83 (app. s, 1H), 5.83 (d, *J* = 6.6 Hz, 1H), 5.38 (d, *J* = 12.0 Hz, 1H), 5.23 (br. d, *J* = 12.0 Hz, 1H), 4.23-4.08 (comp. m, 2H), 4.06 (app. t, *J* = 7.6 Hz, 1H), 2.98 (app. dd, *J* = 18.4, 7.6 Hz, 1H), 2.72 (app. d, *J* = 18.4 Hz, 1H), 1.23 (t, *J* = 7.1 Hz, 3H).

^{13}C NMR (125 MHz, $CDCl_3$, 50 °C): δ 164.0, 153.5, 144.1, 140.8, 137.5, 136.5, 135.7, 131.3, 128.7, 128.4, 128.3, 127.3, 118.4, 116.0, 69.0, 67.9, 60.6, 43.9, 37.8, 14.3.

IR (ATR, neat): 2979, 1709, 1629, 1477, 1280, 752 cm^{-1}.

HRMS (ESI+): *m/z* calc'd for $(M + Na)^+$ $[C_{22}H_{20}BrNO_4 + Na]^+$: 464.0468 found 464.0466.

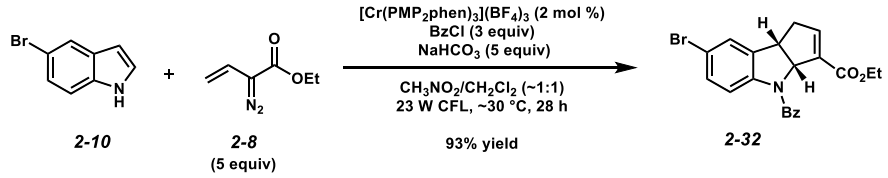

2-10 *2-8* (5 equiv) *2-32*

Indoline 2-32. According to General Procedure A, 5-bromoindole (**2-10**, 28.5 mg, 0.145 mmol), $NaHCO_3$ (61.1 mg, 0.727 mmol) and $[Cr(PMP_2phen)_3](BF_4)_3$ (2.2 mg, 0.00145 mmol) were added to a flame-dried 1-dram borosilicate vial. The reagents were suspended in CH_3NO_2 (0.727 mL), and to this suspension were added benzoyl chloride (50.7 µL, 0.436 mmol) and vinyl diazoacetate **2-8** (0.436 mL, 1.0 M in CH_2Cl_2, 0.436 mmol). The reaction mixture was irradiated with a 23 W CFL bulb while stirring. After 8 h, extra charges of vinyl diazoacetate **2-8** (0.291 mL, 1.0 M in CH_2Cl_2, 0.291 mmol) and $[Cr(PMP_2phen)_3](BF_4)_3$ (2.2 mg, 0.00145 mmol) were added, and irradiation was continued. At the 28 h timepoint, the solvent was removed via rotary evaporation. The crude residue was dissolved in CH_2Cl_2 (~1 mL), and the solution was passed through a SiO_2 plug (0.5 x 3 cm), using CH_2Cl_2 as eluent (~8 mL). The filtrate was concentrated in vacuo, and the residue was purified by silica gel flash chromatography (4:1 hexanes/EtOAc eluent) to afford indoline **2-32** (55.7 mg, 93% yield) as a white solid.

TLC: R_f = 0.28 in 4:1 hexanes/EtOAc, visualized by UV.

^{1}H NMR (400 MHz, $CDCl_3$): δ 7.57 (d, *J* = 8.0 Hz, 2H), 7.50-7.40 (comp. m, 3H), 7.31 (s, 1H), 7.18 (d, *J* = 8.5 Hz, 1H), 7.18-6.96 (br. m, 1H), 6.86-6.80 (m, 1H), 6.02 (app. d, *J* = 5.9 Hz, 1H), 4.20-4.09 (comp. m, 3H), 2.99 (app. ddt, *J* = 18.3, 7.4, 2.0 Hz, 1H), 2.77 (app. d, *J* = 18.3 Hz, 1H), 1.22 (t, *J* = 7.1 Hz, 3H).

^{13}C NMR (100 MHz, $CDCl_3$): δ 170.0, 163.7, 144.7, 141.2, 138.1, 136.9, 135.0, 131.0, 130.5, 128.5, 128.0, 127.5, 118.3, 116.6, 69.6, 60.7, 43.6, 37.4, 14.3.

IR (ATR, neat): 2980, 1715, 1651, 1469, 1378, 728 cm^{-1}.

HRMS (ESI+): *m/z* calc'd for $(M + Na)^+$ $[C_{21}H_{18}BrNO_3 + Na]^+$: 434.0362, found 434.0358.

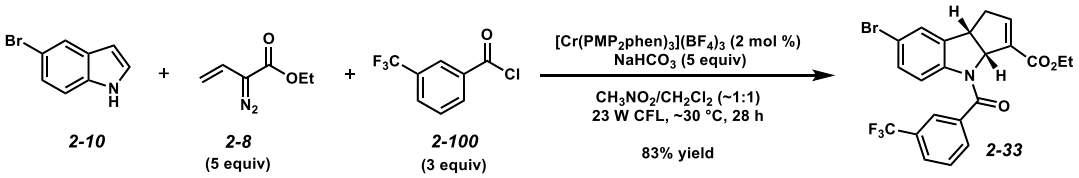

Indoline 2-33. According to a modified General Procedure A, 5-bromoindole (**2-10**, 26.3 mg, 0.134 mmol), $NaHCO_3$ (56.3 mg, 0.671 mmol), and $[Cr(PMP_2phen)_3](BF_4)_3$ (2.0 mg, 0.00134 mmol) were added to a flame-dried 1-dram borosilicate vial. The reagents were suspended in CH_3NO_2 (0.670 mL), and to this suspension were added 3-(trifluoromethyl)benzoyl chloride (**2-100**, 59.9 µL, 0.397 mmol) and vinyl diazoacetate **2-8** (0.402 mL, 1.0 M in CH_2Cl_2, 0.402 mmol). The reaction mixture was irradiated with a 23 W CFL bulb while stirring. After 8 h, second charges of vinyl diazoacetate **2-8** (0.268 mL, 1.0 M in CH_2Cl_2, 0.268 mmol) and $[Cr(PMP_2phen)_3](BF_4)_3$ (2.0 mg, 0.00134 mmol) were added, and irradiation was continued. At the 20 h timepoint, third charges of vinyl diazoacetate **2-8** (0.134 mL, 1.0 M in CH_2Cl_2, 0.134 mmol) and $[Cr(PMP_2phen)_3](BF_4)_3$ (2.0 mg, 0.00134 mmol) were added, and irradiation was continued. At the 28 h timepoint, the solvent was removed via rotary evaporation. The crude residue was

dissolved in CH_2Cl_2 (~1 mL), and the solution was passed through a SiO_2 plug (0.5 x 3 cm), using CH_2Cl_2 as eluent (~8 mL). The filtrate was concentrated in vacuo, and the residue was purified by silica gel flash chromatography (6:1 hexanes/EtOAc eluent) to afford indoline **2-33** (53.2 mg, 83% yield) as a yellow oil.

TLC: R_f = 0.45 in 4:1 hexanes/EtOAc, visualized by UV.

^{1}H NMR (400 MHz, $CDCl_3$): δ 7.87 (s, 1H), 7.81 (d, *J* = 7.7 Hz, 1H), 7.73 (d, *J* = 7.7 Hz, 1H), 7.58 (app. t, *J* = 7.7 Hz, 1H), 7.53-7.22 (br. m, 1H), 7.35 (s, 1H), 7.29-7.21 (m, 1H), 6.85-6.80 (m, 1H), 5.85 (app. d, *J* = 5.5 Hz, 1H), 4.18-4.09 (comp. m, 3H), 3.00 (app. ddt, *J* = 18.4, 7.3, 2.0 Hz, 1H), 2.79 (app. d, *J* = 18.4 Hz, 1H), 1.21 (t, *J* = 7.1 Hz, 3H).

^{13}C NMR (100 MHz, $CDCl_3$): δ 168.5, 163.4, 145.0, 140.9, 137.9, 137.7, 134.4, 131.7, 131.3, 130.8 (q, *J* = 32.4 Hz), 129.0, 127.6, 127.0 (q, *J* = 3.7 Hz), 126.6 (q, *J* = 271 Hz), 125.1 (q, *J* = 3.7 Hz), 118.5, 117.1, 70.0, 60.7, 43.7, 37.3, 14.3.

IR (ATR, neat): 2983, 1715, 1651, 1470, 1384, 822 cm^{-1}.

HRMS (ESI+): *m/z* calc'd $(M + H)^+$ $[C_{22}H_{17}BrF_3NO_3 + H]^+$: 480.0417 found 480.0414.

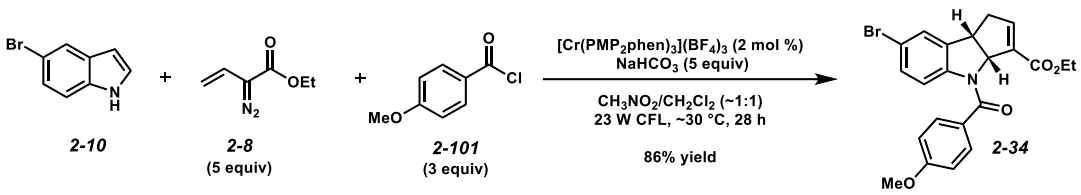

Indoline 2-34. According to a modified General Procedure A, 5-bromoindole (**2-10**, 24.8 mg, 0.126 mmol), $NaHCO_3$ (53.1 mg, 0.632 mmol), and $[Cr(PMP_2phen)_3](BF_4)_3$ (1.9 mg, 0.00126 mmol) were added to a flame-dried 1-dram borosilicate vial. The reagents were suspended in CH_3NO_2 (0.630 mL), and to this suspension were added 4-methoxybenzoyl chloride (**2-101**, 51.2 µL, 0.378 mmol) and vinyl diazoacetate **2-8** (0.378 mL, 1.0 M in CH_2Cl_2, 0.378 mmol). The reaction mixture was irradiated with a 23 W CFL bulb while stirring. After 8 h, second charges of vinyl diazoacetate **2-8** (0.252 mL, 1.0 M in CH_2Cl_2, 0.252 mmol) and $[Cr(PMP_2phen)_3](BF_4)_3$ (1.9 mg, 0.00126 mmol) were added, and irradiation was continued. At the 20 h timepoint, third charges of vinyl diazoacetate **2-8** (0.126 mL, 1.0 M in CH_2Cl_2, 0.126 mmol) and $[Cr(PMP_2phen)_3](BF_4)_3$ (1.9 mg, 0.00126 mmol) were added, and irradiation was continued. At the 28 h timepoint, the solvent was removed via rotary evaporation. The crude residue was dissolved in CH_2Cl_2 (~1 mL), and the solution was passed through a SiO_2 plug (0.5 x 3 cm), using CH_2Cl_2 as eluent (~8 mL). The filtrate was concentrated in vacuo, and the residue was purified by silica gel flash chromatography (2:1 hexanes/Et_2O eluent) to afford indoline **2-34** (48.3 mg, 86% yield) as a colorless oil. (49.8 mg total mass was isolated. This included 1.5 mg starting acid chloride, which was chromatographically inseparable from the product.)

TLC: R_f = 0.21 in 4:1 hexanes/EtOAc, visualized by UV.

^{1}H NMR (400 MHz, $CDCl_3$): δ 7.56 (d, *J* = 8.7 Hz, 2H), 7.31 (s, 1H), 7.22-7.12 (comp. m, 2H), 6.94 (d, *J* = 8.7 Hz, 2H), 6.85-6.80 (m, 1H), 6.03 (dd, *J* = 7.2, 1.6 Hz, 1H), 4.13 (app. q, *J* = 7.1, 3H), 3.86 (s, 3H), 2.99 (app. ddt, *J* = 18.3, 7.5, 2.0 Hz, 1H), 2.77 (app. d, *J* = 18.3 Hz, 1H), 1.20 (t, *J* = 7.1 Hz, 3H).

^{13}C NMR (100 MHz, $CDCl_3$): δ 170.0, 163.8, 161.4, 144.6, 141.5, 138.0, 135.1, 131.0, 130.2, 129.2, 127.5, 118.1, 116.3, 113.7, 69.7, 60.6, 55.5, 43.6, 37.5, 14.3.

IR (ATR, neat): 2933, 1715, 1644, 1606, 1252, 877 cm^{-1}.

HRMS (ESI+): *m/z* calc'd for $(M + Na)^+$ $[C_{22}H_{20}BrNO_4 + Na]^+$: 464.0468, found 464.0469.

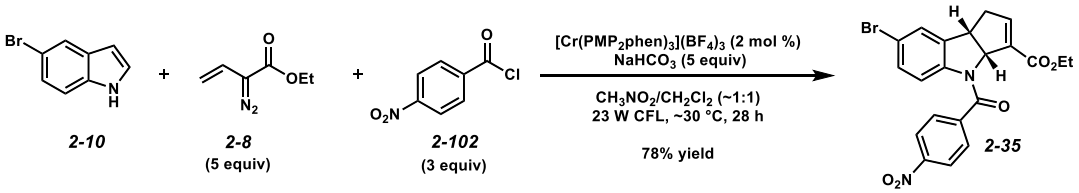

Indoline 2-35. According to a modified General Procedure A, 5-bromoindole (**2-10**, 26.6 mg, 0.136 mmol), $NaHCO_3$ (57.1 mg, 0.680 mmol), and $[Cr(PMP_2phen)_3](BF_4)_3$ (2.0 mg, 0.00136 mmol) were added to a flame-dried 1-dram borosilicate vial. The reagents were suspended in CH_3NO_2 (0.680 mL), and to this suspension were added 4-nitrobenzoyl chloride (**2-102**, 75.7 mg, 0.408 mmol) and vinyl diazoacetate **2-8** (0.408 mL, 1.0 M in CH_2Cl_2, 0.408 mmol). The reaction mixture was irradiated with a 23 W CFL bulb while stirring. After 8 h, second charges of vinyl diazoacetate **2-8** (0.272 mL, 1.0 M in CH_2Cl_2, 0.272 mmol) and $[Cr(PMP_2phen)_3](BF_4)_3$ (2.0 mg, 0.00136 mmol) were added, and irradiation was continued. At the 20 h timepoint, third charges of vinyl diazoacetate **2-8** (0.136 mL, 1.0 M in CH_2Cl_2, 0.136 mmol) and $[Cr(PMP_2phen)_3](BF_4)_3$ (2.0 mg, 0.00136 mmol) were added, and irradiation was continued. At the 28 h timepoint, the

solvent was removed via rotary evaporation. The crude residue was dissolved in CH_2Cl_2 (~1 mL), and the solution was passed through a SiO_2 plug (0.5 x 3 cm), using CH_2Cl_2 as eluent (~8 mL). The filtrate was concentrated in vacuo, and the residue was purified by silica gel flash chromatography (2:1 hexanes/Et_2O eluent) to afford indoline **2-35** (48.3 mg, 78% yield) as a white solid.

TLC: R_f = 0.27 in 4:1 hexanes/EtOAc, visualized by UV.

^{1}H NMR (400 MHz, $CDCl_3$): δ 8.31 (d, *J* = 8.5 Hz, 2H), 7.80 (d, *J* = 8.5 Hz, 2H), 7.70-7.41 (br. m, 1H), 7.36 (s, 1H), 7.30 (d, *J* = 7.6 Hz, 1H), 6.85-6.80 (m, 1H), 5.79 (br. s, 1H), 4.22-4.08 (comp. m, 3H), 3.00 (app. ddt, *J* = 18.4, 7.3, 2.0 Hz, 1H), 2.81 (app. d, *J* = 18.4 Hz, 1H), 1.22 (t, *J* = 7.1 Hz, 3H).

^{13}C NMR (100 MHz, $CDCl_3$): δ 163.4, 148.7, 145.2, 142.9, 140.7, 137.8, 134.0, 131.4, 129.4, 127.6, 123.7, 118.7, 117.4, 70.1, 60.8, 43.7, 37.4, 14.3 (*1 carbon not detected*).

IR (ATR, neat): 2925, 1713, 1652, 1521, 1346, 734 cm^{-1}.

HRMS (ESI+): *m/z* calc'd for $(M + Na)^+$ $[C_{21}H_{17}BrN_2O_5 + Na]^+$: 479.0213, found 479.0216.

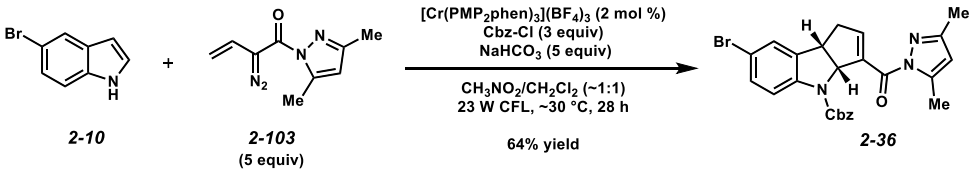

2-10 + *2-103* (5 equiv) → *2-36*

Indoline 2-36. According to a modified General Procedure A, 5-bromoindole (**2-10**, 18.1 mg, 0.0923 mmol), $NaHCO_3$ (38.8 mg, 0.462 mmol), and $[Cr(PMP_2phen)_3](BF_4)_3$ (1.4 mg, 0.000923 mmol) were added to a flame-dried 1-dram borosilicate vial. The reagents were suspended in

CH_3NO_2 (0.462 mL), and to this suspension were added benzyl chloroformate (39.5 µL, 0.277 mmol) and vinyl diazoamide **2-103** (0.277 mL, 1.0 M in CH_2Cl_2, 0.277 mmol). The reaction mixture was irradiated with a 23 W CFL bulb while stirring. After 8 h, second charges of vinyl diazoamide **2-103** (0.185 mL, 1.0 M in CH_2Cl_2, 0.185 mmol) and $[Cr(PMP_2phen)_3](BF_4)_3$ (1.4 mg, 0.000923 mmol) were added, and irradiation was continued. At the 20 h timepoint, a third charge of $[Cr(PMP_2phen)_3](BF_4)_3$ (1.4 mg, 0.000923 mmol) was added, and irradiation was continued. At the 28 h timepoint, the solvent was removed via rotary evaporation. The crude residue was dissolved in CH_2Cl_2 (~1 mL), and the solution was passed through a SiO_2 plug (0.5 x 3 cm), using CH_2Cl_2 as eluent (~8 mL). The filtrate was concentrated in vacuo, and the residue was purified by silica gel flash chromatography (9:1 hexanes/EtOAc eluent) to afford indoline **2-36** (24.5 mg, 64% yield) as an off-white solid.

TLC: R*f* = 0.25 in 4:1 hexanes/EtOAc, visualized by UV.

^{1}H NMR (400 MHz, CDCl3): δ 7.70 (br. s, 1H), 7.39-7.25 (comp. m, 5H), 7.25-7.08 (comp. m, 2H), 6.41 (app. s, 1H), 6.05 (d, *J* = 8.6 Hz, 1H), 5.91 (s, 1H), 5.23 (d, *J* = 12.6 Hz, 1H), 4.71-4.33 (br. m, 1H), 4.19 (app. t, *J* = 8.7 Hz, 1H), 3.18 (app. dd, *J* = 17.0, 8.8 Hz, 1H), 2.74 (app. d, *J* = 17.0 Hz, 1H), 2.47 (s, 3H), 2.17 (s, 3H).

^{13}C NMR (100 MHz, CDCl3): δ 167.1, 152.5, 144.1, 140.4, 139.0, 138.7, 137.2, 136.0, 131.2, 128.8, 128.6, 128.2, 128.0, 127.4, 117.4, 115.6, 111.2, 72.5, 67.2. 42.9, 40.2, 14.3, 14.0.

IR (ATR, neat): 3409, 2928, 1737, 1710, 1480, 1346, 814 cm^{-1}.

HRMS (ESI+): *m/z* calc'd for $(M + H)^+$ $[C25H22BrN3O3 + H]^+$: 492.0917, found 492.0895.

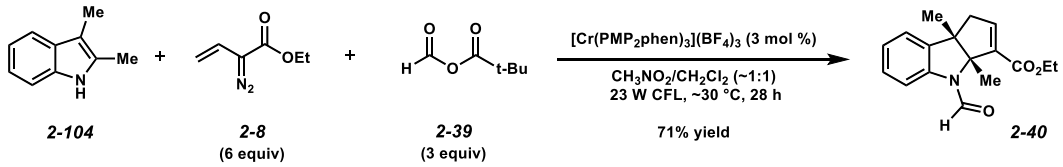

Indoline 2-40. According to General Procedure B, in a flame-dried 1-dram borosilicate vial, trimethylacetic formic anhydride (**2-39**, 78.1 mg, 0.600 mmol) was dissolved in CH_3NO_2 (1.00 mL). To this solution were added 2,3-dimethylindole (**2-104**, 29.1 mg, 0.200 mmol), $[Cr(PMP_2phen)_3](BF_4)_3$ (3.0 mg, 0.00200 mmol), and vinyl diazoacetate **2-8** (0.600 mL, 1.0 M in CH_2Cl_2, 0.600 mmol). The reaction mixture was irradiated with a 23 W CFL bulb while stirring. After 8 h, second charges of vinyl diazoacetate **2-8** (0.400 mL, 1.0 M in CH_2Cl_2, 0.400 mmol) and $[Cr(PMP_2phen)_3](BF_4)_3$ (3.0 mg, 0.00200 mmol) were added, and irradiation was continued. At the 24 h timepoint, third charges of vinyl diazoacetate **2-8** (0.200 mL, 1.0 M in CH_2Cl_2, 0.200 mmol) and $[Cr(PMP_2phen)_3](BF_4)_3$ (3.0 mg, 0.00200 mmol) were added, and irradiation was continued. At the 28 h timepoint, the solvent was removed via rotary evaporation. The crude residue was dissolved in CH_2Cl_2 (~1 mL), and the solution was passed through a SiO_2 plug (0.5 x 3 cm), using CH_2Cl_2 as eluent (~8 mL). The filtrate was concentrated in vacuo, and the residue was purified by silica gel flash chromatography (4:1 hexanes/EtOAc eluent) to afford indoline **2-40** (40.6 mg, 71% yield) as a colorless oil.

TLC: R_f = 0.23 in 3:1 hexanes/EtOAc, visualized by UV.

^{1}H NMR (400 MHz, $CDCl_3$): δ 8.91 (s, 1H), 8.14 (d, *J* = 8.0 Hz, 1H), 7.25-7.15 (comp. m, 2H), 7.08 (t, *J* = 7.3 Hz, 1H), 6.86-6.82 (m, 1H), 4.22-4.11 (comp. m, 2H), 2.95 (app. dd, *J* = 18.5, 3.1 Hz, 1H), 2.64 (app. d, *J* = 18.5 Hz, 1H), 1.75 (s, 3H), 1.28 (s, 3H), 1.27 (t, *J* = 7.1 Hz, 3H).

^{13}C NMR (100 MHz, $CDCl_3$): δ 163.4, 161.6, 144.7, 139.6, 138.5, 137.6, 128.4, 124.6, 122.5, 117.3, 77.3, 60.7, 55.4, 43.9, 22.6, 19.0, 14.2.

IR (ATR, neat): 2978, 1709, 1669, 1414, 757 cm^{-1}.

HRMS (ESI+): *m/z* calc'd for $(M+H)^+$ $[C_{17}H_{19}NO_3 + H]^+$: 286.1438, found 286.1434.

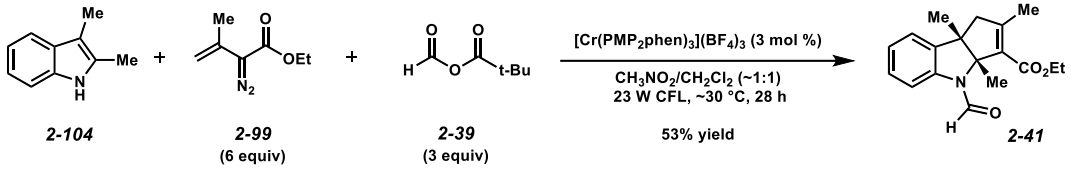

Indoline 2-41. According to General Procedure B, in a flame-dried 1-dram borosilicate vial, trimethylacetic formic anhydride (**2-39**, 53.5 mg, 0.411 mmol) was dissolved in CH_3NO_2 (0.685 mL). To this solution were added 2,3-dimethylindole (**2-104**, 19.9 mg, 0.137 mmol), $[Cr(PMP_2phen)_3](BF_4)_3$ (2.1 mg, 0.00137 mmol), and vinyl diazoacetate **2-99** (0.411 mL, 1.0 M in CH_2Cl_2, 0.411 mmol). The reaction mixture was irradiated with a 23 W CFL bulb while stirring. After 8 h, second charges of vinyl diazoacetate **2-99** (0.274 mL, 1.0 M in CH_2Cl_2, 0.274 mmol) and $[Cr(PMP_2phen)_3](BF_4)_3$ (2.1 mg, 0.00137 mmol) were added, and irradiation was continued. At the 24 h timepoint, third charges of vinyl diazoacetate **2-99** (0.137 mL, 1.0 M in CH_2Cl_2, 0.137 mmol) and $[Cr(PMP_2phen)_3](BF_4)_3$ (2.1 mg, 0.00137 mmol) were added, and irradiation was continued. At the 28 h timepoint, the solvent was removed via rotary evaporation. The crude residue was dissolved in CH_2Cl_2 (~1 mL), and the solution was passed through a SiO_2 plug (0.5 x 3 cm), using CH_2Cl_2 as eluent (~8 mL). The filtrate was concentrated in vacuo, and the residue was purified by silica gel flash chromatography (4:1 hexanes/EtOAc eluent) to afford indoline **2-41** (21.6 mg, 53% yield) as a white solid.

TLC: R_f = 0.23 in 3:1 hexanes/EtOAc, visualized by UV.

^{1}H NMR (400 MHz, $CDCl_3$): δ 8.81 (s, 1H), 8.10 (d, *J* = 8.0 Hz, 1H), 7.22 (app. t, *J* = 8.0 Hz, 1H), 7.17 (d, *J* = 7.3 Hz, 1H), 7.07 (app. t, *J* = 7.3 Hz, 1H), 4.29-4.13 (comp. m, 2H), 2.86 (d, *J* = 17.9 Hz, 1H), 2.67 (d, *J* = 17.9 Hz, 1H), 2.03 (s, 3H), 1.74 (s, 3H), 1.31 (t, *J* = 7.1 Hz, 3H), 1.22 (s, 3H).

^{13}C NMR (100 MHz, $CDCl_3$): δ 164.6, 161.5, 156.7, 139.7, 138.9, 129.8, 128.3, 124.5, 122.4, 117.4, 79.1, 60.4, 53.2, 50.4, 22.4, 19.2, 17.5, 14.3.

IR (ATR, neat): 2977, 1701, 1669, 1597, 757 cm^{-1}.

HRMS (ESI+): *m/z* calc'd for $(M + Na)^+$ $[C_{18}H_{21}NO_3 + Na]^+$: 322.1414, found 322.1407.

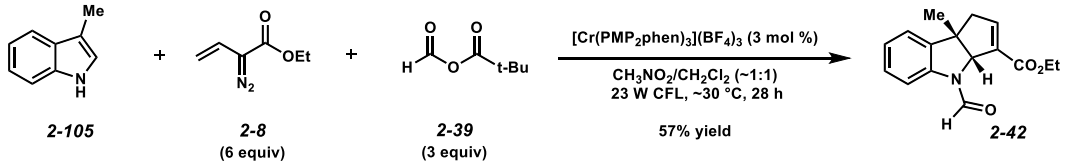

Indoline 2-42. According to General Procedure B, in a flame-dried 1-dram borosilicate vial, trimethylacetic formic anhydride (**2-39**, 60.5 mg, 0.465 mmol) was dissolved in CH_3NO_2 (0.775 mL). To this solution were added 3-methylindole (**2-105**, 20.3 mg, 0.155 mmol), $[Cr(PMP_2phen)_3](BF_4)_3$ (2.3 mg, 0.00155 mmol), and vinyl diazoacetate **2-8** (0.465 mL, 1.0 M in CH_2Cl_2, 0.465 mmol). The reaction mixture was irradiated with a 23 W CFL bulb while stirring. After 8 h, second charges of vinyl diazoacetate **2-8** (0.310 mL, 1.0 M in CH_2Cl_2, 0.310 mmol) and $[Cr(PMP_2phen)_3](BF_4)_3$ (2.3 mg, 0.00155 mmol) were added, and irradiation was continued. At the 24 h timepoint, third charges of vinyl diazoacetate **2-8** (0.155 mL, 1.0 M in CH_2Cl_2, 0.155

mmol) and $[Cr(PMP_2phen)_3](BF_4)_3$ (2.3 mg, 0.00155 mmol) were added, and irradiation was continued. At the 28 h timepoint, the solvent was removed via rotary evaporation. The crude residue was dissolved in CH_2Cl_2 (~1 mL), and the solution was passed through a SiO_2 plug (0.5 x 3 cm), using CH_2Cl_2 as eluent (~8 mL). The filtrate was concentrated in vacuo, and the residue was purified by silica gel flash chromatography (2:1 hexanes/Et_2O eluent) to afford indoline **2-42** (24.1 mg, 57% yield) as a yellow oil.

TLC: R_f = 0.25 in 3:1 hexanes/EtOAc, visualized by UV.

^{1}H NMR (400 MHz, $CDCl_3$): δ 8.89 (s, 1H), 8.03 (d, *J* = 8.0 Hz, 1H), 7.25-7.18 (comp. m, 2H), 7.10 (app. td, *J* = 7.3, 1.0 Hz, 1H), 6.87 (app. s, 1H), 5.15-5.10 (m, 1H), 4.22 (app. qd, *J* = 7.1, 2.0 Hz, 2H), 2.99 (app. dt, *J* = 18.9, 2.2 Hz, 1H), 2.79 (app. dt, *J* = 18.9, 2.2 Hz, 1H), 1.50 (s, 3H), 1.30 (t, *J* = 7.1 Hz, 3H).

^{13}C NMR (100 MHz, $CDCl_3$): δ 164.0, 161.9, 146.3, 139.9, 139.1, 134.5, 128.5, 125.1, 122.9, 117.6, 74.5, 61.0, 51.7, 46.5, 26.6, 14.3.

IR (ATR, neat): 2959, 1711, 1676, 1484, 756 cm^{-1}.

HRMS (ESI+): *m/z* calc'd for $(M + Na)^+$ $[C_{16}H_{17}NO_3 + Na]^+$: 294.1101, found 294.1096.

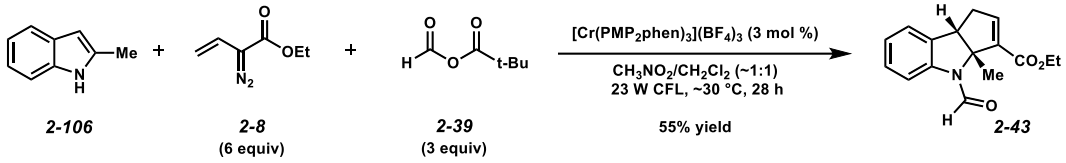

Indoline 2-43. According to General Procedure B, in a flame-dried 1-dram borosilicate vial, trimethylacetic formic anhydride (**2-39**, 60.5 mg, 0.465 mmol) was dissolved in CH_3NO_2 (0.775 mL). To this solution were added 2-methylindole (**2-106**, 20.3 mg, 0.155 mmol), $[Cr(PMP_2phen)_3](BF_4)_3$ (2.3 mg, 0.00155 mmol), and vinyl diazoacetate **2-8** (0.465 mL, 1.0 M in CH_2Cl_2, 0.465 mmol). The reaction mixture was irradiated with a 23 W CFL bulb while stirring. After 8 h, second charges of vinyl diazoacetate **2-8** (0.310 mL, 1.0 M in CH_2Cl_2, 0.310 mmol) and $[Cr(PMP_2phen)_3](BF_4)_3$ (2.3 mg, 0.00155 mmol) were added, and irradiation was continued. At the 24 h timepoint, third charges of vinyl diazoacetate **2-8** (0.155 mL, 1.0 M in CH_2Cl_2, 0.155 mmol) and $[Cr(PMP_2phen)_3](BF_4)_3$ (2.3 mg, 0.00155 mmol) were added, and irradiation was continued. At the 28 h timepoint, the solvent was removed via rotary evaporation. The crude residue was dissolved in CH_2Cl_2 (~1 mL), and the solution was passed through a SiO_2 plug (0.5 x 3 cm), using CH_2Cl_2 as eluent (~8 mL). The filtrate was concentrated in vacuo, and the residue was purified by silica gel flash chromatography (2:1 hexanes/Et_2O eluent) to afford indoline **2-43** (23.2 mg, 55% yield) as a pink oil.

TLC: R_f = 0.24 in 3:1 hexanes/EtOAc, visualized by UV.

^{1}H NMR (400 MHz, $CDCl_3$): δ 9.03 (s, 1H), 8.18 (d, *J* = 8.0 Hz, 1H), 7.24 (app. t, *J* = 8.0 Hz, 1H), 7.16 (d, *J* = 7.3 Hz, 1H), 7.08 (app. t, *J* = 7.3 Hz, 1H), 6.89 (app. t, *J* = 2.2 Hz, 1H), 4.20 (q,

J = 7.1 Hz, 2H), 3.77 (d, *J* = 7.9 Hz, 1H), 3.07 (ddd, *J* = 18.9, 7.9, 2.2 Hz, 1H), 2.73 (app. d, *J* = 18.9 Hz, 1H), 1.91 (s, 3H), 1.29 (t, *J* = 7.1 Hz, 3H).

^{13}C NMR (100 MHz, $CDCl_3$): δ 163.6, 161.5, 145.4, 140.8, 137.1, 133.1, 128.5, 124.6, 123.9, 117.4, 76.8, 60.8, 53.3, 37.4, 24.2, 14.3.

IR (ATR, neat): 2922, 1709, 1669, 1483, 755 cm^{-1}.

HRMS (ESI+): *m/z* calc'd for $(M + Na)^+$ $[C_{16}H_{17}NO_3 + Na]^+$: 294.1101, found 294.1098.

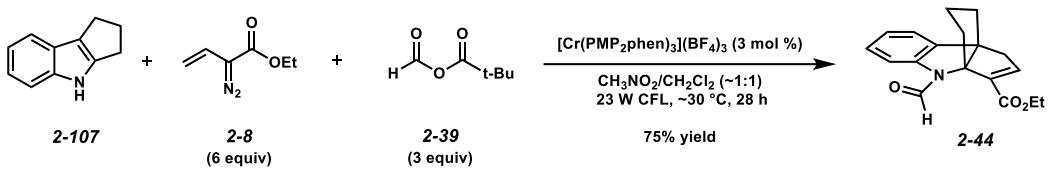

Indoline 2-44. According to General Procedure B, in a flame-dried 1-dram borosilicate vial, trimethylacetic formic anhydride (**2-39**, 67.1 mg, 0.516 mmol) was dissolved in CH_3NO_2 (0.860 mL). To this solution were added indole **2-107** (27.1 mg, 0.172 mmol), $[Cr(PMP_2phen)_3](BF_4)_3$ (2.6 mg, 0.00172 mmol), and vinyl diazoacetate **2-8** (0.516 mL, 1.0 M in CH_2Cl_2, 0.516 mmol). The reaction mixture was irradiated with a 23 W CFL bulb while stirring. After 8 h, second charges of vinyl diazoacetate **2-8** (0.344 mL, 1.0 M in CH_2Cl_2, 0.344 mmol) and $[Cr(PMP_2phen)_3](BF_4)_3$ (2.6 mg, 0.00172 mmol) were added, and irradiation was continued. At the 24 h timepoint, third charges of vinyl diazoacetate **2-8** (0.172 mL, 1.0 M in CH_2Cl_2, 0.172 mmol) and $[Cr(PMP_2phen)_3](BF_4)_3$ (2.6 mg, 0.00172 mmol) were added, and irradiation was continued. At the 28 h timepoint, the solvent was removed via rotary evaporation. The crude residue was dissolved in CH_2Cl_2 (~1 mL), and the solution was passed through a SiO_2 plug (0.5 x 3 cm), using CH_2Cl_2 as eluent (~8 mL). The filtrate was concentrated in vacuo, and the residue was purified

by silica gel flash chromatography (4:1 hexanes/EtOAc eluent) to afford indoline **2-44** (38.3 mg, 75% yield) as a colorless oil.

TLC: R_f = 0.37 in 3:1 hexanes/EtOAc, visualized by UV.

^{1}H NMR (400 MHz, $CDCl_3$): δ 9.12 (s, 1H), 8.17 (d, *J* = 8.0 Hz, 1H), 7.25-7.15 (comp. m, 2H), 7.10 (app. t, *J* = 7.3 Hz, 1H), 6.86 (app. t, *J* = 2.4 Hz, 1H), 4.30-4.17 (comp. m, 2H), 2.91 (dd, *J* = 19.5, 2.4 Hz, 1H), 2.79 (dd, *J* = 19.5, 2.4 Hz, 1H), 2.48-2.30 (comp. m, 2H), 2.10-1.93 (comp. m, 2H), 1.83-1.64 (comp. m, 2H), 1.31 (t, *J* = 7.1 Hz, 3H).

^{13}C NMR (100 MHz, $CDCl_3$): δ 164.0, 162.5, 146.7, 141.3, 137.5, 136.7, 128.3, 125.1, 123.3, 117.3, 87.8, 65.5, 61.0, 47.2, 41.6, 40.7, 26.7, 14.3.

IR (ATR, neat): 2957, 1709, 1671, 1240, 700 cm^{-1}.

HRMS (ESI+): *m/z* calc'd for $(M + Na)^+$ $[C_{18}H_{19}NO_3 + Na]^+$: 320.1257, found 320.1255.

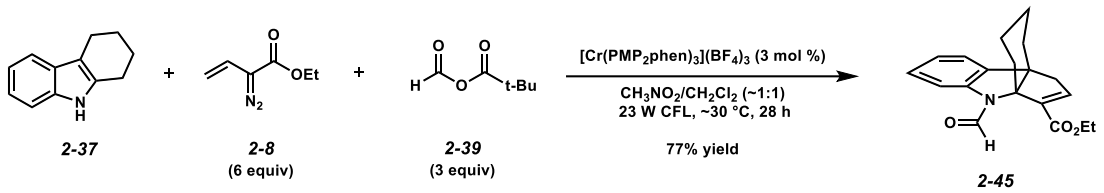

Indoline 2-45. According to General Procedure B, in a flame-dried 1-dram borosilicate vial, trimethylacetic formic anhydride (**2-39**, 70.3 mg, 0.540 mmol) was dissolved in CH_3NO_2 (0.90 mL). To this solution were added tetrahydrocarbazole **2-37** (30.9 mg, 0.180 mmol), $[Cr(PMP_2phen)_3](BF_4)_3$ (2.7 mg, 0.00180 mmol), and vinyl diazoacetate **2-8** (0.540 mL, 1.0 M in CH_2Cl_2, 0.540 mmol). The reaction mixture was irradiated with a 23 W CFL bulb while stirring. After 8 h, second charges of vinyl diazoacetate **2-8** (0.360 mL, 1.0 M in CH_2Cl_2, 0.360 mmol) and

$[Cr(PMP_2phen)_3](BF_4)_3$ (2.7 mg, 0.00180 mmol) were added, and irradiation was continued. At the 24 h timepoint, third charges of vinyl diazoacetate **2-8** (0.180 mL, 1.0 M in CH_2Cl_2, 0.180 mmol) and $[Cr(PMP_2phen)_3](BF_4)_3$ (2.7 mg, 0.00180 mmol) were added, and irradiation was continued. At the 28 h timepoint, the solvent was removed via rotary evaporation. The crude residue was dissolved in CH_2Cl_2 (~1 mL), and the solution was passed through a SiO_2 plug (0.5 x 3 cm), using CH_2Cl_2 as eluent (~8 mL). The filtrate was concentrated in vacuo, and the residue was purified by silica gel flash chromatography (4:1 hexanes/EtOAc eluent) to afford indoline **2-45** (42.9 mg, 77% yield) as a yellow oil.

TLC: R_f = 0.28 in 3:1 hexanes/EtOAc, visualized by UV.

^{1}H NMR (400 MHz, $CDCl_3$): δ 8.93 (s, 1H), 8.16 (d, *J* = 8.0 Hz, 1H), 7.23 (app. t, *J* = 8.0 Hz, 1H), 7.15 (d, *J* = 7.1 Hz, 1H), 7.08 (app. t, *J* = 7.1 Hz, 1H), 6.91 (app. s, 1H), 4.18 (q, *J* = 7.1 Hz, 2H), 2.85 (app. d, *J* = 18.7 Hz, 1H), 2.75 (app. d, *J* = 18.7 Hz, 1H), 2.59 (app. dt, *J* = 15.0, 5.0 Hz, 1H), 2.11-1.99 (m, 1H), 1.92-1.83 (m, 1H), 1.72-1.62 (m, 1H), 1.57-1.30 (comp. m, 4H), 1.28 (t, *J* = 7.1 Hz, 3H).

^{13}C NMR (100 MHz, $CDCl_3$): δ 163.7, 161.7, 145.7, 140.2, 138.5, 137.5, 128.3, 124.7, 122.4, 117.5, 60.7, 55.0, 43.0, 32.4, 29.0, 18.7, 17.7, 14.5, 14.3.

IR (ATR, neat): 2935, 1709, 1669, 1481, 1379, 753 cm^{-1}.

HRMS (ESI+): *m/z* calc'd for $(M + H)^+$ $[C_{19}H_{21}NO_3 + H]^+$: 312.1594, found 312.1591.

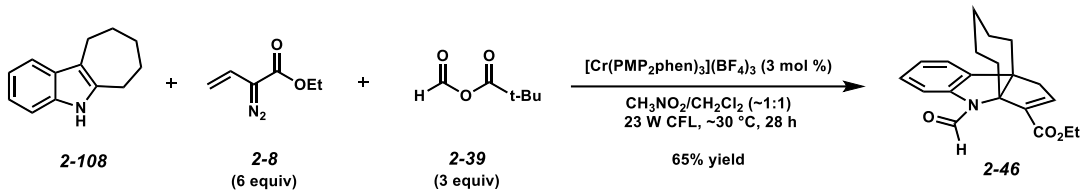

Indoline 2-46. According to General Procedure B, in a flame-dried 1-dram borosilicate vial, trimethylacetic formic anhydride (**2-39**, 54.3 mg, 0.417 mmol) was dissolved in CH_3NO_2 (0.695 mL). To this solution were added indole **2-108** (25.7 mg, 0.139 mmol), $[Cr(PMP_2phen)_3](BF_4)_3$ (2.1 mg, 0.00139 mmol), and vinyl diazoacetate **2-8** (0.417 mL, 1.0 M in CH_2Cl_2, 0.417 mmol). The reaction mixture was irradiated with a 23 W CFL bulb while stirring. After 8 h, second charges of vinyl diazoacetate **2-8** (0.278 mL, 1.0 M in CH_2Cl_2, 0.278 mmol) and $[Cr(PMP_2phen)_3](BF_4)_3$ (2.1 mg, 0.00139 mmol) were added, and irradiation was continued. At the 24 h timepoint, third charges of vinyl diazoacetate **2-8** (0.139 mL, 1.0 M in CH_2Cl_2, 0.139 mmol) and $[Cr(PMP_2phen)_3](BF_4)_3$ (2.1 mg, 0.00139 mmol) were added, and irradiation was continued. At the 28 h timepoint, the solvent was removed via rotary evaporation. The crude residue was dissolved in CH_2Cl_2 (~1 mL), and the solution was passed through a SiO_2 plug (0.5 x 3 cm), using CH_2Cl_2 as eluent (~8 mL). The filtrate was concentrated in vacuo, and the residue was purified by silica gel flash chromatography (4:1 hexanes/EtOAc eluent) to afford indoline **2-46** (29.3 mg, 65% yield) as a white solid.

TLC: R_f = 0.40 in 3:1 hexanes/EtOAc, visualized by UV.

^{1}H NMR (400 MHz, $CDCl_3$): δ 8.97 (s, 1H), 8.26 (d, *J* = 8.0 Hz, 1H), 7.23 (app. td, *J* = 8.0, 2.0 Hz, 1H), 7.16-7.06 (comp. m, 2H), 6.92 (app. t, *J* = 2.6 Hz, 1H), 4.17 (q, *J* = 7.1 Hz, 2H), 2.82 (app. d, *J* = 2.6 Hz, 2H), 2.78-2.69 (m, 1H), 2.28-2.15 (m, 1H), 2.13 (app. dd, *J* = 9.5, 5.2 Hz, 1H)

1.86 (app. dd, *J* = 9.5, 5.2 Hz, 1H), 1.64-1.47 (comp. m, 4H), 1.46-1.35 (m, 1H), 1.26 (t, *J* = 7.1 Hz, 3H), 0.99 (app. q, *J* = 9.5 Hz, 1H).

^{13}C NMR (100 MHz, $CDCl_3$): δ 163.7, 162.6, 145.6, 140.7, 137.9, 136.9, 128.4, 124.7, 122.9, 117.2, 82.5, 60.7, 60.6, 46.9, 39.9, 32.9, 30.8, 24.6, 24.0, 14.3.

IR (ATR, neat): 2928, 1709, 1668, 1483, 756 cm^{-1}.

HRMS (ESI+): *m/z* calc'd for $(M + H)^+$ $[C_{20}H_{23}NO_3 + H]^+$: 326.1751, found 326.1745.

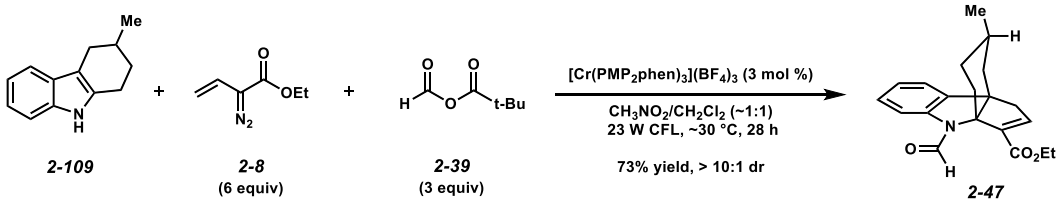

Indoline 2-47. According to General Procedure B, to a flame-dried 1-dram borosilicate vial, trimethylacetic formic anhydride (**2-39**, 64.0 mg, 0.492 mmol) was dissolved in CH_3NO_2 (0.82 mL). To this solution were added tetrahydrocarbazole **2-109** (30.4 mg, 0.164 mmol), $[Cr(PMP_2phen)_3](BF_4)_3$ (2.5 mg, 0.00164 mmol), and vinyl diazoacetate **2-8** (0.492 mL, 1.0 M in CH_2Cl_2, 0.492 mmol). The reaction mixture was irradiated with a 23 W CFL bulb while stirring. After 8 h, second charges of vinyl diazoacetate **2-8** (0.328 mL, 1.0 M in CH_2Cl_2, 0.328 mmol) and $[Cr(PMP_2phen)_3](BF_4)_3$ (2.5 mg, 0.00164 mmol) were added, and irradiation was continued. At the 24 h timepoint, third charges of vinyl diazoacetate **2-8** (0.164 mL, 1.0 M in CH_2Cl_2, 0.164 mmol) and $[Cr(PMP_2phen)_3](BF_4)_3$ (2.5 mg, 0.00164 mmol) were added, and irradiation was continued. At the 28 h timepoint, the solvent was removed via rotary evaporation. The crude residue was dissolved in CH_2Cl_2 (~1 mL), and the solution was passed through a SiO_2 plug (0.5 x 3 cm), using CH_2Cl_2 as eluent (~8 mL). The filtrate was concentrated in vacuo, and the crude ^{1}H

NMR indicated a >10:1 dr of the indoline cycloadduct. The material was purified by silica gel flash chromatography (4:1 hexanes/EtOAc eluent) to afford indoline **2-47** (38.8 mg, 73% yield, >10:1 dr) as a colorless oil. The major diastereomer was further isolated by preparatory TLC (6:1 hexanes/EtOAc eluent) for analytical characterization.

TLC: R_f = 0.33 in 3:1 hexanes/EtOAc, visualized by UV.

^{1}H NMR (400 MHz, $CDCl_3$):

Major Diastereomer: δ 8.92 (s, 1H), 8.16 (d, *J* = 8.0 Hz, 1H), 7.22 (app. t, *J* = 8.0 Hz, 1H), 7.13 (d, *J* = 7.1 Hz, 1H), 7.06 (app. t, *J* = 7.1 Hz, 1H), 6.82 (app. s, 1H), 4.22-4.11 (comp. m, 2H), 2.92-2.72 (comp. m, 3H), 1.98 (dd, *J* = 13.8, 2.6 Hz, 1H), 1.93-1.84 (m, 1H), 1.76-1.48 (comp. m, 2H), 1.27 (t, *J* = 7.1 Hz, 3H), 1.14-0.97 (comp. m, 2H), 0.91 (d, *J* = 6.3 Hz, 3H).

Minor Diastereomer: Identified by a methyl doublet at 0.85 ppm.

^{13}C NMR (100 MHz, $CDCl_3$): δ 163.5, 161.4, 144.2, 139.7, 139.5, 138.5, 128.2, 124.6, 121.7, 117.6, 76.4, 60.7, 55.4, 42.1, 39.9, 30.2, 27.4, 27.2, 22.2, 14.2.

IR (ATR, neat): 2925, 1709, 1669, 1480, 753 cm^{-1}.

HRMS (ESI+): *m/z* calc'd for $(M + H)^+$ $[C_{20}H_{23}NO_3 + H]^+$: 326.1751, found 326.1747.

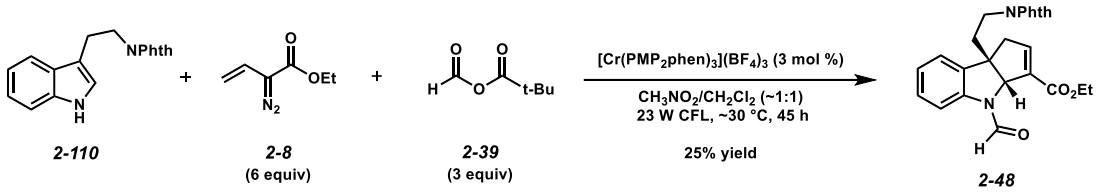

Indoline 2-48. According to General Procedure B, in a flame-dried 1-dram borosilicate vial, trimethylacetic formic anhydride (**2-39**, 41.4 mg, 0.318 mmol) was dissolved in CH_3NO_2 (0.530 mL). To this solution were added *N*-phthalimidotryptamine (**2-110**, 30.8 mg, 0.106 mmol), $[Cr(PMP_2phen)_3](BF_4)_3$ (1.6 mg, 0.00106 mmol), and vinyl diazoacetate **2-8** (0.318 mL, 1.0 M in CH_2Cl_2, 0.318 mmol). The reaction mixture was irradiated with a 23 W CFL bulb while stirring. After 8 h, second charges of vinyl diazoacetate **2-8** (0.212 mL, 1.0 M in CH_2Cl_2, 0.212 mmol) and $[Cr(PMP_2phen)_3](BF_4)_3$ (1.6 mg, 0.00106 mmol) were added, and irradiation was continued. At the 24 h timepoint, third charges of vinyl diazoacetate **2-8** (0.106 mL, 1.0 M in CH_2Cl_2, 0.106 mmol) and $[Cr(PMP_2phen)_3](BF_4)_3$ (1.6 mg, 0.00106 mmol) were added, and irradiation was continued. At the 45 h timepoint, the solvent was removed via rotary evaporation. The crude residue was dissolved in CH_2Cl_2 (~1 mL), and the solution was passed through a SiO_2 plug (0.5 x 3 cm), using CH_2Cl_2 as eluent (~8 mL). The filtrate was concentrated in vacuo, and the residue was purified by silica gel flash chromatography (2:1 hexanes/EtOAc eluent) to afford indoline **2-48** (11.6 mg, 25% yield) as a yellow oil.

TLC: R_f = 0.31 in 2:1 hexanes/EtOAc, visualized by UV.

^{1}H NMR (400 MHz, $CDCl_3$): δ 8.94 (s, 1H), 8.03 (d, *J* = 8.0 Hz, 1H), 7.83-7.75 (comp. m, 2H), 7.72-7.64 (comp. m, 2H), 7.27 (d, *J* = 7.1 Hz, 1H), 7.22 (app. t, *J* = 8.0 Hz, 1H), 7.11 (app. t, *J* = 7.1 Hz, 1H), 6.88 (app. s, 1H), 5.45 (s, 1H), 4.30-4.17 (comp. m, 2H), 3.68-3.57 (m, 1H), 3.56-

3.44 (m, 1H), 2.99 (app. d, *J* = 19.1 Hz, 1H), 2.88 (app. d, *J* = 19.1 Hz, 1H), 2.36-2.26 (m, 1H), 2.18-2.07 (m, 1H), 1.32 (t, *J* = 7.1 Hz, 3H).

^{13}C NMR (100 MHz, $CDCl_3$): δ 168.1, 163.8, 161.7, 145.7, 139.7, 136.7, 134.5, 134.2, 132.1, 128.9, 125.3, 123.4, 117.8, 72.2, 61.1, 54.1, 45.7, 37.6, 34.2, 14.3 (*1 carbon not detected*).

IR (ATR, neat): 2927, 1771, 1712, 1677, 1483, 721 cm^{-1}.

HRMS (ESI+): *m/z* calc'd for $(M + Na)^+$ $[C_{25}H_{22}N_2O_5 + Na]^+$: 453.1421, found 453.1418.

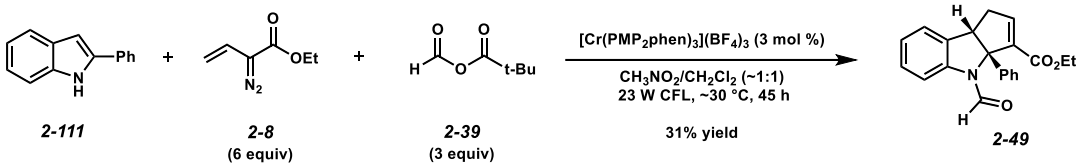

Indoline 2-49. According to General Procedure B, in a flame-dried 1-dram borosilicate vial, trimethylacetic formic anhydride (**2-39**, 62.1 mg, 0.477 mmol) was dissolved in CH_3NO_2 (0.795 mL). To this solution were added 3-phenylindole (**2-111**, 30.7 mg, 0.159 mmol), $[Cr(PMP_2phen)_3](BF_4)_3$ (2.4 mg, 0.00159 mmol), and vinyl diazoacetate **2-8** (0.477 mL, 1.0 M in CH_2Cl_2, 0.477 mmol). The reaction mixture was irradiated with a 23 W CFL bulb while stirring. After 8 h, second charges of vinyl diazoacetate **2-8** (0.318 mL, 1.0 M in CH_2Cl_2, 0.318 mmol) and $[Cr(PMP_2phen)_3](BF_4)_3$ (2.4 mg, 0.00159 mmol) were added, and irradiation was continued. At the 24 h timepoint, third charges of vinyl diazoacetate **2-8** (0.159 mL, 1.0 M in CH_2Cl_2, 0.159 mmol) and $[Cr(PMP_2phen)_3](BF_4)_3$ (2.4 mg, 0.00159 mmol) were added, and irradiation was continued. At the 45 h timepoint, the solvent was removed via rotary evaporation. The crude residue was dissolved in CH_2Cl_2 (~1 mL), and the solution was passed through a SiO_2 plug (0.5 x 3 cm), using CH_2Cl_2 as eluent (~8 mL). The filtrate was concentrated in vacuo, and the residue

was purified by silica gel flash chromatography (2:1 hexanes/Et_2O eluent) to afford indoline **2-49** (16.2 mg, 31% yield) as a yellow oil.

TLC: R_f = 0.38 in 3:1 hexanes/EtOAc, visualized by UV.

^{1}H NMR (400 MHz, $CDCl_3$): δ 8.66 (s, 1H), 8.31 (d, *J* = 8.0 Hz, 1H), 7.42-7.34 (comp. m, 2H), 7.35-7.26 (comp. m, 5H), 7.17-7.12 (comp. m, 2H), 4.20 (q, *J* = 7.1 Hz, 2H), 3.97 (d, *J* = 7.9 Hz, 1H), 3.03 (ddd, *J* = 18.8, 7.9, 2.1 Hz, 1H), 2.75 (app. dd, *J* = 18.8, 3.1 Hz, 1H), 1.25 (t, *J* = 7.1 Hz, 3H).

^{13}C NMR (100 MHz, $CDCl_3$): δ 163.5, 163.2, 149.1, 141.4, 141.3, 135.1, 132.4, 129.2, 128.7, 128.1, 126.3, 124.9, 123.9, 117.2, 82.5, 61.0, 57.9, 37.5, 14.3.

IR (ATR, neat): 2979, 1712, 1672, 1483, 736 cm^{-1}.

HRMS (ESI+): *m/z* calc'd for $(M + Na)^+$ $[C_{21}H_{19}NO_3 + Na]^+$: 356.1257, found 356.1254.

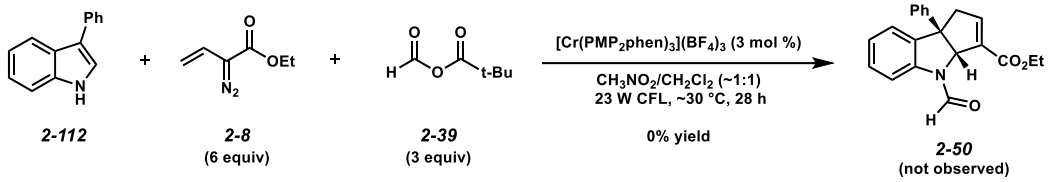

Indoline 2-50. According to a modified General Procedure B, to a flame-dried 1-dram borosilicate vial open to air, trimethylacetic formic anhydride (**2-39**, 50.8 mg, 0.390 mmol) was dissolved in CH_3NO_2 (0.650 mL). To this solution were added 3-phenylindole (**2-112**, 25.1 mg, 0.130 mmol), $[Cr(PMP_2phen)_3](BF_4)_3$ (2.0 mg, 0.00130 mmol), and vinyl diazoacetate **2-8** (0.390 mL, 1.0 M solution in CH_2Cl_2, 0.390 mmol). The vial was then capped, and the reaction mixture was

irradiated with a 23 W CFL bulb while stirring. After 8 h, second charges of vinyl diazoacetate **2-8** (0.260 mL, 1.0 M solution in CH_2Cl_2, 0.260 mmol) and $[Cr(PMP_2phen)_3](BF_4)_3$ (2.0 mg, 0.00130 mmol), were added, and irradiation was continued. After 28 h total, the solvent was removed by rotary evaporation. The crude residue was then dissolved in CH_2Cl_2 (~1 mL), and the solution was passed through a SiO_2 plug (0.5 x 3 cm), using CH_2Cl_2 as eluent (~8 mL). The filtrate was concentrated in vacuo, and the residue was analyzed by ^1H NMR. Cycloadduct **2-50** was not observed.

Formylation Conditions on C2/C3-Unsubstituted Indole

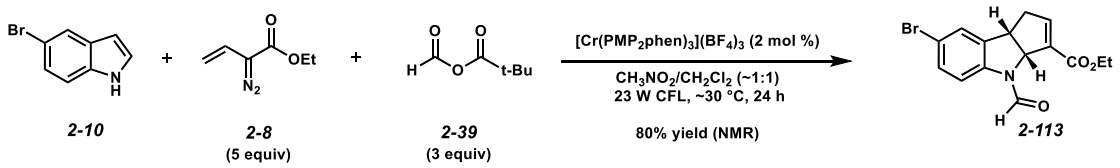

Indoline 2-113. According to a modified General Procedure B, in a flame-dried 1-dram borosilicate vial, trimethylacetic formic anhydride (**2-39**, 29.9 mg, 0.230 mmol) was dissolved in CH_3NO_2 (0.383 mL). To this solution were added 5-bromoindole (**2-10**, 15.0 mg, 0.0765 mmol), $[Cr(PMP_2phen)_3](BF_4)_3$ (1.1 mg, 0.000765 mmol), and vinyl diazoacetate **2-8** (0.230 mL, 1.0 M in CH_2Cl_2, 0.230 mmol). The reaction mixture was irradiated with a 23 W CFL bulb while stirring. After 8 h, second charges of vinyl diazoacetate **2-8** (0.153 mL, 1.0 M in CH_2Cl_2, 0.153 mmol) and $[Cr(PMP_2phen)_3](BF_4)_3$ (1.1 mg, 0.000765 mmol) were added, and irradiation was continued. At the 24 h timepoint, the solvent was removed via rotary evaporation. The crude residue was dissolved in CH_2Cl_2 (~1 mL), and the solution was passed through a SiO_2 plug (0.5 x 3 cm), using CH_2Cl_2 as eluent (~8 mL). The filtrate was concentrated in vacuo, and the crude residue was analyzed by ^1H NMR using CH_2Br_2 as an internal standard. Cycloadduct **2-113** was observed in 80% NMR yield.

γ-Substituted Diazo Reagent Evaluation

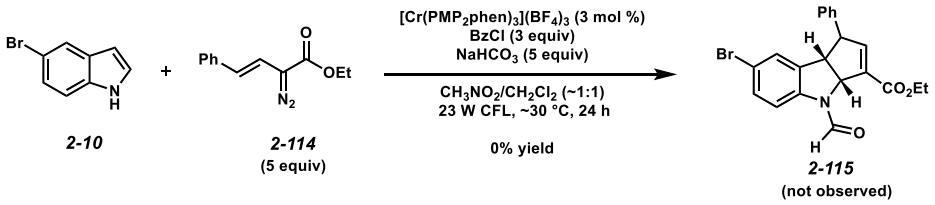

Indoline 2-115. According to General Procedure A, 5-bromoindole (**2-10**, 10.0 mg, 0.0510 mmol), $NaHCO_3$ (21.4 mg, 0.255 mmol), and $[Cr(PMP_2phen)_3](BF_4)_3$ (1.1 mg, 0.000765 mmol) were added to a flame-dried 1-dram borosilicate vial open to air. The reagents were suspended in CH_3NO_2 (0.255 mL), and to this suspension were added benzoyl chloride (17.8 μL, 0.153 mmol) and vinyl diazoacetate **2-114** (0.153 mL, 1.0 M solution in CH_2Cl_2, 0.153 mmol). The vial was then capped, and the reaction mixture was irradiated with a 23 W CFL bulb while stirring. After 8 h, second charges of vinyl diazoacetate **2-114** (0.102 mL, 1.0 M solution in CH_2Cl_2, 0.102 mmol) and $[Cr(PMP_2phen)_3](BF_4)_3$ (1.1 mg, 0.000765 mmol) were added, and irradiation was continued. After 24 h total, solvent was removed by rotary evaporation. The crude residue was then dissolved in CH_2Cl_2 (~1 mL), and the solution was passed through a SiO_2 plug (0.5 x 3 cm), using CH_2Cl_2 as eluent (~8 mL). The filtrate was concentrated in vacuo, and the residue was analyzed by ^1H NMR. Cycloadduct **2-115** was not observed.

2.12.5. Cycloaddition Product Diversification

Suzuki Coupling—4-methoxyphenylboronic acid

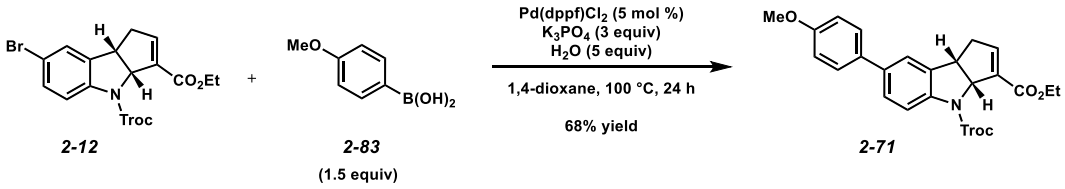

Coupling product 2-71. A vial charged with indoline **2-12** (39.1 mg, 0.0809 mmol), 4-methoxyphenylboronic acid (**2-83**, 18.4 mg, 0.121 mmol), K_3PO_4 (51.5 mg, 0.243 mmol), and $Pd(dppf)Cl_2$ (3.0 mg, 0.00404 mmol) in 1,4-dioxane (0.323 mL) and H_2O (7.3 µL, 0.404 mmol) was degassed with argon for 15 min at 23 °C. The reaction mixture was then heated to 100 °C and stirred for 24 h, at which point the reaction had proceeded to completion as determined by TLC. The reaction mixture was diluted with EtOAc (2 mL) and filtered through a celite plug (0.5 x 2 cm), eluting with EtOAc (15 mL). The filtrate was washed sequentially with H_2O (3 x 10 mL) and brine (10 mL). The organic layer was dried over Na_2SO_4 and concentrated in vacuo. The crude reside was purified by flash chromatography (2:1 hexanes/Et_2O eluent) to afford coupling product **2-71** (28.1 mg, 68% yield) as a white solid.

TLC R_f: 0.38 in 1:1 hexanes/Et_2O, visualized by UV, stained blue in Hanessian's stain.

^{1}H NMR (400 MHz, $CDCl_3$): δ 7.89-7.62 (br. m, 1H), 7.47 (d, *J* = 8.8 Hz, 2H), 7.43 (d, *J* = 8.4 Hz, 1H), 7.36 (s, 1H), 6.96 (d, *J* = 8.8 Hz, 2H), 6.86 (app. s, 1H), 5.93 (app. d, *J* = 6.2 Hz, 1H),

5.38-4.53 (comp. m, 2H), 4.26-4.11 (comp. m, 3H), 3.85 (s, 3H), 3.06 (app. ddt, *J* = 18.3, 7.7, 2.0 Hz, 1H), 2.85 (app. d, *J* = 18.3 Hz, 1H), 1.27 (t, *J* = 7.1 Hz, 3H).

^{13}C NMR (125 MHz, 50 °C, $CDCl_3$): δ 164.0, 159.4, 151.9, 144.8, 139.6, 137.4, 136.0, 135.3, 133.7, 128.1, 127.1, 122.6, 117.4, 114.5, 95.6, 75.8, 69.2, 60.6, 55.5, 44.0, 37.9, 14.4.

IR (ATR, neat): 2953, 1720, 1609, 1485, 1254, 822 cm^{-1}.

HRMS (ESI+): *m/z* calc'd for $(M + H)^+$ $[C_{24}H_{22}Cl_3NO_5 + H]^+$: 510.0636, found 510.0628.

Suzuki Coupling—Indole boronate

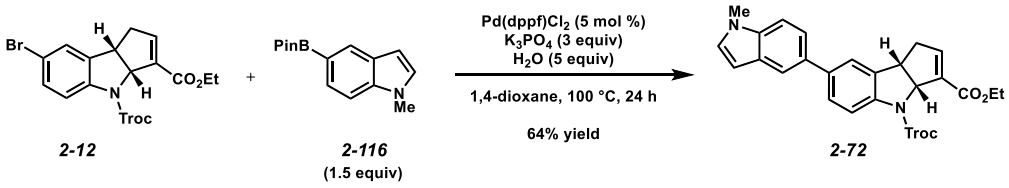

Coupling product 2-72. A vial charged with indoline **2-12** (35.6 mg, 0.0736 mmol), *N*-Me indole boronate (**2-116**, 28.4 mg, 0.110 mmol), K_3PO_4 (46.9 mg, 0.221 mmol), and $Pd(dppf)Cl_2$ (2.7 mg, 0.00368 mmol) in 1,4-dioxane (0.294 mL) and H_2O (6.6 µL, 0.368 mmol) was degassed with argon for 15 min at 23 °C. The reaction mixture was then heated to 100 °C and stirred for 24 h, at which point the reaction had proceeded to completion as determined by TLC. The reaction mixture was diluted with EtOAc (2 mL) and filtered through a celite plug (0.5 x 2 cm), eluting with EtOAc (15 mL). The filtrate was washed sequentially with H_2O (3 x 10 mL) and brine (10 mL). The organic layer was dried over Na_2SO_4 and concentrated in vacuo. The crude reside was purified by flash chromatography (2:1 hexanes/EtOAc eluent) to afford coupling product **2-72** (25.1 mg, 64% yield) as a white solid.

TLC R_f: 0.46 in 2:1 hexanes/EtOAc, visualized by UV, stained blue in Hanessian's stain.

^{1}H NMR (500 MHz, 50 °C, C_6D_6): δ 8.21-8.08 (br. m, 1H), 7.89 (s, 1H), 7.55 (d, *J* = 8.4 Hz, 1H), 7.49 (dd, *J* = 8.5, 1.4 Hz, 1H), 7.32 (s, 1H), 7.11 (d, *J* = 8.5 Hz, 1H), 6.62 (d, *J* = 3.0 Hz, 1H), 6.54 (d, *J* = 3.0 Hz, 1H), 6.51-6.45 (m, 1H), 5.87 (d, *J* = 7.1 Hz, 1H), 5.47-4.94 (br. m, 1H), 4.76 (d, *J* = 11.9 Hz, 1H), 4.09-3.91 (comp. m, 2H), 3.55-3.47 (m, 1H), 3.04 (s, 3H), 2.34-2.22 (comp. m, 2H), 1.00 (t, *J* = 7.0 Hz, 3H).

^{13}C NMR (125 MHz, 50 °C, C_6D_6): δ 163.7, 151.9, 144.5, 139.9, 139.4, 136.9, 136.1, 135.5, 133.2, 129.9, 129.4, 123.3, 121.7, 119.8, 117.5, 109.7, 101.9, 96.3, 75.9, 69.4, 60.3, 44.0, 37.7, 32.2, 14.3 (*1 carbon not detected*).

IR (ATR, neat): 2980, 2950, 1716, 1633, 1479 cm^{-1}.

HRMS (ESI+): *m/z* calc'd for $(M + H)^+$ $[C_{26}H_{23}Cl_3N_2O_4 + H]^+$: 533.0796, found 533.0786.

(3+2) Cycloaddition Reaction—Nitrile Oxide

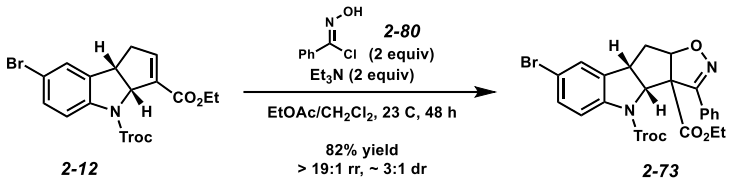

Cycloadduct 2-73. According to a modification of a procedure by Benltifa and co-workers,[33] in a flame-dried flask under argon, to a solution of indoline **2-12** (40.4 mg, 0.0835 mmol) and iminoyl chloride **2-80** (13.0 mg, 0.0835 mmol) in EtOAc (0.334 mL) at room temperature was added a solution of Et_3N (11.6 µL, 0.0835 mmol) in CH_2Cl_2 (0.334 mL) dropwise over 30 min. Triethylammonium chloride precipitated from the reaction mixture over time. After 8 h, an additional charge of iminoyl chloride **2-80** (13.0 mg, 0.0835 mmol) was added to the reaction

mixture, followed by the addition of a solution of Et_3N (11.6 µL, 0.0835 mmol) in CH_2Cl_2 (0.334 mL) over 30 min. After 48 h total, H_2O (5 mL) was added, and the layers were separated. The aqueous layer was then extracted with EtOAc (3 x 10 mL). The combined organic layers were washed sequentially with H_2O (15 mL) and brine (15 mL), and then dried over Na_2SO_4 and concentrated in vacuo. The crude residue was purified by flash chromatography (2:1 hexanes/Et_2O eluent) to afford cycloadduct **2-73** (41.3 mg, 82% yield, ~3:1 dr) as a white solid.

TLC R_f: 0.41 in 1:1 hexanes/Et_2O, visualized by UV, stained blue in Hanessian's stain.

^{1}H NMR (400 MHz, C_6D_6):

Major Diastereomer: δ 8.05 (d, *J* = 8.6 Hz, 1H), 7.08 (dd, *J* = 8.6, 0.8 Hz, 1H), 7.06-6.90 (comp. m, 3H), 6.81 (app. dd, *J* = 8.2, 1.4 Hz, 2H), 6.31 (app. t, *J* = 1.5 Hz, 1H), 5.37 (d, *J* = 8.8 Hz, 1H), 5.29 (d, *J* = 12.2 Hz, 1H), 4.27 (d, *J* = 12.2 Hz, 1H), 4.07 (q, *J* = 7.1 Hz, 2H), 3.89 (app. dd, *J* = 7.4, 1.6 Hz, 1H), 3.22 (app. t, *J* = 7.5 Hz, 1H), 2.05-1.85 (comp. m, 2H), 1.00 (t, *J* = 7.1 Hz, 3H).

Minor Diastereomer: δ 7.63 (d, *J* = 8.6 Hz, 1H), 7.14 (dd, *J* = 8.6, 0.8 Hz, 1H), 7.06-6.90 (comp. m, 3H), 6.81 (app. dd, *J* = 8.2, 1.4 Hz, 2H), 6.38 (app. t, *J* = 1.5 Hz, 1H), 5.48 (d, *J* = 8.8 Hz, 1H), 4.86 (d, *J* = 12.2 Hz, 1H), 4.32 (d, *J* = 12.2 Hz, 1H), 4.12 (q, *J* = 7.2 Hz, 2H), 3.96 (app. dd, *J* = 7.4, 1.6 Hz, 1H), 3.22 (app. t, *J* = 7.5 Hz, 1H), 2.05-1.85 (comp. m, 2H), 1.11 (t, *J* = 7.2 Hz, 3H).

^{13}C NMR (125 MHz, 50 °C, C_6D_6, *both diastereomers*): δ 172.1, 171.3, 158.9, 158.7, 151.9, 150.8, 142.8, 141.5, 135.1, 134.1, 131.68, 131.65, 130.2, 130.1, 128.8, 128.7, 127.6, 127.4, 127.2, 127.1, 116.9 (2), 116.0, 115.9, 96.1, 95.5, 94.4, 94.0, 75.7, 74.9, 73.3, 72.0, 62.2, 62.1, 60.2, 59.8, 45.5, 44.9, 33.1, 32.4, 14.2, 14.1 (*2 carbons not detected*).

IR (ATR, neat): 2980, 1727, 1477, 1157, 822 cm^{-1}.

HRMS (ESI+): *m/z* calc'd for $(M + H)^+$ $[C_{24}H_{20}BrCl_3N_2O_5 + H]^+$: 600.9694, found 600.9675.

Relative stereochemistries of the major/minor diastereomers were not ascertained.

(3+2) Cycloaddition Reaction—Glycine Imine

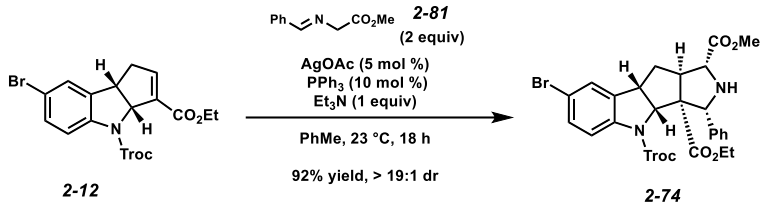

Cycloadduct 2-74. According to a modification of a procedure by Mancebo-Aracil and co-workers,[34] to a flame-dried flask wrapped in aluminum foil under argon, AgOAc (0.6 mg, 0.00367 mmol) and PPh_3 (1.9 mg, 0.00734 mmol) were suspended in toluene (0.734 mL) at 23 °C, and the suspension was stirred for 15 min. A solution of indoline **2-12** (35.5 mg, 0.0734 mmol) and imine acetate **2-81** (26.0 mg, 0.147 mmol) in toluene (0.734 mL) at room temperature was then added dropwise to the stirring mixture of AgOAc/PPh_3 at room temperature over 10 min. Et_3N (10.2 µL, 0.0734 mmol) was then added to the reaction mixture, and the resulting mixture was stirred to reaction completion, as determined by TLC. The reaction mixture was diluted with EtOAc (2 mL) and filtered through a celite plug (0.5 x 2 cm, eluting with 10 mL EtOAc), and the filtrate was concentrated in vacuo. The crude residue was purified by flash chromatography (4:1 hexane/Et_2O eluent) to afford cycloadduct **2-74** (44.6 mg, 92% yield, >19:1 dr) as a colorless oil.

TLC R_f: 0.35 in 1:1 hexanes/Et_2O, visualized by UV, stained blue in Hanessian's stain.

^{1}H NMR (400 MHz, $CDCl_3$): δ 7.77-7.51 (br. m, 1H), 7.39 (s, 1H), 7.36 (d, *J* = 5.7 Hz, 1H), 7.30-7.20 (comp. m, 5H), 5.75 (d, *J* = 9.1 Hz, 1H), 5.33-4.63 (br. m, 2H), 4.39 (br. s, 1H), 4.17-4.07

(br. m, 1H), 3.75 (s, 3H), 3.75-3.56 (br. m, 2H), 3.44-3.32 (br. m, 1H), 2.96 (br. d, J = 8.8 Hz, 1H), 2.61 (br. s, 1H), 2.45-2.28 (br. m, 2H), 0.81 (t, J = 7.1 Hz, 3H).

^{13}C NMR (125 MHz, 50 °C, $CDCl_3$): δ 173.2, 172.7, 152.4, 140.8, 140.7, 138.4, 131.5, 128.2, 127.9, 127.6, 127.2, 118.8, 117.7, 95.2, 75.7, 72.7, 70.7, 66.8, 64.4, 61.4, 55.9, 52.3, 47.1, 32.9, 13.6.

IR (ATR, neat): 3356, 2953, 1727, 1477, 754 cm^{-1}.

HRMS (ESI+): *m/z* calc'd for $(M + H)^+$ $[C_{27}H_{26}BrCl_3N_2O_6 + H]^+$: 659.0113, found 659.0092.

The relative stereochemistry of cycloadduct **2-74** was assigned by analogy to a similar Ag-catalyzed (3+2) cycloaddition by Guo and coworkers,[35] where the stereochemistry was confirmed by X-ray analysis.

Conjugate Reduction

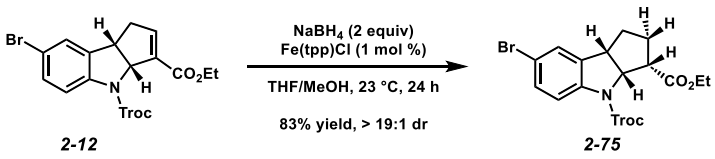

Saturated ester 2-75. According to a modification of a procedure by Sakaki and co-workers,[29] in an argon-filled glove box a 2-dram vial was charged with Fe(tpp)Cl (0.4 mg, 0.631 μmol). The vial was removed from the glovebox and equipped to a Schlenk line under argon. The Fe complex was then dissolved in THF (0.315 mL) and MeOH (0.315 mL, distilled over MS3Å) at 23 °C. In a separate flame-dried vial, indoline **2-12** (30.5 mg, 0.0631 mmol) and $NaBH_4$ (4.8 mg, 0.126 mmol) were suspended in THF (0.315 mL) at 23 °C. The solution of the Fe(tpp)Cl complex was then added dropwise to the indoline mixture over 15 min, and the resulting mixture was stirred at

room temperature. After 24 h, the reaction mixture was quenched by the addition of sat. aq. NH_4Cl (10 mL), and the mixture was extracted with EtOAc (3 x 10 mL). The combined organic extracts were washed sequentially with H_2O (20 mL) and brine (20 mL), and then dried over Na_2SO_4 and concentrated in vacuo. The crude residue was purified by flash chromatography (9:1 hexane/Et_2O eluent) to afford saturated ester **2-75** (25.4 mg, 83% yield, >19:1 dr) as a colorless oil.

Ester **2-75** appears as an approx. 3:1 mixture of major and minor rotamers in the ^{1}H NMR spectrum. The signals begin to coalesce at elevated temperatures.

TLC R_f: 0.65 in 2:1 hexanes/Et_2O, visualized by UV, stained blue in Hanessian's stain.

^{1}H NMR (400 MHz, $CDCl_3$):

Major rotamer: δ 7.70 (d, *J* = 8.6 Hz, 1H), 7.34 (app. d, *J* = 8.6 Hz, 1H), 7.28 (app. s, 1H), 5.23 (app. d, *J* = 8.6 Hz, 1H), 4.93 (d, *J* = 11.8 Hz, 1H), 4.75 (d, *J* = 11.8 Hz, 1H), 4.14 (app. q, *J* = 7.1 Hz, 2H), 4.01 (app. t, *J* = 7.9 Hz, 1H), 3.19 (app. d, *J* = 7.9 Hz, 1H), 2.20-2.07 (m, 1H), 2.03-1.86 (comp. m, 2H), 1.85-1.69 (comp. m, 1H), 1.27 (app. t, *J* = 7.1 Hz, 3H).

Minor rotamer (diagnostic signals): δ 7.53 (d, *J* = 8.5 Hz, 1H), 5.15-5.07 (m, 1H), 4.97-4.86 (comp. m, 2H), 4.20 (app. q, *J* = 7.2 Hz, 2H), 3.96-3.84 (m, 1H), 3.04-2.95 (m, 1H), 2.35-2.24 (br. m, 1H).

^{13}C NMR (125 MHz, 50 °C, $CDCl_3$): δ 173.8, 141.5, 136.6, 131.0, 127.6, 116.5, 116.3, 95.2, 75.0, 67.0, 61.0, 52.4, 45.6, 32.8, 28.8, 14.4 (*1 carbon not detected*).

IR (ATR, neat): 2956, 1723, 1479, 1396, 1136 cm^{-1}.

HRMS (ESI+): *m/z* calc'd for $(M + H)^+$ $[C_{17}H_{17}BrCl_3NO_4 + H]^+$: 483.9479, found 483.9472.

The relative stereochemistry of the major diastereomer of saturated ester **2-75** was confirmed through 2D NOESY NMR analysis.

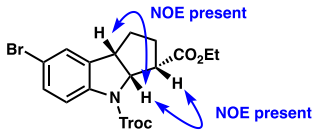

Reduction

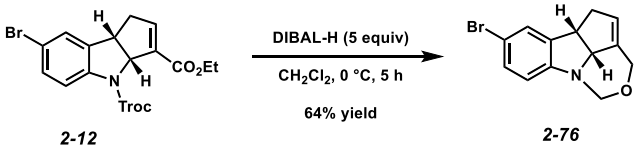

2-12 2-76

Aminal 2-76. In a flame-dried flask under argon, to a solution of indoline **2-12** (30.0 mg, 0.0620 mmol) in CH_2Cl_2 (0.620 mL) at 0 °C was added DIBAL-H (0.310 mL, 1.0 M in hexanes, 0.310 mmol). The reaction mixture was stirred at 0 °C for 5 h, at which point the starting material was consumed as determined by TLC. The reaction mixture was diluted with Et_2O (15 mL) and quenched by the addition of sat. aq. Rochelle's salt (15 mL). The biphasic mixture was stirred for 1 h at room temperature. The layers were then separated, and the aqueous layer was extracted with Et_2O (3 x 10 mL). The combined organic extracts were washed with brine (15 mL), dried over Na_2SO_4, and concentrated in vacuo. The crude residue was purified by flash chromatography (4:1 hexanes/Et_2O eluent) to afford aminal **2-76** (11.0 mg, 64% yield) as a white solid.

TLC R_f: 0.43 in 2:1 hexanes/Et_2O, visualized by UV, stained blue in Hanessian's stain.

^{1}H NMR (400 MHz, $CDCl_3$): δ 7.25 (s, 1H), 7.24 (d, *J* = 8.4 Hz, 1H), 6.59 (d, *J* = 8.4 Hz, 1H), 5.68-5.57 (m, 1H), 5.20 (d, *J* = 11.5 Hz, 1H), 4.77 (d, *J* = 11.5 Hz, 1H), 4.64 (d, *J* = 6.8 Hz, 1H), 4.46 (d, *J* = 12.2 Hz, 1H), 4.29 (d, *J* = 12.2 Hz, 1H), 3.80 (app. t, *J* = 6.8 Hz, 1H), 2.95-2.85 (m, 1H), 2.49 (app. d, *J* = 16.4 Hz, 1H).

^{13}C NMR (100 MHz, $CDCl_3$): δ 148.1, 138.0, 136.0, 131.0, 128.2, 125.2, 111.9, 111.6, 76.5, 70.4, 67.5, 43.5, 38.5.

IR (ATR, neat): 2919, 2849, 1473, 1027, 810 cm^{-1}.

HRMS (ESI+): *m/z* calc'd for $(M + H)^+$ $[C_{13}H_{12}BrNO + H]^+$: 278.0175, found 278.0172.

Allylic Oxidation

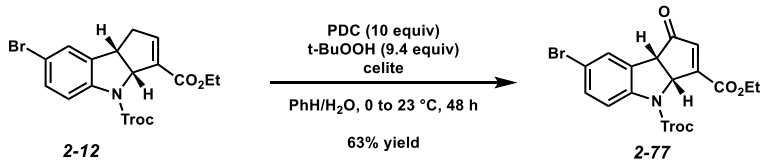

Enone 2-77. According to a modification of a procedure by Guandalini and coworkers,[27] indoline **2-12** (45.2 mg, 0.0934 mmol), celite (0.163 g, 1.75 g/mmol of **2-12**), and PDC (0.176 g, 0.467 mmol) were dissolved in benzene (1.00 mL) and cooled to 0 °C. *t*-BuOOH (60.1 µL, 70% wt. in H_2O, 0.439 mmol) was then added at 0 °C with vigorous stirring. The reaction mixture was allowed to warm to 23 °C and stir for 24 h. After 24 h, second charges of PDC (0.176 g, 0.467 mmol) and *t*-BuOOH (60.1 µL, 70% wt. in H_2O, 0.439 mmol) were added at 23 °C, and the mixture was stirred for an additional 24 h. After 48 h total, the reaction mixture was diluted with Et_2O (~ 20 mL), and the solids were removed by vacuum filtration using a Buchner funnel, rinsing with Et_2O (~ 20 mL). The filtrate was then dried over $MgSO_4$ and concentrated in vacuo. The crude residue was purified by flash chromatography (2:1 hexanes/Et_2O eluent) to afford enone **2-77** (29.3 mg, 63% yield) as a white solid.

TLC R_f: 0.47 in 1:1 hexanes/Et_2O, visualized by UV, stained blue in Hanessian's stain.

^{1}H NMR (400 MHz, $CDCl_3$): δ 7.60 (br. s, 1H), 7.58 (s, 1H), 7.42 (dd, *J* = 8.7, 1.4 Hz, 1H), 6.68 (d, *J* = 1.0 Hz, 1H), 5.97 (dd, *J* = 6.7, 1.0 Hz, 1H), 5.33-4.49 (br. m, 2H), 4.32 (q, *J* = 7.1 Hz, 2H), 4.24 (d, *J* = 6.7 Hz, 1H), 1.34 (t, *J* = 7.1 Hz, 3H).

^{13}C NMR (125 MHz, 50 °C, $CDCl_3$): δ 201.6, 163.6, 160.5, 151.6, 139.6, 137.2, 132.7, 128.7, 128.1, 118.8, 117.5, 95.0, 76.0, 63.5, 62.3, 52.2, 14.2.

IR (ATR, neat): 2982, 1725, 1613, 1477, 1250, 820 cm^{-1}.

HRMS (ESI+): *m/z* calc'd for $(M + H)^+$ $[C_{17}H_{13}BrCl_3NO_5 + H]^+$: 495.9115, found 495.9106.

Removal of Troc Group

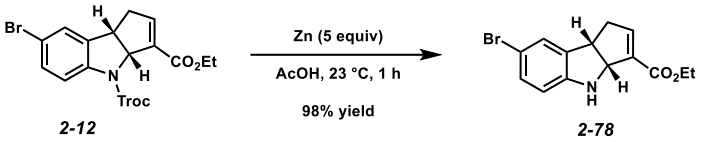

N-H Indoline 2-78. To a solution of indoline **2-12** (30.5 mg, 0.0631 mmol) in AcOH (0.631 mL) in a flame-dried vial under argon at 23 °C was added zinc dust (20.6 mg, 0.315 mmol), and the resulting mixture was stirred for 1 h. Upon completion, the reaction mixture was concentrated in vacuo. The crude residue was suspended in EtOAc (~2 mL), and the mixture was passed through a celite plug (0.5 x 2 cm), eluting with EtOAc (~10 mL). The filtrate was then washed sequentially with sat. aq. $NaHCO_3$ (20 mL), H_2O (20 mL), and brine (20 mL), and then dried over Na_2SO_4 and concentrated in vacuo. The crude residue was then purified by flash chromatography (4:1 hexanes/EtOAc eluent) to afford N-H indoline **2-78** (19.0 mg, 98% yield) as a yellow oil.

TLC R_f: 0.54 in 2:1 hexanes/Et_2O, visualized by UV, stained blue in Hanessian's stain.

^{1}H NMR (400 MHz, $CDCl_3$): δ 7.16 (s, 1H), 7.10 (d, *J* = 8.3 Hz, 1H), 6.86 (app. s, 1H), 6.46 (d, *J* = 8.3 Hz, 1H), 5.02 (d, *J* = 8.4 Hz, 1H), 4.60 (br. s, 1H), 4.22 (q, *J* = 7.1 Hz, 2H), 4.04 (app. t, *J* =

8.2 Hz, 1H), 3.05 (app. dd, *J* = 18.7, 8.2 Hz, 1H), 2.69 (app. d, *J* = 18.7 Hz, 1H), 1.30 (t, *J* = 7.1 Hz, 1H).

^{13}C NMR (100 MHz, $CDCl_3$): δ 164.7, 148.7, 144.5, 136.0, 134.6, 130.9, 127.5, 111.1, 109.9, 67.9, 60.7, 44.5, 40.1, 14.4.

IR (ATR, neat): 3391, 2926, 1704, 1478, 808 cm^{-1}.

HRMS (ESI+): *m/z* calc'd for $(M + H)^+$ $[C_{14}H_{14}BrNO_2 + H]^+$: 308.0281, found 308.0273.

Deprotection of Formyl Group

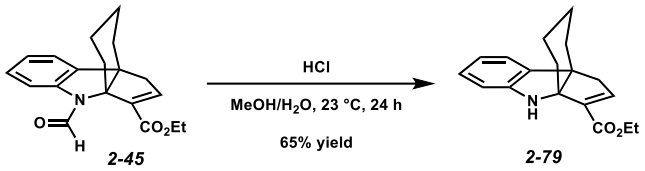

N-H Indoline 2-79. According to a modification of a procedure by Sheehan and Yang,[36] in a flame-dried flask under argon, indoline **2-45** (36.5 mg, 0.117 mmol) was dissolved in a 12:1 mixture of MeOH/conc. HCl (0.500 mL) at 23 °C. The reaction mixture was stirred for 24 h. The mixture was then neutralized with sat. aq. $NaHCO_3$ (2 mL) and extracted with EtOAc (3 x 10 mL). The combined organic extracts were washed with brine (20 mL), dried over $MgSO_4$, and concentrated in vacuo. The crude residue was purified by flash chromatography (4:1 hexanes/EtOAc eluent) to afford N-H indoline **2-79** (21.5 mg, 65% yield) as a yellow oil.

TLC: R_f = 0.43 in 4:1 hexanes/EtOAc, visualized by UV.

^{1}H NMR (400 MHz, $CDCl_3$): δ 7.03 (app. t, *J* = 7.4 Hz, 2H), 6.76 (app. s, 1H), 6.71 (app. t, *J* = 7.4 Hz, 1H), 6.62 (d, *J* = 7.4 Hz, 1H), 4.77 (br. s, 1H), 4.15 (q, *J* = 7.1 Hz, 2H), 2.81-2.69 (comp. m, 2H), 2.38 (app. d, *J* = 13.0 Hz, 1H), 1.92 (app. d, *J* = 13.0 Hz, 1H), 1.62-1.34 (comp. m, 6H), 1.27 (t, *J* = 7.1 Hz, 3H).

^{13}C NMR (100 MHz, $CDCl_3$): δ 164.5, 148.8, 142.6, 139.8, 138.5, 127.8, 122.4, 118.7, 109.9, 74.4, 60.3, 53.3, 41.3, 33.7, 32.6, 20.8, 19.6, 14.4.

IR (ATR, neat): 3376, 2930, 1700, 1242, 743 cm^{-1}.

HRMS (ESI+): *m/z* calc'd for $(M + H)^+$ $[C_{18}H_{21}NO_2 + H]^+$: 284.1645, found 284.1640.

2.12.6. Photocatalyst Monitoring Experiments

Evaluation of $[Cr(PMP_2phen)_3]^{3+}$

Procedure: $[Cr(PMP_2phen)_3](BF_4)_3$ (2.5 mg, 0.00166 mmol) was dissolved in CH_2Cl_2 (8.3 mL). A baseline UV-Vis measurement was then taken. BzCl (57.9 μL, 0.498 mmol, 300 equiv) was then added to the mixture. The solution was then placed in the photobox and irradiated by a 23 W CFL bulb for 18 h, withdrawing aliquots of the solution at 1, 2, 4, and 24 h timepoints, and measuring their UV-Vis absorbances. The data is recorded below.

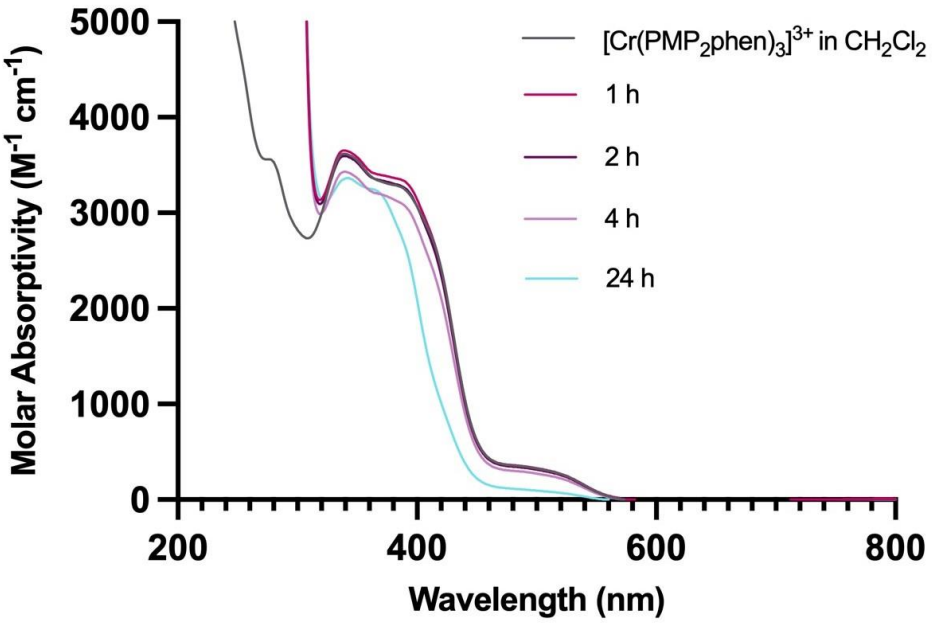

Figure 2.12.2. $[Cr(PMP_2phen)_3](BF_4)_3$ and 300 equiv of BzCl in CH_2Cl_2 irradiated with a 23 W CFL bulb over time.

Evaluation of $[Ru(bpz)_3]^{2+}$

Procedure: $[Ru(bpz)_3](PF_6)_2$ (8.6 mg, 0.010 mmol) was dissolved in acetonitrile (50 mL). A baseline UV-Vis measurement was then taken. BzCl (0.348 mL, 3.00 mmol, 300 equiv) was then added to the mixture, and another baseline measurement (0 h timepoint) was taken. Half of the solution (25 mL) was then placed in the photobox and irradiated by a 23 W CFL bulb for 24 h, withdrawing aliquots of the solution at 1, 2, 4, and 24 h timepoints, and measuring their UV-Vis absorbances. The other half of the solution (25 mL) was kept in the dark for 24 h, withdrawing aliquots at the same timepoints and measuring their UV-Vis absorbances. The data is recorded below.

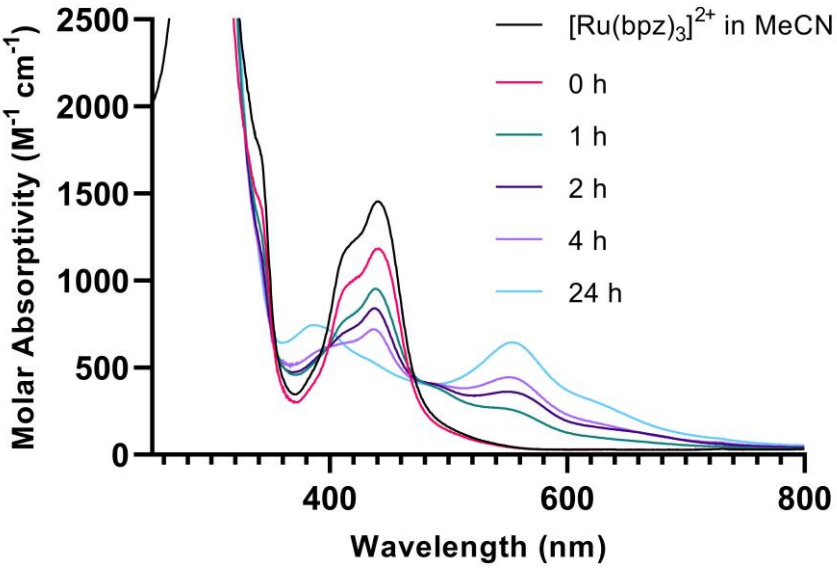

Figure 2.12.3. $[Ru(bpz)_3](PF_6)_2$ and 300 equiv of BzCl in acetonitrile irradiated with a 23 W CFL bulb over time.

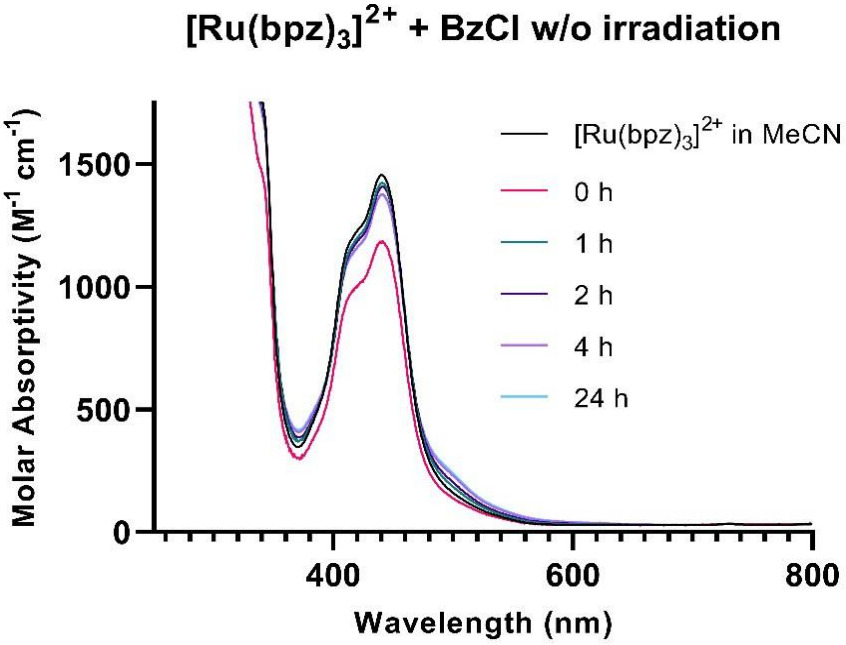

Figure 2.12.4. $[Ru(bpz)_3](PF_6)_2$ and 300 equiv of BzCl in acetonitrile over time.

Procedure: A solution of benzoyl chloride (0.348 mL, 3.00 mol) in acetonitrile (50 mL) was irradiated over the course of 24 h. No appreciable change between the 0 h timepoint and 24 h timepoint was observed.

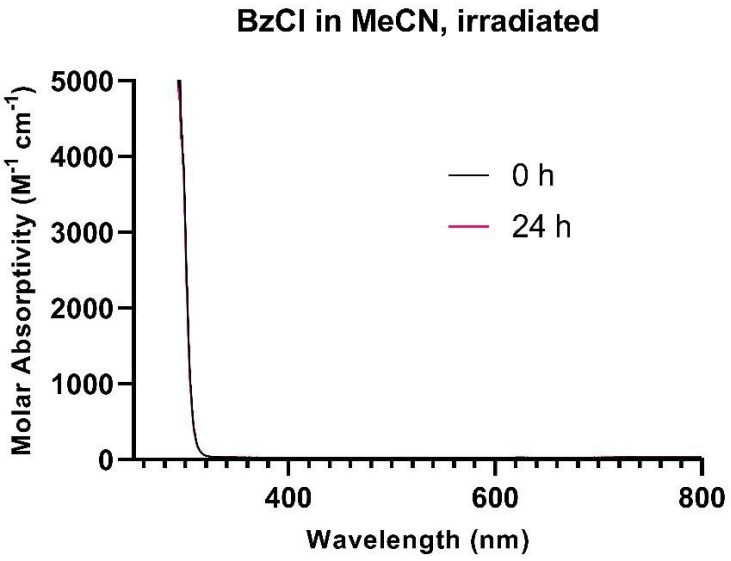

Figure 2.12.5. BzCl in acetonitrile irradiated with a 23 W CFL bulb over 24 h. (Lines are overlapping.)

2.12.7. Mechanistic Experiments

Reaction of N-Substituted Indoles & Evaluation of Indole Protection

Reaction of Troc-Protected Indole

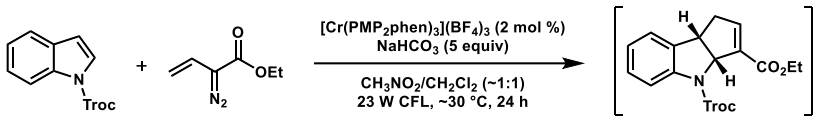

2-51 | *2-8* (5 equiv) | *2-16* (not observed)

According to a modified General Procedure A, indole **2-51** (30.0 mg, 0.103 mmol), $NaHCO_3$ (43.1 mg, 0.515 mmol), and $[Cr(PMP_2phen)_3](BF_4)_3$ (1.5 mg, 0.00103 mmol) were added to a flame-dried 1-dram borosilicate vial. The reagents were suspended in CH_3NO_2 (0.515 mL), and to this solution was added vinyl diazoacetate **2-8** (0.309 mL, 1.0 M in CH_2Cl_2, 0.309 mmol). The reaction mixture was irradiated with a 23 W CFL bulb while stirring. After 8 h, second charges of vinyl diazoacetate **2-8** (0.206 mL, 1.0 M in CH_2Cl_2, 0.206 mmol) and $[Cr(PMP_2phen)_3](BF_4)_3$ (1.5 mg, 0.00103 mmol) were added, and irradiation was continued. At the 24 h timepoint, the solvent was removed via rotary evaporation. The crude residue was dissolved in CH_2Cl_2 (~1 mL), and the solution was passed through a SiO_2 plug (0.5 x 3 cm), using CH_2Cl_2 as eluent (~8 mL). The filtrate was concentrated in vacuo, and the residue was analyzed by ^1H NMR using CH_2Br_2 as an internal standard, where there was a >95% recovery of indole **2-51** and no formation of indoline **2-16**.

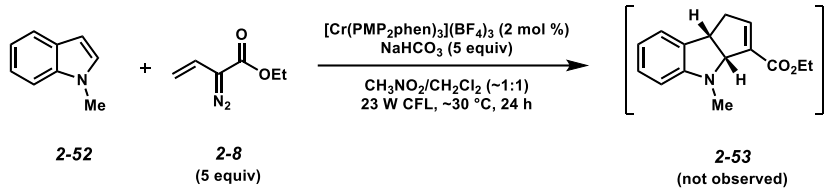

2-52 *2-8* (5 equiv) *2-53* (not observed)

According to a modified General Procedure A, indole **2-52** (14.6 μL, 0.117 mmol) was added to a flame-dried 1-dram borosilicate vial. This was dissolved in CH_3NO_2 (0.585 mL), and to this solution was added and $[Cr(PMP_2phen)_3](BF_4)_3$ (1.7 mg, 0.00117 mmol) and vinyl diazoacetate **2-8** (0.351 mL, 1.0 M in CH_2Cl_2, 0.351 mmol). The reaction mixture was irradiated with a 23 W CFL bulb while stirring. After 8 h, second charges of vinyl diazoacetate **2-8** (0.234 mL, 1.0 M in CH_2Cl_2, 0.234 mmol) and $[Cr(PMP_2phen)_3](BF_4)_3$ (1.7 mg, 0.00117 mmol) were added, and irradiation was continued. At the 24 h timepoint, the solvent was removed via rotary evaporation. The crude residue was dissolved in CH_2Cl_2 (~1 mL), and the solution was passed through a SiO_2 plug (0.5 x 3 cm), using CH_2Cl_2as eluent (~8 mL). The filtrate was concentrated in vacuo, and the residue was analyzed by ^1H NMR using CH_2Br_2as an internal standard, where there was a >95% recovery of indole **2-52** and no formation of indoline **2-53**.

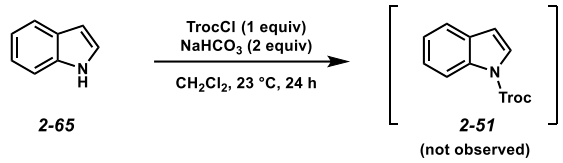

Indole **2-65** (15.0 mg, 0.128 mmol) and $NaHCO_3$ (21.5 mg, 0.256 mmol) were added to a flame-dried 1-dram borosilicate vial. The reagents were suspended in CH_2Cl_2 (1.28 mL), and to this solution was added 2,2,2-trichloroethoxycarbonyl chloride (17.6 µL, 0.128 mmol). The reaction stirred at room temperature for 24 h, at which point the solvent was removed via rotary evaporation. The crude residue was dissolved in CH_2Cl_2 (~1 mL), and the solution was passed through a SiO_2 plug (0.5 x 3 cm), using CH_2Cl_2as eluent (~8 mL). The filtrate was concentrated in vacuo, and the residue was analyzed by ^1H NMR using CH_2Br_2 (8.9 µL) as an internal standard. Indole **2-51** was not observed; a 50% yield recovery of indole **2-65** was determined.

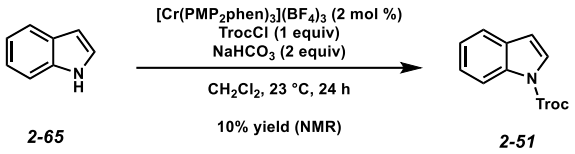

Indole **2-65** (15.0 mg, 0.128 mmol), $NaHCO_3$ (53.8 mg, 0.640 mmol), and $[Cr(PMP_2phen)_3](BF_4)_3$ (1.9 mg, 0.00128 mmol) were added to a flame-dried 1-dram borosilicate vial. The reagents were suspended in CH_3NO_2 (0.640 mL) and CH_2Cl_2 (0.640 mL), and to this solution was added 2,2,2-trichloroethoxycarbonyl chloride (52.8 µL, 0.384 mmol). The reaction mixture was irradiated with a 23 W CFL bulb while stirring. At the 24 h timepoint, the solvent was removed via rotary

evaporation. The crude residue was dissolved in CH_2Cl_2 (~1 mL), and the solution was passed through a SiO_2 plug (0.5 x 3 cm), using CH_2Cl_2 as eluent (~8 mL). The filtrate was concentrated in vacuo, and the residue was analyzed by ^1H NMR using CH_2Br_2 (8.9 µL) as an internal standard. Indole **2-51** was observed in 10% yield; a 62% yield recovery of indole **2-65** was determined.

Evaluation of Cycloaddition in Presence of Triplet Quencher

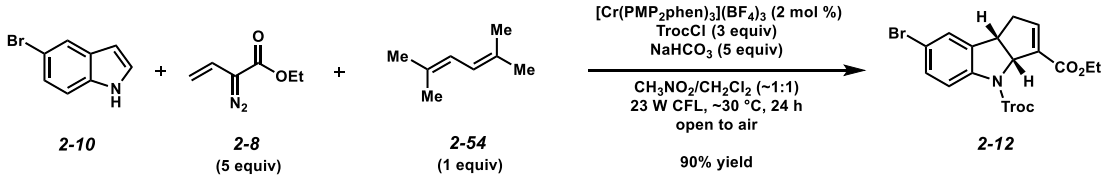

2-10 | *2-8* (5 equiv) | *2-54* (1 equiv) | *2-12*

Procedure: According to General Procedure A, 5-bromoindole (**2-10**, 10.1 mg, 0.0515 mmol), $NaHCO_3$ (21.6 mg, 0.258 mmol), and $[Cr(PMP_2phen)_3](BF_4)_3$ (0.8 mg, 0.000515 mmol) were added to a flame- dried 1-dram borosilicate vial. The reagents were suspended in CH_3NO_2 (0.258 mL), and to this suspension were added 2,2,2-trichloroethoxycarbonyl chloride (21.3 µL, 0.155 mmol), 2,5-dimethyl-2,4-hexadiene (**2-54**, 7.3 µL, 0.0515 mmol), and vinyl diazoacetate **2-8** (0.155 mL, 1.0 M in CH_2Cl_2, 0.155 mmol). The reaction mixture was irradiated with a 23 W CFL bulb while stirring. After 8 h, second charges of vinyl diazoacetate **2-8** (0.103 mL, 1.0 M in CH_2Cl_2, 0.103 mmol) and $[Cr(PMP_2phen)_3](BF_4)_3$ (0.8 mg, 0.000515 mmol) were added, and irradiation was continued. At the 24 h timepoint, the solvent was removed via rotary evaporation. The crude residue was dissolved in CH_2Cl_2 (~1 mL), and the solution was passed through a SiO_2 plug (0.5 x 3 cm), using CH_2Cl_2 as eluent (~8 mL). The filtrate was concentrated in vacuo, and

the crude residue was analyzed via ^{1}H NMR using CH_2Br_2 as an internal standard. Cycloadduct **2-12** was observed in 90% yield.

Competition Experiments

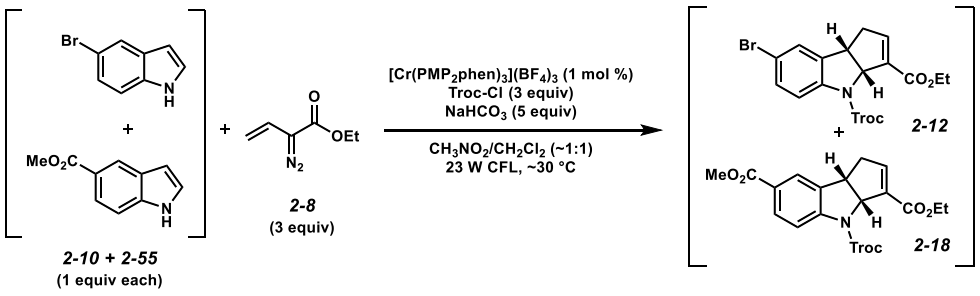

time (h)	yield *2-12* (%)	yield *2-18* (%)
1	10	6
2	19	12
3	28	19
4	33	23

Procedure: According to General Procedure A, 5-bromoindole (**2-10**, 20.0 mg, 0.102 mmol), 5-methoxycarbonylindole (**2-55**, 17.9 mg, 0.102 mmol), $NaHCO_3$ (42.0 mg, 0.500 mmol), 4,4'-di-*tert*-butylbiphenyl (27.2 mg, 0.102 mmol) and $[Cr(PMP_2phen)_3](BF_4)_3$ (1.5 mg, 0.00102 mmol) were added to a flame-dried 1-dram borosilicate vial. The reagents were suspended in CH_3NO_2 (0.510 mL), and to this suspension were added 2,2,2-trichloroethoxycarbonyl chloride (42.1 µL, 0.306 mmol) and vinyl diazoacetate **2-8** (0.306 mL, 1.00 M in CH_2Cl_2, 0.306 mmol). The reaction mixture was irradiated with a 23 W CFL bulb while stirring. Aliquots of 25 µL were taken at various timepoints. Aliquots were dissolved in EtOAc (0.2 mL) and passed through a silica plug (0.5 x 0.5 cm), using EtOAc as eluent (2 mL). The aliquots were then directly analyzed via GC assay using 4,4'-di-*tert*-butylphenyl as an internal standard (added at the beginning).

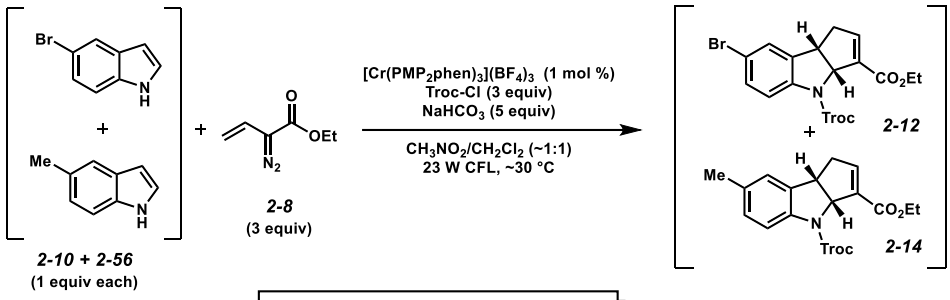

time (h)	yield *2-12* (%)	yield *2-14* (%)
1	0	20
2	< 5	34
3	< 5	53
4	5	65

Procedure: According to General Procedure A, 5-bromoindole (**2-10**, 20.0 mg, 0.102 mmol), 5-methylindole (**2-56**, 13.4 mg, 0.102 mmol), $NaHCO_3$ (42.0 mg, 0.500 mmol), 4,4'-di-*tert*-butylbiphenyl (27.2 mg, 0.102 mmol) and $[Cr(PMP_2phen)_3](BF_4)_3$ (1.5 mg, 0.00102 mmol) were added to a flame-dried 1-dram borosilicate vial. The reagents were suspended in CH_3NO_2 (0.510 mL), and to this suspension were added 2,2,2-trichloroethoxycarbonyl chloride (42.1 µL, 0.306 mmol) and vinyl diazoacetate **2-8** (0.306 mL, 1.00 M in CH_2Cl_2, 0.306 mmol). The reaction mixture was irradiated with a 23 W CFL bulb while stirring. Aliquots of 25 µL were taken at various timepoints. Aliquots were dissolved in EtOAc (0.2 mL) and passed through a silica plug (0.5 x 0.5 cm), using EtOAc as eluent (2 mL). The aliquots were then directly analyzed via GC assay using 4,4'-di-*tert*-butylphenyl as an internal standard (added at the beginning).

Stern-Volmer Quenching Experiments & Additional Mechanism Tests

For 5-bromoindole (**2-10**) and $[Cr(PMP_2phen)_3](BF_4)_3$, samples were prepared by adding solutions of $[Cr(PMP_2phen)_3](BF_4)_3$ and **2-10** in CH_3NO_2 to obtain a total volume of 3 mL. The concentration of $[Cr(PMP_2phen)_3](BF_4)_3$ was 1.67×10^{-5} M. Samples were irradiated at 400 nm, and emission was detected at 752 nm. For ethyl vinyldiazoacetate (**2-8**) and $[Cr(PMP_2phen)_3](BF_4)_3$, samples were prepared by adding solutions of $[Cr(PMP_2phen)_3](BF_4)_3$ and **2-8** in CH_3NO_2 to obtain a total volume of 3 mL. The concentration of $[Cr(PMP_2phen)_3](BF_4)_3$ was 1.67×10^{-5} M. Samples were irradiated at 400 nm, and emission was detected at 752 nm.

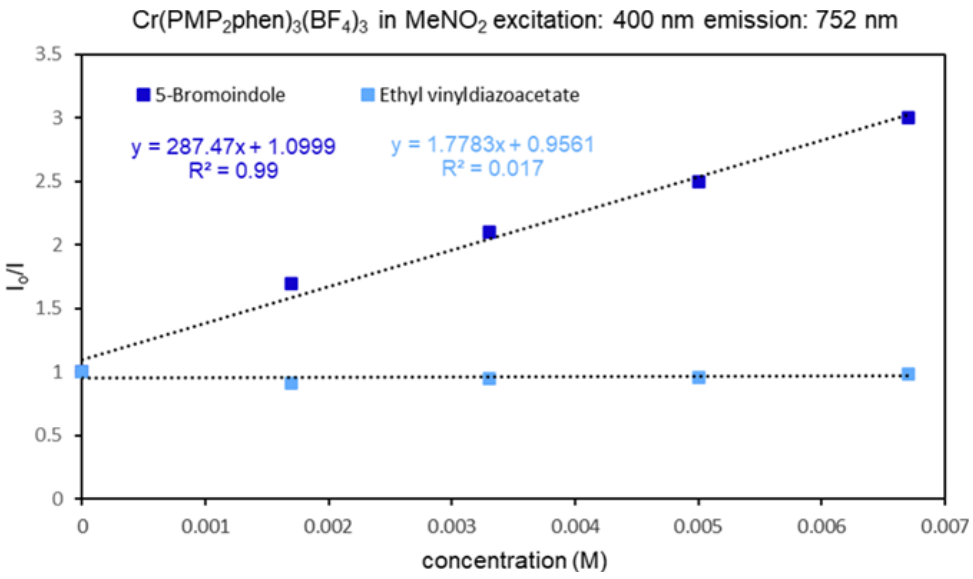

Figure 2.12.6. Stern-Volmer analysis: quenching of excited state of $[Cr(PMP_2phen)_3](BF_4)_3$ by 5- bromoindole at the 752 nm emission band.

A similar analysis was performed on a second emission band at 464 nm. For 5-bromoindole (**2-10**) and $[Cr(PMP_2phen)_3](BF_4)_3$, samples were prepared by adding solutions of $[Cr(PMP_2phen)_3](BF_4)_3$ and **2-10** in CH_3NO_2 to obtain a total volume of 3 mL. The concentration of $[Cr(PMP_2phen)_3](BF_4)_3$ was 8.33×10^{-6} M. Samples were irradiated at 400 nm, and emission was detected at 464 nm. For ethyl vinyldiazoacetate (**2-8**) and $[Cr(PMP_2phen)_3](BF_4)_3$, samples were prepared by adding solutions of $[Cr(PMP_2phen)_3](BF_4)_3$ and **2-8** in CH_3NO_2 to obtain a total volume of 3 mL. The concentration of $[Cr(PMP_2phen)_3](BF_4)_3$ was 8.33×10^{-6} M. Samples were irradiated at 400 nm, and emission was detected at 464 nm.

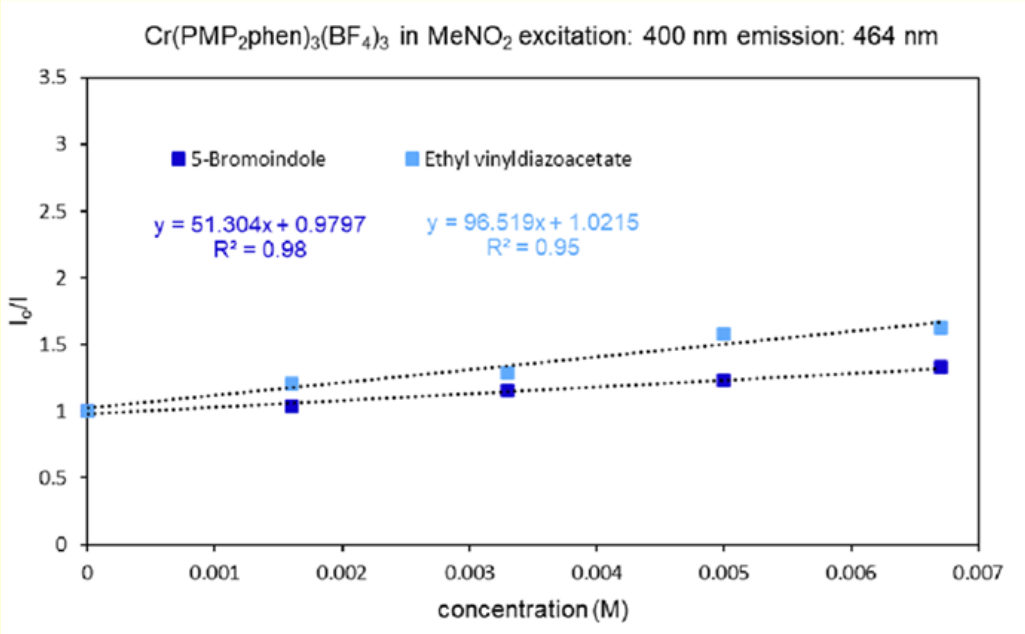

Figure 2.12.7. Stern-Volmer analysis: quenching of excited state of $[Cr(PMP_2phen)_3](BF_4)_3$ by ethyl vinyldiazoacetate at the 464 emission band.

Note: Cr(III) complexes such as these octahedral polypyridyl species are appreciated to possess two main emission bands, broadly representing the $^2E/^2T_1$ and ^4T excited states, at ~750 nm and ~400-500 nm respectively.[6,25] The $^2E/^2T_1$ state is responsible for electron transfer processes, while the ^4T has been attributed to energy transfer type processes. In *Figure 2.12.6*, we observe significant quenching of the electron-transfer excited state (measured at 752 nm) by indole **2-10** with strong linear correlation, consistent with our proposed mechanism (initiation via single electron oxidation of the indole substrate). Both indole **2-10** and vinyl diazoacetate **2-8** also appear to quench the ^4T excited state (measured at 464 nm),[26] although not as pronounced (*Figure 2.12.7*). We do not believe these quenching actions lead to product formation. These actions likely result in unproductive background processes that arise from energy transfer, including relaxation, nonspecific decomposition, or pyrazole formation. The rearrangement of a vinyl diazoacetate to pyrazole, which is observed, proceeds through two pericyclic reactions that do not require but may be impacted by energy transfer events.[37] We also observe additional nonspecific decomposition of vinyl diazoacetate **2-8**, contributing to the need for excess equivalents in the cycloaddition.

Gryko Competition Experiments:

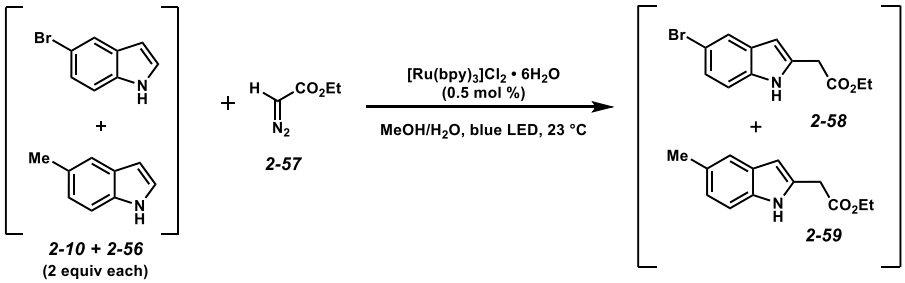

time (h)	yield *2-58* (%)	yield *2-59* (%)
1	13	7
2	20	14
4	24	16
6	26	19

Procedure: According to a procedure reported by Gryko and coworkers,[11] 5-methylindole (**2-56**, 42.5 mg, 0.324 mmol), 5-bromoindole (**2-10**, 63.5 mg, 0.324 mmol), and $Ru(bpy)_3Cl_2 \cdot 6H_2O$ (0.6 mg, 0.000810 mmol) were added to a flame-dried 2-dram borosilicate vial. The reagents were suspended in MeOH and H_2O (10:1, 1.80 mL), and argon was bubbled through the reaction for 10 min. To this suspension were then added ethyl diazoacetate (**2-57**, 20.0 µL, ~85 wt. %, 0.162 mmol) and dodecyl acetate (43.0 µL, 0.162 mmol). The reaction mixture was irradiated under a stream of Ar with a 160 W blue LED light. Aliquots of 30 µL were taken at various timepoints. The aliquots were directly analyzed via ^1H NMR analysis.

Intramolecular Cycloadditions

Substrate synthesis:

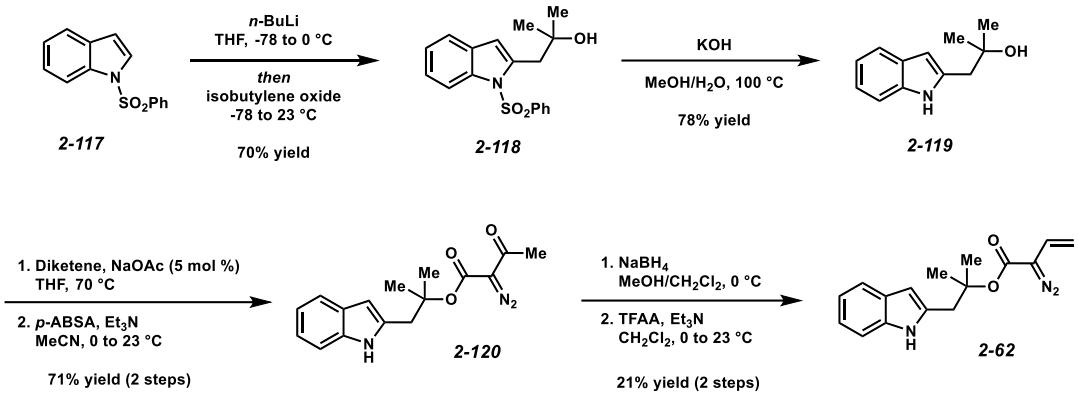

Alcohol 2-118. According to a modification of a reported procedure by Chikkade and coworkers,[38] to a solution of 1-phenylsulfonylindole (**2-117**, 1.80 g, 6.99 mmol) in THF (27.9 mL, 0.250 M) cooled to -78 ºC was added *n*-butyllithium (3.36 mL, 2.5 M in hexanes, 8.39 mmol) dropwise over 10 min. The solution was stirred for 1.5 h at -78 ºC, and then was warmed to 0 ºC and stirred for 1 h. The solution was cooled back to -78 ºC, and isobutylene oxide (0.745 mL, 8.39 mmol) was added dropwise. The reaction mixture was warmed to room temperature and stirred overnight. After 16 h, the reaction mixture was quenched by the addition of sat. aq. NH_4Cl (10 mL). THF was removed by rotary evaporation, and the mixture was extracted with EtOAc (3 x 30 mL). The combined organic layers were washed sequentially with H_2O (10 mL) and brine (10 mL), and then dried over Na_2SO_4 and concentrated in vacuo. The crude residue was purified by silica gel flash chromatography (4:1 → 2:1 hexanes/EtOAc eluent) to afford the indolyl alcohol (**2-118**, 1.60 g, 70% yield, R_f = 0.16 in 4:1 hexanes/EtOAc) as an orange oil.

A solution of sulfonylindole **2-118** (6.79 g, 20.6 mmol) and KOH (5.78 g, 103 mmol) in MeOH/H_2O (3:1, 103 mL, 0.2 M) was refluxed for 8 h. The reaction mixture was cooled to 23 ºC and quenched by the addition of sat. aq. NH_4Cl (30 mL). The mixture was extracted with EtOAc (3 x 50 mL). The combined organic layers were washed sequentially with H_2O (30 mL) and brine (30 mL), and then dried over Na_2SO_4 and concentrated in vacuo. The crude residue was purified via silica gel flash chromatography (3:1 hexanes/EtOAc eluent) to afford deprotected indole **2-119** (3.04 g, 78% yield) as a pale yellow solid.

TLC: R_f = 0.35 in 2:1 hexanes/EtOAc, visualized by UV.

^{1}H NMR (400 MHz, $CDCl_3$): δ 8.63 (br. s, 1H), 7.55 (d, *J* = 7.9 Hz, 1H), 7.33 (d, *J* = 7.2 Hz, 1H), 7.13 (app. t, *J* = 7.2 Hz, 1H), 7.07 (app. t, *J* = 7.9 Hz, 1H), 6.26 (s, 1H), 2.91 (s, 2H), 1.29 (s, 6H).

Diazo ketoester 2-120. Following a procedure reported by Doyle and coworkers,[39] a solution of indole **2-119** (3.04 g, 16.1 mmol) and NaOAc (79.0 mg, 0.963 mmol) in THF (4.60 mL) was heated to reflux. A solution of diketene (1.49 mL, 19.3 mmol) in THF (2.14 mL) was then added dropwise to the reaction mixture over 30 min. The reaction mixture was refluxed for 4 h, and then cooled to room temperature. The reaction mixture was then partitioned between Et_2O (25 mL) and brine (25 mL). The aqueous layer was extracted with Et_2O (3 x 25 mL), and the organic layers were combined, dried over $MgSO_4$, and concentrated in vacuo. The crude ketoester (R_f = 0.41 in 4:1 hexanes/EtOAc) was taken forward without further purification.

To a stirring solution of the ketoester (assume 16.1 mmol) in acetonitrile (13.4 mL) at 0 ºC was added Et_3N (2.92 mL, 20.9 mmol) dropwise. A solution of *p*-ABSA (5.03 g, 20.9 mmol) in acetonitrile (10.7 mL) was then added dropwise to the reaction mixture over 30 min. The resulting mixture was then warmed to room temperature and stirred for 3 h. The reaction mixture was then

filtered through a Buchner funnel to remove the *p*-ABSA byproducts, and the filtrate was concentrated in vacuo. The crude residue was purified via silica gel flash chromatography (4:1 hexanes/EtOAc eluent) to afford α-diazo ketoester **2-120** (3.42 g, 71% yield over 2 steps) as a yellow oil.

TLC: R_f = 0.45 in 4:1 hexanes/EtOAc, visualized by UV.

^{1}H NMR (400 MHz, $CDCl_3$): δ 8.62 (br. s, 1H), 7.55 (d, *J* = 7.7 Hz, 1H), 7.34 (d, *J* = 7.3 Hz, 1H), 7.14 (app. t, *J* = 7.3 Hz, 1H), 7.07 (app. t, *J* = 7.7 Hz, 1H), 6.29 (s, 1H), 3.21 (s, 2H), 2.45 (s, 3H), 1.61 (s, 6H).

Vinyl diazoester 2-62. To a solution of α-diazo ketoester **2-120** (300 mg, 1.00 mmol) in MeOH/CH_2Cl_2 (1:1, 4.0 mL) at 0 ºC was added $NaBH_4$ (45.4 mg, 1.20 mmol) portionwise. After addition, the reaction mixture was warmed to room temperature and stirred for 3 h, monitoring progress by TLC. The reaction mixture was then diluted with H_2O (10 mL) and extracted with EtOAc (3 x 10 mL). The combined organic layers were washed with brine (10 mL), dried over $MgSO_4$, and concentrated in vacuo. The crude alcohol product (R_f = 0.20 in 3:1 hexanes/EtOAc) was taken forward without further purification.

According to a modification of a procedure by Rianelli and coworkers,[40] to a solution of the crude alcohol (assume 1.00 mmol) in CH_2Cl_2 (8.33 mL) at 0 °C was added triethylamine (0.697 mL, 5.00 mmol) and trifluoroacetic anhydride (0.153 mL, 1.10 mmol) sequentially. The reaction mixture was warmed to room temperature and stirred for 2 h. The reaction mixture was then concentrated in vacuo, and the crude residue was purified via silica gel flash chromatography (6:1 hexanes/Et_2O eluent) to afford vinyl diazoester **2-62** (59.2 mg, 21% yield over 2 steps) as an orange oil.

TLC: R_f = 0.55 in 4:1 hexanes/EtOAc, visualized by UV.

^{1}H NMR (400 MHz, $CDCl_3$): δ 7.98 (br. s, 1H), 7.56 (d, *J* = 7.7 Hz, 1H), 7.33 (d, *J* = 7.8 Hz, 1H), 7.15 (app. t, *J* = 7.7 Hz, 1H), 7.09 (app. t, *J* = 7.8 Hz, 1H), 6.33-6.28 (m, 1H), 6.14 (dd, *J* = 10.9, 17.4 Hz, 1H), 5.13 (d, *J* = 10.9 Hz, 1H), 4.86 (d, *J* = 17.4 Hz, 1H), 3.26 (s, 2H), 1.58 (s, 6H).

^{13}C NMR (100 MHz, $CDCl_3$): δ 136.0, 134.3, 128.6, 121.5, 120.5, 120.1, 119.8, 110.7, 107.8, 102.8, 83.7, 40.4, 26.6 (*2 carbons not detected: carbonyl and diazo*).

IR (ATR, neat): 3399, 2924, 2854, 2087, 1785, 1406, 1168, 740 cm^{-1}.

HRMS (ESI+): *m/z* calc'd for $(M + Na)^+$ $[C_{16}H_{17}N_3O_2 + Na]^+$: 306.1213, found 306.1209.

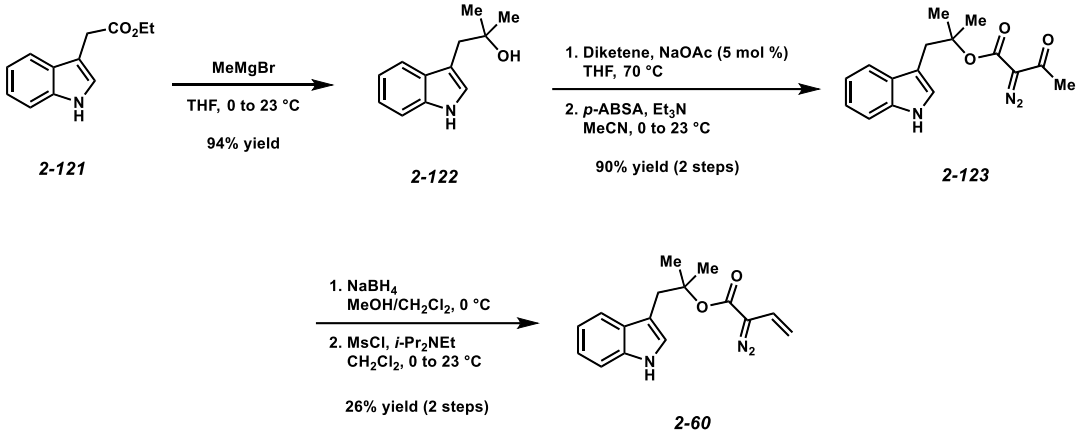

Alcohol 2-122. According to a known procedure by Maskeri and coworkers,[41] to a solution of ethyl 2-(1*H*-indol-3-yl)acetate (**2-121**, 1.55 g, 7.63 mmol) in THF (25.4 mL) at 0 °C was added methylmagnesium bromide (8.13 mL, 3.0 M in Et_2O, 24.4 mmol) dropwise. The reaction mixture was then warmed to room temperature and stirred for 2 h. The reaction mixture was then quenched with sat. aq. NH_4Cl (20 mL), and the layers were separated. The aqueous layer was extracted with EtOAc (3 x 30 mL). The combined organic layers were washed with brine (20 mL), dried over $MgSO_4$, and concentrated in vacuo. The resulting alcohol (**2-122**, 1.31 g, 94% yield, R_f = 0.24 in 4:1 hexanes/EtOAc) required no further purification. The spectroscopic data were in accordance with the published values.[41]

Diazo ketoester 2-123. Following a procedure reported by Doyle and coworkers,[39] a solution of indole **2-122** (1.11 g, 5.89 mmol) and NaOAc (28.9 mg, 0.353 mmol) in THF (1.68 mL, 3.5 M) was heated to reflux. A solution of diketene (0.500 mL, 6.48 mmol) in THF (0.697 mL, 9.3 M) was then added dropwise to the reaction mixture over 30 min. The resulting mixture was refluxed for 4 h and then cooled to room temperature. The reaction mixture was partitioned between Et_2O (25 mL) and brine (25 mL). The aqueous layer was extracted with Et_2O (3 x 25 mL), and the

organic layers were combined, dried over $MgSO_4$, and concentrated in vacuo. The crude ketoester (1.58 g, R_f = 0.33 in 2:1 hexanes/EtOAc) was not further purified. A portion of the ketoester (1.08 g) was carried forward.

To a stirring solution of the crude ketoester (1.08 g, assume 3.95 mmol) in acetonitrile (3.29 mL) at 0 ºC was added Et_3N (0.716 mL, 5.14 mmol) dropwise. A solution of *p*-ABSA (1.23 g, 5.14 mmol) in acetonitrile (3.43 mL) was then added dropwise to the reaction mixture over 30 min. The resulting mixture was then warmed to room temperature and stirred for 3 h. The reaction mixture was then filtered through a Buchner funnel to remove the *p*-ABSA byproducts, and the filtrate was concentrated in vacuo. The crude residue was purified via silica gel flash chromatography (4:1 hexanes/EtOAc eluent) to afford α-diazo ketoester **2-123** (1.08 g, 90% yield over 2 steps) as a yellow oil.

TLC: R_f = 0.56 in 2:1 hexanes/EtOAc, visualized by UV.

^{1}H NMR (400 MHz, $CDCl_3$): δ 8.08 (br. s, 1H), 7.61 (app. t, *J* = 7.9 Hz, 1H), 7.37 (d, *J* = 7.9 Hz, 1H), 7.23-7.08 (comp. m, 2H), 7.02 (d, *J* = 7.7 Hz, 1H), 3.29 (s, 2H), 2.44 (s, 3H), 1.59 (s, 6H).

Diazoester 2-60. To a solution of α-diazo ketoester **2-123** (1.07 g, 3.57 mmol) in MeOH/CH_2Cl_2 (1:1, 14 mL) at 0 ºC was added $NaBH_4$ (162 mg, 4.29 mmol) portionwise. After addition, the reaction mixture was warmed to room temperature and stirred for 3 h, monitoring progress by TLC. The reaction mixture was then diluted with H_2O (20 mL) and extracted with EtOAc (3 x 20 mL). The combined organic layers were washed with brine (20 mL), dried over $MgSO_4$, and concentrated in vacuo. The crude alcohol product (760 mg, approx. 90:10 alcohol/ketoester **2-123**, R_f = 0.30 in 4:1 hexanes/EtOAc) was not further purified. A portion of the crude alcohol product (690 mg) was carried forward.

To a solution of the crude alcohol (690 mg, assume 2.29 mmol) in CH_2Cl_2 (19 mL) at 0 °C was added *i*-Pr_2NEt (2.01 mL, 11.5 mmol) and MsCl (0.213 mL, 2.75 mmol) sequentially. The reaction mixture was warmed to room temperature and stirred for 2 h. The reaction mixture was then concentrated in vacuo, and the crude residue was purified via silica gel flash chromatography (8:1 hexanes/Et_2O eluent) to afford vinyl diazoester **2-60** (239 mg, 26% yield over 2 steps) as an orange oil.

TLC: R_f = 0.55 in 2:1 hexanes/Et_2O, visualized by UV.

^{1}H NMR (400 MHz, C_6D_6): δ 7.63-7.55 (m, 1H), 7.25-7.18 (comp. m, 2H), 7.08-7.00 (m, 1H), 6.74 (br. s, 1H), 6.52 (app. d, *J* = 2.4 Hz), 6.22 (dd, *J* = 17.4, 11.0 Hz, 1H), 4.84 (d, *J* = 11.0 Hz, 1H), 4.62 (d, *J* = 17.4 Hz, 1H), 3.18 (s, 2H), 1.46 (s, 6H).

^{13}C NMR (100 MHz, C_6D_6): δ 164.0, 136.3, 128.9, 123.7, 122.0, 121.3, 119.8, 119.7, 111.4, 111.3, 107.0, 84.7, 36.5, 26.4 (*1 carbon not detected: diazo*).

IR (ATR, neat): 3412, 2950, 2086, 1692, 1309, 1111, 743 cm^{-1}.

HRMS (ESI+): *m/z* calc'd for $(M + Na)^+$ $[C_{16}H_{17}N_3O_2 + Na]^+$: 306.1213, found 306.1209.

Intramolecular cycloaddition reactions

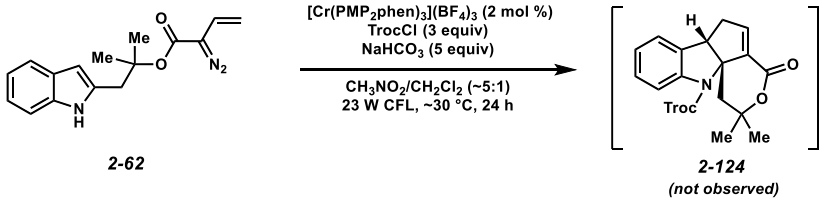

In a 1-dram borosilicate vial, $[Cr(PMP_2phen)_3](BF_4)_3$ (1.6 mg, 0.00106 mmol) and $NaHCO_3$ (29.6 mg, 0.352 mmol) were suspended in CH_3NO_2 (0.250 mL). 2,2,2-Trichloroethoxycarbonyl chloride (29.1 μL, 0.212 mmol) and the solution of diazoester **2-62** (20.0 mg in 0.14 mL CH_2Cl_2, 0.0706 mmol) were added. The reaction mixture was irradiated with a 23 W CFL bulb while stirring. After 8 h, a second charge of $[Cr(PMP_2phen)_3](BF_4)_3$ (1.6 mg, 0.00106 mmol) was added. After 24 h total, the solvent was removed via rotary evaporation. The crude residue was dissolved in CH_2Cl_2 (~1 mL), and the solution was passed through a silica plug (0.5 x 3 cm), using CH_2Cl_2/EtOAc as eluent (~10 mL, 1:1). The filtrate was concentrated in vacuo, and the residue was analyzed by ^1H NMR. Cycloadduct **2-124** was not observed.

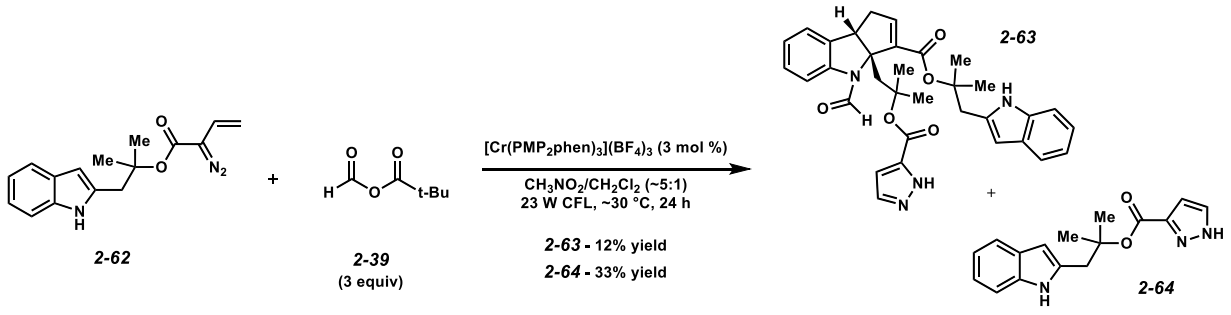

In a 1-dram borosilicate vial, trimethylacetic formic anhydride (**2-39**, 52.4 mg, 0.402 mmol) was dissolved in CH_3NO_2 (0.670 mL). $[Cr(PMP_2phen)_3](BF_4)_3$ (3.0 mg, 0.00201 mmol) was then added, followed by a solution of diazoester **2-62** (38.0 mg, 0.134 mmol) in CH_2Cl_2 (0.134 mL). The reaction mixture was irradiated with a 23 W CFL bulb while stirring. After 8 h, a second charge of $[Cr(PMP_2phen)_3](BF_4)_3$ (3.0 mg, 0.00201 mmol) was added. After 24 h total, the solvent was removed via rotary evaporation. The crude residue was dissolved in CH_2Cl_2 (~1 mL), and the solution was passed through a silica plug (0.5 x 3 cm), using CH_2Cl_2/EtOAc as eluent (~10 mL, 1:1). The filtrate was concentrated in vacuo, and the residue was purified via flash chromatography (4:1 → 2:1 EtOAc/hexanes eluent) to afford cycloadduct **2-63** (9.0 mg, 12% yield) as a yellow oil, and a pyrazole byproduct (**2-64,** 33% NMR yield using CH_2Br_2 (9.3 μL, 0.134 mmol) as the internal standard) as a beige solid.

Cycloadduct 2-63

TLC R_f = 0.20 in 1:1 hexanes/EtOAc, visualized by UV.

^{1}H NMR (400 MHz, $CDCl_3$): δ 9.24 (s, 1H), 8.30 (d, *J* = 8.1 Hz, 1H), 7.98 (br. s, 1H), 7.64 (app. s, 1H), 7.50 (d, *J* = 7.8 Hz, 1H), 7.35-7.17 (comp. m, 2H), 7.16-6.98 (comp. m, 4H), 6.79 (app. s, 1H), 6.75 (app. s, 1H), 6.26 (s, 1H), 4.57 (app. d, *J* = 8.4 Hz, 1H), 3.38 (app. d, *J* = 14.6 Hz, 1H),

3.17 (app. d, *J* = 14.6 Hz, 1H), 3.09 (app. d, *J* = 16.0 Hz, 1H), 3.00 (app. dd, *J* = 18.2, 8.4 Hz, 1H), 2.89 (app. d, *J* = 16.0 Hz, 1H), 2.60 (app. d, *J* = 18.2, 8.4 Hz, 1H), 1.66 (s, 3H), 1.62 (s, 3H), 1.58 (s, 3H), 1.53 (s, 3H).

^{13}C NMR (100 MHz, $CDCl_3$): δ 164.0, 162.3, 146.9, 140.4, 138.4, 136.0, 134.2, 133.4, 128.63, 128.56, 124.9, 124.0, 121.5, 120.0, 119.8, 117.7, 110.8, 108.5, 102.8, 84.2, 83.5, 79.4, 48.9, 45.2, 39.6, 38.7, 31.1, 27.8, 27.4, 26.6 (*3 carbons not detected)*.

IR (ATR, neat): 3270, 2928, 1704, 1656, 1596, 1461, 1133, 755 cm^{-1}.

HRMS (ESI+): *m/z* calc'd for $(M + H)^+$ $[C_{33}H_{34}N_4O_5 + H]^+$: 567.2602, found 567.2588.

Pyrazole 2-64

TLC R_f = 0.15 in 4:1 hexanes/EtOAc, visualized by UV.

^{1}H NMR (400 MHz, $CDCl_3$): δ 9.72 (br. s, 1H), 7.67 (d, *J* = 2.4 Hz, 1H), 7.55 (d, *J* = 7.5 Hz, 1H), 7.31 (d, *J* = 7.9 Hz, 1H), 7.10 (app. t, *J* = 7.5 Hz, 1H), 7.05 (app. t, *J* = 7.9 Hz, 1H), 6.91 (d, *J* = 2.4 Hz, 1H), 6.32 (s, 1H), 3.18 (s, 2H), 1.67 (s, 6H).

^{13}C NMR (100 MHz, $CDCl_3$): δ 160.7, 136.8, 135.4, 128.2, 121.1, 120.0, 119.4, 110.7, 108.4, 102.6, 83.8, 41.9, 25.5 (*2 carbons not detected).*

IR (ATR, neat): 3344, 2926, 1711, 1459, 1168, 740 cm^{-1}.

HRMS (ESI+): *m/z* calc'd for $(M + Na)^+$ $[C_{16}H_{17}N_3O_2 + Na]^+$: 306.1213, found 306.1209.

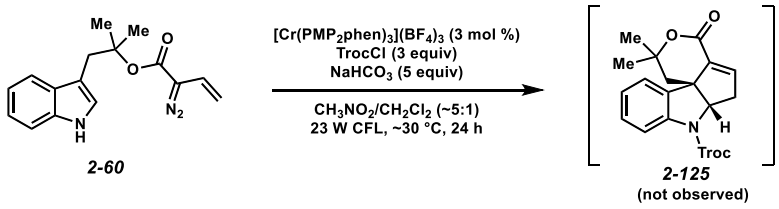

Procedure: An approx. 0.8 M solution of diazoester **2-60** (239 mg, 0.845 mmol) in CH_2Cl_2 (0.845 mL) was prepared for test reactions. In a 1-dram borosilicate vial, $[Cr(PMP_2phen)_3](BF_4)_3$ (1.1 mg, 0.000750 mmol) and $NaHCO_3$ (21.0 mg, 0.250 mmol) were suspended in CH_3NO_2 (0.25 mL). 2,2,2-Trichloroethoxycarbonyl chloride (20.6 μL, 0.150 mmol) and the solution of diazoester **2-60** (0.0500 mL, ~0.8 M in CH_2Cl_2, 0.0400 mmol) were added. The reaction mixture was irradiated with a 23 W CFL bulb while stirring. After 8 h, a second charge of $[Cr(PMP_2phen)_3](BF_4)_3$ (1.1 mg, 0.000750 mmol) was added. After 24 h total, the solvent was removed via rotary evaporation. The crude residue was dissolved in CH_2Cl_2 (~1 mL), and the solution was passed through a silica plug (0.5 x 3 cm), using CH_2Cl_2/EtOAc as eluent (~10 mL, 1:1). The filtrate was concentrated in vacuo, and the residue was analyzed by ^1H NMR. Cycloadduct **2-125** was not observed.

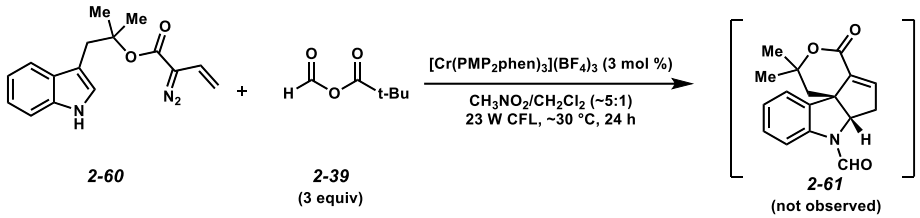

In a 1-dram borosilicate vial, trimethylacetic formic anhydride (**2-39**, 19.5 mg, 0.150 mmol) was dissolved in CH_3NO_2 (0.250 mL). $[Cr(PMP_2phen)_3](BF_4)_3$ (1.1 mg, 0.000750 mmol) was then added, followed by the solution of diazoester **2-60** (0.0500 mL, ~0.8 M in CH_2Cl_2, 0.0400 mmol). The reaction mixture was irradiated with a 23 W CFL bulb while stirring. After 8 h, a second charge of $[Cr(PMP_2phen)_3](BF_4)_3$ (1.1 mg, 0.000750 mmol) was added. After 24 h total, the solvent was removed via rotary evaporation. The crude residue was dissolved in CH_2Cl_2 (~1 mL), and the solution was passed through a silica plug (0.5 x 3 cm), using CH_2Cl_2/EtOAc as eluent (~10 mL, 1:1). The filtrate was concentrated in vacuo, and the residue was analyzed by ^1H NMR. Cycloadduct **2-61** was not observed.

2.12.8. Cyclic Voltammetry of Corresponding Indoles:

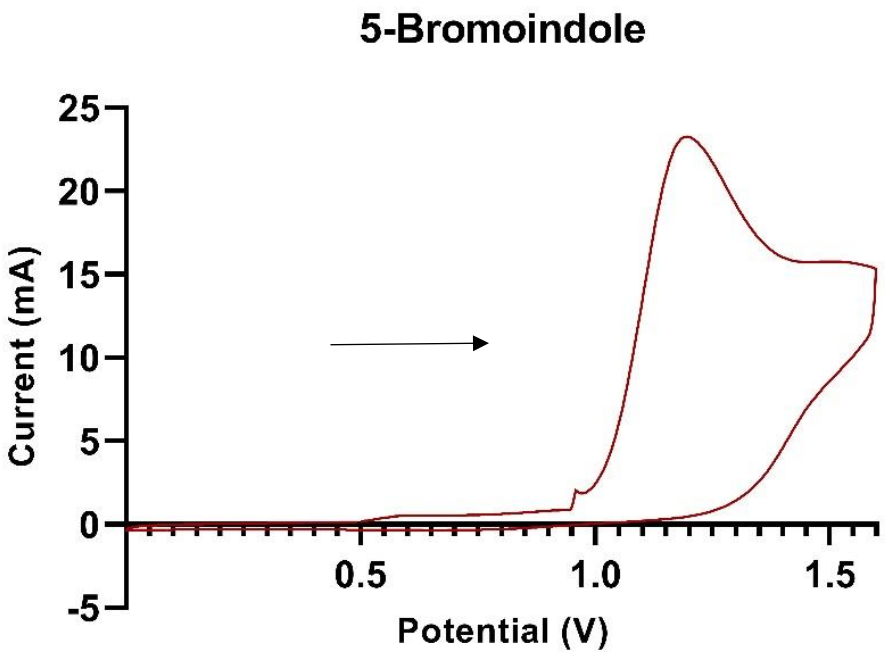

Figure 2.12.8. Cyclic voltammogram of indole **2-10** (5 mM) recorded at ambient temperature in CH_3CN containing 0.25 M Bu_4NPF_6, glassy carbon working electrode measured at a scan rate of 100 mV/s and referenced to Fc/Fc^+. The arrow displays the scan direction.

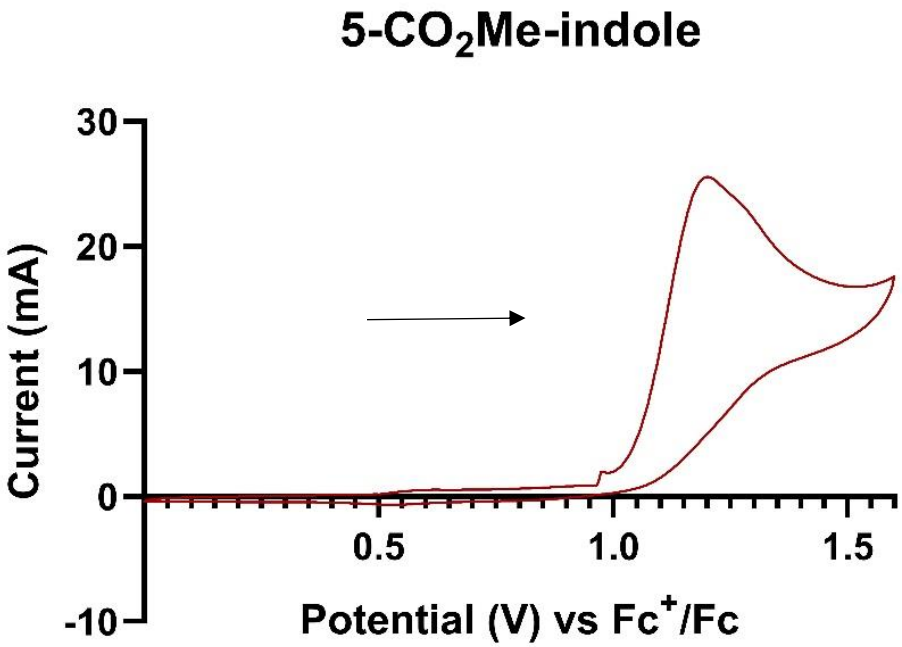

Figure 2.12.9. Cyclic voltammogram of indole **2-55** (5 mM) recorded at ambient temperature in CH_3CN containing 0.25 M Bu_4NPF_6, glassy carbon working electrode measured at a scan rate of 100 mV/s and referenced to Fc/Fc^+. The arrow displays the scan direction.

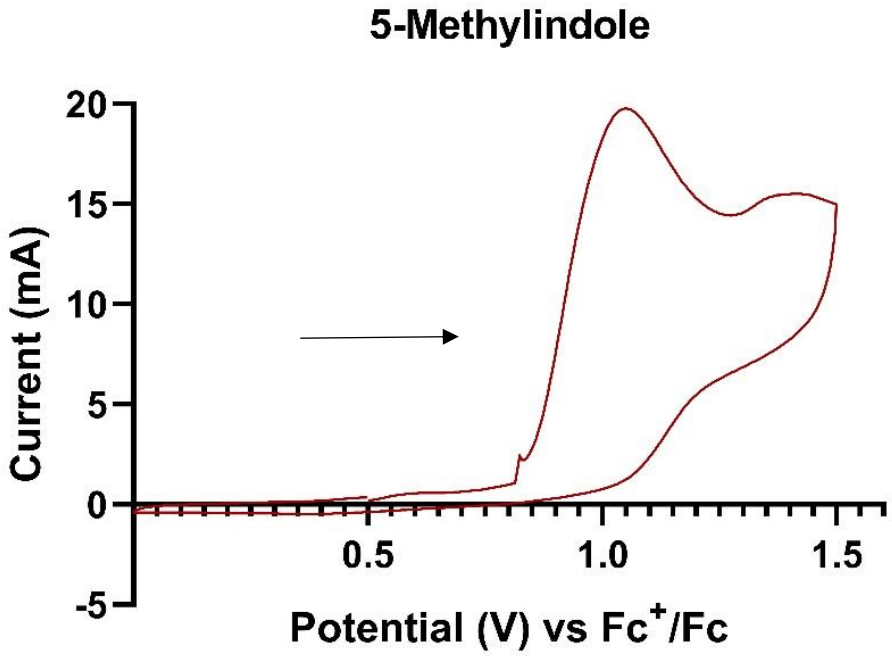

Figure 2.12.10. Cyclic voltammogram of indole **2-56** (5 mM) recorded at ambient temperature in CH_3CN containing 0.25 M Bu_4NPF_6, glassy carbon working electrode measured at a scan rate of 100 mV/s and referenced to Fc/Fc^+. The arrow displays the scan direction.

2.12.9. Characterization of Potential Pyrazole Byproducts

Pyrazole byproducts can be formed by light-mediated rearrangement of the diazo reagent. Protected pyrazoles were independently synthesized from ethyl 1*H*-pyrazole-3-carboxylate[42] and acylating agent/base to ascertain their presence/absence in samples. Only pyrazole **2-127** was observed in a couple of purified compounds (**2-18**, **2-25**).

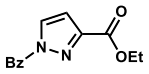

2-126

TLC R_f: 0.41 in 1:1 hexanes/Et_2O, visualized by UV, stained blue in Hanessian's stain.

^{1}H NMR (400 MHz, $CDCl_3$): δ 8.45 (d, *J* = 2.8 Hz, 1H), 8.19 (d, *J* = 8.6 Hz, 2H), 7.64 (t, *J* = 7.4 Hz, 1H), 7.52 (app. t, *J* = 7.9 Hz, 2H), 6.99 (d, *J* = 2.8 Hz, 1H), 4.42 (q, *J* = 7.1 Hz, 2H), 1.40 (t, *J* = 7.1 Hz, 3H).

^{13}C NMR (100 MHz, $CDCl_3$): δ 166.2, 161.7, 148.2, 133.9, 132.2, 131.9, 130.4, 128.5, 110.8, 61.8, 14.4.

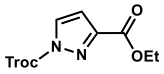

2-127

TLC R_f: 0.56 in 1:1 hexanes/Et_2O, visualized by UV, stained blue in Hanessian's stain.

^{1}H NMR (400 MHz, $CDCl_3$): δ 8.22 (d, *J* = 2.9 Hz, 1H), 6.96 (d, *J* = 2.9 Hz, 1H), 5.09 (s, 2H), 4.43 (q, *J* = 7.2 Hz, 2H), 1.40 (t, *J* = 7.2 Hz, 3H).

^{13}C NMR (100 MHz, $CDCl_3$): δ 161.3, 149.4, 147.5, 132.7, 111.5, 93.7, 76.6, 62.0, 14.4.

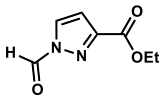

2-128

TLC R_f: 0.32 in 1:1 hexanes/Et_2O, visualized by UV, stained blue in Hanessian's stain.

^{1}H NMR (400 MHz, $CDCl_3$): δ 9.26 (s, 1H), 8.23 (d, *J* = 2.8 Hz, 1H), 7.01 (dd, *J* = 2.8, 1.1 Hz, 1H), 4.47 (q, *J* = 7.1 Hz, 2H), 1.43 (t, *J* = 7.1 Hz, 3H).

^{13}C NMR (100 MHz, $CDCl_3$): δ 161.2, 160.2, 149.4, 128.3, 112.2, 62.1, 14.4.

(*Unformylated pyrazole is present in this sample*.)

2.12.10. Starting Material Synthesis

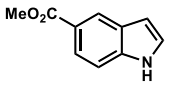

2-55

Indole 2-55. Prepared according to the procedure reported by Kong and coworkers.[43]

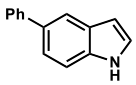

2-88

Indole 2-88. Prepared according to the procedure reported by Shao and coworkers.[44]

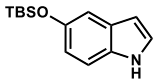

2-89

Indole 2-89. Prepared according to the procedure reported by Ito and coworkers.[45]

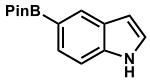

2-91

Indole 2-91. Prepared according to the procedure reported by Prieto and coworkers.[46]

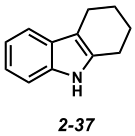

2-37

Indole 2-37. Prepared according to the procedure reported by Dalvi and Lokhande.[47]

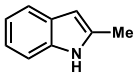

2-106

Indole 2-106. Prepared according to the procedure reported by Zhang and Yu.[48]

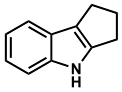

2-107

Indole 2-107. Prepared according to the procedure reported by Matsumoto and coworkers.[49]

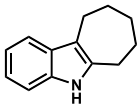

2-108

Indole 2-108. Prepared according to the procedure reported by Matsumoto and coworkers.[50]

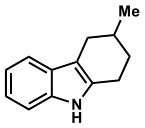

2-109

Indole 2-109. Prepared according to the procedure reported by Matsumoto and coworkers.[51]

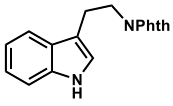

2-110

Indole 2-110. Prepared according to the procedure reported by Feng and coworkers.[52]

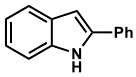

2-111

Indole 2-111. Prepared according to the procedure reported by Gaikwad and coworkers.[53]

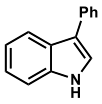

2-112

Indole 2-112. Prepared according to the procedure reported by Zhou and coworkers.[54]

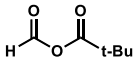

2-39

Trimethylacetic formic anhydride (2-39). Prepared according to the procedure reported by Vlietstra and coworkers.[22]

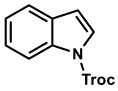

2-51

Indole 2-51. Prepared according to the procedure reported by Yuan and coworkers.[55]

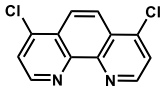

2-82

4,7-dichloro-1,10-phenanthroline (2-82). Prepared according to the procedure reported by Altman and Buchwald.[56]

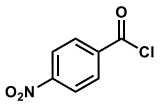

2-102

4-Nitrobenzoyl chloride (2-102). Prepared according to the procedure reported by Otevrel and coworkers.[57]

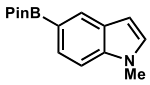

2-116

1-methyl-5-(4,4,5,5-tetramethyl-1,3,2-dioxaborolan-2-yl)-1*H*-indole (2-116). Prepared according to the procedure reported by Ha and coworkers.[58]

2-80

Benzohydroximoyl chloride (2-80). Prepared according to the procedure reported by Lemercier and Pierce.[59]

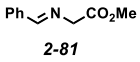

2-81

Methyl 2-(benzylidienamino)acetate (2-81). Prepared according to the procedure reported by Lasch and Heinrich.[60]

2,4,6-Tris(4-methoxyphenyl)pyrylium tetrafluoroborate ($(OMe)_3TPP(BF_4)$). Prepared according to the procedure reported by Krappitz and coworkers.[61]

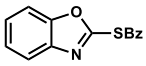

5-(benzoxazole-2-yl)thiobenzoate. Prepared according to the procedure reported by Ueda and coworkers.[62]

Pentafluorophenyl benzoate. Prepared according to the procedure reported by Igolen and Morin.[63]

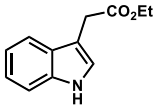

2-121

Indole 2-121. Prepared according to the procedure reported by Leitch and coworkers.[64]

Diazocarbonyl Synthesis:

General Notes: After synthesizing, vinyl diazocarbonyl compounds were stored in a -20 °C freezer as a 1.0 M solution in CH_2Cl_2. Diazo compounds are toxic, irritants, and many compounds are explosive. Care should be taken when handling and synthesizing diazo compounds. For several of these compounds, the ^{13}C NMR signal for the CN_2 carbon atom was not observed; this phenomenon is common and is due to the long relaxation time due to the enhanced negative partial charge on this atom.[65]

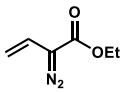

2-8

Diazoester 2-8. Prepared according to the procedure reported by Davies and coworkers.[66]

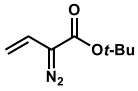

2-96

Diazoester 2-96. Prepared according to the procedure reported by Schwartz and coworkers.[67]

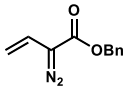

2-97

Diazoester 2-97. Prepared according to the procedure reported by Sarabia and coworkers.[8]

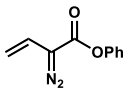

2-98

Diazoester 2-98. Prepared according to the procedure reported by Sarabia and coworkers.[8]

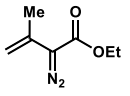

2-99

Diazoester 2-99. Prepared according to the procedure reported by Jadhav and coworkers.[68]

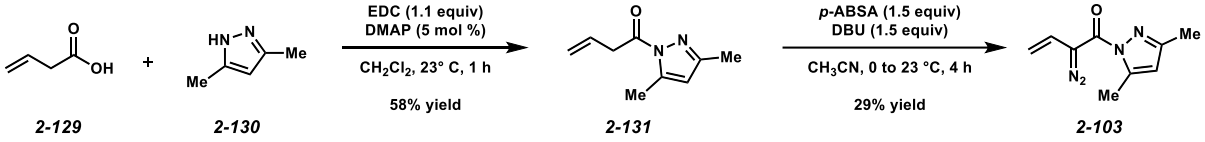

2-129 *2-130* *2-131* *2-103*

Diazoamide 2-103. Following a modified procedure from Feng and coworkers,[69] to a solution of 3-butenoic acid (**2-129**, 0.443 mL, 5.20 mmol) and 3,5-dimethylpyrazole (**2-130**, 500 mg, 5.20 mmol) in CH_2Cl_2 (10.4 mL) at 23 °C were added 1-ethyl-3-(3-dimethylaminopropyl)carbodiimide (1.10 g, 5.72 mmol) and 4-dimethylaminopyridine (31.8 mg, 0.260 mmol). The reaction mixture was then stirred at room temperature for 1 h. Brine (10 mL) was added to the reaction mixture, the layers were separated, and the aqueous layer was extracted with CH_2Cl_2 (3 x 10 mL). The organic layers were combined, dried over Na_2SO_4, and concentrated in vacuo. The crude residue was purified via silica gel flash chromatography (9:1 hexanes/EtOAc eluent) to afford amide **2-131** (495mg, R_f = 0.35 in 9:1 hexanes/EtOAc, 58% yield) as a colorless oil, which was carried to the next reaction.

Continuing the modified procedure from Feng and coworkers,[69] to a solution of amide **2-131** (495 mg, 3.01 mmol) and *p*-acetamidobenzenesulfonyl azide (1.09 g, 4.52 mmol) in CH_3CN

(30 mL) at 0 °C was added 1,8-diazabicyclo[5.4.0]undec-7-ene (0.675 mL, 4.52 mmol) dropwise. The reaction mixture was slowly warmed to room temperature and stirred for 4 h. The solvent was then evaporated, and the residue was dissolved in Et_2O (10 mL) and sat. aq. NH_4Cl (10 mL). The layers were separated, and the aqueous layer was extracted with Et_2O (3 x 10 mL). The organic layers were combined, washed with brine (10 mL), dried over $MgSO_4$, and concentrated in vacuo. The crude residue was purified via silica gel flash chromatography (9:1 hexanes/Et_2O eluent) to afford vinyl diazoamide **2-103** (165 mg, 29% yield) as an orange oil.

TLC: R_f = 0.52 in 4:1 hexanes/EtOAc, visualized by UV.

^{1}H NMR (400 MHz, CDCl3): δ 6.61 (dd, *J* = 17.1, 10.6 Hz, 1H), 5.95 (s, 1H), 5.19 (d, *J* = 10.6 Hz, 1H), 4.78 (d, *J* = 17.1 Hz, 1H), 2.53 (s, 3H), 2.22 (s, 3H).

^{13}C NMR (100 MHz, CDCl3): δ 150.8, 144.0, 122.3, 110.5, 107.0, 14.1, 13.9 (*2 carbons not detected*).

IR (ATR, neat): 2927, 2095, 1710, 1665, 1352 cm^{-1}.

HRMS (ESI+): *m/z* calc'd for $(M + H)^+$ $[C_9H_{10}N_4O + H]^+$: 191.0927, found 191.0918.

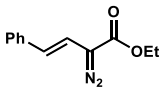

2-114

Diazoester 2-114. Prepared according to the procedure reported by Loy and coworkers.[70]

2.13. References and Notes

[1] Gall, B. K.; Smith, A. K.; Ferreira, E. M. *Angew. Chem. Int. Ed.* **2022**, *61*, e202212187.

[2] For select reviews, see: (a) Narayanam, J. M. R.; Stephenson, C. R. J. *Chem. Soc. Rev.* **2011**, *40*, 102-113. (b) Prier, C. K.; Rankic, D. A.; MacMillan, D. W. C. *Chem. Rev.* **2013**, *113*, 5322-5363. (c) Romero, N. A.; Nicewicz, D. A. *Chem. Rev.* **2016**, *116*, 10075-10166. (d) Bell, J. D.; Murphy, J. A. *Chem. Soc. Rev*. **2021**, *50*, 9540-9685.

[3] For select reviews on earth-abundant photocatalysis, see: (a) Larsen, C. B.; Wenger, O. S. *Chem. Eur. J*. **2018**, *24*, 2039-2058. (b) Wenger, O. S. *J. Am. Chem. Soc*. **2018**, *140*, 13522-13533. (c) Hockin, B. M.; Li, C.; Robertson, N.; Zysman-Coleman, E. *Catal. Sci. Technol.* **2019**, *9*, 889-915.

[4] McDaniel, A, M.; Tseng, H.-W.; Damrauer, N. H.; Shores, M. P. *Inorg. Chem.* **2010**, *49*, 7981-7991.

[5] (a) Stevenson, S. M.; Shores, M. P.; Ferreira, E. M. *Angew. Chem. Int. Ed.* **2015**, *54*, 6506-6510. (b) Higgins, R. F.; Fatur, S. M.; Shepard, S. G.; Stevenson, S. M.; Boston, D. J.; Ferreira, E. M.; Damrauer, N. H.; Rappé, A. K.; Shores, M. P. *J. Am. Chem. Soc*. **2016**, *138*, 5451-5464.

[6] (a) Stevenson, S. M.; Higgins, R. F.; Shores, M. P.; Ferreira, E. M. *Chem. Sci*. **2017**, *8*, 654-660. (b) Higgins, R. F.; Fatur, S. M.; Damrauer, N. H.; Ferreira, E. M.; Rappé, A. K.; Shores, M. P. *ACS Catal*. **2018**, *8*, 9216-9225.

[7] Sarabia, F. J.; Ferreira, E. M. *Org. Lett*. **2017**, *19*, 2865-2868.

[8] Sarabia, F. J.; Li, Q.; Ferreira, E. M. *Angew. Chem. Int. Ed.* **2018**, *57*, 11015-11019.

[9] (a) Saxton, J. E. in *The Alkaloids: Chemistry and Biology* (Ed: Cordell, G. A.), Academic Press: San Diego, CA, 1998, Vol. 51, Ch. 1. (b) Kam, T.-S.; Lim, K.-H. in *The Alkaloids: Chemistry and*

Biology (Ed: Cordell, G. A.), Elsevier, Amsterdam: 2008, Vol. 66, Ch. 1. (c) Cuendet, M.; Pezzuto, J. M. in *Modern Alkaloids: Structure, Isolation, Synthesis and Biology* (Eds: Fattorusso, E.; Taglialatela-Scafati, O.), Wiley-VCH, Weinheim: 2008, Ch. 2. (d) Podoll, J. D.; Liu, Y.; Chang, L.; Walls, S.; Wang, W.; Wang, X. *Proc. Natl. Acad. Sci. USA* **2013**, *110*, 15573-15578. (e) Liu, X.-Y.; Qin, Y. *Acc. Chem. Res.* **2019**, *52*, 1877-1891.

[10] (a) Romero, N. A.; Margrey, K. A.; Tay, N. E.; Nicewicz, D. A. *Science* **2015**, *349*, 1326-1330. (b) Holmberg-Douglas, N.; Onuska, N. P. R.; Nicewicz, D. A. *Angew. Chem. Int. Ed*. **2020**, *59*, 7425-7429.

[11] Ciszewski, Ł. W.; Durka, J.; Gryko, D. *Org. Lett*. **2019**, *21*, 7028-7032.

[12] For select examples of intramolecular cycloadditions, see: (a) Zhu, M.; Zheng, C.; Zhang, X.; You, S.-L. *J. Am. Chem. Soc.* **2019**, *141*, 2636-2644. (b) Rolka, A. B.; Koenig, B. *Org. Lett.* **2020**, *22*, 5035-5040. (c) Oderinde, M. S.; Mao, E.; Ramirez, A.; Pawluczyk, J.; Jorge, C.; Cornelius, L. A. M.; Kempson, J.; Vetrichelvan, M.; Pitchai, M.; Gupta, A.; Gupta, A. K.; Meanwell, N. A.; Mathur, A.; Dhar, T. G. M. *J. Am. Chem. Soc.* **2020**, *142*, 3094-3103. For select examples of intermolecular examples, see: (d) Oderinde, M. S.; Ramirez, A.; Murali Dhar, T. G.; Cornelius, L. A. M.; Jorge, C.; Aulakh, D.; Sandhu, B.; Pawluczyk, J.; Sarjeant, A. A.; Meanwell, N. A.; Mathur, A.; Kempson, J. *J. Org. Chem.* **2021**, *86*, 1730-1747. (e) Ma, J.; Schäfers, F.; Daniliuc, C.; Bergander, K.; Strassert, C. A.; Glorius, F. *Angew. Chem. Int. Ed.* **2020**, *59*, 9639-9645. For select examples of intramolecular cyclizations, see: (f) Wu, K.; Du, Y.; Wang, T. *Org. Lett.* **2017**, *19*, 5669-5672. (g) Gentry, E. C.; Rono, L. J.; Hale, M. E.; Matsuura, R.; Knowles, R. R. *J. Am. Chem. Soc*. **2018**, *140*, 3394-3402.

[13] (a) Gieseler, A.; Steckhan, E.; Wiest, O. *Synlett* **1990**, 275-277. (b) Gieseler, A.; Steckhan, E.; Wiest, O.; Knoch, F. *J. Org. Chem.* **1991**, *56*, 1405-1411. (c) Wiest, O.; Steckhan, E.; Grein, F. *J. Org. Chem.* **1992**, *57*, 4034-4037. (d) Wiest, O.; Steckhan, E. *Tetrahedron Lett.* **1993**, *34*, 6391-6394. (e) Haberl, U.; Steckhan, E.; Blechert, S.; Wiest, O. *Chem. Eur. J.* **1999**, *5*, 2859-2865. (f) Peglow, T.; Blechert, S.; Steckhan, E. *Chem. Commun.* **1999**, 433-434. (g) Pitre, S. P.; Scaiano, J. C.; Yoon, T. P. *ACS Catal*. **2017**, *7*, 6440-6444.

[14] (a) Lian, Y.; Davies, H. M. L. *J. Am. Chem. Soc*. **2010**, *132*, 440-441. (b) Jing, C.; Cheng, Q.-Q.; Deng, Y.; Arman, H.; Doyle, M. P. *Org. Lett.* **2016**, *18*, 4550-4553.

[15] Indole dearomatization via (3+2) cycloaddition can also be achieved through alternative methods, including by opening strained rings or by conjugate addition into an electron deficient C2–C3 π bond. For select examples, see: (a) Xiong, H.; Xu, H.; Liao, S.; Xie, Z.; Tang, Y. *J. Am. Chem. Soc*. **2013**, *135*, 7851-7854. (b) Awata, A.; Arai, T. *Angew. Chem. Int. Ed*. **2014**, *53*, 10462-10465. (c) Chai, Z.; Zhu, Y.-M.; Yang, P.-J.; Wang, S.; Wang, S.; Liu, Z.; Yang, G. *J. Am. Chem. Soc*. **2015**, *137*, 10088-10091. (d) Wang, H.; Zhang, J.; Tu, Y.; Zhang, J. *Angew. Chem. Int. Ed*. **2019**, *58*, 5422-5426.

[16] Reduction potentials are reported vs. the saturated calomel electrode (SCE).

[17] Roth, H. G.; Romero, N. A.; Nicewicz, D. A. *Synlett* **2015**, *27*, 714.

[18] Running experiments for longer did not increase the yield.

[19] Devery, J. J., III; Douglas, J. J.; Nguyen, J. D.; Cole, K. P.; Flowers, R. A., II; Stephenson, C. R. J. *Chem. Sci.* **2015**, *6*, 537-541.

[20] Schultz, D. M.; Sawicki, J. W.; Yoon, T. P. *Beilstein J. Org. Chem.* **2015**, *11*, 61-65.

[21] Bowden, K.; Braude, E. A.; Jones, E. R. H. *J. Chem. Soc.* **1946**, 948-952.

[22] Vlietstra, E. J.; Zwikker, J. A.; Nolte, R. J. M.; Drenth, W. *Recl. Trav. Chim. Pays. Bas*. **1982**, *101*, 460-462.

[23] For recent examples of use, see: (a) Nicolaou, K. C.; Chen, Q.; Li, R.; Anami, Y.; Tsuchikama, K. *J. Am. Chem. Soc*. **2020**, *142*, 20201-20207. (b) Kovacevic, L. S.; Idziak, C.; Markevicius, A.; Scullion, C.; Corr, M. J.; Kennedy, A. R.; Tuttle, T.; Murphy, J. A. *Angew. Chem. Int. Ed.* **2012**, *51*, 8516-8519. (c) Caspi, D. D.; Zhang, H.; Virgil, S. C.; Piller, F. M.; Stoltz, B. M. *Heterocycles* **2012**, *86*, 1003-1008.

[24] (a) Zhu, M.; Zheng, C.; Zhang, X.; You, S.-L. *J. Am. Chem. Soc*. **2019**, *141*, 2636-2644. (b) Zhu, M.; Xu, H.; Zhang, X.; Zheng, C.; You, S.-L. *Angew. Chem. Int. Ed.* **2021**, *60*, 7036-7040.

[25] (a) Bürgin, T. H.; Glaser, F.; Wenger, O. S. *J. Am. Chem. Soc.* **2022**, *144*, 14181-14194. (b) Otto, S.; Grabolle, M.; Förster, C.; Kreitner, C.; Resch-Genger, U.; Heinze, K. *Angew. Chem. Int. Ed.* **2015**, *54*, 11572-11576.

[26] For an example of vinyl diazoacetate quenching a photocatalyst excited state, see: Li, W.; Zhou, L. *Org. Lett.* **2021**, *23*, 4279-4283.

[27] Guandalini, L.; Dei, S.; Gualtieri, F.; Romanelli, M. N.; Scapecchi, S.; Teodori, E.; Varani, K. *Helv. Chim. Acta* **2002**, *85*, 96-107.

[28] For a similar observation of this intramolecular cyclization/reduction, see: Baylis, A. M.; Davies, M. P. H.; Thomas, E. J. *Org. Biomol. Chem*. **2007**, *5*, 3139-3155.

[29] Sakaki, S.; Kojima, T.; Arai, T. *J. Chem. Soc., Dalton Trans.* **1994**, 7-11.

[30] (a) Jäger, V.; Colinas, P. A. in *Synthetic Applications of 1,3-Dipolar Cycloaddition Chemistry Toward Heterocycles and Natural Products* (Eds: Padwa, A.; Pearson, W. H.), John Wiley & Sons, New York: 2002, Ch. 6. (b) Barr, D. A.; Grigg, R.; Gunaratne, N.; Kemp, J.; McMeekin, P.;

Sridharan, V. *Tetrahedron* **1988**, *44*, 557-570. (c) Casas, J.; Grigg, R.; Nájera, C.; Sansano, J. *Eur. J. Org. Chem*. **2001**, 1971-1982.

[31] Connelly, N. G. Geiger, W. E. *Chem. Rev.* **1996**, *96*, 877-910.

[32] Bradley K. Gall is acknowledged for catalyst development. Cr catalyst development is thoroughly described in Chapter 2 of his dissertation: Gall, B. K. Chromium(III) Photocatalysis: Catalyst Design and Reaction Development. Ph.D. Dissertation, University of Georgia, Athens, GA, 2021.

[33] Benltifa, M.; Vidal, S.; Gueyrard, D.; Goekjian, P. G.; Msaddek, M.; Praly, J.-P. *Tetrahedron Lett.* **2006**, *47*, 6143-6147.

[34] Mancebo-Aracil, J.; Martín-Rodríguez, M.; Nájera, C.; Sansano, J. M.; Costa, P. R. R.; Crizanto de Lima, E.; Dias, A. G. *Tetrahedron: Asymmetry* **2012**, *23*, 1596-1606.

[35] Gao, X.; Xia, M.; Yuan, C.; Zhou, L.; Sun, W.; Li, C.; Wu, B.; Zhu, D.; Zhang, C.; Zheng, B.; Wang, D.; Guo, H. *ACS Catal*. **2019**, *9*, 1645-1654.

[36] Sheehan, J. C.; Yang, D.-D. H. *J. Am. Chem. Soc.* **1958**, *80*, 1154-1158.

[37] Taylor, E. C.; Turchi, I. J. *Chem. Rev.* **1979**, *79*, 181-231.

[38] Chikkade, P. K.; Shimizu, Y.; Kanai, M. *Chem. Sci.* **2014**, *5*, 1585-1590.

[39] Doyle, M. P.; Winchester, W. R.; Protopopova, M. N.; Kazala, A. P.; Westrum, L. J. *Org. Synth.* **1996**, *73*, 13.

[40] Rianelli, R. d. S.; da Silva, F. d. C.; de Souza, M. C. B. V.; Ferreira, V. F. *Lett. Org. Chem.* **2006**, *3*, 73.

[41] Maskeri, M. A.; O'Connor, M. J.; Jaworski, A. A.; Davies, A. V.; Scheidt, K. A. *Angew. Chem. Int. Ed.* **2018**, *57*, 17225-17229.

[42] Fatin-Rouge, N.; Tóth, É.; Perret, D.; Backer, R. H.; Merbach, A. E.; Bünzli, J.-C. G. *J. Am Chem. Soc*. **2000**, *122*, 10810-10820.

[43] Kong, A.; Han, X.; Lu, X. *Org. Lett*. **2006**, *8*, 1339-1342.

[44] Shao, G.; Shi, G.; Zhang, Y.; Pan, S.; Guan, X. *Org. Lett.* **2015**, *17*, 2652-2655.

[45] Ito, F.; Shudo, K.; Yamaguchi, K. *Tetrahedron* **2011**, *67*, 1805-1811.

[46] Prieto, M.; Zurita, E.; Rosa, E.; Muñoz, L.; Lloyd-Williams, P.; Giralt, E. *J. Org. Chem.* **2004**, *69*, 6812-6820.

[47] Dalvi, B. A.; Lokhande, P. D. *Tetrahedron Lett*. **2018**, *59*, 2145-2149.

[48] Zhang, S.; Yu, Z. *Org. Biomol. Chem.* **2016**, *14*, 10511-10515.

[49] (a) Matsumoto, K.; Tanaka, A.; Yukio, I.; Toda, M.; Bulman, R. A. *Heterocycl. Commun.* **2003**, *9*, 9-12. (b) Bergès, J.; García, B.; Muñiz, K. *Angew. Chem. Int. Ed*. **2018**, *57*, 15891-15895.

[50] (a) Matsumoto, K.; Tanaka, A.; Yukio, I.; Toda, M.; Bulman, R. A. *Heterocycl. Commun.* **2003**, *9*, 9-12. (b) Tong, S.; Xu, Z.; Mamboury, M.; Wang, Q.; Zhu, J. *Angew. Chem. Int. Ed*. **2015**, *54*, 11809-11812.

[51] (a) Matsumoto, K.; Tanaka, A.; Yukio, I.; Toda, M.; Bulman, R. A. *Heterocycl. Commun.* **2003**, *9*, 9-12. (b) Dalvi, B. A.; Lokhande, P. D. *Tetrahedron Lett*. **2018**, *59*, 2145-2149.

[52] Feng, P.; Fan, Y.; Xue, F.; Liu, W.; Li, S.; Shi, Y. *Org. Lett.* **2011**, *13*, 5827-5829.

[53] Gaikwad, R.; Bobde, Y.; Ganesh, R.; Patel, T.; Rathore, A.; Ghosh, B.; Das, K.; Gayen, S. *Synth. Commun.* **2019**, *49*, 2258-2269.

[54] Zhou, N.; Zhao, J.; Sun, C.; Lai, Y.; Ruan, Z.; Feng, P. *J. Org. Chem*. **2021**, *86*, 16059-16067.

[55] Yuan, Y.-A.; Lu, D.-F.; Chen, Y.-R.; Xu, H. *Angew. Chem. Int. Ed.* **2016**, *55*, 534-538.

[56] (a) Altman, R. A.; Buchwald, S. L. *Org. Lett.* **2006**, *8*, 2779-2782. A different workup was followed in the dichlorination reaction, see: (b) Molock, F. F.; Boykin, D. W. *J. Heterocycl. Chem.* **1983**, *20*, 681-686.

[57] (a) Otevrel, J.; Mandelova, Z.; Pesko, M.; Gui, J.; Kralova, L.; Sersen, F.; Vejsova, M.; Kalinowski, D. S.; Kovacevic, Z.; Coffey, A.; Csollei, J.; Richardson, D. R.; Jampilek, J. *Molecules* **2010**, *15*, 8122-8142. (b) Zaragoza, F. *J. Org. Chem*. **2015**, *80*, 10370-10374.

[58] (a) Ha, P. T.; Nguyen, O. T. K.; Huynh, K. D.; Phan, N. T. S. *Synlett* **2018**, *29*, 2031-2034. (b) Nemoto, K.; Tanaka, S.; Konno, M.; Onozawa, S.; Chiba, M.; Tanaka, Y.; Sasaki, Y.; Okubo, R.; Hattori, T. *Tetrahedron* **2016**, *72*, 734-745.

[59] (a) Lemercier, B. C.; Pierce, J. G. *J. Org. Chem.* **2014**, *79*, 2321-2330. (b) Ismail, T.; Shafi, S.; Singh, P. P.; Qazi, N. A.; Sawant, S. D.; Ali, I.; Khan, I. A.; Kumar, H. M. S.; Qazi, G. N.; Alam, M. S. *Indian J. Chem. Sect. B*. **2008**, *47*, 740-747.

[60] Lasch, R.; Heinrich, M. R. *Tetrahedron* **2015**, *71*, 4282-4295.

[61] Krappitz, T.; Jovic, K.; Feist, F.; Frisch, H.; Rigoglioso, V. P.; Blinco, J. P.; Boydston, A. J.; Barner-Kowollik, C. *J. Am. Chem. Soc*. **2019**, *141*, 16605-16609.

[62] (a) Ueda, M.; Seki, K.; Imai, Y. *Synthesis* **1981**, 991-993. (b) Nishio, T.; Shiwa, K. *Heterocycles* **2004**, *62*, 313-324.

[63] Igolen, J.; Morin, C. *J. Org. Chem.* **1980**, *45*, 4802-4804.

[64] Leitch, J. A.; McMullin, C. L.; Mahon, M. F.; Bhonoah, Y.; Frost, C. G. *ACS Catal*. **2017**, *7*, 2616-2623.

[65] (a) Kappe, T.; Lang, G.; Pongratz, E. *J. Chem. Soc., Chem Commun.* **1984**, 338-339. (b) Schmitz, A.; Kraatz, U.; Korte, F. *Heterocycles* **1978**, *10*, 199-205.

[66] (a) Davies, H. M. L.; Cantrell, W. R., Jr.; Romines, K. R.; Baum, J. S. *Org. Synth.* **1992**, *70*, 93. (b) Davies, H. M. L.; Houghland, P. W.; Cantrell, W. R., Jr. *Synth. Commun*. **1992**, *22*, 971-978. (c) Jadhav, A. M.; Pagar, V. V.; Liu, R.-S. *Angew. Chem. Int. Ed*. **2012**, *51*, 11809-11813.

[67] Schwartz, B. D.; Denton, J. R.; Lian, Y.; Davies, H. M. L.; Williams, C. M. *J. Am. Chem. Soc.* **2009**, *131*, 8329-8332.

[68] Jadhav, A. M.; Pagar, V. V.; Liu, R.-S. *Angew. Chem. Int. Ed.* **2012**, *51*, 11809-11813.

[69] Lin, X.; Tang, Y.; Yang, W.; Tan, F.; Lin, L.; Liu, X.; Feng, X. *J. Am. Chem. Soc*. **2018**, *140*, 3299-3305.

[70] Loy, N. S. Y.; Singh, A.; Xu, X.; Park, C.-M. *Angew. Chem. Int. Ed.* **2013**, *52*, 2212-2216.

CHAPTER 3

ACCESS TO HIGHLY FUNCTIONALIZED AMINO-INDOLINES VIA RUTHENIUM(II) PHOTOREDOX CATALYSIS: A DEAROMATIVE (3 + 2) CYCLOADDITION WITH INDOLAMINES AND VINYL DIAZOACETATES

3.1. Introduction

During our studies concerning the development of a more active Cr-based photooxidant, we observed that amine substrates, even protected amines, performed poorly.[1] This report disclosed a dearomative (3 + 2) cycloaddition between indoles and vinyl diazoacetates to yield highly functionalized indoline products (*Scheme 3.1.1*). While most of our tested substrates—containing a variety of functional groups—were moderate to high yielding, indolamine substrates afforded low yields or were non-reactive (e.g., **3-1**→**3-4**, 25% yield).

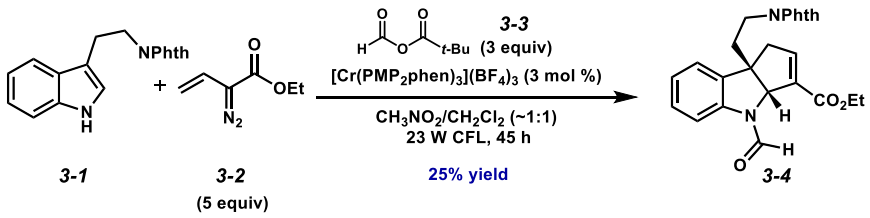

Scheme 3.1.1. Indolamines performing poorly with Cr(III) photocatalyst.

Highly functionalized indoline substrates are a prevalent core in a number of pertinent natural products and bioactive molecules, with the majority biosynthetically derived from tryptophan (*Figure 3.1.1*).[2] Likewise, these compounds contain C2 and C3 disubstitution, which can require arduous methods for synthetic acquisition.[3] We were inspired to pursue these functionalized amino-indoline cores via our recently developed visible light-mediated, Cr(III)-photocatalyzed cycloaddition, which tolerated C2/C3 substitution.[4] If the yield of indolamine substrates could be improved, we would be able to access these valuable adducts in a one-step process under mild, visible light-mediated conditions. Importantly, refining this reaction would necessitate a modification to the current conditions in order to obtain these amino-indoline cores in acceptable yields.

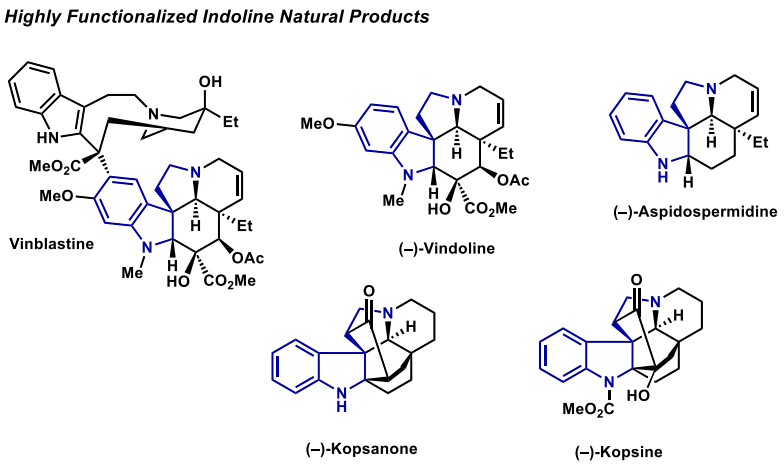

Figure 3.1.1. Relevant natural products containing densely substituted tryptophan cores.

To our knowledge, there is limited success employing these tryptophan derivatives in an intermolecular photocatalytic cycloaddition strategy.[5] This chapter will disclose a method for utilizing protected indolamines in a photoredox-catalyzed dearomative (3 + 2) cycloaddition with vinyl diazoacetates by employing Ru(II) photocatalysis.

3.2. Preliminary Experiments

3.2.1. Photocatalyst Optimization

Our original Cr(III) conditions afforded 25% yield of cycloaddition product **3-4** (*Table 3.2.1, entry 1*) with the phthalimide-tryptamine derivative (**3-1**). While we were not certain what the cause of this incompatibility was, we hypothesized that it could be due to competitive oxidation of the protected amine *N*-lone pair. We began our studies by analyzing various photocatalysts with the previous conditions established for C2/C3-substituted indoles (i.e., trimethylacetic formic anhydride, **3-3**, no base, CH_3NO_2, and white light irradiation). Other chromium catalysts were tested (*entry 2*), as well as various organic photocatalysts (*entries 3 to 7*). Ruthenium and iridium catalysts were also screened (*entries 8 to 11*), and we were delighted to observe that $[Ir(dFCF_3ppy)_2(5,5'\text{-}dCF_3bpy)](PF_6)$ (*entry 9*) and $[Ru(bpz)_3](PF_6)_2$ (*entry 11*), both commonly employed photooxidants, afforded a significant increase in yield of amino-indoline product **3-4**: 63% and 62%, respectively. As $[Ru(bpz)_3](PF_6)_2$ is more accessible synthetically,[6] it was utilized as a viable photocatalyst in further cycloadditions.

Table 3.2.1. Photocatalyst optimization.

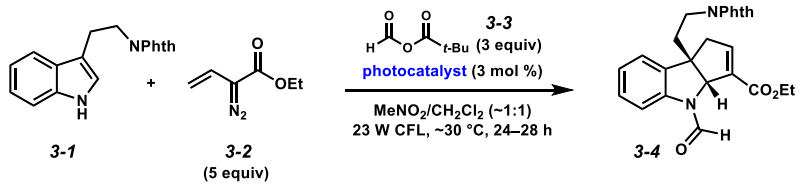

entry	photocatalyst	^{1}H NMR yield (%)
1	$[Cr(PMP_2phen)_3](BF_4)_3$	25
2	$[Cr(Ph_2phen)_3](BF_4)_3$	trace
3	4-CzIPN	trace
4	DCA	10
5	Mes-Acr(BF_4)	trace
6	TPP(BF_4)	trace
7	$(OMe)_3$TPP(BF_4)	10
8	$[Ir(dFCF_3ppy)_2(bpy)](PF_6)$	15
9	$[Ir(dFCF_3ppy)_2(5,5'\text{-}dCF_3bpy)](PF_6)$	63
10	$[Ru(bpy)_3]Cl_2$	15
11	$[Ru(bpz)_3](PF_6)_2$	62

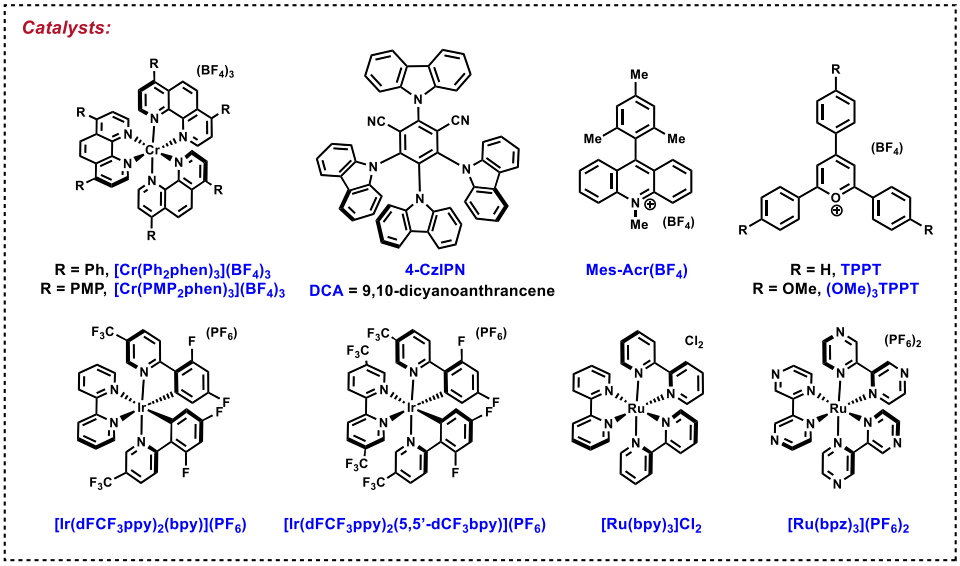

3.2.2. Deviations from Standard Conditions

Deviations from the established conditions were explored and are shown in *Table 3.2.2*. We were curious if conversion and/ yield could be further improved in this reaction. Changing the solvent to methylene chloride only (*entry 1*) reduced the yield significantly, likely due to the

insolubility of $[Ru(bpz)_3](PF_6)_2$ in methylene chloride. Other polar solvents (*entries 2, 3*) did not improve conversion or yield either. While other light sources were not as successful as white light (*entries 4, 5*), they still promoted moderate reactivity. When the reaction was performed in the dark, trace conversion and no product was observed (*entry 6*). Less equivalents of vinyl diazoacetate **3-2** (*entry 9*) or catalyst (*entry 7*) also resulted in diminished yields. Without Ru photocatalyst present, no product was observed (*entry 8*). Other acylating reagents (i.e., TrocCl) were employed, but conversion or yield did not improve (*entries 10, 11*). Finally, in an attempt to advance the reaction to full conversion, the reaction was performed for 45 h, adding extra amounts of catalyst and vinyl diazoacetate **3-2**, with little effect on conversion and yield observed (*entry 12*).

Table 3.2.2. Deviations from standard conditions.

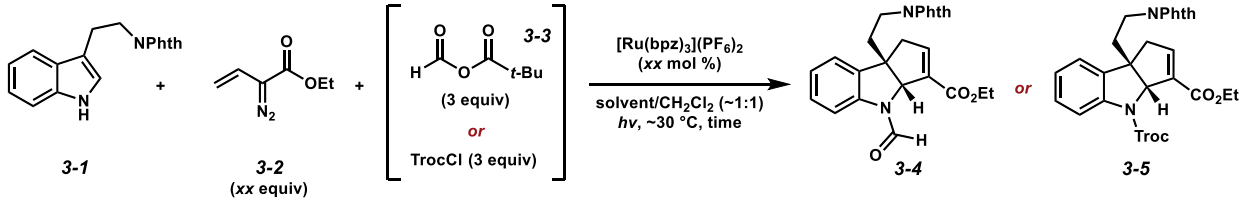

entry	solvent	*hv*	Ru (mol %)	additions (Ru)	VDA (equiv)	PG	time (h)	*3-1* conv (%)	*3-4/3-5* ^{1}H NMR yield (%)[a]
1	CH_2Cl_2	23 W CFL	3	2	5	*3-3*	24	38	30
2	MeCN	23 W CFL	3	2	5	*3-3*	24	50	48
3	Acetone	23 W CFL	3	2	5	*3-3*	24	48	43
4	$MeNO_2$	blue LEDs	3	2	5	*3-3*	24	55	49
5	$MeNO_2$	NUV	3	2	5	*3-3*	24	24	20
6	$MeNO_2$	no hv	3	2	5	*3-3*	24	<10	0
7	$MeNO_2$	23 W CFL	0.5	1	5	*3-3*	24	38	30
8	$MeNO_2$	23 W CFL	0	0	5	*3-3*	24	15	0
9	$MeNO_2$	23 W CFL	3	2	2	*3-3*	24	75	42
10	$MeNO_2$	23 W CFL	3	2	5	TrocCl	24	46	33
11[b]	$MeNO_2$	23 W CFL	3	2	5	TrocCl	24	57	38
12	$MeNO_2$	23 W CFL	6	4	6	*3-3*	48	80	65

[a] CH_2Br_2 was used as an internal standard. [b] 5 equiv of $NaHCO_3$ was also added.

3.3. UV-vis Studies on Catalyst Stability

In the previously mentioned report employing Cr photocatalysis, an *in situ* acylation of the cycloadduct was necessary to prevent competitive oxidation between starting material and product. This competitive oxidation issue was noted by Steckhan and coworkers in 1990, when they disclosed a photocatalyzed (4 + 2) cycloaddition between indoles and cyclohexadienes.[7] The authors circumvented this issue by *in situ* protection of the indoline (4 + 2) cycloaddition product with an acyl chloride (*see Steckhan and Yoon examples, Chapter 1*). We found BzCl and TrocCl to be optimal acylating agents in our cycloaddition, and trimethylacetic formic anhydride (**3-3**) to be the optimal protecting group for C2/C3-substituted indoles. Interestingly, during an early catalyst screen, $[Ru(bpz)_3](PF_6)_2$ was observed to be unusually inadequate.[8] When we subjected the Ru catalyst to excess BzCl and irradiation over 24 h, we observed a significant change in the UV-vis absorbance (*Figure 3.3.1a*). We initially hypothesized that this change in catalyst absorbance was due to acylation of the bipyrazine ligand framework, although we have not been able to characterize the products of this reaction. Likely, multiple acylation events could be occurring, making characterization difficult. After observing excellent reactivity with the Ru catalyst using the conditions shown in *Table 3.2.1*, we were curious about catalyst stability to trimethylacetic formic anhydride (**3-3**). When $[Ru(bpz)_3](PF_6)_2$ was irradiated in the presence of excess **3-3** over 24 h, only a small change in the UV-vis absorbance was observed (*Figure 3.3.1b*). We attribute this in part to reactivity differences between BzCl and **3-3**; however, HCl produced from BzCl may be more detrimental to the catalyst than we had originally anticipated.

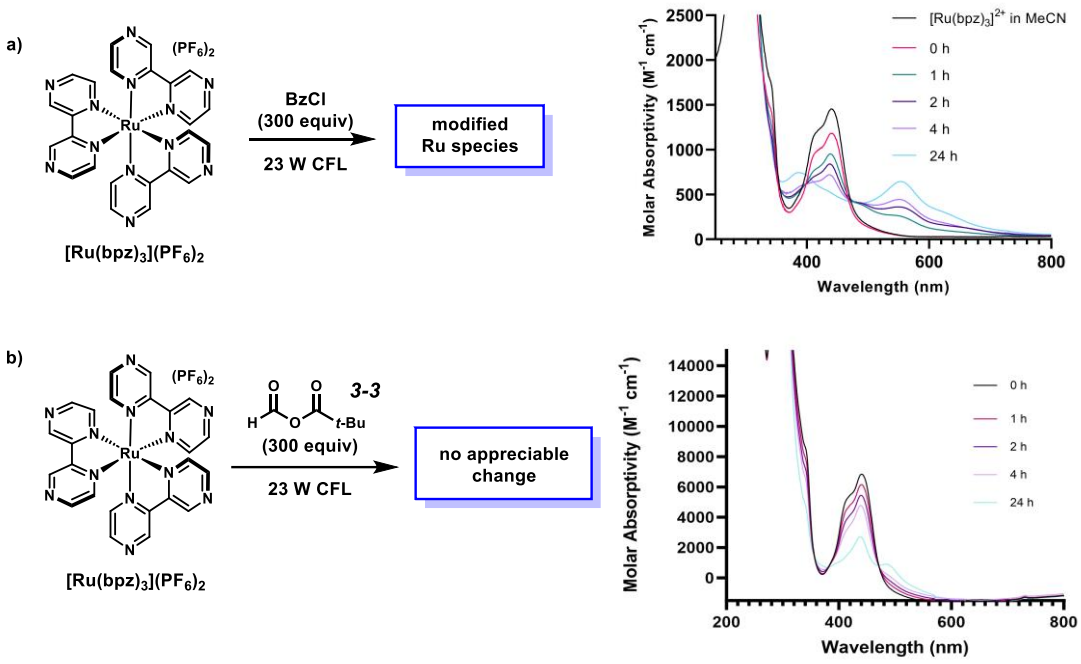

*Figure 3.3.1. UV-vis absorption of $[Ru(bpz)_3](PF_6)_2$ irradiated with (a) BzCl (300 equiv) and (b) trimethylacetic formic anhydride (**3-3**, 300 equiv) over 24 h.*

Other acyl chlorides (*see Experimental Section 3.10.7*) were irradiated with $[Ru(bpz)_3](PF_6)_2$ and found to also change the catalyst absorbance significantly. The differences in the change in absorption between the acyl chlorides tested seems to suggest that acylation (i.e., different absorption character, different acylation products) does plays a role in the change in catalyst.

3.4. Scope of the Reaction

With the optimized conditions in hand, various tryptophan derivatives were tested and found to perform well in the reaction. The scope of indolamines investigated in the reaction is depicted in *Schemes 3.4.1* and *3.4.2*. Carbamate and amide protecting groups (including phthalimide, Boc, Alloc, Cbz, and Troc, **3-4–3-9**) afforded moderate to excellent yields of the cycloaddition products from the respective protected tryptamines. Pivalyl- (**3-10**) and acetyl- (**3-11**) protected tryptamines performed poorly. Indoles with methylene and ethylene carbamate substitutions at C2 and C5 (**3-13–3-15**) were also tolerated. A secondary carbamate tested afforded cycloadduct **3-12** in moderate yield. *N*,*N*-Dibenzyl tryptamine was also assessed in the reaction and no cycloaddition product was observed (*see Experimental Section*), indicating a withdrawing group is essential to deactivate the lone pair on the nitrogen atom and avoid unproductive oxidation. When additional substitution was also introduced at C2 on tryptamine derivatives (e.g., **3-16**), a noticeable increase in yield was observed. Several different carbamate and amide groups were tested with this additional C2 substitution, and all exhibited excellent reactivity (**3-16–3-20**).

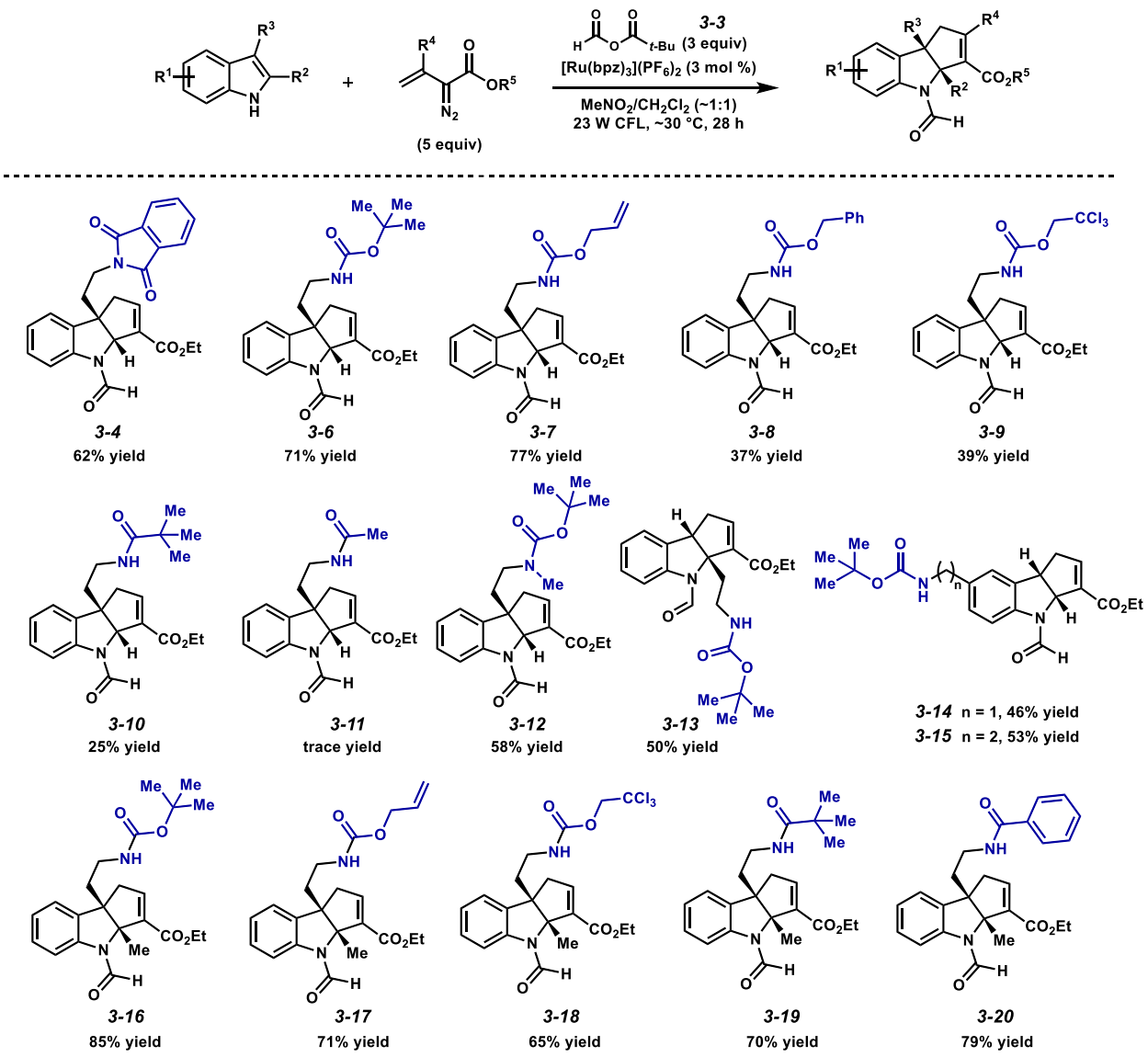

Scheme 3.4.1. Scope of (3 + 2) cycloaddition of indolamines and vinyl diazoacetates employing Ru photocatalysis.

Other vinyl diazoacetates were also accommodated in this reaction (**3-21**, **3-22**), including substitution at the β-position (**3-21**) and different ester substitution (**3-22**). L-Tryptophan derivatives were next evaluated. Several different carbamate groups afforded moderate to good yields of cycloadduct (**3-23**–**3-25**), but with little to no diastereoselectivity. Amide and phthalimide protecting groups were also tested and only furnished low to trace yields of product (*see Experimental Section*), with sterics possibly playing a role in diminished reactivity. A cyclic protecting group was also employed (**3-26**) and performed well, while also imparting some diastereoselectivity (2:1 dr).

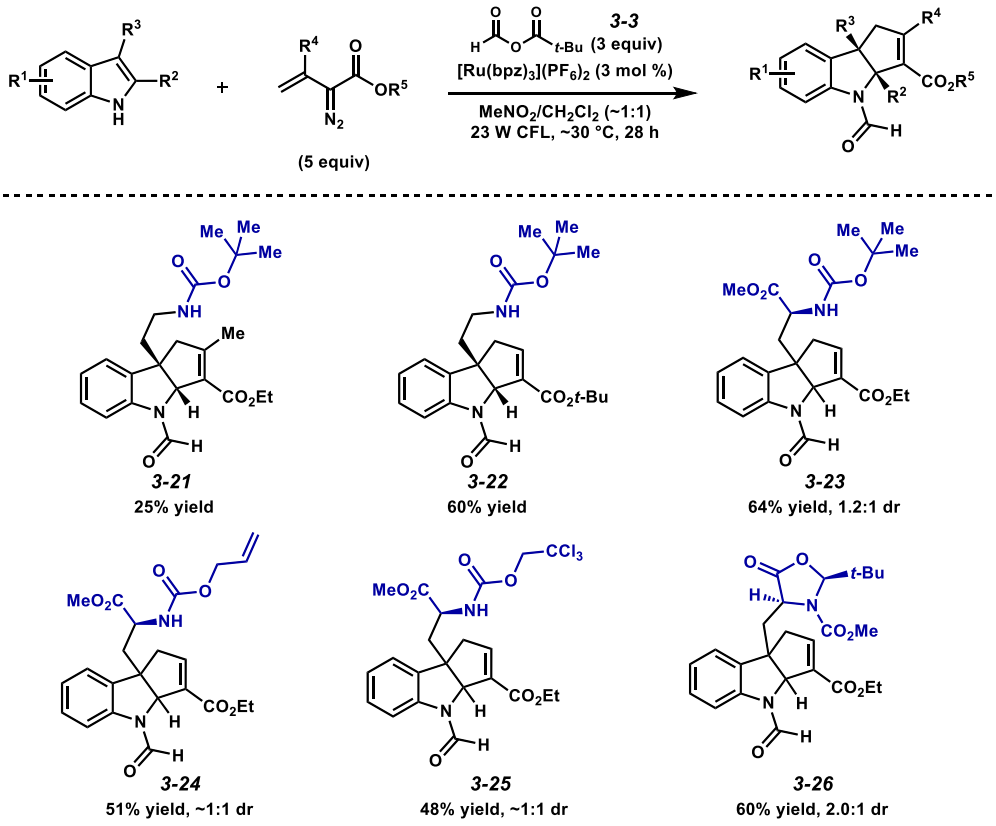

Scheme 3.4.2. Extended scope of the cycloaddition reaction.

3.5. Product Derivatization

A few product derivatizations were next investigated (*Scheme 3.5.1*). When indoline **3-6** was subjected to mildly acidic conditions, compound **3-28** was observed with moderate diastereoselectivity (1.5:1 dr) and yield (*Scheme 3.5.1a*). Employing indoline **3-7** (*Scheme 3.5.1b*), we were able to selectively deprotect the allyl carbamate using Pd(0) π-allyl conditions, while the formyl group remained intact. Notably, the vinylogous amide was the major product observed (**3-30**). Other Alloc deprotection conditions were tried and all yielded either decomposition products, vinylogous amide product, or **3-28**, indicating that the free amine may be somewhat unstable in the presence of the nearby α,β-unsaturated ester.[9] Additionally, we were able to selectively deformylate under acidic conditions, preserving the allyl carbamate (**3-29**).

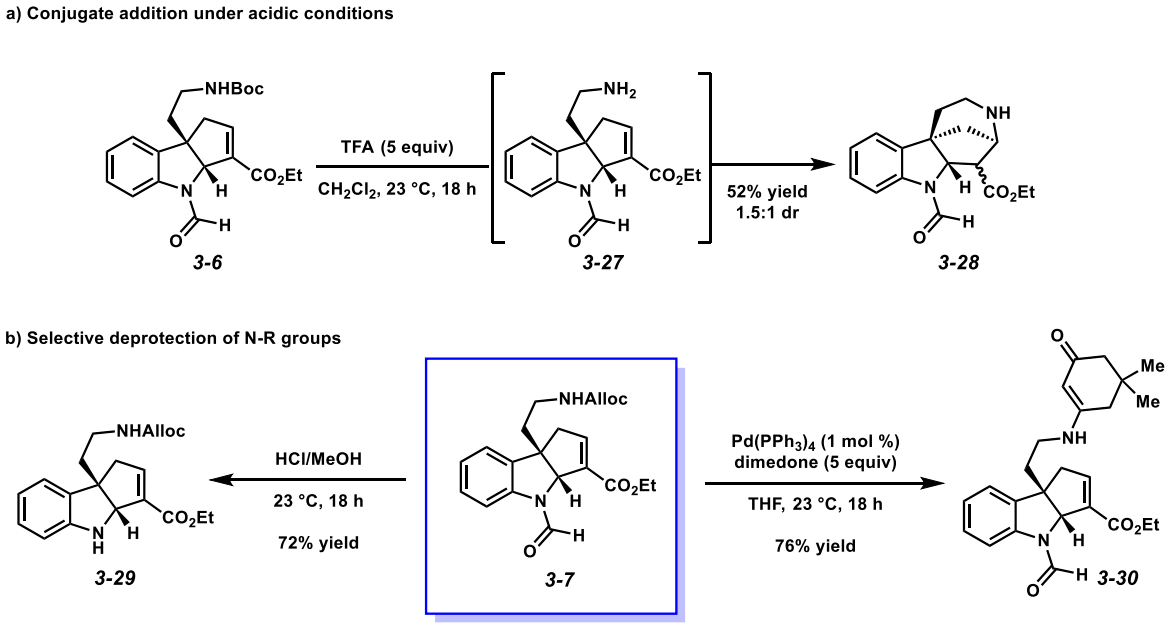

Scheme 3.5.1. (a) Deprotection of the Boc carbamate and conjugate addition. (b) Selective deprotection of the allyl carbamate or formamide.

3.6. Non-Amine Examples

We were also interested in demonstrating the utility of this method with other, non-aminated indoles using trimethylacetic formic anhydride **3-3** with $[Ru(bpz)_3](PF_6)_2$. Indolines **3-31–3-35** (*Scheme 3.6.1*) were afforded in excellent yields when subjected to the reaction conditions.

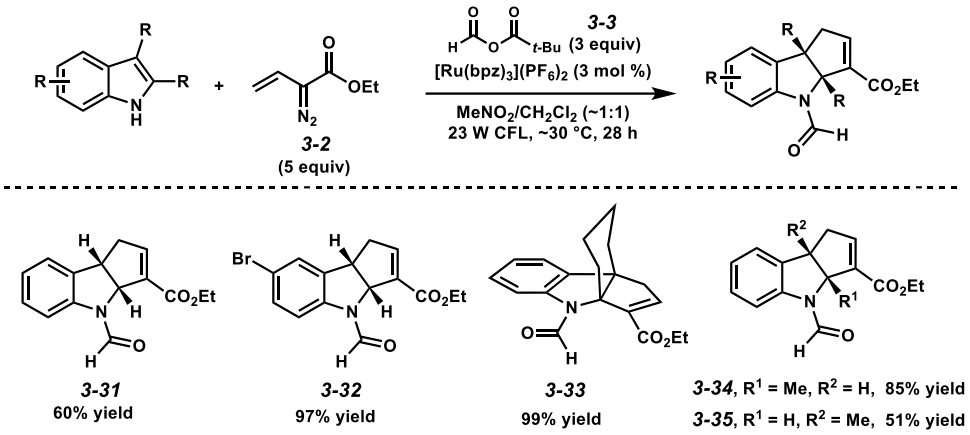

Scheme 3.6.1. Demonstrated method with non-aminated substrates.

3.7. Mechanistic Experiments

An interesting phenomenon we observed in several of these amine-containing substrates was incomplete conversion of the starting indole, even though the indoline cycloadducts were furnished in moderate to excellent yield. We were curious what could be contributing to this lack of complete conversion and slower reactivity. UV-vis studies employing trimethylacetic formic anhydride (**3-3**) without base in the presence of $[Ru(bpz)_3](PF_6)_2$ implicated that catalyst decomposition by the protecting group is no longer a significant problem (*vide supra, Figure*

3.3.1). The lower reactivity could be attributed to a number of issues, and some of our hypotheses as to why were: radical cation stabilization from the protected amine or catalyst degradation via the amine. We first wanted to investigate the possibility of radical cation stabilization (**3-36→3-37**, *Scheme 3.7.1*) slowing reactivity. Indoles that yielded **3-38**, **3-39**, and **3-40** were tested as electronically different substrates (*Scheme 3.7.1*). No perceivable trend was observed, leading us to conclude that stabilization from the amide is likely not deterring reaction progress.

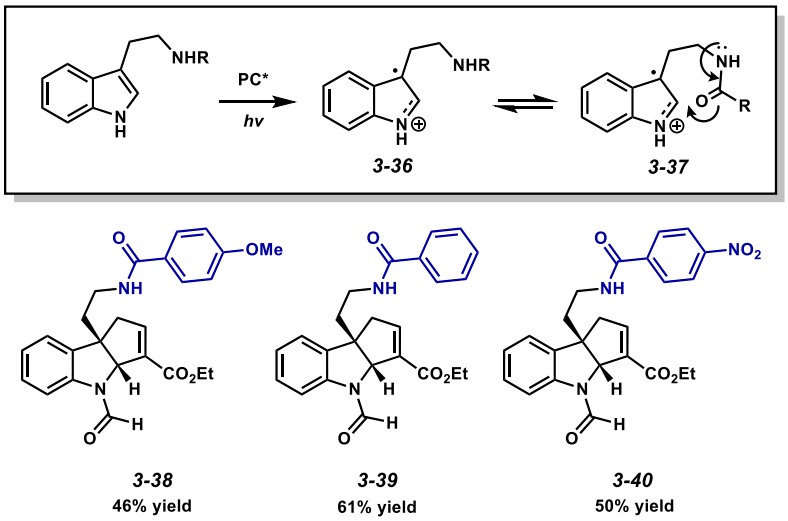

Scheme 3.7.1. Effect of electronic tuning of amine protecting group.

We next wanted to test the presence of an external amine in the reaction with non-aminated indole (*Scheme 3.7.2*). When carbamate **3-42** was subjected to the reaction conditions with indole **3-41**, 53% yield of cycloaddition product (**3-35**) was afforded (*Scheme 3.7.2a*); an almost identical result as when the reaction was run without external amine (51% yield, *vide supra, Scheme 3.6.1*). Additionally, when $[Ru(bpz)_3](PF_6)_2$ was irradiated for 24 h in the presence of external amine **3-42**, no significant change in the UV-vis was observed (*Scheme 3.7.2b*). These results seem to indicate that the protected amine is likely not interfering with the catalyst in a detrimental manner.

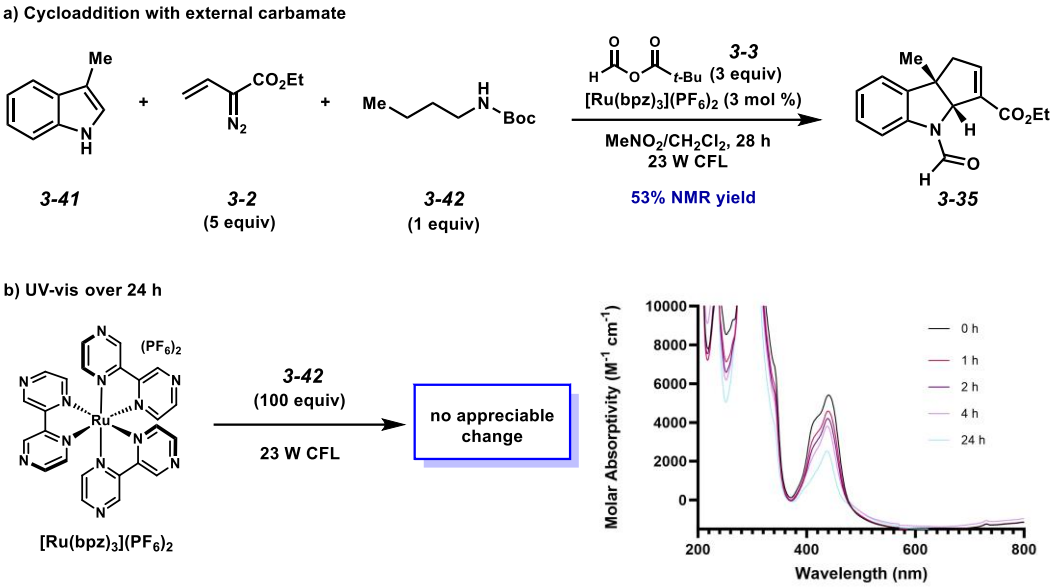

Scheme 3.7.2. (a) Addition of external amine with Ru conditions and (b) Ru stability to amine.

Similarly, we were interested in determining the cause of the Cr catalyst incompatibility with these substrates (*Scheme 3.7.3*). Carbamate **3-42** was again subjected to the reaction with indole **3-41**, employing $[Cr(PMP_2phen)_3](BF_4)_3$ as the photocatalyst. 32% yield of cycloaddition product (**3-35**) was observed (*Scheme 3.7.3a*), a moderate decrease from our result without external amine (57% yield, *see Chapter 2*). While the presence of **3-42** does seem to affect reaction efficiency, it is not an on-off switch like we presumed. Additionally, when $[Cr(PMP_2phen)_3](BF_4)_3$ was irradiated for 24 h in the presence of external amine **3-42**, no change whatsoever was observed in the UV-vis absorbance (*Scheme 3.7.3b*).

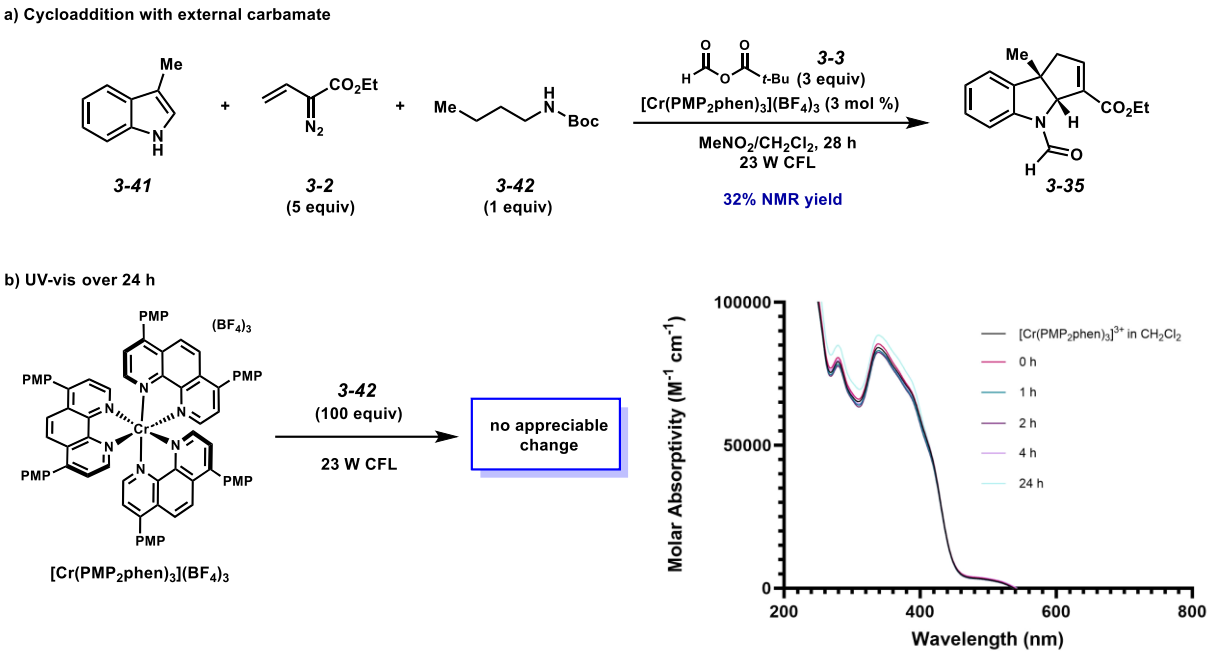

Scheme 3.7.3. (a) Addition of external amine with Cr conditions and (b) Cr stability to amine.

3.8. Proposed Catalytic Cycle

We next surmised that conversion issues could arise from facile intramolecular electron transfer from the indole radical cation to the protected amine.[10] While amine substrates do not seem to degrade the photocatalyst (Ru or Cr, *vide supra*), they can slow radical cation reaction rates through this intramolecular electron transfer, requiring a catalyst with high efficiency for the reaction to proceed to the cycloadduct.[11] Based on our results and previous findings,[1,8] we believe the reaction mechanism proceeds through the catalytic cycle shown in *Scheme 3.8.1*. Excited Ru(II) can oxidize the indolamine (**3-43**) to generate a reactive radical cation (**3-44**) and reduced Ru(I). This radical cation could then be intercepted by the diazoester (**3-2**) to generate intermediate **3-47**, followed by radical cyclization to **3-48**. Reduction of the indoline radical cation by Ru(I), or through propagation, would afford fused indoline **3-49**. Formylation would then generate the

final product **3-50** and drive the cycloadduct oxidation potential above that of starting indole. The radical cation generated after oxidation (**3-44**) could undergo intramolecular electron transfer to the protected amine (**3-45**→**3-46**). To close the cycle, oxygen, or **3-46**, can regenerate ground state Ru(II).

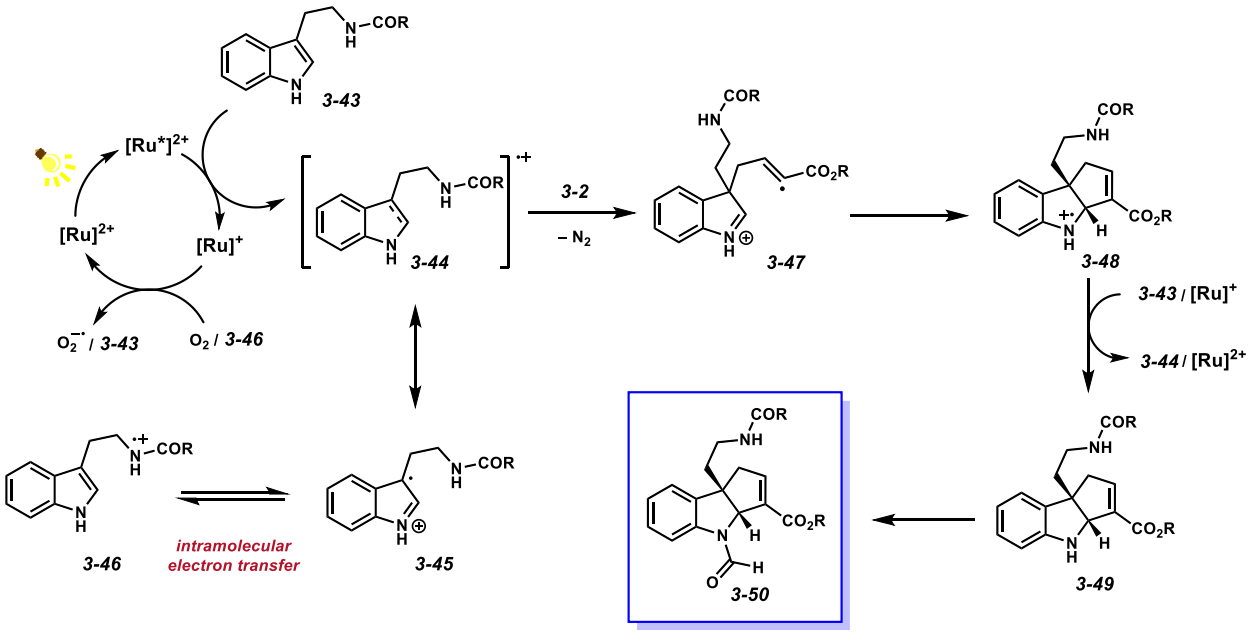

Scheme 3.8.1. Proposed catalytic cycle.

3.9. Conclusion and Project Outlook

In conclusion, we have disclosed a dearomative (3 + 2) photocatalyzed cycloaddition between protected tryptophan or tryptamine derivatives and vinyl diazoacetates. The subsequent amino-indoline products have significant value in their potential to be utilized as intermediates toward relevant natural products. Extending the scope of this reaction to this useful functional group, through exploring catalyst tolerance, has also been accomplished. Further studies

investigating diastereoselectivity in this reaction, as well as investigating this method with various peptide sequences, are underway.

The future of the photocatalysis project within our lab lies in three separate directions. First, our interest in developing *earth-abundant* metal photocatalysts is still ongoing. The continuous development of chromium(III) photocatalysts and expansion of the reaction profile of these Cr photocatalysts are fundamental goals. Second, there remains a gap in the literature of indole-based dearomative cycloadditions invoking PET processes. There is ample opportunity for continued exploration of these dearomative reactions to access important structural motifs. Finally, there are motivations to continue exploring radical cation reactions coupled with vinyldiazo reactants. These cycloadditions have the potential to add a number of new methods and interesting structures to the literature (*see Chapter 4*).

3.10. Experimental Section

3.10.1. Materials and Methods

$[Ru(bpz)_3](PF_6)_2$ was prepared according to the procedure by Yoon and coworkers.[12] Reactions to synthesize substrates were performed under argon atmosphere unless otherwise noted. Reactions to synthesize (3+2) cycloadducts were performed open to air. Dichloromethane, tetrahydrofuran, dimethylformamide, and toluene were purified by passing through activated alumina columns. 1,4-Dioxane was distilled over CaH_2 and stored over 3Å molecular sieves. Methanol (certified ACS grade) was stored over 3Å molecular sieves. Nitromethane (99%), acetonitrile (HPLC grade), and acetone (HPLC grade) were used as received. Commercially available chemicals were purchased from Alfa Aesar (Ward Hill, MA), Sigma-Aldrich (St. Louis, MO), Oakwood Products (West Columbia, SC), Strem (Newburport, MA), and TCI America (Portland, OR). Qualitative TLC analysis was performed on 250 mm thick, 60 Å, glass backed, F254 silica (SiliCycle, Quebec City, Canada). Visualization was accomplished with UV light and/or exposure to cerium ammonium molybdate (Hanessian's Stain), $KMnO_4$, or *p*-anisaldehyde stain solutions followed by heating. Flash chromatography was performed using SiliCycle silica gel (230-400 mesh). ^1H NMR spectra were acquired on either a Bruker AVANCE III HD NMR (at 400 MHz) or a Bruker AVANCE NEO NMR (at 900 MHz) and are reported relative to $SiMe_4$ (δ 0.00). ^{13}C NMR spectra were acquired on either a Bruker AVANCE III HD NMR (at 100 MHz) or a Bruker AVANCE NEO NMR (at 226 MHz) and are reported relative to $SiMe_4$ (δ 0.0). All IR spectra were obtained on a Thermo Nicolet iS10 spectrometer and are reported in wavenumbers (ν). High resolution mass spectrometry (HRMS) data were acquired via electrospray ionization (ESI) using a ThermoFisher Orbitrap Q-Exactive. Catalyst absorbance measurements were taken

on a Varian Cary 5000 UV-Visible-NIR spectrophotometer. Reactions under near-UV irradiation (NUV) were performed in a Luzchem photoreactor (LZC-ORG) equipped with 10 lamps of wavelengths 419, 350, and 300 nm. Reactions under blue LED irradiation were performed using a 390 nm Kessil PR160L LED PhotoReaction light. Irradiation with visible light was performed with one 23 W compact fluorescent light bulb (EcoSmart 23 W bright white CFL spiral bulb, 1600 lumens). Cycloadditions using all modes of irradiation were performed using borosilicate vials. The internal temperature of the photobox was measured at approximately 30 °C.

3.10.2. Optimization Experiments

Table 3.2.1 (recreated). Catalyst Optimization.

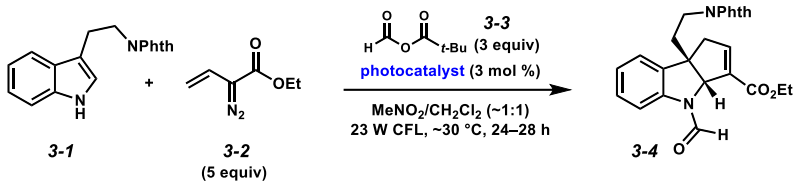

entry	photocatalyst	^{1}H NMR yield (%)
1	$[Cr(PMP_2phen)_3](BF_4)_3$	25
2	$[Cr(Ph_2phen)_3](BF_4)_3$	trace
3	4-CzIPN	trace
4	DCA	10
5	Mes-Acr(BF_4)	trace
6	TPP(BF_4)	trace
7	$(OMe)_3$TPP(BF_4)	10
8	$[Ir(dFCF_3ppy)_2(bpy)](PF_6)$	15
9	$[Ir(dFCF_3ppy)_2(5,5'\text{-}dCF_3bpy)](PF_6)$	63 [a]
10	$[Ru(bpy)_3]Cl_2$	15
11	$[Ru(bpz)_3](PF_6)_2$	62 [a]

[a] Isolated yields

General procedure for catalyst optimization: In a flame-dried 1-dram borosilicate vial open to air, trimethylacetic formic anhydride (**3-3**, 3.0 equiv) was dissolved in CH_3NO_2 (0.20 M with respect to indole substrate). To this solution were added indole (**3-1**, 1.0 equiv), photocatalyst (1.5 mol %), and vinyl diazoacetate **3-2** (3.0 equiv, 1.0 M solution in CH_2Cl_2). The vial was then capped, and the reaction mixture was irradiated with a 23 W CFL bulb while stirring. After 8 h, second charges of vinyl diazoacetate **3-2** (2.0 equiv, 1.0 M solution in CH_2Cl_2) and photocatalyst (1.5 mol %) were added, and irradiation was continued. At the 24 h timepoint, the solvent was removed by rotary evaporation. The crude residue was then dissolved in CH_2Cl_2 (~1 mL), and the solution was passed through a SiO_2 plug (0.5 x 3 cm), eluting with ~4 mL CH_2Cl_2, then ~4 mL EtOAc. The filtrate was concentrated in vacuo, and the crude residue was analyzed by ^{1}H NMR using CH_2Br_2 as an internal standard. Entries 9 and 11 were determined via isolated yields.

Table 3.2.1 (recreated). Deviation from standard conditions.

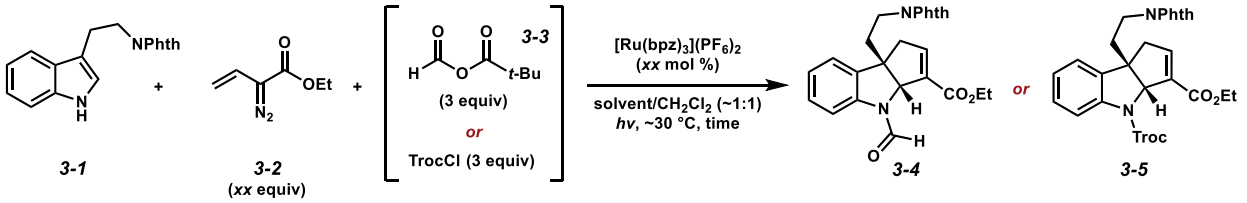

entry	solvent	*hv*	Ru (mol %)	additions (Ru)	VDA (equiv)	PG	time (h)	*3-1* conv (%)	*3-4/3-5* ^{1}H NMR yield (%)[a]
1	CH_2Cl_2	23 W CFL	3	2	5	*3-3*	24	38	30
2	MeCN	23 W CFL	3	2	5	*3-3*	24	50	48
3	Acetone	23 W CFL	3	2	5	*3-3*	24	48	43
4	$MeNO_2$	blue LEDs	3	2	5	*3-3*	24	55	49
5	$MeNO_2$	NUV	3	2	5	*3-3*	24	24	20
6	$MeNO_2$	no hv	3	2	5	*3-3*	24	<10	0
7	$MeNO_2$	23 W CFL	0.5	1	5	*3-3*	24	38	30
8	$MeNO_2$	23 W CFL	0	0	5	*3-3*	24	15	0
9	$MeNO_2$	23 W CFL	3	2	2	*3-3*	24	75	42
10	$MeNO_2$	23 W CFL	3	2	5	TrocCl	24	46	33
11[b]	$MeNO_2$	23 W CFL	3	2	5	TrocCl	24	57	38
12	$MeNO_2$	23 W CFL	6	4	6	*3-3*	48	80	65

[a] CH_2Br_2 was used as an internal standard. [b] 5 equiv of $NaHCO_3$ was also added.

Standard procedure for the analysis of conditions deviations: In a flame-dried 1-dram borosilicate vial open to air, either trimethylacetic formic anhydride (**3-3**, 3.0 equiv) or TrocCl (3.0 equiv) was dissolved in the indicated solvent (0.20 M with respect to indole substrate). To this solution were added indole **3-1**, $[Ru(bpz)_3](PF_6)_2$ (1.5 mol %), and vinyl diazoacetate **3-2** (3.0 equiv, 1.0 M solution in CH_2Cl_2). The vial was then capped, and the reaction mixture was irradiated with the indicated light source while stirring. After 8 h, second charges of vinyl diazoacetate **3-2** (2.0 equiv, 1.0 M solution in CH_2Cl_2) and $[Ru(bpz)_3](PF_6)_2$ (1.5 mol %) were added, and irradiation was continued. At the 24 h timepoint, the solvent was removed by rotary evaporation. The crude residue was then dissolved in CH_2Cl_2 (~1 mL), and the solution was passed through a SiO_2 plug (0.5 x 3 cm), eluting with ~4 mL CH_2Cl_2, then ~4 mL EtOAc. The filtrate was concentrated in vacuo, and the crude residue was analyzed by ^{1}H NMR using CH_2Br_2 as an internal standard to determine conversion of starting material and yield of cycloaddition product.

Notes on deviation:

Entry 6: The reaction vial was covered with aluminum foil and placed in a sealed box and stirred.

Entry 7: $[Ru(bpz)_3](PF_6)_2$ (0.5 mol %) was added at the beginning of the reaction. No second charge of Ru was added.

Entry 8: No $[Ru(bpz)_3](PF_6)_2$ was added to the reaction mixture.

*Entry 9: Only 2.0 equiv of vinyl diazoacetate **3-2** were added at the 0 h timepoint. No second charge of reactant **3-2** was added.*

Entry 11: $NaHCO_3$ (5.0 equiv) was also added to the reaction mixture at the 0 h timepoint.

*Entry 12: The reaction mixture was irradiated for 48 h total. After the first and second charges of Ru and vinyl diazoacetate **3-2**, third charges of $[Ru(bpz)_3](PF_6)_2$ (1.5 mol %) and vinyl diazoacetate **3-2** (1.0 equiv) were added at the 24 h timepoint. A fourth charge of $[Ru(bpz)_3](PF_6)_2$ (1.5 mol %) was added at the 32 h timepoint.*

3.10.3. Photocatalyzed Cycloaddition Reactions

General Procedure:

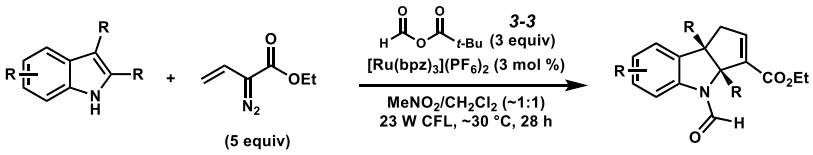

In a flame-dried 1-dram borosilicate vial open to air, trimethylacetic formic anhydride (3.0 equiv) was dissolved in CH_3NO_2 (0.20 M with respect to indole substrate). To this solution were added indole substrate (1.0 equiv), $[Ru(bpz)_3](PF_6)_2$ (1.5 mol %), and vinyl diazoacetate reagent (3.0 equiv, 1.0 M solution in CH_2Cl_2). The vial was then capped, and the reaction mixture was irradiated with a 23 W CFL bulb while stirring. After 8 h, second charges of vinyl diazoacetate reagent (2.0 equiv, 1.0 M solution in CH_2Cl_2) and $[Ru(bpz)_3](PF_6)_2$ (1.5 mol %) were added, and irradiation was continued. Reaction progress was monitored by TLC. When determined complete, the solvent was removed by rotary evaporation. The crude residue was then dissolved in CH_2Cl_2 (~1 mL), and the solution was passed through a SiO_2 plug (0.5 x 3 cm), eluting with ~4 mL CH_2Cl_2, then ~4 mL EtOAc. The filtrate was concentrated in vacuo, and a ^1H NMR spectrum was acquired using CH_2Br_2 as an internal standard to determine conversion and crude yield. The crude residue was then purified by silica gel flash chromatography to afford pure indoline product.

Note: Under the optimized conditions, several of the C3-substituted indole substrates were not fully consumed. Attempts to increase conversion (e.g., increased catalyst loadings) did not appreciably improve the isolated yield of the cycloadduct. See Table 3.2.1, entry 11 (62% yield with 3 mol % Ru) and Table 3.2.2, entry 12 (65% yield with 6 mol % Ru).

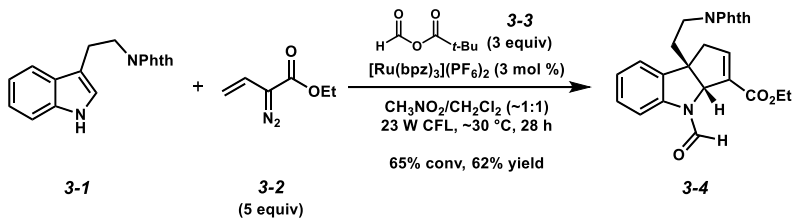

Indoline 3-4. In a flame-dried 1-dram borosilicate vial open to air, trimethylacetic formic anhydride (**3-3**, 42.6 mg, 0.327 mmol) was dissolved in CH_3NO_2 (0.545 mL). To this solution were added indole **3-1** (31.5 mg, 0.109 mmol), $[Ru(bpz)_3](PF_6)_2$ (1.4 mg, 0.00164 mmol), and ethyl vinyl diazoacetate (**3-2**, 0.327 mL, 1.0 M solution in CH_2Cl_2, 0.327 mmol). The vial was then capped, and the reaction mixture was irradiated with a 23 W CFL bulb while stirring. After 8 h, second charges of ethyl vinyl diazoacetate (**3-2**, 0.218 mL, 1.0 M solution in CH_2Cl_2, 0.218 mmol) and $[Ru(bpz)_3](PF_6)_2$ (1.4 mg, 0.00164 mmol) were added, and irradiation was continued. Reaction progress was monitored by TLC. At the 28 h timepoint, the solvent was removed by rotary evaporation. The crude residue was then dissolved in CH_2Cl_2 (~1 mL), and the solution was passed through a SiO_2 plug (0.5 x 3 cm), eluting with ~4 mL CH_2Cl_2, then ~4 mL EtOAc. The filtrate was concentrated in vacuo, and the residue was purified by silica gel flash chromatography (3:1 hexanes/EtOAc eluent) to afford indoline **3-4** (29.0 mg, 62% yield) as a yellow oil. The characterization data was consistent with the data from the previous report.[1]

^{1}H NMR (400 MHz, $CDCl_3$): δ 8.94 (s, 1H), 8.03 (d, *J* = 8.0 Hz, 1H), 7.86-7.73 (comp. m, 2H), 7.73-7.61 (comp. m, 2H), 7.27-7.24 (m, 1H), 7.21 (app. t, *J* = 8.0 Hz, 1H), 7.11 (app. t, *J* = 7.4 Hz, 1H), 6.88 (app. s, 1H), 5.45 (s, 1H), 4.31-4.15 (comp. m, 2H), 3.71-3.57 (m, 1H), 3.55-3.45 (m, 1H), 2.99 (app. d, *J* = 18.8 Hz, 1H), 2.87 (app. d, *J* = 18.8 Hz, 1H), 2.39-2.25 (m, 1H), 2.19-2.07 (m, 1H), 1.32 (t, *J* = 7.2 Hz, 3H).

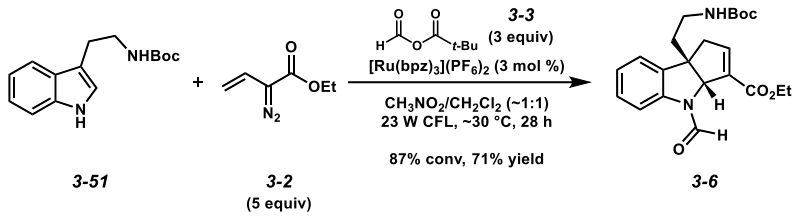

Indoline 3-6. In a flame-dried 1-dram borosilicate vial open to air, trimethylacetic formic anhydride (**3-3**, 38.3 mg, 0.294 mmol) was dissolved in CH_3NO_2 (0.490 mL). To this solution were added indole **3-51** (25.5 mg, 0.0980 mmol), $[Ru(bpz)_3](PF_6)_2$ (1.3 mg, 0.00147 mmol), and ethyl vinyl diazoacetate (**3-2**, 0.294 mL, 1.0 M solution in CH_2Cl_2, 0.294 mmol). The vial was then capped, and the reaction mixture was irradiated with a 23 W CFL bulb while stirring. After 8 h, second charges of ethyl vinyl diazoacetate (**3-2**, 0.196 mL, 1.0 M solution in CH_2Cl_2, 0.196 mmol) and $[Ru(bpz)_3](PF_6)_2$ (1.3 mg, 0.00147 mmol) were added, and irradiation was continued. Reaction progress was monitored by TLC. At the 28 h timepoint, the solvent was removed by rotary evaporation. The crude residue was then dissolved in CH_2Cl_2 (~1 mL), and the solution was passed through a SiO_2 plug (0.5 x 3 cm), eluting with ~4 mL CH_2Cl_2, then ~4 mL EtOAc. The filtrate was concentrated in vacuo, and the residue was purified by silica gel flash chromatography (2:1 hexanes/EtOAc eluent) to afford indoline **3-6** (27.9 mg, 71% yield) as a yellow solid.

TLC R_f: 0.21 in 2:1 hexanes/EtOAc, visualized by UV, stained blue in Hanessian's stain.

^{1}H NMR (400 MHz, $CDCl_3$): δ 8.89 (s, 1H), 8.03 (d, *J* = 8.0 Hz, 1H), 7.29-7.21 (m, 1H), 7.18 (d, *J* = 7.5 Hz, 1H), 7.11 (app. t, *J* = 7.5 Hz, 1H), 6.86 (app. s, 1H), 5.30 (s, 1H), 4.42 (br. s, 1H), 4.26-

4.14 (comp. m, 2H), 3.16-3.00 (br. m, 1H), 2.99-2.83 (br. m, 1H), 2.96 (app. d, *J* = 18.5 Hz, 1H), 2.86 (app. d, *J* = 18.5 Hz, 1H), 2.11-1.95 (comp. m, 2H), 1.42 (s, 9H), 1.30 (t, *J* = 7.1 Hz, 3H).

^{13}C NMR (100 MHz, $CDCl_3$): δ 163.8, 161.6, 156.0, 145.8, 139.7, 137.4, 134.4, 128.9, 125.2, 123.4, 117.8, 79.7, 72.6, 61.0, 54.1, 45.3, 39.6, 37.2, 28.5, 14.3.

IR (ATR, neat): 3368, 2978, 1710, 1678, 1502, 1248 cm^{-1}.

HRMS (ESI+): *m/z* calc'd for $(M + Na)^+$ $[C_{22}H_{28}N_2O_5 + Na]^+$: 423.1890, found 423.1882.

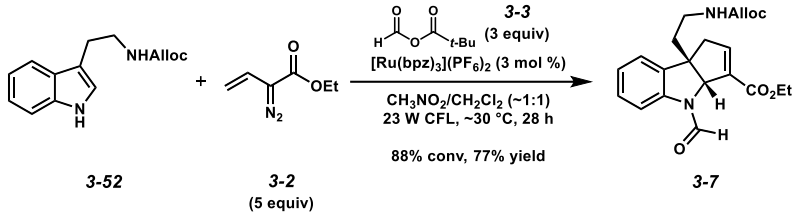

Indoline 3-7. In a flame-dried 1-dram borosilicate vial open to air, trimethylacetic formic anhydride (**3-3**, 33.2 mg, 0.255 mmol) was dissolved in CH_3NO_2 (0.426 mL). To this solution were added indole **3-52** (20.8 mg, 0.0851 mmol), $[Ru(bpz)_3](PF_6)_2$ (1.1 mg, 0.00128 mmol), and ethyl vinyl diazoacetate (**3-2**, 0.255 mL, 1.0 M solution in CH_2Cl_2, 0.255 mmol). The vial was then capped, and the reaction mixture was irradiated with a 23 W CFL bulb while stirring. After 8 h, second charges of ethyl vinyl diazoacetate (**3-2**, 0.170 mL, 1.0 M solution in CH_2Cl_2, 0.170 mmol) and $[Ru(bpz)_3](PF_6)_2$ (1.1 mg, 0.00128 mmol) were added, and irradiation was continued. Reaction progress was monitored by TLC. At the 28 h timepoint, the solvent was removed by rotary evaporation. The crude residue was then dissolved in CH_2Cl_2 (~1 mL), and the solution was passed through a SiO_2 plug (0.5 x 3 cm), eluting with ~4 mL CH_2Cl_2, then ~4 mL EtOAc.

The filtrate was concentrated in vacuo, and the residue was purified by silica gel flash chromatography (2:1 hexanes/EtOAc eluent) to afford indoline **3-7** (25.2 mg, 77% yield) as an orange oil.

TLC R*f*: 0.15 in 2:1 hexanes/EtOAc, visualized by UV, stained blue in Hanessian's stain.

^{1}H NMR (400 MHz, $CDCl_3$): δ 8.89 (s, 1H), 8.04 (d, *J* = 8.0 Hz, 1H), 7.31-7.21 (m, 1H), 7.19 (d, *J* = 7.4 Hz, 1H), 7.12 (app. t, *J* = 7.4 Hz, 1H), 6.87 (app. s, 1H), 5.88 (app. ddd, *J* = 16.6, 10.4, 5.3 Hz, 1H), 5.30 (s, 1H), 5.27 (d, *J* = 16.7 Hz, 1H), 5.20 (d, *J* = 10.4 Hz, 1H), 4.59 (br. s, 1H), 4.52 (d, *J* = 5.9 Hz, 2H), 4.32-4.08 (comp. m, 2H), 3.24-3.07 (m, 1H), 3.05-2.89 (m, 1H), 2.97 (app. d, *J* = 18.4 Hz, 1H), 2.85 (app. d, *J* = 18.4 Hz, 1H), 2.21-1.94 (comp. m, 2H), 1.30 (t, *J* = 7.1 Hz, 3H).

^{13}C NMR (100 MHz, $CDCl_3$): δ 163.8, 161.6, 156.3, 145.7, 139.7, 137.2, 134.4, 132.9, 129.0, 125.2, 123.4, 117.9, 117.8, 72.6, 65.7, 61.1, 54.1, 45.4, 39.6, 37.6, 14.3.

IR (ATR, neat): 3343, 2931, 1710, 1691, 1502, 1246 cm^{-1}.

HRMS (ESI+): *m/z* calc'd for $(M + Na)^+$ $[C_{21}H_{24}N_2O_5 + Na]^+$: 407.1577, found 407.1565.

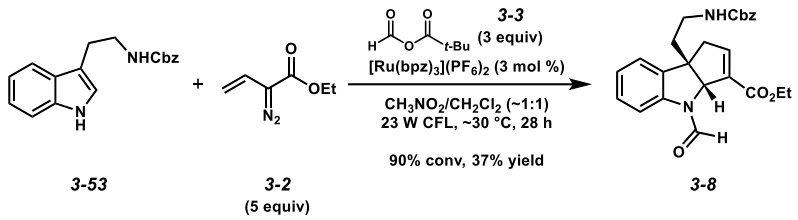

Indoline 3-8. In a flame-dried 1-dram borosilicate vial open to air, trimethylacetic formic anhydride (**3-3**, 34.7 mg, 0.267 mmol) was dissolved in CH_3NO_2 (0.445 mL). To this solution were added indole **3-53** (26.2 mg, 0.0890 mmol), $[Ru(bpz)_3](PF_6)_2$ (1.2 mg, 0.00134 mmol), and ethyl vinyl diazoacetate (**3-2**, 0.267 mL, 1.0 M solution in CH_2Cl_2, 0.267 mmol). The vial was then capped, and the reaction mixture was irradiated with a 23 W CFL bulb while stirring. After 8 h, second charges of ethyl vinyl diazoacetate (**3-2**, 0.178 mL, 1.0 M solution in CH_2Cl_2, 0.178 mmol) and $[Ru(bpz)_3](PF_6)_2$ (1.2 mg, 0.00134 mmol) were added, and irradiation was continued. Reaction progress was monitored by TLC. At the 28 h timepoint, the solvent was removed by rotary evaporation. The crude residue was then dissolved in CH_2Cl_2 (~1 mL), and the solution was passed through a SiO_2 plug (0.5 x 3 cm), eluting with ~4 mL CH_2Cl_2, then ~4 mL EtOAc. The filtrate was concentrated in vacuo, and the residue was purified by silica gel flash chromatography (2:1 hexanes/EtOAc eluent) to afford indoline **3-8** (14.4 mg, 37% yield) as a yellow oil.

TLC R_f: 0.13 in 2:1 hexanes/EtOAc, visualized by UV, stained blue in Hanessian's stain.

^{1}H NMR (400 MHz, $CDCl_3$): δ 8.88 (s, 1H), 8.04 (d, *J* = 8.0 Hz, 1H), 7.40-7.26 (comp. m, 6H), 7.18 (d, *J* = 8.2 Hz, 1H), 7.15-7.06 (m, 1H), 6.86 (app. s, 1H), 5.30 (s, 1H), 5.06 (s, 2H), 4.63 (br.

s, 1H), 4.22-4.15 (comp. m, 2H), 3.22-3.07 (br. m, 1H), 3.04-2.92 (br. m, 1H), 2.96 (app. d, J = 18.7 Hz, 1H), 2.85 (app. d, J = 18.7 Hz, 1H), 2.15-1.99 (comp. m, 2H), 1.30 (t, J = 7.2 Hz, 1H).

^{13}C NMR (100 MHz, $CDCl_3$): δ 163.8, 161.6, 156.4, 145.7, 139.7, 137.2, 134.4, 129.0, 128.7, 128.3, 128.2, 125.2, 123.4, 117.8, 72.6, 66.9, 61.1, 54.1, 45.3, 39.6, 37.6, 14.3. (*1 carbon not detected*).

IR (ATR, neat): 3339, 2929, 1710, 1691, 1483, 1246 cm^{-1}.

HRMS (ESI+): *m/z* calc'd for $(M + Na)^+$ $[C_{25}H_{26}N_2O_5 + Na]^+$: 457.1734, found 457.1722.

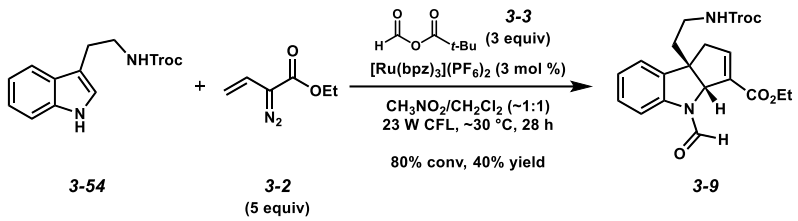

Indoline 3-9. In a flame-dried 1-dram borosilicate vial open to air, trimethylacetic formic anhydride (**3-3**, 33.8 mg, 0.260 mmol) was dissolved in CH_3NO_2 (0.434 mL). To this solution were added indole **3-54** (29.1 mg, 0.0867 mmol), $[Ru(bpz)_3](PF_6)_2$ (1.1 mg, 0.00130 mmol), and ethyl vinyl diazoacetate (**3-2**, 0.260 mL, 1.0 M solution in CH_2Cl_2, 0.260 mmol). The vial was then capped, and the reaction mixture was irradiated with a 23 W CFL bulb while stirring. After 8 h, second charges of ethyl vinyl diazoacetate (**3-2**, 0.173 mL, 1.0 M solution in CH_2Cl_2, 0.173 mmol) and $[Ru(bpz)_3](PF_6)_2$ (1.1 mg, 0.00130 mmol) were added, and irradiation was continued. Reaction progress was monitored by TLC. At the 28 h timepoint, the solvent was removed by rotary evaporation. The crude residue was then dissolved in CH_2Cl_2 (~1 mL), and the solution

was passed through a SiO_2 plug (0.5 x 3 cm), eluting with ~4 mL CH_2Cl_2, then ~4 mL EtOAc. The filtrate was concentrated in vacuo, and the residue was purified by silica gel flash chromatography (2:1 hexanes/EtOAc eluent) to afford indoline **3-9** (16.3 mg, 40% yield) as a yellow oil.

TLC R_f: 0.19 in 2:1 hexanes/EtOAc, visualized by UV, stained blue in Hanessian's stain.

^{1}H NMR (400 MHz, $CDCl_3$): δ 8.90 (s, 1H), 8.05 (d, *J* = 8.0 Hz, 1H), 7.30-7.21 (m, 1H), 7.19 (d, *J* = 7.5 Hz, 1H), 7.13 (app. t, *J* = 7.5 Hz, 1H), 6.87 (app. s, 1H), 5.32 (s, 1H), 4.93-4.77 (m, 1H), 4.76-4.60 (comp. m, 2H), 4.28-4.13 (comp. m, 2H), 3.18 (app. quint, *J* = 7.5 Hz, 1H), 3.02 (app. quint, *J* = 7.5 Hz, 1H), 2.99 (app. d, *J* = 18.7 Hz, 1H), 2.85 (app. d, *J* = 18.7 Hz, 1H), 2.20-2.02 (comp. m, 2H), 1.30 (t, *J* = 7.2 Hz, 3H).

^{13}C NMR (100 MHz, $CDCl_3$): δ 163.7, 161.6, 154.6, 145.6, 139.7, 137.0, 134.4, 129.1, 125.3, 123.4, 117.9, 95.6, 74.6, 72.5, 61.1, 54.1, 45.5, 39.4, 37.8, 14.3.

IR (ATR, neat): 3338, 2927, 1721, 1710, 1483, 1245 cm^{-1}.

HRMS (ESI+): *m/z* calc'd for $(M + Na)^+$ $[C_{20}H_{21}Cl_3N_2O_5 + Na]^+$: 497.0408, found 497.0399.

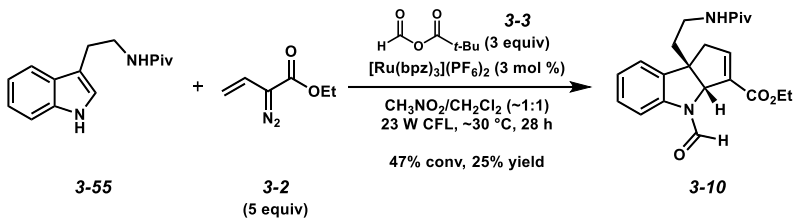

Indoline 3-10. In a flame-dried 1-dram borosilicate vial open to air, trimethylacetic formic anhydride (**3-3**, 36.3 mg, 0.279 mmol) was dissolved in CH_3NO_2 (0.465 mL). To this solution were added indole **3-55** (22.7 mg, 0.0929 mmol), $[Ru(bpz)_3](PF_6)_2$ (1.2 mg, 0.00139 mmol), and ethyl vinyl diazoacetate (**3-2**, 0.279 mL, 1.0 M solution in CH_2Cl_2, 0.279 mmol). The vial was then capped, and the reaction mixture was irradiated with a 23 W CFL bulb while stirring. After 8 h, second charges of ethyl vinyl diazoacetate (**3-2**, 0.186 mL, 1.0 M solution in CH_2Cl_2, 0.186 mmol) and $[Ru(bpz)_3](PF_6)_2$ (1.2 mg, 0.00139 mmol) were added, and irradiation was continued. Reaction progress was monitored by TLC. At the 28 h timepoint, the solvent was removed by rotary evaporation. The crude residue was then dissolved in CH_2Cl_2 (~1 mL), and the solution was passed through a SiO_2 plug (0.5 x 3 cm), eluting with ~4 mL CH_2Cl_2, then ~4 mL EtOAc. The filtrate was concentrated in vacuo, and the residue was purified by silica gel flash chromatography (2:1 hexanes/EtOAc eluent) to afford indoline **3-10** (9.1 mg, 25% yield) as a yellow oil.

TLC R_f: 0.10 in 2:1 hexanes/EtOAc, visualized by UV, stained blue in Hanessian's stain.

^{1}H NMR (400 MHz, $CDCl_3$): δ 8.90 (s, 1H), 8.05 (d, *J* = 8.0 Hz, 1H), 7.32-7.25 (m, 1H), 7.21 (d, *J* = 7.6 Hz, 1H), 7.12 (app. t, *J* = 7.6 Hz, 1H), 6.87 (app. s, 1H), 5.53 (br. s, 1H), 5.34 (s, 1H), 4.28-4.14 (comp. m, 2H), 3.21-3.04 (m, 1H), 3.01-2.88 (m, 1H), 2.96 (app. d, *J* = 19.0 Hz, 1H), 2.87 (app. d, *J* = 19.0 Hz, 1H), 2.07 (app. t, *J* = 7.6 Hz, 1H), 1.30 (t, *J* = 7.1 Hz, 1H), 1.11 (s, 9H).

^{13}C NMR (100 MHz, $CDCl_3$): δ 166.2, 163.8, 161.6, 145.8, 139.7, 137.5, 134.3, 129.0, 125.2, 123.5, 117.9, 72.5, 61.1, 54.3, 45.3, 39.3, 38.7, 36.3, 27.6, 14.3.

IR (ATR, neat): 3350, 2925, 1721, 1672, 1485, 1247 cm^{-1}.

HRMS (ESI+): *m/z* calc'd for $(M + Na)^+$ $[C_{22}H_{28}N_2O_4 + Na]^+$: 407.1941, found 407.1934.

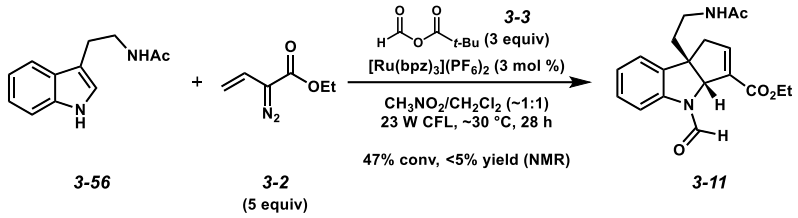

Indoline 3-11. In a flame-dried 1-dram borosilicate vial open to air, trimethylacetic formic anhydride (**3-3**, 35.1 mg, 0.270 mmol) was dissolved in CH_3NO_2 (0.450 mL). To this solution were added indole **3-56** (18.2 mg, 0.0900 mmol), $[Ru(bpz)_3](PF_6)_2$ (1.2 mg, 0.00135 mmol), and ethyl vinyl diazoacetate (**3-2**, 0.270 mL, 1.0 M solution in CH_2Cl_2, 0.270 mmol). The vial was then capped, and the reaction mixture was irradiated with a 23 W CFL bulb while stirring. After 8 h, second charges of ethyl vinyl diazoacetate (**3-2**, 0.180 mL, 1.0 M solution in CH_2Cl_2, 0.180 mmol) and $[Ru(bpz)_3](PF_6)_2$ (1.2 mg, 0.00135 mmol) were added, and irradiation was continued. Reaction progress was monitored by TLC. At the 28 h timepoint, the solvent was removed by rotary evaporation. The crude residue was then dissolved in CH_2Cl_2 (~1 mL), and the solution was passed through a SiO_2 plug (0.5 x 3 cm), eluting with ~4 mL CH_2Cl_2, then ~4 mL EtOAc. The filtrate was concentrated in vacuo, and the residue was analyzed by ^{1}H NMR using CH_2Br_2 as an internal standard and only trace product (<5% yield) was observed.

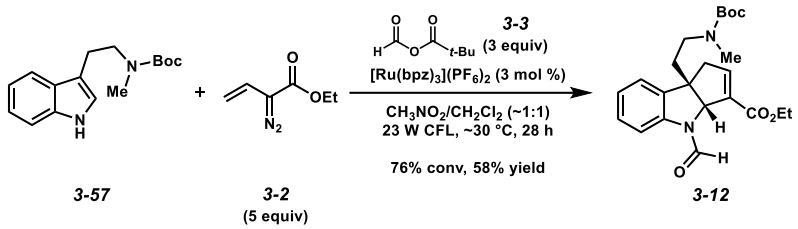

Indoline 3-12. In a flame-dried 1-dram borosilicate vial open to air, trimethylacetic formic anhydride (**3-3**, 35.0 mg, 0.269 mmol) was dissolved in CH_3NO_2 (0.449 mL). To this solution were added indole **3-57** (24.6 mg, 0.0897 mmol), $[Ru(bpz)_3](PF_6)_2$ (1.2 mg, 0.00135 mmol), and ethyl vinyl diazoacetate (**3-2**, 0.269 mL, 1.0 M solution in CH_2Cl_2, 0.269 mmol). The vial was then capped, and the reaction mixture was irradiated with a 23 W CFL bulb while stirring. After 8 h, second charges of ethyl vinyl diazoacetate (**3-2**, 0.179 mL, 1.0 M solution in CH_2Cl_2, 0.179 mmol) and $[Ru(bpz)_3](PF_6)_2$ (1.2 mg, 0.00135 mmol) were added, and irradiation was continued. Reaction progress was monitored by TLC. At the 28 h timepoint, the solvent was removed by rotary evaporation. The crude residue was then dissolved in CH_2Cl_2 (~1 mL), and the solution was passed through a SiO_2 plug (0.5 x 3 cm), eluting with ~4 mL CH_2Cl_2, then ~4 mL EtOAc. The filtrate was concentrated in vacuo, and the residue was purified by silica gel flash chromatography (2:1 hexanes/EtOAc eluent) to afford indoline **3-12** (21.5 mg, 58% yield) as a yellow oil.

TLC R_f: 0.25 in 2:1 hexanes/EtOAc, visualized by UV, stained blue in Hanessian's stain.

^{1}H NMR (400 MHz, $CDCl_3$): δ 8.90 (s, 1H), 8.04 (d, *J* = 8.0 Hz, 1H), 7.29-7.23 (m, 1H), 7.19 (d, *J* = 7.5 Hz, 1H), 7.12 (app. t, *J* = 7.5 Hz, 1H), 6.88 (app. s, 1H), 5.29 (s, 1H), 4.28-4.15 (comp. m,

2H), 3.32-3.09 (br. m, 1H), 3.00-2.87 (br. m, 1H), 2.97 (app. d, *J* = 18.1 Hz, 1H), 2.87 (app. d, *J* = 18.1 Hz, 1H), 2.74 (s, 3H), 2.13-1.90 (comp. m, 2H), 1.42 (s, 9H), 1.30 (t, *J* = 7.1 Hz, 1H).

^{13}C NMR (100 MHz, $CDCl_3$): δ 163.8, 161.6, 155.6, 145.9, 139.6, 134.4, 128.9, 125.2, 123.3, 117.8, 79.8, 72.5, 61.4, 61.0, 54.0, 45.3, 34.6, 28.6, 14.3 (*2 carbons not detected*).

IR (ATR, neat): 2977, 1710, 1678, 1483, 1391, 1246 cm^{-1}.

HRMS (ESI+): *m/z* calc'd for $(M + Na)^+$ $[C_{23}H_{30}N_2O_5 + Na]^+$: 437.2047, found 437.2036.

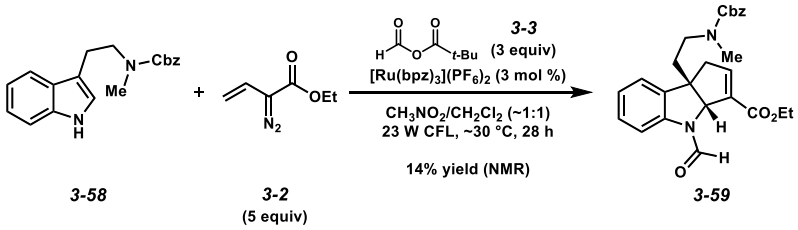

Indoline 3-59. In a flame-dried 1-dram borosilicate vial open to air, trimethylacetic formic anhydride (**3-3**, 40.2 mg, 0.309 mmol) was dissolved in CH_3NO_2 (0.515 mL). To this solution were added indole **3-58** (31.7 mg, 0.103 mmol), $[Ru(bpz)_3](PF_6)_2$ (1.3 mg, 0.00155 mmol), and ethyl vinyl diazoacetate (**3-2**, 0.309 mL, 1.0 M solution in CH_2Cl_2, 0.309 mmol). The vial was then capped, and the reaction mixture was irradiated with a 23 W CFL bulb while stirring. After 8 h, second charges of ethyl vinyl diazoacetate (**3-2**, 0.206 mL, 1.0 M solution in CH_2Cl_2, 0.206 mmol) and $[Ru(bpz)_3](PF_6)_2$ (1.3 mg, 0.00155 mmol) were added, and irradiation was continued. Reaction progress was monitored by TLC. At the 28 h timepoint, the solvent was removed by rotary evaporation. The crude residue was then dissolved in CH_2Cl_2 (~1 mL), and the solution was passed through a SiO_2 plug (0.5 x 3 cm), eluting with ~4 mL CH_2Cl_2, then ~4 mL EtOAc.

The filtrate was concentrated in vacuo, and the residue was analyzed by ^{1}H NMR (indoline **3-59**, 14% yield) using CH_2Br_2 as an internal standard.

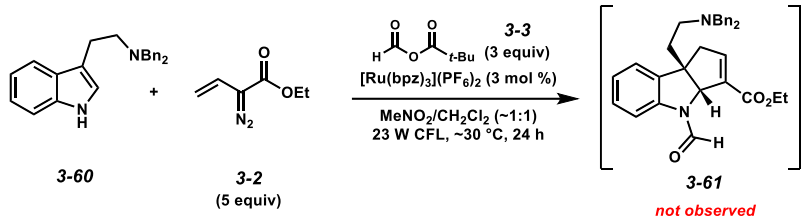

Indoline 3-61. In a flame-dried 1-dram borosilicate vial open to air, trimethylacetic formic anhydride (**3-3**, 37.7 mg, 0.290 mmol) was dissolved in CH_3NO_2 (0.483 mL). To this solution were added indole **3-60** (32.9 mg, 0.0966 mmol), $[Ru(bpz)_3](PF_6)_2$ (1.3 mg, 0.00145 mmol), and ethyl vinyl diazoacetate (**3-2**, 0.290 mL, 1.0 M solution in CH_2Cl_2, 0.290 mmol). The vial was then capped, and the reaction mixture was irradiated with a 23 W CFL bulb while stirring. After 8 h, second charges of ethyl vinyl diazoacetate (**3-2**, 0.193 mL, 1.0 M solution in CH_2Cl_2, 0.193 mmol) and $[Ru(bpz)_3](PF_6)_2$ (1.3 mg, 0.00145 mmol) were added, and irradiation was continued. Reaction progress was monitored by TLC. At the 24 h timepoint, the solvent was removed by rotary evaporation. The crude residue was then dissolved in CH_2Cl_2 (~1 mL), and the solution was passed through a SiO_2 plug (0.5 x 3 cm), eluting with ~4 mL CH_2Cl_2, then ~4 mL EtOAc. The filtrate was concentrated in vacuo, and the residue was analyzed by ^{1}H NMR using CH_2Br_2 as an internal standard. Indoline **3-61** was not observed.

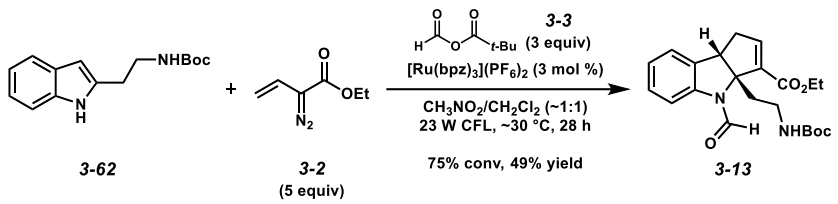

Indoline 3-13. In a flame-dried 1-dram borosilicate vial open to air, trimethylacetic formic anhydride (**3-3**, 30.7 mg, 0.236 mmol) was dissolved in CH_3NO_2 (0.394 mL). To this solution were added indole **3-62** (20.5 mg, 0.0787 mmol), $[Ru(bpz)_3](PF_6)_2$ (1.0 mg, 0.00118 mmol), and ethyl vinyl diazoacetate (**3-2**, 0.236 mL, 1.0 M solution in CH_2Cl_2, 0.236 mmol). The vial was then capped, and the reaction mixture was irradiated with a 23 W CFL bulb while stirring. After 8 h, second charges of ethyl vinyl diazoacetate (**3-2**, 0.157 mL, 1.0 M solution in CH_2Cl_2, 0.157 mmol) and $[Ru(bpz)_3](PF_6)_2$ (1.0 mg, 0.00118 mmol) were added, and irradiation was continued. Reaction progress was monitored by TLC. At the 28 h timepoint, the solvent was removed by rotary evaporation. The crude residue was then dissolved in CH_2Cl_2 (~1 mL), and the solution was passed through a SiO_2 plug (0.5 x 3 cm), eluting with ~4 mL CH_2Cl_2, then ~4 mL EtOAc. The filtrate was concentrated in vacuo, and the residue was purified by silica gel flash chromatography (2:1 hexanes/EtOAc eluent) to afford indoline **3-13** (15.6 mg, 49% yield) as a yellow oil.

TLC R_f: 0.29 in 2:1 hexanes/EtOAc, visualized by UV, stained blue in Hanessian's stain.

^{1}H NMR (400 MHz, $CDCl_3$): δ 9.06 (s, 1H), 8.21 (d, *J* = 8.0 Hz, 1H), 7.23 (app. t, *J* = 8.0 Hz, 1H), 7.16 (d, *J* = 7.4 Hz, 1H), 7.09 (app. t, *J* = 7.4 Hz, 1H), 6.99-6.91 (m, 1H), 4.59 (br. s, 1H),

4.27-4.16 (comp. m, 2H), 4.09 (app. d, J = 8.4 Hz, 1H), 3.26-3.01 (comp. m, 3H), 2.76-2.57 (comp. m, 2H), 2.54-2.37 (m, 1H), 1.42 (s, 9H), 1.29 (t, J = 7.1 Hz, 1H).

^{13}C NMR (100 MHz, $CDCl_3$): δ 164.0, 161.7, 155.9, 147.5, 140.7, 135.6, 133.1, 128.5, 124.8, 124.1, 117.5, 79.7, 79.2, 61.0, 50.5, 39.3, 37.1, 36.3, 28.5, 14.3.

IR (ATR, neat): 3369, 2978, 1710, 1672, 1483, 1379 cm^{-1}.

HRMS (ESI+): *m/z* calc'd for $(M + Na)^+$ $[C_{22}H_{28}N_2O_5 + Na]^+$: 423.1890, found 423.1878.

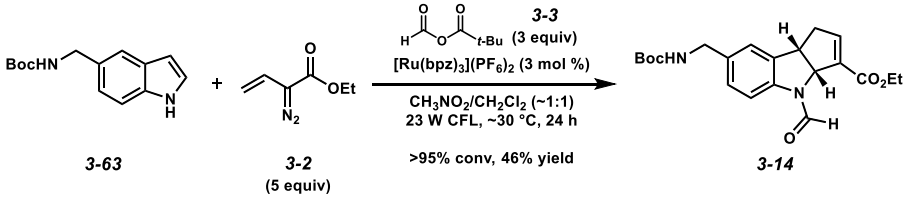

Indoline 3-14. In a flame-dried 1-dram borosilicate vial open to air, trimethylacetic formic anhydride (**3-3**, 43.3 mg, 0.333 mmol) was dissolved in CH_3NO_2 (0.555 mL). To this solution were added indole **3-63** (27.4 mg, 0.111 mmol), $[Ru(bpz)_3](PF_6)_2$ (1.4 mg, 0.00167 mmol), and ethyl vinyl diazoacetate (**3-2**, 0.333 mL, 1.0 M solution in CH_2Cl_2, 0.333 mmol). The vial was then capped, and the reaction mixture was irradiated with a 23 W CFL bulb while stirring. After 8 h, second charges of ethyl vinyl diazoacetate (**3-2**, 0.222 mL, 1.0 M solution in CH_2Cl_2, 0.222 mmol) and $[Ru(bpz)_3](PF_6)_2$ (1.4 mg, 0.00167 mmol) were added, and irradiation was continued. Reaction progress was monitored by TLC. At the 24 h timepoint, the solvent was removed by rotary evaporation. The crude residue was then dissolved in CH_2Cl_2 (~1 mL), and the solution was passed through a SiO_2 plug (0.5 x 3 cm), eluting with ~4 mL CH_2Cl_2, then ~4 mL EtOAc.

The filtrate was concentrated in vacuo, and the residue was purified by silica gel flash chromatography (2:1 hexanes/EtOAc eluent) to afford indoline **3-14** (19.8 mg, 46% yield) as a yellow oil.

TLC R_f: 0.18 in 2:1 hexanes/EtOAc, visualized by UV, stained blue in Hanessian's stain.

^{1}H NMR (400 MHz, $CDCl_3$): δ 8.89 (s, 1H), 7.97 (d, *J* = 8.1 Hz, 1H), 7.15 (s, 1H), 7.13 (d, *J* = 8.1 Hz, 1H), 6.97-6.87 (m, 1H), 5.57 (d, *J* = 8.0 Hz, 1H), 4.81 (br. s, 1H), 4.36-4.11 (comp. m, 5H), 3.09 (app. dd, *J* = 19.0, 8.2 Hz, 1H), 2.79 (app. d, *J* = 19.0 Hz, 1H), 1.46 (s, 9H), 1.30 (t, *J* = 7.2 Hz, 1H).

^{13}C NMR (100 MHz, $CDCl_3$): δ 163.9, 161.8, 156.0, 146.3, 139.4, 135.9, 134.8, 127.8, 123.7, 117.6, 79.7, 68.4, 61.0, 44.6, 43.3, 39.3, 28.6, 14.3 (*1 carbon not detected*).

IR (ATR, neat): 3350, 2978, 1710, 1678, 1492, 1251 cm^{-1}.

HRMS (ESI+): *m/z* calc'd for $(M + H)^+$ $[C_{21}H_{26}N_2O_5 + H]^+$: 387.1915, found 387.1898.

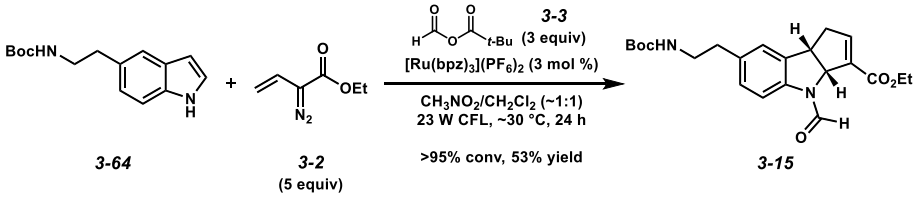

Indoline 3-15. In a flame-dried 1-dram borosilicate vial open to air, trimethylacetic formic anhydride (**3-3**, 48.4 mg, 0.372 mmol) was dissolved in CH_3NO_2 (0.620 mL). To this solution were added indole **3-64** (32.4 mg, 0.124 mmol), $[Ru(bpz)_3](PF_6)_2$ (1.6 mg, 0.00186 mmol), and

ethyl vinyl diazoacetate (**3-2**, 0.372 mL, 1.0 M solution in CH_2Cl_2, 0.372 mmol). The vial was then capped, and the reaction mixture was irradiated with a 23 W CFL bulb while stirring. After 8 h, second charges of ethyl vinyl diazoacetate (**3-2**, 0.248 mL, 1.0 M solution in CH_2Cl_2, 0.248 mmol) and $[Ru(bpz)_3](PF_6)_2$ (1.6 mg, 0.00186 mmol) were added, and irradiation was continued. Reaction progress was monitored by TLC. At the 24 h timepoint, the solvent was removed by rotary evaporation. The crude residue was then dissolved in CH_2Cl_2 (~1 mL), and the solution was passed through a SiO_2 plug (0.5 x 3 cm), eluting with ~4 mL CH_2Cl_2, then ~4 mL EtOAc. The filtrate was concentrated in vacuo, and the residue was purified by silica gel flash chromatography (2:1 hexanes/EtOAc eluent) to afford indoline **3-15** (26.1 mg, 53% yield) as a yellow solid.

TLC R_f: 0.14 in 2:1 hexanes/EtOAc, visualized by UV, stained blue in Hanessian's stain.

^{1}H NMR (400 MHz, $CDCl_3$): δ 8.89 (s, 1H), 7.95 (d, *J* = 8.0 Hz, 1H), 7.05 (d, *J* = 8.0 Hz, 1H), 7.04 (s, 1H), 6.96-6.87 (m, 1H), 5.57 (d, *J* = 8.2 Hz, 1H), 4.52 (br. s, 1H), 4.28-4.13 (comp. m, 3H), 3.43-3.23 (comp. m, 2H), 3.09 (app. dd, *J* = 19.0, 8.2 Hz, 1H), 2.87-2.68 (comp. m, 3H), 1.43 (s, 9H), 1.31 (t, *J* = 7.2 Hz, 3H).

^{13}C NMR (100 MHz, $CDCl_3$): δ 164.0, 161.7, 156.0, 146.3, 138.6, 135.9, 135.9, 134.8, 128.9, 124.6, 117.6, 79.4, 68.4, 61.0, 43.3, 42.1, 39.3, 36.0, 28.6, 14.3.

IR (ATR, neat): 3371, 2977, 1710, 1672, 1501, 1257 cm^{-1}.

HRMS (ESI+): *m/z* calc'd for $(M + H)^+$ $[C_{22}H_{28}N_2O_5 + H]^+$: 401.2071, found 401.2051.

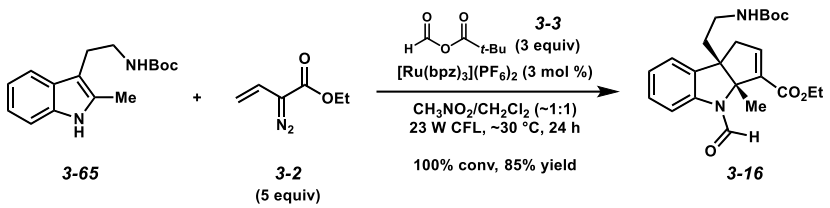

Indoline 3-16. In a flame-dried 1-dram borosilicate vial open to air, trimethylacetic formic anhydride (**3-3**, 41.4 mg, 0.318 mmol) was dissolved in CH_3NO_2 (0.530 mL). To this solution were added indole **3-65** (29.1 mg, 0.106 mmol), $[Ru(bpz)_3](PF_6)_2$ (1.4 mg, 0.00159 mmol), and ethyl vinyl diazoacetate (**3-2**, 0.318 mL, 1.0 M solution in CH_2Cl_2, 0.318 mmol). The vial was then capped, and the reaction mixture was irradiated with a 23 W CFL bulb while stirring. After 8 h, second charges of ethyl vinyl diazoacetate (**3-2**, 0.212 mL, 1.0 M solution in CH_2Cl_2, 0.212 mmol) and $[Ru(bpz)_3](PF_6)_2$ (1.4 mg, 0.00159 mmol) were added, and irradiation was continued. Reaction progress was monitored by TLC. At the 24 h timepoint, the solvent was removed by rotary evaporation. The crude residue was then dissolved in CH_2Cl_2 (~1 mL), and the solution was passed through a SiO_2 plug (0.5 x 3 cm), eluting with ~4 mL CH_2Cl_2, then ~4 mL EtOAc. The filtrate was concentrated in vacuo, and the residue was purified by silica gel flash chromatography (2:1 hexanes/EtOAc eluent) to afford indoline **3-16** (37.4 mg, 85% yield) as a colorless oil.

TLC R_f: 0.16 in 2:1 hexanes/EtOAc, visualized by UV, stained blue in Hanessian's stain.

^{1}H NMR (400 MHz, $CDCl_3$): 8.87 (s, 1H), 8.16 (d, J = 8.0 Hz, 1H), 7.28-7.21 (m, 1H), 7.19 (d, J = 7.6 Hz, 1H), 7.08 (app. t, J = 7.6 Hz, 1H), 6.81 (app. s, 1H), 4.39 (br. m, 1H), 4.24-4.06 (comp. m, 2H), 3.16-3.03 (br. m, 1H), 3.02-2.92 (m, 1H), 2.95 (app. d, J =18.3 Hz, 1H), 2.68 (app. d, J =

18.3 Hz, 1H), 1.98-1.73 (comp. m, 2H), 1.82 (s, 3H), 1.42 (s, 9H), 1.29-1.21 (br. t, J = 7.4 Hz, 3H).

^{13}C NMR (100 MHz, $CDCl_3$): δ 163.2, 161.1, 156.0, 144.0, 140.3, 137.7, 135.3, 128.9, 124.4, 123.5, 117.5, 77.9, 60.7, 57.2, 41.7, 36.9, 35.7, 28.5, 18.5, 14.2 (*1 carbon not detected*).

IR (ATR, neat): 3372, 2977, 1710, 1665, 1381, 1246 cm^{-1}.

HRMS (ESI+): *m/z* calc'd for $(M + H)^+$ $[C_{23}H_{30}N_2O_5 + H]^+$: 415.2227, found 415.2211.

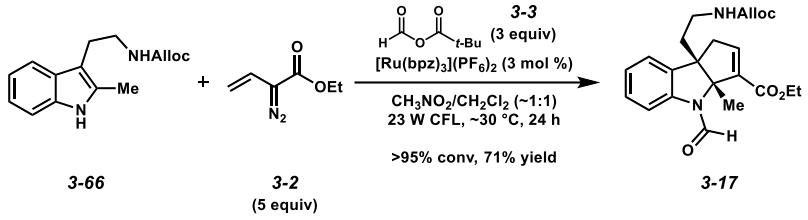

Indoline 3-17. In a flame-dried 1-dram borosilicate vial open to air, trimethylacetic formic anhydride (**3-3**, 46.1 mg, 0.354 mmol) was dissolved in CH_3NO_2 (0.590 mL). To this solution were added indole **3-66** (30.5 mg, 0.118 mmol), $[Ru(bpz)_3](PF_6)_2$ (1.5 mg, 0.00177 mmol), and ethyl vinyl diazoacetate (**3-2**, 0.354 mL, 1.0 M solution in CH_2Cl_2, 0.354 mmol). The vial was then capped, and the reaction mixture was irradiated with a 23 W CFL bulb while stirring. After 8 h, second charges of ethyl vinyl diazoacetate (**3-2**, 0.236 mL, 1.0 M solution in CH_2Cl_2, 0.236 mmol) and $[Ru(bpz)_3](PF_6)_2$ (1.5 mg, 0.00177 mmol) were added, and irradiation was continued. Reaction progress was monitored by TLC. At the 24 h timepoint, the solvent was removed by rotary evaporation. The crude residue was then dissolved in CH_2Cl_2 (~1 mL), and the solution was passed through a SiO_2 plug (0.5 x 3 cm), eluting with ~4 mL CH_2Cl_2, then ~4 mL EtOAc. The filtrate was concentrated in vacuo, and the residue was purified by silica gel flash

chromatography (2:1 to 1:1 hexanes/EtOAc eluent) to afford indoline **3-17** (33.2 mg, 71% yield) as a yellow solid.

TLC R_f: 0.16 in 2:1 hexanes/EtOAc, visualized by UV, stained blue in Hanessian's stain.

^{1}H NMR (400 MHz, $CDCl_3$): δ 8.87 (s, 1H), 8.16 (d, *J* = 8.1 Hz, 1H), 7.31-7.21 (m, 1H), 7.19 (d, *J* = 7.5 Hz, 1H), 7.09 (app. t, *J* = 7.5 Hz, 1H), 6.81 (app. s, 1H), 5.87 (app. ddd, *J* = 17.1, 10.8, 5.5 Hz, 1H), 5.27 (d, *J* = 17.3 Hz, 1H), 5.20 (d, *J* = 10.4 Hz, 1H), 4.61 (br. s, 1H), 4.58-4.45 (comp. m, 2H), 4.23-4.09 (comp. m, 2H), 3.24-3.07 (m, 1H), 3.05-2.89 (m, 1H), 2.95 (app. d, *J* = 18.0 Hz, 1H), 2.67 (app. d, *J* = 18.0 Hz, 1H), 2.01-1.80 (comp. m, 2H), 1.83 (s, 3H), 1.26 (t, *J* = 7.4 Hz, 3H).

^{13}C NMR (100 MHz, $CDCl_3$): δ 163.2, 161.1, 156.4, 143.9, 140.3, 137.7, 135.2, 132.9, 129.0, 124.5, 123.3, 117.9, 117.6, 77.8, 65.7, 60.8, 57.2, 41.8, 37.4, 35.7, 18.4, 14.2.

IR (ATR, neat): 3342, 2981, 1710, 1725, 1665, 1390 cm^{-1}.

HRMS (ESI+): *m/z* calc'd for $(M + H)^+$ $[C_{22}H_{26}N_2O_5 + H]^+$: 399.1914, found 399.1896.

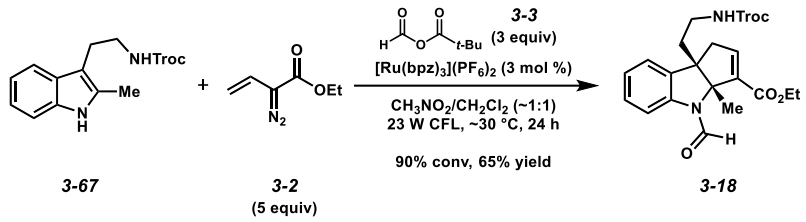

Indoline 3-18. In a flame-dried 1-dram borosilicate vial open to air, trimethylacetic formic anhydride (**3-3**, 39.0 mg, 0.300 mmol) was dissolved in CH_3NO_2 (0.500 mL). To this solution were added indole **3-67** (35.0 mg, 0.100 mmol), $[Ru(bpz)_3](PF_6)_2$ (1.3 mg, 0.00150 mmol), and ethyl vinyl diazoacetate (**3-2**, 0.300 mL, 1.0 M solution in CH_2Cl_2, 0.300 mmol). The vial was then capped, and the reaction mixture was irradiated with a 23 W CFL bulb while stirring. After 8 h, second charges of ethyl vinyl diazoacetate (**3-2**, 0.200 mL, 1.0 M solution in CH_2Cl_2, 0.200 mmol) and $[Ru(bpz)_3](PF_6)_2$ (1.3 mg, 0.00150 mmol) were added, and irradiation was continued. Reaction progress was monitored by TLC. At the 24 h timepoint, the solvent was removed by rotary evaporation. The crude residue was then dissolved in CH_2Cl_2 (~1 mL), and the solution was passed through a SiO_2 plug (0.5 x 3 cm), eluting with ~4 mL CH_2Cl_2, then ~4 mL EtOAc. The filtrate was concentrated in vacuo, and the residue was purified by silica gel flash chromatography (2:1 to 1:1 hexanes/EtOAc eluent) to afford indoline **3-18** (31.8 mg, 65% yield) as a yellow solid.

TLC R_f: 0.23 in 2:1 hexanes/EtOAc, visualized by UV, stained blue in Hanessian's stain.

^{1}H NMR (400 MHz, $CDCl_3$): δ 8.88 (s, 1H), 8.17 (d, *J* = 8.1 Hz, 1H), 7.31-7.25 (m, 1H), 7.20 (d, *J* = 7.5 Hz, 1H), 7.10 (app. t, *J* = 7.5 Hz, 1H), 6.81 (app. s, 1H), 4.87 (br. s, 1H), 4.74-4.62 (comp. m, 2H), 4.24-4.09 (comp. m, 2H), 3.31-3.13 (m, 1H), 3.07-2.92 (m, 1H), 2.97 (app. d, *J* = 18.3 Hz,

1H), 2.68 (app. d, *J* = 18.3 Hz, 1H), 2.07-1.82 (comp. m, 2H), 1.84 (s, 3H), 1.26 (t, *J* = 7.1 Hz, 3H).

^{13}C NMR (100 MHz, $CDCl_3$): δ 163.2, 161.1, 154.6, 143.8, 140.3, 137.7, 135.0, 129.1, 124.6, 123.3, 117.6, 95.6, 77.8, 74.6, 60.8, 57.1, 41.9, 37.6, 35.5, 18.4, 14.2.

IR (ATR, neat): 3338, 2981, 1725, 1710, 1665, 1390 cm^{-1}.

HRMS (ESI+): *m/z* calc'd for $(M + H)^+$ $[C_{21}H_{23}Cl_3N_2O_5 + H]^+$: 489.0745, found 489.0727.

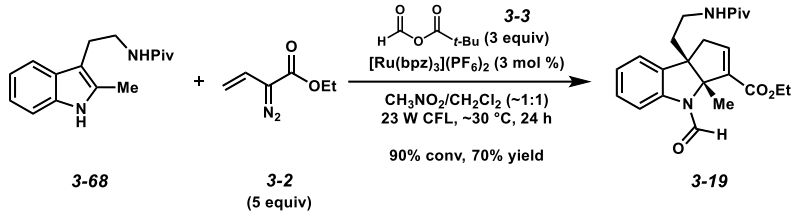

Indoline 3-19. In a flame-dried 1-dram borosilicate vial open to air, trimethylacetic formic anhydride (**3-3**, 46.1 mg, 0.354 mmol) was dissolved in CH_3NO_2 (0.590 mL). To this solution were added indole **3-68** (30.6 mg, 0.118 mmol), $[Ru(bpz)_3](PF_6)_2$ (1.5 mg, 0.00177 mmol), and ethyl vinyl diazoacetate (**3-2**, 0.354 mL, 1.0 M solution in CH_2Cl_2, 0.354 mmol). The vial was then capped, and the reaction mixture was irradiated with a 23 W CFL bulb while stirring. After 8 h, second charges of ethyl vinyl diazoacetate (**3-2**, 0.236 mL, 1.0 M solution in CH_2Cl_2, 0.236 mmol) and $[Ru(bpz)_3](PF_6)_2$ (1.5 mg, 0.00177 mmol) were added, and irradiation was continued. Reaction progress was monitored by TLC. At the 24 h timepoint, the solvent was removed by rotary evaporation. The crude residue was then dissolved in CH_2Cl_2 (~1 mL), and the solution was passed through a SiO_2 plug (0.5 x 3 cm), eluting with ~4 mL CH_2Cl_2, then ~4 mL EtOAc.

The filtrate was concentrated in vacuo, and the residue was purified by silica gel flash chromatography (2:1 to 1:1 hexanes/EtOAc eluent) to afford indoline **3-19** (32.7 mg, 70% yield) as an off-white solid.

TLC R*f*: 0.12 in 2:1 hexanes/EtOAc, visualized by UV, stained blue in Hanessian's stain.

^{1}H NMR (400 MHz, $CDCl_3$): δ 8.87 (s, 1H), 8.16 (d, *J* = 8.0 Hz, 1H), 7.27-7.22 (m, 1H), 7.21 (d *J* = 7.5 Hz, 1H), 7.09 (app. t, *J* = 7.5 Hz, 1H), 6.80 (app. s, 1H), 5.54 (br. s, 1H), 4.23-4.09 (comp. m, 2H), 3.28-3.14 (m, 1H), 3.08-2.92 (m, 1H), 2.96 (app. d, *J* = 18.3 Hz, 1H), 2.68 (app. d, *J* = 18.3 Hz, 1H), 1.95-1.80 (comp. m, 2H), 1.84 (s, 3H), 1.26 (t, *J* = 7.2 Hz, 3H), 1.11 (s, 9H).

^{13}C NMR (100 MHz, $CDCl_3$): δ 178.8, 163.2, 161.1, 143.9, 140.4, 137.7, 135.4, 128.9, 124.4, 123.4, 117.5, 77.8, 60.7, 57.4, 41.8, 38.7, 36.0, 35.4, 27.6, 18.5, 14.2.

IR (ATR, neat): 3357, 2976, 1710, 1672, 1482, 1381 cm^{-1}.

HRMS (ESI+): *m/z* calc'd for $(M + Na)^+$ $[C_{23}H_{30}N_2O_4 + Na]^+$: 421.2098, found 421.2077.

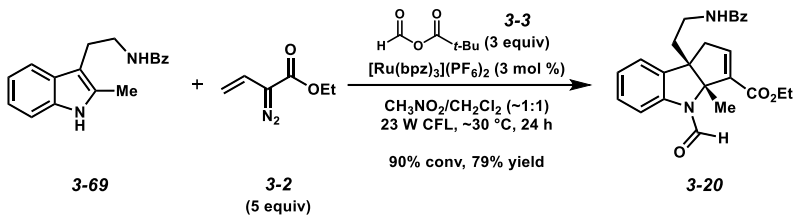

Indoline 3-20. In a flame-dried 1-dram borosilicate vial open to air, trimethylacetic formic anhydride (**3-3**, 41.8 mg, 0.321 mmol) was dissolved in CH_3NO_2 (0.535 mL). To this solution were added indole **3-69** (29.8 mg, 0.107 mmol), $[Ru(bpz)_3](PF_6)_2$ (1.4 mg, 0.00161 mmol), and ethyl vinyl diazoacetate (**3-2**, 0.321 mL, 1.0 M solution in CH_2Cl_2, 0.321 mmol). The vial was then capped, and the reaction mixture was irradiated with a 23 W CFL bulb while stirring. After 8 h, second charges of ethyl vinyl diazoacetate (**3-2**, 0.214 mL, 1.0 M solution in CH_2Cl_2, 0.214 mmol) and $[Ru(bpz)_3](PF_6)_2$ (1.4 mg, 0.00161 mmol) were added, and irradiation was continued. Reaction progress was monitored by TLC. At the 24 h timepoint, the solvent was removed by rotary evaporation. The crude residue was then dissolved in CH_2Cl_2 (~1 mL), and the solution was passed through a SiO_2 plug (0.5 x 3 cm), eluting with ~4 mL CH_2Cl_2, then ~4 mL EtOAc. The filtrate was concentrated in vacuo, and the residue was purified by silica gel flash chromatography (2:1 to 1:1 hexanes/EtOAc eluent) to afford indoline **3-20** (35.2 mg, 79% yield) as a white, airy solid.

TLC R_f: 0.45 in 1:1 hexanes/EtOAc, visualized by UV, stained blue in Hanessian's stain.

^{1}H NMR (400 MHz, $CDCl_3$): δ 8.87 (s, 1H), 8.17 (d, *J* = 8.0 Hz, 1H), 7.66 (d, *J* = 7.5 Hz, 2H), 7.47 (t, *J* = 7.5 Hz, 1H), 7.39 (app. t, *J* = 7.5 Hz, 2H), 7.29-7.20 (comp. m, 2H), 7.08 (app. t, *J* = 7.5 Hz, 1H), 6.81 (app. s, 1H), 6.19 (br. s, 1H), 4.25-4.07 (comp. m, 2H), 3.48-3.33 (m, 1H), 3.32-

3.19 (m, 1H), 2.99 (app. d, J = 18.2 Hz, 1H), 2.72 (app. d, J = 18.2 Hz, 1H), 2.09-1.88 (comp. m, 2H), 1.84 (s, 3H), 1.25 (t, J = 7.2 Hz, 3H).

^{13}C NMR (100 MHz, $CDCl_3$): δ 167.6, 163.2, 161.2, 143.9, 140.3, 137.7, 135.4, 134.3, 131.7, 128.9, 128.7, 126.9, 124.5, 123.5, 117.6, 77.9, 60.7, 57.4, 41.8, 36.4, 35.3, 18.5, 14.2.

IR (ATR, neat): 3330, 2981, 1721, 1710, 1658, 1390 cm^{-1}.

HRMS (ESI+): *m/z* calc'd for $(M + Na)^+$ $[C_{25}H_{26}N_2O_4 + Na]^+$: 441.1785, found 441.1766.

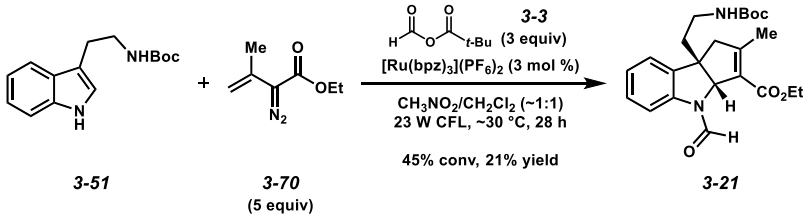

Indoline 3-21. In a flame-dried 1-dram borosilicate vial open to air, trimethylacetic formic anhydride (**3-3**, 39.0 mg, 0.300 mmol) was dissolved in CH_3NO_2 (0.500 mL). To this solution were added indole **3-51** (26.0 mg, 0.0999 mmol), $[Ru(bpz)_3](PF_6)_2$ (1.3 mg, 0.00150 mmol), and ethyl alkenyl diazoacetate **3-70** (0.300 mL, 1.0 M solution in CH_2Cl_2, 0.300 mmol). The vial was then capped, and the reaction mixture was irradiated with a 23 W CFL bulb while stirring. After 8 h, second charges of ethyl alkenyl diazoacetate **3-70** (0.200 mL, 1.0 M solution in CH_2Cl_2, 0.200 mmol) and $[Ru(bpz)_3](PF_6)_2$ (1.3 mg, 0.00150 mmol) were added, and irradiation was continued. Reaction progress was monitored by TLC. At the 28 h timepoint, the solvent was removed by rotary evaporation. The crude residue was then dissolved in CH_2Cl_2 (~1 mL), and the solution was passed through a SiO_2 plug (0.5 x 3 cm), eluting with ~4 mL CH_2Cl_2, then ~4 mL EtOAc.

The filtrate was concentrated in vacuo, and the residue was purified by silica gel flash chromatography (2:1 hexanes/EtOAc eluent) to afford indoline **3-21** (8.6 mg, 21% yield) as a yellow oil.

TLC R_f: 0.24 in 2:1 hexanes/EOAc, visualized by UV, stained blue in Hanessian's stain.

^{1}H NMR (400 MHz, $CDCl_3$): δ 8.80 (s, 1H), 8.00 (d, *J* = 8.0 Hz, 1H), 7.26-7.21 (m, 1H), 7.17 (d, *J* = 7.5 Hz, 1H), 7.10 (app. t, *J* = 7.5 Hz, 1H), 5.32 (s, 1H), 4.41 (br. s, 1H), 4.31-4.16 (comp. m, 2H), 3.12-3.00 (m, 1H), 2.99-2.80 (comp. m, 3H), 2.06 (s, 3H), 2.05-1.92 (comp. m, 2H), 1.42 (s, 9H), 1.33 (t, *J* = 7.1 Hz, 3H).

^{13}C NMR (100 MHz, $CDCl_3$): δ 164.7, 161.6, 157.9, 156.0, 139.7, 137.9, 128.8, 126.4, 125.1, 123.4, 118.0, 79.6, 74.6, 60.6, 51.7, 51.5, 39.4, 37.2, 28.5, 16.9, 14.4.

IR (ATR, neat): 3340, 2970, 1710, 1691, 1483, 1247 cm^{-1}.

HRMS (ESI+): *m/z* calc'd for $(M + Na)^+$ $[C_{23}H_{30}N_2O_5 + Na]^+$: 437.2047, found 437.2038.

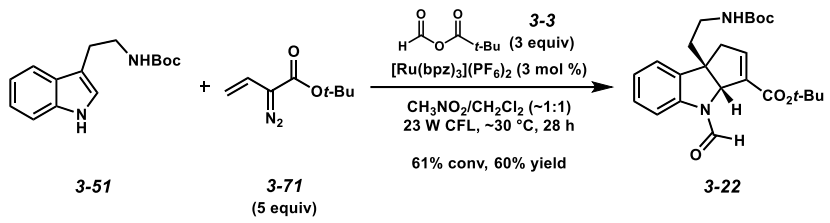

Indoline 3-22. In a flame-dried 1-dram borosilicate vial open to air, trimethylacetic formic anhydride (**3-3**, 38.0 mg, 0.292 mmol) was dissolved in CH_3NO_2 (0.486 mL). To this solution were added indole **3-51** (25.3 mg, 0.0972 mmol), $[Ru(bpz)_3](PF_6)_2$ (1.3 mg, 0.00146 mmol), and *t*-butyl vinyl diazoacetate (**3-71**, 0.292 mL, 1.0 M solution in CH_2Cl_2, 0.292 mmol). The vial was then capped, and the reaction mixture was irradiated with a 23 W CFL bulb while stirring. After 8 h, second charges of *t*-butyl vinyl diazoacetate (**3-71**, 0.194 mL, 1.0 M solution in CH_2Cl_2, 0.194 mmol) and $[Ru(bpz)_3](PF_6)_2$ (1.3 mg, 0.00146 mmol) were added, and irradiation was continued. Reaction progress was monitored by TLC. At the 28 h timepoint, the solvent was removed by rotary evaporation. The crude residue was then dissolved in CH_2Cl_2 (~1 mL), and the solution was passed through a SiO_2 plug (0.5 x 3 cm), eluting with ~4 mL CH_2Cl_2, then ~4 mL EtOAc. The filtrate was concentrated in vacuo, and the residue was purified by silica gel flash chromatography (2:1 hexanes/EtOAc eluent) to afford indoline **3-22** (25.1 mg, 60% yield) as a yellow oil.

TLC R_f: 0.32 in 2:1 hexanes/EtOAc, visualized by UV, stained blue in Hanessian's stain.

^{1}H NMR (400 MHz, $CDCl_3$): δ 8.88 (s, 1H), 8.04 (d, *J* = 8.0 Hz, 1H), 7.29-7.21 (m, 1H), 7.18 (d, *J* = 7.5 Hz, 1H), 7.11 (app. t, *J* = 7.5 Hz, 1H), 6.77 (app. s, 1H), 5.25 (s, 1H), 4.41 (br. s, 1H), 3.16-

2.99 (m, 1H), 2.97-2.84 (m, 1H), 2.93 (app. d, J = 18.4 Hz, 1H), 2.82 (app. d, J = 18.4 Hz, 1H), 2.13-1.94 (comp. m, 2H), 1.49 (s, 9H), 1.42 (s, 9H).

^{13}C NMR (100 MHz, $CDCl_3$): δ 163.2, 161.7, 145.0, 139.7, 135.8, 128.9, 125.1, 123.4, 117.8, 82.7, 81.9, 72.6, 54.1, 45.1, 39.6, 29.8, 28.5, 28.3 (*2 carbons not detected*).

IR (ATR, neat): 3359, 2977, 1709, 1679, 1483, 1366 cm^{-1}.

HRMS (ESI+): *m/z* calc'd for $(M + Na)^+$ $[C_{24}H_{32}N_2O_5 + Na]^+$: 451.2203, found 451.2191.

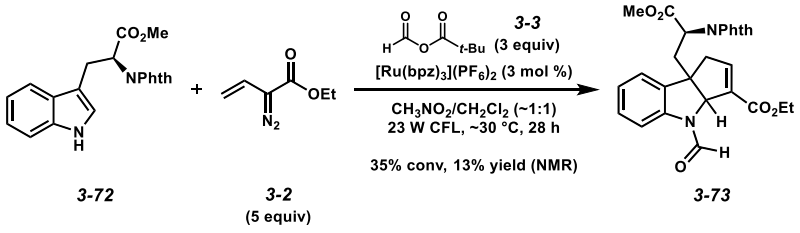

Indoline 3-73. In a flame-dried 1-dram borosilicate vial open to air, trimethylacetic formic anhydride (**3-3**, 33.6 mg, 0.258 mmol) was dissolved in CH_3NO_2 (0.431 mL). To this solution were added indole **3-72** (30.0 mg, 0.0861 mmol), $[Ru(bpz)_3](PF_6)_2$ (1.1 mg, 0.00129 mmol), and ethyl vinyl diazoacetate (**3-2**, 0.258 mL, 1.0 M solution in CH_2Cl_2, 0.258 mmol). The vial was then capped, and the reaction mixture was irradiated with a 23 W CFL bulb while stirring. After 8 h, second charges of ethyl vinyl diazoacetate (**3-2**, 0.172 mL, 1.0 M solution in CH_2Cl_2, 0.172 mmol) and $[Ru(bpz)_3](PF_6)_2$ (1.1 mg, 0.00129 mmol) were added, and irradiation was continued. Reaction progress was monitored by TLC. At the 28 h timepoint, the solvent was removed by rotary evaporation. The crude residue was then dissolved in CH_2Cl_2 (~1 mL), and the solution was passed through a SiO_2 plug (0.5 x 3 cm), eluting with ~4 mL CH_2Cl_2, then ~4 mL EtOAc.

The filtrate was concentrated in vacuo, and the residue was analyzed by ^{1}H NMR (indoline **3-73**, 13% yield) using CH_2Br_2 as an internal standard.

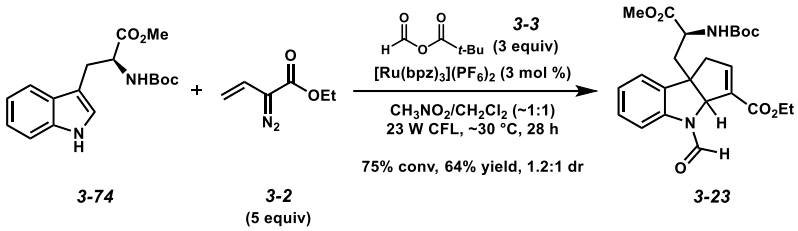

Indoline 3-23. In a flame-dried 1-dram borosilicate vial open to air, trimethylacetic formic anhydride (**3-3**, 36.3 mg, 0.279 mmol) was dissolved in CH_3NO_2 (0.465 mL). To this solution were added indole **3-74** (29.6 mg, 0.0930 mmol), $[Ru(bpz)_3](PF_6)_2$ (1.2 mg, 0.00140 mmol), and ethyl vinyl diazoacetate (**3-2**, 0.279 mL, 1.0 M solution in CH_2Cl_2, 0.279 mmol). The vial was then capped, and the reaction mixture was irradiated with a 23 W CFL bulb while stirring. After 8 h, second charges of ethyl vinyl diazoacetate (**3-2**, 0.186 mL, 1.0 M solution in CH_2Cl_2, 0.186 mmol) and $[Ru(bpz)_3](PF_6)_2$ (1.2 mg, 0.00140 mmol) were added, and irradiation was continued. Reaction progress was monitored by TLC. At the 28 h timepoint, the solvent was removed by rotary evaporation. The crude residue was then dissolved in CH_2Cl_2 (~1 mL), and the solution was passed through a SiO_2 plug (0.5 x 3 cm), eluting with ~4 mL CH_2Cl_2, then ~4 mL EtOAc. The filtrate was concentrated in vacuo, and the residue was purified by silica gel flash chromatography (2:1 hexanes/EtOAc eluent) to afford indoline **3-23** (27.1 mg, 64% yield, 1.2:1 dr) as a yellow oil.

TLC R_f: 0.17 in 2:1 hexanes/EtOAc, visualized by UV, stained blue in Hanessian's stain.

^{1}H NMR (400 MHz, $CDCl_3$, *mixture of two diastereomers*): δ 8.85 (s, 0.45H), 8.84 (s, 0.55H), 8.03 (app. d, *J* = 8.0 Hz, 1H), 7.34-7.26 (m, 1H), 7.20 (app. d, *J* = 7.5 Hz, 1H), 7.16-7.03 (m, 1H), 6.85 (app. s, 1H), 5.40 (s, 0.55H), 5.32 (s, 0.45H), 4.99-4.87 (br. m, 0.45H), 4.87-4.73 (br. m, 0.55H), 4.45 (br. s, 0.45H), 4.26-4.14 (comp. m, 2H), 4.01 (br. s, 0.55H), 3.61 (s, 1.35H), 3.56 (s, 1.65H), 3.03-2.85 (comp. m, 2H), 2.48-2.32 (m, 1H), 2.27-2.08 (m, 1H), 1.44 (s, 4.95H), 1.42 (s, 4.05H), 1.32-1.25 (m, 3H).

^{13}C NMR (100 MHz, $CDCl_3$, *mixture of two diastereomers*): δ 172.9, 172.5, 163.7, 161.65, 161.56, 155.2, 145.7, 145.3, 139.9, 139.6, 137.0, 136.7, 134.5, 134.1, 129.1, 125.1, 125.0, 124.1, 123.6, 117.9, 80.6, 72.7, 72.2, 61.02, 60.97, 54.1, 52.74, 52.70, 51.4, 45.9, 44.5, 41.3, 40.6, 28.4, 14.3.

IR (ATR, neat): 3350, 2979, 1721, 1688, 1484, 1247 cm^{-1}.

HRMS (ESI+): *m/z* calc'd for $(M + Na)^+$ $[C_{24}H_{30}N_2O_7 + Na]^+$: 481.1945, found 481.1930.

Optical rotation: $[\alpha]_D^{23}$ = +11.0 (*c* = 0.50, CH_2Cl_2).

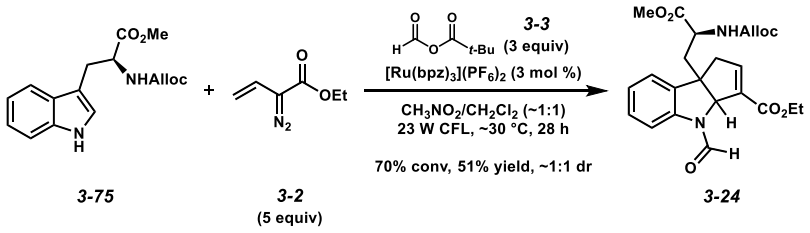

Indoline 3-24. In a flame-dried 1-dram borosilicate vial open to air, trimethylacetic formic anhydride (**3-3**, 33.7 mg, 0.259 mmol) was dissolved in CH_3NO_2 (0.431 mL). To this solution were added indole **3-75** (26.1 mg, 0.0863 mmol), $[Ru(bpz)_3](PF_6)_2$ (1.1 mg, 0.00129 mmol), and ethyl vinyl diazoacetate (**3-2**, 0.259 mL, 1.0 M solution in CH_2Cl_2, 0.259 mmol). The vial was

then capped, and the reaction mixture was irradiated with a 23 W CFL bulb while stirring. After 8 h, second charges of ethyl vinyl diazoacetate (**3-2**, 0.173 mL, 1.0 M solution in CH_2Cl_2, 0.173 mmol) and $[Ru(bpz)_3](PF_6)_2$ (1.1 mg, 0.00129 mmol) were added, and irradiation was continued. Reaction progress was monitored by TLC. At the 28 h timepoint, the solvent was removed by rotary evaporation. The crude residue was then dissolved in CH_2Cl_2 (~1 mL), and the solution was passed through a SiO_2 plug (0.5 x 3 cm), eluting with ~4 mL CH_2Cl_2, then ~4 mL EtOAc. The filtrate was concentrated in vacuo, and the residue was purified by silica gel flash chromatography (2:1 hexanes/EtOAc eluent) to afford indoline **3-24** (19.5 mg, 51% yield, ~1:1 dr) as a yellow oil.

TLC R_f: 0.10 in 2:1 hexanes/EtOAc, visualized by UV, stained blue in Hanessian's stain.

^{1}H NMR (400 MHz, $CDCl_3$, *mixture of two diastereomers*): δ 8.84 (s, 0.5H), 8.82 (s, 0.5H), 8.04 (app. d, *J* = 8.0 Hz, 1H), 7.34-7.04 (comp. m, 3H), 6.85 (app. s, 1H), 6.00-5.77 (m, 1H), 5.40 (s, 0.5H), 5.308 (s, 0.5H), 5.306 (app. d, *J* = 17.5 Hz, 1H), 5.24 (app. d, *J* = 10.3 Hz, 1H), 5.09-4.84 (br. m, 1H), 4.62-4.42 (comp. m, 2H), 4.29-4.11 (comp. m, 2H), 4.06 (br. s, 1H), 3.62 (s, 1.5H), 3.57 (s, 1.5H), 3.07-2.76 (comp. m, 2H), 2.54-2.35 (m, 1H), 2.27-2.11 (m, 1H), 1.30 (t, *J* = 7.4 Hz, 3H).

^{13}C NMR (100 MHz, $CDCl_3$, *mixture of two diastereomers*): δ 172.6, 172.3, 163.7, 161.6, 155.5, 145.5, 145.1, 140.0, 139.7, 134.5, 134.1, 132.5, 125.2, 125.1, 124.0, 123.5, 118.3, 118.0, 117.9, 72.9, 72.2, 66.3, 61.1, 54.1, 52.8, 51.8, 46.1, 45.1, 41.6, 40.7, 14.3.

IR (ATR, neat): 3336, 2952, 1722, 1710, 1691, 1247 cm^{-1}.

HRMS (ESI+): *m/z* calc'd for $(M + H)^+$ $[C_{23}H_{26}N_2O_7 + H]^+$: 443.1813, found 443.1792.

Optical rotation: $[\alpha]_D^{23}$ = +21.6 (c = 0.50, CH_2Cl_2).

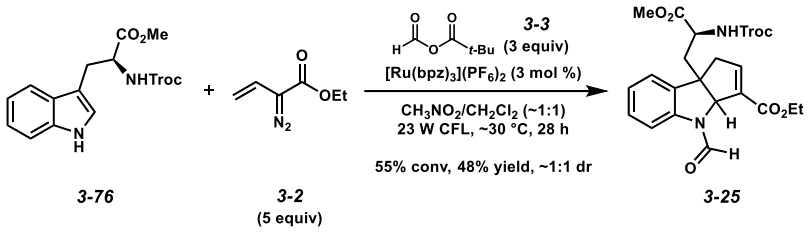

Indoline 3-25. In a flame-dried 1-dram borosilicate vial open to air, trimethylacetic formic anhydride (**3-3**, 32.3 mg, 0.248 mmol) was dissolved in CH_3NO_2 (0.413 mL). To this solution were added indole **3-76** (32.5 mg, 0.0826 mmol), $[Ru(bpz)_3](PF_6)_2$ (1.1 mg, 0.00124 mmol), and ethyl vinyl diazoacetate (**3-2**, 0.248 mL, 1.0 M solution in CH_2Cl_2, 0.248 mmol). The vial was then capped, and the reaction mixture was irradiated with a 23 W CFL bulb while stirring. After 8 h, second charges of ethyl vinyl diazoacetate (**3-2**, 0.165 mL, 1.0 M solution in CH_2Cl_2, 0.165 mmol) and $[Ru(bpz)_3](PF_6)_2$ (1.1 mg, 0.00124 mmol) were added, and irradiation was continued. Reaction progress was monitored by TLC. At the 28 h timepoint, the solvent was removed by rotary evaporation. The crude residue was then dissolved in CH_2Cl_2 (~1 mL), and the solution was passed through a SiO_2 plug (0.5 x 3 cm), eluting with ~4 mL CH_2Cl_2, then ~4 mL EtOAc. The filtrate was concentrated in vacuo, and the residue was purified by silica gel flash chromatography (2:1 hexanes/EtOAc eluent) to afford indoline **3-25** (21.2 mg, 48% yield, ~1:1 dr) as a yellow oil.

TLC R_f: 0.21 in 2:1 hexanes/EtOAc, visualized by UV, stained blue in Hanessian's stain.

^{1}H NMR (400 MHz, $CDCl_3$, *mixture of two diastereomers*): δ 8.86 (app. s, 1H), 8.04 (app. d, *J* = 8.0 Hz, 1H), 7.34-7.08 (comp. m, 3H), 6.85 (app. s, 1H), 5.40 (s, 0.5H), 5.36-5.19 (br. m, 1H), 5.33 (s, 0.5H), 4.86-4.56 (comp. m, 2H), 4.50 (br. s, 0.5H), 4.32-4.10 (comp. m, 2H), 4.06 (br. s, 0.5H), 3.64 (s, 1.5H), 3.59 (s, 1.5H), 3.07-2.80 (comp. m, 2H), 2.62-2.38 (m, 1H), 2.33-2.18 (m, 1H), 1.39-1.17 (m, 3H).

^{13}C NMR (100 MHz, $CDCl_3$, *mixture of two diastereomers*): δ 172.1, 171.7, 163.6, 161.6, 154.1, 145.4, 145.0, 139.7, 136.5, 134.6, 134.2, 129.4, 125.3, 125.1, 123.9, 123.5, 118.0, 95.3, 74.9, 74.8, 72.7, 72.2, 61.1, 54.1, 53.0, 52.2, 52.1, 46.2, 45.1, 41.4, 40.6, 14.3.

IR (ATR, neat): 3331, 2954, 1726, 1710, 1678, 1270 cm^{-1}.

HRMS (ESI+): *m/z* calc'd for $(M + H)^+$ $[C_{22}H_{23}Cl_3N_2O_7 + H]^+$: 533.0644, found 533.0621.

Optical rotation: $[\alpha]_D^{23}$ = +12.4 (*c* = 0.50, CH_2Cl_2).

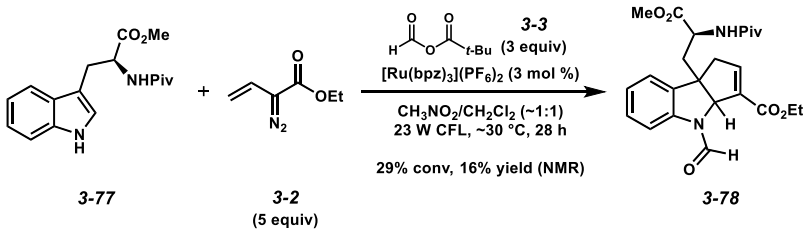

Indoline 3-78. In a flame-dried 1-dram borosilicate vial open to air, trimethylacetic formic anhydride (**3-3**, 47.8 mg, 0.367 mmol) was dissolved in CH_3NO_2 (0.610 mL). To this solution were added indole **3-77** (37.0 mg, 0.122 mmol), $[Ru(bpz)_3](PF_6)_2$ (1.6 mg, 0.00183 mmol), and ethyl vinyl diazoacetate (**3-2**, 0.367 mL, 1.0 M solution in CH_2Cl_2, 0.367 mmol). The vial was

then capped, and the reaction mixture was irradiated with a 23 W CFL bulb while stirring. After 8 h, second charges of ethyl vinyl diazoacetate (**3-2**, 0.244 mL, 1.0 M solution in CH_2Cl_2, 0.244 mmol) and $[Ru(bpz)_3](PF_6)_2$ (1.6 mg, 0.00183 mmol) were added, and irradiation was continued. Reaction progress was monitored by TLC. At the 28 h timepoint, the solvent was removed by rotary evaporation. The crude residue was then dissolved in CH_2Cl_2 (~1 mL), and the solution was passed through a SiO_2 plug (0.5 x 3 cm), eluting with ~4 mL CH_2Cl_2, then ~4 mL EtOAc. The filtrate was concentrated in vacuo, and the residue was analyzed by ^1H NMR (indoline **3-78**, 16% yield) using CH_2Br_2 as an internal standard.

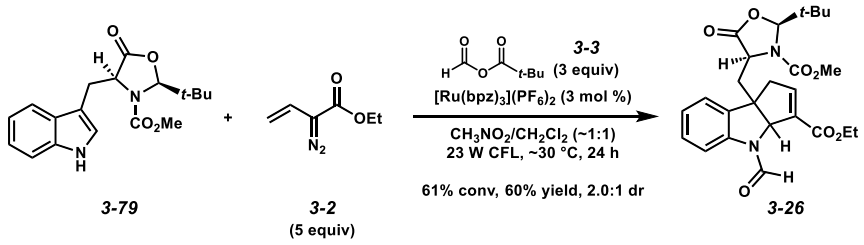

Indoline 3-26. In a flame-dried 1-dram borosilicate vial open to air, trimethylacetic formic anhydride (**3-3**, 48.4 mg, 0.372 mmol) was dissolved in CH_3NO_2 (0.620 mL). To this solution were added indole **3-79** (41.1 mg, 0.124 mmol), $[Ru(bpz)_3](PF_6)_2$ (1.6 mg, 0.00186 mmol), and ethyl vinyl diazoacetate (**3-2**, 0.372 mL, 1.0 M solution in CH_2Cl_2, 0.372 mmol). The vial was then capped, and the reaction mixture was irradiated with a 23 W CFL bulb while stirring. After 8 h, second charges of ethyl vinyl diazoacetate (**3-2**, 0.248 mL, 1.0 M solution in CH_2Cl_2, 0.248 mmol) and $[Ru(bpz)_3](PF_6)_2$ (1.6 mg, 0.00186 mmol) were added, and irradiation was continued. Reaction progress was monitored by TLC. At the 24 h timepoint, the solvent was removed by rotary evaporation. The crude residue was then dissolved in CH_2Cl_2 (~1 mL), and the solution

was passed through a SiO_2 plug (0.5 x 3 cm), eluting with ~4 mL CH_2Cl_2, then ~4 mL EtOAc. The filtrate was concentrated in vacuo, and the residue was purified by silica gel flash chromatography (3:1 hexanes/EtOAc eluent) to afford indoline **3-26** (34.7 mg, 59% yield, 2.0:1 dr) as a yellow solid.

TLC R_f: 0.30 in 2:1 hexanes/EtOAc, visualized by UV, stained blue in Hanessian's stain.

^{1}H NMR (400 MHz, $CDCl_3$, *mixture of two diastereomers*): 8.89 (s, 0.33H), 8.86 (s, 0.67H), 8.04 (d, *J* = 8.5 Hz, 0.33H), 8.02 (d, *J* = 8.5 Hz, 0.67H), 7.35-7.26 (comp. m, 2H), 7.20-7.05 (m, 1H), 6.90 (app. s, 0.33H), 6.86 (app. s, 0.67H), 6.00 (s, 0.67H), 5.78 (br. s, 0.33H), 5.51 (s, 0.33H), 5.49 (s, 0.67H), 4.34 (app. d, *J* = 8.4 Hz, 0.33H), 4.30-4.13 (comp. m, 2H), 4.08-3.89 (br. m, 0.67H), 3.67 (s, 1H), 3.58 (s, 2H), 3.40-3.26 (m, 0.33H), 3.13-3.01 (m, 1H), 3.05-2.90 (m, 0.67H), 2.49-2.17 (comp. m, 2H), 1.31 (app. t, *J* = 7.3 Hz, 3H), 0.94 (app. s, 9H).

^{13}C NMR (100 MHz, $CDCl_3$, *mixture of two diastereomers*): δ 173.2, 172.7, 163.9, 163.8, 162.5, 162.1, 156.2, 146.1, 145.0, 139.6, 135.0, 129.3, 129.2, 125.0, 124.9, 124.0, 117.9, 96.6, 96.5, 71.0, 61.1, 54.7, 54.55, 54.48, 54.3, 53.7, 53.5, 43.1, 42.3, 37.28, 37.25, 25.0, 14.4.

IR (ATR, neat): 2975, 1787, 1721, 1710, 1678, 1483 cm^{-1}.

HRMS (ESI+): *m/z* calc'd for $(M + H)^+$ $[C_{25}H_{30}N_2O_7 + H]^+$: 471.2126, found 471.2106.

Optical rotation: $[\alpha]_D^{23}$ = +26.2 (*c* = 0.50, CH_2Cl_2).

3.10.4. Product Derivatizations

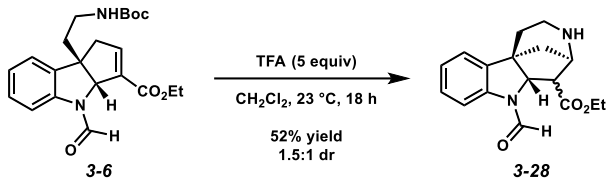

N-H cyclization product 3-28. In a flame-dried flask under argon, to a solution of indoline **3-6** (68.8 mg, 0.172 mmol) in CH_2Cl_2 (0.344 mL) at 23 °C was added trifluoroacetic acid (65.9 μL, 0.860 mmol), and the resulting reaction mixture was stirred overnight. The reaction was determined to be complete by TLC after 18 h. The reaction mixture was concentrated, then dissolved in CH_2Cl_2 (1 mL) and neutralized with sat. aq. $NaHCO_3$ (1 mL). The layers were separated, and the aqueous layer was extracted with CH_2Cl_2 (3 x 2 mL). The organic layers were then combined and washed with brine (2 mL), dried over Na_2SO_4, and concentrated in vacuo. The crude residue was purified via silica gel flash chromatography (1:1 hexanes/EtOAc w/ 1% Et_3N eluent) to afford indoline **3-28** (27.0 mg, 52%, 1.5:1 dr) as a yellow solid.

TLC R_f: 0.08 in 1:1 hexanes/EtOAc, visualized by UV, stained blue in Hanessian's stain.

^{1}H NMR (400 MHz, $CDCl_3$, *mixture of two diastereomers*): δ 9.00 (s, 0.60H), 8.70 (s, 0.40H), 8.13 (d, *J* = 7.9 Hz, 0.40H), 7.23-7.16 (m, 0.60H), 7.20 (app. t, *J* = 7.2 Hz, 1H), 7.14 (app. d, *J* = 7.9 Hz, 1H), 7.07 (app. t, *J* = 7.2 Hz, 1H), 4.90 (d, *J* = 5.0 Hz, 0.60H), 4.84 (d, *J* = 5.0 Hz, 0.40H), 4.43-4.17 (comp. m, 2H), 3.93 (app. s, 0.40H), 3.88 (app. s, 0.60H), 3.39-3.31 (m, 1H), 3.29 (app. dt, *J* = 12.5, 5.0 Hz, 0.60H), 3.11 (app. ddd, *J* = 19.0, 12.5, 5.0 Hz, 1H), 2.76 (app. dt, *J* = 12.5,

5.0 Hz, 0.40H), 2.38-2.23 (m, 1H), 2.04 (br. s, 1H), 1.90-1.62 (comp. m, 3H), 1.44-1.27 (comp. m, 3H).

^{13}C NMR (100 MHz, $CDCl_3$, *mixture of two diastereomers*): δ 171.5, 171.4, 161.0, 157.9, 140.9, 140.6, 136.5, 136.0, 128.5, 128.3, 124.8, 124.4, 123.7, 122.4, 116.7, 109.4, 68.3, 67.9, 61.7, 61.2, 61.0, 59.9, 58.3, 57.9, 54.1, 53.3, 47.5, 46.4, 40.1, 39.8, 32.6, 32.3, 14.5.

IR (ATR, neat): 2930, 1726, 1672, 1353, 1182 cm^{-1}.

HRMS (ESI+): *m/z* calc'd for $(M + H)^+$ $[C_{17}H_{20}N_2O_3 + H]^+$: 301.1547, found 301.1532.

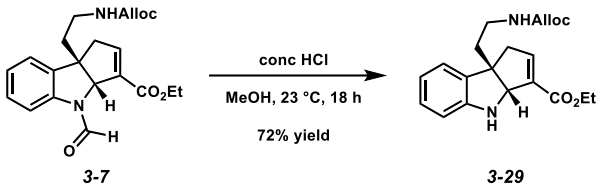

3-7 *3-29*

N-H indoline 3-29. According to a modification of a procedure by Sheehan and Yang,[13] in a round-bottomed flask under argon, indoline **3-7** (32.8 mg, 0.0853 mmol) was dissolved in a 12:1 mixture of MeOH/conc. HCl (0.200 mL). The reaction mixture was stirred at 23 °C for 18 h, and then the mixture was neutralized with sat. aq. $NaHCO_3$ (1 mL) and extracted with EtOAc (3 x 5 mL). The combined organic phases were washed with brine (10 mL), dried over $MgSO_4$, and concentrated in vacuo. The crude residue was purified by flash chromatography (2:1 hexanes/EtOAc eluent) to afford N-H indoline **3-29** (21.9 mg, 72% yield) as a pale-yellow solid.

TLC R_f: 0.43 in 2:1 hexanes/EtOAc, visualized by UV, stained blue in Hanessian's stain.

^{1}H NMR (400 MHz, $CDCl_3$): δ 7.06 (app. t, *J* = 8.4 Hz, 1H), 7.05 (d, *J* = 7.5 Hz, 1H), 6.79 (app. s, 1H), 6.75 (app. t, *J* = 7.5 Hz, 1H), 6.63 (app. d, *J* = 7.8 Hz, 1H), 5.90 (app. ddd, *J* = 16.3, 10.8, 5.5 Hz, 1H), 5.27 (app. d, *J* = 18.1 Hz, 1H), 5.26 (s, 1H), 5.19 (app. d, *J* = 10.4 Hz, 1H), 4.69 (br. s, 2H), 4.52 (app. d, *J* = 5.5 Hz, 2H), 4.25-4.14 (app. q, *J* = 6.9 Hz,, 2H), 3.32-3.17 (m, 1H), 2.97-2.85 (m, 1H), 2.91 (app. d, *J* = 18.3 Hz, 1H), 2.77 (app. d, *J* = 18.3 Hz, 1H), 2.01 (app. t, *J* = 6.9 Hz, 2H), 1.29 (t, *J* = 7.2 Hz, 3H).

^{13}C NMR (100 MHz, $CDCl_3$): δ 164.7, 156.4, 149.3, 143.9, 135.5, 133.7, 133.2, 128.7, 123.5, 119.3, 117.6, 110.4, 71.8, 65.5, 60.6, 55.5, 46.7, 39.7, 38.1, 14.4.

IR (ATR, neat): 3381, 2927, 1721, 1710, 1483, 1245 cm^{-1}.

HRMS (ESI+): *m/z* calc'd for $(M + H)^+$ $[C_{20}H_{24}N_2O_4 + H]^+$: 357.1809, found 357.1791.

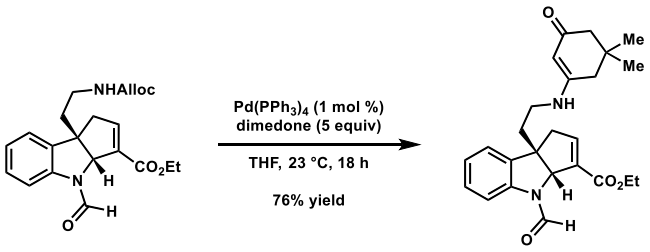

3-7 *3-30*

Indoline 3-30. To a solution of indoline **3-7** (32.8 mg, 0.0853 mmol) in THF (0.427 mL) at 23 °C was added dimedone (59.8 mg, 0.427 mmol) and $Pd(PPh_3)_4$ (1.0 mg, 0.000853 mmol). The reaction mixture was sparged with argon for 5 min and then stirred overnight at room temperature. After 18 h, the mixture was concentrated in vacuo, and the crude residue was purified by silica gel

flash chromatography (20:1 CH_2Cl_2/MeOH w/ 1% Et_3N eluent) to afford indoline **3-30** (27.5 mg, 76% yield) as an orange solid.

TLC R_f: 0.45 in 10:1 CH_2Cl_2/MeOH, visualized by UV.

^{1}H NMR (400 MHz, $CDCl_3$): δ 8.90 (s, 1H), 8.06 (d, *J* = 8.0 Hz, 1H), 7.30 (app. t, *J* = 8.0 Hz, 1H), 7.22-7.08 (comp. m, 2H), 6.87 (app. s, 1H), 5.27 (s, 1H), 5.03 (s, 1H), 4.31-4.16 (comp. m, 2H), 4.03 (br. s, 1H), 3.20-3.05 (m, 1H), 3.04-2.90 (comp. m, 2H), 2.82 (app. d, *J* = 18.3 Hz, 1H), 2.15 (app. s, 4H), 1.97 (app. d, *J* = 5.2 Hz, 2H), 1.31 (t, *J* = 7.2 Hz, 3H), 1.03 (app. s, 6H).

^{13}C NMR (100 MHz, $CDCl_3$): δ 196.9, 163.7, 161.9, 161.5, 145.5, 139.7, 136.9, 134.3, 129.3, 125.4, 123.4, 118.0, 96.0, 72.6, 61.1, 54.1, 50.4, 45.7, 43.7, 39.5, 37.9, 32.9, 28.4, 14.3 (*1 carbon not detected*).

IR (ATR, neat): 3258, 2955, 1710, 1678, 1547,1274 cm^{-1}.

HRMS (ESI+): *m/z* calc'd for $(M + H)^+$ $[C_{25}H_{30}N_2O_4 + H]^+$: 423.2278, found 423.2259.

3.10.5. Non-amine-based examples

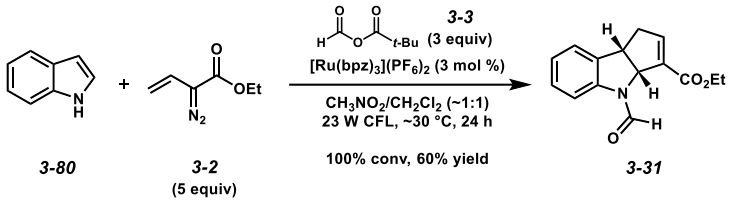

Indoline 3-31. In a flame-dried 1-dram borosilicate vial open to air, trimethylacetic formic anhydride (**3-3**, 60.9 mg, 0.468 mmol) was dissolved in CH_3NO_2 (0.780 mL). To this solution were added indole (**3-80**, 18.3 mg, 0.156 mmol), $[Ru(bpz)_3](PF_6)_2$ (2.0 mg, 0.00234 mmol), and ethyl vinyl diazoacetate (**3-2**, 0.468 mL, 1.0 M solution in CH_2Cl_2, 0.468 mmol). The vial was then capped, and the reaction mixture was irradiated with a 23 W CFL bulb while stirring. After 8 h, second charges of ethyl vinyl diazoacetate (**3-2**, 0.312 mL, 1.0 M solution in CH_2Cl_2, 0.312 mmol) and $[Ru(bpz)_3](PF_6)_2$ (2.0 mg, 0.00234 mmol) were added, and irradiation was continued. Reaction progress was monitored by TLC. At the 24 h timepoint, the solvent was removed by rotary evaporation. The crude residue was then dissolved in CH_2Cl_2 (~1 mL), and the solution was passed through a SiO_2 plug (0.5 x 3 cm), using CH_2Cl_2 as eluent (~8 mL). The filtrate was concentrated in vacuo, and the residue was purified by silica gel flash chromatography (3:1 hexanes/EtOAc eluent) to afford indoline **3-31** (24.2 mg, 60% yield) as a beige solid.

TLC R_f: 0.34 in 2:1 hexanes/EtOAc, visualized by UV, stained blue in Hanessian's stain.

^{1}H NMR (400 MHz, $CDCl_3$): δ 8.92 (s, 1H), 8.03 (d, *J* = 8.0 Hz, 1H), 7.26-7.16 (comp. m, 2H), 7.10 (app. t, *J* = 7.6 Hz, 1H), 6.97-6.88 (m, 1H), 5.58 (d, *J* = 8.2 Hz, 1H), 4.33-4.12 (comp. m, 3H), 3.11 (app. dd, *J* = 18.9, 8.2 Hz, 1H), 2.81 (app. d, *J* = 18.9 Hz, 1H), 1.31 (t, *J* = 7.1 Hz, 3H).

^{13}C NMR (100 MHz, $CDCl_3$): δ 164.0, 161.9, 146.3, 140.1, 135.4, 134.8, 128.5, 125.0, 124.3, 117.7, 68.2, 61.0, 43.4, 39.4, 14.3.

IR (ATR, neat): 2980, 1711, 1678, 1483, 1390, 1258 cm^{-1}.

HRMS (ESI+): *m/z* calc'd for $(M + H)^+$ $[C_{15}H_{15}NO_3 + H]^+$: 258.1125, found 258.1112.

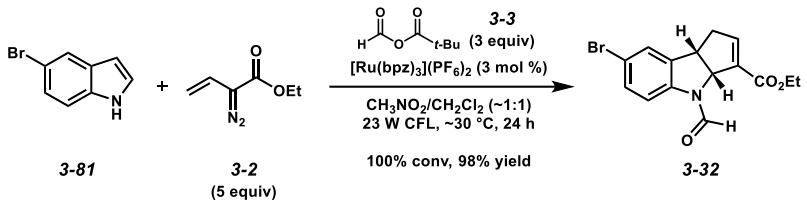

Indoline 3-32. In a flame-dried 1-dram borosilicate vial open to air, trimethylacetic formic anhydride (**3-3**, 40.6 mg, 0.312 mmol) was dissolved in CH_3NO_2 (0.520 mL). To this solution were added indole **3-81** (20.3 mg, 0.104 mmol), $[Ru(bpz)_3](PF_6)_2$ (1.3 mg, 0.00156 mmol), and ethyl vinyl diazoacetate (**3-2**, 0.312 mL, 1.0 M solution in CH_2Cl_2, 0.312 mmol). The vial was then capped, and the reaction mixture was irradiated with a 23 W CFL bulb while stirring. After 8 h, second charges of ethyl vinyl diazoacetate (**3-2**, 0.208 mL, 1.0 M solution in CH_2Cl_2, 0.208 mmol) and $[Ru(bpz)_3](PF_6)_2$ (1.3 mg, 0.00156 mmol) were added, and irradiation was continued. Reaction progress was monitored by TLC. At the 24 h timepoint, the solvent was removed by rotary evaporation. The crude residue was then dissolved in CH_2Cl_2 (~1 mL), and the solution was passed through a SiO_2 plug (0.5 x 3 cm), using CH_2Cl_2 as eluent (~8 mL). The filtrate was

concentrated in vacuo, and the residue was purified by silica gel flash chromatography (3:1 hexanes/EtOAc eluent) to afford indoline **3-32** (34.1 mg, 98% yield) as a white solid.

TLC R_f: 0.31 in 2:1 hexanes/EtOAc, visualized by UV, stained blue in Hanessian's stain.

^{1}H NMR (400 MHz, $CDCl_3$): δ 8.90 (s, 1H), 7.93 (d, *J* = 8.7 Hz, 1H), 7.34 (d, *J* = 8.7 Hz, 1H), 7.32 (s, 1H), 6.97-6.87 (m, 1H), 5.58 (d, *J* = 8.2 Hz, 1H), 4.30-4.13 (comp. m, 3H), 3.10 (app. dd, *J* = 18.9, 8.2 Hz, 1H), 2.79 (app. d, *J* = 18.9 Hz, 1H), 1.31 (t, *J* = 7.2 Hz, 3H).

^{13}C NMR (100 MHz, $CDCl_3$): δ 163.8, 161.8, 146.2, 139.2, 137.6, 134.7, 131.4, 127.5, 119.0, 117.2, 68.4, 61.1, 43.3, 39.3, 14.3.

IR (ATR, neat): 2981, 1710, 1678, 1478, 1380, 1251 cm^{-1}.

HRMS (ESI+): *m/z* calc'd for $(M + H)^+$ $[C_{15}H_{14}BrNO_3 + H]^+$: 336.0230, found 336.0215.

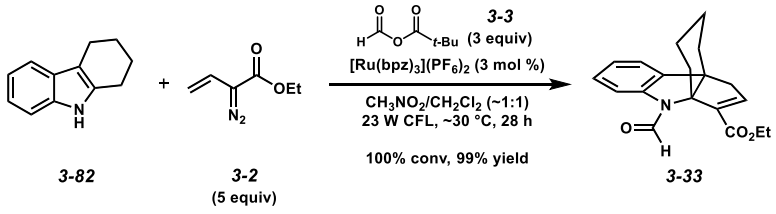

Indoline 3-33. In a flame-dried 1-dram borosilicate vial open to air, trimethylacetic formic anhydride (**3-3**, 47.2 mg, 0.363 mmol) was dissolved in CH_3NO_2 (0.605 mL). To this solution were added indole **3-82** (20.7 mg, 0.121 mmol), $[Ru(bpz)_3](PF_6)_2$ (1.6 mg, 0.00182 mmol), and ethyl vinyl diazoacetate (**3-2**, 0.363 mL, 1.0 M solution in CH_2Cl_2, 0.363 mmol). The vial was

then capped, and the reaction mixture was irradiated with a 23 W CFL bulb while stirring. After 8 h, second charges of ethyl vinyl diazoacetate (**3-2**, 0.242 mL, 1.0 M solution in CH_2Cl_2, 0.242 mmol) and $[Ru(bpz)_3](PF_6)_2$ (1.6 mg, 0.00182 mmol) were added, and irradiation was continued. Reaction progress was monitored by TLC. At the 28 h timepoint, the solvent was removed by rotary evaporation. The crude residue was then dissolved in CH_2Cl_2 (~1 mL), and the solution was passed through a SiO_2 plug (0.5 x 3 cm), using CH_2Cl_2 as eluent (~8 mL). The filtrate was concentrated in vacuo, and the residue was purified by silica gel flash chromatography (3:1 hexanes/EtOAc eluent) to afford indoline **3-33** (37.4 mg, 99% yield) as a yellow oil. The characterization data was consistent with the data from the previous report.[1]

^{1}H NMR (400 MHz, $CDCl_3$): δ 8.93 (s, 1H), 8.17 (d, *J* = 8.0 Hz, 1H), 7.23 (app. t, *J* = 8.0 Hz, 1H), 7.15 (d, *J* = 7.4 Hz, 1H), 7.08 (app. t, *J* = 7.4 Hz, 1H), 6.91 (app. t, *J* = 2.6 Hz, 1H), 4.19 (app. q, *J* = 7.2 Hz, 2H), 2.85 (dd, *J* = 18.8, 2.6 Hz, 1H), 2.75 (dd, *J* = 18.8, 2.6 Hz, 1H), 2.60 (app. dt, *J* = 15.2, 5.2 Hz, 1H), 2.05 (ddd, *J* = 19.3, 15.2, 5.2 Hz, 1H), 1.93-1.81 (m, 1H), 1.80-1.62 (comp. m, 2H), 1.54-1.38 (comp. m, 3H), 1.29 (t, *J* = 7.2 Hz, 3H).

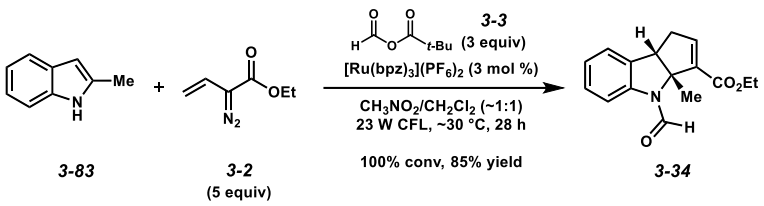

Indoline 3-34. In a flame-dried 1-dram borosilicate vial open to air, trimethylacetic formic anhydride (**3-3**, 48.0 mg, 0.369 mmol) was dissolved in CH_3NO_2 (0.615 mL). To this solution were added 2-methyl indole (**3-83**, 16.2 mg, 0.123 mmol), $[Ru(bpz)_3](PF_6)_2$ (1.6 mg, 0.00185 mmol), and ethyl vinyl diazoacetate (**3-2**, 0.369 mL, 1.0 M solution in CH_2Cl_2, 0.369 mmol). The vial was then capped, and the reaction mixture was irradiated with a 23 W CFL bulb while stirring. After 8 h, second charges of ethyl vinyl diazoacetate (**3-2**, 0.246 mL, 1.0 M solution in CH_2Cl_2, 0.246 mmol) and $[Ru(bpz)_3](PF_6)_2$ (1.6 mg, 0.00185 mmol) were added, and irradiation was continued. Reaction progress was monitored by TLC. At the 28 h timepoint, the solvent was removed by rotary evaporation. The crude residue was then dissolved in CH_2Cl_2 (~1 mL), and the solution was passed through a SiO_2 plug (0.5 x 3 cm), using CH_2Cl_2 as eluent (~8 mL). The filtrate was concentrated in vacuo, and the residue was purified by silica gel flash chromatography (3:1 hexanes/EtOAc eluent) to afford indoline **3-34** (28.4 mg, 85% yield) as a yellow oil. The characterization data was consistent with the data from the previous report.[1]

^{1}H NMR (400 MHz, $CDCl_3$): δ 9.03 (s, 1H), 8.18 (d, *J* = 8.0 Hz, 1H), 7.24-7.19 (m, 1H), 7.16 (d, *J* = 7.4 Hz, 1H), 7.09 (app. t, *J* = 7.4 Hz, 1H), 6.93-6.84 (m, 1H), 4.20 (app. q, *J* = 7.1 Hz, 2H), 3.77 (app. d, *J* = 8.0 Hz, 1H), 3.07 (app. dd, *J* = 18.6, 8.0 Hz, 1H), 2.72 (app. d, *J* = 18.6 Hz, 1H), 1.92 (s, 3H), 1.29 (t, *J* = 7.1 Hz, 3H).

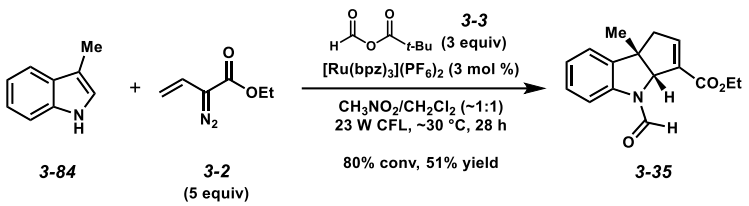

Indoline 3-35. In a flame-dried 1-dram borosilicate vial open to air, trimethylacetic formic anhydride (**3-3**, 43.3 mg, 0.333 mmol) was dissolved in CH_3NO_2 (0.555 mL). To this solution were added 3-methyl indole (**3-84**, 14.5 mg, 0.111 mmol), $[Ru(bpz)_3](PF_6)_2$ (1.4 mg, 0.00167 mmol), and ethyl vinyl diazoacetate (**3-2**, 0.333 mL, 1.0 M solution in CH_2Cl_2, 0.333 mmol). The vial was then capped, and the reaction mixture was irradiated with a 23 W CFL bulb while stirring. After 8 h, second charges of ethyl vinyl diazoacetate (**3-2**, 0.222 mL, 1.0 M solution in CH_2Cl_2, 0.222 mmol) and $[Ru(bpz)_3](PF_6)_2$ (1.4 mg, 0.00167 mmol) were added, and irradiation was continued. Reaction progress was monitored by TLC. At the 28 h timepoint, the solvent was removed by rotary evaporation. The crude residue was then dissolved in CH_2Cl_2 (~1 mL), and the solution was passed through a SiO_2 plug (0.5 x 3 cm), using CH_2Cl_2 as eluent (~8 mL). The filtrate was concentrated in vacuo, and the residue was purified by silica gel flash chromatography (3:1 hexanes/EtOAc eluent) to afford indoline **3-35** (15.4 mg, 51% yield) as a yellow oil. The characterization data was consistent with the data from the previous report.[1]

^{1}H NMR (400 MHz, $CDCl_3$): δ 8.89 (s, 1H), 8.03 (d, *J* = 8.0 Hz, 1H), 7.24 (app. t, *J* = 7.4 Hz, 1H), 7.20 (d, *J* = 7.4 Hz, 1H), 7.11 (app. t, *J* = 8.0 Hz, 1H), 6.88 (app. s, 1H), 5.12 (s, 1H), 4.23 (app. q, *J* = 7.0 Hz, 2H), 2.99 (app. d, *J* = 18.9 Hz, 1H), 2.79 (app. d, *J* = 18.9 Hz, 1H), 1.51 (s, 3H), 1.31 (t, *J* = 7.2 Hz, 3H).

3.10.6. Mechanistic Experiments

External Amine Component:

Without external carbamate:

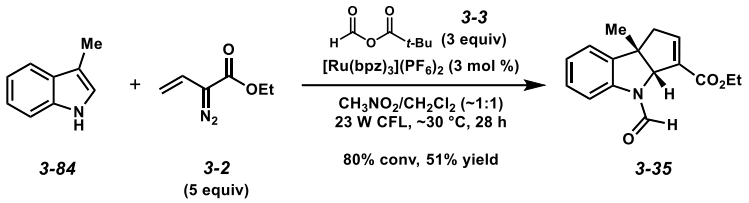

With external carbamate:

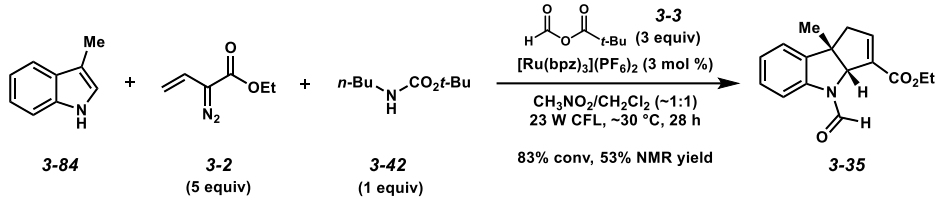

Indoline 3-35. In a flame-dried 1-dram borosilicate vial open to air, trimethylacetic formic anhydride (**3-3**, 38.7 mg, 0.297 mmol) was dissolved in CH_3NO_2 (0.496 mL). To this solution were added 3-methyl indole (**3-84**, 13.0 mg, 0.0991 mmol), *t*-butyl carbamate **3-42** (17.2 mg, 0.0991 mmol), $[Ru(bpz)_3](PF_6)_2$ (1.3 mg, 0.00149 mmol), and ethyl vinyl diazoacetate (**3-2**, 0.297 mL, 1.0 M solution in CH_2Cl_2, 0.297 mmol). The vial was then capped, and the reaction mixture was irradiated with a 23 W CFL bulb while stirring. After 8 h, second charges of ethyl vinyl

diazoacetate (**3-2**, 0.198 mL, 1.0 M solution in CH_2Cl_2, 0.198 mmol) and $[Ru(bpz)_3](PF_6)_2$ (1.3 mg, 0.00149 mmol) were added, and irradiation was continued. Reaction progress was monitored by TLC. At the 24 h timepoint, the solvent was removed by rotary evaporation. The crude residue was then dissolved in CH_2Cl_2 (~1 mL), and the solution was passed through a SiO_2 plug (0.5 x 3 cm), using CH_2Cl_2 as eluent (~8 mL). The filtrate was concentrated in vacuo, and the crude residue was analyzed by ^1H NMR (indoline **3-35**, 53% yield) using CH_2Br_2 as an internal standard.

Without external carbamate:[1]

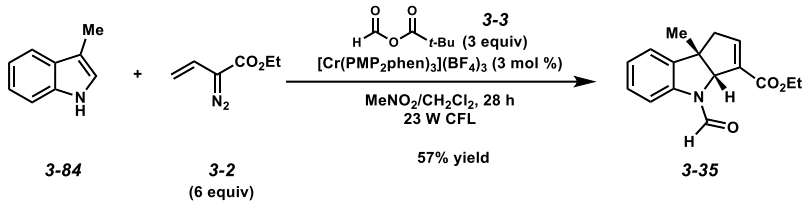

With external carbamate:

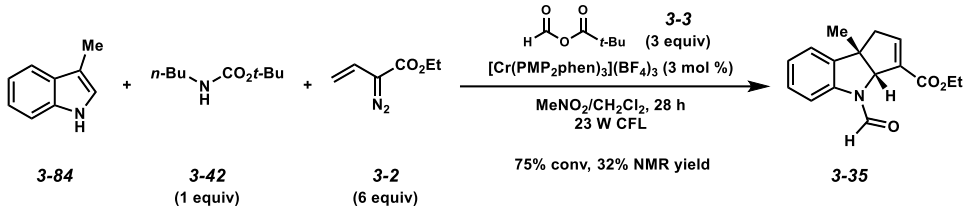

Indoline 3-35. In a flame-dried 1-dram borosilicate vial open to air, trimethylacetic formic anhydride (**3-3**, 47.0 mg, 0.361 mmol) was dissolved in CH_3NO_2 (0.600 mL). To this solution were added 3-methyl indole (**3-84**, 15.8 mg, 0.120 mmol), *t*-butyl carbamate **3-42** (20.8 mg, 0.120 mmol), $[Cr(PMP_2phen)_3](BF_4)_3$ (1.8 mg, 0.00120 mmol), and ethyl vinyl diazoacetate (**3-2**, 0.361 mL, 1.0 M solution in CH_2Cl_2, 0.361 mmol). The vial was then capped, and the reaction mixture was irradiated with a 23 W CFL bulb while stirring. After 8 h, second charges of ethyl vinyl diazoacetate (**3-2**, 0.240 mL, 1.0 M solution in CH_2Cl_2, 0.240 mmol) and $[Cr(PMP_2phen)_3](BF_4)_3$ (1.8 mg, 0.00120 mmol) were added, and irradiation was continued. At the 24 h timepoint, third charges of ethyl vinyl diazoacetate (0.120 mL, 1.0 M solution in CH_2Cl_2, 0.120 mmol) and

$[Cr(PMP_2phen)_3](BF_4)_3$ (1.8 mg, 0.00120 mmol) were added, and irradiation was continued. At the 28 h timepoint, the solvent was removed by rotary evaporation. The crude residue was then dissolved in CH_2Cl_2 (~1 mL), and the solution was passed through a SiO_2 plug (0.5 x 3 cm), using CH_2Cl_2 as eluent (~8 mL). The filtrate was concentrated in vacuo, and the crude residue was analyzed by ^1H NMR (indoline **3-35**, 32% yield) using CH_2Br_2 as an internal standard.

Examining Electronic Stabilization of Radical Cation:

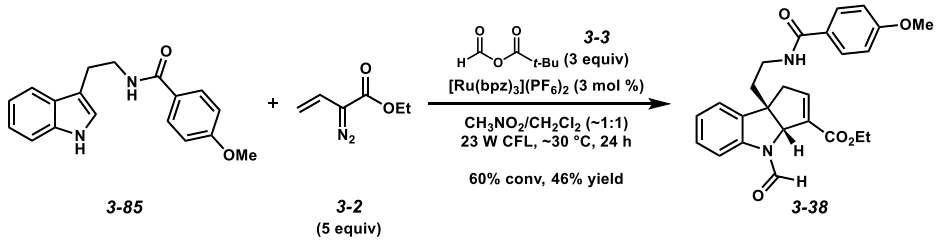

Indoline 3-38. In a flame-dried 1-dram borosilicate vial open to air, trimethylacetic formic anhydride (**3-3**, 39.4 mg, 0.303 mmol) was dissolved in CH_3NO_2 (0.505 mL). To this solution were added indole **3-85** (29.8 mg, 0.101 mmol), $[Ru(bpz)_3](PF_6)_2$ (1.3 mg, 0.00152 mmol), and ethyl vinyl diazoacetate (**3-2**, 0.303 mL, 1.0 M solution in CH_2Cl_2, 0.303 mmol). The vial was then capped, and the reaction mixture was irradiated with a 23 W CFL bulb while stirring. After 8 h, second charges of ethyl vinyl diazoacetate (**3-2**, 0.202 mL, 1.0 M solution in CH_2Cl_2, 0.202 mmol) and $[Ru(bpz)_3](PF_6)_2$ (1.3 mg, 0.00152 mmol) were added, and irradiation was continued. Reaction progress was monitored by TLC. At the 24 h timepoint, the solvent was removed by rotary evaporation. The crude residue was then dissolved in CH_2Cl_2 (~1 mL), and the solution was passed through a SiO_2 plug (0.5 x 3 cm), eluting with ~4 mL CH_2Cl_2, then ~4 mL EtOAc. The filtrate was concentrated in vacuo, and the residue was purified by silica gel flash chromatography (2:1 → 1:2 hexanes/EtOAc eluent) to afford indoline **3-38** (20.4 mg, 46% yield) as a yellow oil.

TLC R_f: 0.13 in 1:1 hexanes/EtOAc, visualized by UV, stained blue in Hanessian's stain.

^{1}H NMR (400 MHz, $CDCl_3$): δ 8.89 (s, 1H), 8.07 (d, *J* = 8.0 Hz, 1H), 7.58 (d, *J* = 8.3 Hz, 2H), 7.31-7.19 (comp. m, 2H), 7.11 (app. t, *J* = 7.6 Hz, 1H), 6.95-6.78 (comp. m, 3H), 5.91 (br. s, 1H), 5.37 (s, 1H), 4.32-4.12 (comp. m, 2H), 3.84 (s, 3H), 3.55-3.40 (m, 1H), 3.30-3.15 (m, 1H), 3.00 (app. d, *J* = 18.8 Hz, 1H), 2.90 (app. d, *J* = 18.8 Hz, 1H), 2.28-2.09 (comp. m, 2H), 1.30 (t, *J* = 7.3 Hz, 1H).

^{13}C NMR (100 MHz, $CDCl_3$): δ 167.1, 163.8, 162.4, 161.7, 145.8, 139.7, 137.5, 134.3, 129.0, 128.7, 126.4, 125.3, 123.6, 117.9, 113.9, 72.5, 61.1, 55.5, 54.4, 45.5, 39.3, 36.7, 14.3.

IR (ATR, neat): 3451, 2931, 1710, 1688, 1631, 1253 cm^{-1}.

HRMS (ESI+): *m/z* calc'd for $(M + Na)^+$ $[C_{25}H_{26}N_2O_5 + Na]^+$: 457.1734, found 457.1711.

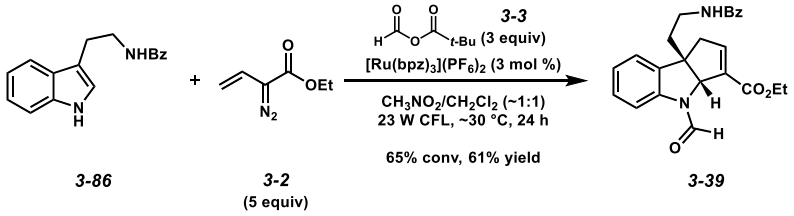

Indoline 3-39. In a flame-dried 1-dram borosilicate vial open to air, trimethylacetic formic anhydride (**3-3**, 45.7 mg, 0.351 mmol) was dissolved in CH_3NO_2 (0.585 mL). To this solution were added indole **3-86** (30.8 mg, 0.117 mmol), $[Ru(bpz)_3](PF_6)_2$ (1.5 mg, 0.00176 mmol), and ethyl vinyl diazoacetate (**3-2**, 0.351 mL, 1.0 M solution in CH_2Cl_2, 0.351 mmol). The vial was then capped, and the reaction mixture was irradiated with a 23 W CFL bulb while stirring. After 8 h, second charges of ethyl vinyl diazoacetate (**3-2**, 0.234 mL, 1.0 M solution in CH_2Cl_2, 0.234 mmol) and $[Ru(bpz)_3](PF_6)_2$ (1.5 mg, 0.00176 mmol) were added, and irradiation was continued.

Reaction progress was monitored by TLC. At the 24 h timepoint, the solvent was removed by rotary evaporation. The crude residue was then dissolved in CH_2Cl_2 (~1 mL), and the solution was passed through a SiO_2 plug (0.5 x 3 cm), eluting with ~4 mL CH_2Cl_2, then ~4 mL EtOAc. The filtrate was concentrated in vacuo, and the residue was purified by silica gel flash chromatography (2:1→1:2 hexanes/EtOAc eluent) to afford indoline **3-39** (28.6 mg, 60% yield) as a yellow oil.

TLC R_f: 0.13 in 1:1 hexanes/EtOAc, visualized by UV, stained blue in Hanessian's stain.

^{1}H NMR (400 MHz, $CDCl_3$): δ 8.89 (s, 1H), 8.07 (d, *J* = 8.0 Hz, 1H), 7.62 (d, *J* = 7.5 Hz, 2H), 7.48 (t, *J* = 7.5 Hz, 1H), 7.40 (app. t, *J* = 7.5 Hz, 2H), 7.31-7.20 (comp. m, 2H), 7.11 (app. t, *J* = 7.6 Hz, 1H), 6.88 (app. s, 1H), 6.02 (br. s, 1H), 5.38 (s, 1H), 4.29-4.10 (comp. m, 2H), 3.61-3.45 (m, 1H), 3.30-3.15 (m, 1H), 3.00 (app. d, *J* = 18.9 Hz, 1H), 2.91 (app. d, *J* = 18.9 Hz, 1H), 2.21 (app. t, *J* = 7.6 Hz, 2H), 1.31 (t, *J* = 7.2 Hz, 3H).

^{13}C NMR (100 MHz, $CDCl_3$): δ 167.6, 163.8, 161.7, 145.8, 139.7, 137.4, 134.3, 134.2, 131.7, 129.1, 128.7, 126.9, 125.3, 123.5, 117.9, 72.5, 61.1, 54.3, 45.5, 39.3, 36.7, 14.3.

IR (ATR, neat): 3331, 2926, 1710, 1678, 1665, 1483 cm^{-1}.

HRMS (ESI+): *m/z* calc'd for $(M + Na)^+$ $[C_{24}H_{24}N_2O_4 + Na]^+$: 427.1628, found 427.1610.

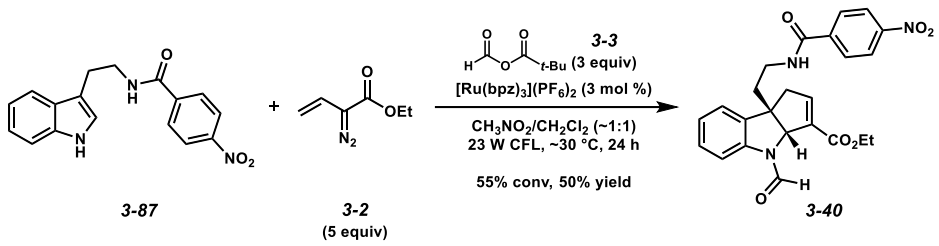

Indoline 3-40. In a flame-dried 1-dram borosilicate vial open to air, trimethylacetic formic anhydride (**3-3**, 33.1 mg, 0.254 mmol) was dissolved in CH_3NO_2 (0.424 mL). To this solution were added indole **3-87** (26.2 mg, 0.0847 mmol), $[Ru(bpz)_3](PF_6)_2$ (1.1 mg, 0.00127 mmol), and ethyl vinyl diazoacetate reagent (**3-2**, 0.254 mL, 1.0 M solution in CH_2Cl_2, 0.254 mmol). The vial was then capped, and the reaction mixture was irradiated with a 23 W CFL bulb while stirring. After 8 h, second charges of ethyl vinyl diazoacetate (**3-2**, 0.169 mL, 1.0 M solution in CH_2Cl_2, 0.169 mmol) and $[Ru(bpz)_3](PF_6)_2$ (1.1 mg, 0.00127 mmol) were added, and irradiation was continued. Reaction progress was monitored by TLC. At the 24 h timepoint, the solvent was removed by rotary evaporation. The crude residue was then dissolved in CH_2Cl_2 (~1 mL), and the solution was passed through a SiO_2 plug (0.5 x 3 cm), eluting with ~4 mL CH_2Cl_2, then ~4 mL EtOAc. The filtrate was concentrated in vacuo, and the residue was purified by silica gel flash chromatography (2:1 → 1:2 hexanes/EtOAc eluent) to afford indoline **3-40** (19.2 mg, 50% yield) as a yellow oil.

TLC R_f: 0.10 in 1:1 hexanes/EtOAc, visualized by UV, stained blue in Hanessian's stain.

^{1}H NMR (400 MHz, $CDCl_3$): δ 8.89 (s, 1H), 8.24 (d, *J* = 8.6 Hz, 2H), 8.05 (d, *J* = 8.1 Hz, 1H), 7.74 (d, *J* = 8.6 Hz, 2H), 7.33-7.18 (comp. m, 2H), 7.11 (app. t, *J* = 7.5 Hz, 1H), 6.89 (app. s, 1H), 6.09 (br. s, 1H), 5.38 (s, 1H), 4.31-4.11 (comp. m, 2H), 3.68-3.53 (m, 1H), 3.32-3.16 (m, 1H), 3.02

(app. d, *J* = 18.7 Hz, 1H), 2.90 (app. d, *J* = 18.7 Hz, 1H), 2.31-2.12 (comp. m, 2H), 1.30 (t, *J* = 7.2 Hz, 3H).

^{13}C NMR (100 MHz, $CDCl_3$): δ 165.4, 163.7, 161.7, 149.8, 145.7, 139.7, 137.4, 134.2, 129.2, 128.8, 128.2, 125.4, 123.9, 123.5, 118.0, 72.5, 61.1, 54.3, 45.7, 39.1, 37.1, 14.3.

IR (ATR, neat): 3330, 2926, 1710, 1672, 1599, 1483 cm^{-1}.

HRMS (ESI+): *m/z* calc'd for $(M + Na)^+$ $[C_{24}H_{23}N_3O_6 + Na]^+$: 427.1479, found 472.1458.

Inert Atmosphere:

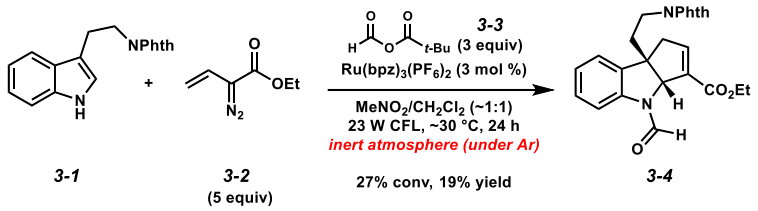

In a flame-dried 1-dram borosilicate vial evacuated and backfilled 3x with argon, trimethylacetic formic anhydride (**3-3**, 40.6 mg, 0.312 mmol) was dissolved in degassed CH_3NO_2 (0.520 mL). To this solution were added indole **3-1** (30.1 mg, 0.104 mmol), $[Ru(bpz)_3](PF_6)_2$ (1.3 mg, 0.00156 mmol), and ethyl vinyl diazoacetate reagent (**3-2**, 0.312 mL, 1.0 M solution in CH_2Cl_2, 0.312 mmol). The vial was then capped, and the reaction mixture was irradiated with a 23 W CFL bulb while stirring. After 8 h, second charges of ethyl vinyl diazoacetate reagent (**3-2**, 0.208 mL, 1.0 M solution in CH_2Cl_2, 0.208 mmol) and $[Ru(bpz)_3](PF_6)_2$ (1.3 mg, 0.00156 mmol) were added under argon, and irradiation was continued. At the 24 h timepoint, the solvent was removed by rotary evaporation. The crude residue was then dissolved in CH_2Cl_2 (~1 mL), and the solution was passed through a SiO_2 plug (0.5 x 3 cm), eluting with ~4 mL CH_2Cl_2, then ~4 mL EtOAc. The filtrate was concentrated in vacuo, and the residue was analyzed by ^1H NMR (indoline **3-4**, 27% conversion, 19% yield) using CH_2Br_2 as an internal standard.

3.10.7. Photocatalyst Monitoring Experiments

Evaluation of $[Ru(bpz)_3]^{2+}$ in MeCN

Procedure: $[Ru(bpz)_3](PF_6)_2$ (2.3 mg, 0.00266 mmol) was dissolved in acetonitrile (13.3 mL). A baseline UV-Vis measurement was then taken (0 h timepoint). The solution was then irradiated in the photobox by a 23 W CFL bulb for 24 h, withdrawing aliquots of the solution at 1, 2, 4, and 24 h timepoints, and measuring their UV-Vis absorbances. The data is recorded below.

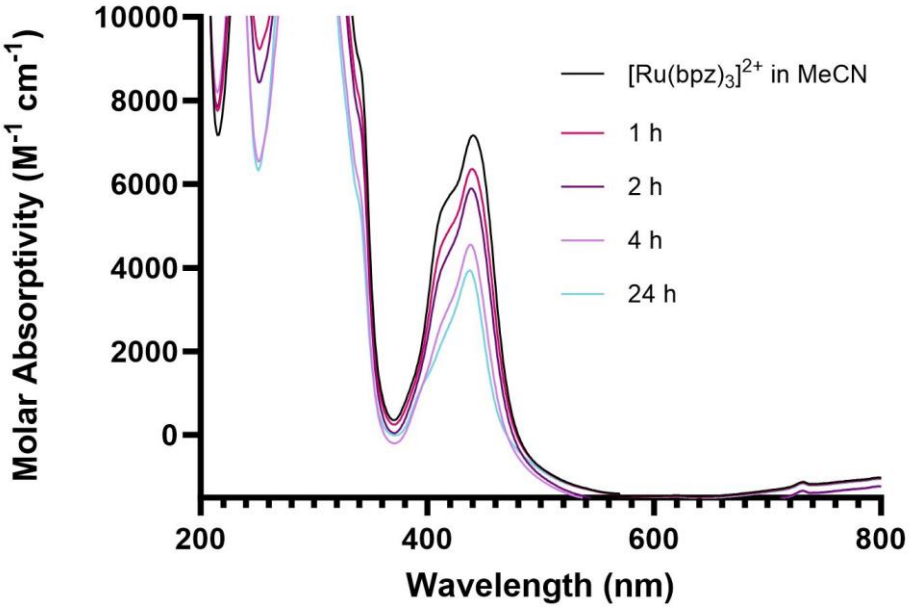

Figure 3.10.1. $[Ru(bpz)_3](PF_6)_2$ in acetonitrile irradiated with a 23 W CFL bulb over time.

*Evaluation of $[Ru(bpz)_3]^{2+}$ with Trimethylacetic Formic Anhyrdride (**3-3**)*

Procedure: $[Ru(bpz)_3](PF_6)_2$ (2.3 mg, 0.00266 mmol) was dissolved in acetonitrile (13.3 mL). Trimethylacetic formic anhydride (**3-3**, 104 mg, 0.798 mmol, 300 equiv) was then added to the mixture, and a baseline measurement (0 h timepoint) was taken. The solution was then irradiated in the photobox by a 23 W CFL bulb for 24 h, withdrawing aliquots of the solution at 1, 2, 4, and 24 h timepoints, and measuring their UV-Vis absorbances. The data is recorded below.

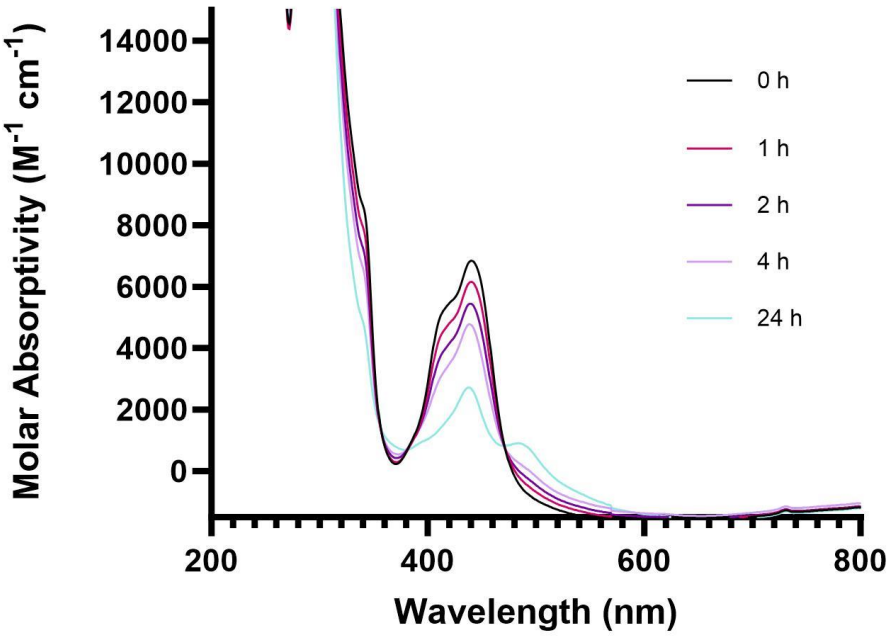

*Figure 3.10.2. $[Ru(bpz)_3](PF_6)_2$ and 300 equiv of **3-3** in acetonitrile irradiated with a 23 W CFL bulb over time.*

Evaluation of $[Ru(bpz)_3]^{2+}$ with other acyl chlorides

Isobutyryl Chloride:

Procedure: $[Ru(bpz)_3](PF_6)_2$ (2.3 mg, 0.00266 mmol) was dissolved in acetonitrile (13.3 mL). Isobutyryl chloride (83.3 µL, 0.798 mmol, 300 equiv) was then added to the mixture, and a baseline measurement (0 h timepoint) was taken. The solution was then irradiated in the photobox by a 23 W CFL bulb for 24 h, withdrawing aliquots of the solution at 1, 2, 4, and 24 h timepoints, and measuring their UV-Vis absorbances. The data is recorded below.

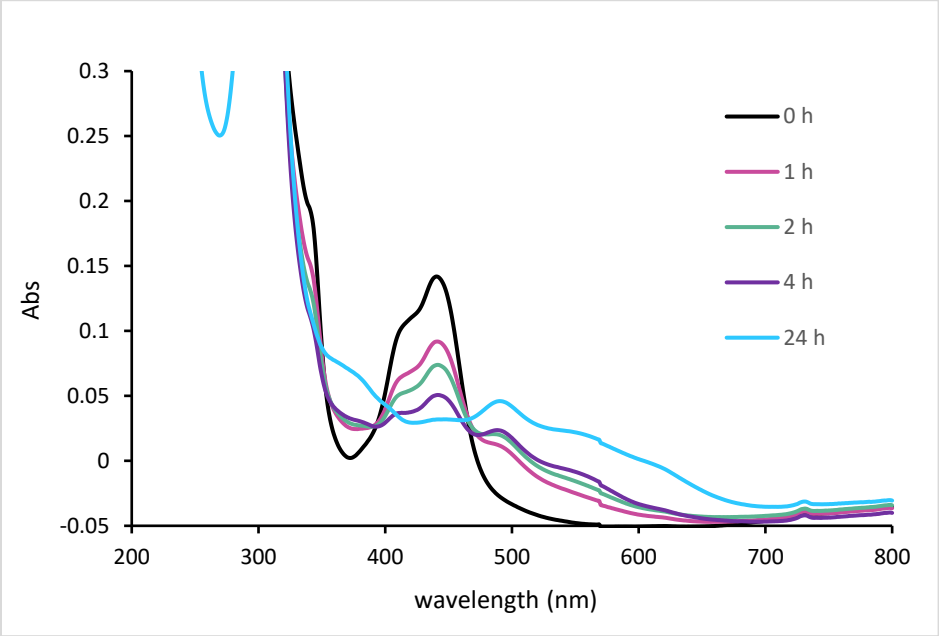

Figure 3.10.3. $[Ru(bpz)_3](PF_6)_2$ and 300 equiv of isobutyryl chloride in acetonitrile irradiated with a 23 W CFL bulb over time.

TrocCl:

Procedure: $[Ru(bpz)_3](PF_6)_2$ (2.3 mg, 0.00266 mmol) was dissolved in acetonitrile (13.3 mL). TrocCl (0.110 mL, 0.798 mmol, 300 equiv) was then added to the mixture, and a baseline measurement (0 h timepoint) was taken. The solution was then irradiated in the photobox by a 23 W CFL bulb for 24 h, withdrawing aliquots of the solution at 1, 2, 4, and 24 h timepoints, and measuring their UV-Vis absorbances. The data is recorded below.

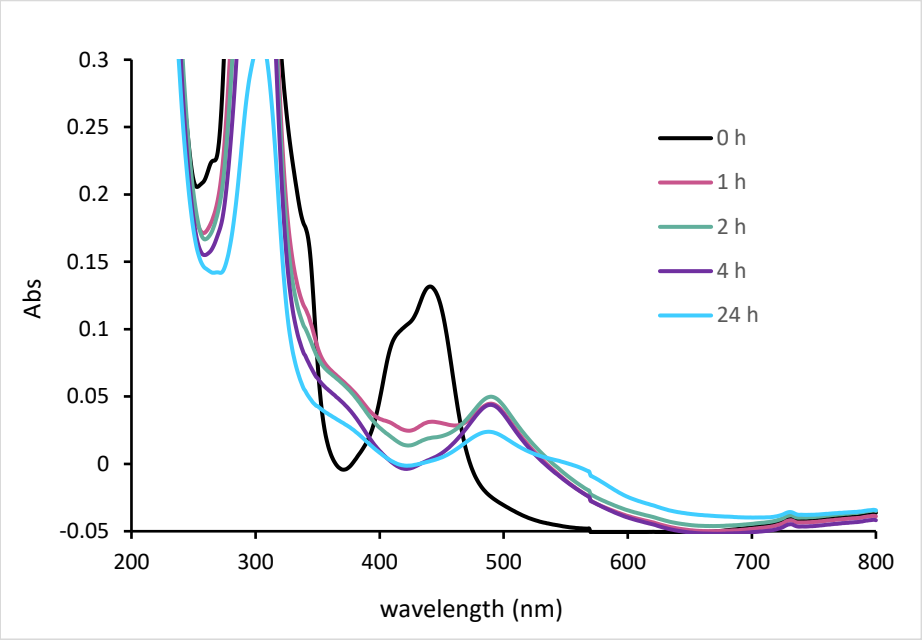

Figure 3.10.4. $[Ru(bpz)_3](PF_6)_2$ and 300 equiv of TrocCl in acetonitrile irradiated with a 23 W CFL bulb over time.

Evaluation of $[Ru(bpz)_3]^{2+}$ with another mixed anhydride

Benzoic pivalic anhydride:

Procedure: $[Ru(bpz)_3](PF_6)_2$ (2.3 mg, 0.00266 mmol) was dissolved in acetonitrile (13.3 mL). benzoic pivalic anhydride (165 mg, 0.798 mmol, 300 equiv) was then added to the mixture, and a baseline measurement (0 h timepoint) was taken. The solution was then irradiated in the photobox by a 23 W CFL bulb for 24 h, withdrawing aliquots of the solution at 1, 2, 4, and 24 h timepoints, and measuring their UV-Vis absorbances. The data is recorded below.

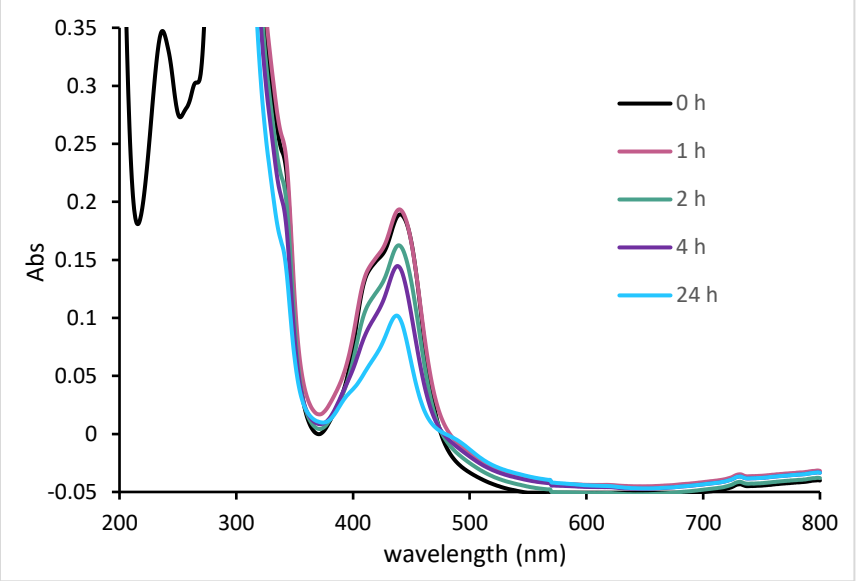

Figure 3.10.5. $[Ru(bpz)_3](PF_6)_2$ and 300 equiv of benzoic pivalic anhydride in acetonitrile irradiated with a 23 W CFL bulb over time.

*Evaluation of $[Ru(bpz)_3]^{2+}$ with External Carbamate (**3-42**)*

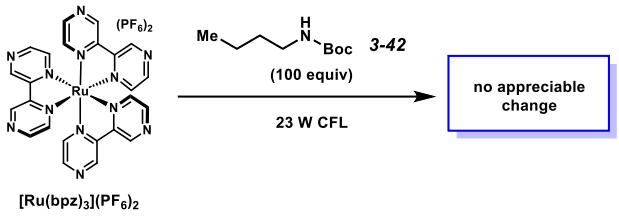

Procedure: $[Ru(bpz)_3](PF_6)_2$ (3.0 mg, 0.00347 mmol) was dissolved in acetonitrile (17.3 mL). Carbamate **3-42** (60.1 mg, 0.347 mmol, 100 equiv) was then added to the mixture, and a baseline measurement (0 h timepoint) was taken. The solution was then irradiated in the photobox by a 23 W CFL bulb for 24 h, withdrawing aliquots of the solution at 1, 2, 4, and 24 h timepoints, and measuring their UV-Vis absorbances. The data is recorded below.

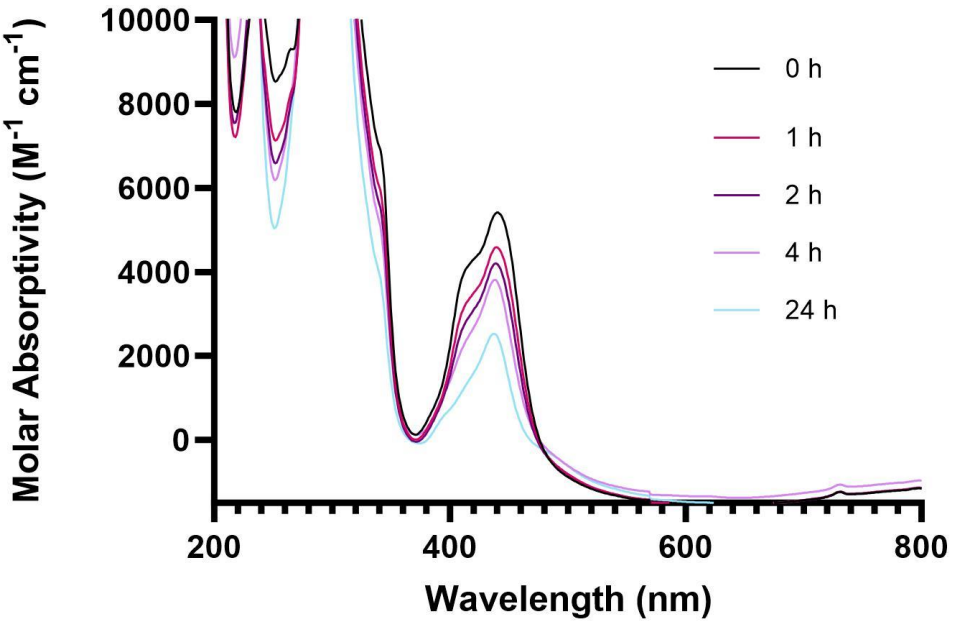

*Figure 3.10.6. $[Ru(bpz)_3](PF_6)_2$ and 100 equiv of **3-42** in acetonitrile irradiated with a 23 W CFL bulb over time.*

*Evaluation of $[Cr(PMP_2phen)_3]^{3+}$ with External Carbamate (**3-42**)*

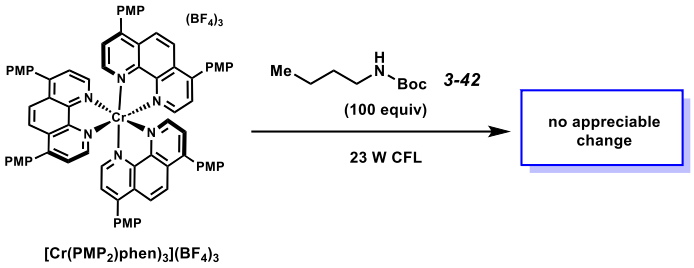

Procedure: $[Cr(PMP_2phen)_3](BF_4)_3$ (2.5 mg, 0.00166 mmol) was dissolved in CH_2Cl_2 (8.3 mL). A baseline UV-Vis measurement was then taken. Carbamate **3-42** (28.8 mg, 0.166 mmol, 100 equiv) was then added to the mixture, and another baseline measurement (0 h timepoint) was taken. The solution was then irradiated in the photobox by a 23 W CFL bulb for 24 h, withdrawing aliquots of the solution at 1, 2, 4, and 24 h timepoints, and measuring their UV-Vis absorbances. The data is recorded below.

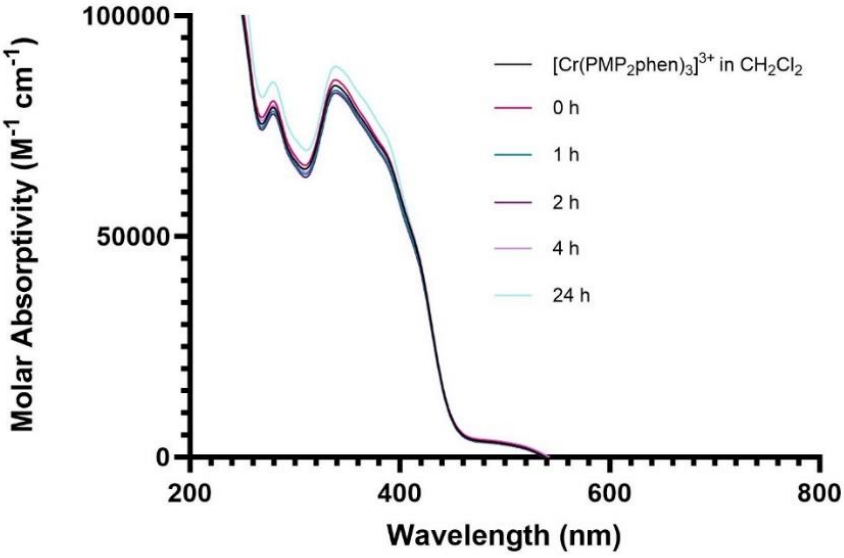

*Figure 3.10.7. $[Cr(PMP_2phen)_3](BF_4)_3$ and 100 equiv of **3-42** in CH_2Cl_2 irradiated with a 23 W CFL bulb over time*

3.10.8. Starting Material Synthesis

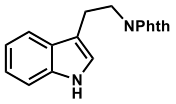

3-1

Indole 3-1. Prepared according to the procedure reported by Feng and coworkers.[14]

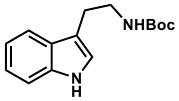

3-51

Indole 3-51. Prepared according to the procedure reported by Unhale and coworkers.[15] The characterization data was consistent with those reported by Shaikh and coworkers.[16]

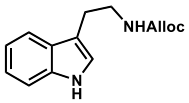

3-52

Indole 3-52. Prepared according to the procedure reported by Tyson and coworkers.[17]

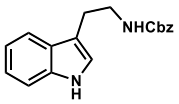

3-53

Indole 3-53. Prepared according to the procedure reported by Carr and coworkers.[18] The characterization data was consistent with those reported by Kandukuri and coworkers.[19]

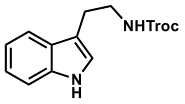

3-54

Indole 3-54. Prepared according to the procedure reported by Yang and coworkers.[20]

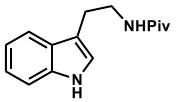

3-55

Indole 3-55. Prepared according to the procedure reported by Oliveira and coworkers.[21]

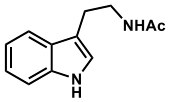

3-56

Indole 3-56. Prepared according to the procedure reported by Huber and coworkers.[22]

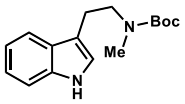

3-57

Indole 3-57. Prepared according to the procedure reported by De and coworkers, substituting Boc_2O for CbzCl in the final step.[23] The characterization data was consistent with those reported by Snell and coworkers.[24]

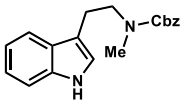

3-58

Indole 3-58. Prepared according to the procedure reported by De and coworkers.[23]

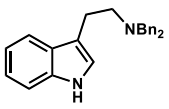

3-60

Indole 3-60. Prepared according to the procedure reported by de la Fuente and Domínguez.[25]

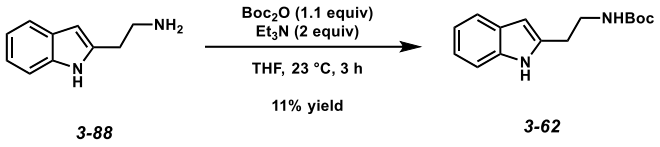

3-88 *3-62*

Indole 3-62. Indole **3-88** was prepared as crude material, according to a procedure reported by Schlegel and coworkers.[26] To a solution of 2-(1*H*-indol-2-yl)ethan-1-amine (**3-88**, 250 mg, 1.56 mmol) and triethylamine (435 μL, 3.12 mmol) in THF (1.5 mL) was added a solution of di-*tert*-butyl dicarbonate (375 mg, 1.72 mmol) in THF (1.5 mL) at room temperature. The reaction mixture was stirred for 3 h. After the reaction was complete, the reaction mixture was concentrated, and the crude residue was purified via silica gel flash chromatography (4:1 hexanes/EtOAc eluent) to afford indole **3-62** (43.4 mg, 11% yield) as a beige solid.

TLC R_f: 0.36 in 4:1 hexanes/EtOAc, visualized by UV, stained blue in Hanessian's stain.

^{1}H NMR (900 MHz, $CDCl_3$): δ 8.30 (br. s, 1H), 7.55 (d, *J* = 7.8 Hz, 1H), 7.31 (d, *J* = 8.0 Hz, 1H), 7.14 (app. t, *J* = 7.4 Hz, 1H), 7.09 (app. t, *J* = 7.4 Hz, 1H), 6.29 (s, 1H), 4.74 (br. s, 1H), 3.55-3.41 (comp. m, 2H), 3.03-2.87 (comp. m, 2H), 1.44 (s, 9H).

^{13}C NMR (226 MHz, $CDCl_3$): δ 156.3, 136.5, 136.2, 128.8, 121.5, 120.0, 119.9, 110.7, 100.6, 79.8, 40.0, 29.2, 28.5.

IR (ATR, neat): 3406, 2977, 1691, 1512, 1366, 1275 cm^{-1}.

HRMS (ESI+): *m/z* calc'd for $(M + H)^+$ $[C_{15}H_{20}N_2O_2 + H]^+$: 261.1598, found 261.1585.

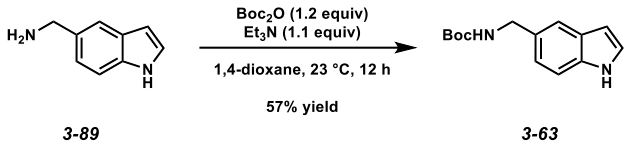

Indole 3-63. Indole **3-89** was prepared according to a procedure reported by Utsumi and coworkers.[27] To a solution of (1*H*-indol-5-yl)methanamine (**3-89**, 363 mg, 2.48 mmol) and triethylamine (381 μL, 2.73 mmol) in 1,4-dioxane (2 mL) was added a solution of di-*tert*-butyl dicarbonate (650 mg, 2.98 mmol) in 1,4-dioxane (2 mL) at room temperature. The reaction mixture was then stirred overnight. After the reaction was complete, the reaction mixture was concentrated and the crude residue was purified via silica gel flash chromatography (4:1 hexanes/EtOAc eluent) to afford indole **3-63** (350 mg, 57% yield, R_f = 0.24 in 4:1 hexanes/EtOAc eluent) as an orange oil. The characterization data was consistent with a procedure reported by Trabbic and coworkers.[28]

^{1}H NMR (400 MHz, $CDCl_3$): δ 8.41 (br. s, 1H), 7.55 (s, 1H), 7.34 (d, *J* = 8.4 Hz, 1H), 7.20 (app. s, 1H), 7.12 (d, *J* = 8.4 Hz, 1H), 6.52 (app. s, 1H), 4.87 (br. s, 1H), 4.48-4.29 (comp. m, 2H), 1.49 (s, 9H).

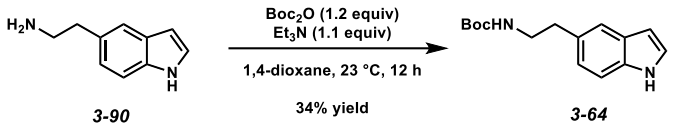

Indole 3-64. Indole **3-90** was prepared according to a procedure reported by Mehndiratta and coworkers.[29] To a solution of 2-(1*H*-indol-5-yl)ethan-1-amine (**3-90**, 179 mg, 1.12 mmol) and triethylamine (169 μL, 1.21 mmol) in 1,4-dioxane (1 mL) was added a solution of di-*tert*-butyl dicarbonate (288 mg, 1.32 mmol) in 1,4-dioxane (1 mL) at room temperature. The reaction mixture was then stirred overnight. After the reaction was complete, the reaction mixture was concentrated and the crude residue was purified via silica gel flash chromatography (3:1 hexanes/EtOAc eluent) to afford indole **3-64** (99.0 mg, 34% yield) as a clear oil.

TLC R_f: 0.50 in 2:1 hexanes/EtOAc, visualized by UV, stained blue in Hanessian's stain.

^{1}H NMR (400 MHz, $CDCl_3$): δ 8.34 (br. s, 1H), 7.46 (s, 1H), 7.33 (d, *J* = 8.4 Hz, 1H), 7.20 (app. s, 1H), 7.03 (d, *J* = 8.4 Hz, 1H), 6.51 (app. s, 1H), 4.59 (br. s, 1H), 3.54-3.28 (m, 2H), 2.89 (t, *J* = 7.0 Hz, 2H), 1.45 (s, 9H).

^{13}C NMR (100 MHz, $CDCl_3$): δ 156.2, 134.8, 130.2, 128.3, 124.7, 123.1, 120.6, 111.3, 102.3, 79.2, 42.5, 36.3, 28.6.

IR (ATR, neat): 3409, 2977, 1709, 1691, 1529, 1366 cm^{-1}.

HRMS (ESI+): *m/z* calc'd for $(M + Na)^+$ $[C_{15}H_{20}N_2O_2 + Na]^+$: 283.1417, found 283.1412.

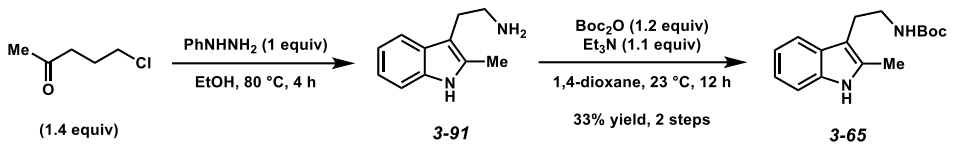

Indole 3-65. According to a procedure reported by Montgomery and coworkers,[30] to a solution of 5-chloro-2-pentanone (98.6 mg, 0.818 mmol) in EtOH (3 mL) was added phenylhydrazine (57.4 μL, 0.583 mmol), and the mixture was heated at 80 °C and stirred for 4 h. After the reaction was complete, the solution was cooled to room temperature and concentrated in vacuo to afford indole **3-91** as a purple oil. The crude material was carried forward without further purification. The crude residue was dissolved in 1,4-dioxane (0.5 mL), and Et_3N (89.5 μL, 0.642 mmol) was added. A solution of di-*tert*-butyl dicarbonate (153 mg, 0.701 mmol) in 1,4-dioxane (0.5 mL) was then added to the reaction mixture, and the reaction was stirred overnight at room temperature. After 12 h, the reaction mixture was concentrated, and the crude residue was purified via silica gel flash chromatography (3:1 hexanes/EtOAc eluent) to afford indole **3-65** (53.2 mg, 33% yield over 2 steps) as an orange solid.

TLC R*f*: 0.52 in 2:1 hexanes/EtOAc, visualized by UV, stained blue in Hanessian's stain.

^{1}H NMR (400 MHz, $CDCl_3$): δ 7.90 (br. s, 1H), 7.50 (d, *J* = 7.4 Hz, 1H), 7.27 (d, *J* = 7.0 Hz, 1H), 7.13 (app. t, *J* = 7.0 Hz, 1H), 7.08 (app. t, *J* = 7.4 Hz, 1H), 4.58 (br. s, 1H), 3.44-3.22 (m, 2H), 2.90 (br. t, *J* = 6.8 Hz, 2H), 2.38 (s, 3H), 1.45 (s, 9H).

^{13}C NMR (100 MHz, $CDCl_3$): δ 156.1, 135.4, 132.1, 128.7, 121.2, 119.4, 118.0, 110.4, 108.7, 79.1, 41.1, 28.6, 24.7, 11.7.

IR (ATR, neat): 3405, 2977, 1691, 1678, 1462, 1366 cm^{-1}.

HRMS (ESI+): *m/z* calc'd for $(M + Na)^+$ $[C_{16}H_{22}N_2O_2 + Na]^+$: 297.1573, found 297.1564.

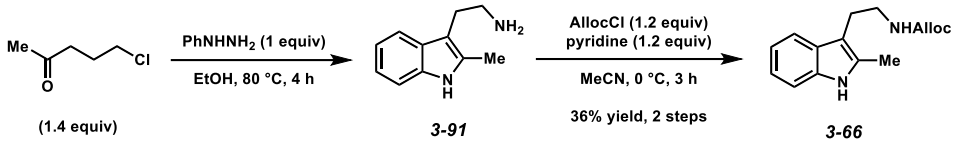

Indole 3-66. According to a procedure reported by Montgomery and coworkers,[30] to a solution of 5-chloro-2-pentanone (1.04 mL, 9.16 mmol) in EtOH (33 mL) was added phenylhydrazine (0.643 mL, 6.54 mmol), and the mixture was heated at 80 °C and stirred for 4 h. After the reaction was complete, the solution was cooled to room temperature and concentrated in vacuo to afford indole **3-91** as a purple oil. The crude residue was carried forward without further purification. The crude indole was dissolved in CH_3CN (33 mL) and cooled to 0 °C. Allyl chloroformate (0.837 mL, 7.87 mmol) and pyridine (0.632 mL, 7.81 mmol) were then added to the solution, and the resulting mixture was stirred for 3 h at 0 °C. After the reaction was complete, the reaction mixture was diluted with EtOAc (20 mL), 5% aq. citric acid (10 mL) was added, and the mixture was allowed to warm to room temperature. The layers were separated, and the aqueous layer was extracted with EtOAc (3 x 20 mL). The organic layers were combined, washed with brine (20 mL), dried over $MgSO_4$, and concentrated in vacuo. The crude residue was purified via silica gel flash chromatography (4:1→2:1 hexanes/EtOAc eluent) to afford indole **3-66** (614 mg, 36% yield over 2 steps) as an orange oil.

TLC R_f: 0.42 in 2:1 hexanes/EtOAc, visualized by UV, stained blue in Hanessian's stain.

^{1}H NMR (400 MHz, $CDCl_3$): δ 7.94 (br. s, 1H), 7.51 (d, *J* = 7.5 Hz, 1H), 7.25 (d, *J* = 7.5 Hz, 1H), 7.12 (app. quint, *J* = 7.5 Hz, 2H), 6.01-5.84 (m, 1H), 5.30 (app. d, *J* = 17.2 Hz, 1H), 5.21 (app. d, *J* = 10.4 Hz, 1H), 4.81 (br. s, 1H), 4.59 (app. s, 2H), 3.51-3.35 (m, 2H), 2.93 (t, *J* = 6.8 Hz, 2H), 2.37 (s, 3H).

^{13}C NMR (100 MHz, $CDCl_3$): δ 156.5, 135.4, 133.1, 132.2, 128.6, 121.2, 119.5, 117.9, 117.7, 110.4, 108.4, 65.5, 41.5, 24.7, 11.7.

IR (ATR, neat): 3400, 2939, 1709, 1691, 1462 cm^{-1}.

HRMS (ESI+): *m/z* calc'd for $(M + Na)^+$ $[C_{15}H_{18}N_2O_2 + Na]^+$: 281.1260, found 281.1252.

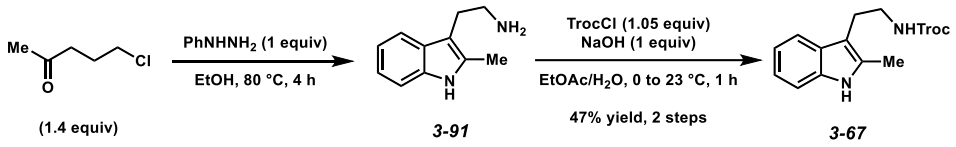

Indole 3-67. According to a procedure reported by Montgomery and coworkers,[30] to a solution of 5-chloro-2-pentanone (1.22 mL, 10.7 mmol) in EtOH (38 mL) was added phenylhydrazine (0.750 mL, 7.63 mmol), and the mixture was heated at 80 °C and stirred for 4 h. After the reaction was complete, the solution was cooled to room temperature and concentrated in vacuo to afford indole **3-91** as a purple oil. The crude residue was carried forward without further purification. The crude indole was dissolved in EtOAc (13 mL) and cooled to 0 °C. NaOH (7.63 mL, 1 M in H_2O, 7.63 mmol) and 2,2,2-trichloroethyl chloroformate (1.10 mL, 8.01 mmol) were then added, and the reaction mixture was warmed to room temperature and stirred for 1 h. After the reaction was complete, the reaction mixture was diluted with EtOAc (20 mL), the layers were separated, and

the aqueous layer was extracted with EtOAc (3 x 20 mL). The organic layers were combined, washed with brine (20 mL), dried over $MgSO_4$, and concentrated in vacuo. The crude residue was purified via silica gel flash chromatography (2:1 hexanes/EtOAc eluent) to afford indole **3-67** (1.25 g, 47% yield over 2 steps) as a yellow oil. Indole **3-67** was found to be susceptible to rapid decomposition and was best stored in a frozen benzene matrix.

TLC R_f: 0.51 in 2:1 hexanes/EtOAc, visualized by UV, stained blue in Hanessian's stain.

^{1}H NMR (400 MHz, $CDCl_3$): δ 7.82 (br. s, 1H), 7.50 (d, *J* = 7.8 Hz, 1H), 7.28 (d, *J* = 7.8 Hz, 1H), 7.14 (app. t, *J* = 7.2 Hz, 1H), 7.09 (app. t, *J* = 7.2 Hz, 1H), 5.01 (br. s, 1H), 4.72 (s, 2H), 3.57-3.42 (m, 2H), 2.95 (t, *J* = 6.7 Hz, 2H), 2.40 (s, 3H).

^{13}C NMR (100 MHz, $CDCl_3$): δ 154.7, 135.4, 132.2, 128.6, 121.5, 119.7, 117.9, 110.4, 108.3, 95.8, 74.6, 41.8, 24.7, 11.8.

IR (ATR, neat): 3399, 2946, 1737, 1725, 1535 cm^{-1}.

HRMS (ESI+): *m/z* calc'd for $(M + Na)^+$ $[C_{14}H_{15}Cl_3N_2O_2 + Na]^+$: 371.0091, found 371.0084.

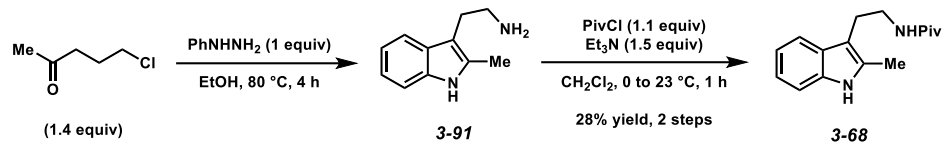

Indole 3-68. According to a procedure reported by Montgomery and coworkers,[30] to a solution of 5-chloro-2-pentanone (1.12 mL, 9.88 mmol) in EtOH (35 mL) was added phenylhydrazine (0.694 mL, 7.06 mmol), and the mixture was heated at 80 °C and stirred for 4 h. After the reaction was complete, the solution was cooled to room temperature and concentrated in vacuo to afford indole **3-91** as a purple oil. The crude residue was carried forward without further purification. The crude indole was dissolved in CH_2Cl_2 (12 mL) and cooled to 0 °C. Et_3N (1.48 mL, 10.6 mmol) and pivaloyl chloride (0.951 mL, 7.72 mmol) were then added, and the reaction mixture was warmed to room temperature and stirred for 1 h. After the reaction was complete, water was added (10 mL), the layers were separated, and the aqueous layer was extracted with CH_2Cl_2 (3 x 20 mL). The organic layers were combined, washed with brine (20 mL), dried over Na_2SO_4, and concentrated in vacuo. The crude residue was purified via silica gel flash chromatography (2:1 hexanes/EtOAc eluent) to afford indole **3-68** (503 mg, 28% yield over 2 steps) as a white solid.

TLC R_f: 0.23 in 2:1 hexanes/EtOAc, visualized by UV, stained blue in Hanessian's stain.

^{1}H NMR (400 MHz, $CDCl_3$): δ 8.20 (br. s, 1H), 7.52 (d, *J* = 7.8 Hz, 1H), 7.29 (d, *J* = 7.8 Hz, 1H), 7.13 (app. t, *J* = 7.2 Hz, 1H), 7.09 (app. t, *J* = 7.3 Hz, 1H), 5.76 (br. s, 1H) 3.53 (app. q, *J* = 6.2 Hz, 2H), 2.93 (t, *J* = 6.7 Hz, 2H), 2.39 (s, 3H), 1.12 (s, 9H).

^{13}C NMR (100 MHz, $CDCl_3$): δ 178.6, 135.5, 132.1, 128.7, 121.2, 119.4, 117.9, 110.5, 108.6, 40.1, 38.7, 27.6, 24.2, 11.8.

IR (ATR, neat): 3400, 2967, 1649, 1461, 1300 cm^{-1}.

HRMS (ESI+): *m/z* calc'd for $(M + Na)^+$ $[C_{16}H_{22}N_2O + Na]^+$: 281.1624, found 281.1611.

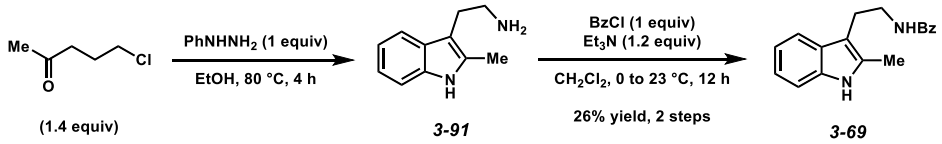

Indole 3-69. According to a procedure reported by Montgomery and coworkers,[30] to a solution of 5-chloro-2-pentanone (1.15 mL, 10.1 mmol) in EtOH (36 mL) was added phenylhydrazine (0.711 mL, 7.23 mmol), and the mixture was heated at 80 °C and stirred for 4 h. After the reaction was complete, the solution was cooled to room temperature and concentrated in vacuo to afford indole **3-91** as a purple oil. The crude residue was carried forward without further purification. The crude indole was dissolved in CH_2Cl_2 (18 mL) and cooled to 0 °C. Et_3N (1.21 mL, 8.68 mmol) and BzCl (0.840 mL, 7.23 mmol) were then added, and the reaction mixture was allowed to warm to room temperature and stirred overnight. After the reaction was complete, the reaction mixture was diluted with CH_2Cl_2 (10 mL), washed with H_2O (20 mL), dried over Na_2SO_4, and concentrated in vacuo. The crude residue was purified via silica gel flash chromatography (2:1 hexanes/EtOAc eluent) to afford indole **3-69** (517 mg, 26% yield over 2 steps) as an airy, white solid.

TLC R_f: 0.16 in 2:1 hexanes/EtOAc, visualized by UV, stained blue in Hanessian's stain.

^{1}H NMR (400 MHz, $CDCl_3$): δ 8.27 (br. s, 1H), 7.66 (d, *J* = 7.5 Hz, 2H), 7.54 (d, *J* = 7.9 Hz, 1H), 7.46 (app. t, *J* = 7.5 Hz, 1H), 7.36 (app. t, *J* = 7.5 Hz, 2H), 7.27 (d, *J* = 7.3 Hz, 1H), 7.14 (app. t, *J*

= 7.3 Hz, 1H), 7.08 (app. t, *J* = 7.9 Hz, 1H), 6.35 (br. s, 1H), 3.72 (app. q, *J* = 6.6 Hz, 2H), 3.04 (t, *J* = 6.6 Hz, 2H), 2.34 (s, 3H).

^{13}C NMR (100 MHz, $CDCl_3$): δ 167.7, 135.5, 134.7, 132.3, 131.4, 128.63, 128.58, 126.9, 121.2, 119.4, 117.8, 110.6, 108.3, 40.6, 24.1, 11.6.

IR (ATR, neat): 3295, 2936, 1665, 1501, 1303 cm^{-1}.

HRMS (ESI+): *m/z* calc'd for $(M + H)^+$ $[C_{18}H_{18}N_2O + H]^+$: 279.1492, found 279.1480.

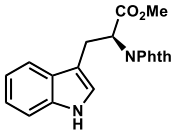

3-72

Indole 3-72. Prepared according to the procedure reported by Alqahtani and coworkers.[31]

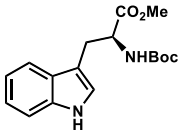

3-74

Indole 3-74. Prepared according to the procedure reported by Sacco and coworkers.[32]

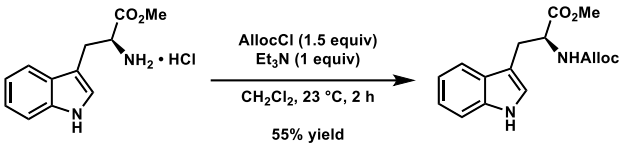

Indole 3-75. According to a procedure reported by Ruiz-Sanchis and coworkers,[33] to a solution of L-tryptophan methyl ester hydrochloride (**3-92**, 100 mg, 0.393 mmol) and Et_3N (54.8 μL, 0.393 mmol) in CH_2Cl_2 (2 mL) was added allyl chloroformate (62.7 μL, 0.590 mmol) and the reaction was stirred at room temperature for 2 h. Once the reaction was determined to be completed by TLC, the reaction mixture was diluted with CH_2Cl_2 (5 mL), washed with brine (2 x 5 mL), dried over Na_2SO_4, and concentrated in vacuo. The crude residue was purified silica gel chromatography (2:1 hexanes/EtOAc eluent) to afford indole **3-75** (65.0 mg, 55% yield) as a colorless oil.

TLC R_f: 0.28 in 2:1 hexanes/EtOAc, visualized by UV, stained blue in Hanessian's stain.

^{1}H NMR (900 MHz, $CDCl_3$): δ 8.19 (br. s, 1H), 7.55 (d, *J* = 7.9 Hz, 1H), 7.34 (d, *J* = 8.1 Hz, 1H), 7.20 (app. t, *J* = 7.5 Hz, 1H), 7.12 (app. t, *J* = 7.5 Hz, 1H), 6.99 (s, 1H), 5.97-5.82 (m, 1H), 5.31 (br. s, 1H), 5.28 (app. d, *J* = 17.1 Hz, 1H), 5.20 (app. d, *J* = 10.5 Hz, 1H), 4.75-4.67 (m, 1H), 4.63-4.51 (comp. m, 2H), 3.68 (s, 3H), 3.38-3.23 (comp. m, 2H).

^{13}C NMR (226 MHz, $CDCl_3$): δ 172.6, 155.8, 136.3, 132.8, 127.7, 122.9, 122.4, 119.8, 118.7, 117.9, 111.4, 110.0, 65.9, 54.6, 52.5, 28.1.

IR (ATR, neat): 3349, 2951, 1725, 1710, 1691, 1229 cm^{-1}.

HRMS (ESI+): *m/z* calc'd for $(M + H)^+$ $[C_{16}H_{18}N_2O_4 + H]^+$: 303.1339, found 303.1325.

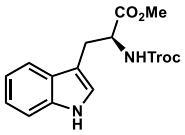

3-76

Indole 3-76. Prepared according to the procedure reported by Ruiz-Sanchis and coworkers.[33] The characterization data was consistent with a procedure reported by Tirotta and coworkers.[34]

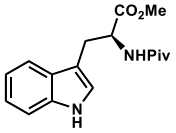

3-77

Indole 3-77. Prepared according to the procedure reported by Guerrero and Correa.[35]

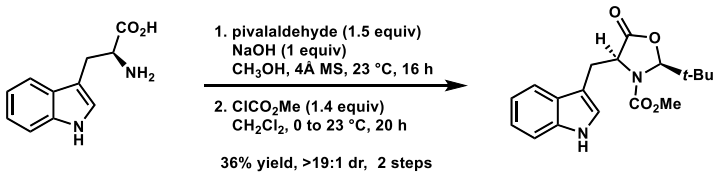

3-93 *3-79*

Indole 3-79. According to a procedure reported by Zhang and Finn,[36] to a solution of NaOH (98.0 mg, 2.45 mmol) in MeOH (6.1 mL) was added L-tryptophan (**3-93**, 500 mg, 2.45 mmol) and pivalaldehyde (398 μL, 3.66 mmol), followed by 4Å MS (~1 g). The reaction mixture stirred at room temperature for 16 h. After the reaction was complete, the mixture was filtered, and the filtrate was concentrated. The crude residue was then dissolved in CH_2Cl_2 (13 mL) and cooled to 0 °C. To this solution was added methyl chloroformate (266 μL, 3.44 mmol) and the reaction mixture was stirred at 0 °C for 4 h, then allowed to warm to room temperature and stirred overnight.

After 20 h total reaction time, the reaction mixture was filtered through a fritted funnel, and the filtrate was concentrated. The crude residue was purified via silica gel chromatography (2:1:1 hexanes/EtOAc/CH_2Cl_2 w/ 1% Et_3N eluent) to afford indole **3-79** (292 mg, 36% yield, >19:1 dr, over 2 steps) as a white solid.

TLC R*f*: 0.51 in 2:1 hexanes/EtOAc, visualized by UV, stained blue in Hanessian's stain.

^{1}H NMR (400 MHz, $CDCl_3$): δ 8.14 (br. s, 1H), 7.73 (d, *J* = 7.6 Hz, 1H), 7.35 (d, *J* = 8.0 Hz, 1H), 7.19 (app. t, *J* = 7.1 Hz, 1H), 7.17-7.10 (comp. m, 2H), 5.54 (s, 1H), 4.57 (app. t, *J* = 6.1 Hz, 1H), 3.65 (s, 3H), 3.37 (app. d, *J* = 6.1 Hz, 2H), 1.01 (s, 9H).

^{13}C NMR (100 MHz, $CDCl_3$): δ 172.4, 156.7, 136.3, 127.5, 123.8, 122.1, 119.7, 118.7, 111.4, 110.8, 96.1, 57.6, 53.3, 37.2, 29.2, 25.0.

IR (ATR, neat): 3411, 2958, 1787, 1725, 1443, 1366 cm^{-1}.

HRMS (ESI+): *m/z* calc'd for $(M + Na)^+$ $[C_{18}H_{22}N_2O_4 + Na]^+$: 353.1472, found 353.1458.

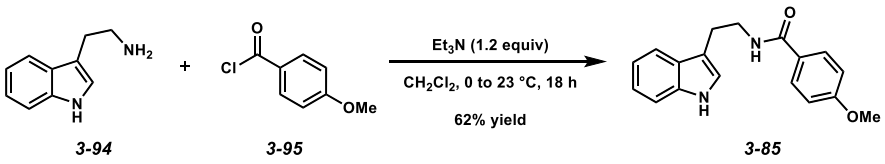

Indole 3-85. Indole **3-85** was synthesized according to a procedure reported by Wu and coworkers.[37] To a solution of tryptamine (**3-94**, 200 mg, 1.25 mmol) and triethylamine (209 μL, 1.50 mmol) in CH_2Cl_2 (3 mL) was added 4-methoxybenzoyl chloride (**3-95**, 169 μL, 1.25 mmol) at 0 °C. The reaction mixture was allowed to warm to room temperature and stirred overnight. After 18 h, the reaction mixture was diluted with CH_2Cl_2 (5 mL) and washed with H_2O (2 x 5 mL),

dried over Na_2SO_4, and concentrated in vacuo. The crude residue was purified silica gel chromatography (2:1 hexanes/EtOAc eluent) to afford indole **3-85** (229 mg, 62% yield, R_f = 0.25 in 2:1 hexanes/EtOAc eluent) as a white solid. The characterization data was consistent with a procedure reported by Veatch and Alexanian.[38]

^{1}H NMR (400 MHz, $CDCl_3$): δ 8.08 (br. s, 1H), 7.66 (d, *J* = 8.1 Hz, 1H), 7.63 (d, *J* = 8.3 Hz, 2H), 7.39 (d, *J* = 8.1 Hz, 1H), 7.23 (app. t, *J* = 7.6 Hz, 1H), 7.14 (app. t, *J* = 7.6 Hz, 1H), 7.08 (s, 1H), 6.87 (d, *J* = 8.3 Hz, 2H), 6.13 (br. s, 1H), 3.83 (s, 3H), 3.79 (app. q, *J* = 6.8 Hz, 2H), 3.10 (app. t, *J* = 6.8 Hz, 2H).

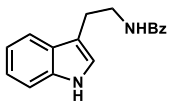

3-86

Indole 3-86. Prepared according to the procedure reported by Wu and coworkers.[37]

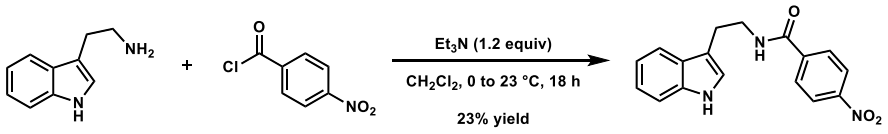

3-94 *3-96* *3-87*

Indole 3-87. Indole **3-87** was synthesized according to a procedure reported by Wu and coworkers.[37] To a solution of tryptamine (**3-94**, 200 mg, 1.25 mmol) and triethylamine (209 μL, 1.50 mmol) in CH_2Cl_2 (3 mL) was added 4-nitrobenzoyl chloride (**3-96**, 232 mg, 1.25 mmol) at 0 °C. The reaction mixture was allowed to warm to room temperature and stirred overnight. After

18 h, the reaction mixture was diluted with CH_2Cl_2 (5 mL) and washed with H_2O (2 x 5 mL), dried over Na_2SO_4, and concentrated in vacuo. The crude residue was purified silica gel chromatography (2:1 hexanes/EtOAc eluent) to afford indole **3-87** (90.5 mg, 23% yield) as a yellow solid.

TLC R_f: 0.21 in 2:1 hexanes/EtOAc, visualized by UV, stained blue in Hanessian's stain.

^{1}H NMR (400 MHz, $CDCl_3$): δ 8.23 (d, *J* = 8.3 Hz, 2H), 8.08 (br. s, 1H), 7.79 (d, *J* = 8.3 Hz, 2H), 7.64 (d, *J* = 8.0 Hz, 1H), 7.41 (d, *J* = 8.0 Hz, 1H), 7.24 (app. t, *J* = 7.6 Hz, 1H), 7.15 (app. t, *J* = 7.6 Hz, 1H), 7.10 (s, 1H), 6.22 (br. s, 1H), 3.83 (app. q, *J* = 6.2 Hz, 2H), 3.13 (app. t, *J* = 6.2 Hz, 2H).

^{13}C NMR (100 MHz, $(CD_3)_2SO$): δ 172.1, 164.5, 148.9, 140.3, 136.2, 128.6, 127.2, 123.5, 122.7, 120.9, 118.2, 111.7, 111.4, 40.4, 25.0.

IR (ATR, neat): 3044, 1641, 1598, 1535, 1345 cm^{-1}.

HRMS (ESI+): *m/z* calc'd for $(M + Na)^+$ $[C_{17}H_{15}N_3O_3 + Na]^+$: 332.1006, found 332.0991.

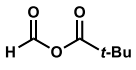

3-3

Trimethylacetic formic anhydride (3-3). Prepared according to the procedure reported by Vlietstra and coworkers.[39]

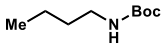

3-42

Carbamate 3-42. Prepared according to the procedure reported by Siddaiah and coworkers.[40] Spectroscopic data was consistent with a report by Li and coworkers.[41]

Diazocarbonyl Synthesis

General Notes: After synthesizing, vinyl diazocarbonyl compounds were stored in a -20 °C freezer as a 1.0 M solution in CH_2Cl_2. Diazo compounds are toxic, irritants, and many compounds are explosive. Care should be taken when handling and synthesizing diazo compounds.

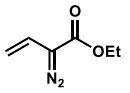

3-2

Diazoester 3-2. Prepared according to the procedure reported by Davies and coworkers.[42]

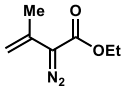

3-70

Diazoester 3-70. Prepared according to the procedure reported by Jadhav and coworkers,[43] which they had applied to the synthesis of 2-diazo-7-methyl-3-methyleneoct-6-enoate. Acetone was instead used as the initial electrophile.

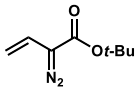

3-71

Diazoester 3-71. Prepared according to the procedure reported by Schwartz and coworkers.[44]

3.11. References and Notes

[1] Gall, B. K.; Smith, A. K. Ferreira, E. M. *Angew. Chem. Int. Ed.* **2022**, *61*, e2022121.

[2] (a) Saxtonin, J. E. *The Alkaloids: Chemistry and Biology*, Vol. 51(Ed.: Cordell, G. A.), Academic Press, San Diego, 1998, Ch. 1. (b) Kam, T.-S.; Lim, K.-H. in *The Alkaloids: Chemistry and Biology*, Vol. 66 (Ed.: Cordell, G. A.), Elsevier, Amsterdam, 2008, Ch. 1. (c) Cuendet, M.; Pezzutoin, J. M. Modern Alkaloids: Structure, Isolation, Biology (Ed.: Fattorusso, E.; Taglialatela-Scafati, O.), Wiley-VCH, Weinheim, 2008, Ch. 2. (d) Liu, X.-Y.; Qin, Y. *Acc. Chem. Res*. **2019**, *52*, 1877-1891. (e) Ishikawa, H.; Elliott, G. I.; Velcicky, J.; Choi, Y.; Boger, D. L. *J. Am. Chem. Soc*. **2006**, *128*, 10596-10612. (f) Martin, G.; Angyal, P.; Egyed, O.; Varga, S.; Soós. T. *Org. Lett.* **2020**, *22*, 4675-4679. (g) Qin, B.; Wang, Y.; Wang, X.; Jia, Y. *Org. Chem. Front.* **2021**, *8*, 369-383.

[3] Nondearomative C2/C3-functionalization has been accomplished employing C-H functionalization. For select examples, see: (a) Antos, J. M.; Francis, M. B. *J. Am. Chem. Soc.* **2004**, *126*, 10256-10257. (b) Ruiz-Rodríguez, J.; Albericio, F.; Lavilla, R. *Chem. Eur. J.* **2010**, *16*, 1124-1127. (c) Ruan, Z.; Sauermann, N.; Manoni, E.; Ackermann, L. *Angew. Chem. Int. Ed.* **2017**, *56*, 3172-3176. (d) Schischko, A.; Ren, H.; Kaplaneris, N.; Ackermann, L. *Angew. Chem. Int. Ed*. **2017**, *56*, 1576-1580.

[4] For select examples of tryptophan functionalization reactions that invoke photoredox catalysis, see: (a) Lima, R. N.; Delgado, J. A. C.; Bernardi, D. I.; Berlinck, R. G. S.; Kaplaneris, N.; Ackermann, L.; Paixão, M. W. *Chem. Commun*. **2021**, *57*, 5758-5761. (b) Li, Y.; Vaz, R. J.; Olson, S. H.; Munson, M.; Paras, N. A.; Conrad, J. *Eur. J. Org. Chem.* **2020**, *2020*, 5828-5832. (c) Lee, J. C.; Cuthbertson, J. D.; Mitchell, N. J. *Org. Lett*. **2023**, *25*, 5459-5464.

[5] Indolamines have been employed in dearomative spirocyclization reactions. For select examples, see: (a) Gao, F.; Yang, C.; Gao, G.-L.; Zheng, L.; Xia, W. *Org. Lett.* **2015**, *17*, 3478-3481. (b) Zhang, M.; Duan, Y.; Li, W.; Cheng, Y.; Zhu, C. *Chem. Commun.* **2016**, *52*, 4761-4763. (c) Wang, Q.; Qu, Y.; Xia, Q.; Song, H.; Song, H.; Liu, Y.; Wang, Q. *Adv. Synth. Catal*. **2018**, *360*, 2879-2884. (d) Wu, K.; Du, Y.; Wang, T. *Org. Lett.* **2017**, *19*, 5669-5672. (e) Gentry, E. C.; Rono, L. J.; Hale, M. E.; Matsuura, R.; Knowles, R. R. *J. Am. Chem. Soc.* **2018**, *140*, 3394-3402.

[6] Lies, S. D.; Lin, S.; Yoon, T. P. *Org. Synth.* **2016**, *93*, 178-199.

[7] (a) Gieseler, A.; Steckhan, E.; Wiest, O. *Synlett* **1990**, 275-277. (b) Geiseler, A.; Steckhan, E.; Wiest, O.; Knoch, F. *J. Org. Chem.* **1991**, *56*, 1405-1411. (c) Wiest, O.; Steckhan, E.; Grein, F. *J. Org. Chem*. **1992**, *57*, 4034-4037. (d) Wiest, O.; Steckhan, E. *Tetrahedron Lett*. **1993**, *34*, 6391-6394. (e) Peglow, T.; Blechert, S.; Steckhan, E. *Chem. Commun*. **1999**, 433-434. (f) Haberl, U.; Steckhan, E.; Blechert, S.; Wiest, O. *Chem. Eur. J.* **1999**, *5*, 2859-2865. (g) Pitre, S. P.; Scaiano, J. C.; Yoon, T. P. *ACS Catal*. **2017**, *7*, 6440-6444.

[8] $[Ru(bpz)_3](PF_6)_2$ is a known photooxidant, prevalent in a number of radical cation photocatalyzed methods. For more information, see: (a) Lin, S.; Ischay, M. A.; Fry, C. G.; Yoon, T. P. *J. Am. Chem. Soc.* **2011**, *133*, 19350-19353. (b) Yoon, T. P. *ACS Catal.* **2013**, *3*, 895-902.

[9] Other conditions that were tried included malonates with base, hydrosilanes, and other cyclic enones.

[10] (a) Shono, T.; Matsumura, Y.; Tsubata, K. *J. Am. Chem. Soc.* **1981**, *103*, 1172-1176. (b) Moeller, K. D.; Sharif, T.; Marzabadi, M. R. *Tetrahedron Lett*. **1989**, *30*, 1213-1216. (c) Moeller, K. D.; Wang, P. W.; Tarazi, S.; Marzabadi, M. R.; Wong, P. L. *J. Org. Chem.* **1991**, *56*, 1058-1067. (d) Duan, S.; Moeller, K. D. *J. Am. Chem. Soc.* **2002**, *124*, 9368-9369. (e) Okada, Y.; Chiba, K. *Chem. Rev.* **2018**, *118*, 4592-4630.

[11] The quantum yield of $[Ru(bpz)_3](PF_6)_2$ in the (3+2) cycloaddition between *trans*-anethole and ethyl vinyl diazoacetate is Φ(63.8%). The quantum yield of $[Cr(PMP_2phen)_3](BF_4)_3$ in the same reaction is Φ(15.9%). For more information, see: Gall, B. K. Chromium(III) Photocatalysis: Catalyst Design and Reaction Development. Ph.D. Dissertation, University of Georgia, Athens, GA, 2021.

[12] Schultz, D. M.; Sawicki, J. W.; Yoon, T. P. *Beilstein J. Org. Chem.* **2015**, *11*, 61-65.

[13] Sheehan, J. C.; Yang, D.-D. H. *J. Am. Chem. Soc.* **1958**, *80*, 1154-1158.

[14] Feng, P.; Fan, Y.; Xue, F.; Liu, W.; Li, S.; Shi, Y. *Org. Lett.* **2011**, *13*, 5827-5829.

[15] Unhale; R. A.; Sadhu; M. M.; Singh, V. K. *Org. Lett.* **2022**, *24*, 3319-3324.

[16] Shaikh, R. S.; Ghosh, I.; König, B. *Chem. Eur. J.* **2017**, *23*, 12120-12124.

[17] Tyson, E. L.; Niemeyer, Z. L; Yoon, T. P. *J. Org. Chem.* **2014**, *79*, 1427-1436.

[18] Carr, G.; Chung, M. K. W.; Mauk, A. G.; Andersen, R. J. *J. Med. Chem.* **2008**, *51*, 2634-2637.

[19] Kandukuri, S. R.; Schiffner, J. A.; Oestreich, M. *Angew. Chem. Int. Ed.* **2012**, *51*, 1265-1269.

[20] Yang, Y.; Jiang, X.; Qing, F.-L. *J. Org. Chem.* **2012**, *77*, 7538-7547.

[21] Oliveira, R. R. B.; Brito, T. B.; Nepel, A.; Costa, E. V.; Barison, A.; Nunes, R. S.; Santos, R. L. C.; Cavalcanti, S. C. H. *Med. Chem. (Sharjah, UAE)* **2014**, *10*, 580-587.

[22] Huber, T.; Schneider, L.; Präg, A.; Gerhardt, S.; Einsle, O.; Müller, M. *ChemCatChem* **2014**, *6*, 2248-2252.

[23] De, S.; Das, M. K.; Bhunia, S.; Bisai, A. *Org. Lett.* **2015**, *17*, 5922-5925.

[24] Snell, R. H.; Woodward, R. L.; Willis, M. C. *Angew. Chem. Int. Ed.* **2011**, *50*, 9116-9119.

[25] de la Fuente, M. C.; Domínguez, D. *Tetrahedron* **2011**, *67*, 3997-4001.

[26] Schlegel, M.; Coburger, P.; Schneider, C. *Chem. Eur. J.* **2018**, *24*, 14207-14212.

[27] Utsumi, T.; Noda, K.; Kawauchi, D.; Ueda, H.; Tokuyama, H. *Adv. Synth. Catal.* **2020**, *362*, 3583-3588.

[28] Trabbic, C. J.; Overmeyer, J. H.; Alexander, E. M.; Crissman, E. J.; Kvale, H. M.; Smith, M. A.; Erhardt, P. W.; Maltese, W. A. *J. Med. Chem.* **2015**, *58*, 2489-2512.

[29] Mehndiratta, S.; Wang R.-S.; Huang, H.-L.; Su, C.-J.; Hsu, C.-M.; Wu, Y.-W.; Pan, S.-L.; Liou, J.-P. *Eur. J. Med. Chem.* **2017**, *134*, 13-23.

[30] Montgomery, T. D.; Nibbs, A. E.; Zhu, Y.; Rawal, V. H. *Org. Lett*. **2014**, *16*, 3480-3483.

[31] Alqahtani, N.; Porwal, S. K.; James, E. D.; Bis, D. M.; Karty, J. A.; Lane, A. L.; Viswanathan, R. *Org. Biomol. Chem*. **2015**, *13*, 7177-7192.

[32] Sacco, M. D.; Defrees, K.; Zhang, X.; Lawless, W.; Nwanochie, E.; Balsizer, A.; Darch, S. E.; Renslo, A. R.; Chen, Y. *ACS Infect. Dis.* **2022**, *8*, 1231-1240.

[33] Ruiz-Sanchis, P.; Savina, S. A.; Acosta, G. A.; Albericio, F.; Álvarez, M. *Eur. J. Org. Chem*. **2012**, *2012*, 67-73.

[34] Tirotta, I.; Fifer, N. L.; Eakins, J.; Hutton, C. A. *Tetrahedron Lett.* **2013,** *54*, 618-620.

[35] Guerrero, I.; Correa, A. *Org. Lett.* **2020**, *22*, 1754-1759.

[36] Zhang, L.; Finn, J. M. *J. Org. Chem.* **1995**, *60*, 5719-5720.

[37] Wu, G.; Lv, T.; Mo, W.; Yang, X.; Gao, Y.; Chen, H. *Tetrahedron Lett*. **2017**, *58*, 1395-1398.

[38] Veatch, A. M.; Alexanian, E. J. *Chem. Sci*. **2020**, *11*, 7210-7213.

[39] Vlietstra, E. J.; Zwikker, J. W.; Nolte, R. J. M.; Drenth, W. *Recl. Trav. Chim. Pays. Bas.* **1982**, *101*, 460-462.

[40] Siddaiah, V.; Basha, G. M.; Rao, G. P.; Prasad, U. V.; Rao, R. S. *Chem. Lett.* **2010**, *39*, 1127-1129.

[41] Li, P.; Ma, N.; Wang, Z.; Dai, Q.; Hu, C. *J. Org. Chem*. **2018**, *83*, 8233-8240.

[42] (a) Davies, H. M. L.; Cantrell, W. R., Jr.; Romines, K. R.; Baum, J. S. *Org. Synth.* **1992**, *70*, 93. (b) Davies, H. M. L.; Hougland, P. W.; Cantrell, W. R., Jr. *Synth. Commun*. **1992**, *22*, 971-978.

[43] (a) Jadhav, A. M.; Pagar, V. V.; Liu, R.-S. *Angew. Chem. Int. Ed.* **2012**, *51*, 11809-11813. (b) Padwa, A.; Kulkarni, Y. S.; Zhang, Z. *J. Org. Chem.* **1990**, *55*, 4144-4153.

[44] Schwartz, B. D.; Denton, J. R.; Lian, Y.; Davies, H. M. L.; Williams, C. M. *J. Am. Chem. Soc.* **2009**, *131*, 8329-8332.

CHAPTER 4

DISTONIC RADICAL CATIONS FROM AMINOCYCLOPROPANES AND THEIR APPLICATION IN A (3 + 3) CYCLOADDITION WITH VINYL DIAZOACETATES

4.1. Introduction: Distonic Radical Ions

Distonic radical ions can be classified by separation of charge and radical sites—as such, the charge and radical density are located on different atoms.[1] The aminocyclopropane functional group represents a unique coupling partner in organic reaction methodology. While the generation of carbon centered radicals by photocatalytic means are prominent in modern synthetic chemistry, *N*-centered radicals remain less studied. By leveraging the lone-pair of an electron-rich amine to undergo single electron oxidation, the resulting amino-radical cation can participate in a number of various radical or cascade reaction pathways to synthesize complex molecules in a step-economical procedure. Attaching a highly strained cyclopropyl unit to this system could allow for facile radical ring-opening, resulting in a *distonic radical cation* that is highly reactive.

4.1.1. Reactivity of Distonic Radical Cations from Aminocyclopropanes

In 1997, Cha and coworkers developed a method for rapid ring-opening of aminocyclopropanes through photooxidation (*Scheme 4.1.1*).[2] When cyclopropylamine **4-1** was exposed to stoichiometric DCB (1,4-dicyanobenzene) and UV irradiation, oxidation (**4-2**) of the lone pair on nitrogen occurred. This led to facile ring opening (**4-3**), followed by a 1,5-hydrogen atom transfer (HAT) (**4-4**). Reduction (**4-5**) and hydrolysis further led to isolation of ketone **4-6**.

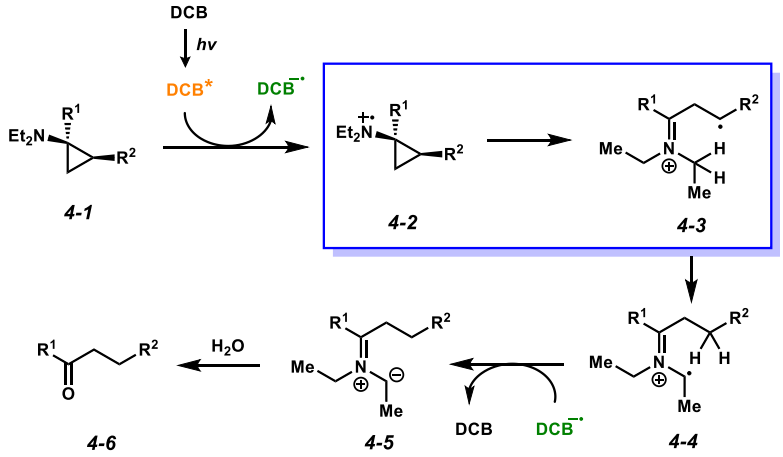

Scheme 4.1.1. Early report of the photooxidation of aminocyclopropanes.

Shortly after this report, Cha extended this method to an intramolecular radical cyclization (*Scheme 4.1.2*).[3] By including a tethered alkene on the aminocyclopropane (**4-7**), after oxidation and ring-opening, the radical cation produced could undergo a *5-exo-trig* radical cyclization with the pendant alkene (**4-9**) instead of 1,5-HAT (**4-8**). When smaller alkyl groups were employed at R^1 and R^2 (e.g., acyclic propyl and pentyl groups) the dual annulation product (**4-10**) could be obtained in 60% yield, as one stereoisomer. When R^1 was a bulkier alkyl group (e.g., cyclopentane), stereochemistry imposed during the second cyclization was eroded due to

competing steric interactions between R^1 and the diethylimine group. Drawbacks to this approach include limitations arising from the intramolecular nature of the cyclization. Stoichiometric photocatalyst and harsh UV light were also necessary.

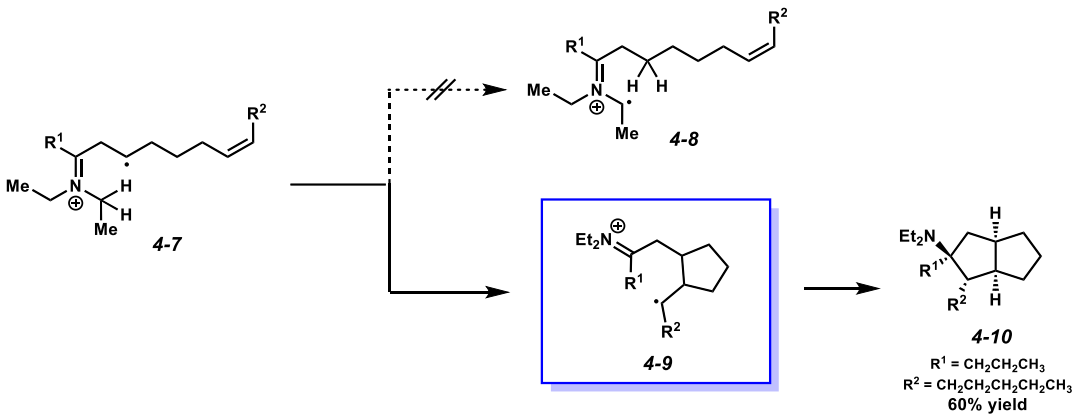

Scheme 4.1.2. Cha's intramolecular (3 + 2) annulation cascade.

In 2012, Zheng reported the first use of aminocyclopropanes in a visible light-promoted, photoredox reaction.[4] Up to this point, amines typically had been used as sacrificial electron donors in photoredox catalytic systems. This study explored the use of amine lone pairs as a sacrificial donor and as a substrate, by invoking an irreversible ring-opening cascade process. Zheng reported cyclopropylamines (**4-11**) could be employed in an intermolecular (3 + 2) photocatalytic cycloaddition with styrenes (**4-12**) to generate functionalized cyclopentanes (**4-13**, *Scheme 4.1.3*). In the past, amine lone pairs required UV light and a highly oxidizing photosensitizer in stoichiometric amounts (*vide supra*);[2,3] however, catalytic $[Ru(bpz)_3](PF_6)_2$, in the presence of white light, was found to be reactive with electron rich cyclopropylamines. In the initial screening process, degassing of the solvent and the reaction mixture were found to be crucial for obtaining high yield of cycloadduct **4-13**. If air was present, only moderate yields of

cycloadduct were afforded. The distonic radical intermediate is highly reactive and can be rapidly intercepted by oxygen.

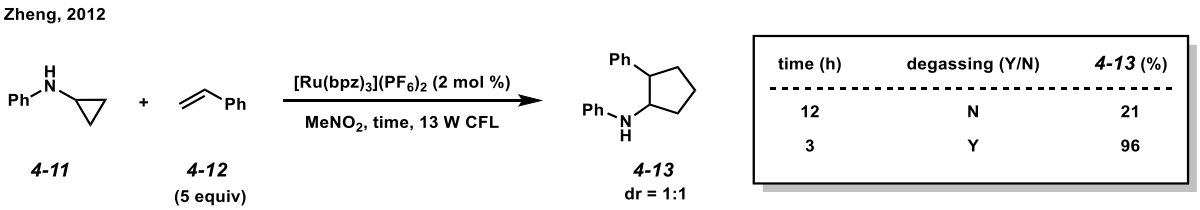

Scheme 4.1.3. Zheng's seminal report utilizing cyclopropylamine to generate highly reactive distonic radical cations via visible light-mediated photocatalysis.

The proposed mechanism is shown in *Scheme 4.1.4*. Upon excitation of the Ru(II) photocatalyst, single electron oxidation of the lone pair on nitrogen of **4-11** generates radical cation **4-14** and reduced Ru(I). **4-14** then undergoes a ring-opening sequence to generate distonic radical intermediate **4-15**. This intermediate is highly reactive and will react with oxygen rapidly to afford cyclic peroxide, thus the need for excessive degassing.[5] This radical cation intermediate can then react with styrene in a Giese-type addition to generate radical cation **4-16**. Subsequent radical cyclization (**4-17**) and reduction affords product **4-13** and ground-state Ru(II), closing the catalytic cycle and regenerating the photocatalyst.

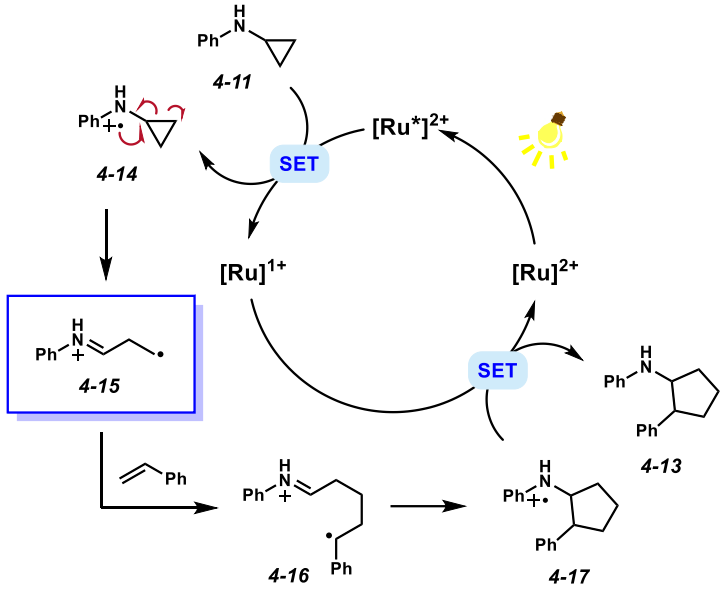

Scheme 4.1.4. Proposed catalytic cycle of (3 + 2) cycloaddition with aminocyclopropanes and electron-rich alkenes.

The scope of this reaction was limited to aryl cyclopropylamines (**4-18** or **4-19**, *Scheme 4.1.5a*). The aryl group effectively lowers the oxidation potential of the *N*-lone pair within the window of the Ru photocatalyst potential. Different functional groups were tolerated on the aryl group (**4-22**), as well as naphthyl (**4-23**) and pyridyl (**4-24**) substrates. An area of concern was the lack of diastereoselectivity with these substrates. It was hypothesized that a bicyclic system could impart some selectivity through steric bias. Indeed, when bicyclic substrates (**4-19**) were tested in the reaction, moderate to excellent diastereoselectivity was observed (**4-25**–**4-27**). To rationalize this selectivity, a model was proposed (*Scheme 4.1.5b*).[6] One model of the two chair transition states (**4-28**→**4-29**) is more favorable due to the minimization of the steric interactions between R^1 and the Ph group (**4-30**→**4-31**).

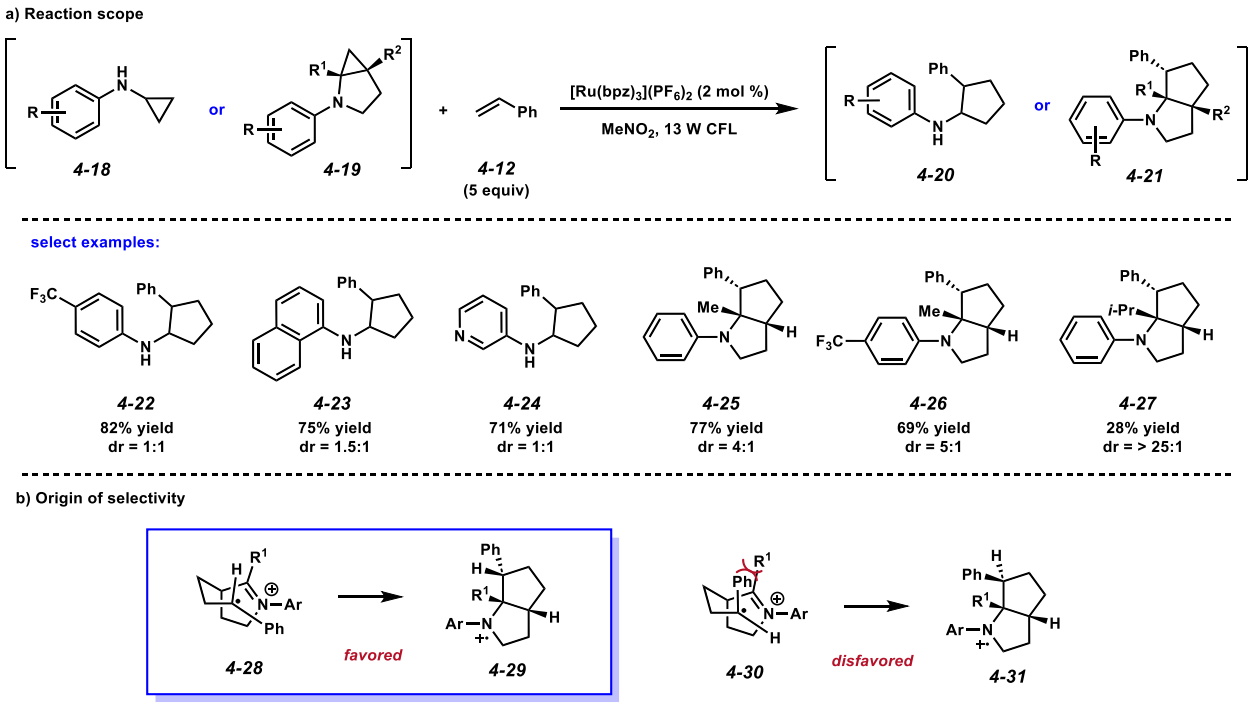

Scheme 4.1.5. (a) Select scope of the reaction. (b) Explanation of diastereoselectivity in bicyclic examples.

Zheng and coworkers furthered the scope of this reaction in 2014 with a follow-up study in which they disclosed a photocatalytic (3 + 2) cycloaddition between cyclopropylamines and alkynes (*Scheme 4.1.6*).[7] While internal alkynes were not tolerated, electron-rich alkynes, enynes, and diynes were successful in the reaction with moderate to complete regioselectivity. Several strategies were employed to induce diastereoselectivity. Using bulky alkene tethers in enyne derivatives (**4-34**) imparted moderate selectivity, although chemoselectivity favored the alkene in these examples (**4-35**). Pre-functionalizing the cyclopropyl unit (**4-36**) only imparted mild selectivity (**4-37**).

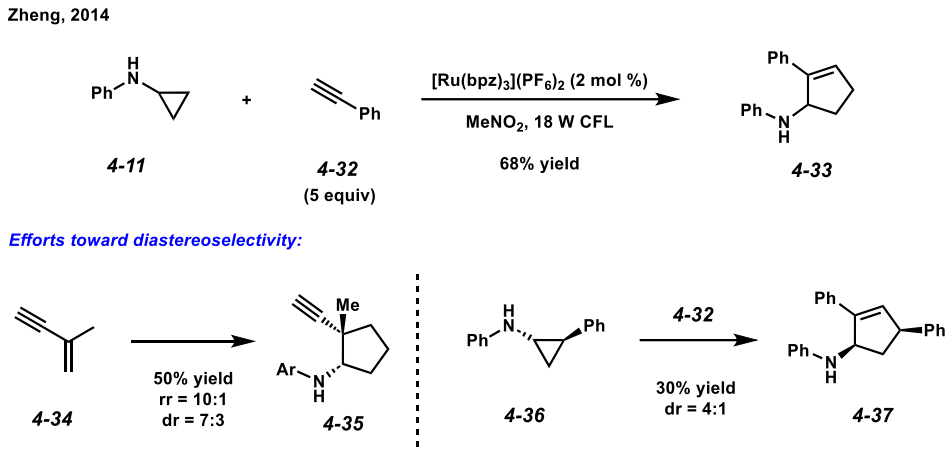

Scheme 4.1.6. Radical cycloaddition with alkyne derivatives.

4.1.2. Diastereoselective Cycloadditions

While Zheng discovered this highly reactive intermediate could be generated from visible light and employed in intermolecular reactions, there remained a gap in producing highly stereoselective cycloaddition products from this method. In 2019, the Waser group were attempting to invoke cyclopropenes (**4-38**) in a (3 + 2) cycloaddition with cyclopropylamines to synthesize bicyclo[3.1.0]hexanes (**4-39**, *Scheme 4.1.7*).[8] In the course of their optimization studies, they found several photocatalysts to be proficient in initiating oxidation depending on the substrate, including $[Ru(bpz)_3](PF_6)_2$, $[Ir(dtbbpy)(ppy)_2](PF_6)$, and organic photocatalysts 4-CzIPN (2,4,5,6-tetrakis (9*H*-carbazol-9-yl) isophthalonitrile) and 4DPAIPN (1,3-dicyano-2,4,5,6-tetrakis(diphenylamino)-benzene). Bis-substitution on the methylene of the cyclopropene was required and typically were electron withdrawing groups (either ester, **4-40**, or fluorine, **4-42**). Bulky substitution on the aryl group attached to the cyclopropene (**4-41**), as well as on the aryl of the cyclopropylamine (**4-42**), impacted selectivity. This approach rendered diastereoselective substrates and allowed for lower loadings of coupled alkene; however, a more general approach

was still necessary as conditions changed per substrate, and the products (bicyclo[3.1.0]hexanes, **4-39**) were very specific.

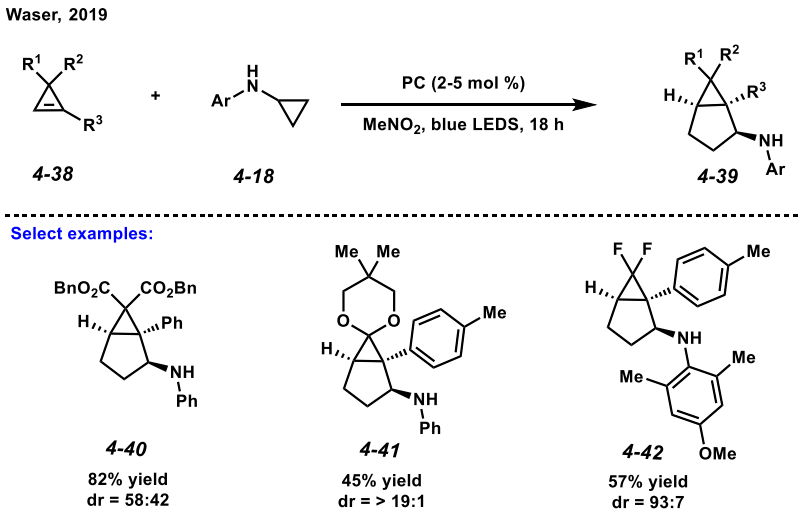

Scheme 4.1.7. Diastereoselectivity induced via substrate control.

In 2021, Aggarwal and coworkers reported a more general method to obtain functionalized cyclopentenes with excellent diastereoselectivity.[9] It was their vision that access to non-styrene-based alkenes (**4-44**) be considered, as well as easing downstream functionalization of the amine component. To this end, *N*-sulfonyl cyclopropylamines (**4-43**) were implemented in a (3 + 2) cycloaddition with electron-deficient alkenes to generate cyclopentanes (**4-45**) in high yields and excellent diastereoselectivities using visible light photoredox catalysis (*Scheme 4.1.8*). Considering post-cycloaddition transformations, the amine protecting group was thoroughly scrutinized. A sulfonyl group would be readily cleaved and introduce steric hindrance, but it would also markedly increase the oxidation potential of the amine. However, the addition of a base to engage in an initial deprotonation, rendering an amide anion that could be readily oxidized, could circumvent this issue. Indeed, when sodium phosphate was added to a solution of alkene **4-44** and

aminocyclopropane **4-43** in methylene chloride, with catalytic 4-CzIPN and blue light irradiation, cycloadduct **4-45** was obtained in 52% yield with 4:1 dr. Employing potassium phosphate slightly increased the yield and dr, while lowering the concentration of solvent drastically improved the yield; lowering the concentration would minimize the chances of alkene polymerization. When nosyl was used as the protecting group (**4-46**), cleavage to the free amine could be accomplished in 75% yield (**4-47**).

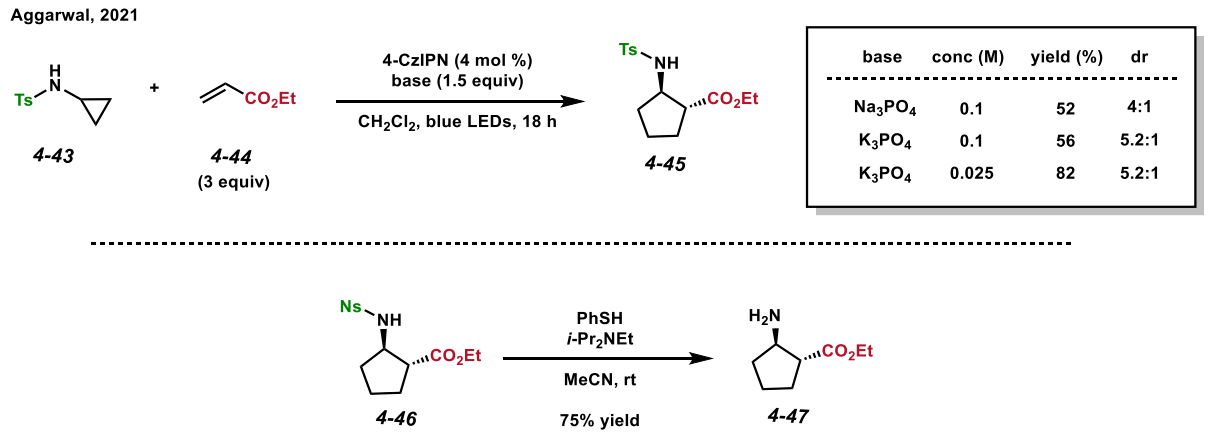

Scheme 4.1.8. Intermolecular (3 + 2) cycloaddition between N-sulfonyl cyclopropylamines and electron-deficient olefins.

The proposed mechanism of this reaction is shown in *Scheme 4.1.9*. After initial deprotonation of the *N*-sulfonyl cyclopropylamine (**4-43**), the resulting anion (**4-48**) can be oxidized through SET by excited 4-CzIPN to afford radical **4-49** and reduced 4-CzIPN. **4-49** can rapidly undergo β-scission to generate intermediate **4-50**, which can be intercepted by ethyl acrylate. After the formation of intermediate **4-51**, this radical can be further reduced to **4-52**, regenerating ground state 4-CzIPN. **4-52** can close the cycle to afford to **4-45** through a *5-exo-trig* radical cyclization. Selectivity in this reaction favors the *trans*-isomer, which is favored due to

minimization steric interactions between the ester and sulfonyl groups in intermediate **4-52**. Employing larger withdrawing groups on the alkene led to increase in dr (> 20:1).

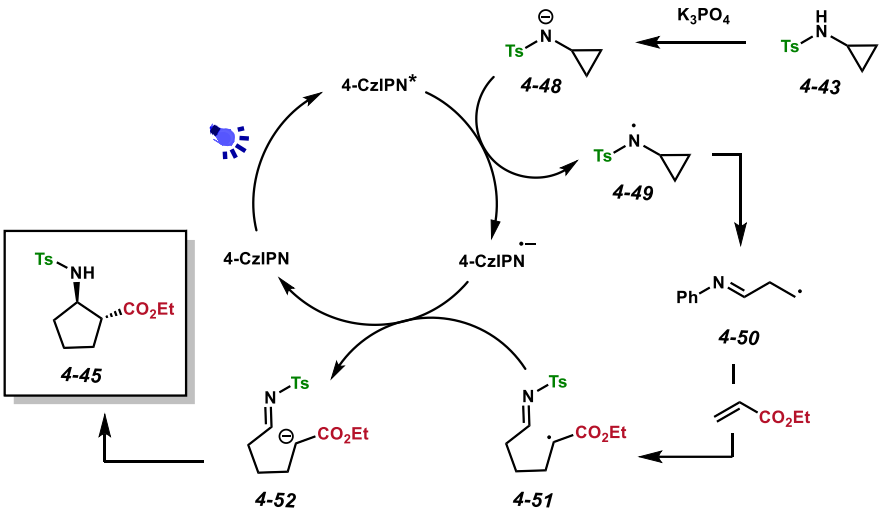

Scheme 4.1.9. Proposed mechanism of Aggarwal's (3 + 2) cycloaddition.

4.1.3. A Diradical-Mediated Cycloaddition

Another interesting procedure was reported by Stephenson and coworkers in 2022.[10] This method is different mechanistically from the radical cation methods otherwise discussed in this chapter, but nonetheless relevant background. Similar to Aggarwal, Stephenson aimed to utilize a substrate that was easier to manipulate after cyclization. The authors sought to use an imine-cyclopropane (**4-53**) as the starting substrate and induce a diradical intermediate (**4-54**) via direct excitation of the imine double bond in the presence of violet light (*Scheme 4.1.10*). When imine **4-53** was exposed to violet light in the presence of styrene, cyclopentane **4-56** was observed. Aldrithiol (2,2′-dipyridyldisulfide) was added to suppress polymerization. This reaction was scalable and ran in continuous flow. The cycloadduct was taken directly on to imine hydrolysis

under acidic conditions, followed by addition of acyl chlorides to form the final amide cyclopentane **4-57**. This method represents a simple procedure for accessing a functionalized free amine (**4-56**) that can be further manipulated towards various amino cyclopentanes.

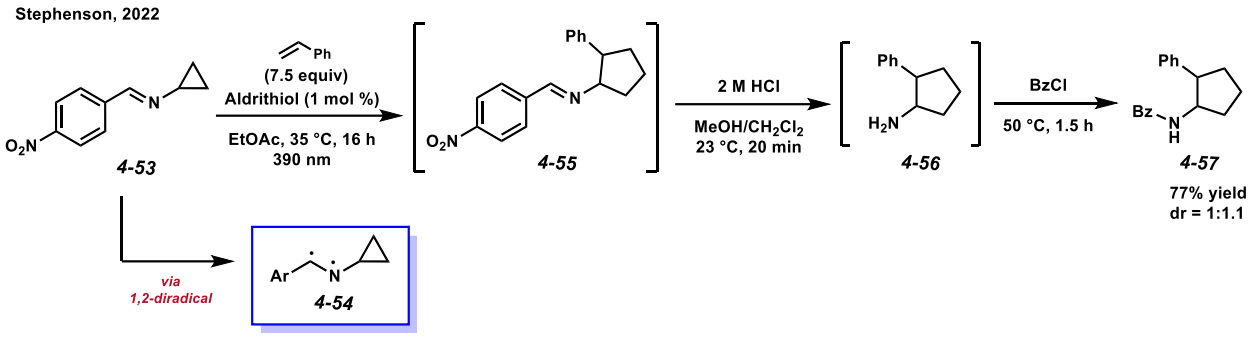

Scheme 4.1.10. Direct excitation of imine-cyclopropanes and application in a (3 + 2) cycloaddition.

4.1.4. Enantioselective Cycloadditions

Several methods have been reported in which aminocyclopentane products can be synthesized from aminocyclopropanes with asymmetric induction. In 2020, Ooi[11] and Jiang[12] separately disclosed the first two enantioselective syntheses of aminocyclopentanes from aminocyclopropanes via visible light photoredox catalysis. Ooi sought to develop an enantioselective transformation that leveraged a directing group that could engage in non-bonding interactions with a chiral photocatalyst (*Scheme 4.1.11*).[11] By using a known cationic Ir photocatalyst (**4-62**), chirality could be introduced from the counterion without affecting photocatalyst efficiency. Pre-organization of the counterion and directing group would allow for photooxidation and radical cyclization to proceed asymmetrically. The authors found that when a urea directing group (**4-58**) was employed with **4-62**, cycloadduct **4-60** could be obtained with

high enantiomeric enrichment. The cyclopentane product was afforded in high yields and dr as well. The urea group could also be readily cleaved without degradation of ee (**4-61**).

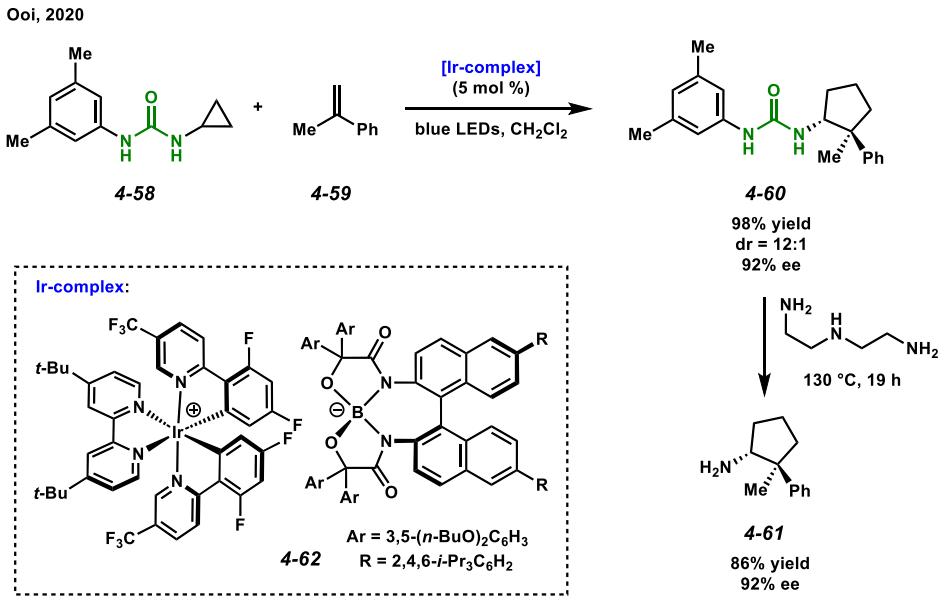

Scheme 4.1.11. Enantioselective cycloaddition through chiral counterion association.

The Jiang group concomitantly reported another enantioselective (3 + 2) cycloaddition strategy using a different catalyst framework.[12] Instead of applying a directing group to the aminocyclopropane, their group sought to employ alkenes substituted with azaarenes (**4-63**) which could be protonated in situ and act as an H-bonding directing group with a chiral Brønsted acid (**4-65**, *Scheme 4.1.12*). The authors found that chiral phosphoric acid **4-65**, with DPZ (5,6-bis(5-methoxythiophen-2-yl)pyrazine-2,3-dicarbonitrile) as the photocatalyst, were sufficient in inducing an asymmetric cycloaddition between a number of azaarene alkenes and aryl aminocyclopropanes to afford amino cyclopentanes (**4-64**) in high yields and ee.

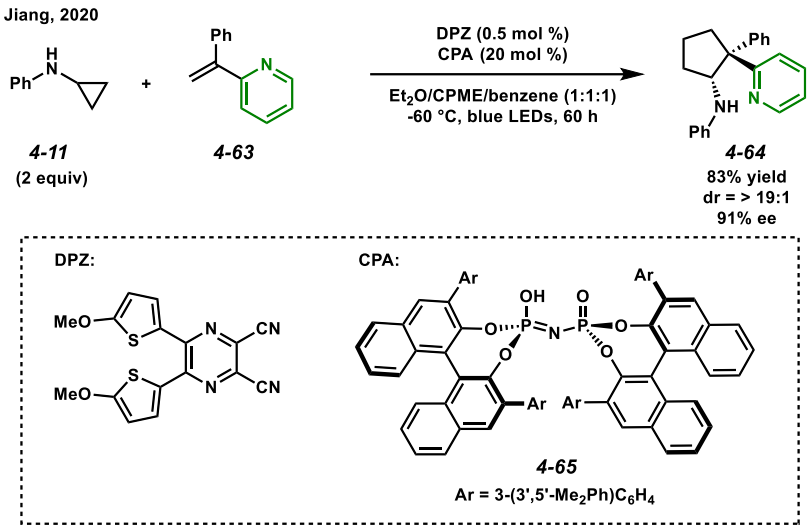

Scheme 4.1.12. Enantioselective cycloaddition through chiral Brønsted acid coordination.

In 2021, Aleman and coworkers reported an enantioselective cycloaddition using an asymmetric photocatalyst (*Scheme 4.1.13*).[13] The synthesis and application of asymmetric rhodium and iridium photocatalysts has been pioneered by the Meggers group.[14] This study also relies on a directing group tethered to the alkene; using unsaturated ketone **4-66**, the chiral Δ-Rh complex can coordinate to the alkene, and after visible light excitation, oxidize the aminocyclopropane (**4-11**). This asymmetric Rh complex will remain bound throughout the catalytic cycle, thus inducing enantioenrichment. While dr was only moderate using this method, **4-67** could be obtained with excellent ee. This method simplified asymmetric approaches towards aminocyclopentanes by implementing one chiral catalyst instead of a dual catalytic system (*vide supra*).

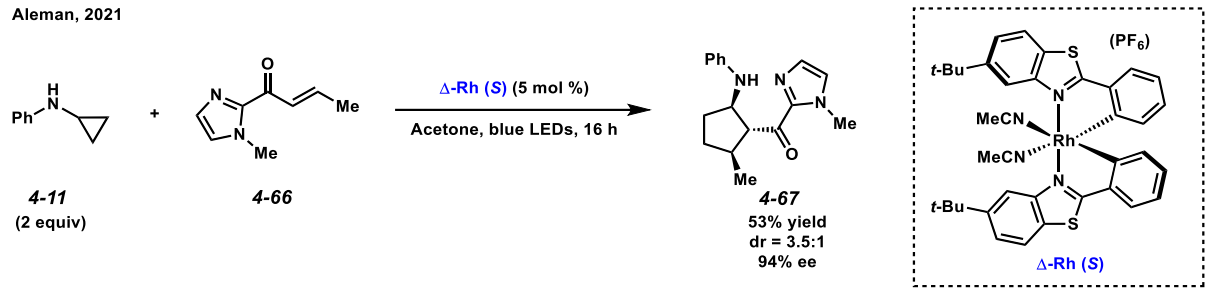

Scheme 4.1.13. Enantioselective cycloaddition using a chiral photocatalyst.

Most recently, Jiang and coworkers have disclosed a follow-up to their previous study (*vide supra*) in which chiral phosphoric acids are employed with the DPZ photocatalyst to achieve asymmetric aminocyclopentanes.[15] This study expanded beyond previously disclosed alkenyl azaarenes as compatible alkenes. Azaarenes were replaced with furanyl esters. After screening a series of chiral Brønsted acids, a chiral SPINOL phosphoric acid was found to be compatible with the new class of alkenes. High dr and ee were obtained using these conditions.

Several strategies have been employed to access derivatives of aminocyclopentanes. Efforts towards accessing these substrates stereoselectively have been accomplished through substrate control and using either dual catalysis or chiral photocatalysts. The future of this field lies in the potential applications of these methods in total synthesis, as well as expansion of substrate scope and coupling partners. Thus far, distonic radical cations from aminocyclopropanes have only been applied in (3 + 2) cycloadditions. To our knowledge, other cycloadditions remain unexplored.

4.2. Project Proposal

In light of our previously reported (3 + 2) cycloadditions between electron-rich alkenes or indoles and vinyl diazoacetates,[16] we began to seek new reactivity that Cr(III) photocatalysts could accomplish. Specifically, we wanted to expand the reaction profile of the newly developed $[Cr(PMP_2phen)_3](BF_4)_3$ photocatalyst. This Cr catalyst can be excited by visible light, and this excited complex has a relatively high reduction potential ($E_{1/2}$ = +1.43 V vs SCE). In theory, this catalyst should be able to oxidize electron rich amine lone pairs (e.g., aniline, $E_{1/2}$ = +0.625 V vs SCE). A specific interest we had was expanding this catalytic system to aminocyclopropanes (**4-11**, $E_{1/2}$ = +0.829 V vs SCE).[17] We were interested in the Cr catalyst's ability to oxidize *N*-atom lone pairs and generate distonic radicals from aminocyclopropanes, complementary to Ru (*Scheme 4.2.1*). Separately, we envisioned a new reaction in which a distonic radical cation, generated from oxidation of aminocyclopropane, could be intercepted by vinyl diazoacetate (**4-68**) and undergo a rapid cycloaddition to yield functionalized amino cyclohexenes (**4-69**).

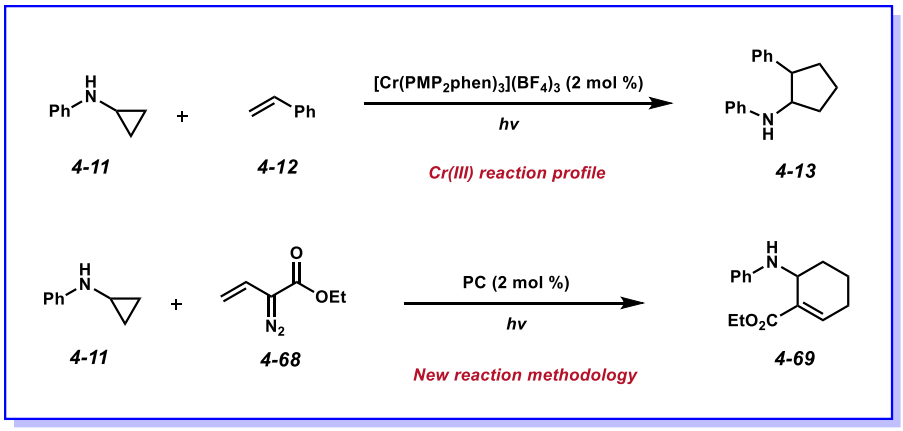

Scheme 4.2.1. Proposed complementary reaction and new methodology.

The desired cycloaddition product would be an interesting scaffold, as highly functionalized amines are present in a number of natural products and biologically active molecules (*Figure 4.2.1*). The product generated from the proposed (3 + 3) cycloaddition could easily be modulated further to afford a library of potentially valuable compounds.[18]

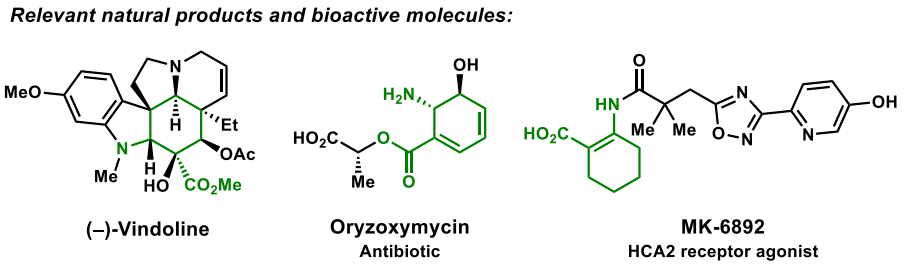

Figure 4.2.1. Applicability of proposed cycloaddition with vinyl diazoacetates.

4.3. Preliminary Experiments

We began our studies by repeating Zheng's conditions[4] and subjecting electron-rich aminocyclopropane **4-70** and styrene **4-12** to irradiation with catalytic $[Ru(bpz)_3](PF_6)_2$ (*Table 4.3.1*). Notably, we initially tested this reaction with white light instead of blue light, as white light is a cheaper source of irradiation. The reactions were set up under argon to avoid distonic radical decomposition. The results with Ru were comparable to Zheng's (85% yield of **4-71**). We next tested Cr's competence in the reaction. These reactions took longer for cyclopropane **4-70** to be consumed and were run for 24 h. We were delighted to observe (3 + 2) cycloaddition product with both Cr(III) photocatalysts tested. While $[Cr(Ph_2phen)_3](BF_4)_3$ only afforded 30% of **4-71**, $[Cr(PMP_2phen)_3](BF_4)_3$ yielded **4-71** in more comparable yields to $[Ru(bpz)_3](BF_4)_2$.

Table 4.3.1. Initial screening of Cr catalyst competency in the (3 + 2) cycloaddition.

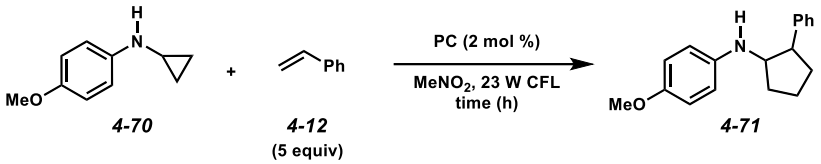

entry	PC	time (h)	conv (%)	yield (%) [a]
1	$[Ru(bpz)_3](PF_6)_2$	3	100	85
2	$[Cr(Ph_2phen)_3](BF_4)_3$	24	55	30
3	$[Cr(PMP_2phen)_3](BF_4)_3$	24	80	60

[a] dr = ~1:1

After proving Cr can generate the desired distonic radical intermediate, we next wanted to test our other intended reaction of coupling distonic radical cations from aminocyclopropanes with vinyl diazoacetate in a (3 + 3) cycloaddition. We initially chose to screen aminocyclopropane **4-70** and **4-11** in the proposed reaction. To our delight, when **4-70** was irradiated with white light in the presence of vinyl diazoacetate **4-68** and photocatalysts, aminocyclohexene **4-72** was observed (*Table 4.3.2*). $[Ru(bpz)_3](PF_6)_2$ and $[Cr(PMP_2phen)_3](BF_4)_3$ afforded comparable yields of **4-72**, while $[Cr(Ph_2phen)_3](BF_4)_3$ was not as adequate.

Table 4.3.2. Preliminary catalyst screen in proposed (3 + 3) cycloaddition.

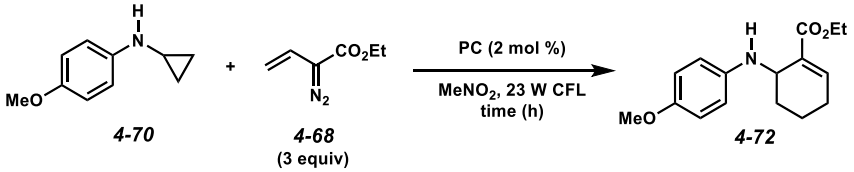

entry	PC	time (h)	conv (%)	yield (%)
1	$[Ru(bpz)_3](PF_6)_2$	20	62	41
2	$[Cr(Ph_2phen)_3](BF_4)_3$	20	20	15
3	$[Cr(PMP_2phen)_3](BF_4)_3$	20	78	37

When **4-11** was tested in the reaction, **4-69** was observed when $[Ru(bpz)_3](PF_6)_2$ and $[Cr(PMP_2phen)_3](BF_4)_3$ were employed, but in diminished yields compared to **4-70** (*Table 4.3.3).*

Table 4.3.3. Preliminary catalyst screen in (3 + 3) cycloaddition.

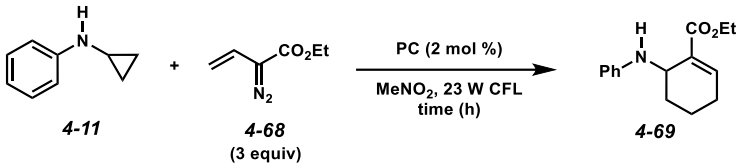

entry	PC	time (h)	conv (%)	yield (%)
1	$[Ru(bpz)_3](PF_6)_2$	20	100	33
2	$[Cr(Ph_2phen)_3](BF_4)_3$	20	50	0
3	$[Cr(PMP_2phen)_3](BF_4)_3$	20	100	36

In 2019, the McNeill group disclosed a photophysical study of cyclopropylamines.[19] They found that more electron-donating groups (i.e., *o*-OMe) on the aryl amine group lead to faster oxidation, but a slower rate of ring-opening. The slower rate of ring-opening alluded to by McNeill may lead to potential reactivity issues. In addition to potential reactivity issue, we observed that **4-70** was not bench stable and readily decomposed when left open to air. To remedy this, we stored **4-70** in a solution in CH_2Cl_2 under argon at –20 °C. This extended the lifetime of the substrate; however, it was still prone to decomposition over time. For optimization studies, we sought to utilize an aminocyclpropane that would be reactive and stable. While cycloproylamine **4-11** was not as reactive as **4-70**, it was significantly more stable and thus applied in further optimization studies.

4.4. Preliminary Reaction Optimization

4.4.1. Peroxide Side-Product

In the proposed (3 + 3) cycloaddition, we observed the desired product with both aminocyclopropanes tested, albeit in moderate to low yields. Another major product was present in these reactions that was eventually identified as peroxide **4-73** (*Scheme 4.4.1*). We were aware of the sensitivity of this reaction, but it was more susceptible to oxidation than we had anticipated. Setting the reactions up under argon, along with sparging of the reaction mixture with an argon balloon, was required to prevent significant formation of **4-73**, although it was still observed in several reactions even after implementing these measures. Only the freeze-pump-thaw (F-P-T) degassing method was sufficient for consistently suppressing formation of the peroxide.

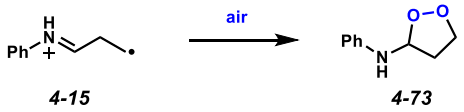

Scheme 4.4.1. Cyclic peroxide side-product observed.

4.4.2. Addition of an Acylating Agent

We began our optimizations with the intention of applying Cr as the photocatalyst for this transformation. The desired product could be isolated, but in quite low yields. We were curious if the product amine could be susceptible to oxidation by the Cr photocatalyst. Acylation of the cycloaddition product *in situ* could prevent further *N*-oxidation. We tested **4-11** and **4-68** in the reaction with addition of trimethylacetic formic anhydride (**4-74**) or TrocCl as acylating agents for

post-cycloaddition amine protection with $[Cr(PMP_2phen)_3](BF_4)_3$ photocatalyst (*Scheme 4.4.2*). Interestingly, we only observed acylated aminocyclopropane (**4-75**) with addition of **4-74**, and a low yielding mixture of acylated cyclopropylamine (**4-76**) and cycloaddition product (**4-69**) with addition of TrocCl and base. Acylation of **4-11** seems to be facile, and once acylated, the *N*-lone pair is likely outside of the oxidation window of the catalyst and cannot be oxidized, making it unreactive.

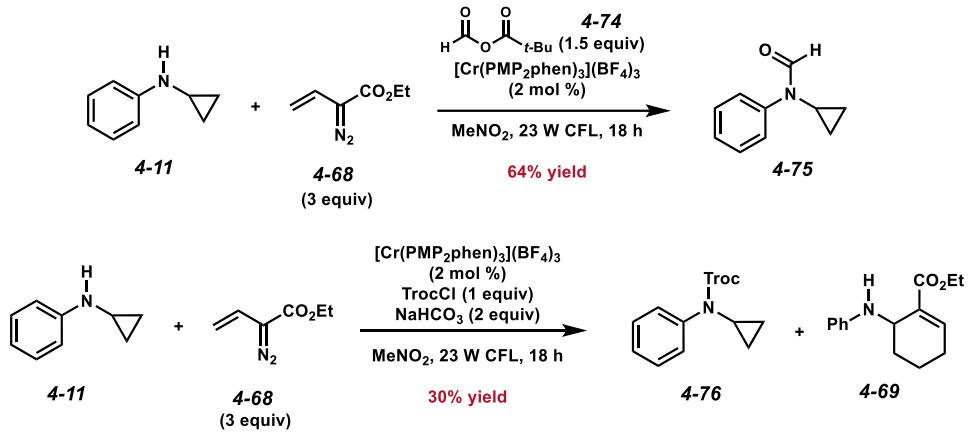

Scheme 4.4.2. Addition of acylating agents.

4.4.3. Optimization with $[Cr(PMP_2phen)_3](BF_4)_3$

Next, we decided to screen other parameters in an attempt to increase the yield of the reaction with Cr photocatalyst (*Table 4.4.1*). Changing the concentration of the reaction failed to increase the yield of **4-69** (*entry 1*). Other solvents did not have a beneficial effect on the reaction (*entries 2, 3*), nor did adding base to the reaction (*entry 4*). After observing significant peroxide formation, we ran the reaction under strictly inert conditions (*entry 5*), which lead to a decrease in the yield of **4-69**. Previous studies of ours have shown that air plays a crucial role in the Cr catalytic

cycle,[20] and air-free conditions may lead to slow catalyst turnover. Due to the desired intermediate being susceptible to oxidation, we concluded that Cr may not be the optimal catalyst for this methodology.

Table 4.4.1. Optimization with [Cr(PMP$_2$phen)$_3$](BF$_4$)$_3$.

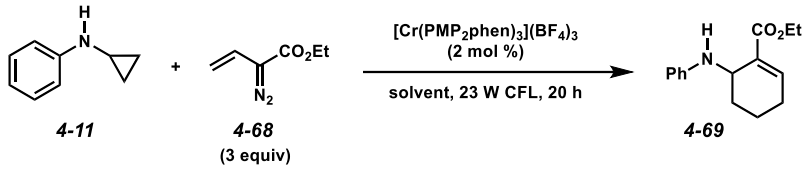

4-11 *4-68* (3 equiv) *4-69*

entry	solvent (M)	degas (Y/N)	conv (%)	yield (%)
1	$MeNO_2$ (0.05)	N	86	24
2	MeCN (0.1)	N	88	31
3	Acetone (0.1)	N	88	22
4 [a]	$MeNO_2$ (0.2)	N	100	0 [b]
5	$MeNO_2$ (0.2)	Y	30	23

[a] $NaHCO_3$ (1 equiv) added. [b] Cyclic peroxide major product.

4.4.4. Catalyst Optimization

We next sought to find the optimal photocatalyst for this novel cycloaddition. The various parameters screened are shown in *Table 4.4.2*. Other organic and transition-metal-based photocatalysts were investigated, with 4-CzIPN (2,4,5,6-tetra(9*H*-carbazol-9-yl)isophthalonitrile) and [Ir(dFCF$_3$ppy)$_2$(5,5'-dCF$_3$bppy)](PF$_6$)$_2$ initially performing the best (*entries 2, 6*). Higher concentration proved to be beneficial (*entries 7, 8*). Changing the light source to a blue LED lamp increased the yield with both catalysts, as well as with [Ru(bpz)$_3$](PF$_6$)$_2$ (*entries 9-11*). Results using the Ir catalyst afforded moderate yields, but these results were difficult to reproduce, and often peroxide side-product was observed in these reactions. The focus was then placed on 4-CzIPN and [Ru(bpz)$_3$](PF$_6$)$_2$ as the optimal catalysts. When reaction times were extended, the

yield was increased to 47% and 53%, respectively (*entries 12, 13*). We believe both catalysts to be sufficient in this reaction and present complementary methods with a commercially available Ru photooxidant and a transition-metal free complex (4-CzIPN). Other additives, solvents, reaction times, and catalyst loading methods were assessed (*see Experimental Section 4.8.2*). Further optimization in future studies to maximize yield should be considered.

Table 4.4.2. Reaction optimization.

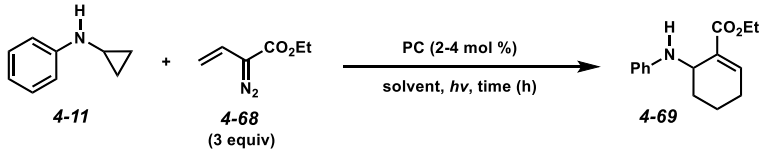

entry	photocatalyst	*hv* (source)	solvent (M)	time (h)	conv (%)	yield (%)
1	Mes-Acr(BF_4)	23 W CFL	$MeNO_2$ (0.1)	20	75	15
2	4-CzIPN	23 W CFL	$MeNO_2$ (0.1)	20	100	35
3	DCA	23 W CFL	$MeNO_2$ (0.1)	20	80	10
4	TPP(BF_4)	23 W CFL	$MeNO_2$ (0.1)	20	80	15
5	$(OMe)_3$TPP(BF_4)	23 W CFL	$MeNO_2$ (0.1)	20	92	30
6	[Ir(dFCF_3ppy)$_2$(5,5'-dCF_3bppy)](PF_6)	23 W CFL	$MeNO_2$ (0.1)	20	100	43
7	4-CzIPN	23 W CFL	$MeNO_2$ (0.2)	3	100	24
8	[Ir(dFCF_3ppy)$_2$(5,5'-dCF_3bppy)](PF_6)	23 W CFL	$MeNO_2$ (0.2)	6	90	47
9	4-CzIPN	blue Kessil	$MeNO_2$ (0.2)	2	100	48
10	[Ir(dFCF_3ppy)$_2$(5,5'-dCF_3bppy)](PF_6)	blue Kessil	$MeNO_2$ (0.2)	2	90	47
11	[Ru(bpz)$_3$](PF_6)$_2$	blue Kessil	$MeNO_2$ (0.2)	2	90	43
12	4-CzIPN	blue Kessil	$MeNO_2$ (0.2)	18	100	47
13	[Ru(bpz)$_3$](PF_6)$_2$	blue Kessil	$MeNO_2$ (0.2)	24	100	53

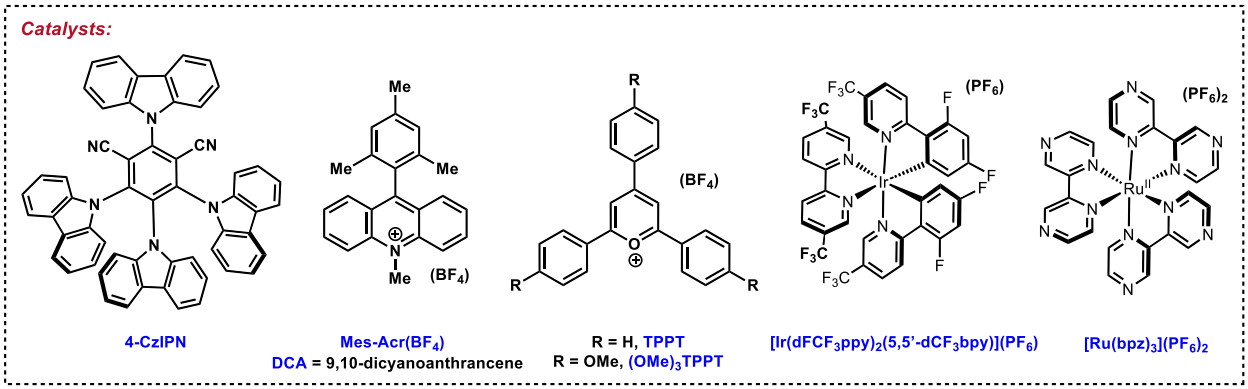

4.5. Scope of the Reaction

The current scope of the reaction is depicted in *Scheme 4.5.1*. Thus far, the scope is very limited. Aminocyclopropanes with aryl substitution were found to work well in the reaction (**4-72**, **4-77**). When trisubstituted aminocyclopropanes were tested, no reaction was observed (**4-83**, *Experimental Section 4.8.4*).

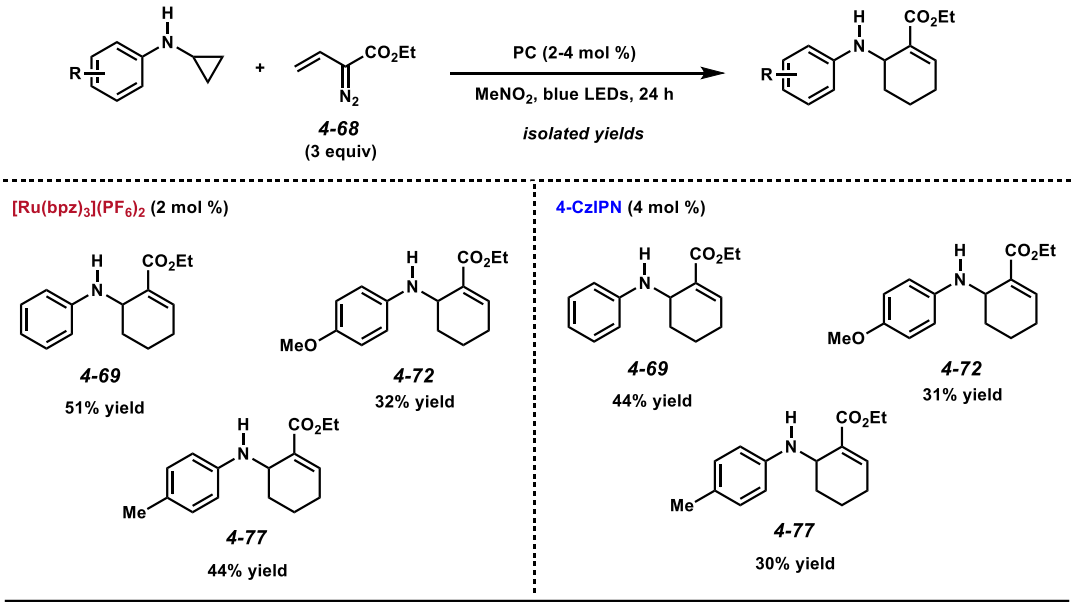

Scheme 4.5.1. Scope of the reaction. Reactions run on a 0.2 mmol scale in a Schlenk tube.

4.6. Proposed Catalytic Cycle

Based on previous reports,[4,16] we propose the catalytic cycle shown in *Scheme 4.6.1*. Both optimal photocatalysts (4-CzIPN or $[Ru(bpz)_3](PF_6)_2$) can be excited in the presence of visible light. The excited catalyst can oxidize cyclopropylamine **4-11** to generate reduced photocatalyst and radical cation **4-14**, which will rapidly ring-open to distonic radical cation **4-15**. This radical

cation can be intercepted by vinyl diazoacetate **4-68**, and after loss of N_2, afford radical cation intermediate **4-78**. This intermediate can undergo radical cyclization (*6-exo-trig*) to yield radical cation **4-79**. Upon SET from reduced photocatalyst, **4-69** is formed and the ground state photocatalyst is regenerated.

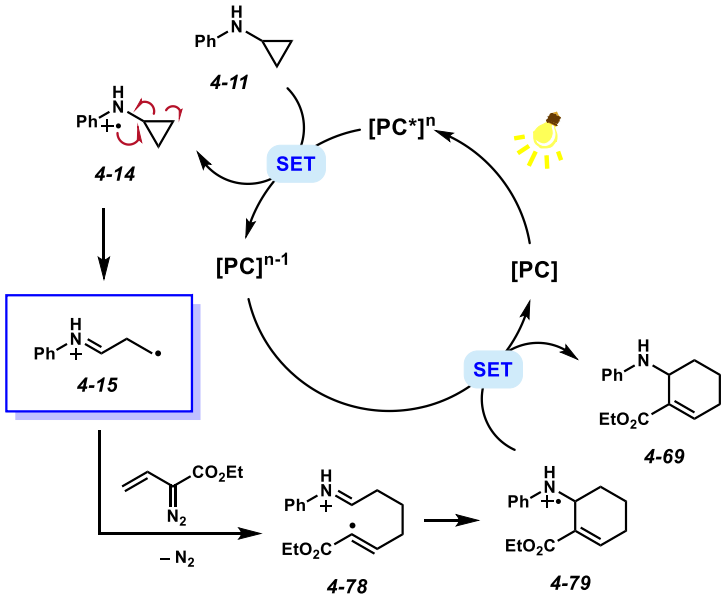

Scheme 4.6.1. Proposed catalytic cycle of novel (3 + 3) cycloaddition with photocatalyst.

4.7. Conclusion and Project Outlook

In this chapter, a novel (3 + 3) cycloaddition between aminocyclopropanes and vinyl diazoacetate has been described. This is accomplished through the formation of a highly reactive radical cation intermediate generated by visible light-mediated photooxidation of electron rich amines. Several photocatalysts can be successfully employed in this reaction including $[Ru(bpz)_3](PF_6)_2$, 4-CzIPN, and even our previously developed Cr catalyst, $[Cr(PMP_2phen)_3](BF_4)_3$, albeit in lower yields. This study is still in the early phases of exploration,

with several questions still unanswered. While proof-of-principle has been established, more optimization seems necessary. This reaction is acutely sensitive to the presence of oxygen, and while a few attempts to alleviate this issue have been made, further efforts to eliminate oxygen would be essential. McNeill and coworkers have tracked the rates of oxidation and ring opening of cyclopropylamines (*Figure 4.7.1*).[19] They found that an *o*-OMe substitution on the aryl group (**4-80**) significantly increased the rate of photooxidation but slowed the rate of ring-opening (*vide supra).* Conversely, *m*-Cl substitution on the aryl group (**4-81**) slowed the rate of photooxidation but increased the rate of ring-opening. While we have only probed methoxy substitution at the *para* position, perhaps substitution at the *ortho* position would be more stable to autoxidation. Substituent effects in our proposed reaction—on reactivity and diastereoselectivity—remain unexplored. This project would benefit greatly from these future studies where substituent effects are investigated on the aniline group (reactivity), the cyclopropyl group (diastereoselectivity), and the vinyldiazo species (reactivity and diastereoselectivity).

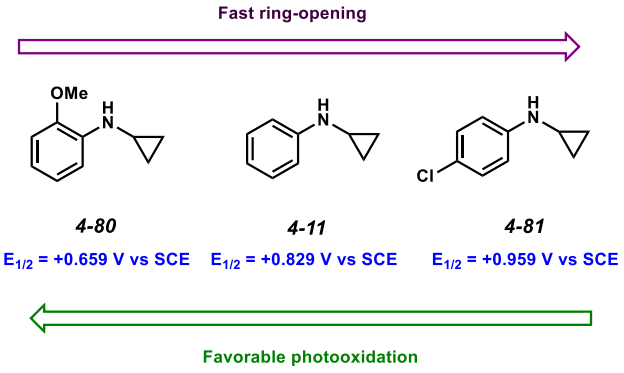

Figure 4.7.1. Substituent effects on cyclopropylamine reactivity.[19]

Other future directions within this project would be in further expanding the scope of Cr(III) photoredox catalysis. This study confirmed the Cr catalyst's ability to oxidize scaffolds (*N*-lone pairs) outside of what had previously been tested (electron-rich alkenes). The product generated from the specific substrate tested in this study was extremely sensitive to oxygen, something we have found to be beneficial in Cr catalytic cycles. In theory, this catalyst could be applicable to a similar scaffold that does not invoke oxygen sensitive intermediates. There is vast potential for future Cr photoredox catalytic systems in further catalyst and methodology development.

4.8. Experimental Section

4.8.1. Materials and Methods

$[Ru(bpz)_3](PF_6)_2$ was prepared according to the procedure by Yoon and coworkers.[21] $[Ru(bpz)_3](BAr^F)_2$ was prepared according to the procedure by Yoon and coworkers.[22] $[Cr(PMP_2phen)_3](BF_4)_3$ was prepared according to the procedure described in Chapter 2.[16b] 4-CzIPN was prepared according to the procedure reported by Kelly and coworkers.[23] Reactions were performed under argon atmosphere unless otherwise noted. Dichloromethane and toluene were purified by passing through activated alumina columns. Nitromethane (99%) and acetonitrile (99%) were used as received. Commercially available chemicals were purchased from Alfa Aesar (Ward Hill, MA), Sigma-Aldrich (St. Louis, MO), Oakwood Products, (West Columbia, SC), Strem (Newburport, MA), and TCI America (Portland, OR). Qualitative TLC analysis was performed on 250 mm thick, 60 Å, glass backed, F254 silica (SiliCycle, Quebec City, Canada). Visualization was accomplished with UV light and/or exposure to potassium bismuth iodide (Dragendorff's reagent), $KMnO_4$, or *p*-anisaldehyde stain solutions followed by heating. Flash chromatography was performed using SiliCycle silica gel (230-400 mesh). ^1H NMR spectra were acquired on either a Bruker AVANCE III HD NMR (at 400 MHz) or a Brucker AVANCE NEO NMR (at 900 MHz) and are reported relative to $SiMe_4$ (δ 0.00). ^{13}C NMR spectra were acquired on either a Bruker AVANCE III HD NMR (at 100 MHz) or a Brucker AVANCE NEO NMR (at 226 MHz) and are reported relative to $SiMe_4$ (δ 0.0). All IR spectra were obtained Thermo Nicolet iS10 spectrometer and are reported in wavenumbers (ν). High resolution mass spectrometry (HRMS) data were acquired via electrospray ionization (ESI) using a ThermoFisher Orbitrap Q-Exactive. Reactions under blue LED irradiation were performed using a 390 nm Kessil PR160L LED PhotoReaction light. Irradiation with visible light was performed with one 23 W compact

fluorescent light bulb (EcoSmart 23 W bright white CFL spiral bulb, 1600 lumens). Cycloadditions using all modes of irradiation were performed using flame-dried borosilicate vials or Schlenk tubes.

Note: Methods of degassing employed were: sparging with argon for an extended amount of time or freeze-pump-thaw. Cycloaddition reaction mixtures were degassed utilizing one of these methods before irradiation unless otherwise noted. Nitromethane was degassed via freeze-pump-thaw before use in cycloaddition reactions unless otherwise noted. Vinyl diazoacetate (**4**-**68**) was not degassed before use in cycloaddition reactions.

4.8.2. Optimization Experiments

Table 4.3.1 (recreated). Initial Probing of (3 + 2) Cycloaddition with Styrene.

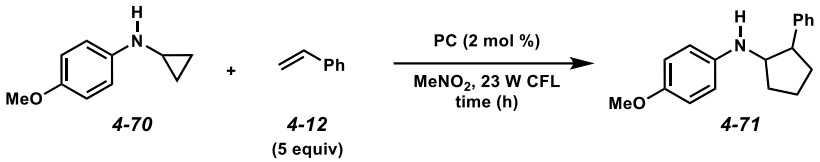

entry	PC	time (h)	conv (%)	yield (%) [a]
1	$[Ru(bpz)_3](PF_6)_2$	3	100	85
2	$[Cr(Ph_2phen)_3](BF_4)_3$	24	55	30
3	$[Cr(PMP_2phen)_3](BF_4)_3$	24	80	60

[a] dr = 1:1

General Procedure: To a flame-dried 1-dram borosilicate vial evacuated and backfilled with argon (3X) was added cyclopropylamine **4-70** (0.0919 mmol) and photocatalyst (0.00184 mmol). The reagents were suspended in CH_3NO_2 (0.919 mL). The reaction mixture was then sparged with argon for 5 minutes. Styrene (**4-12**, 0.460 mmol) was then added, the vial was capped, and the reaction mixture was irradiated with a 23 W CFL bulb while stirring. Once the reaction was determined to be complete by TLC monitoring, the solvent was removed by rotary evaporation. The crude residue was then dissolved in CH_2Cl_2 (~1 mL), and the solution was passed through a SiO_2 plug (0.5 x 3 cm), using CH_2Cl_2 as eluent (~8 mL). The filtrate was concentrated in vacuo, and the crude residue was analyzed by ^1H NMR using CH_2Br_2 as an internal standard.

Table 4.3.2 (recreated). Initial Probing of (3 + 3) Cycloaddition with Vinyl Diazoacetate.

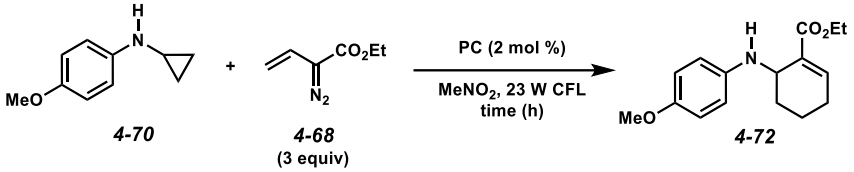

entry	PC	time (h)	conv (%)	yield (%)
1	$[Ru(bpz)_3](PF_6)_2$	20	62	41
2	$[Cr(Ph_2phen)_3](BF_4)_3$	20	20	15
3	$[Cr(PMP_2phen)_3](BF_4)_3$	20	78	37

General Procedure: To a flame-dried 1-dram borosilicate vial evacuated and backfilled with argon (3X) was added cyclopropylamine **4-70** (0.0919 mmol) and photocatalyst (0.00184 mmol). The reagents were suspended in CH_3NO_2 (0.919 mL). Vinyl diazoacetate **4-68** (0.276 mL, 1.0 M solution in CH_2Cl_2, 0.276 mmol) was then added, the vial was capped, and the reaction mixture was irradiated with a 23 W CFL bulb while stirring. At the 20 h timepoint, the solvent was removed by rotary evaporation. The crude residue was then dissolved in CH_2Cl_2 (~1 mL), and the solution was passed through a SiO_2 plug (0.5 x 3 cm), using CH_2Cl_2 as eluent (~8 mL). The filtrate was concentrated in vacuo, and the crude residue was analyzed by ^1H NMR using CH_2Br_2 as an internal standard.

Table 4.3.3 (recreated). Initial Probing of (3 + 3) Cycloaddition with Vinyl Diazoacetate.

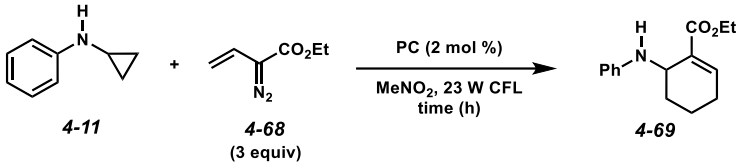

entry	PC	time (h)	conv (%)	yield (%)
1	$[Ru(bpz)_3](PF_6)_2$	20	100	33
2	$[Cr(Ph_2phen)_3](BF_4)_3$	20	50	0
3	$[Cr(PMP_2phen)_3](BF_4)_3$	20	100	36

General Procedure: To a flame-dried 1-dram borosilicate vial evacuated and backfilled with argon (3X) was added cyclopropylamine **4-11** (0.0751 mmol) and photocatalyst (0.00150 mmol). The reagents were suspended in CH_3NO_2 (0.751 mL). Vinyl diazoacetate **4-68** (0.225 mL, 1.0 M solution in CH_2Cl_2, 0.225 mmol) was then added, the vial was capped, and the reaction mixture was irradiated with a 23 W CFL bulb while stirring. At the 20 h timepoint, the solvent was removed by rotary evaporation. The crude residue was then dissolved in CH_2Cl_2 (~1 mL), and the solution was passed through a SiO_2 plug (0.5 x 3 cm), using CH_2Cl_2 as eluent (~8 mL). The filtrate was concentrated in vacuo, and the crude residue was analyzed by ^1H NMR using CH_2Br_2 as an internal standard.

Table 4.4.1 (recreated). [Cr(PMP$_2$phen)$_3$](BF$_4$)$_3$ Optimization.

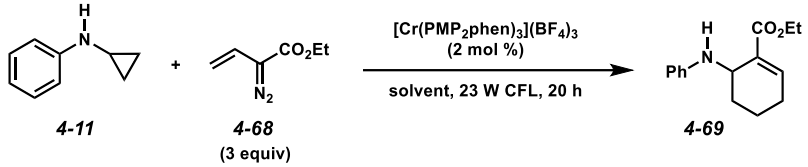

4-11 *4-68* (3 equiv) *4-69*

entry	solvent (M)	degas (Y/N)	conv (%)	yield (%)
1	$MeNO_2$ (0.05)	N	86	24
2	MeCN (0.1)	N	88	31
3	Acetone (0.1)	N	88	22
4 [a]	$MeNO_2$ (0.2)	N	100	0 [b]
5	$MeNO_2$ (0.2)	Y	30	23

[a] $NaHCO_3$ (1 equiv) added. [b] Cyclic peroxide major product.

General Procedure: To a flame-dried 1-dram borosilicate vial evacuated and backfilled with argon (3X) was added cyclopropylamine **4-11** (0.0751 mmol) and [Cr(PMP$_2$phen)$_3$](BF$_4$)$_3$ (0.00150 mmol). The reagents were suspended in CH_3NO_2 (0.751 mL). Vinyl diazoacetate **4-68** (0.225 mL, 1.0 M solution in CH_2Cl_2, 0.225 mmol) was then added, the vial was capped, and the reaction mixture was irradiated with a 23 W CFL bulb while stirring. At the 20 h timepoint, the solvent was removed by rotary evaporation. The crude residue was then dissolved in CH_2Cl_2 (~1 mL), and the solution was passed through a SiO_2 plug (0.5 x 3 cm), using CH_2Cl_2 as eluent (~8 mL). The filtrate was concentrated in vacuo, and the crude residue was analyzed by ^{1}H NMR using CH_2Br_2 as an internal standard.

Entry 1: Reagents suspended in 1.50 mL of CH_3NO_2.

*Entry 4: $NaHCO_3$ (0.0751 mmol) was added to the reaction before suspension in CH_3NO_2 (0.376 mL). Cyclic peroxide **4-73** was observed as the major product.*

Entry 5: CH_3NO_2 (0.376 mL), degassed via F-P-T, was used and the reaction mixture was sparged with argon before irradiation.

Table 4.8.1. Catalyst Optimization.

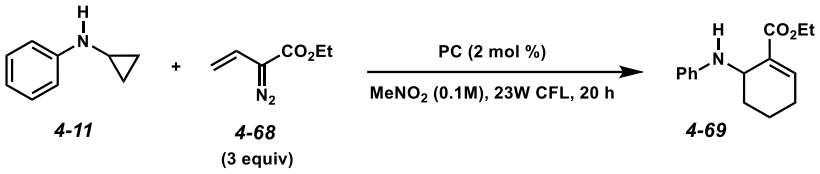

entry	photocatalyst	conv (%)	yield (%)
1	Mes-Acr(BF_4)	75	15
2	4-CzIPN	100	35
3	DCA	80	10
4	TPP(BF_4)	80	15
5	$(OMe)_3$TPP(BF_4)	92	30
6	[Ir(dFCF_3ppy)$_2$(5,5'-dCF_3bppy)](PF_6)	100	43

General Procedure: To a flame-dried 1-dram borosilicate vial evacuated and backfilled with argon (3X) was added cyclopropylamine **4-11** (0.0751 mmol) and photocatalyst (0.00150 mmol). The reagents were suspended in degassed (*via F-P-T*) CH_3NO_2 (0.751 mL). The reaction mixture was then sparged with argon for 5 minutes. Vinyl diazoacetate **4-68** (0.225 mL, 1.0 M solution in CH_2Cl_2, 0.225 mmol) was then added, the vial was capped, and the reaction mixture was irradiated with a 23 W CFL bulb while stirring. At the 20 h timepoint, the solvent was removed by rotary evaporation. The crude residue was then dissolved in CH_2Cl_2 (~1 mL), and the solution was passed through a SiO_2 plug (0.5 x 3 cm), using CH_2Cl_2 as eluent (~8 mL). The filtrate was concentrated in vacuo, and the crude residue was analyzed by ^1H NMR using CH_2Br_2 as an internal standard.

Table 4.8.2. Reaction Optimization.

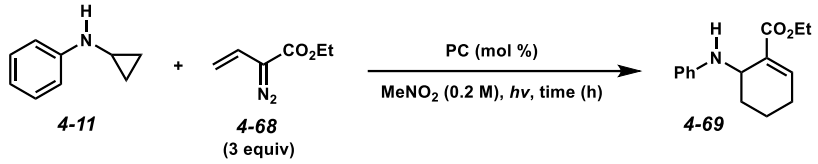

entry	PC (mol %)	*hv*	time (h)	conv (%)	yield(%)
1	4-CzIPN (2)	23 W CFL	3	100	24
2	$[Ir(dFCF_3ppy)_2(5,5'\text{-}dCF_3bppy)](PF_6)$ (2)	23 W CFL	6	90	47
3	4-CzIPN (2)	blue Kessil	2	100	48
4	$[Ir(dFCF_3ppy)_2(5,5'\text{-}dCF_3bppy)](PF_6)$ (2)	blue Kessil	2	90	47
5	$[Ru(bpz)_3](PF_6)_2$ (2)	blue Kessil	2	90	43
6	4-CzIPN (2)	blue Kessil	48	100	51
7	4-CzIPN (4)	blue Kessil	18	100	47
8	$[Ru(bpz)_3](PF_6)_2$ (2)	blue Kessil	24	100	53

General Procedure: To a flame-dried 1-dram borosilicate vial evacuated and backfilled with argon (3X) was added cyclopropylamine **4-11** (0.0751 mmol) and photocatalyst (0.00150 mmol). The reagents were suspended in degassed (*via F-P-T*) CH_3NO_2 (0.376 mL). The reaction mixture was then sparged with argon for 5 minutes. Vinyl diazoacetate **4-68** (0.225 mL, 1.0 M solution in CH_2Cl_2, 0.225 mmol) was then added, the vial was capped, and the reaction mixture was irradiated with a 23 W CFL bulb, or blue Kessil lamp, while stirring. At the timepoint indicated in the table, the solvent was removed by rotary evaporation. The crude residue was then dissolved in CH_2Cl_2 (~1 mL), and the solution was passed through a SiO_2 plug (0.5 x 3 cm), using CH_2Cl_2 as eluent (~8 mL). The filtrate was concentrated in vacuo, and the crude residue was analyzed by ^1H NMR using CH_2Br_2 as an internal standard.

Entry 7: Loading of photocatalyst (4-CzIPN) was changed (0.00300 mmol).

Table 4.8.3. Further Optimization Studies.

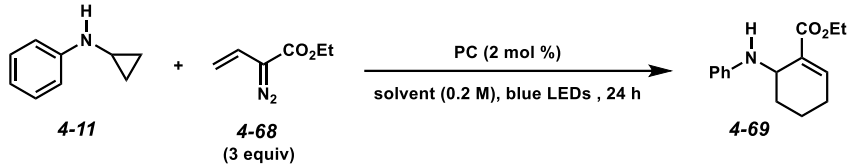

entry	PC	additive (equiv)	solvent	conv (%)	yield(%)
1	$[Ru(bpz)_3](PF_6)_2$	NaBArF (0.05)	$MeNO_2$	95	31
2	$[Ru(bpz)_3](PF_6)_2$	NaBArF (0.05)	CH_2Cl_2	99	40
3	$[Ru(bpz)_3](BArF)_2$	none	$MeNO_2$	100	42
4	$[Ru(bpz)_3](BArF)_2$	none	CH_2Cl_2	100	40
5 [a]	$[Ru(bpz)_3](BArF)_2$	$NaHCO_3$ (1)	$MeNO_2$	79	50
6	$[Ru(bpz)_3](PF_6)_2$	none	MeCN	83	39

[a] Reaction stopped at 3 h timepoint.

General Procedure: To a flame-dried 1-dram borosilicate vial evacuated and backfilled with argon (3X) was added cyclopropylamine **4-11** (0.0751 mmol) and photocatalyst (0.00150 mmol). The reagents were suspended in degassed solvent (*via F-P-T*) (0.376 mL). The reaction mixture was then sparged with argon for 5 minutes. Vinyl diazoacetate **4-68** (0.225 mL, 1.0 M solution in CH_2Cl_2, 0.225 mmol) was then added, the vial was capped, and the reaction mixture was irradiated with a blue Kessil lamp, while stirring. At the 24 h timepoint, the solvent was removed by rotary evaporation. The crude residue was then dissolved in CH_2Cl_2 (~1 mL), and the solution was passed through a SiO_2 plug (0.5 x 3 cm), using CH_2Cl_2 as eluent (~8 mL). The filtrate was concentrated in vacuo, and the crude residue was analyzed by ^1H NMR using CH_2Br_2 as an internal standard.

Entries 1-2: NaBArF (Sodium tetrakis[3,5-bis(trifluoromethyl)phenyl]borate, 0.00376 mmol) was added to the reaction mixture before sparging.

Entry 5: $NaHCO_3$ (0.0751 mmol) was added to the reaction mixture before sparging. The reaction was only irradiated for 3 h.

Addition of Acylation Agents:

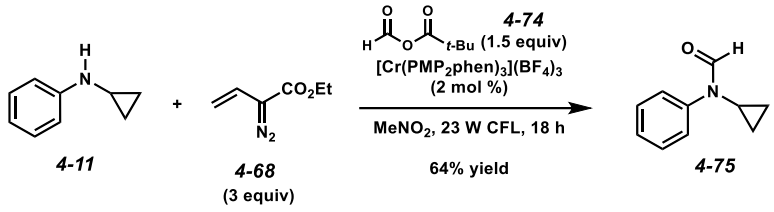

Cyclopropylamine 4-75: To a flame-dried 2-dram vial, evacuated and backfilled with argon (3X), was added cyclopropylamine **4-11** (18.2 mg, 0.137 mmol). The reagent was then suspended in degassed (*via F-P-T*) CH_3NO_2 (1.37 mL), and to this suspension was added trimethylacetic formic anhydride (**4-74**, 26.7 mg, 0.206 mmol), $[Cr(PMP_2phen)_3](BF_4)_3$ (4.1 mg, 0.00274 mmol), and vinyl diazoacetate **4-68** (0.411 mL, 1.0 M solution in CH_2Cl_2, 0.411 mmol). The reaction was then capped and irradiated for 18 h with a 23 W CFL bulb. After 18 h, the solvent was removed by rotary evaporation. The crude residue was then dissolved in CH_2Cl_2 (~1 mL), and the solution was passed through a SiO_2 plug (0.5 x 3 cm), using CH_2Cl_2 and EtOAc as eluent (~8 mL). The filtrate was concentrated in vacuo, and the crude residue was purified by silica gel flash chromatography (4:1 hexanes/EtOAc) to afford formylated cyclopropylamine **4-75** (14.4 mg, 65% yield, 2:1 mixture of rotamers) as a brown oil.

TLC R_f: 0.29 in 4:1 hexanes/EtOAc, visualized by UV.

^{1}H NMR (900 MHz, $CDCl_3$): δ 8.48 (s, 0.33H), 8.38 (s, 0.67H), 7.42 (d, *J* = 7.8 Hz, 0.67H), 7.83 (app. t, *J* = 7.4 Hz, 2H), 7.27-7.24 (m, 0.67H), 7.21 (app. t, *J* = 7.4 Hz, 0.33H), 7.16 (d, *J* = 7.8 Hz, 1.33H), 3.13-3.08 (m, 0.33H), 3.07-3.00 (m, 0.67H), 1.01-0.91 (comp. m, 2H), 0.78-0.68 (m, 0.67H), 0.62-0.53 (comp. m, 1.33H).

^{13}C NMR (226 MHz, $CDCl_3$): δ 164.5, 164.2, 141.1, 140.2, 129.3, 128.7, 126.3, 125.9, 123.8, 123.6, 30.5, 29.7, 27.4, 27.1.

IR (ATR, neat): 3013, 1691, 1678, 1596, 1493, 1344 cm^{-1}.

HRMS (ESI+): *m/z* calc'd for $(M + H)^+$ $[C_{10}H_{11}NO + H]^+$: 162.0913, found 162.0907.

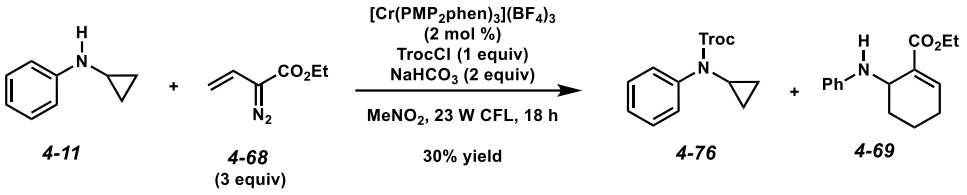

Cyclopropylamine 4-76: To a flame-dried 2-dram vial, evacuated and backfilled with argon (3X), was added cyclopropylamine **4-11** (11.3 mg, 0.0848 mmol). The reagent was then suspended in degassed (*via F-P-T*) CH_3NO_2 (0.848 mL), and to this suspension was added TrocCl (11.7 μL, 0.0848 mmol), $NaHCO_3$ (14.3 mg, 0.170 mmol), $[Cr(PMP_2phen)_3](BF_4)_3$ (2.5 mg, 0.00170 mmol), and vinyl diazoacetate **4-68** (0.254 mL, 1.0 M solution in CH_2Cl_2, 0.254 mmol). The reaction was then capped and irradiated for 18 h with a 23 W CFL bulb. After 18 h, the solvent was removed by rotary evaporation. The crude residue was then dissolved in CH_2Cl_2 (~1 mL), and the solution was passed through a SiO_2 plug (0.5 x 3 cm), using CH_2Cl_2 and EtOAc as eluent (~8 mL). The

filtrate was concentrated in vacuo, and the crude residue was purified by silica gel flash chromatography (9:1 hexanes/EtOAc) to afford a mixture of acylated cyclopropylamine **4-76** (mixture of rotamers) and cycloadduct **4-69** (7.9 mg, 30% yield) as a brown oil.

TLC R_f: 0.49 in 4:1 hexanes/EtOAc, visualized by UV.

4.8.3. Photocatalytic Cycloaddition Reactions

Note: Procedures for scaled-up reactions performed in a Schlenk tube.

General Procedure A:

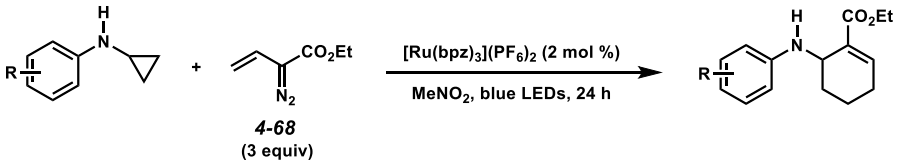

To a flame dried Schlenk tube, evacuated and backfilled with argon (3X), was added cyclopropylamine (1.0 equiv). The reagent was then suspended in degassed (*via F-P-T*) CH_3NO_2 (0.20 M), and to this suspension was added $[Ru(bpz)_3](PF_6)_2$ (2.0 mol %) and vinyl diazoacetate reagent (3.0 equiv, 1.0 M solution in CH_2Cl_2). The reaction mixture was then degassed by freeze-pump-thaw for three cycles. After degassing was complete, the reaction was placed under stagnant argon (by sealing the Schlenk tube after placing it back under argon) and irradiated for 24 h with blue LEDs. After 24 h, the solvent was removed by rotary evaporation. The crude residue was then dissolved in CH_2Cl_2 (~1 mL), and the solution was passed through a SiO_2 plug (0.5 x 3 cm), using CH_2Cl_2 and EtOAc as eluent (~8 mL). The filtrate was concentrated in vacuo, and the crude residue was purified by silica gel flash chromatography to afford pure amine cycloadduct.

General Procedure B:

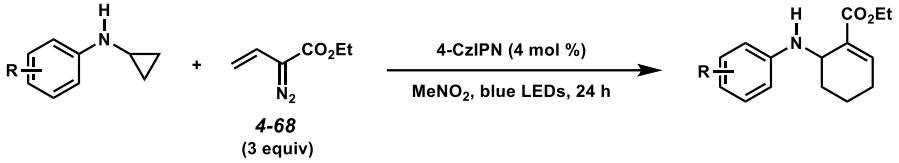

To a flame dried Schlenk tube, evacuated and backfilled with argon (3X), was added cyclopropylamine (1.0 equiv). The reagent was then suspended in degassed (*via F-P-T*) CH_3NO_2 (0.20 M), and to this suspension was added 4-CzIPN (4.0 mol %) and vinyl diazoacetate reagent (3.0 equiv, 1.0 M solution in CH_2Cl_2). The reaction mixture was then degassed by freeze-pump-thaw for three cycles. After degassing was complete, the reaction was placed under stagnant argon (by sealing the Schlenk tube after placing it back under argon) and irradiated for 24 h with blue LEDs. After 24 h, the solvent was removed by rotary evaporation. The crude residue was then dissolved in CH_2Cl_2 (~1 mL), and the solution was passed through a SiO_2 plug (0.5 x 3 cm), using CH_2Cl_2 and EtOAc as eluent (~8 mL). The filtrate was concentrated in vacuo, and the crude residue was purified by silica gel flash chromatography to afford pure amine cycloadduct.

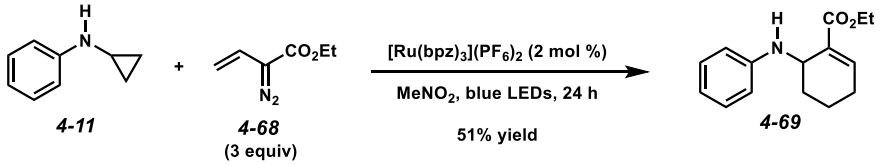

4-11 *4-68* (3 equiv) *4-69*

Cyclohexene Amine 4-69: To a flame dried Schlenk tube, evacuated and backfilled with argon (3X), was added cyclopropylamine **4-11** (0.200 mL, 1.0 M solution in CH_2Cl_2, 0.200 mmol). The reagent was then suspended in degassed (*via F-P-T*) CH_3NO_2 (1.00 mL), and to this suspension was added $[Ru(bpz)_3](PF_6)_2$ (3.5 mg, 0.00400 mmol) and vinyl diazoacetate **4-68** (0.600 mL, 1.0 M solution in CH_2Cl_2, 0.600 mmol). The reaction mixture was then degassed by freeze-pump-thaw for three cycles. After degassing was complete, the reaction was placed under stagnant argon (*vide supra*) and irradiated for 24 h with blue LEDs. After 24 h, the solvent was removed by rotary evaporation. The crude residue was then dissolved in CH_2Cl_2 (~1 mL), and the solution was passed through a SiO_2 plug (0.5 x 3 cm), using CH_2Cl_2 and EtOAc as eluent (~8 mL). The filtrate was concentrated in vacuo, and the crude residue was purified by silica gel flash chromatography (9:1 hexanes/EtOAc eluent) to afford amine **4-69** (24.8 mg, 51% yield) as a light-yellow solid.

TLC R_f: 0.42 in 4:1 hexanes/EtOAc, visualized by UV.

^{1}H NMR (900 MHz, $CDCl_3$): δ 7.16 (app. t, J = 7.6 Hz, 2H), 7.13-7.09 (m, 1H), 6.69 (app. t, J = 7.0 Hz, 1H), 6.66 (d, J = 8.0 Hz, 2H), 4.50-4.45 (br. m, 1H), 4.19-4.11 (comp. m, 2H), 3.62 (br. s, 1H), 2.32 (app. dt, J = 19.9, 5.0 Hz, 1H), 2.19-2.11 (m, 1H), 2.09-2.03 (m, 1H), 1.70-1.60 (comp. m, 2H), 1.50 (app. tt, J = 13.2, 3.8 Hz, 1H), 1.19 (t, J = 7.1 Hz, 3H).

^{13}C NMR (226 MHz, $CDCl_3$): δ 167.0, 147.4, 142.5, 131.8, 129.4, 117.5, 113.6, 60.6, 45.9, 27.2, 25.9, 16.4, 14.3.

IR (ATR, neat): 3389, 2937, 1710, 1599, 1501, 1242 cm^{-1}.

HRMS (ESI+): *m/z* calc'd for $(M + H)^+$ $[C_{15}H_{19}NO_2 + H]^+$: 246.1489, found 246.1480.

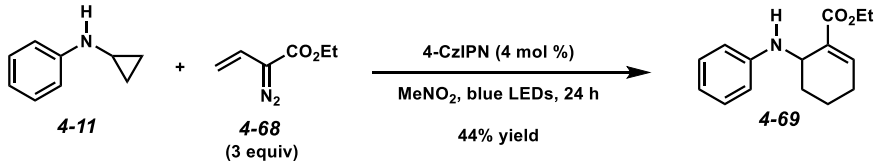

Cyclohexene Amine 4-69: To a flame dried Schlenk tube, evacuated and backfilled with argon (3X), was added cyclopropylamine **4-11** (0.200 mL, 1.0 M solution in CH_2Cl_2, 0.200 mmol). The reagent was then suspended in degassed (*via F-P-T*) CH_3NO_2 (1.00 mL), and to this suspension was added 4-CzIPN (6.3 mg, 0.00800 mmol) and vinyl diazoacetate **4-68** (0.600 mL, 1.0 M solution in CH_2Cl_2, 0.600 mmol). The reaction mixture was then degassed by freeze-pump-thaw for three cycles. After degassing was complete, the reaction was placed under stagnant argon (*vide supra*) and irradiated for 24 h with blue LEDs. After 24 h, the solvent was removed by rotary evaporation. The crude residue was then dissolved in CH_2Cl_2 (~1 mL), and the solution was passed through a SiO_2 plug (0.5 x 3 cm), using CH_2Cl_2 and EtOAc as eluent (~8 mL). The filtrate was concentrated in vacuo, and the crude residue was purified by silica gel flash chromatography (9:1 hexanes/EtOAc eluent) to afford amine **4-69** (21.6 mg, 44% yield) as a light-yellow solid.

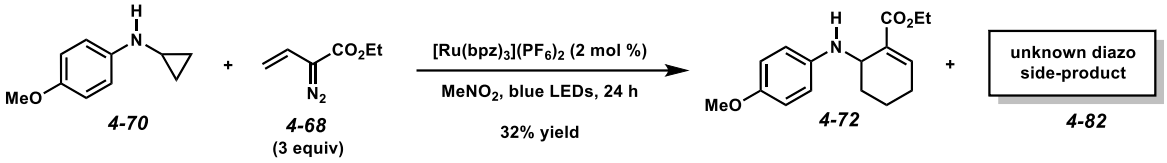

Cyclohexene Amine 4-72: To a flame dried Schlenk tube, evacuated and backfilled with argon (3X), was added cyclopropylamine **4-70** (0.200 mL, 1.0 M solution in CH_2Cl_2, 0.200 mmol). The reagent was then suspended in degassed (*via F-P-T*) CH_3NO_2 (1.00 mL), and to this suspension was added $[Ru(bpz)_3](PF_6)_2$ (3.5 mg, 0.00400 mmol) and vinyl diazoacetate **4-68** (0.600 mL, 1.0 M solution in CH_2Cl_2, 0.600 mmol). The reaction mixture was then degassed by freeze-pump-thaw for three cycles. After degassing was complete, the reaction was placed under stagnant argon (*vide supra*) and irradiated for 24 h with blue LEDs. After 24 h, the solvent was removed by rotary evaporation. The crude residue was then dissolved in CH_2Cl_2 (~1 mL), and the solution was passed through a SiO_2 plug (0.5 x 3 cm), using CH_2Cl_2 and EtOAc as eluent (~8 mL). The filtrate was concentrated in vacuo, and the crude residue was purified by silica gel flash chromatography (6:1 hexanes/EtOAc eluent) to afford an inseparable mixture of amine **4-72** and **4-82** (17.6 mg, 32% yield) as a yellow oil.

TLC R_f: 0.34 in 4:1 hexanes/EtOAc, visualized by UV.

^{1}H NMR (900 MHz, $CDCl_3$, **4-72**): δ 7.11-7.06 (m, 1H), 6.77 (d, J = 8.5 Hz, 2H), 6.65 (d, J = 8.5 Hz, 2H), 4.38-4.32 (br. m, 1H), 4.17-4.13 (comp. m, 2H), 3.74 (s, 3H), 3.36 (br. s, 1H), 2.34-2.77 (m, 1H), 2.17-2.10 (m, 1H), 2.06-1.99 (m, 1H), 1.69-1.58 (comp. m, 2H), 1.50-1.44 (m, 1H), 1.21 (t, J = 7.1 Hz, 2H).

^{1}H NMR (900 MHz, $CDCl_3$, **4-82**): δ 6.59 (app. d, *J* = 2.5 Hz, 1H), 4.94 (d, *J* = 18.2 Hz, 1H), 4.61 (dd, *J* = 18.2, 8.1 Hz, 1H), 4.24-4.18 (comp. m, 4H), 3.57 (app. d, *J* = 8.1 Hz, 1H), 3.50 (app. d, *J* = 20.0 Hz, 1H), 3.26 (app. dt, *J* = 20.0, 2.5 Hz, 1H), 1.29 (t, *J* = 7.2 Hz, 3H), 1.26 (t, *J* = 7.2 Hz, 1H).

^{13}C NMR (226 MHz, $CDCl_3$, *both **4-72** and **4-82***): δ 168.5, 167.1, 163.5, 152.4, 142.2, 141.7, 140.2, 135.5, 132.1, 115.4, 115.0, 103.6, 82.4, 62.3, 60.9, 60.6, 56.0, 47.2, 46.4, 39.4, 27.1, 25.9, 16.4, 14.4, 14.3, 14.2.

IR (ATR, neat): 2933, 1721, 1710, 1512, 1461, 1245 cm^{-1}.

HRMS (ESI+) **4-72**: *m/z* calc'd for $(M + H)^+$ $[C_{16}H_{21}NO_3 + H]^+$: 276.1594, found 276.1586.

HRMS (ESI+) **4-82**: *m/z* calc'd for $(M + Na)^+$ $[C_{12}H_{16}N_2O_4 + Na]^+$: 275.1002, found 275.0996.

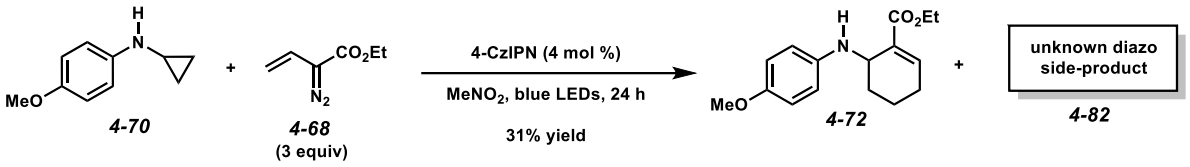

Cyclohexene Amine 4-72: To a flame dried Schlenk tube, evacuated and backfilled with argon (3X), was added cyclopropylamine **4-70** (0.200 mL, 1.0 M solution in CH_2Cl_2, 0.200 mmol). The reagent was then suspended in degassed (*via F-P-T*) CH_3NO_2 (1.00 mL), and to this suspension was added 4-CzIPN (6.3 mg, 0.00800 mmol) and vinyl diazoacetate **4-68** (0.600 mL, 1.0 M solution in CH_2Cl_2, 0.600 mmol). The reaction mixture was then degassed by freeze-pump-thaw for three cycles. After degassing was complete, the reaction was placed under stagnant argon (*vide supra*) and irradiated for 24 h with blue LEDs. After 24 h, the solvent was removed by rotary evaporation. The crude residue was then dissolved in CH_2Cl_2 (~1 mL), and the solution was passed through a SiO_2 plug (0.5 x 3 cm), using CH_2Cl_2 and EtOAc as eluent (~8 mL). The filtrate was concentrated in vacuo, and the crude residue was purified by silica gel flash chromatography (6:1 hexanes/EtOAc eluent) to afford an inseparable mixture of amine **4-72** and **4-82** (17.2 mg, 31% yield) as a yellow oil.

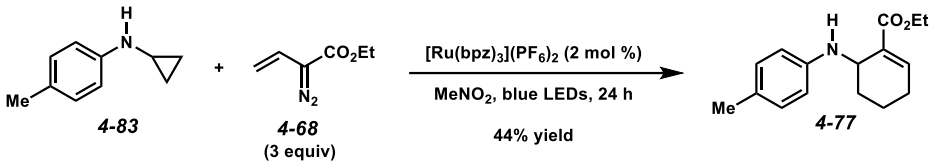

Cyclohexene Amine 4-77: To a flame dried Schlenk tube, evacuated and backfilled with argon (3X), was added cyclopropylamine **4-83** (30.8 mg, 0.209 mmol). The reagent was then suspended in degassed (*via F-P-T*) CH_3NO_2 (1.05 mL), and to this suspension was added $[Ru(bpz)_3](PF_6)_2$ (3.6 mg, 0.00418 mmol) and vinyl diazoacetate **4-68** (0.627 mL, 1.0 M solution in CH_2Cl_2, 0.627 mmol). The reaction mixture was then degassed by freeze-pump-thaw for three cycles. After degassing was complete, the reaction was placed under stagnant argon (*vide supra*) and irradiated for 24 h with blue LEDs. After 24 h, the solvent was removed by rotary evaporation. The crude residue was then dissolved in CH_2Cl_2 (~1 mL), and the solution was passed through a SiO_2 plug (0.5 x 3 cm), using CH_2Cl_2 and EtOAc as eluent (~8 mL). The filtrate was concentrated in vacuo, and the crude residue was purified by silica gel flash chromatography (9:1 hexanes/EtOAc eluent) to afford amine **4-77** (23.9 mg, 44% yield) as a light brown solid.

TLC R*f*: 0.53 in 4:1 hexanes/EtOAc, visualized by UV.

^{1}H NMR (900 MHz, $CDCl_3$): δ 7.12-7.07 (m, 1H), 6.97 (d, *J* = 8.1 Hz, 2H), 6.60 (d, *J* = 8.1 Hz, 2H), 4.48-4.39 (br. m, 1H), 4.20-4.12 (comp. m, 2H), 3.51 (br. s, 1H), 2.31 (app. dt, *J* = 19.8, 5.0 Hz, 1H), 2.23 (s, 3H), 2.17-2.10 (m, 1H), 2.07-2.03 (m, 1H), 1.68-1.58 (comp. m, 2H), 1.48 (app tt, *J* = 13.2, 3.8 Hz, 1H), 1.21 (t, *J* = 7.1 Hz, 3H).

^{13}C NMR (226 MHz, $CDCl_3$): δ 167.1, 145.1, 142.3, 132.0, 129.8, 126.7, 113.9, 60.6, 46.3, 27.0, 25.9, 20.5, 16.4, 14.3.

IR (ATR, neat): 3389, 2936, 1710, 1619, 1524, 1241 cm^{-1}.

HRMS (ESI+): *m/z* calc'd for $(M + H)^+$ $[C_{16}H_{21}NO_2 + H]^+$: 260.1645, found 260.1637.

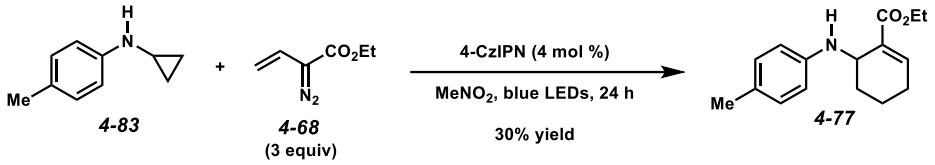

Cyclohexene Amine 4-77: To a flame dried Schlenk tube, evacuated and backfilled with argon (3X), was added cyclopropylamine **4-83** (31.3 mg, 0.213 mmol). The reagent was then suspended in degassed (*via F-P-T*) CH_3NO_2 (1.07 mL), and to this suspension was added 4-CzIPN (6.7 mg, 0.00852 mmol) and vinyl diazoacetate **4-68** (0.639 mL, 1.0 M solution in CH_2Cl_2, 0.639 mmol). The reaction mixture was then degassed by freeze-pump-thaw for three cycles. After degassing was complete, the reaction was placed under stagnant argon (*vide supra*) and irradiated for 24 h with blue LEDs. After 24 h, the solvent was removed by rotary evaporation. The crude residue was then dissolved in CH_2Cl_2 (~1 mL), and the solution was passed through a SiO_2 plug (0.5 x 3 cm), using CH_2Cl_2 and EtOAc as eluent (~8 mL). The filtrate was concentrated in vacuo, and the crude residue was purified by silica gel flash chromatography (9:1 hexanes/EtOAc eluent) to afford amine **4-77** (16.7 mg, 30% yield) as a light brown solid.

4.8.4. Unsuccessful Substrates

Tri-substituted Cyclopropylamine:

To a flame-dried 1-dram borosilicate vial evacuated and backfilled with argon (3X) was added cyclopropylamine **4-84** (8.5 mg, 0.0577 mmol) and $[Ru(bpz)_3](PF_6)_2$ (1.0 mg, 0.00115 mmol). The reagents were suspended in degassed (*via sparging with argon*) CH_3NO_2 (0.289 mL). The reaction mixture was then sparged with argon for 5 minutes. Vinyl diazoacetate **4-68** (0.173 mL, 1.0 M solution in CH_2Cl_2, 0.173 mmol) was then added, the vial was capped, and the reaction mixture was irradiated with a blue Kessil lamp, while stirring. At the 24 h timepoint, the solvent was removed by rotary evaporation. The crude residue was then dissolved in CH_2Cl_2 (~1 mL), and the solution was passed through a SiO_2 plug (0.5 x 3 cm), using CH_2Cl_2 as eluent (~8 mL). The filtrate was concentrated in vacuo, and the crude residue was analyzed by ^1H NMR using CH_2Br_2 as an internal standard. Amine **4-85** was not observed.

4.8.5. Product Stability

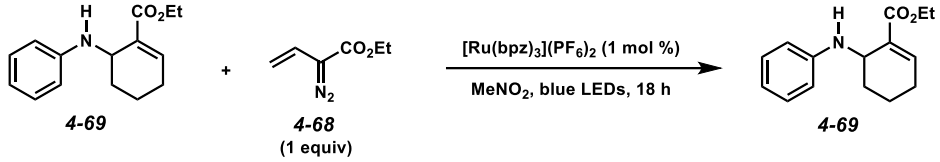

To a flame-dried 1-dram borosilicate vial evacuated and backfilled with argon (3X) was added amine **4-69** (11.5 mg, 0.0469 mmol) and $[Ru(bpz)_3](PF_6)_2$ (0.4 mg, 0.00047 mmol). The reagents were suspended in CH_3NO_2 (0.235 mL). The reaction mixture was then sparged with argon for 5 minutes. Vinyl diazoacetate **4-68** (0.0469 mL, 1.0 M solution in CH_2Cl_2, 0.0469 mmol) was then added, the vial was capped, and the reaction mixture was irradiated with a blue Kessil lamp, while stirring. At the 18 h timepoint, the solvent was removed by rotary evaporation. The crude residue was then dissolved in CH_2Cl_2 (~1 mL), and the solution was passed through a SiO_2 plug (0.5 x 3 cm), using CH_2Cl_2 as eluent (~8 mL). The filtrate was concentrated in vacuo, and the crude residue was analyzed by ^1H NMR using CH_2Br_2 as an internal standard. Minimal loss of material (97% yield of recovered **4-69**) was observed.

4.8.6. Starting Material Synthesis

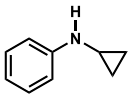

4-11

Aminocyclopropane 4-11. Prepared according to the procedure reported by Pflug and coworkers.[19] Spectroscopic data were consistent with a report by Wimalasena and coworkers.[5a]

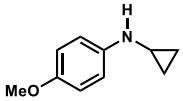

4-70

Aminocyclopropane 4-70. Prepared according to the procedure reported by Pflug and coworkers.[19] Spectroscopic data were consistent with a report by Kuang and coworkers.[24] This compound was found to be prone to rapid oxidation and was stored as a 1.0 M solution in CH_2Cl_2 at –20 °C.

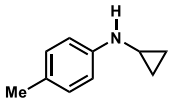

4-83

Aminocyclopropane 4-83. Prepared according to the procedure reported by Pflug and coworkers.[19] Spectroscopic data were consistent with a report by Kuang and coworkers.[24]

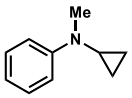

4-84

Aminocyclopropane 4-84. Prepared according to the procedure reported by Nguyen and coworkers.[7b]

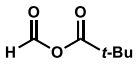

4-74

Trimethylacetic formic anhydride (4-74). Prepared according to the procedure reported by Vlietstra and coworkers.[25]

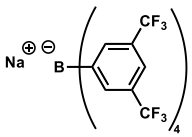

4-86

NaBArF (4-86). Prepared according to the procedure reported by Yakelis and Bergman.[26]

Diazocarbonyl Synthesis:

General Notes: After synthesizing, vinyl diazocarbonyl compounds were stored in a -20 °C freezer as a 1.0 M solution in CH_2Cl_2. Diazo compounds are toxic, irritants, and many compounds are explosive. Care should be taken when handling and synthesizing diazo compounds. For several of these compounds, the ^{13}C NMR signal for the CN_2 carbon atom was not observed; this phenomenon is common and is due to the long relaxation time due to the enhanced negative partial charge on this atom.[27]

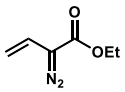

4-68

Diazoester 4-68. Prepared according to the procedure reported by Davies and coworkers.[28]

4.9. References and Notes

[1] For select reviews on distonic radical ions, see: (a) Yates, B. F.; Bouma, W. J.; Radom, L. *Tetrahedron* **1986**, *42*, 6225-6234. (b) Kenttämaa, H. I. *Org. Mass Spectrom*. **1994**, *29*, 1-10. (c) Williams, P. E.; Jankiewicz, B. J.; Yang, L.; Kenttämaa, H. I. *Chem. Rev.* **2013**, *113*, 6949-6985.

[2] Lee, J.; U, J. S.; Blackstock, S. C.; Cha, J. K. *J. Am. Chem. Soc.* **1997**, *119*, 10241-10242.

[3] Ha, J. D.; Lee, J.; Blackstock, S. C.; Cha, J. K. *J. Org. Chem.* **1998**, *63*, 8510-8514.

[4] Maity, S.; Zhu, M.; Shinabery, R. S.; Zheng, N. *Angew. Chem. Int. Ed*. **2012**, *51*, 222-226.

[5] (a) Wimalasena, K.; Wickman, H.; Mahindaratne, M. *Eur. J. Org. Chem*. **2001**, *2001*, 3811-3817. (b) Morris, S. A.; Wang, J.; Zheng, N. *Acc. Chem. Res.* **2016**, *49*, 1957-1968.

[6] Spellmeyer, D. C.; Houk, K. N. *J. Org. Chem.* **1987**, *52*, 959-974.

[7] (a) Nguyen, T. H.; Maity, S.; Zheng, N. *Beilstein J. Org. Chem.* **2014**, *10*, 975-980. (b) Nguyen, T. H.; Morris, S. A.; Zheng, N. *Adv. Synth. Catal.* **2014**, *356*, 2831-2837.

[8] Muriel, B.; Gagnebin, A.; Waser, J. *Chem. Sci*. **2019**, *10*, 10716-10722.

[9] White, D. H.; Noble, A.; Booker-Milburn, K. I.; Aggarwal, V. K. *Org. Lett.* **2021**, *23*, 3038-3042.

[10] Collins, J. L., III; Staveness, D.; Sowden, M. J.; Stephenson, C. R. J. *Org. Lett.* **2022**, *24*, 4344-4348.

[11] Uraguchi, D.; Kimura, Y.; Ueoka, F.; Ooi, T. *J. Am. Chem. Soc.* **2020**, *142*, 19462-19467.

[12] Yin, Y.; Li, Y.; Gonçalves, T. P.; Zhan, Q.; Wang, G.; Zhao, X.; Qiao, B.; Huang, K.-W.; Jiang, Z. *J. Am. Chem. Soc.* **2020**, *142*, 19451-19456.

[13] Mollari, L.; Valle-Amores, M. A.; Martínez-Gualda, A. M.; Marzo, L.; Fraile, A.; Aleman, J. *Chem. Commun*. **2022**, *58*, 1334-1337.

[14] For select reports on chiral rhodium and iridium photocatalysts, see: (a) Huang, X.; Quinn, T. R.; Harms, K.; Webster, R. D.; Zhang, L.; Wiest, O.; Meggers, E. *J. Am. Chem. Soc.* **2017**, *139*, 9120-9123. (b) Zhang, L.; Meggers, E. *Chem. Asian J.* **2017**, *12*, 2335-2342. (c) Jung, H.; Hong, M.; Marchini, M.; Villa, M.; Steinlandt, P. S.; Huang, X.; Hemming, M.; Meggers, E.; Ceroni, P.; Park, J.; Baik, M.-H. *Chem. Sci.* **2021**, *12*, 9673-9681. (d) Steinlandt, P. S.; Zhang, L.; Meggers, E. *Chem. Rev.* **2023**, *123*, 4764-4794.

[15] Dai, Y.; Huang, H.; Liang, S.; Yin, Y.; Ban, X.; Zhao, X.; Jiang, Z. *Org. Lett.* **2023**, *25*, 4551-4555.

[16] (a) Sarabia, F. J.; Li, Q.; Ferreira, E. M. *Angew. Chem. Int. Ed.* **2018**, *57*, 11015-11019. (b) Gall, B. K.; Smith, A. K.; Ferreira, E. M. *Angew. Chem. Int. Ed.* **2022**, *61*, e202212187.

[17] Pavitt, A. S.; Bylaskab, E. J.; Tratnyek, P. G. *Environ. Sci.: Processes Impacts* **2017**, *19*, 339-349.

[18] (a) Saxton, J. E. *In The Alkaloids*; Cordell, G. A., Ed.; Academic Press: New York, 1998; Vol. 51, pp 1-197. (b) Bunnage, M. E.; Ganesh, T.; Masesane, I. B.; Orton, D.; Steel, P. G. *Org. Lett.* **2003**, *5*, 239-242. (c) Shen, H. C.; Ding, F.-X.; Raghavan, S.; Deng, Q.; Luell, S.; Forrest, M. J.; Carballo-Jane, E.; Wilsie, L. C.; Krsmanovic, M. L.; Taggart, A. K.; Wu, K. K.; Wu, T.-J.; Cheng, K.; Ren, N.; Cai, T.-Q.; Chen, Q.; Wang, J.; Wolff, M. S.; Tong, X.; Holt, T. G.; Waters, M. G.; Hammond, M. L.; Tata, J. R.; Colletti, S. L. *J. Med. Chem*. **2010**, *53*, 2666-2670.

[19] Pflug, N. C.; Schmitt, M.; McNeill, K. *Environ. Sci. Technol*. **2019**, *53*, 4813-4822.

[20] (a) Stevenson, S. M.; Shores, M. P.; Ferreira, E. M. *Angew. Chem. Int. Ed.* **2015**, *54*, 6506-6510. (b) Higgins, R. F.; Fatur, S. M.; Shepard, S. G.; Stevenson, S. M.; Boston, D. J.; Ferreira, E. M.; Damrauer, N. H.; Rappé, A. K.; Shores, M. P. *J. Am. Chem. Soc*. **2016**, *138*, 5451-5464. (c) Stevenson, S. M.; Higgins, R. F.; Shores, M. P.; Ferreira, E. M. *Chem. Sci*. **2017**, *8*, 654-660. (d)

Higgins, R. F.; Fatur, S. M.; Damrauer, N. H.; Ferreira, E. M.; Rappé, A. K.; Shores, M. P. *ACS Catal*. **2018**, *8*, 9216-9225.

[21] Schultz, D. M.; Sawicki, J. W.; Yoon, T. P. *Beilstein J. Org. Chem.* **2015**, *11*, 61-65.

[22] Lies, S. D.; Lin, S.; Yoon, T. K. *Org. Synth*. **2016**, *93*, 178-199.

[23] Engle, S. M.; Kirkner, T. R.; Kelly, C. B. *Org. Synth.* **2019**, *96*, 455-473.

[24] Kuang, Y.; Ning, Y.; Zhu, J.; Wang, Y. *Org. Lett.* **2018**, *20*, 2693-2697.

[25] Vlietstra, E. J.; Zwikker, J. A.; Nolte, R. J. M.; Drenth, W. *Recl. Trav. Chim. Pays-Bas* **1982**, *101*, 460-462.

[26] Yakelis, N. A.; Bergman, R. G. *Organometallics* **2005**, *24*, 3579-3581.

[27] (a) Kappe, T.; Lang, G.; Pongratz, E. *J. Chem. Soc., Chem. Commun.* **1984**, 338-339. (b) Schmitz, A.; Kraatz, U.; Korte, F. *Heterocycles* **1978**, *10*, 199-205.

[28] (a) Davies, H. M. L.; Cantrell, W. R., Jr.; Romines, K. R.; Baum, J. S. *Org. Synth.* **1992**, *70*, 93. (b) Davies, H. M. L.; Houghland, P. W.; Cantrell, W. R., Jr. *Synth. Commun*. **1992**, *22*, 971-978. (c) Jadhav, A. M.; Pagar, V. V.; Liu, R.-S. *Angew. Chem. Int. Ed*. **2012**, *51*, 11809-11813.

APPENDICES

APPENDIX A

NMR SPECTRA RELEVANT TO CHAPTER 2

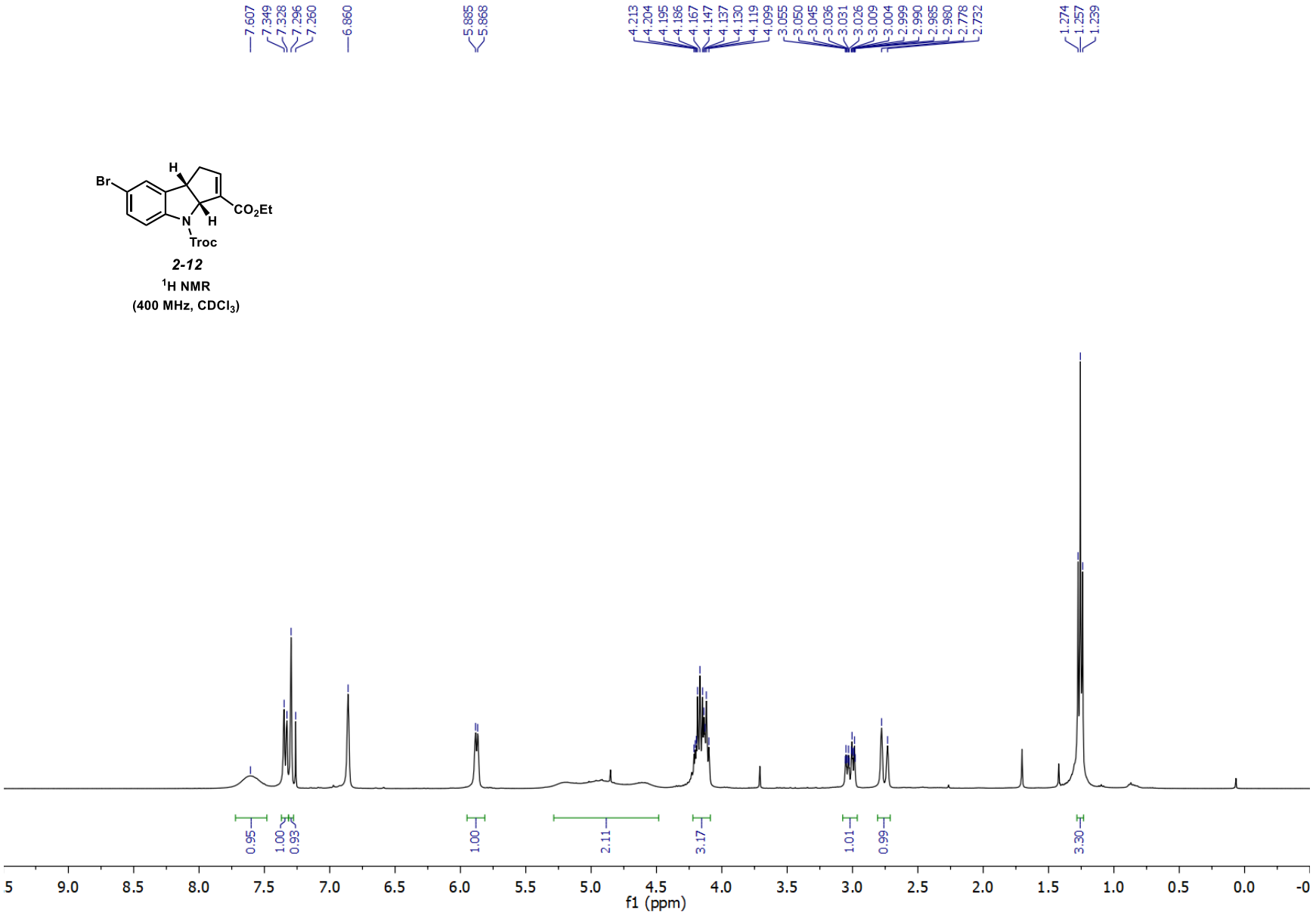
7.607
7.349
7.328
7.296
7.260
6.860
5.885
5.868
4.213
4.204
4.195
4.186
4.167
4.147
4.137
4.130
4.119
4.099
3.055
3.050
3.045
3.036
3.031
3.026
3.009
3.004
2.999
2.990
2.985
2.980
2.778
2.732
1.274
1.257
1.239
Br
H
CO2Et
N
H
Troc
2-12
1H NMR
(400 MHz, CDCl3)
0.95
1.00
0.93
1.00
2.11
3.17
1.01
0.99
3.30
f1 (ppm)

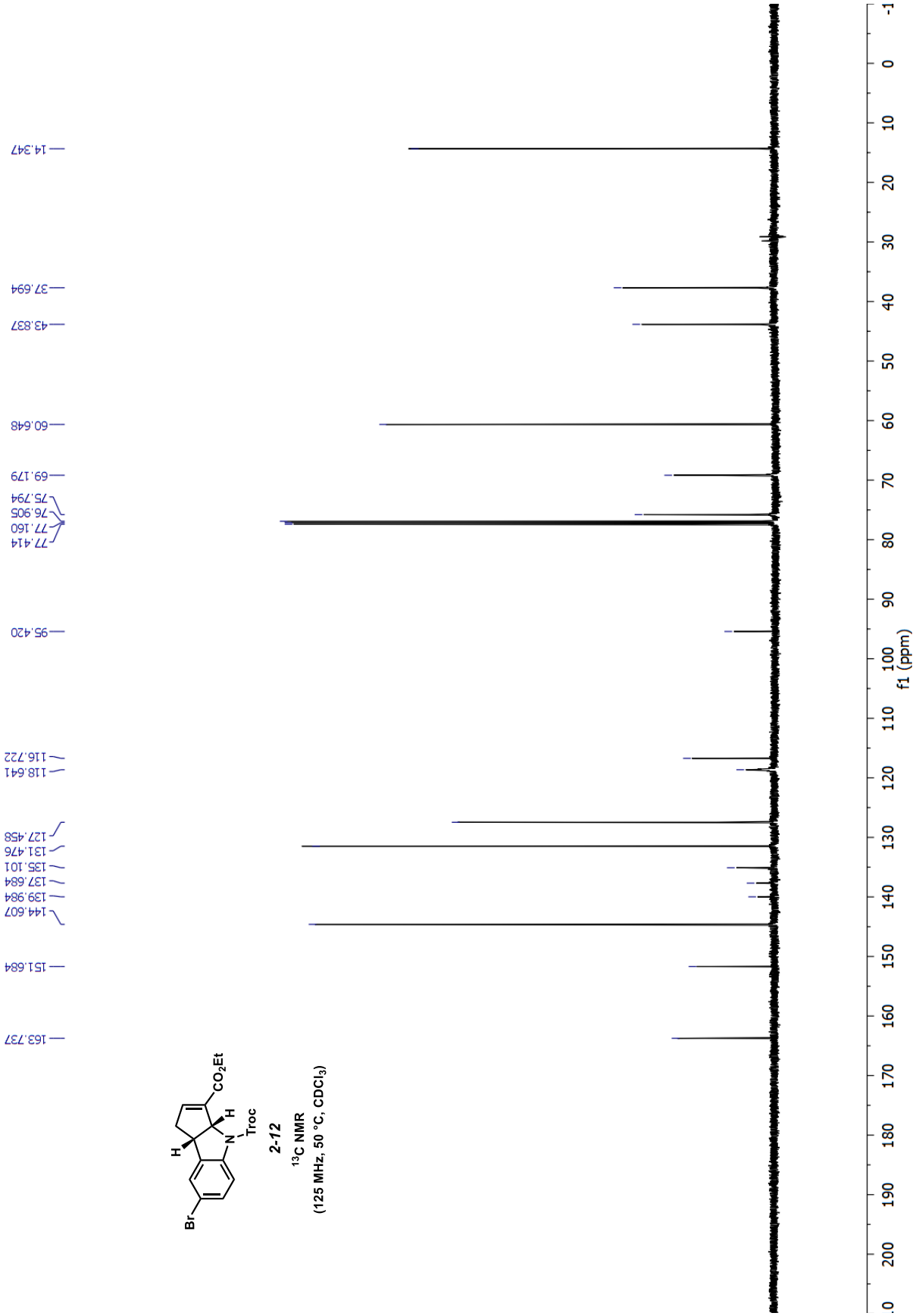
14.347
37.694
43.837
60.648
69.179
75.794
76.905
77.160
77.414
95.420
116.722
118.641
127.458
131.476
135.101
137.684
139.984
144.607
151.684
163.737
f1 (ppm)
2-12
13C NMR
(125 MHz, 50 °C, CDCl3)
CO2Et
H
N
Troc
H
Br

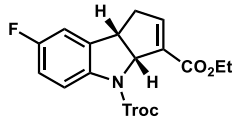

2-13

^{1}H NMR

(400 MHz, $CDCl_3$)

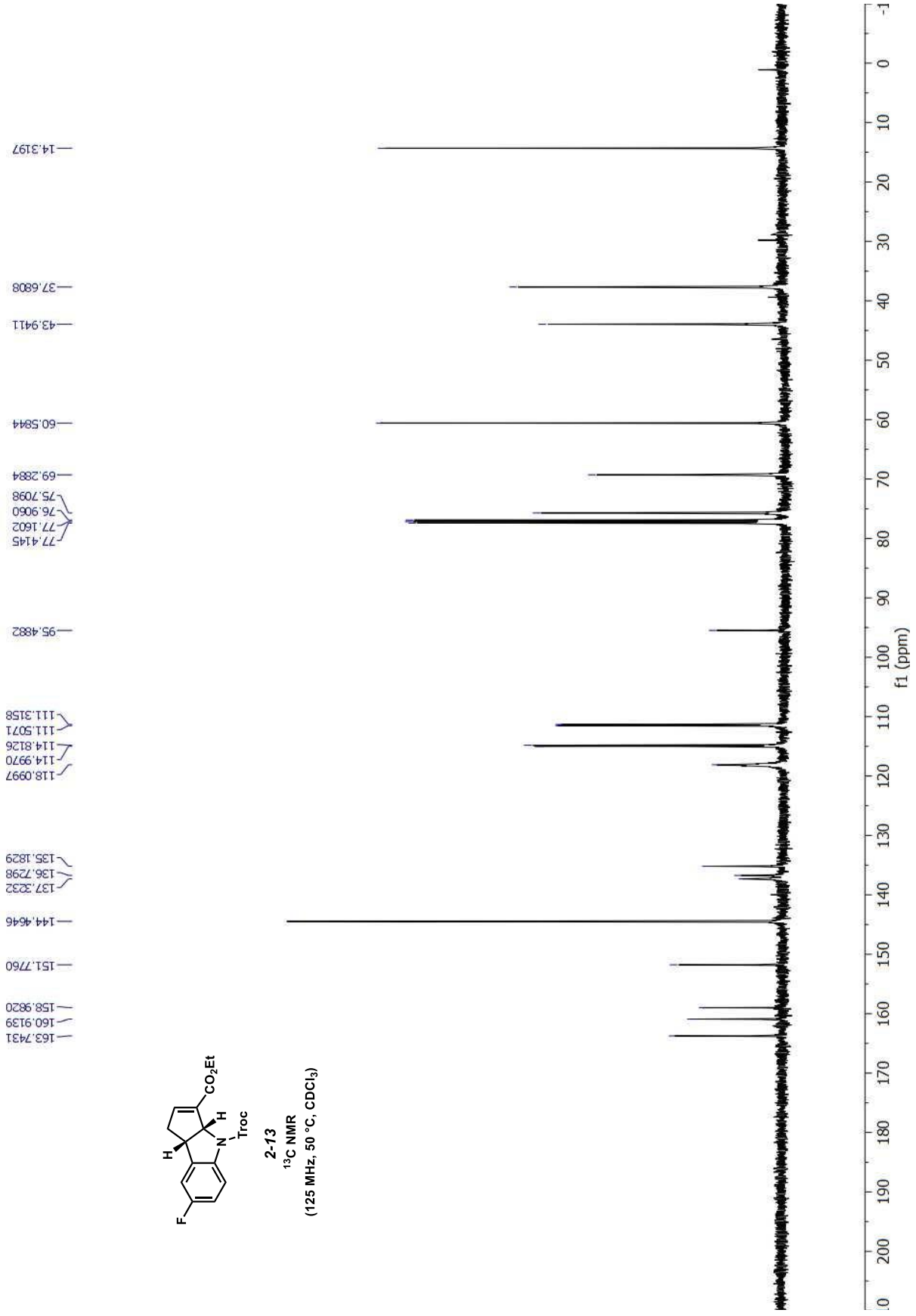
14.3197
37.6808
43.9411
60.5844
69.2884
75.7098
76.9060
77.1602
77.4145
95.4882
111.3158
111.5071
114.8126
114.9970
118.0997
135.1829
136.7298
137.3232
144.4646
151.7760
158.9820
160.9139
163.7431
CO2Et
H
H
N
Troc
F
2-13
13C NMR
(125 MHz, 50 °C, CDCl3)
f1 (ppm)

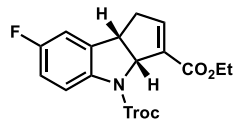

2-13

^{19}F NMR

(376 MHz, $CDCl_3$

C_6H_5F present as reference)

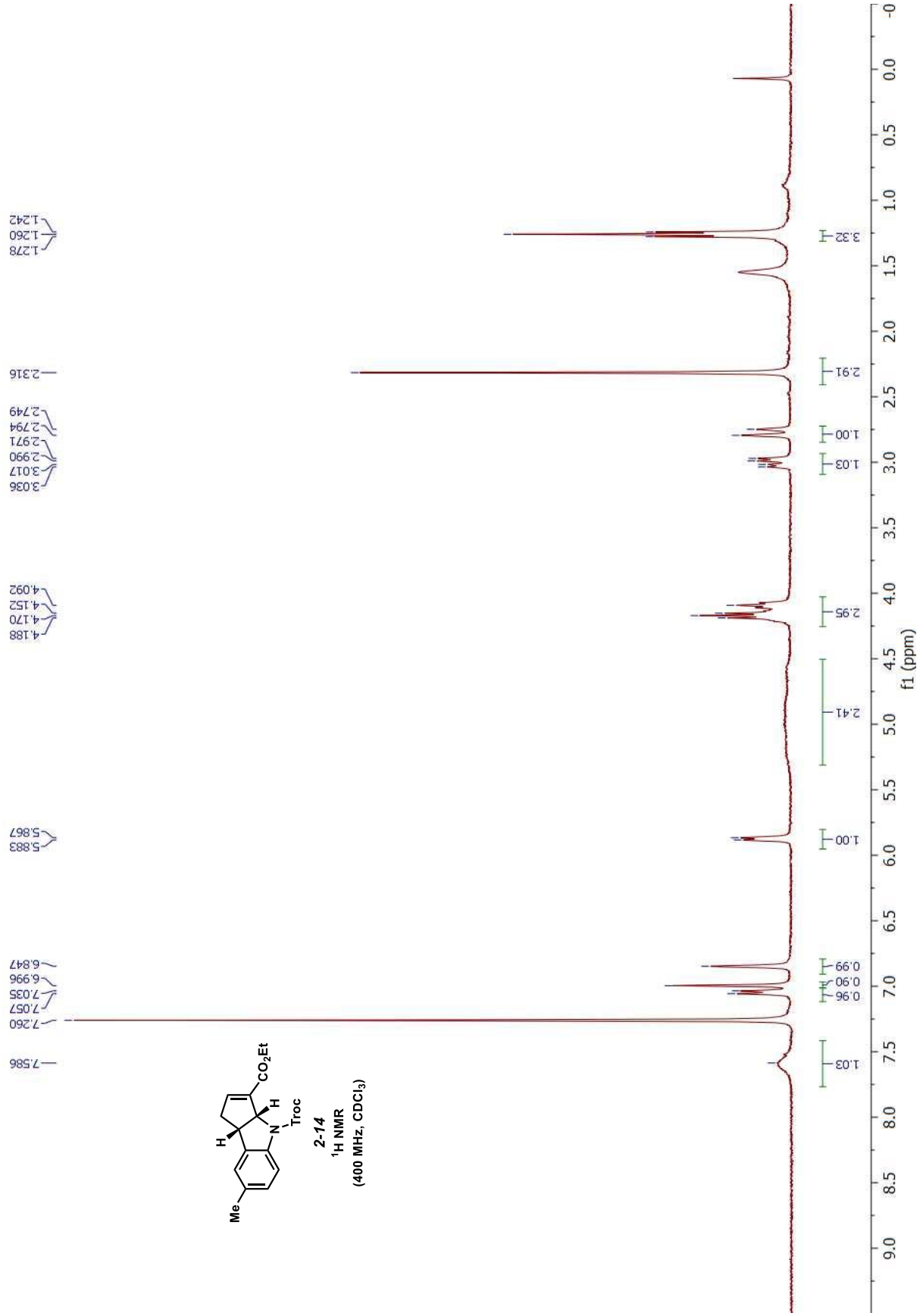
7.586
7.260
7.057
7.035
6.996
6.847
5.883
5.867
4.188
4.170
4.152
4.092
3.036
3.017
2.990
2.971
2.794
2.749
2.316
1.278
1.260
1.242
1.03
0.99
0.90
0.96
1.00
2.41
2.95
1.03
1.00
2.91
3.32
f1 (ppm)
CO2Et
H
N
Troc
H
Me
2-14
1H NMR
(400 MHz, CDCl3)

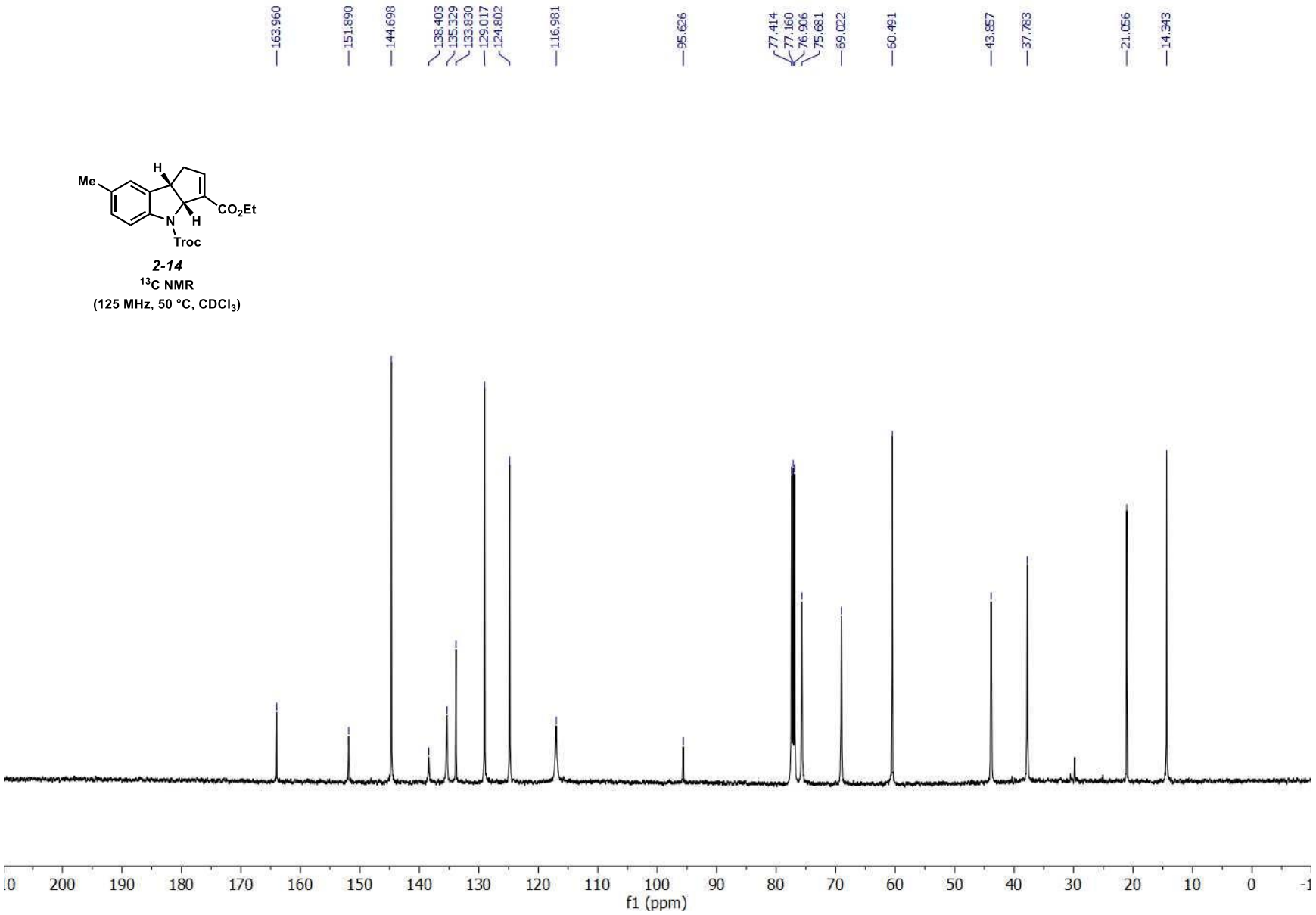
163.960
151.890
144.698
138.403
135.329
133.830
129.017
124.802
116.981
95.626
77.414
77.160
76.906
75.681
69.022
60.491
43.857
37.783
21.056
14.343
Me
H
CO2Et
N
H
Troc
2-14
13C NMR
(125 MHz, 50 °C, CDCl3)
f1 (ppm)

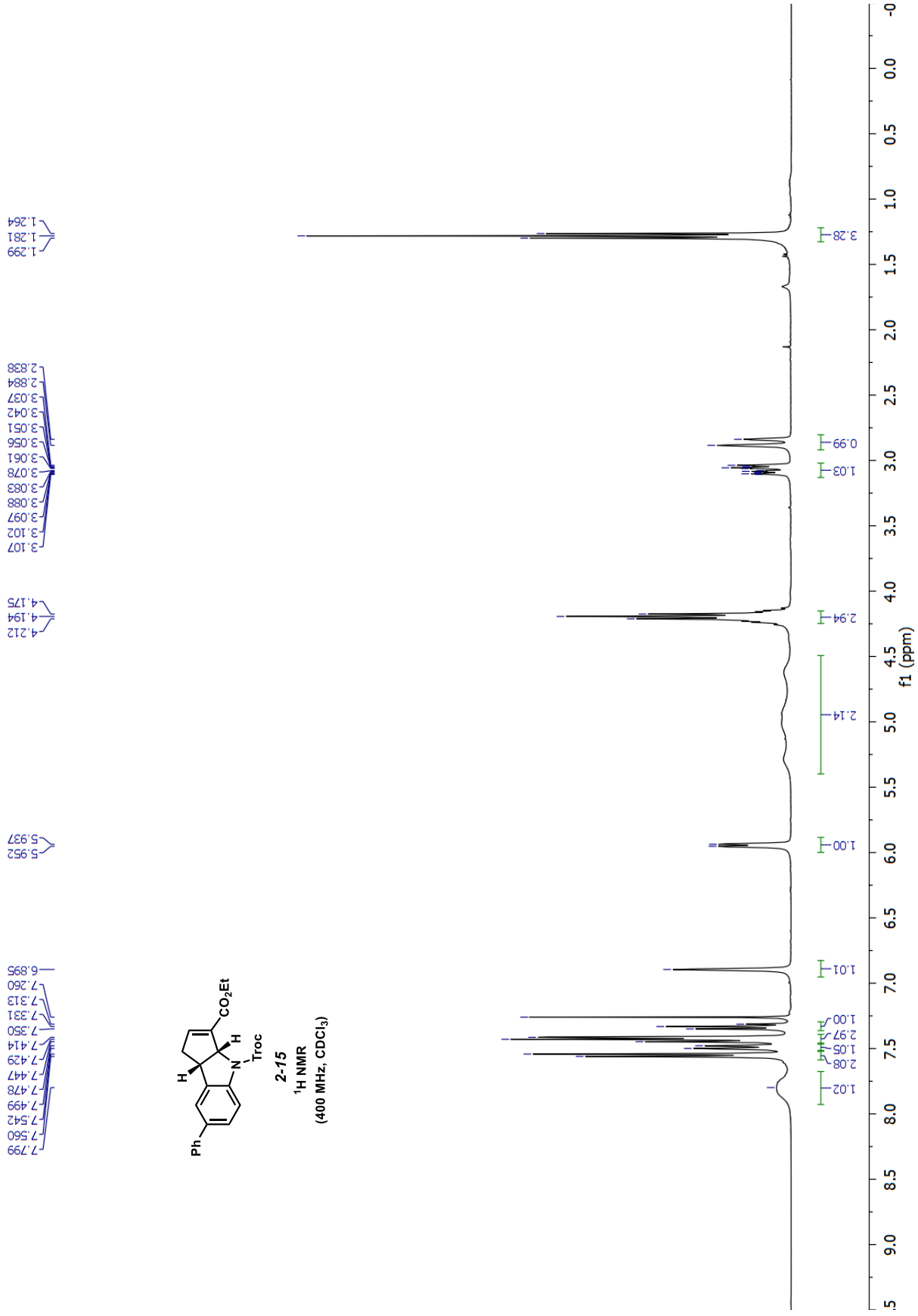
7.799
7.560
7.542
7.499
7.478
7.447
7.429
7.414
7.350
7.331
7.313
7.260
6.895
5.952
5.937
4.212
4.194
4.175
3.107
3.102
3.097
3.088
3.083
3.078
3.061
3.056
3.051
3.042
3.037
2.884
2.838
1.299
1.281
1.264
CO2Et
H
N
Troc
H
Ph
2-15
1H NMR
(400 MHz, CDCl3)
1.02
2.08
1.05
2.97
1.00
1.01
1.00
2.14
2.94
1.03
0.99
3.28
f1 (ppm)

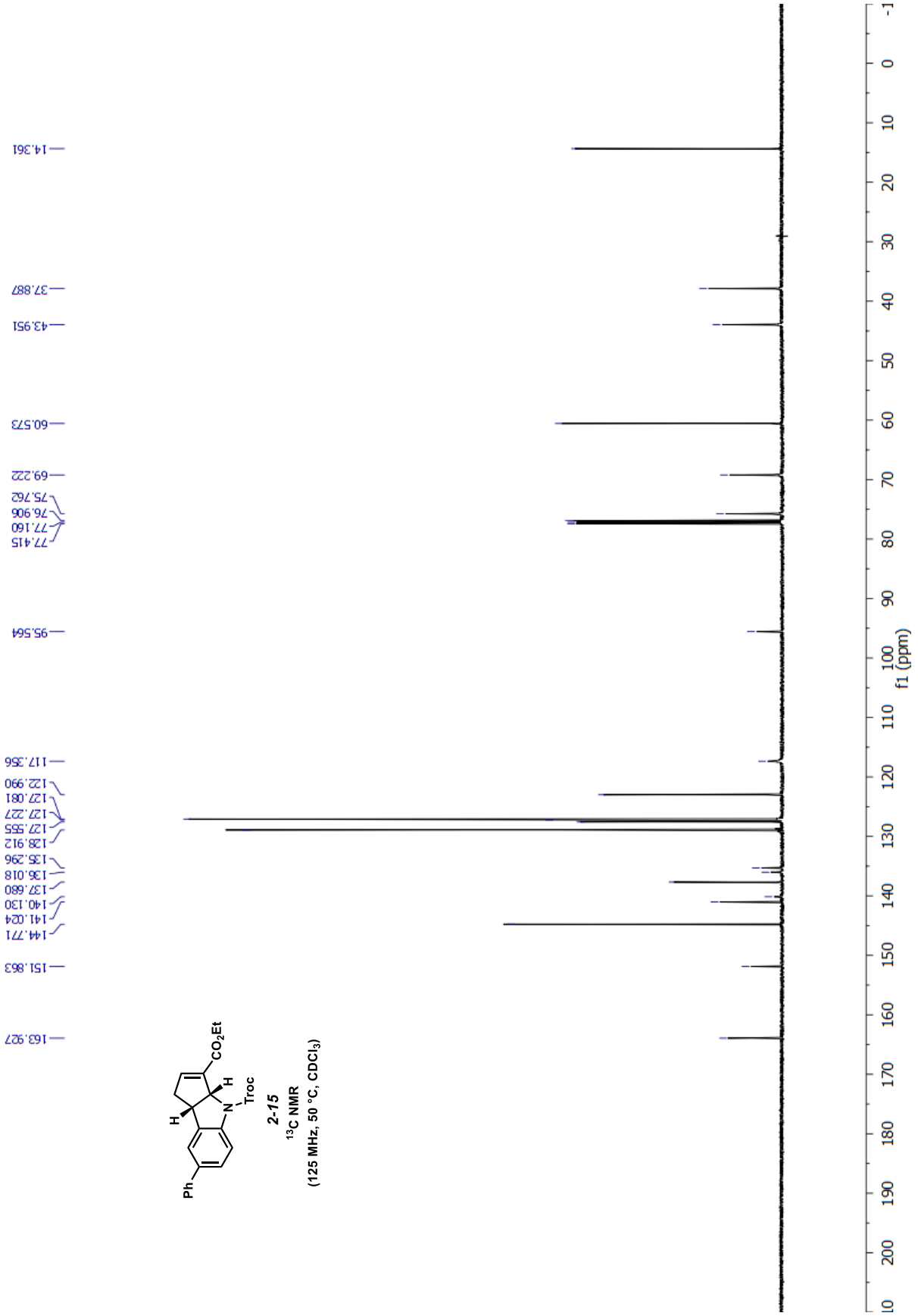
14.361
37.887
43.951
60.573
69.222
75.762
76.906
77.160
77.415
95.564
117.356
122.990
127.081
127.227
127.555
128.912
135.296
136.018
137.680
140.130
141.024
144.771
151.863
163.927
CO2Et
H
N
Troc
H
Ph
2-15
13C NMR
(125 MHz, 50 °C, CDCl3)
f1 (ppm)

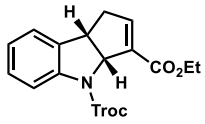

2-16

^{1}H NMR

(400 MHz, $CDCl_3$)

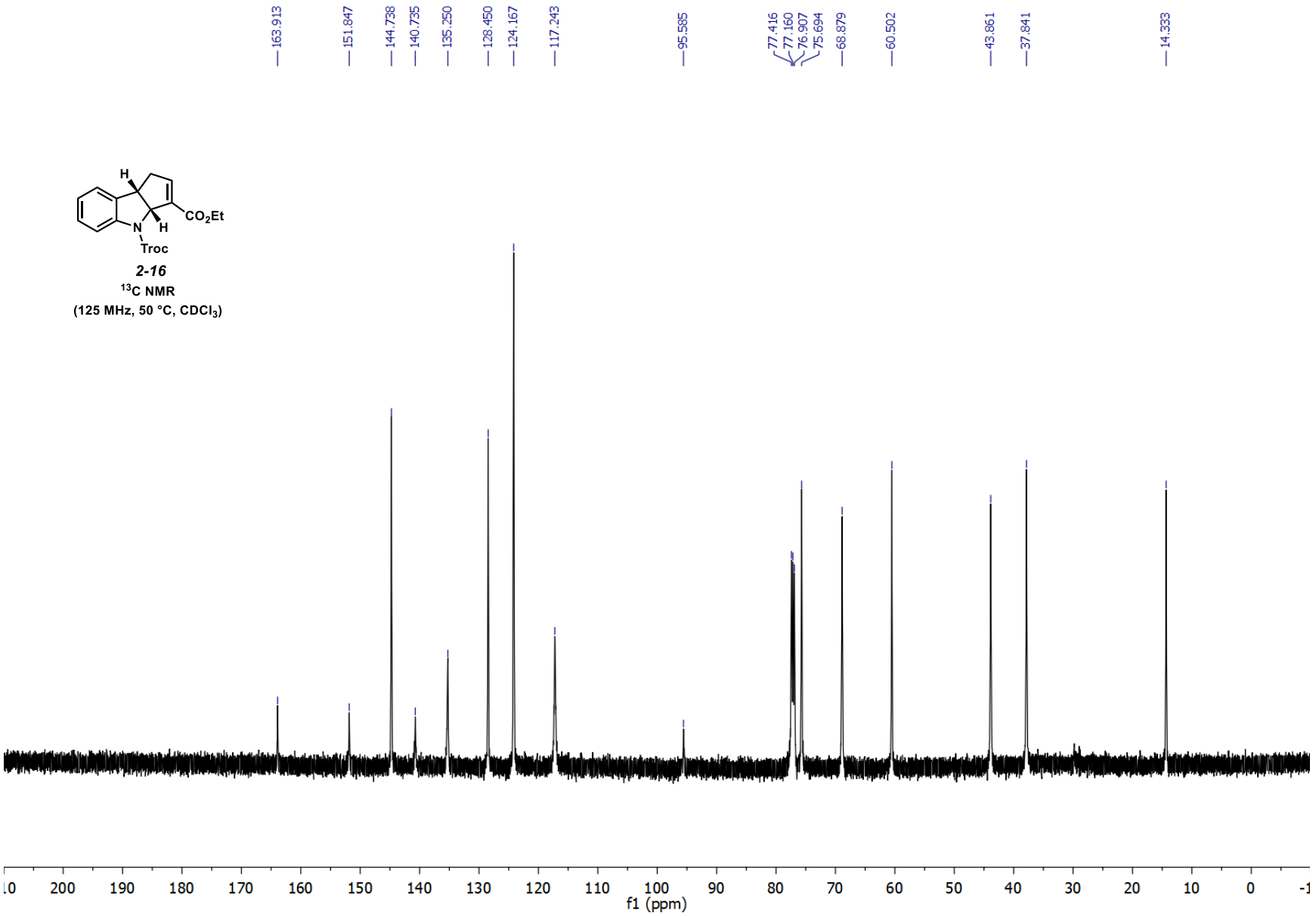
163.913
151.847
144.738
140.735
135.250
128.450
124.167
117.243
95.585
77.416
77.160
76.907
75.694
68.879
60.502
43.861
37.841
14.333
H
CO2Et
N
H
Troc
2-16
13C NMR
(125 MHz, 50 °C, CDCl3)
f1 (ppm)

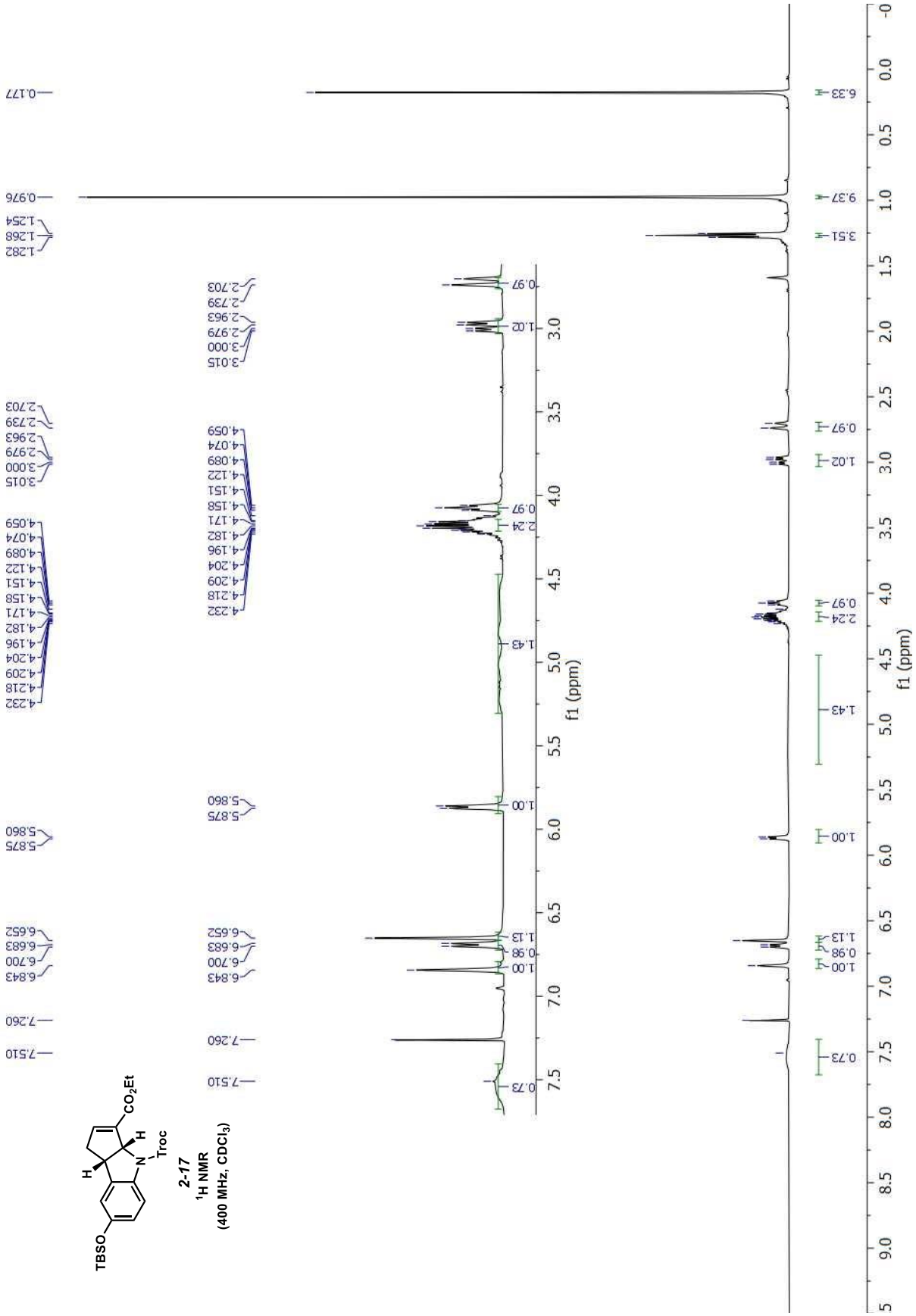
2-17
^{1}H NMR
(400 MHz, CDCl$_3$)
TBSO
Troc
CO$_2$Et
f1 (ppm)

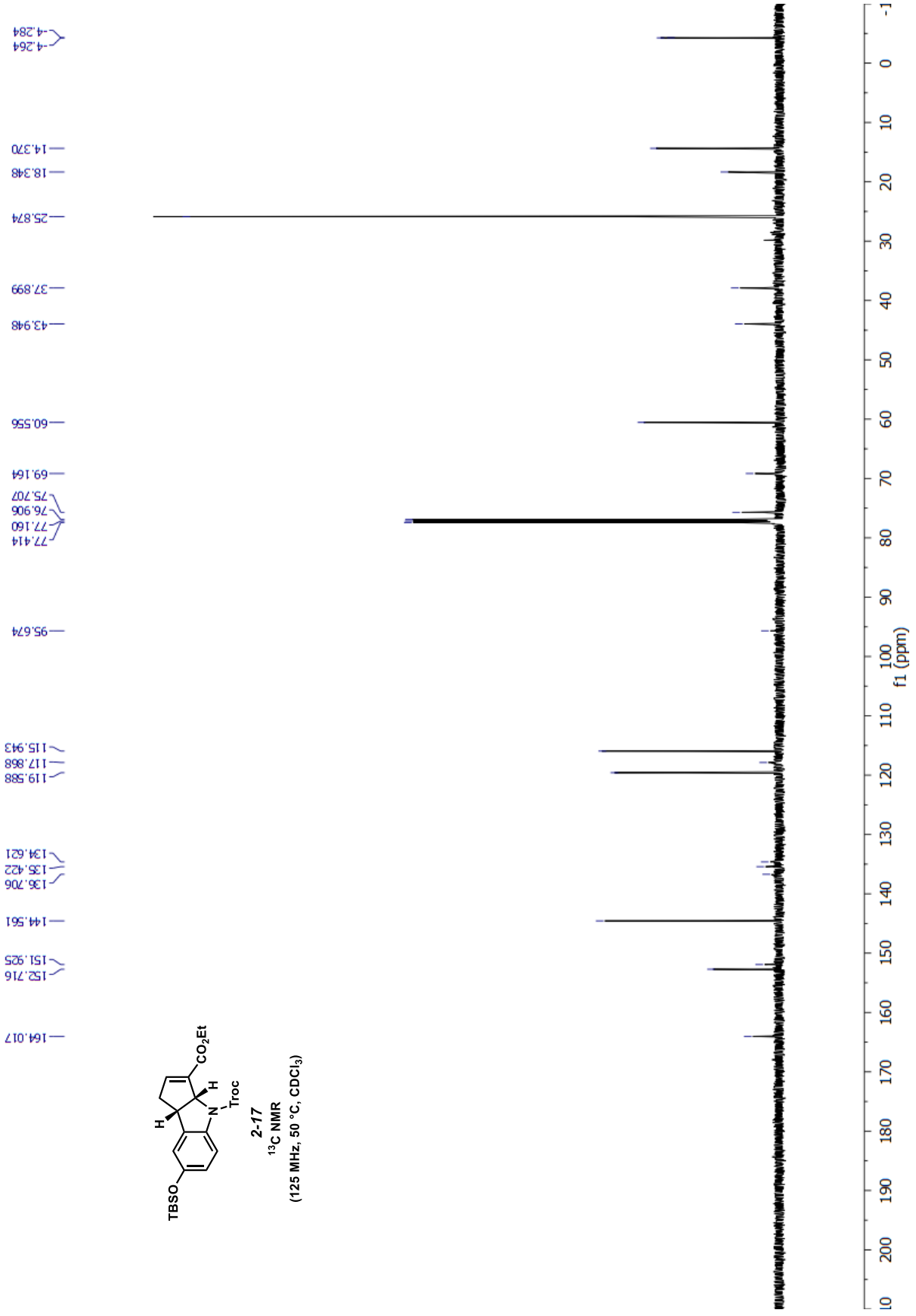
-4.284
-4.264
14.370
18.348
25.874
37.899
43.948
60.556
69.164
75.707
76.906
77.160
77.414
95.674
115.943
117.868
119.588
134.621
135.422
136.706
144.561
151.925
152.716
164.017
TBSO
H
N
H
Troc
CO2Et
2-17
13C NMR
(125 MHz, 50 °C, CDCl3)
f1 (ppm)

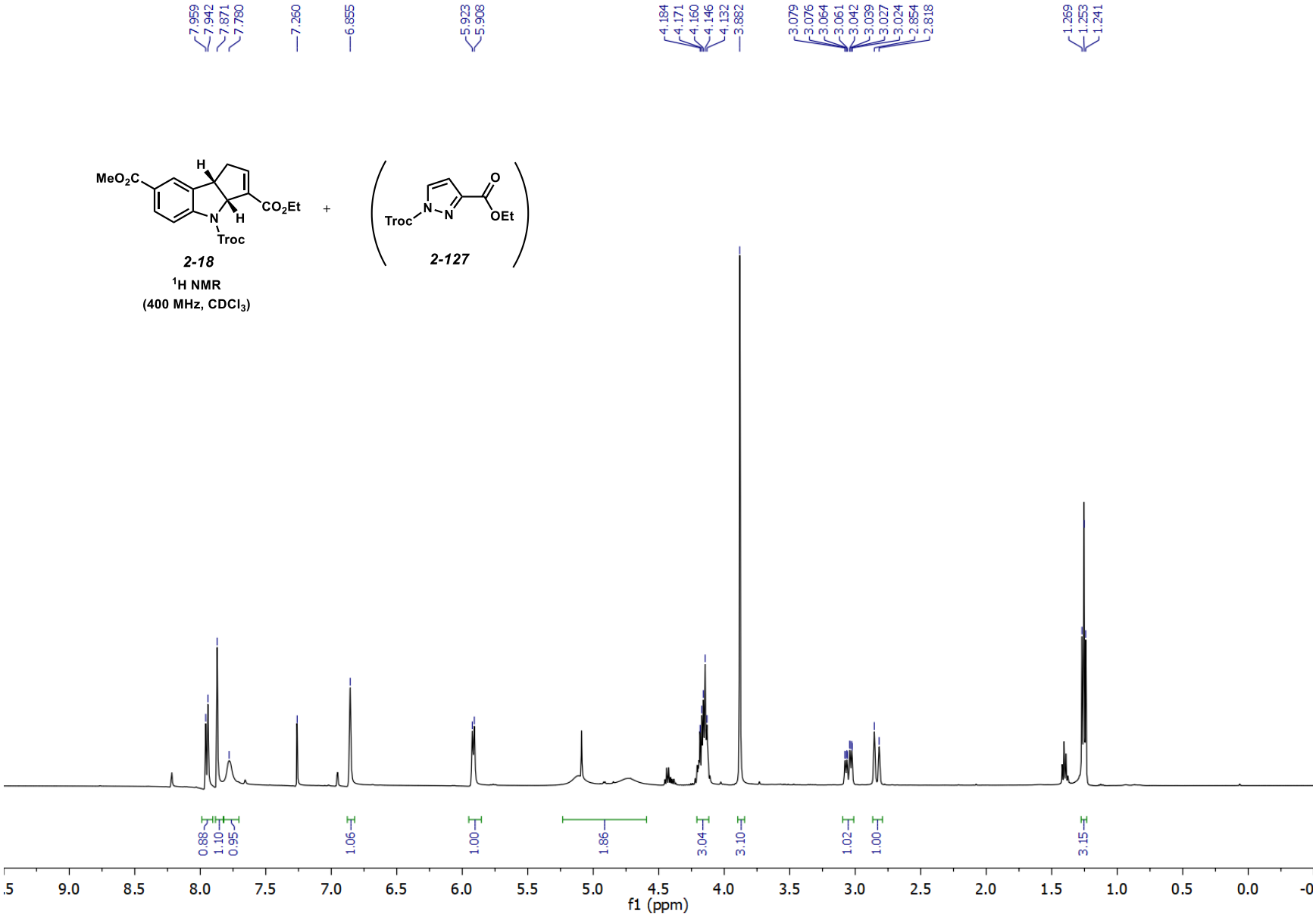
7.959
7.942
7.871
7.780
7.260
6.855
5.923
5.908
4.184
4.171
4.160
4.146
4.132
3.882
3.079
3.076
3.064
3.061
3.042
3.039
3.027
3.024
2.854
2.818
1.269
1.253
1.241
MeO2C
H
CO2Et
N
H
Troc
2-18
+
Troc
N
N
O
OEt
2-127
1H NMR
(400 MHz, CDCl3)
0.88
1.10
0.95
1.06
1.00
1.86
3.04
3.10
1.02
1.00
3.15
f1 (ppm)

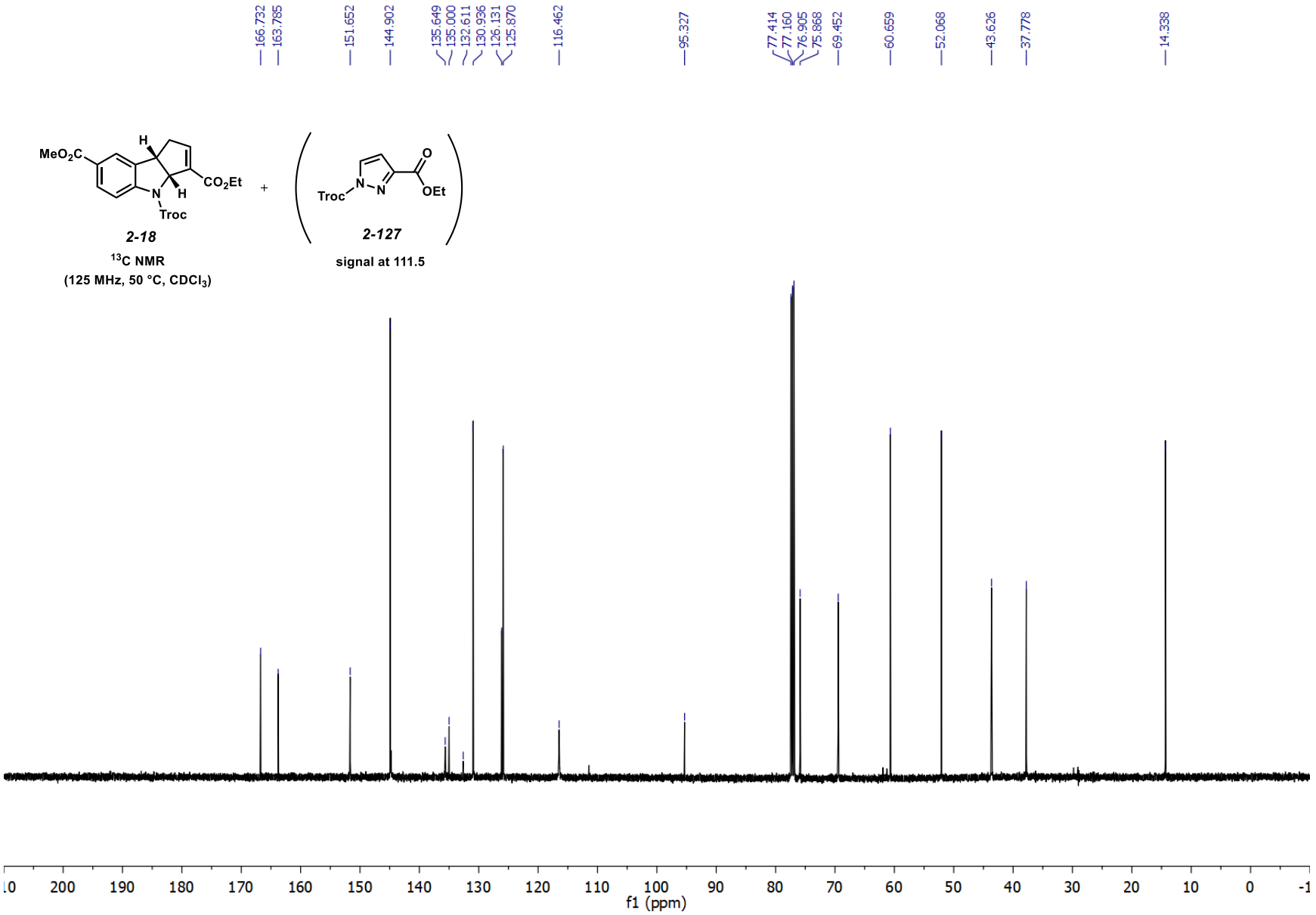
166.732
163.785
151.652
144.902
135.649
135.000
132.611
130.936
126.131
125.870
116.462
95.327
77.414
77.160
76.905
75.868
69.452
60.659
52.068
43.626
37.778
14.338
MeO2C
CO2Et
H
N
H
Troc
2-18
+
Troc
N
N
O
OEt
2-127
signal at 111.5
13C NMR
(125 MHz, 50 °C, CDCl3)
f1 (ppm)

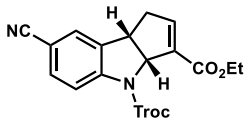

2-19

^{1}H NMR
(400 MHz, $CDCl_3$)

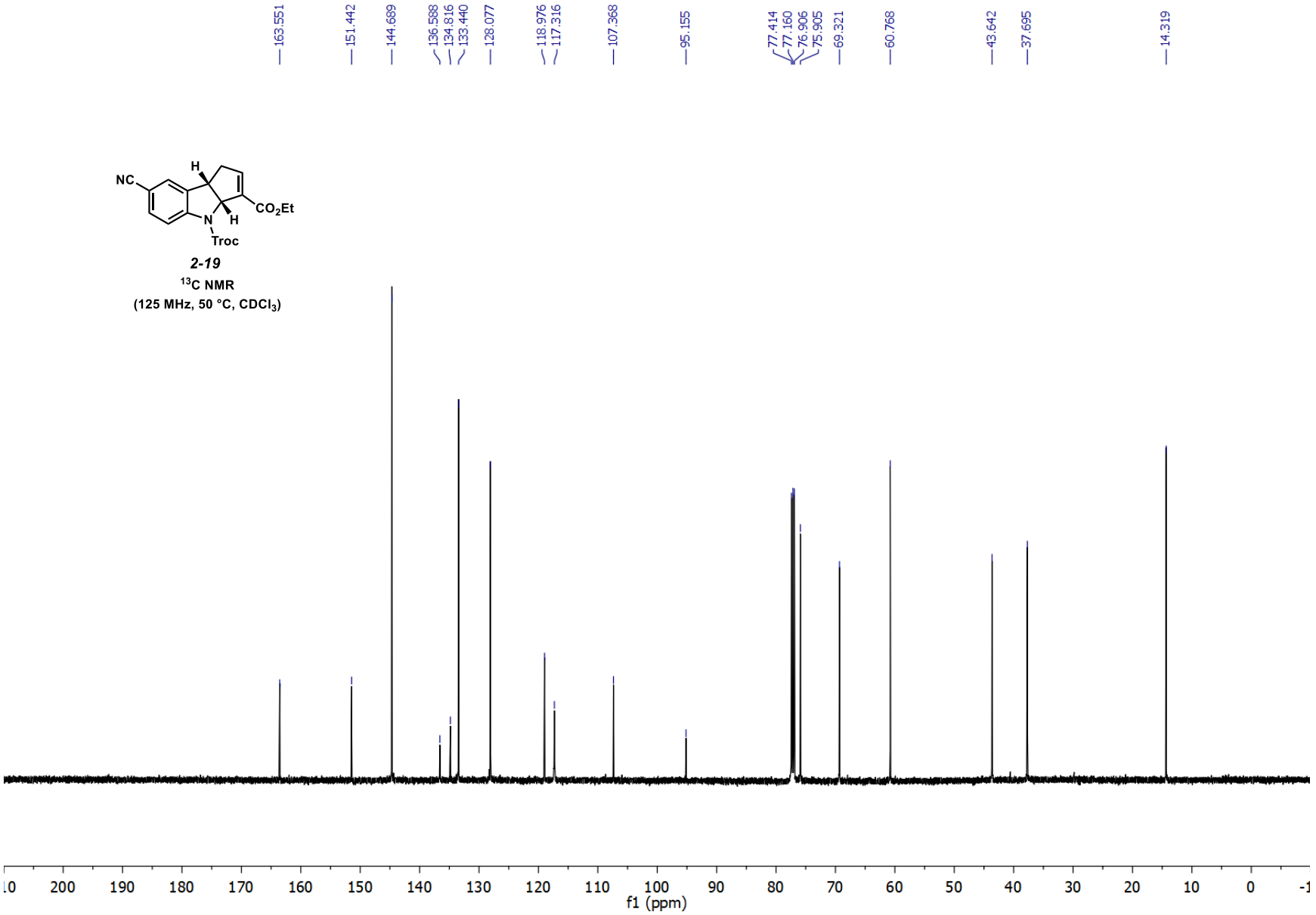
163.551
151.442
144.689
136.588
134.816
133.440
128.077
118.976
117.316
107.368
95.155
77.414
77.160
76.906
75.905
69.321
60.768
43.642
37.695
14.319
NC
H
CO2Et
N
H
Troc
2-19
13C NMR
(125 MHz, 50 °C, CDCl3)
f1 (ppm)

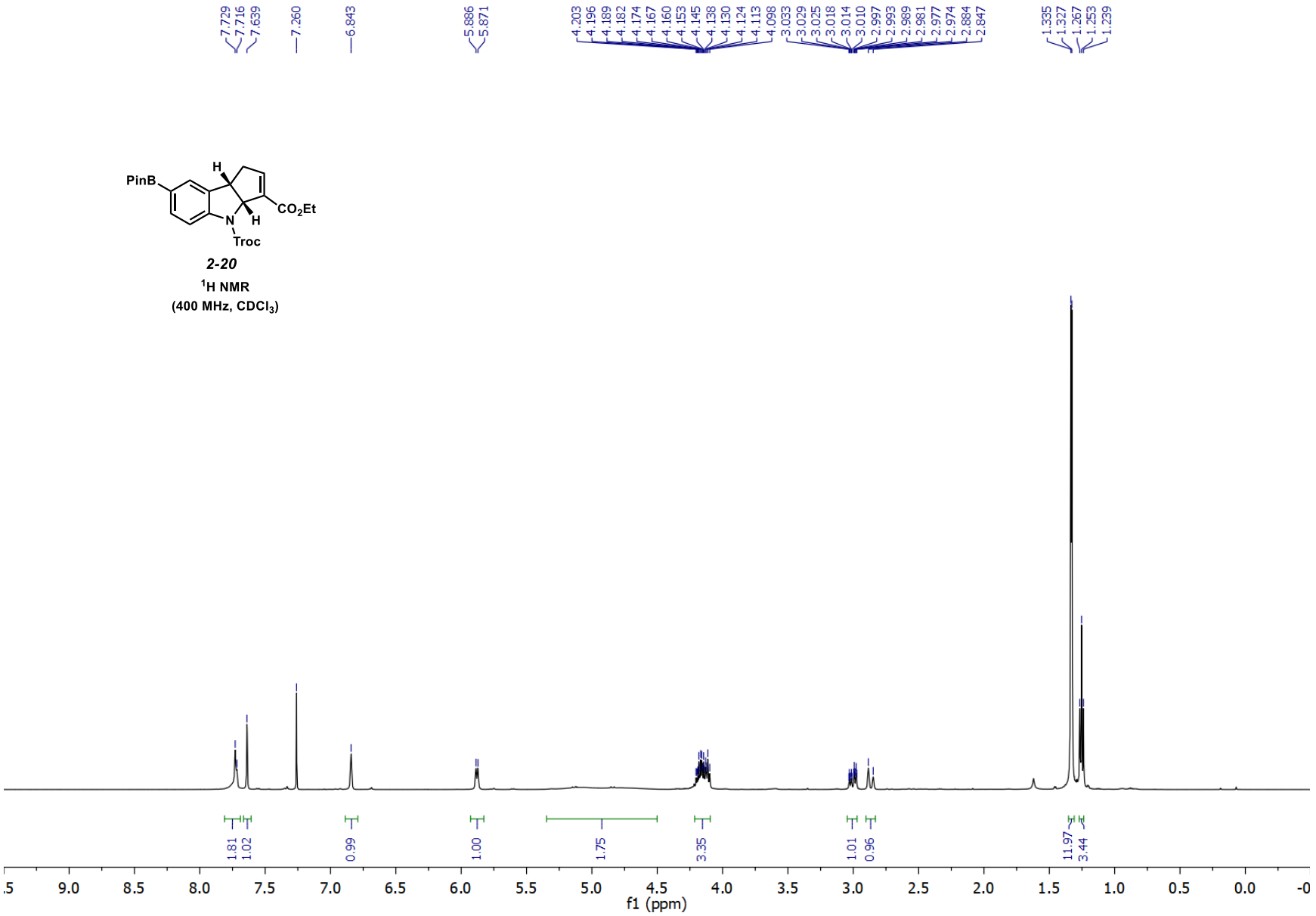
7.729
7.716
7.639
7.260
6.843
5.886
5.871
4.203
4.196
4.189
4.182
4.174
4.167
4.160
4.153
4.145
4.138
4.130
4.124
4.113
4.098
3.033
3.029
3.025
3.018
3.014
3.010
2.997
2.993
2.989
2.981
2.977
2.974
2.884
2.847
1.335
1.327
1.267
1.253
1.239
PinB
H
CO2Et
N
H
Troc
2-20
1H NMR
(400 MHz, CDCl3)
1.81
1.02
0.99
1.00
1.75
3.35
1.01
0.96
11.97
3.44
f1 (ppm)

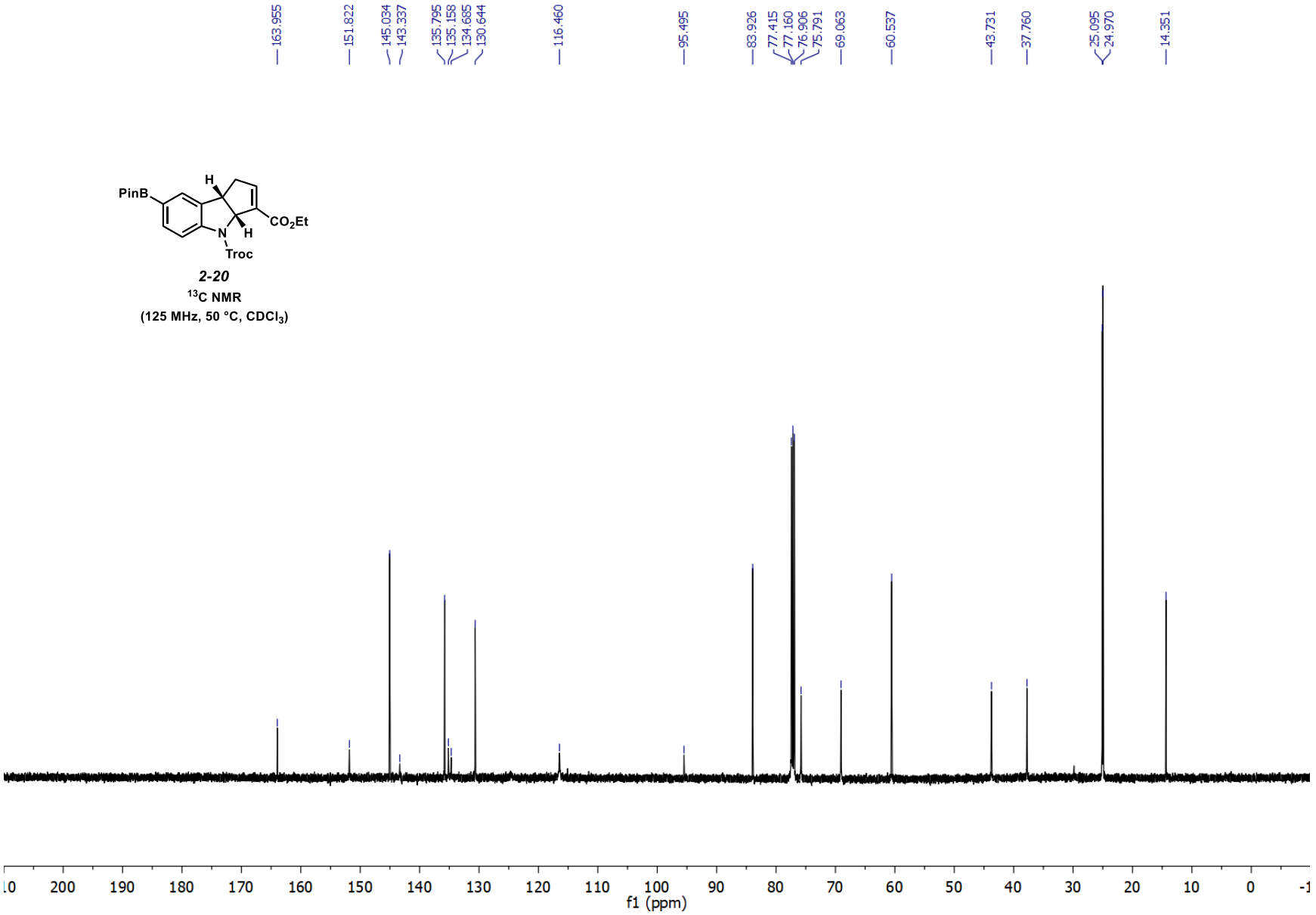
163.955
151.822
145.034
143.337
135.795
135.158
134.685
130.644
116.460
95.495
83.926
77.415
77.160
76.906
75.791
69.063
60.537
43.731
37.760
25.095
24.970
14.351
PinB
H
CO2Et
N
H
Troc
2-20
13C NMR
(125 MHz, 50 °C, CDCl3)
f1 (ppm)

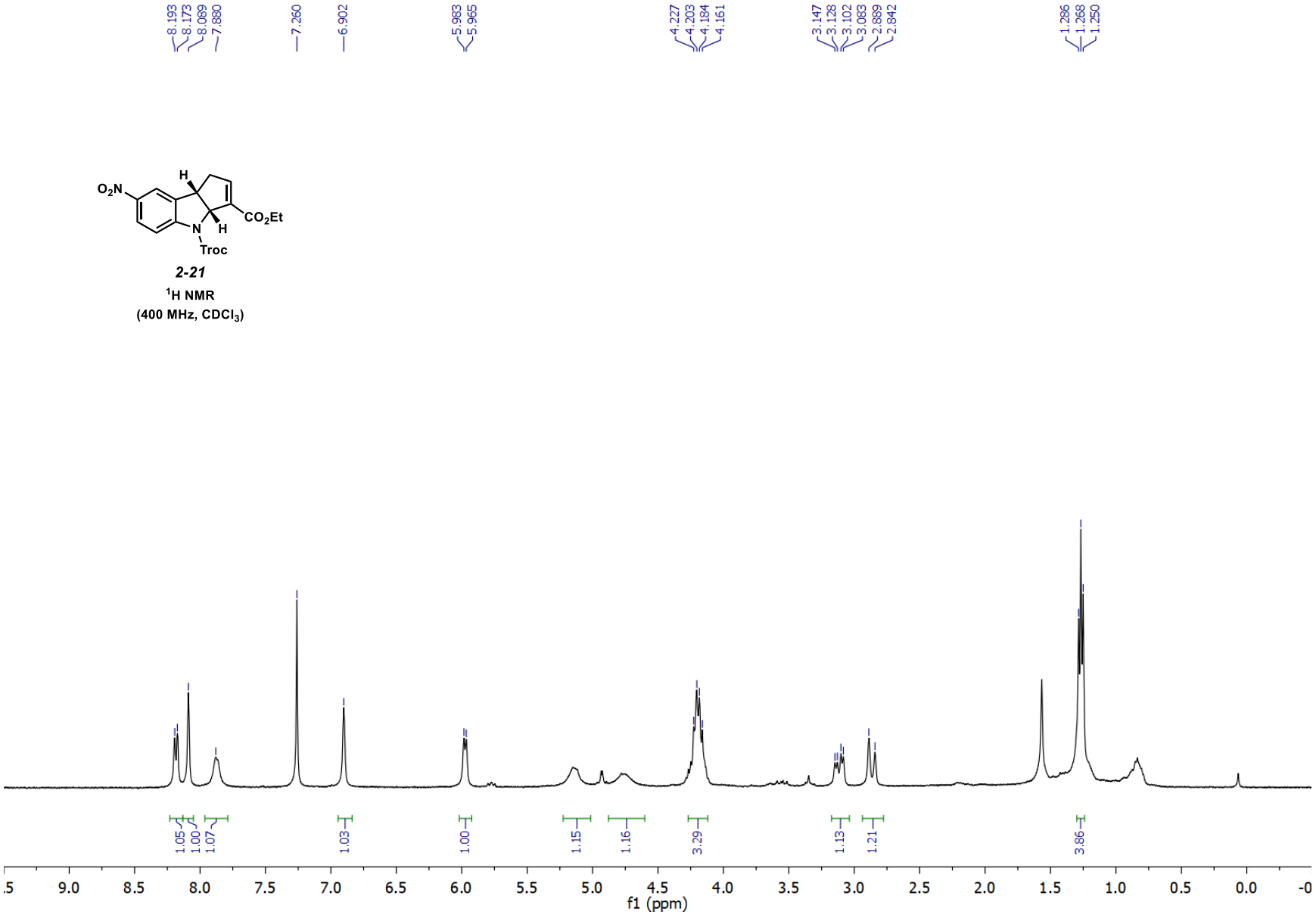
8.193
8.173
8.089
7.880
7.260
6.902
5.983
5.965
4.227
4.203
4.184
4.161
3.147
3.128
3.102
3.083
2.889
2.842
1.286
1.268
1.250
O2N
H
N
H
CO2Et
Troc
2-21
1H NMR
(400 MHz, CDCl3)
1.05
1.00
1.07
1.03
1.00
1.15
1.16
3.29
1.13
1.21
3.86
f1 (ppm)

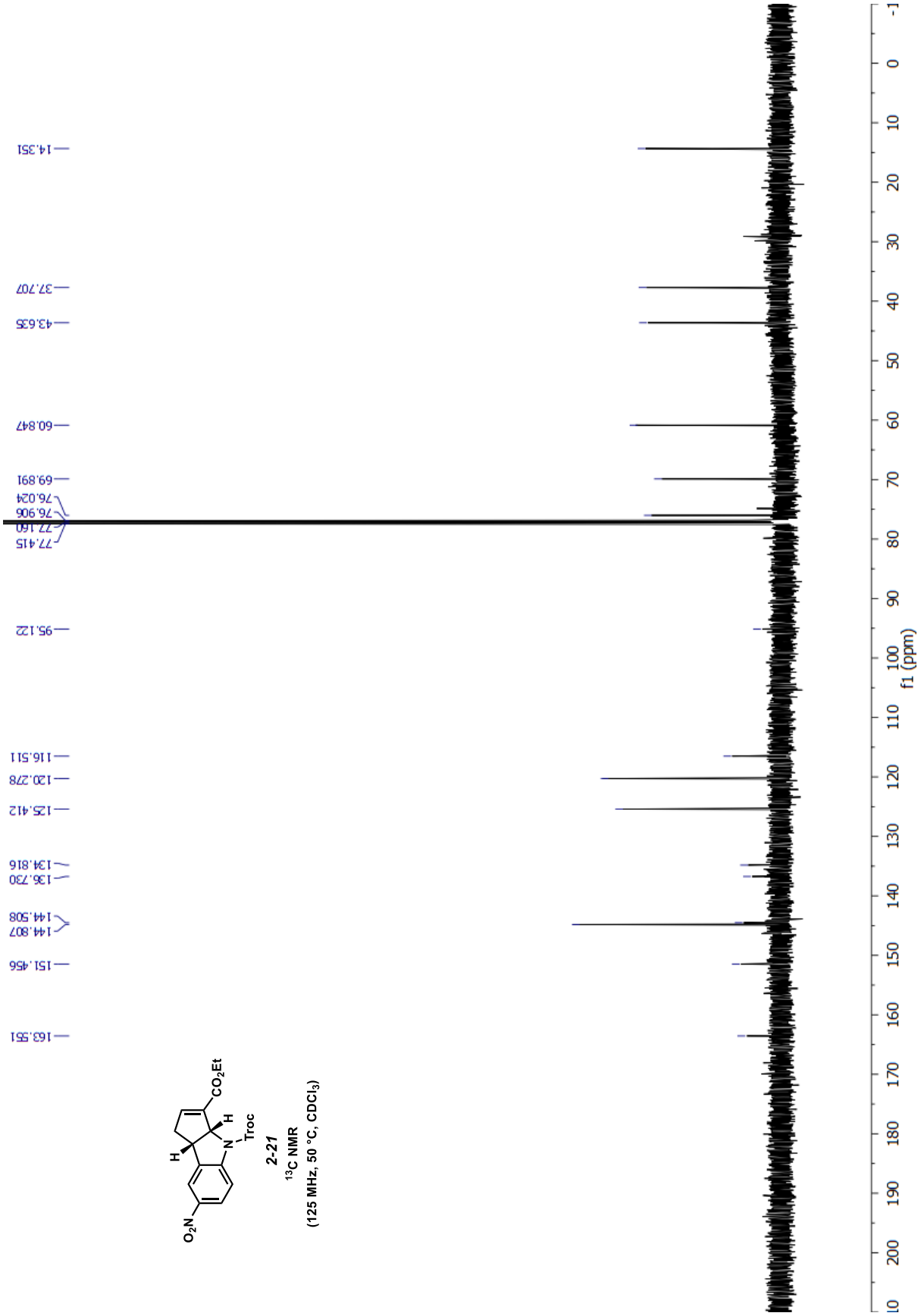
14.351
37.707
43.635
60.847
69.891
76.024
76.906
77.160
77.415
95.122
116.511
130.278
135.412
136.730
144.807
144.508
151.456
163.551
f1 (ppm)
2-21
13C NMR
(125 MHz, 50 °C, CDCl3)

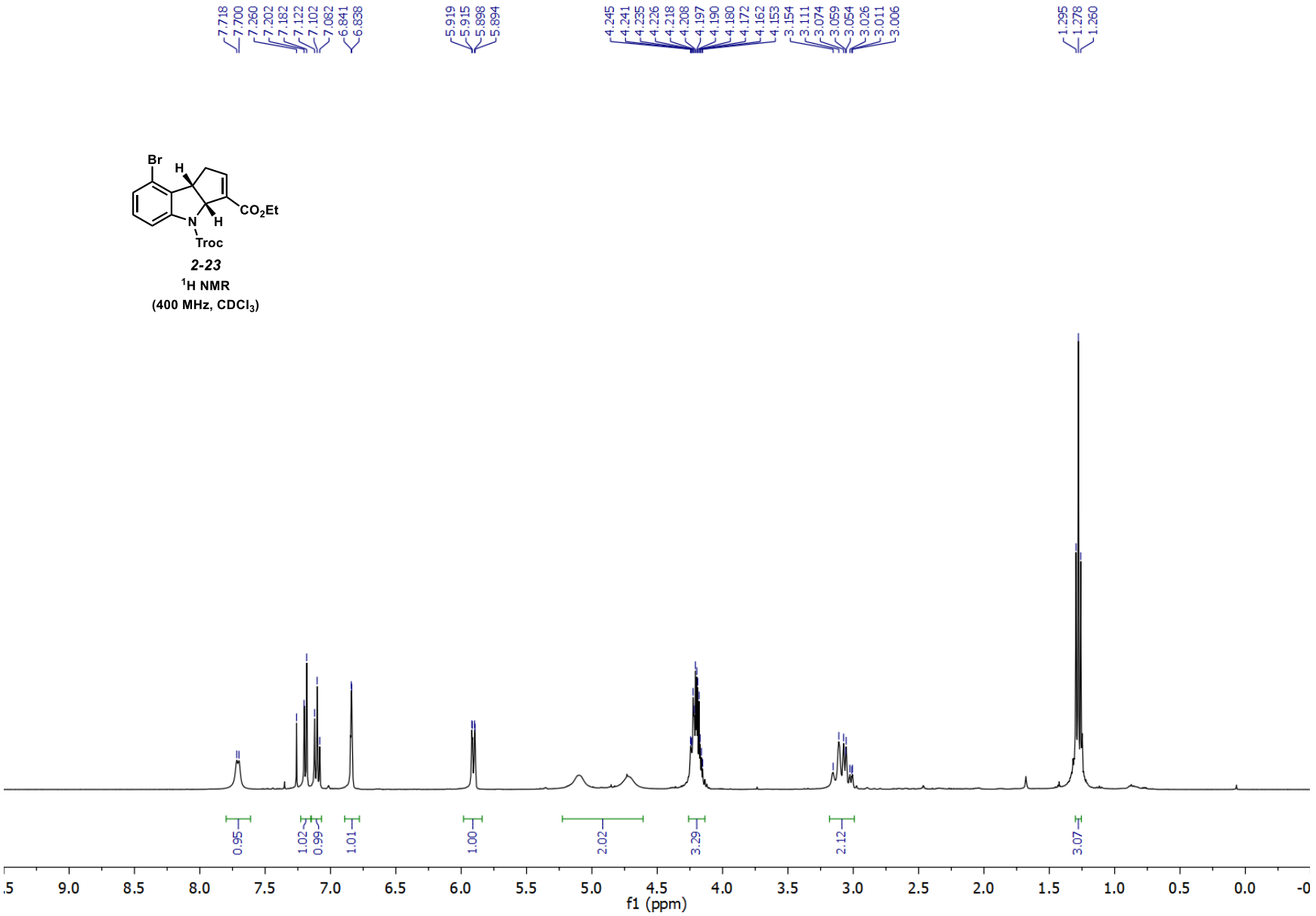
7.718
7.700
7.260
7.202
7.182
7.122
7.102
7.082
6.841
6.838
5.919
5.915
5.898
5.894
4.245
4.241
4.235
4.226
4.218
4.208
4.197
4.190
4.180
4.172
4.162
4.153
3.154
3.111
3.074
3.059
3.054
3.026
3.011
3.006
1.295
1.278
1.260
Br
H
CO2Et
N
H
Troc
2-23
1H NMR
(400 MHz, CDCl3)
0.95
1.02
0.99
1.01
1.00
2.02
3.29
2.12
3.07
f1 (ppm)

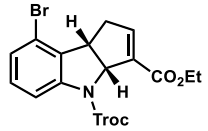

2-23

^{13}C NMR

(125 MHz, 50 °C, $CDCl_3$)

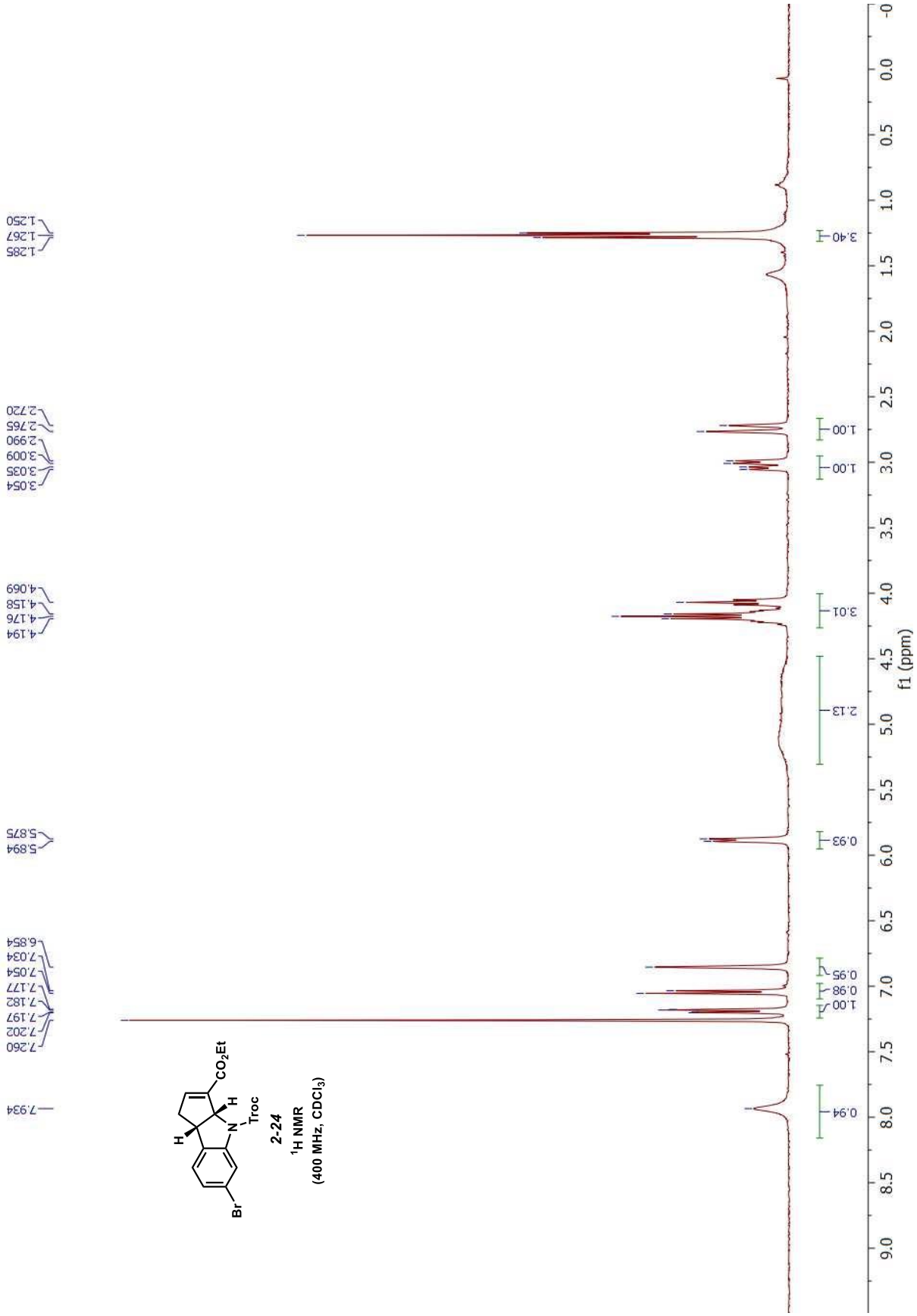
7.934
7.260
7.202
7.197
7.182
7.177
7.054
7.034
6.854
5.894
5.875
4.194
4.176
4.158
4.069
3.054
3.035
3.009
2.990
2.765
2.720
1.285
1.267
1.250
0.94
0.93
2.13
3.01
1.00
1.00
0.95
0.98
1.00
f1 (ppm)
2-24
1H NMR
(400 MHz, CDCl3)
CO2Et
Troc
N
H
H
Br

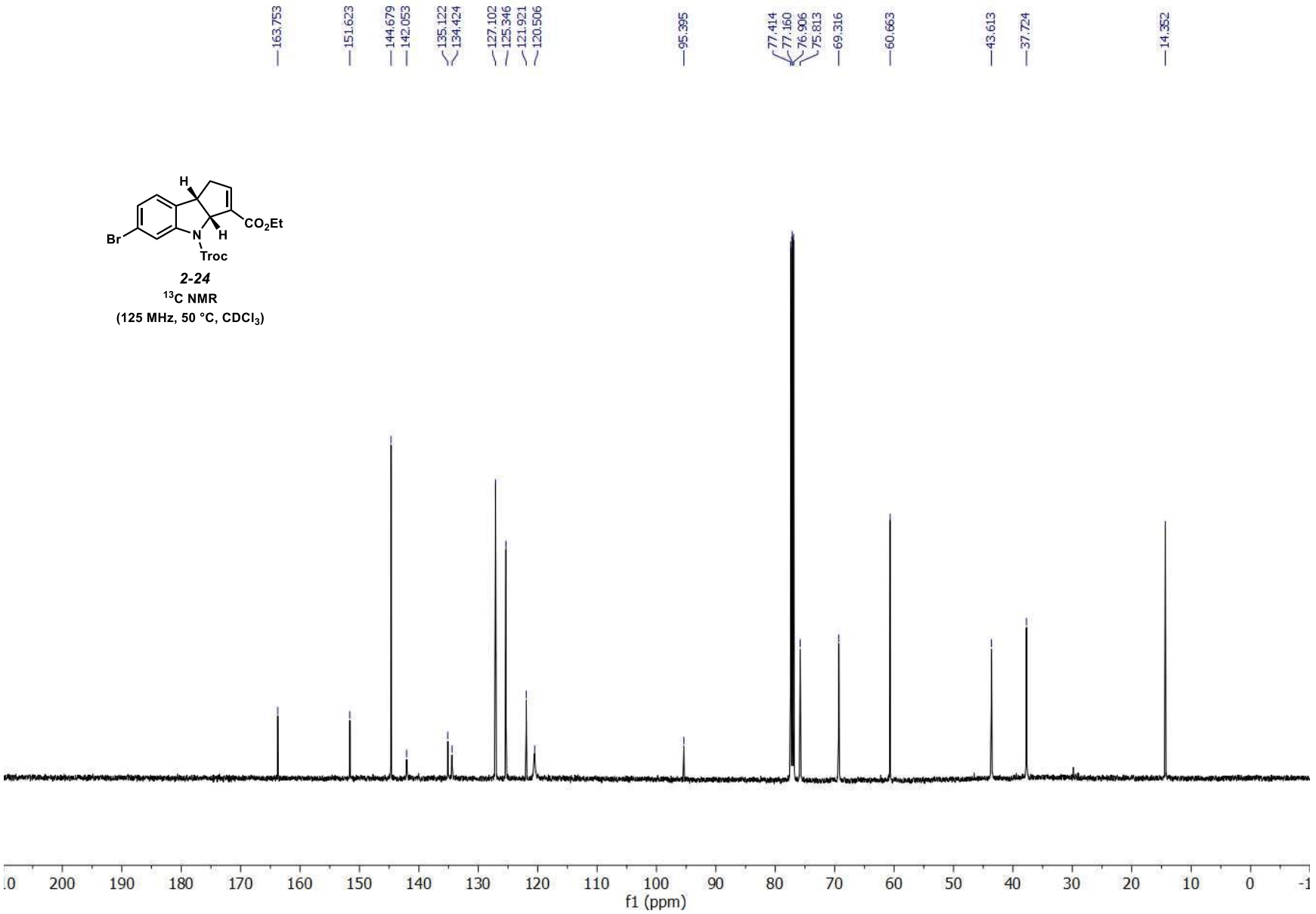
163.753
151.623
144.679
142.053
135.122
134.424
127.102
125.346
121.921
120.506
95.395
77.414
77.160
76.906
75.813
69.316
60.663
43.613
37.724
14.352
H
CO2Et
Br
N
H
Troc
2-24
13C NMR
(125 MHz, 50 °C, CDCl3)
f1 (ppm)

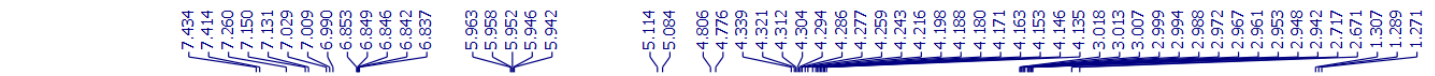

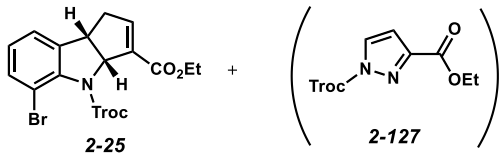

2-25

+

2-127

^{1}H NMR
(400 MHz, $CDCl_3$)

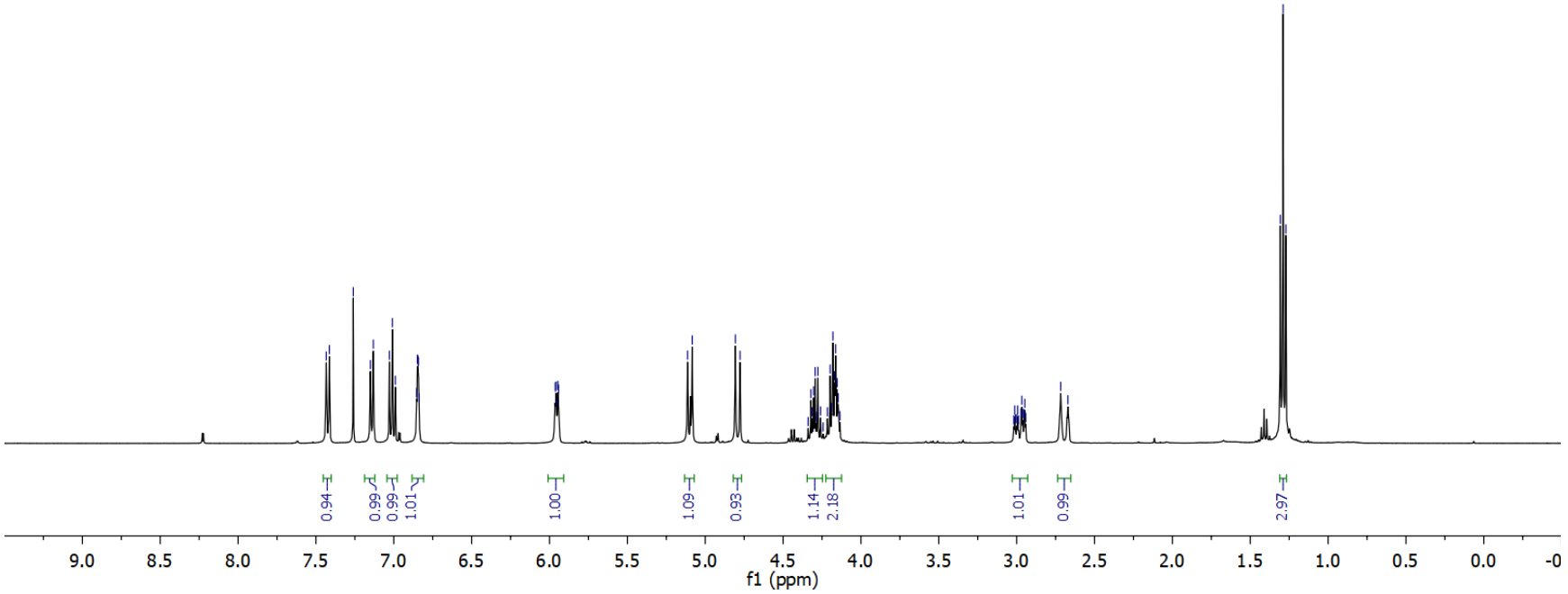

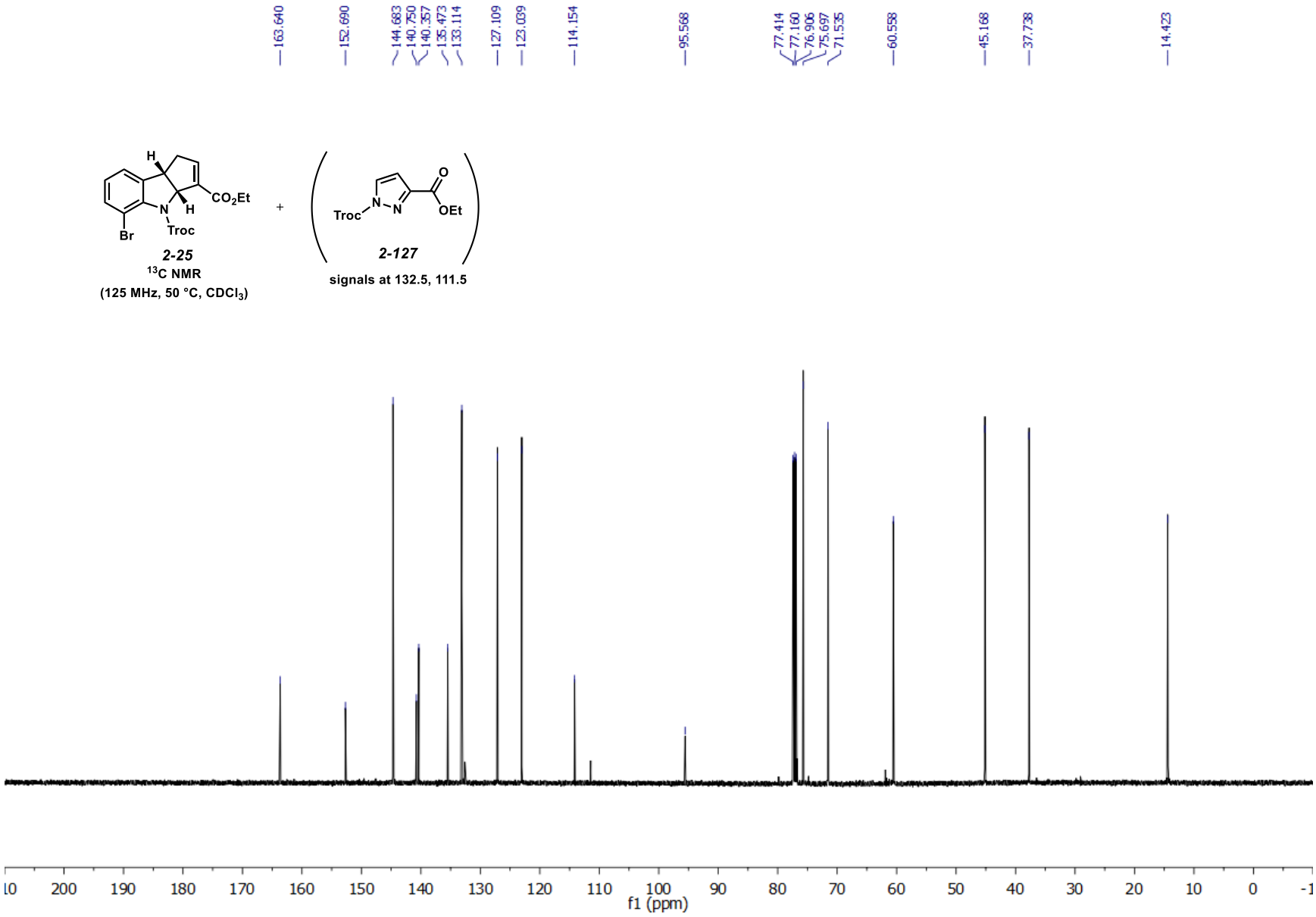
163.640
152.690
144.683
140.750
140.357
135.473
133.114
127.109
123.039
114.154
95.568
77.414
77.160
76.906
75.697
71.535
60.558
45.168
37.738
14.423
H
CO2Et
N
H
Troc
Br
2-25
13C NMR
(125 MHz, 50 °C, CDCl3)
+
O
Troc
N
N
OEt
2-127
signals at 132.5, 111.5
f1 (ppm)

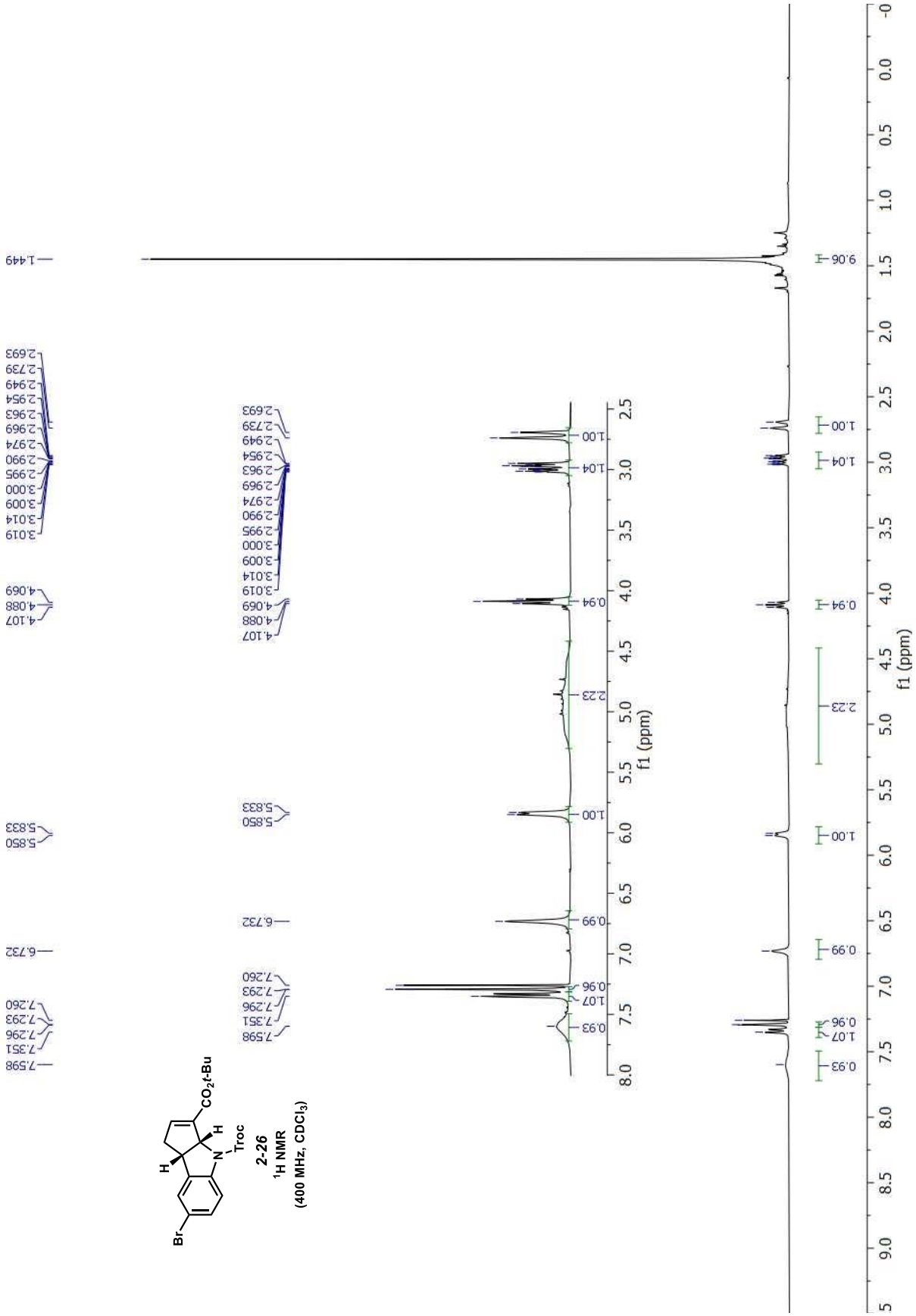
2-26
^{1}H NMR
(400 MHz, CDCl$_3$)
f1 (ppm)

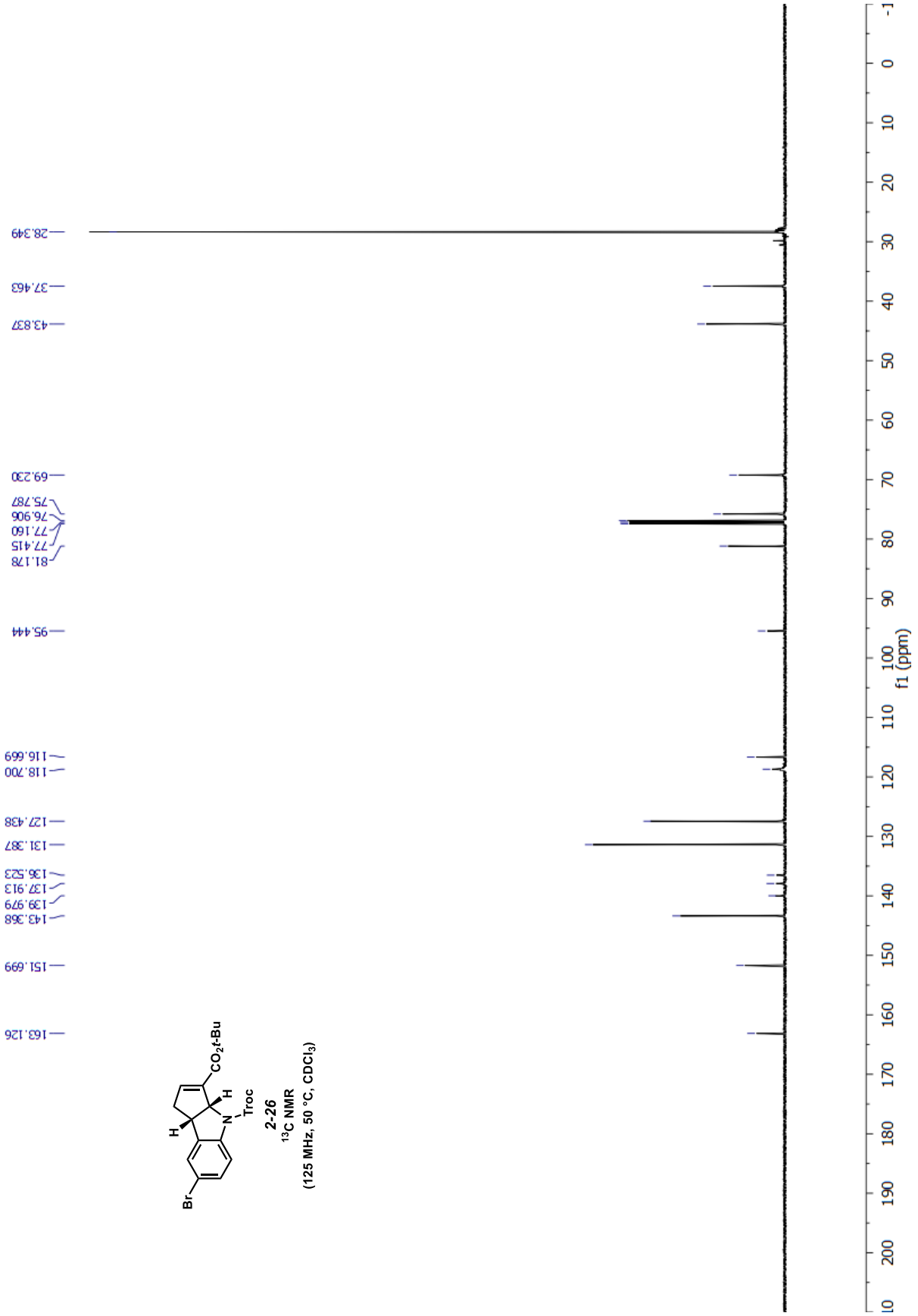
28.349
37.463
43.837
69.230
75.787
76.906
77.160
77.415
81.178
95.444
116.669
118.700
127.438
131.387
136.523
137.913
139.979
143.368
151.699
163.126
f1 (ppm)
CO2t-Bu
H
H
N
Troc
Br
2-26
13C NMR
(125 MHz, 50 °C, CDCl3)

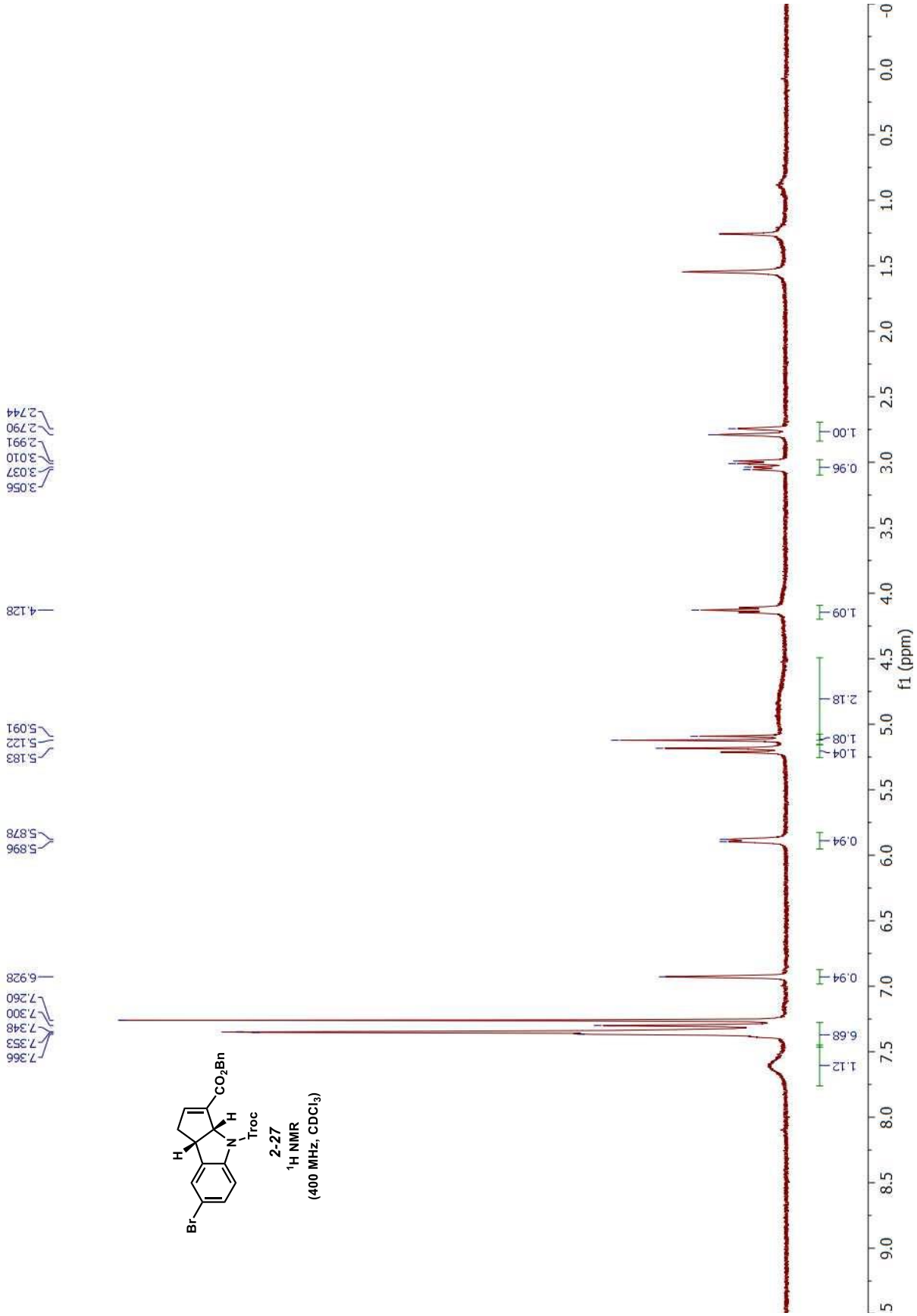
2-27
^{1}H NMR
(400 MHz, $CDCl_3$)
Br
CO_2Bn
Troc
7.366
7.353
7.348
7.300
7.260
6.928
5.896
5.878
5.183
5.122
5.091
4.128
3.056
3.037
3.010
2.991
2.790
2.744
1.00
0.96
1.09
2.18
1.08
1.04
0.94
0.94
6.68
1.12
f1 (ppm)

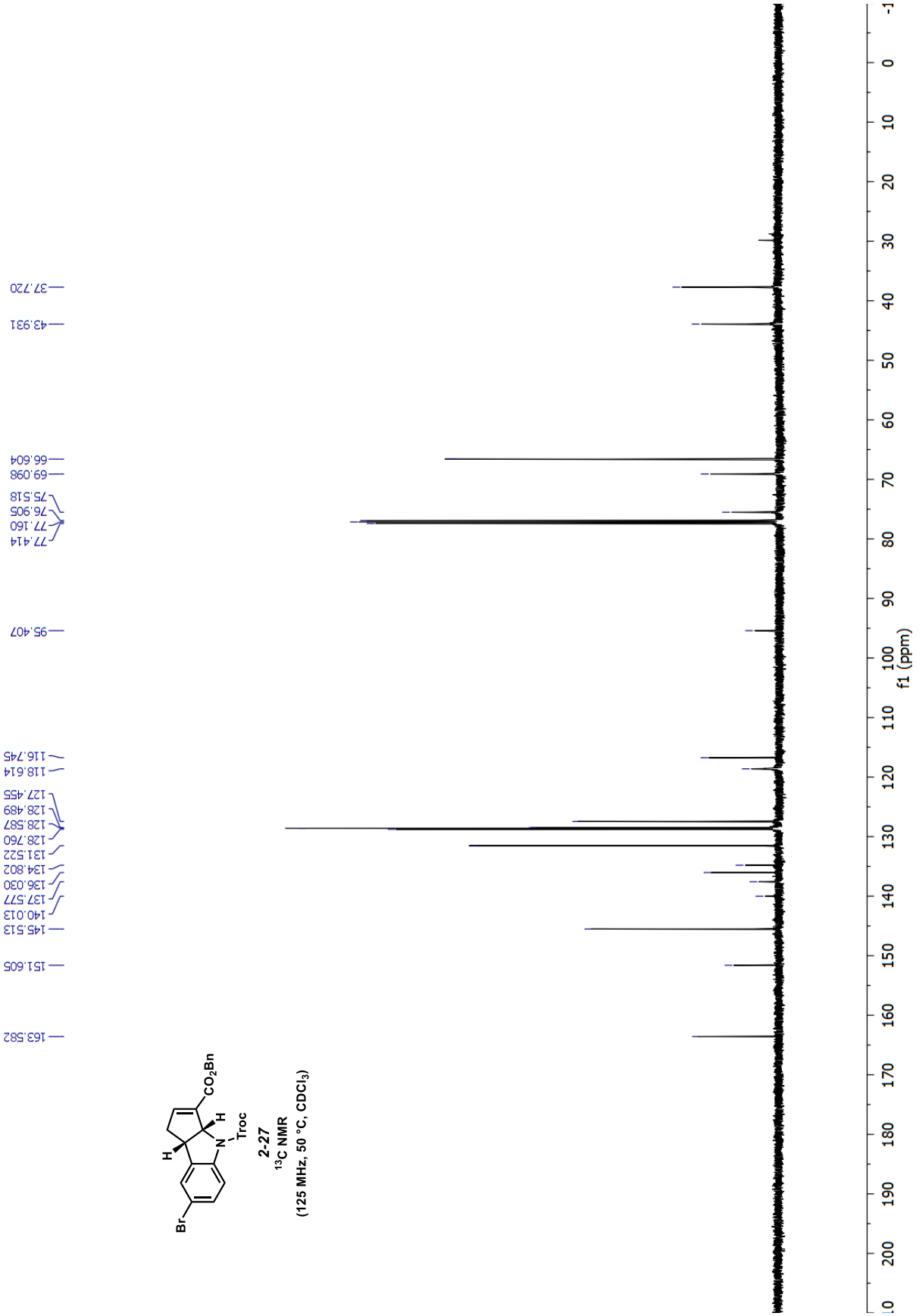
37.720
43.931
66.604
69.098
75.518
76.905
77.160
77.414
95.407
116.745
118.614
127.455
128.489
128.587
128.760
131.522
134.802
136.030
137.577
140.013
145.513
151.605
163.582
CO2Bn
H
N
Troc
H
Br
2-27
13C NMR
(125 MHz, 50 °C, CDCl3)
f1 (ppm)

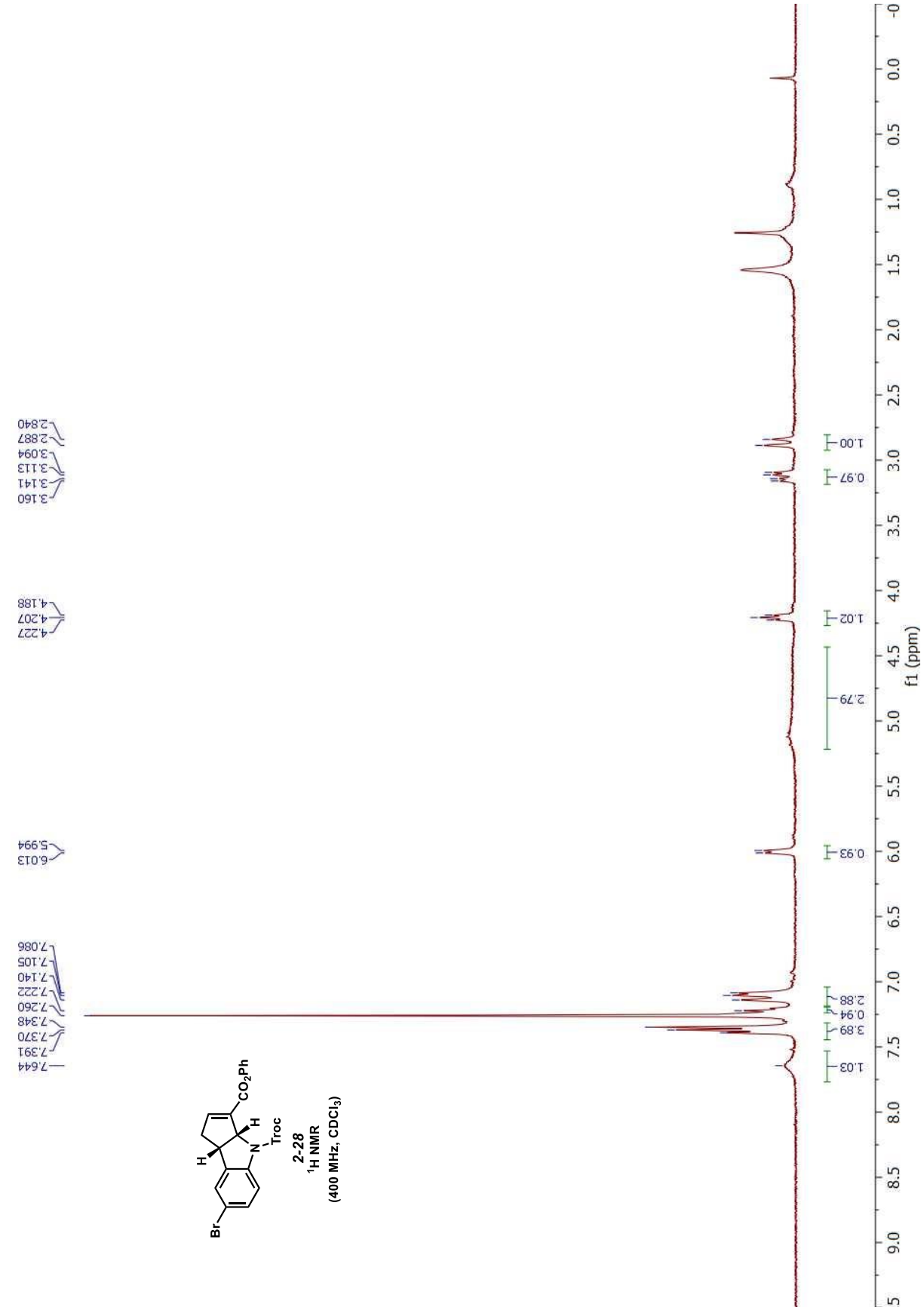
2-28
^{1}H NMR
(400 MHz, CDCl$_3$)
f1 (ppm)

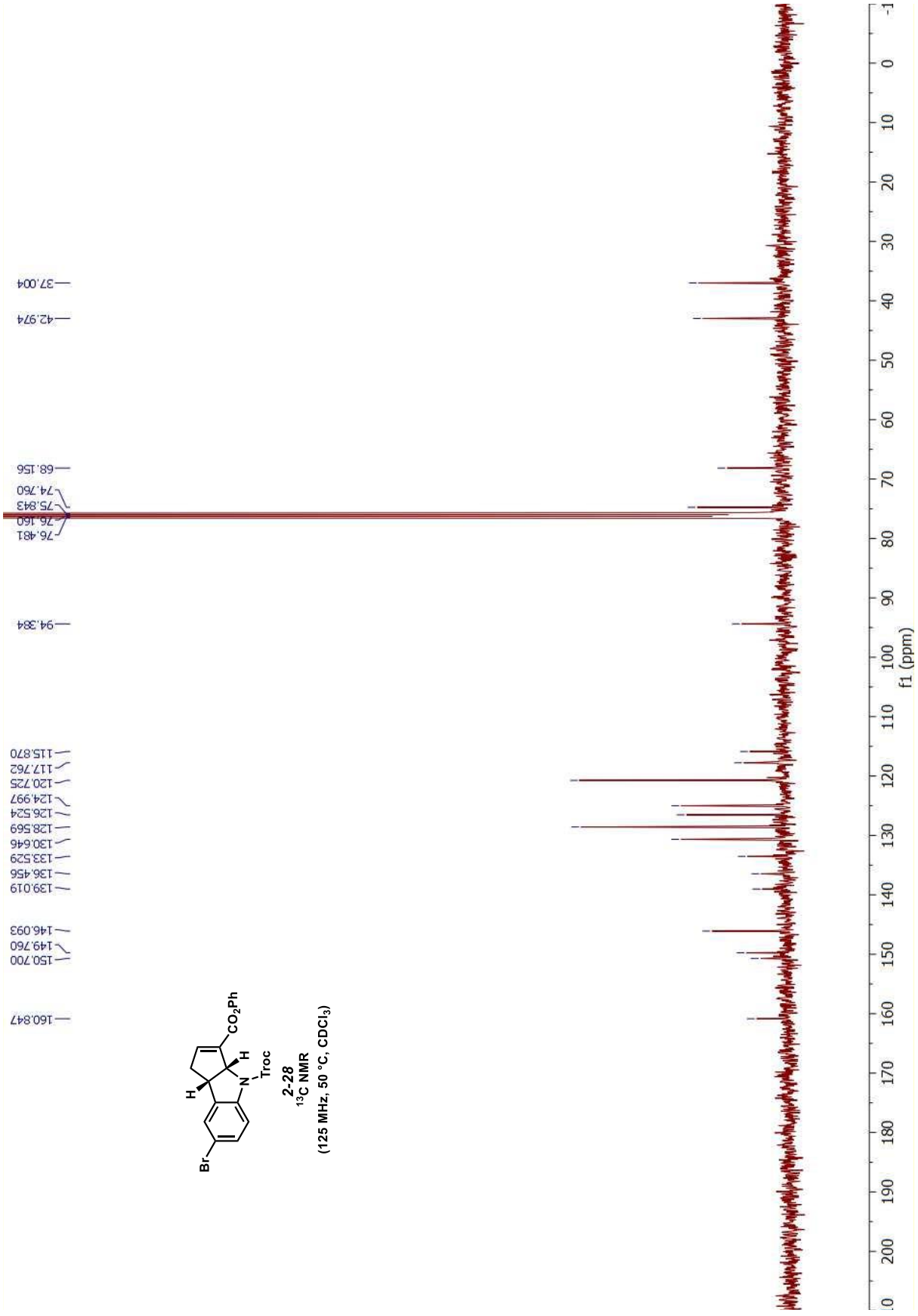
37.004
42.974
68.156
74.760
75.843
76.160
76.481
94.384
115.870
117.762
120.725
124.997
126.524
128.569
130.646
133.529
136.456
139.019
146.093
149.760
150.700
160.847
f1 (ppm)
2-28
13C NMR
(125 MHz, 50 °C, CDCl3)
CO2Ph
Troc
N
H
H
Br

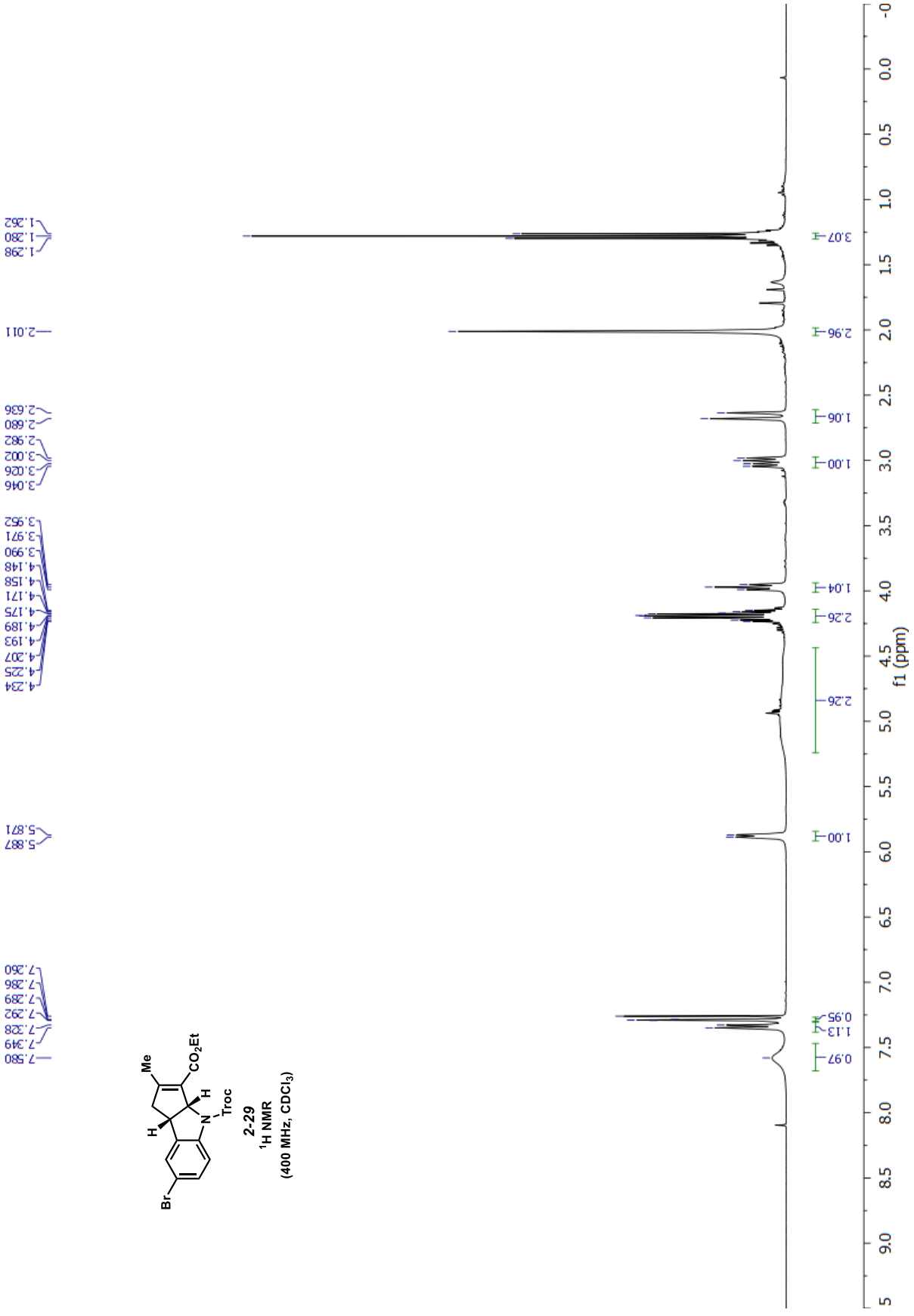
Me
CO2Et
H
N
Troc
H
Br
2-29
1H NMR
(400 MHz, CDCl3)
f1 (ppm)

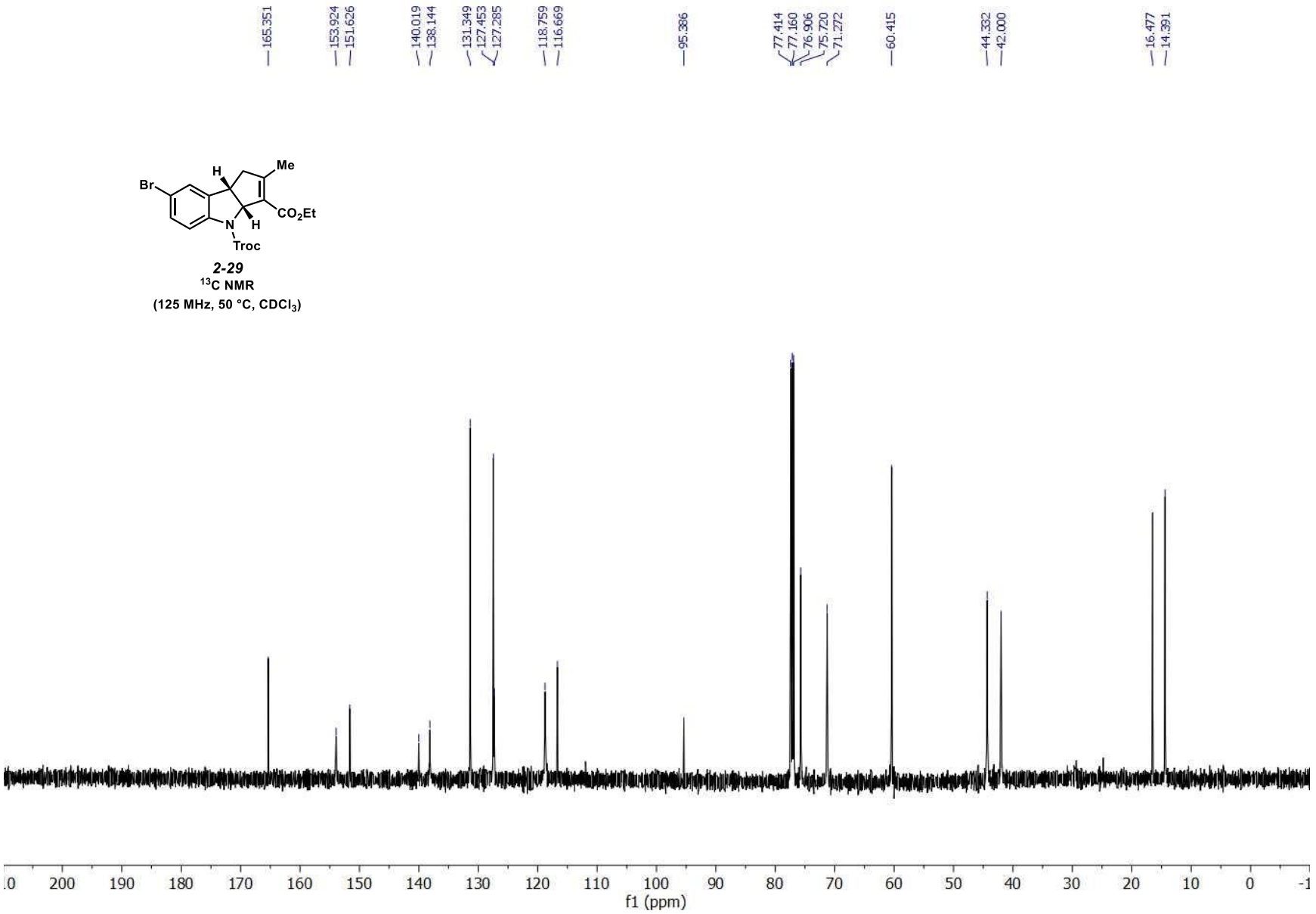
165.351
153.924
151.626
140.019
138.144
131.349
127.453
127.285
118.759
116.669
95.386
77.414
77.160
76.906
75.720
71.272
60.415
44.332
42.000
16.477
14.391
Br
H
Me
CO2Et
N
H
Troc
2-29
13C NMR
(125 MHz, 50 °C, CDCl3)
f1 (ppm)

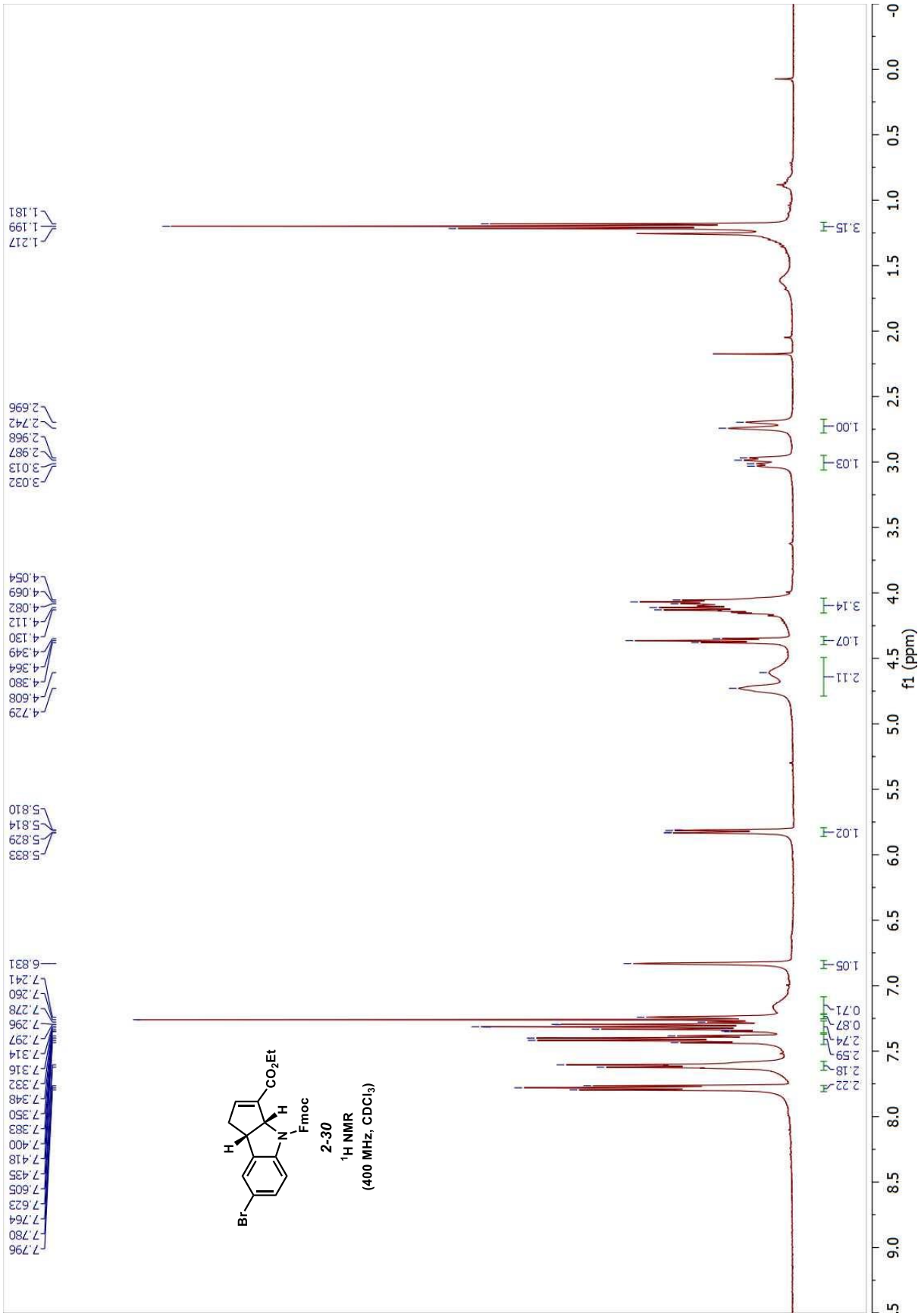
2-30
^{1}H NMR
(400 MHz, CDCl$_3$)
f1 (ppm)

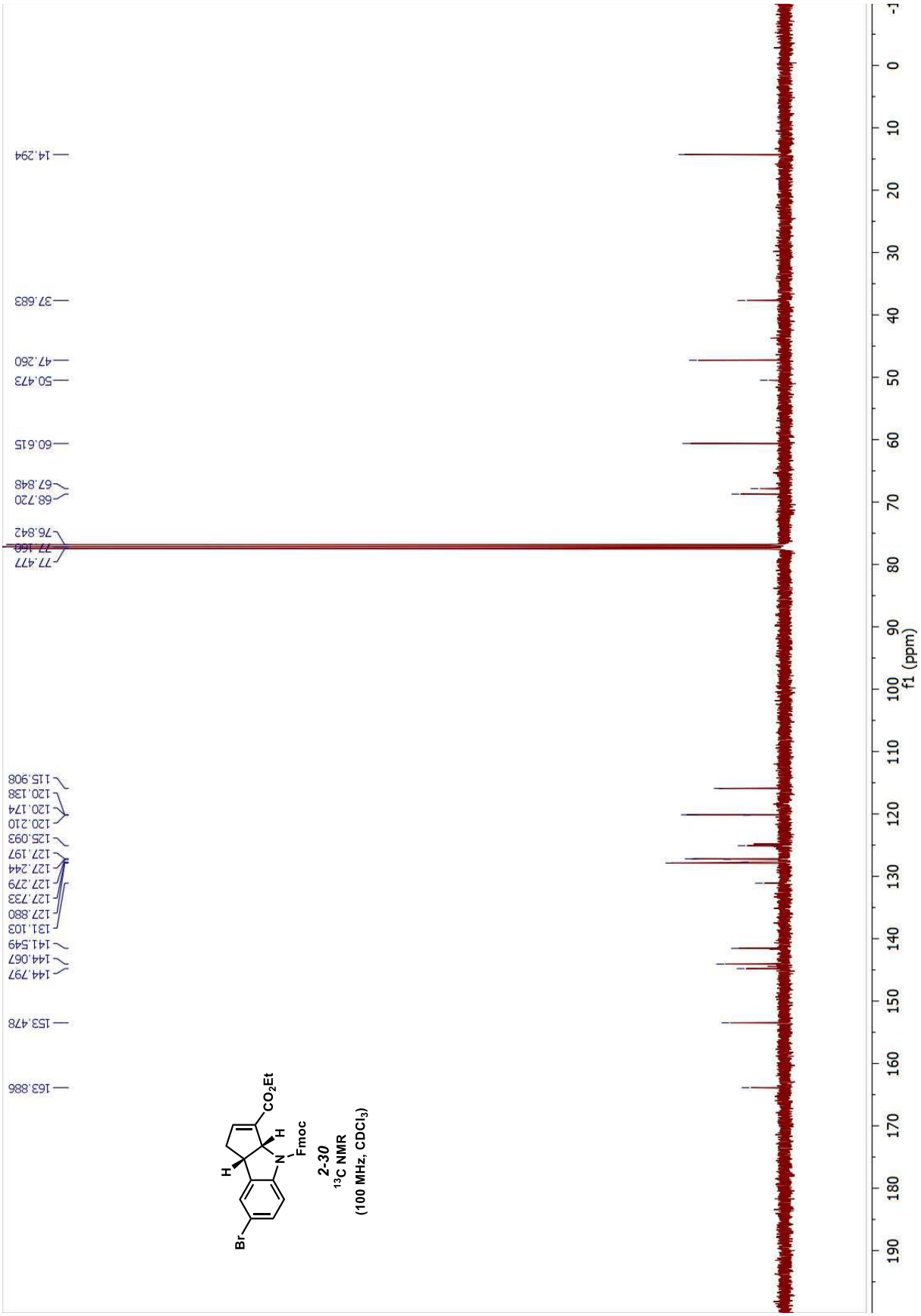
14.294
37.683
47.260
50.473
60.615
67.848
68.720
76.842
77.160
77.477
115.908
120.138
120.174
120.210
125.093
127.197
127.244
127.279
127.733
127.880
131.103
141.549
144.067
144.797
153.478
163.886
CO2Et
H
N
Fmoc
H
Br
2-30
13C NMR
(100 MHz, CDCl3)
f1 (ppm)

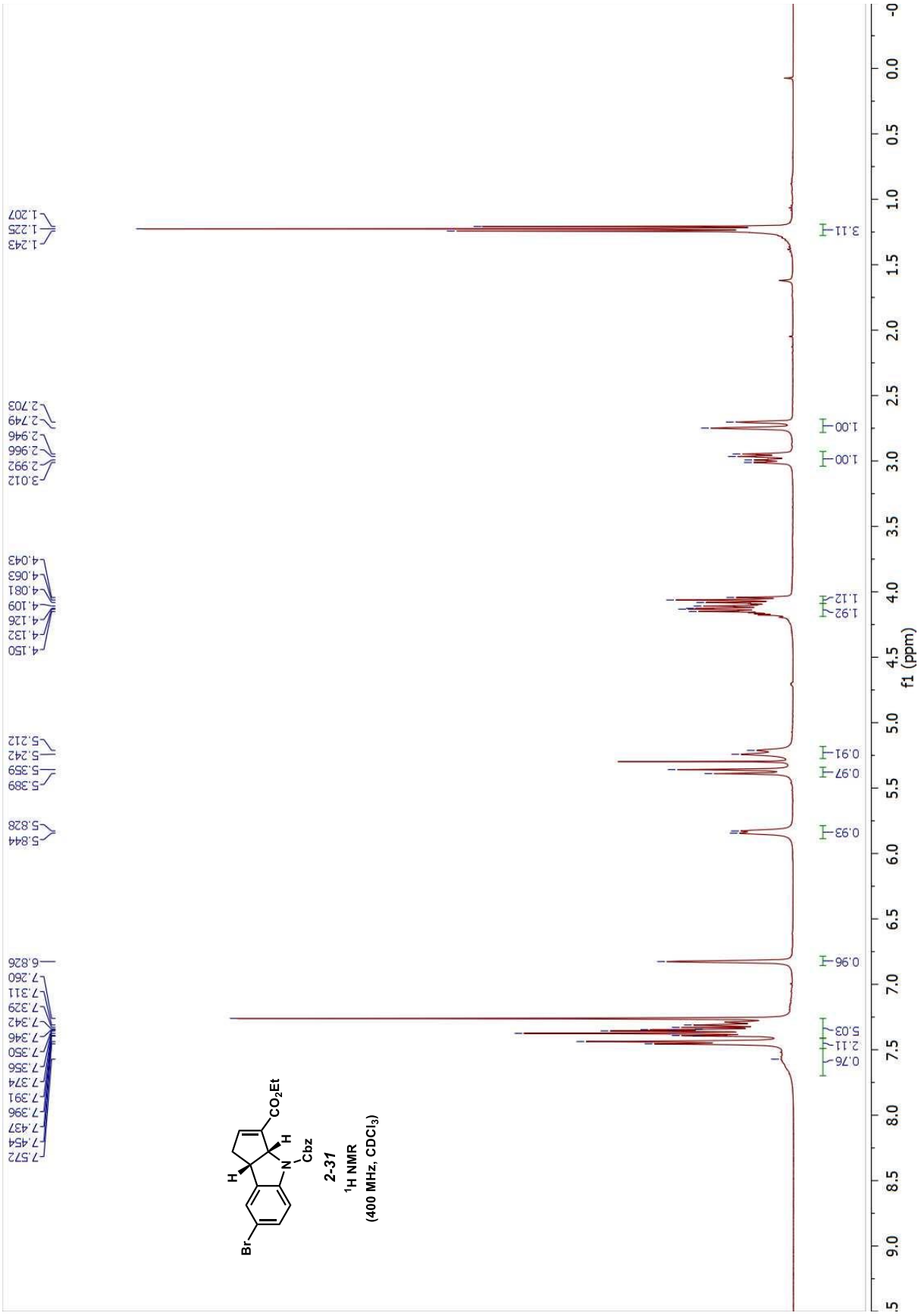
7.572
7.454
7.437
7.396
7.391
7.374
7.356
7.350
7.346
7.342
7.329
7.311
7.260
6.826
5.844
5.828
5.389
5.359
5.242
5.212
4.150
4.132
4.126
4.109
4.081
4.063
4.043
3.012
2.992
2.966
2.946
2.749
2.703
1.243
1.225
1.207
3.11
1.00
1.00
1.92
1.12
0.91
0.97
0.93
0.96
5.03
2.11
0.76
f1 (ppm)
Br
H
N
Cbz
H
CO2Et
2-31
1H NMR
(400 MHz, CDCl3)

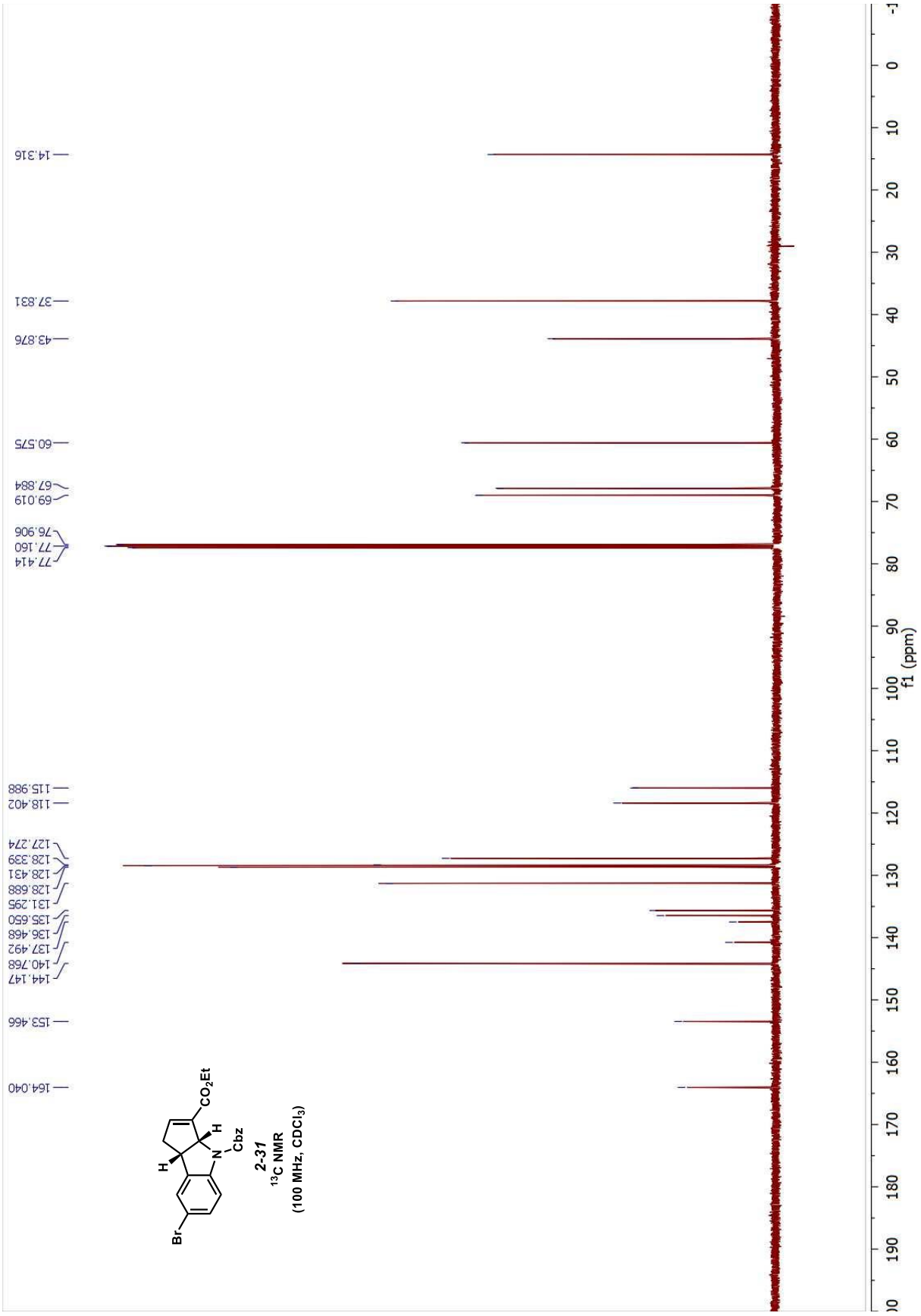
14.316
37.831
43.876
60.575
67.884
69.019
76.906
77.160
77.414
115.988
118.402
127.274
128.339
128.431
128.688
131.295
135.650
136.468
137.492
140.768
144.147
153.466
164.040
CO2Et
H
N
Cbz
H
Br
2-31
13C NMR
(100 MHz, CDCl3)
f1 (ppm)

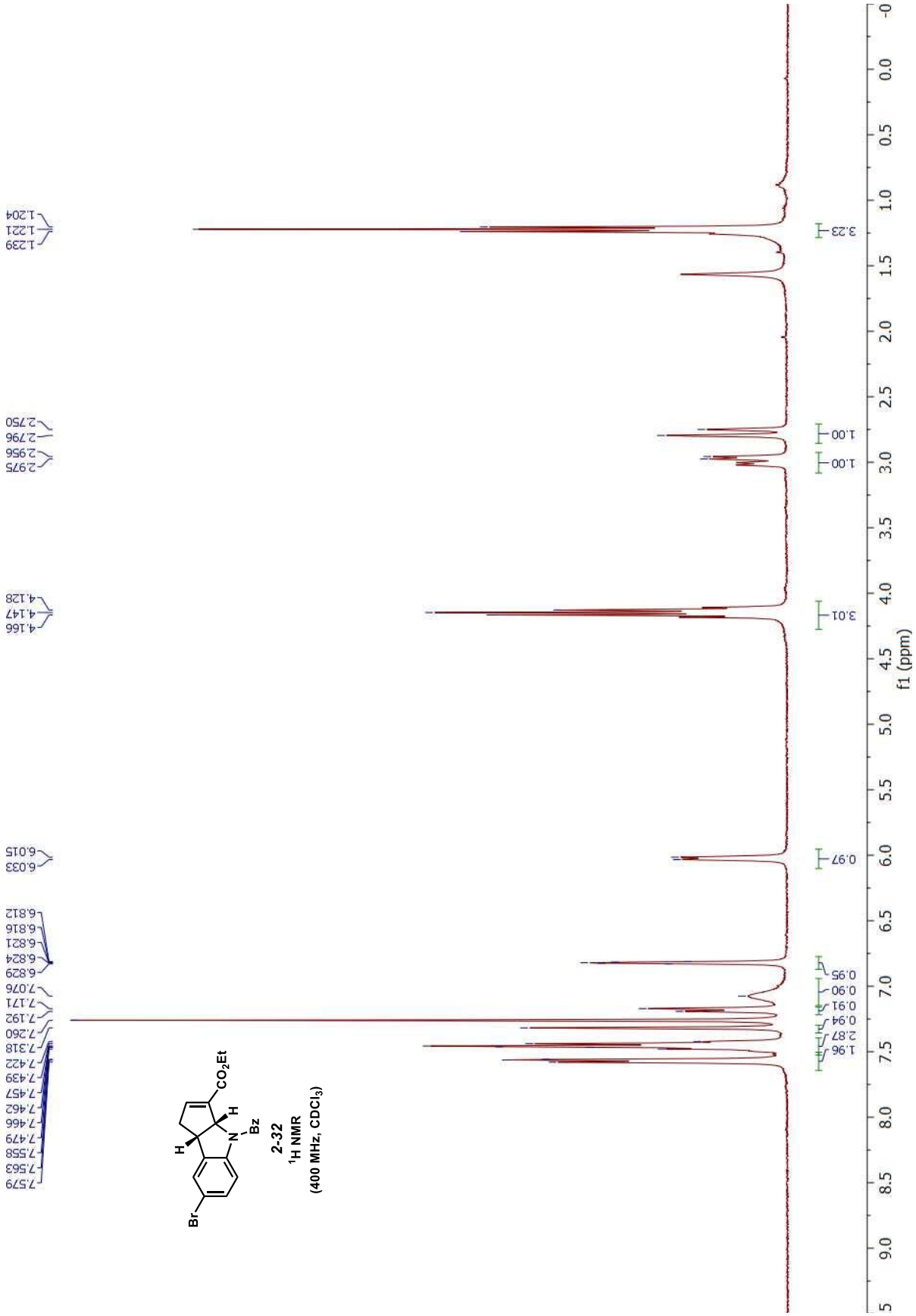
7.579
7.563
7.558
7.479
7.466
7.462
7.457
7.439
7.422
7.318
7.260
7.192
7.171
7.076
6.829
6.824
6.821
6.816
6.812
6.033
6.015
4.166
4.147
4.128
2.975
2.956
2.796
2.750
1.239
1.221
1.204
0.95
0.90
0.91
0.94
2.87
1.96
0.97
3.01
1.00
1.00
3.23
f1 (ppm)
CO2Et
H
N
Bz
H
Br
2-32
1H NMR
(400 MHz, CDCl3)

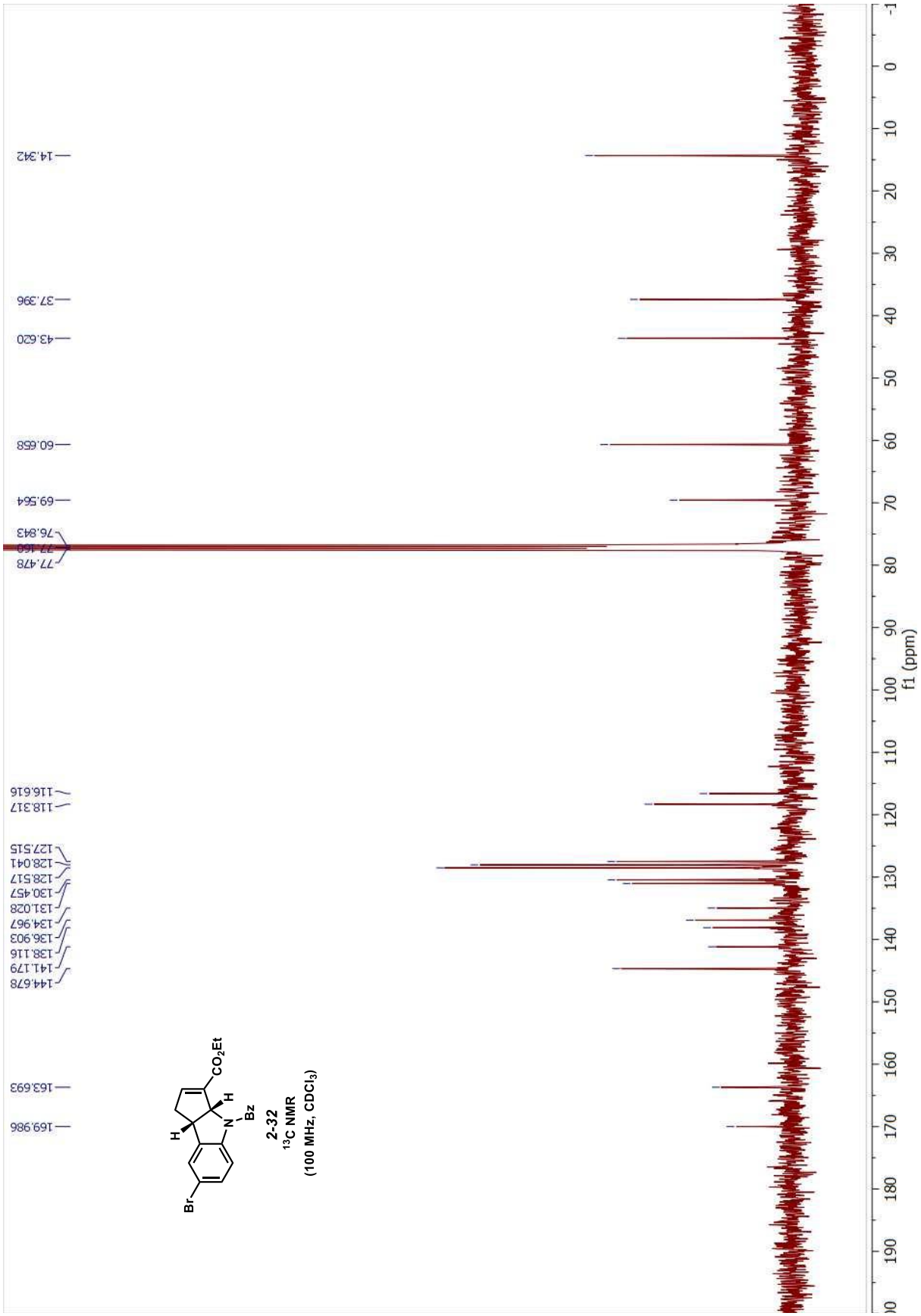
14.342
37.396
43.620
60.658
69.564
76.843
77.160
77.478
116.616
118.317
127.515
128.041
128.517
130.457
131.028
134.967
136.903
138.116
141.179
144.678
163.693
169.986
CO2Et
H
H
N
Bz
Br
2-32
13C NMR
(100 MHz, CDCl3)
f1 (ppm)

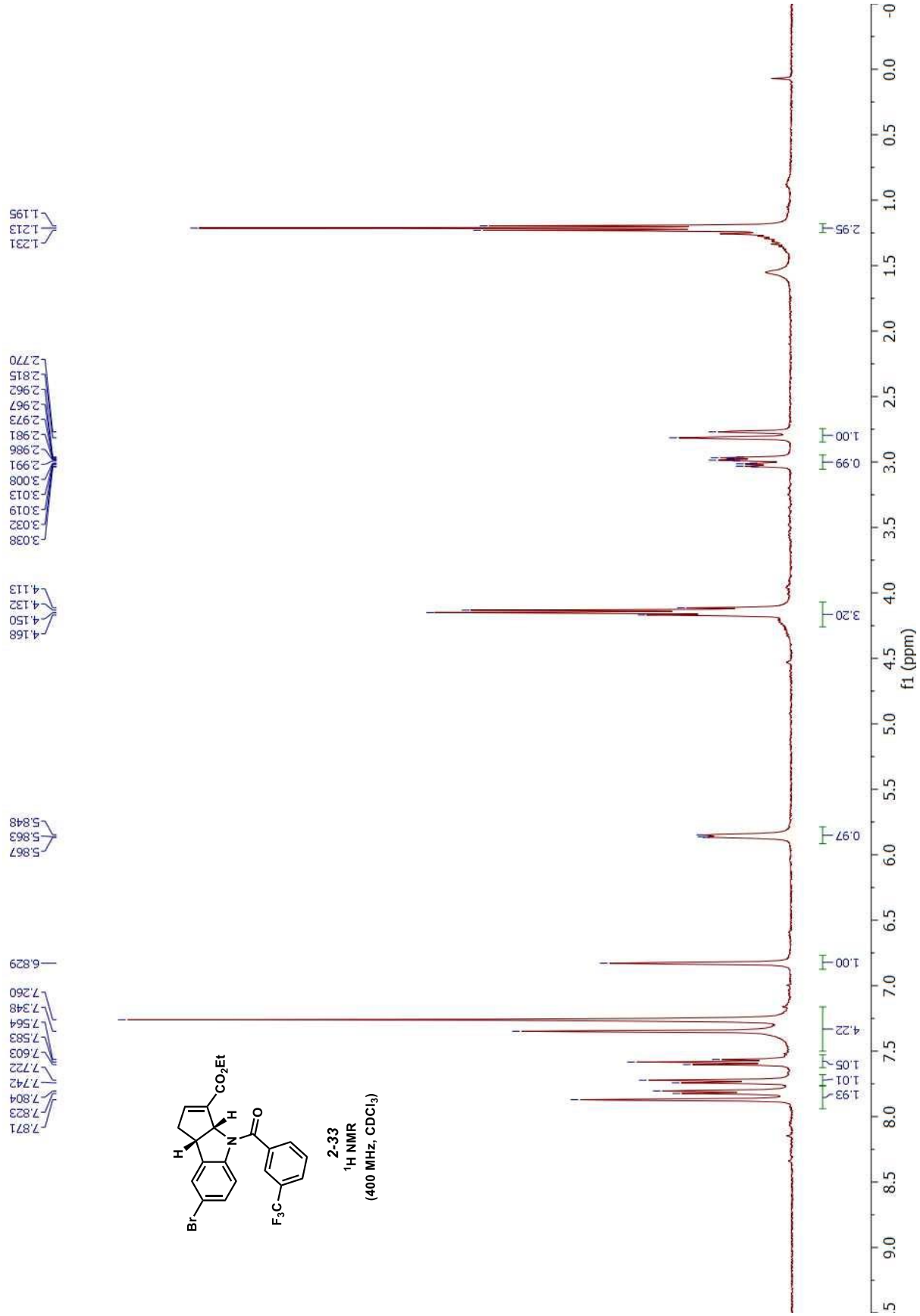
2-33
^{1}H NMR
(400 MHz, $CDCl_3$)
f1 (ppm)

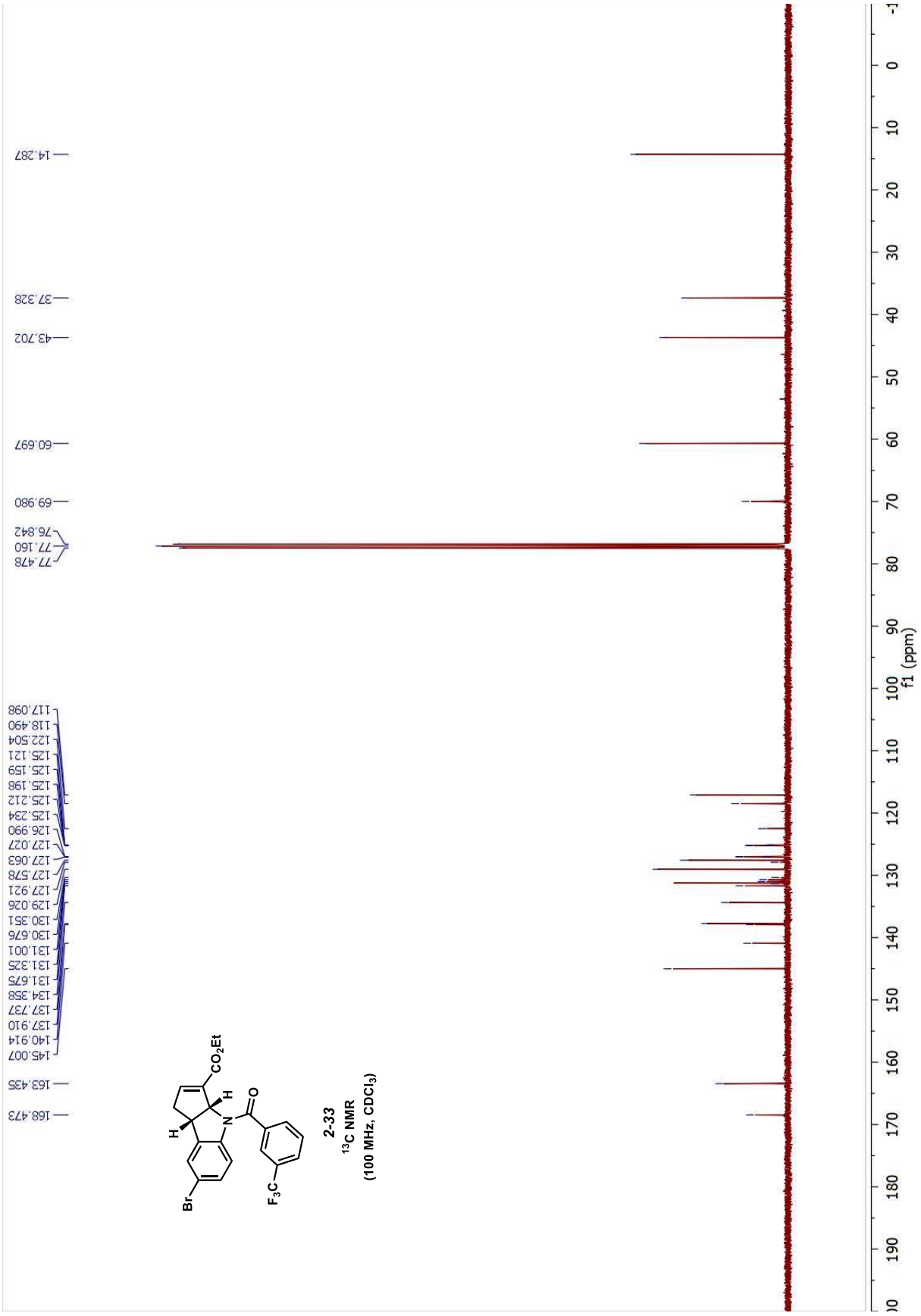
14.287
37.328
43.702
60.697
69.980
76.842
77.160
77.478
117.098
118.490
122.504
125.121
125.159
125.198
125.212
125.234
126.990
127.027
127.063
127.578
127.921
129.026
130.351
130.676
131.001
131.325
131.675
134.358
137.737
137.910
140.914
145.007
163.435
168.473
CO2Et
H
H
N
O
Br
F3C
2-33
13C NMR
(100 MHz, CDCl3)
f1 (ppm)

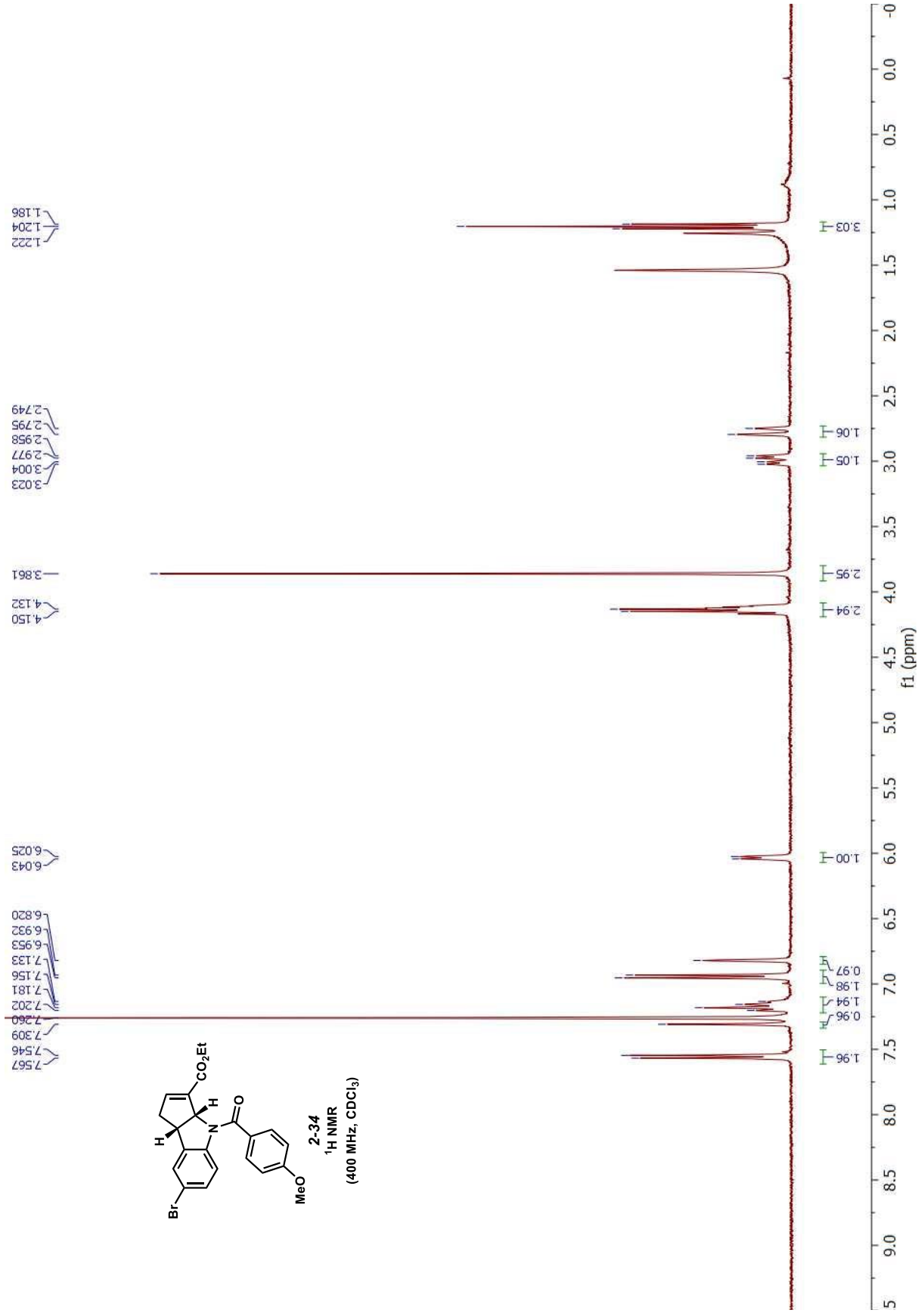
1.186
1.204
1.222
2.749
2.795
2.958
2.977
3.004
3.023
3.861
4.132
4.150
6.025
6.043
6.820
6.932
6.953
7.133
7.156
7.181
7.202
7.260
7.309
7.546
7.567
1.96
0.96
1.94
1.98
0.97
1.00
2.94
2.95
1.05
1.06
3.03
f1 (ppm)
2-34
1H NMR
(400 MHz, CDCl3)
CO2Et
H
N
O
H
Br
MeO

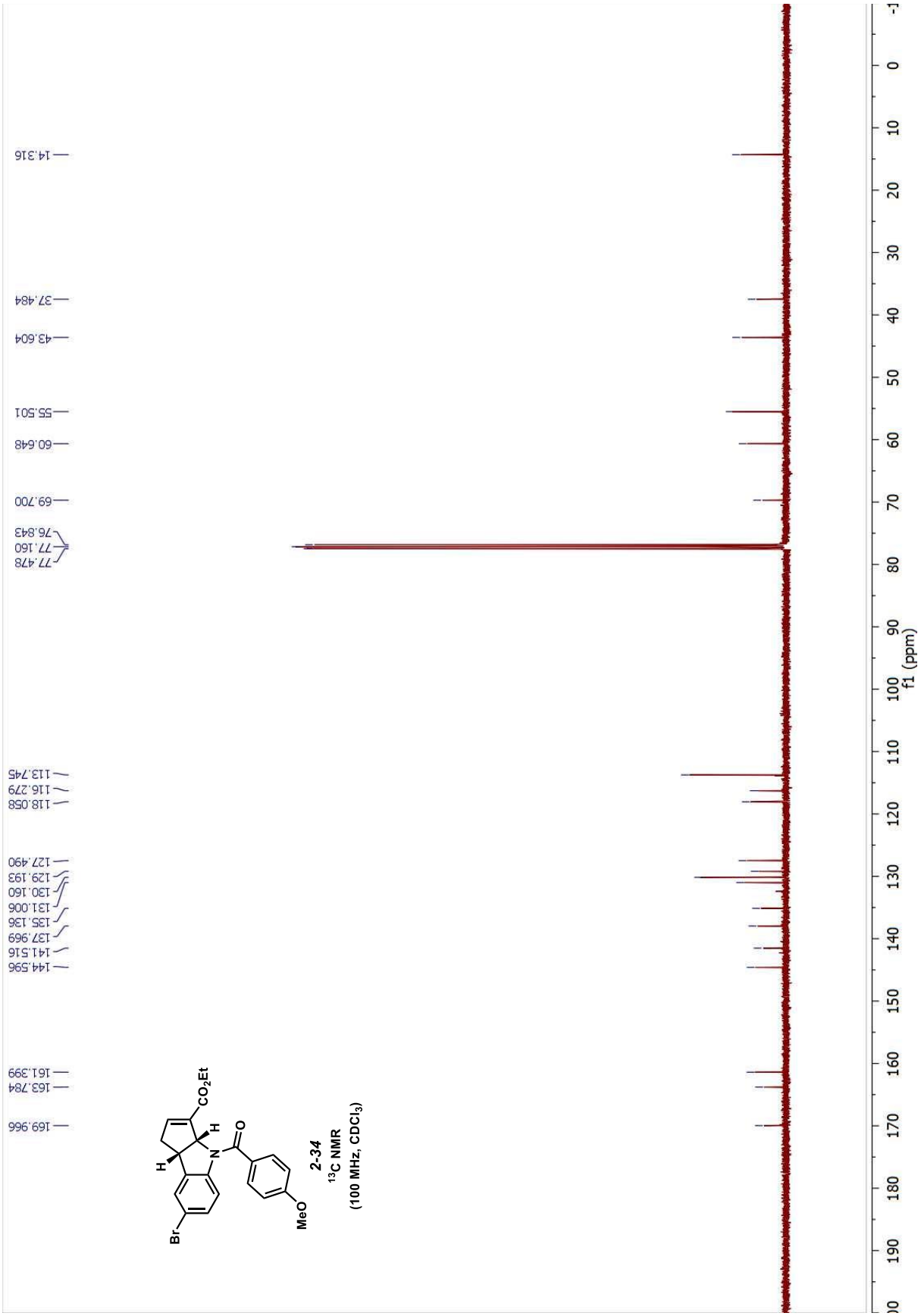
14.316
37.484
43.604
55.501
60.648
69.700
76.843
77.160
77.478
113.745
116.279
118.058
127.490
129.193
130.160
131.006
135.136
137.969
141.516
144.596
161.399
163.784
169.966
f1 (ppm)
CO2Et
H
N
O
H
Br
MeO
2-34
13C NMR
(100 MHz, CDCl3)

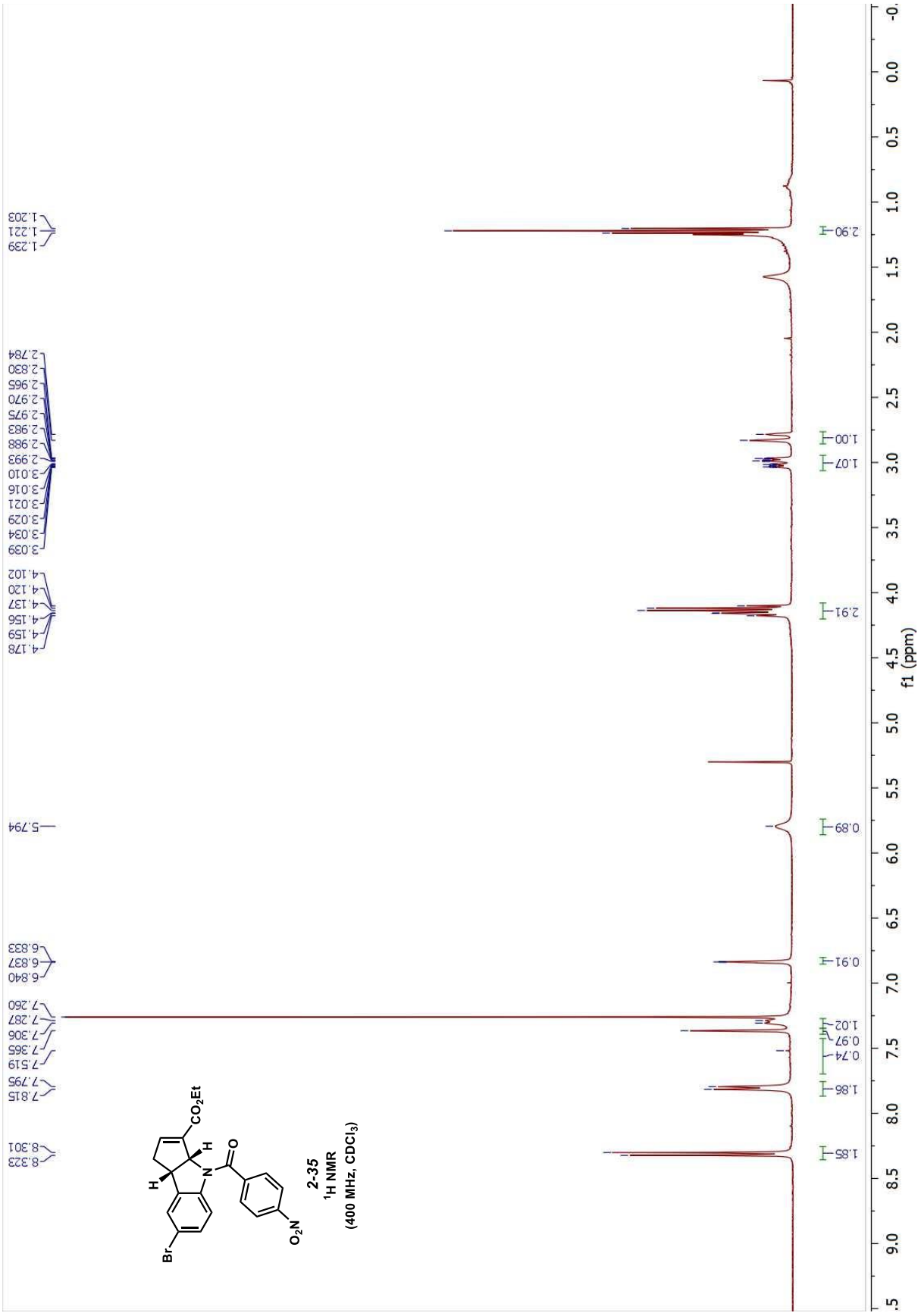
8.323
8.301
7.815
7.795
7.519
7.365
7.306
7.287
7.260
6.840
6.837
6.833
5.794
4.178
4.159
4.156
4.137
4.120
4.102
3.039
3.034
3.029
3.021
3.016
3.010
2.993
2.988
2.983
2.975
2.970
2.965
2.830
2.784
1.239
1.221
1.203
1.85
1.86
0.74
0.97
1.02
0.91
0.89
2.91
1.07
1.00
2.90
f1 (ppm)
2-35
1H NMR
(400 MHz, CDCl3)

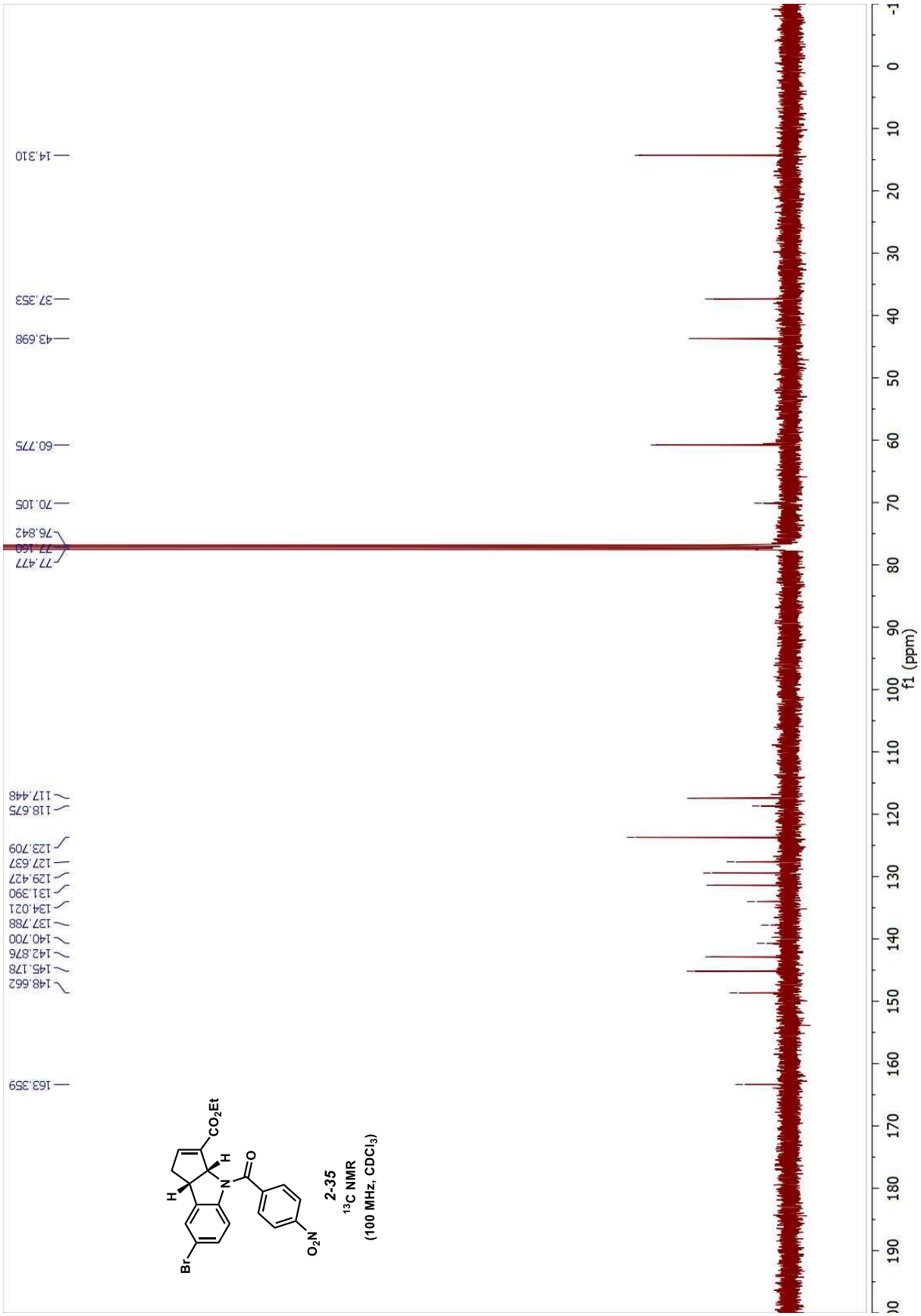
14.310
37.353
43.698
60.775
70.105
76.842
77.160
77.477
117.448
118.675
123.709
127.637
129.427
131.390
134.021
137.788
140.700
142.876
145.178
148.662
163.359
f1 (ppm)
2-35
13C NMR
(100 MHz, CDCl3)

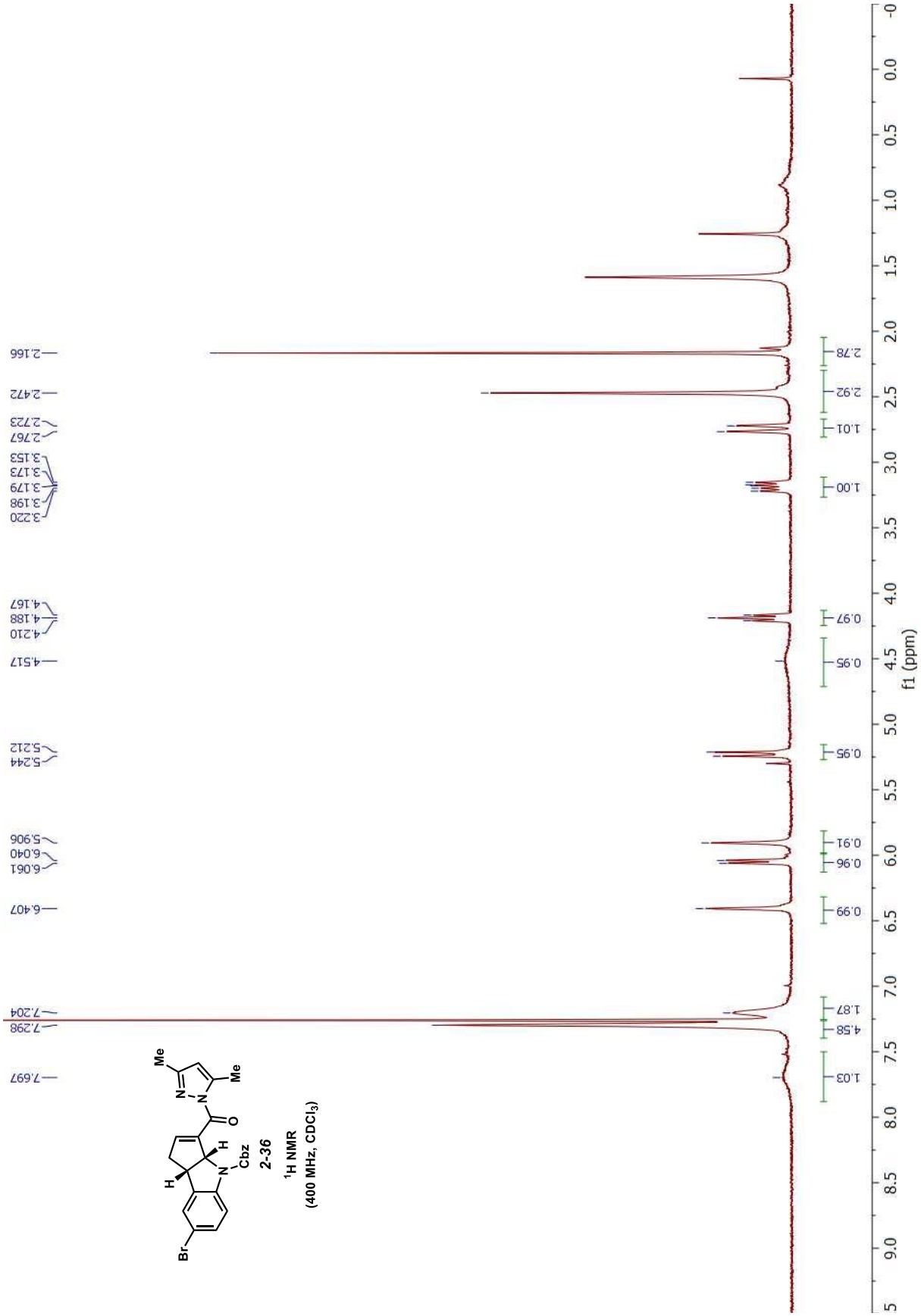
2-36
^{1}H NMR
(400 MHz, CDCl$_3$)
f1 (ppm)

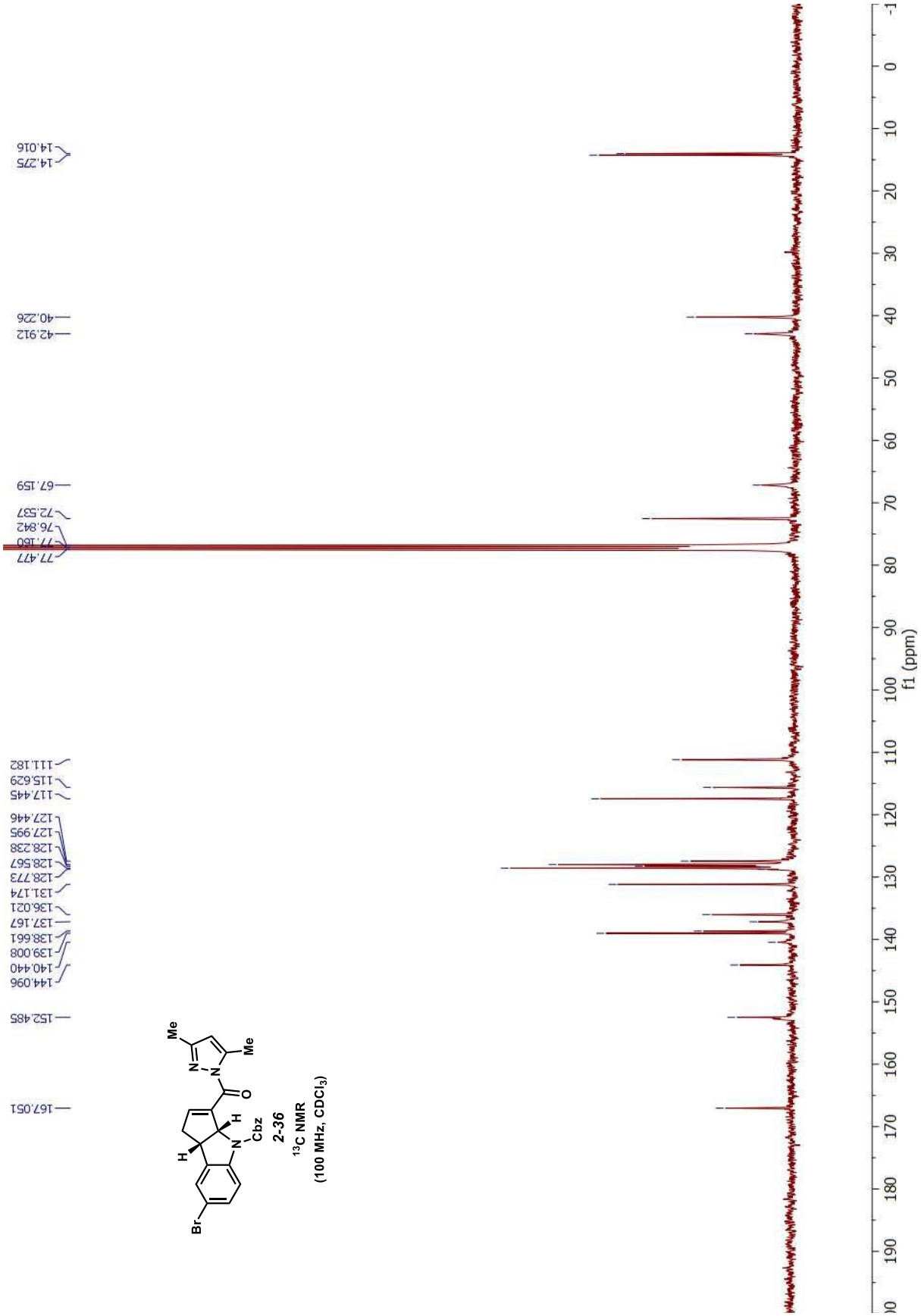
14.016
14.275
40.226
42.912
67.159
72.537
76.842
77.160
77.477
111.182
115.629
117.445
127.446
127.995
128.238
128.567
128.773
131.174
136.021
137.167
138.661
139.008
140.440
144.096
152.485
167.051
Me
Me
O
H
H
N
Cbz
Br
2-36
^{13}C NMR
(100 MHz, $CDCl_3$)
f1 (ppm)

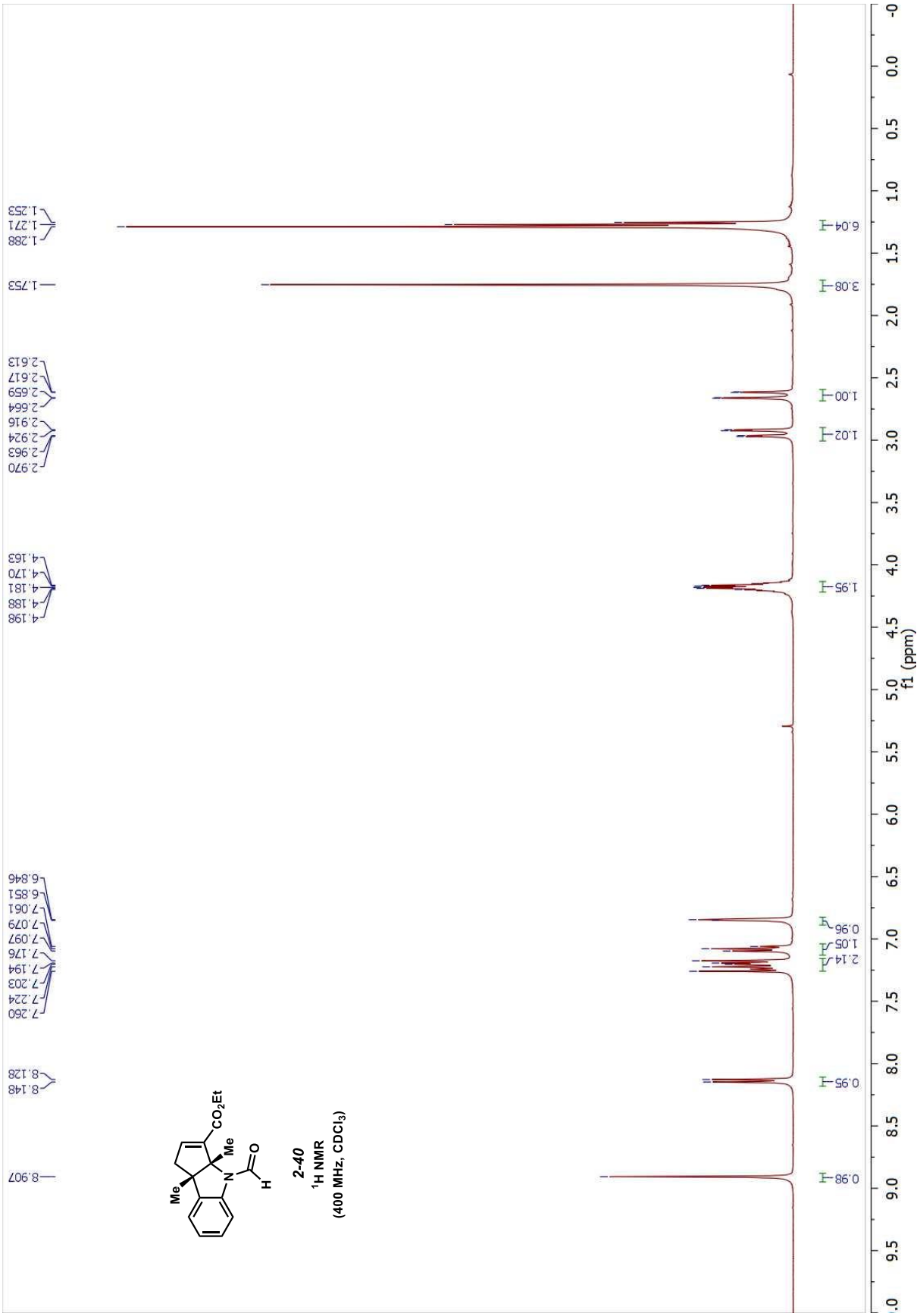
8.907
8.148
8.128
7.260
7.224
7.203
7.194
7.176
7.097
7.079
7.061
6.851
6.846
4.198
4.188
4.181
4.170
4.163
2.970
2.963
2.924
2.916
2.664
2.659
2.617
2.613
1.753
1.288
1.271
1.253
0.98
0.95
2.14
1.05
0.96
1.95
1.02
1.00
3.08
6.04
f1 (ppm)
Me
Me
N
O
H
CO2Et
2-40
1H NMR
(400 MHz, CDCl3)

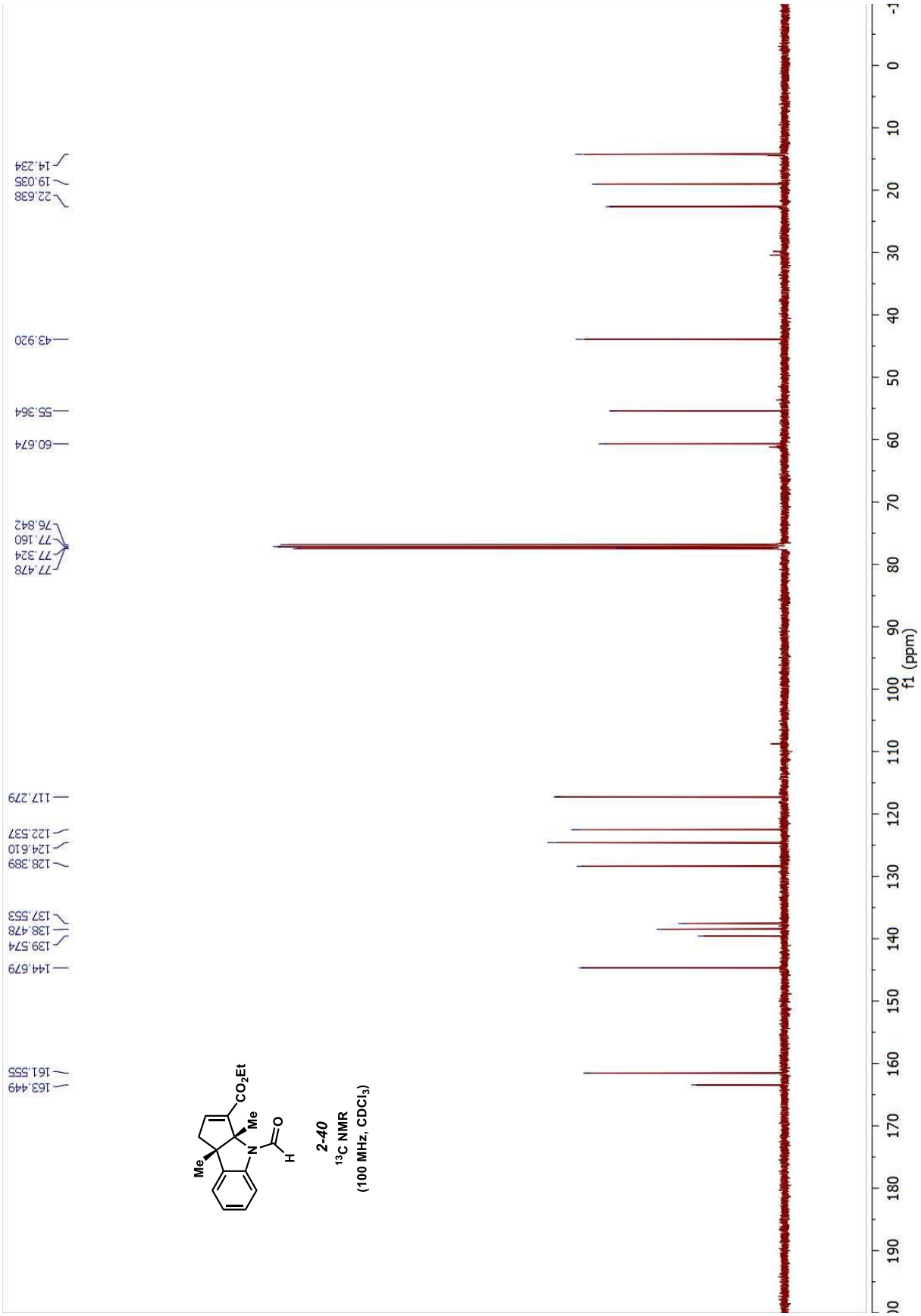
14.234
19.035
22.638
43.920
55.364
60.674
76.842
77.160
77.324
77.478
117.279
122.537
124.610
128.389
137.553
138.478
139.574
144.679
161.555
163.449
f1 (ppm)
2-40
13C NMR
(100 MHz, CDCl3)
CO2Et
Me
Me
N
O
H

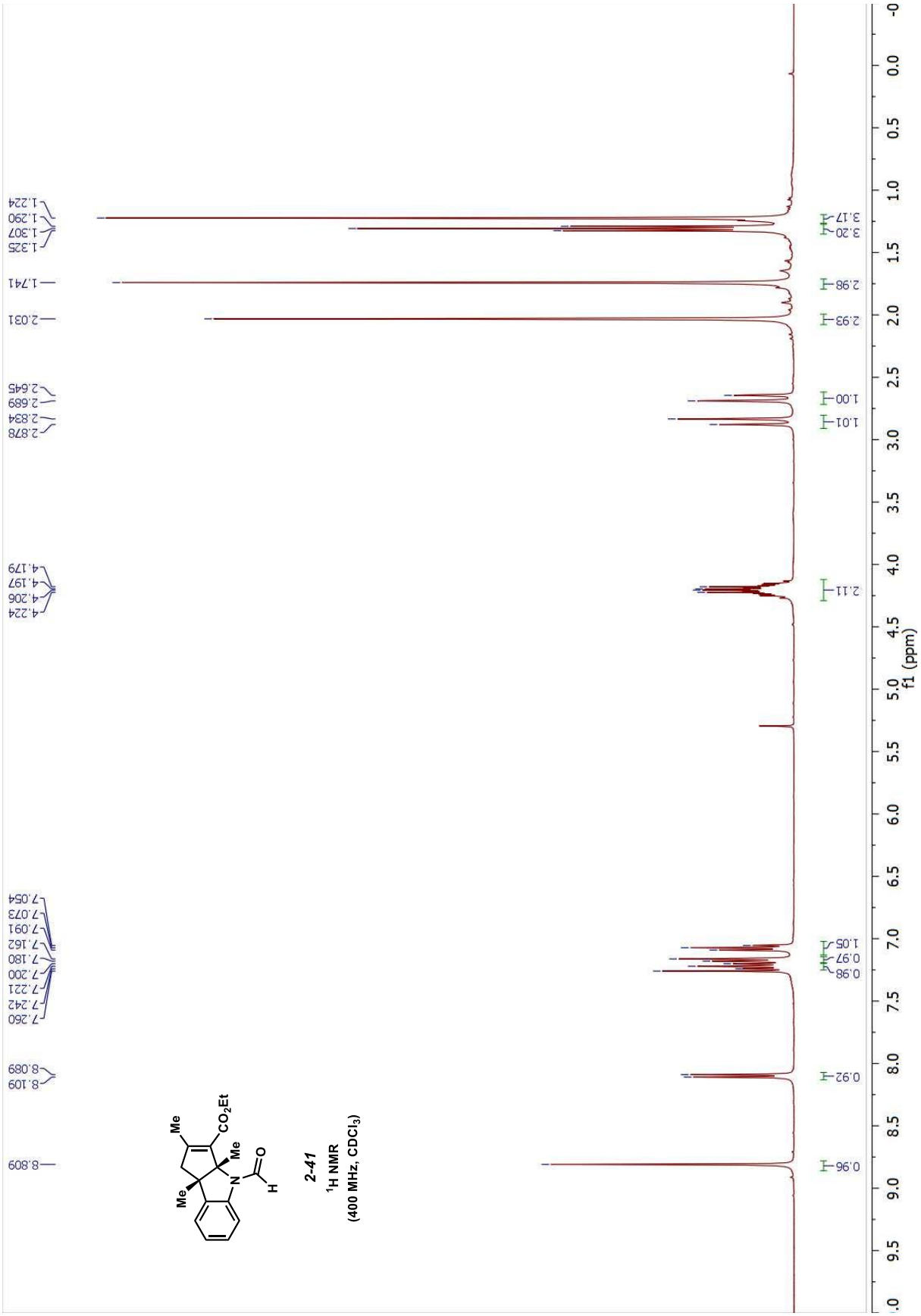
Me
CO2Et
Me
N
O
H
Me
2-41
1H NMR
(400 MHz, CDCl3)
f1 (ppm)

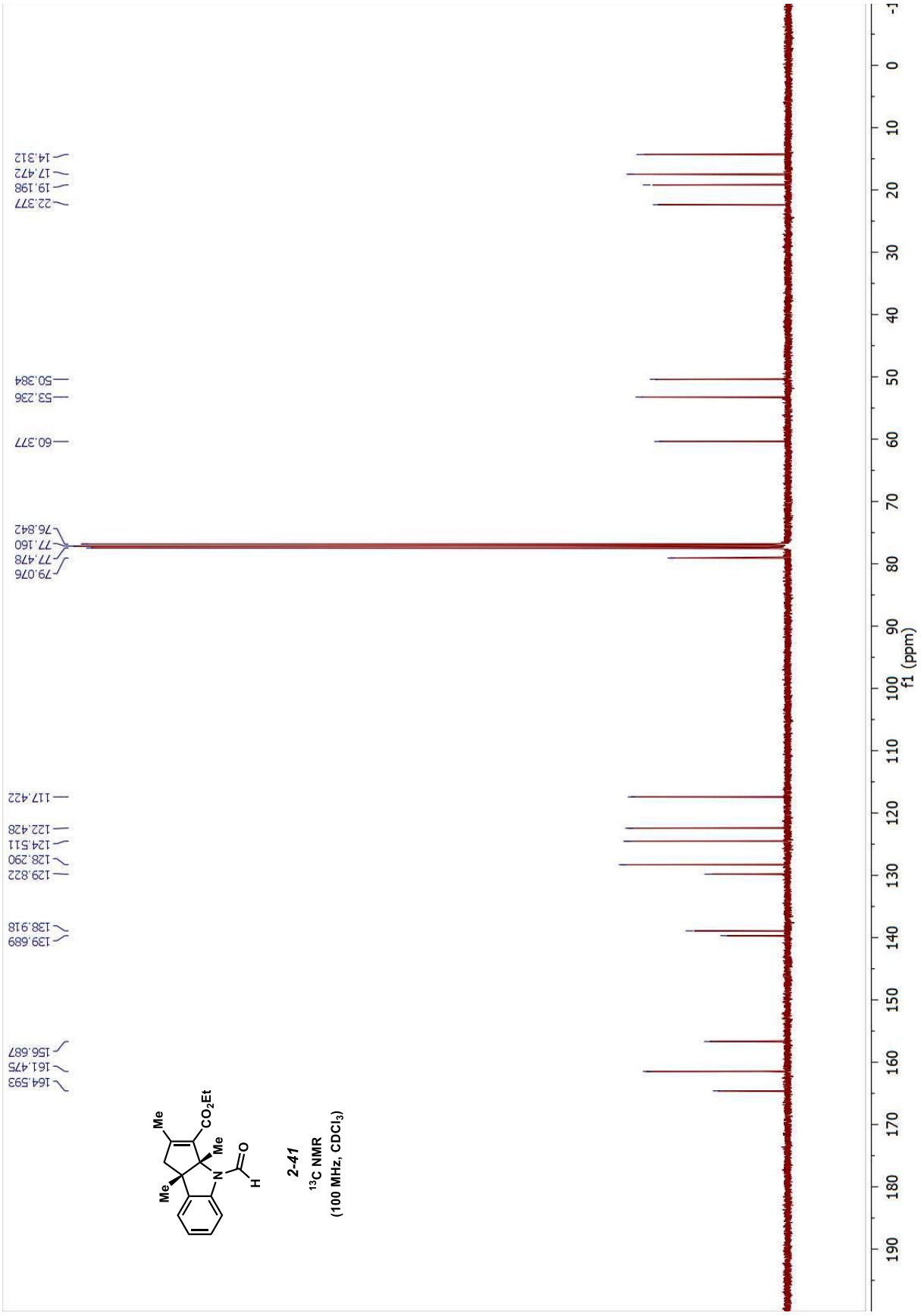
14.312
17.472
19.198
22.377
50.384
53.236
60.377
76.842
77.160
77.478
79.076
117.422
122.428
124.511
128.290
129.822
138.918
139.689
156.687
161.475
164.593
Me
CO2Et
Me
Me
N
O
H
2-41
13C NMR
(100 MHz, CDCl3)
f1 (ppm)

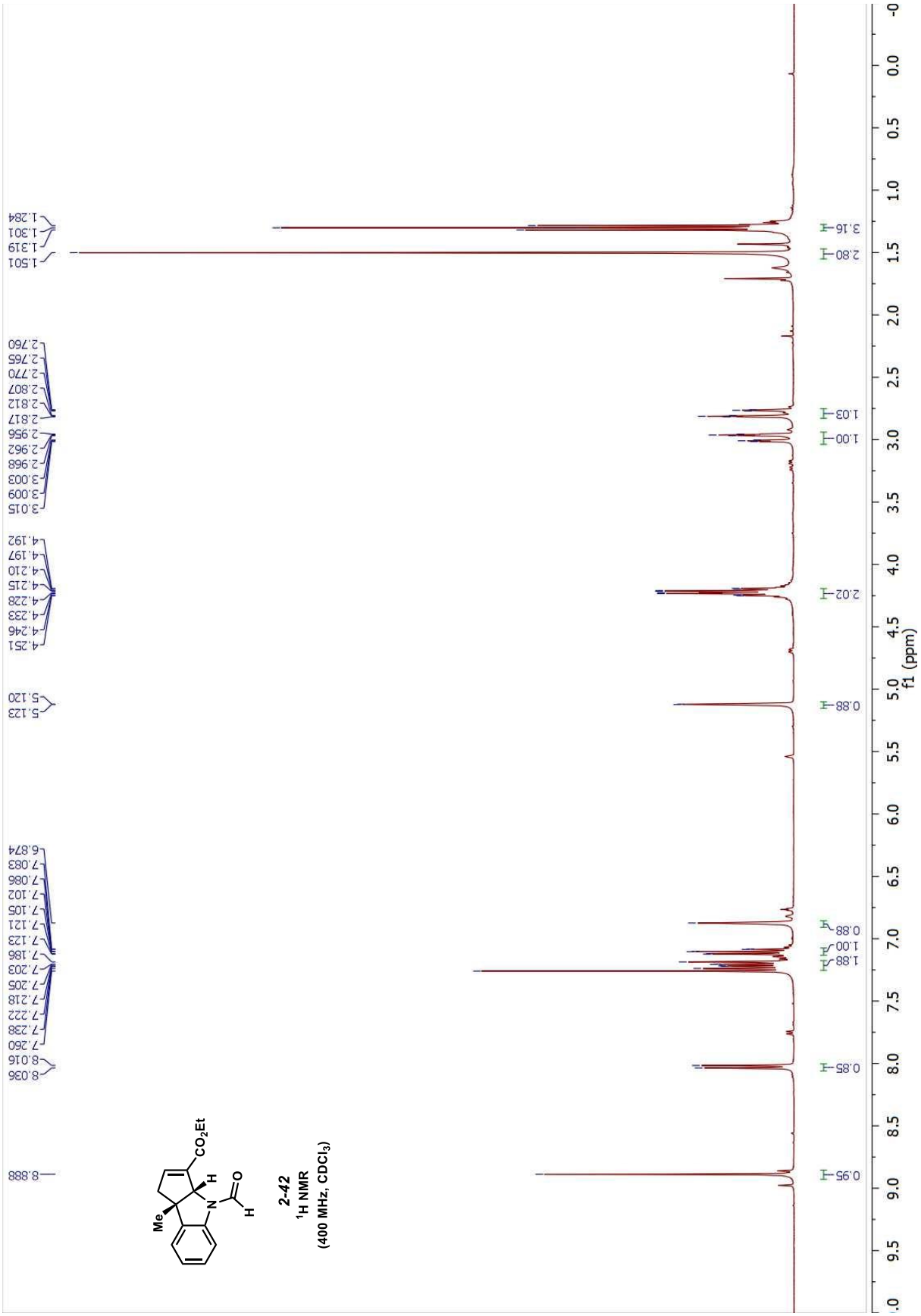
8.888
8.036
8.016
7.260
7.238
7.222
7.218
7.205
7.203
7.186
7.123
7.121
7.105
7.102
7.086
7.083
6.874
5.123
5.120
4.251
4.246
4.233
4.228
4.215
4.210
4.197
4.192
3.015
3.009
3.003
2.968
2.962
2.956
2.817
2.812
2.807
2.770
2.765
2.760
1.501
1.319
1.301
1.284
0.95
0.85
0.88
1.00
1.88
0.88
2.02
1.00
1.03
2.80
3.16
Me
CO2Et
H
N
O
H
2-42
1H NMR
(400 MHz, CDCl3)
f1 (ppm)

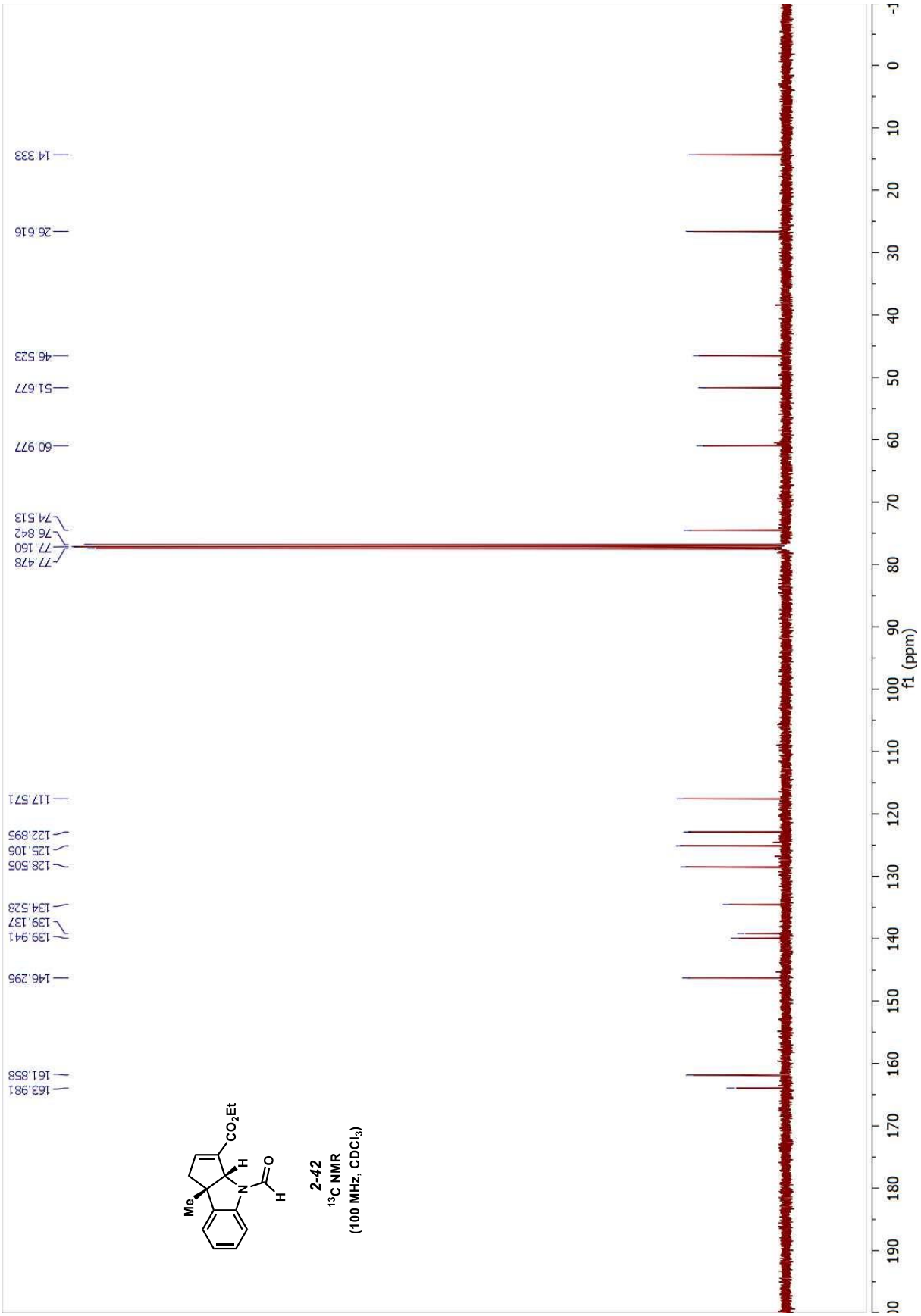
14.333
26.616
46.523
51.677
60.977
74.513
76.842
77.160
77.478
117.571
122.895
125.106
128.505
134.528
139.137
139.941
146.296
161.858
163.981
f1 (ppm)
Me
CO2Et
H
N
O
H
2-42
13C NMR
(100 MHz, CDCl3)

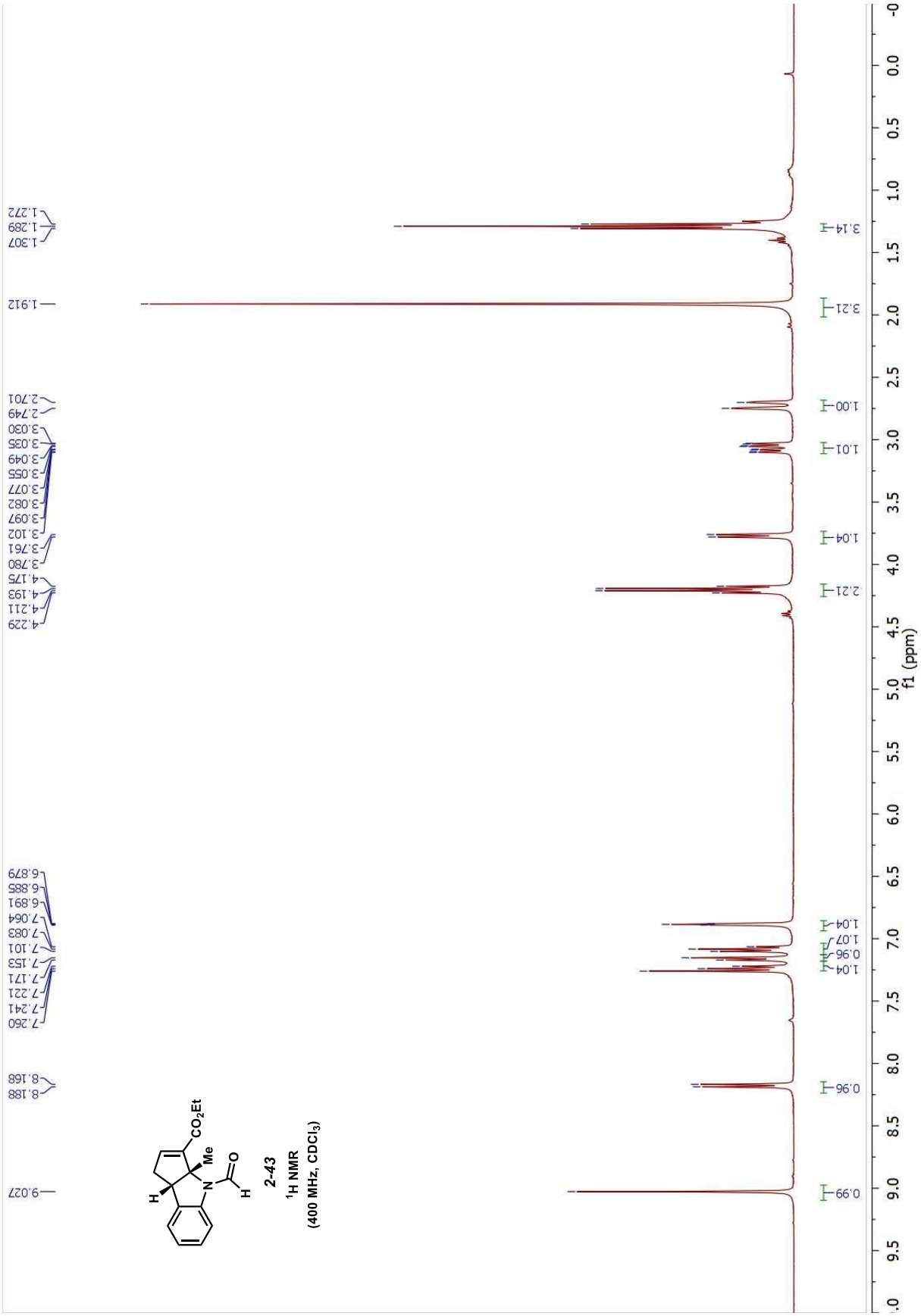
CO2Et
Me
N
O
H
H
2-43
1H NMR
(400 MHz, CDCl3)
f1 (ppm)

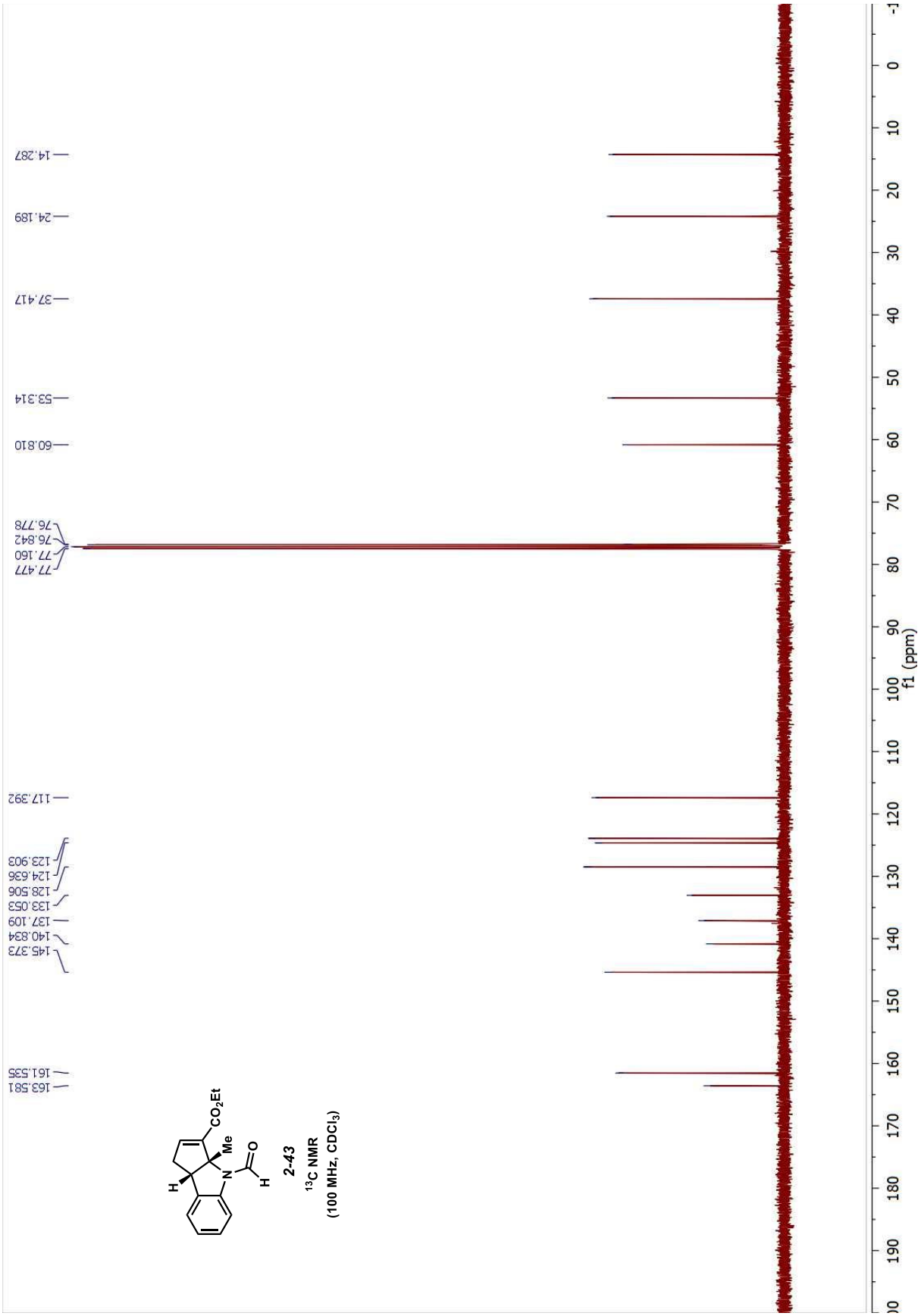
14.287
24.189
37.417
53.314
60.810
76.778
76.842
77.160
77.477
117.392
123.903
124.636
128.506
133.053
137.109
140.834
145.373
161.535
163.581
f1 (ppm)
2-43
13C NMR
(100 MHz, CDCl3)
CO2Et
Me
O
H
N
H

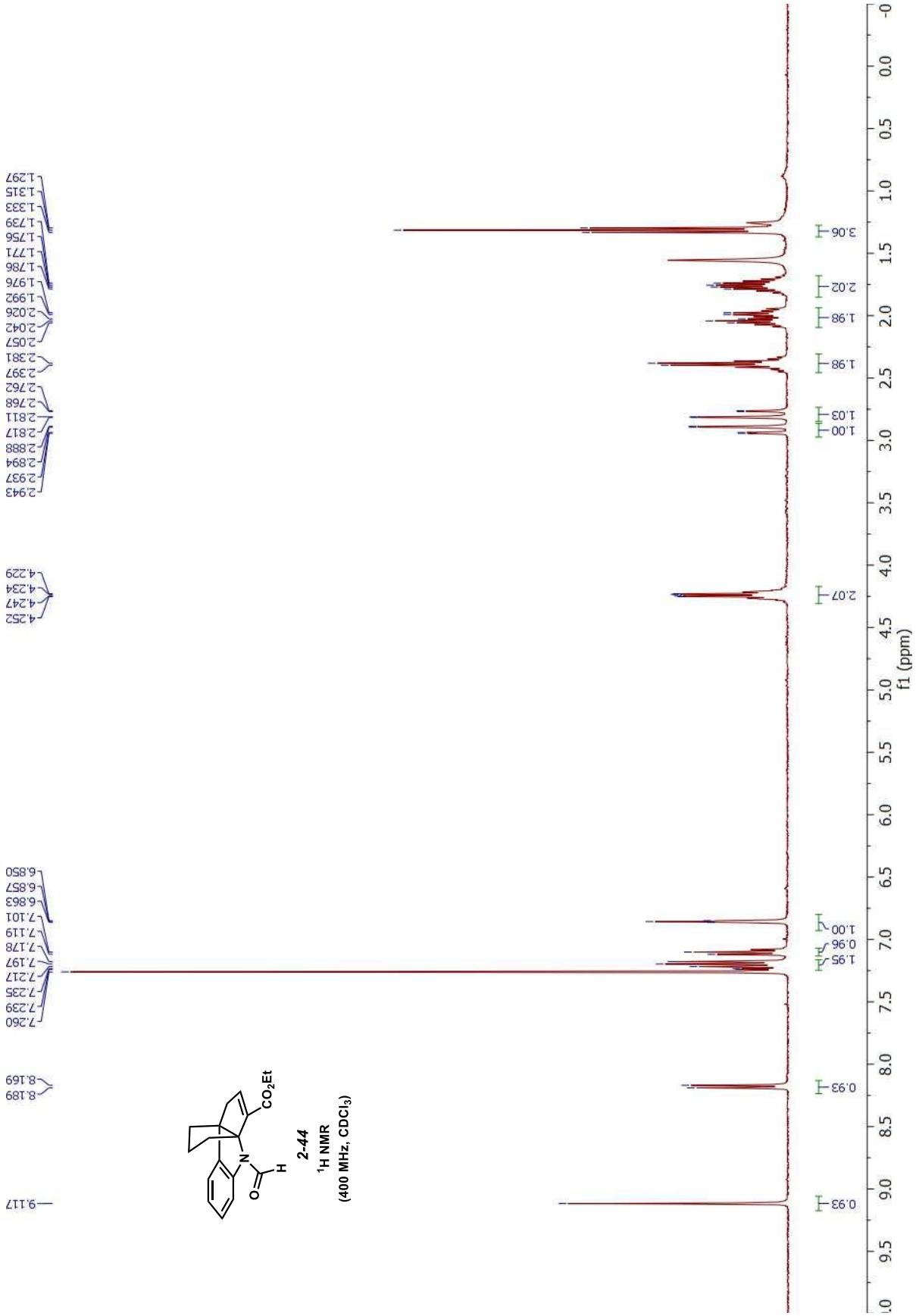
CO2Et
N
O
H
2-44
1H NMR
(400 MHz, CDCl3)
f1 (ppm)

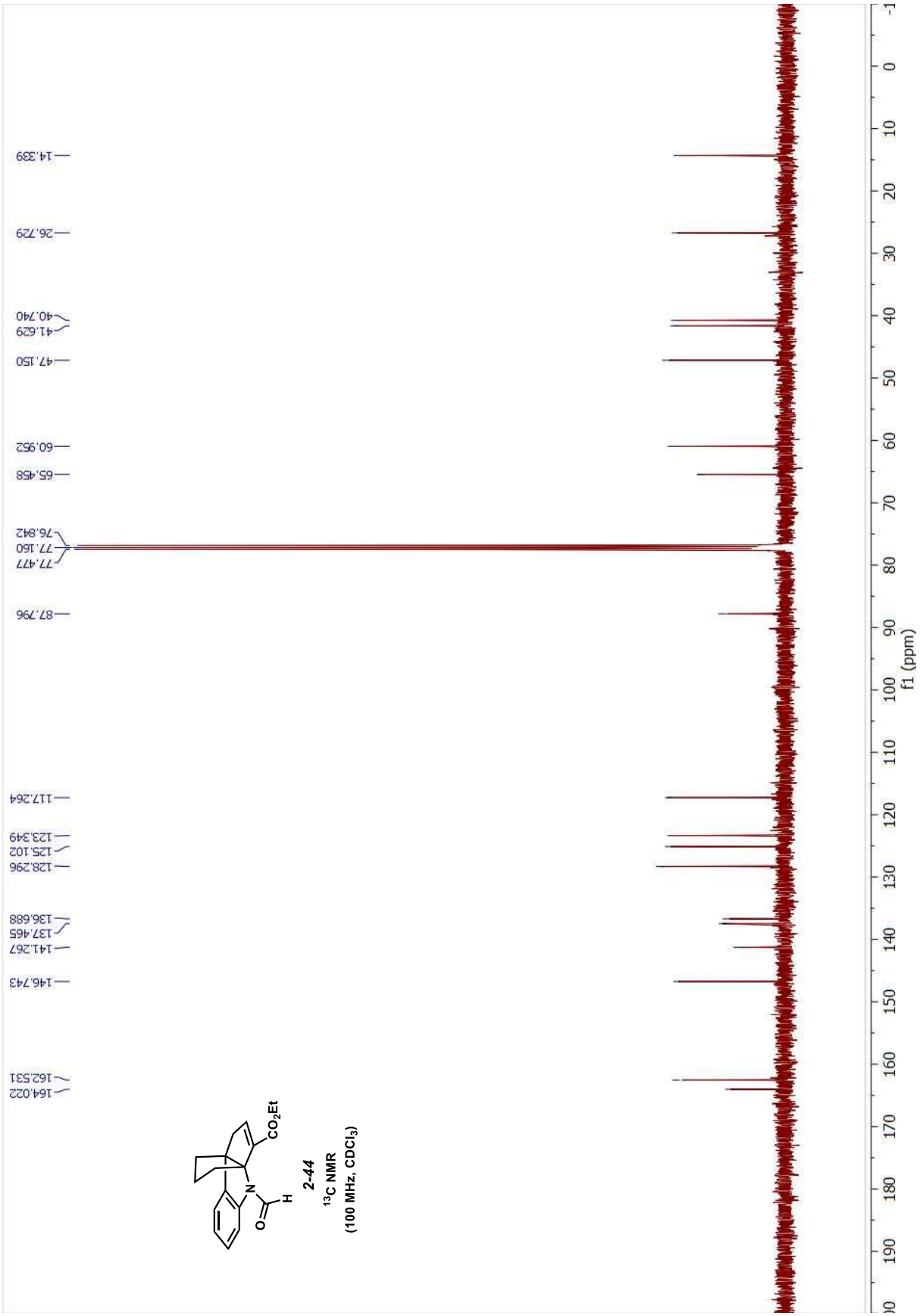
14.339
26.729
40.740
41.629
47.150
60.952
65.458
76.842
77.160
77.477
87.796
117.264
123.349
125.102
128.296
136.688
137.465
141.267
146.743
162.531
164.022
f1 (ppm)
CO2Et
N
H
O
2-44
13C NMR
(100 MHz, CDCl3)

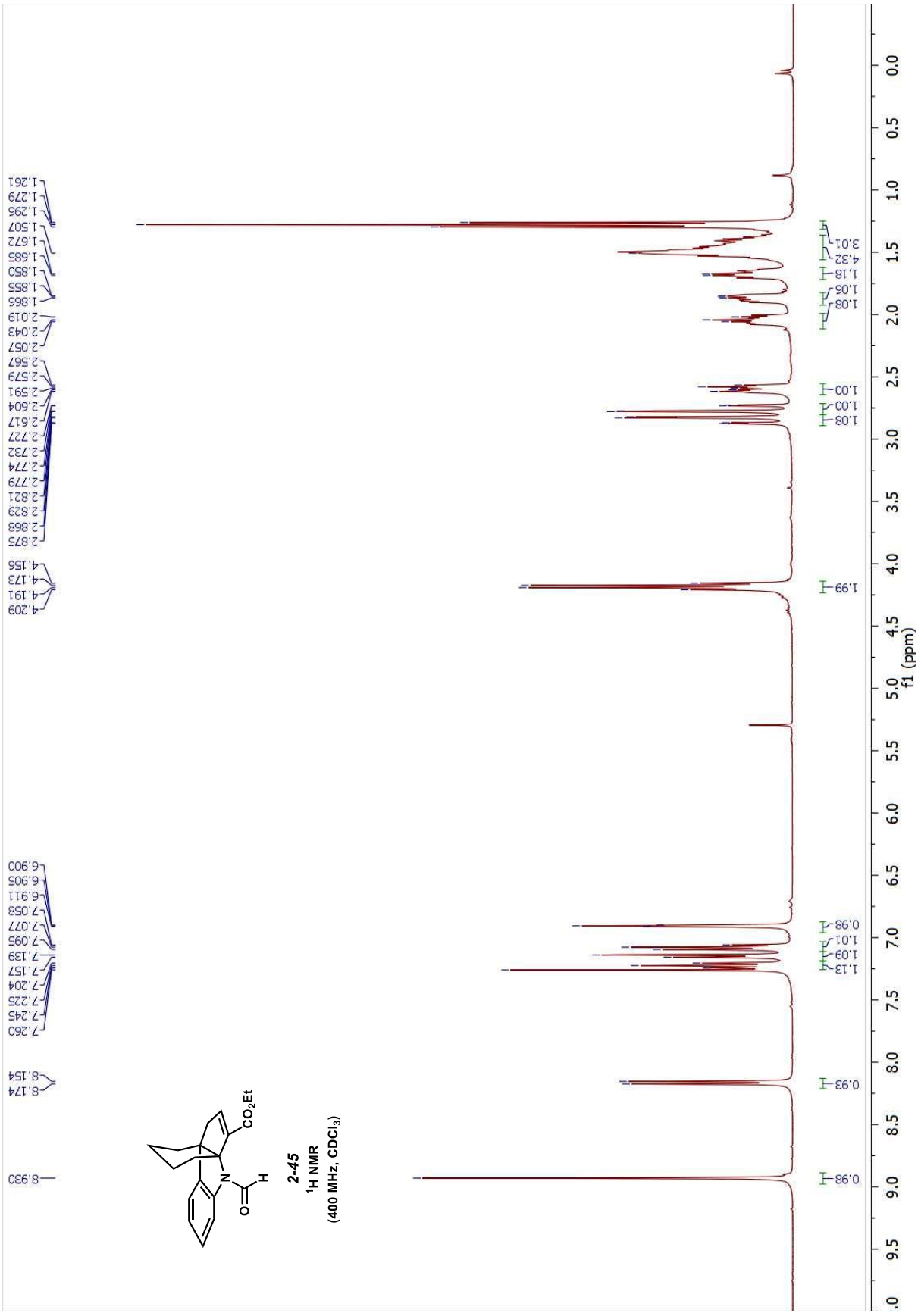
2-45
^{1}H NMR
(400 MHz, $CDCl_3$)
CO_2Et
N
H
O
f1 (ppm)

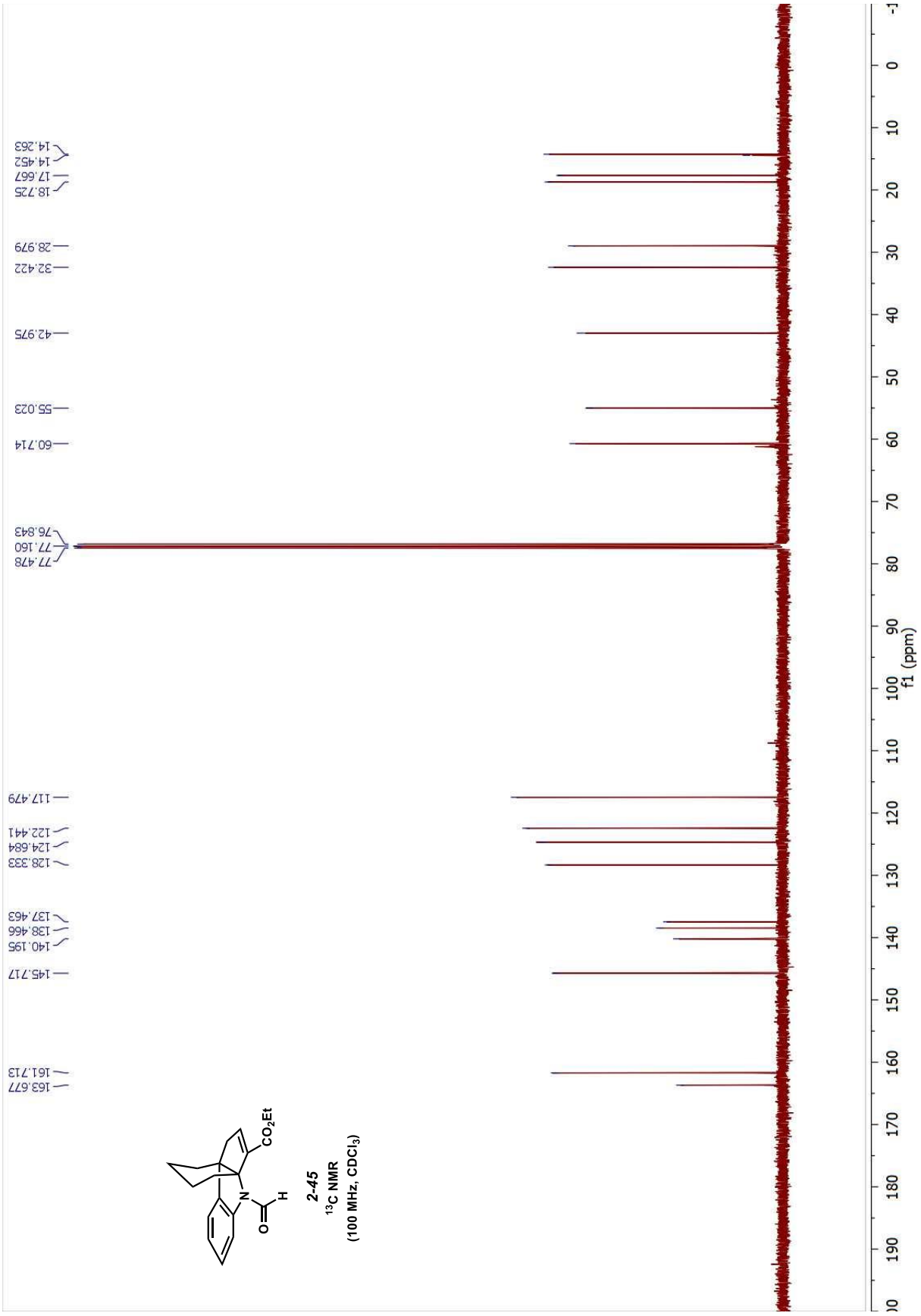
14.263
14.452
17.667
18.725
28.979
32.422
42.975
55.023
60.714
76.843
77.160
77.478
117.479
122.441
124.684
128.333
137.463
138.466
140.195
145.717
161.713
163.677
CO2Et
N
O
H
2-45
13C NMR
(100 MHz, CDCl3)
f1 (ppm)

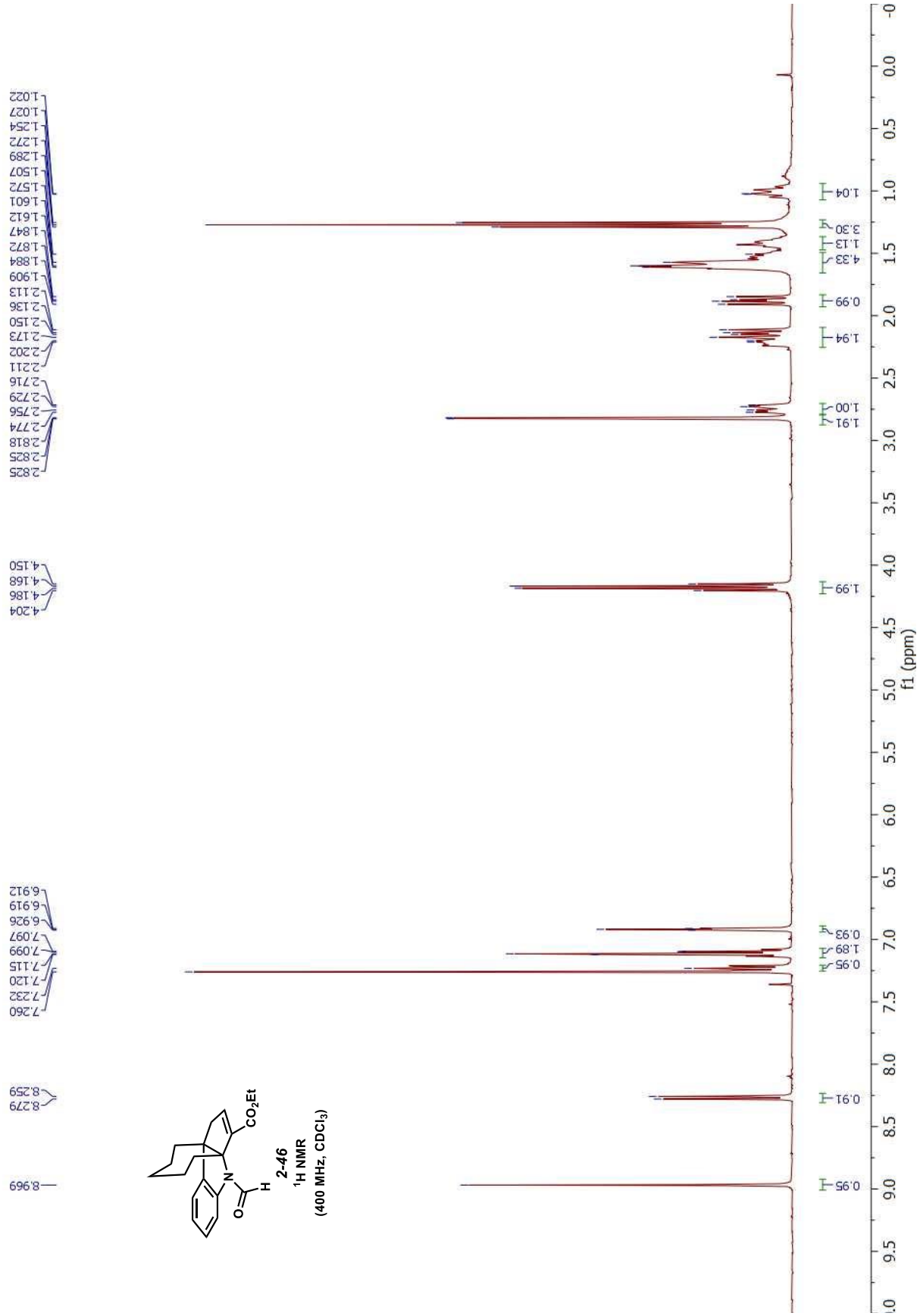
CO2Et
N
H
O
2-46
1H NMR
(400 MHz, CDCl3)
f1 (ppm)

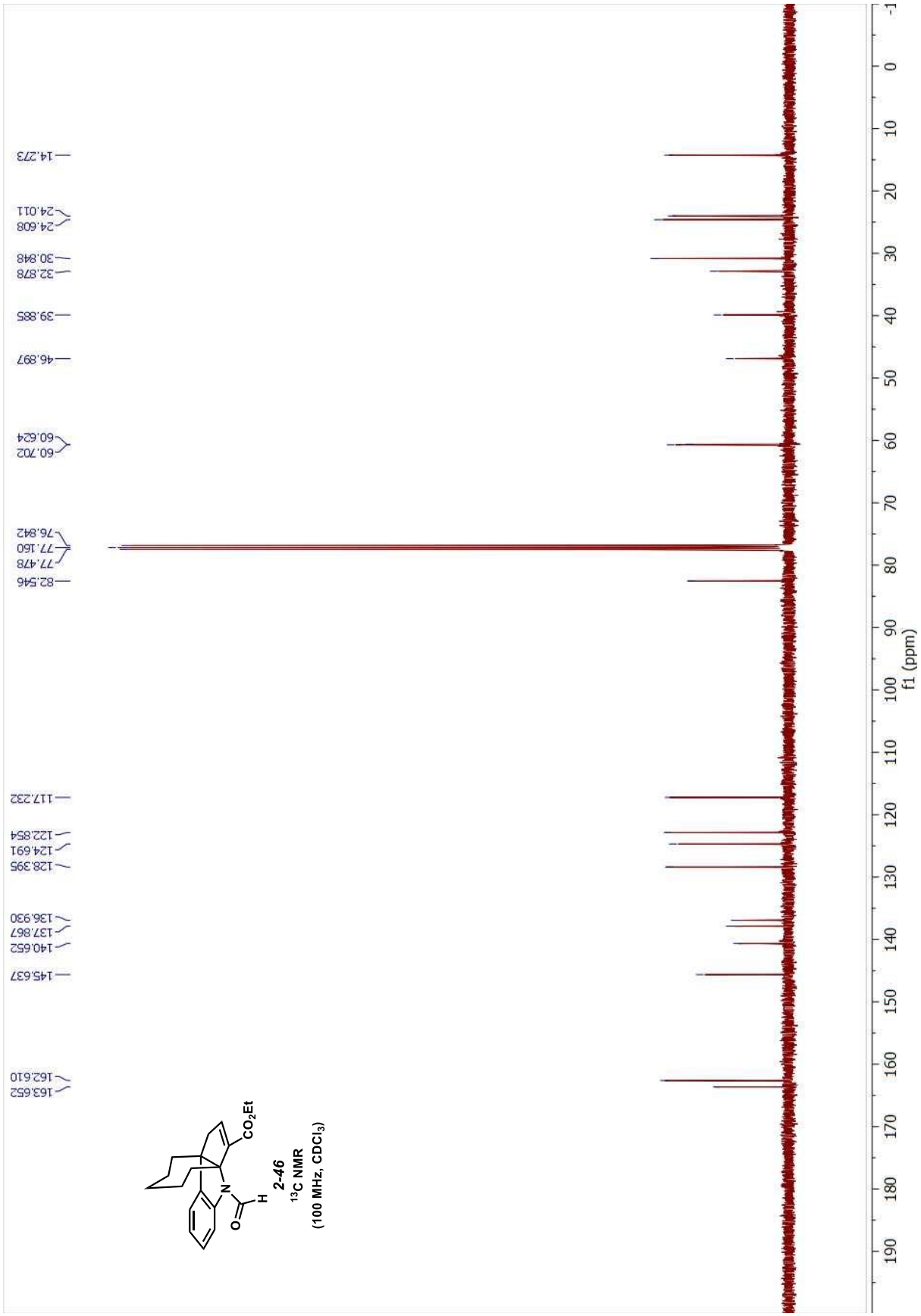
14.273
24.011
24.608
30.848
32.878
39.885
46.897
60.624
60.702
76.842
77.160
77.478
82.546
117.232
122.854
124.691
128.395
136.930
137.867
140.652
145.637
162.610
163.652
f1 (ppm)
CO2Et
N
O
H
2-46
13C NMR
(100 MHz, CDCl3)

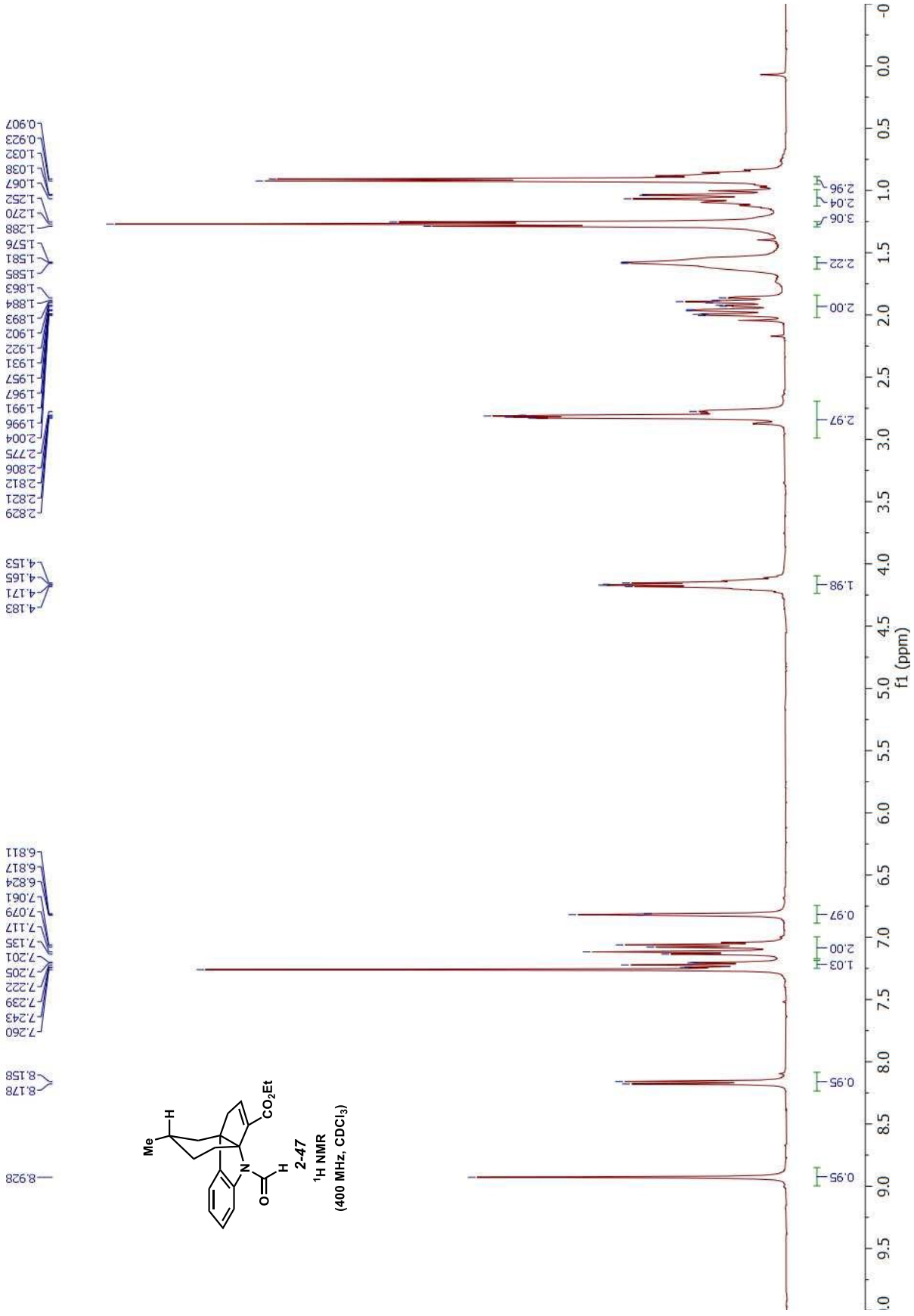
8.928
8.178
8.158
7.260
7.243
7.239
7.222
7.205
7.201
7.135
7.117
7.079
7.061
6.824
6.817
6.811
4.183
4.171
4.165
4.153
2.829
2.821
2.812
2.806
2.775
2.004
1.996
1.991
1.967
1.957
1.931
1.922
1.902
1.893
1.884
1.863
1.585
1.581
1.576
1.288
1.270
1.252
1.067
1.038
1.032
0.923
0.907
0.95
0.95
1.03
2.00
0.97
2.97
1.98
2.00
2.22
3.06
2.04
2.96
f1 (ppm)
Me
H
CO2Et
N
H
O
2-47
1H NMR
(400 MHz, CDCl3)

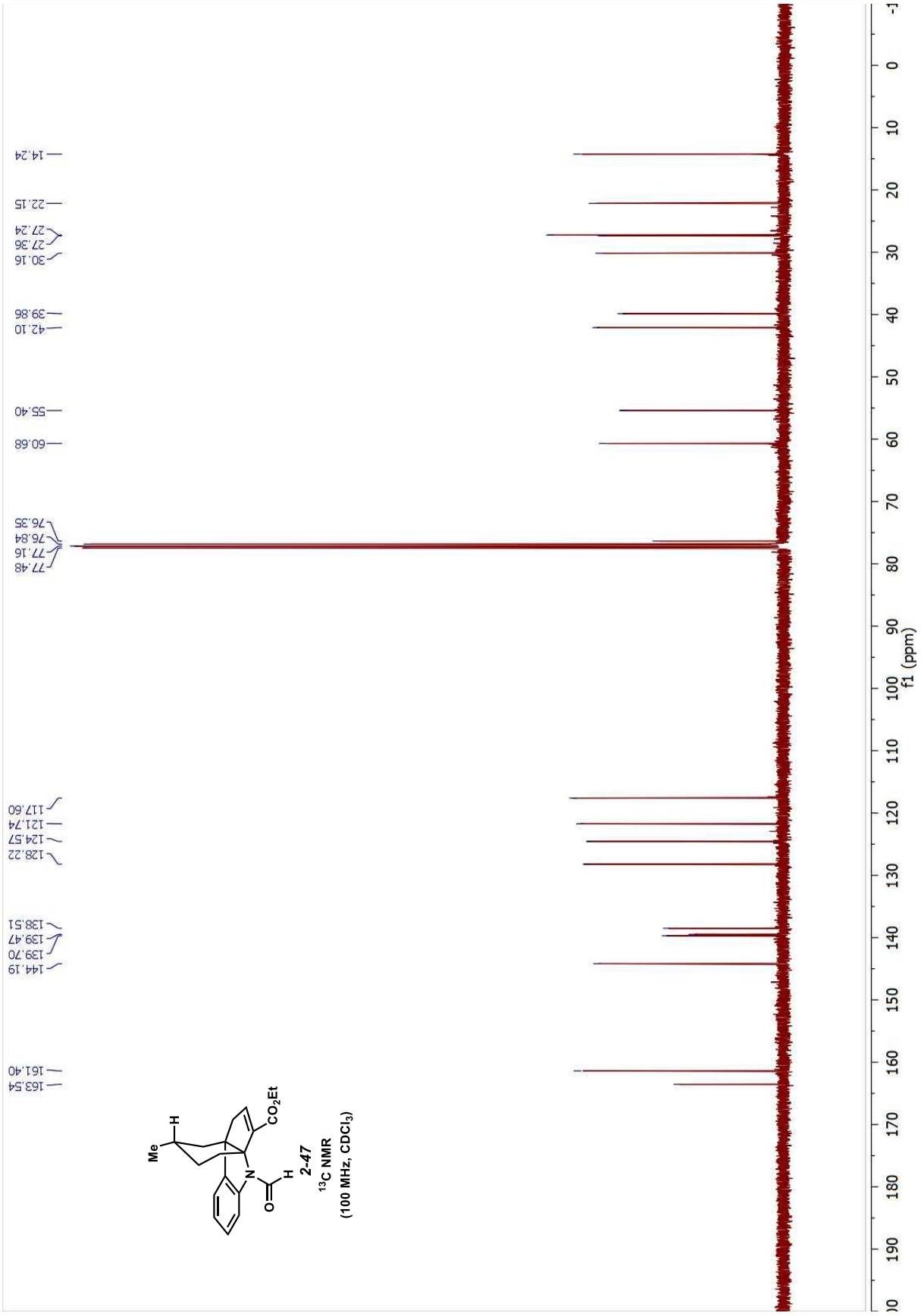
14.24
22.15
27.24
27.36
30.16
39.86
42.10
55.40
60.68
76.35
76.84
77.16
77.48
117.60
121.74
124.57
128.22
138.51
139.47
139.70
144.19
161.40
163.54
f1 (ppm)
Me
H
CO2Et
N
O
H
2-47
13C NMR
(100 MHz, CDCl3)

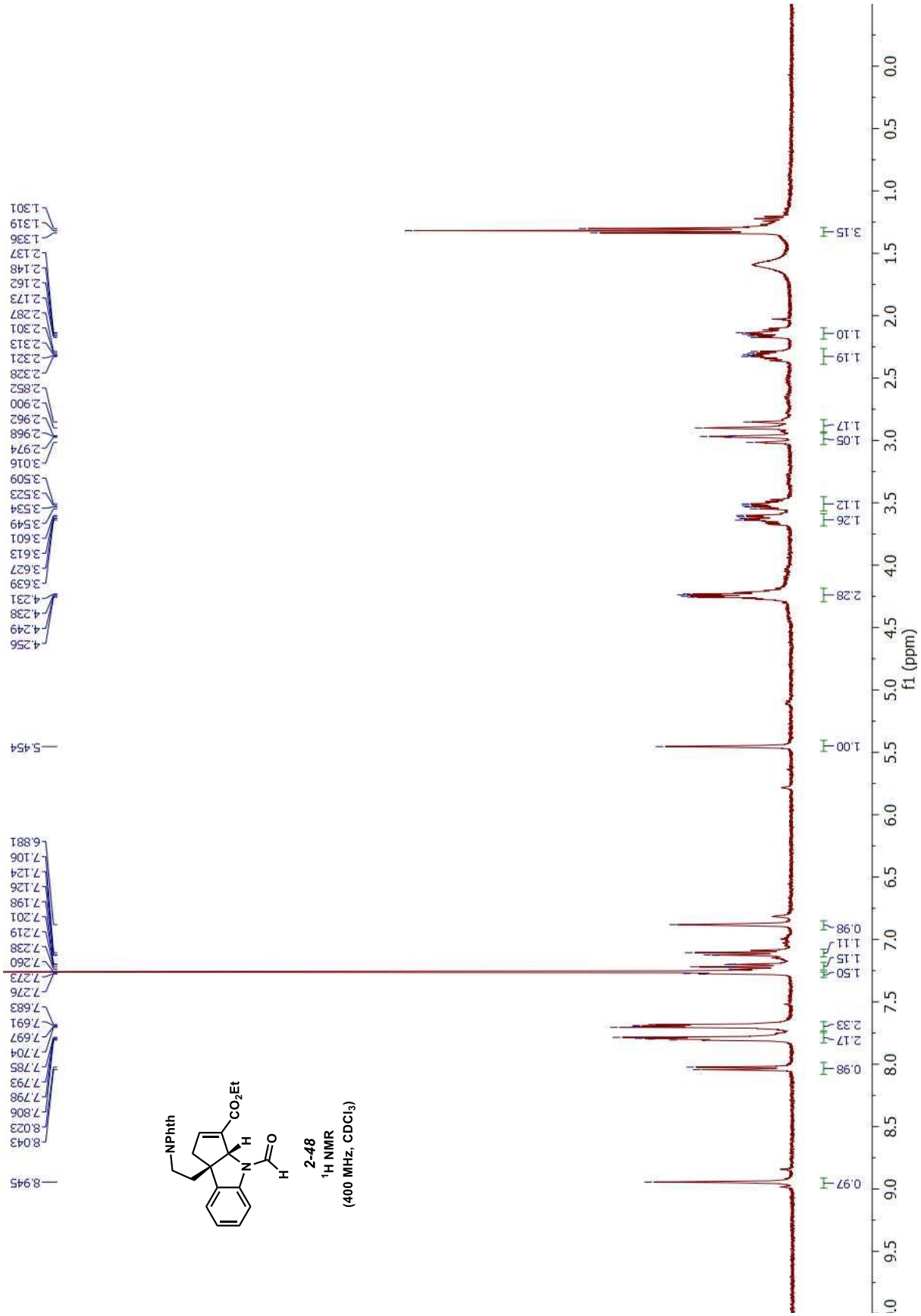
NPhth
CO2Et
H
N
O
H
2-48
1H NMR
(400 MHz, CDCl3)
f1 (ppm)

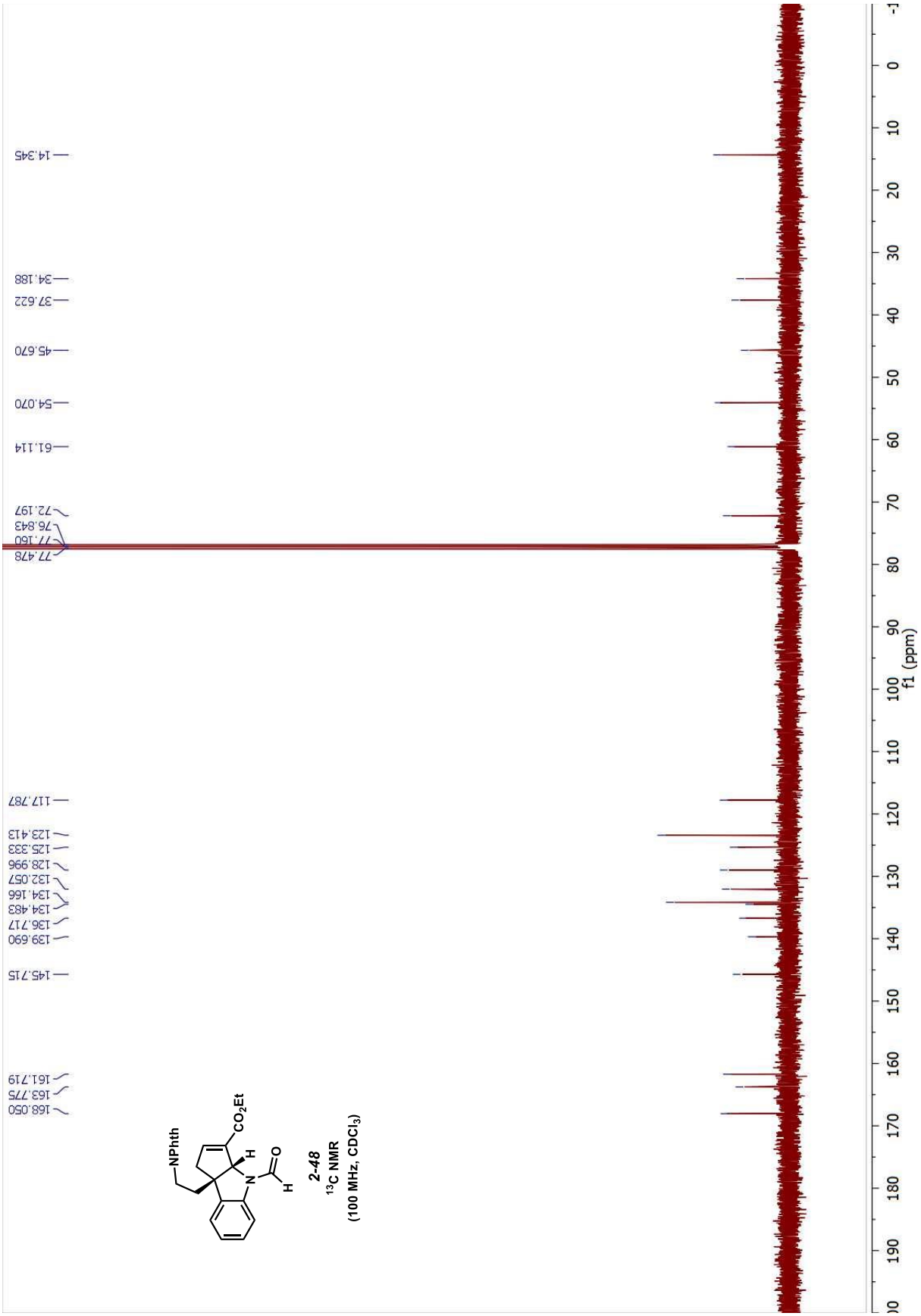
14.345
34.188
37.622
45.670
54.070
61.114
72.197
76.843
77.160
77.478
117.787
123.413
125.333
128.996
132.057
134.166
134.483
136.717
139.690
145.715
161.719
163.775
168.050
NPhth
CO2Et
H
N
O
H
2-48
13C NMR
(100 MHz, CDCl3)
f1 (ppm)

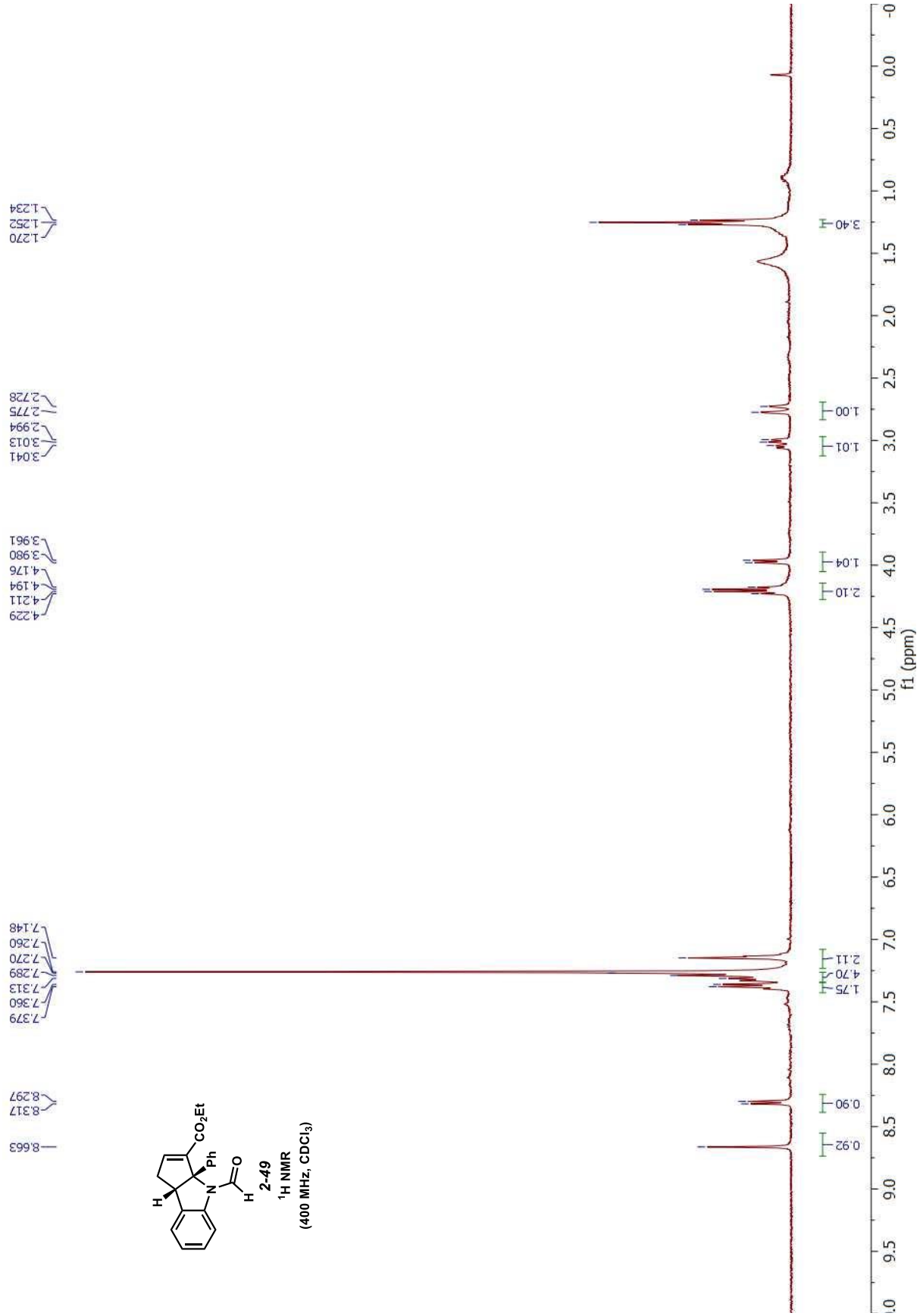
8.663
8.317
8.297
7.379
7.360
7.313
7.289
7.270
7.260
7.148
4.229
4.211
4.194
4.176
3.980
3.961
3.041
3.013
2.994
2.775
2.728
1.270
1.252
1.234
0.92
0.90
2.11
4.70
1.75
2.10
1.04
1.01
1.00
3.40
f1 (ppm)
Ph
CO2Et
N
O
H
H
2-49
1H NMR
(400 MHz, CDCl3)

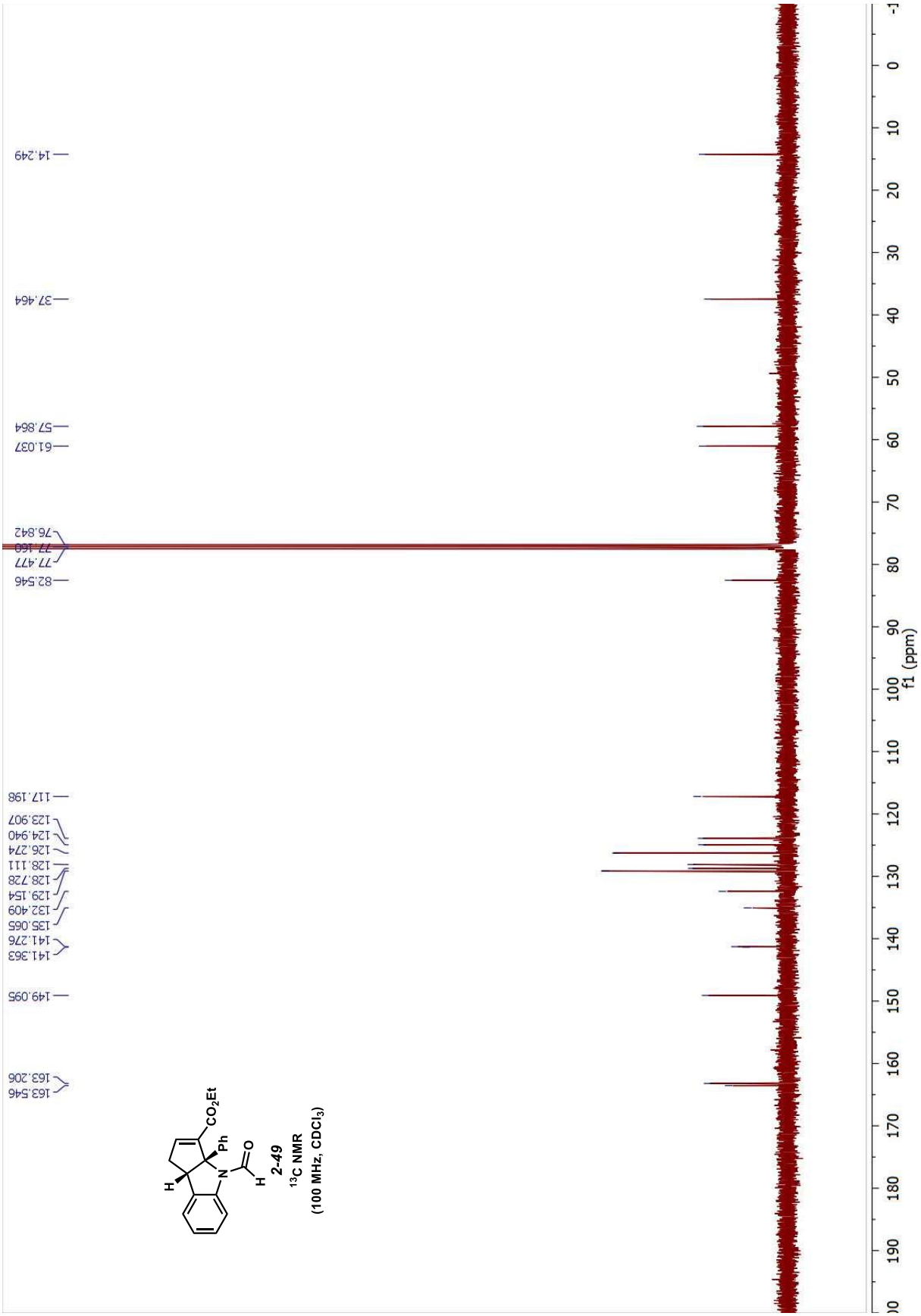
14.249
37.464
57.864
61.037
76.842
77.160
77.477
82.546
117.198
123.907
124.940
126.274
128.111
128.728
129.154
132.409
135.065
141.276
141.363
149.095
163.206
163.546
CO2Et
Ph
N
O
H
H
2-49
13C NMR
(100 MHz, CDCl3)
f1 (ppm)

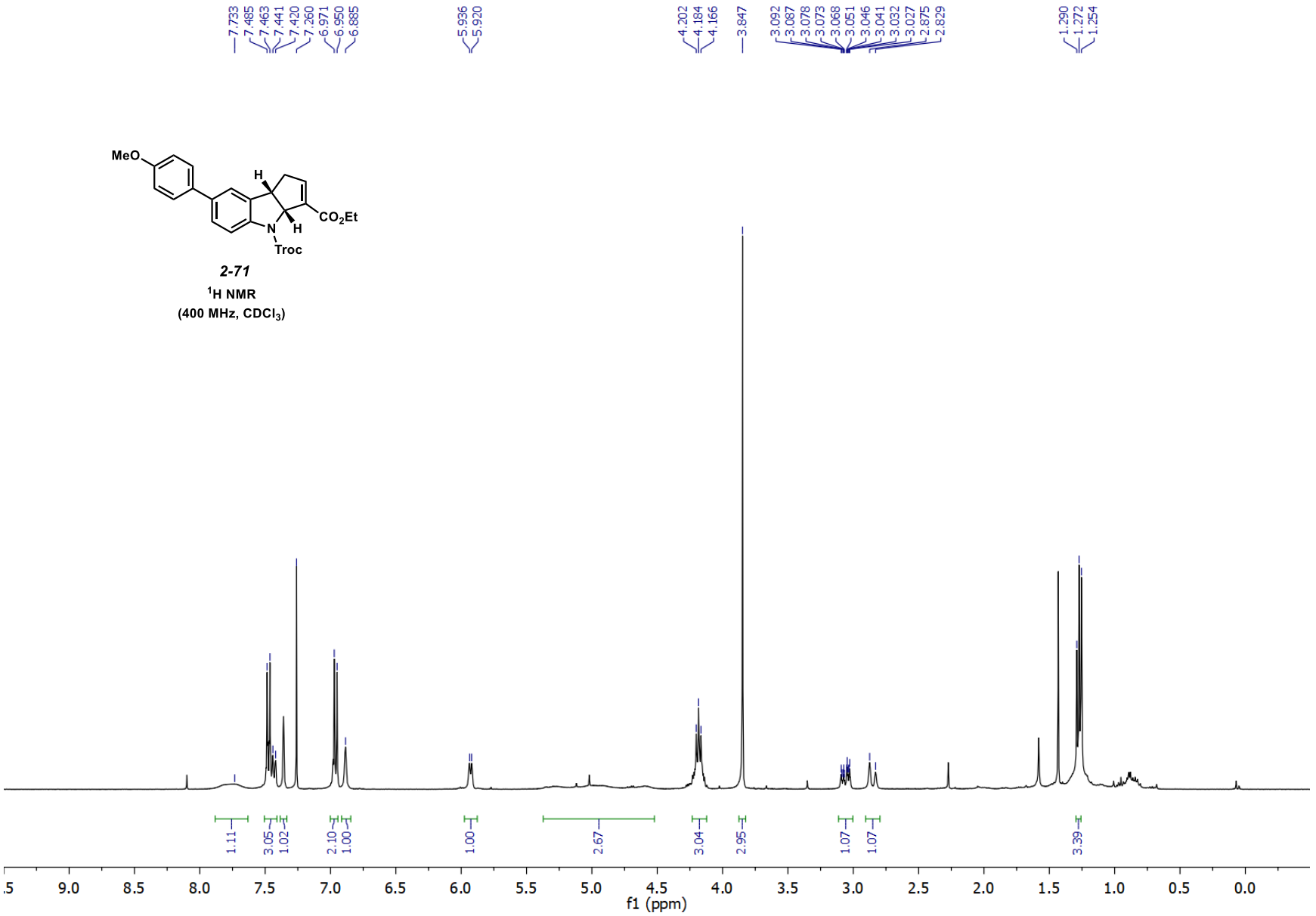
7.733
7.485
7.463
7.441
7.420
7.260
6.971
6.950
6.885
5.936
5.920
4.202
4.184
4.166
3.847
3.092
3.087
3.078
3.073
3.068
3.051
3.046
3.041
3.032
3.027
2.875
2.829
1.290
1.272
1.254
MeO
H
N
H
CO2Et
Troc
2-71
1H NMR
(400 MHz, CDCl3)
1.11
3.05
1.02
2.10
1.00
1.00
2.67
3.04
2.95
1.07
1.07
3.39
f1 (ppm)

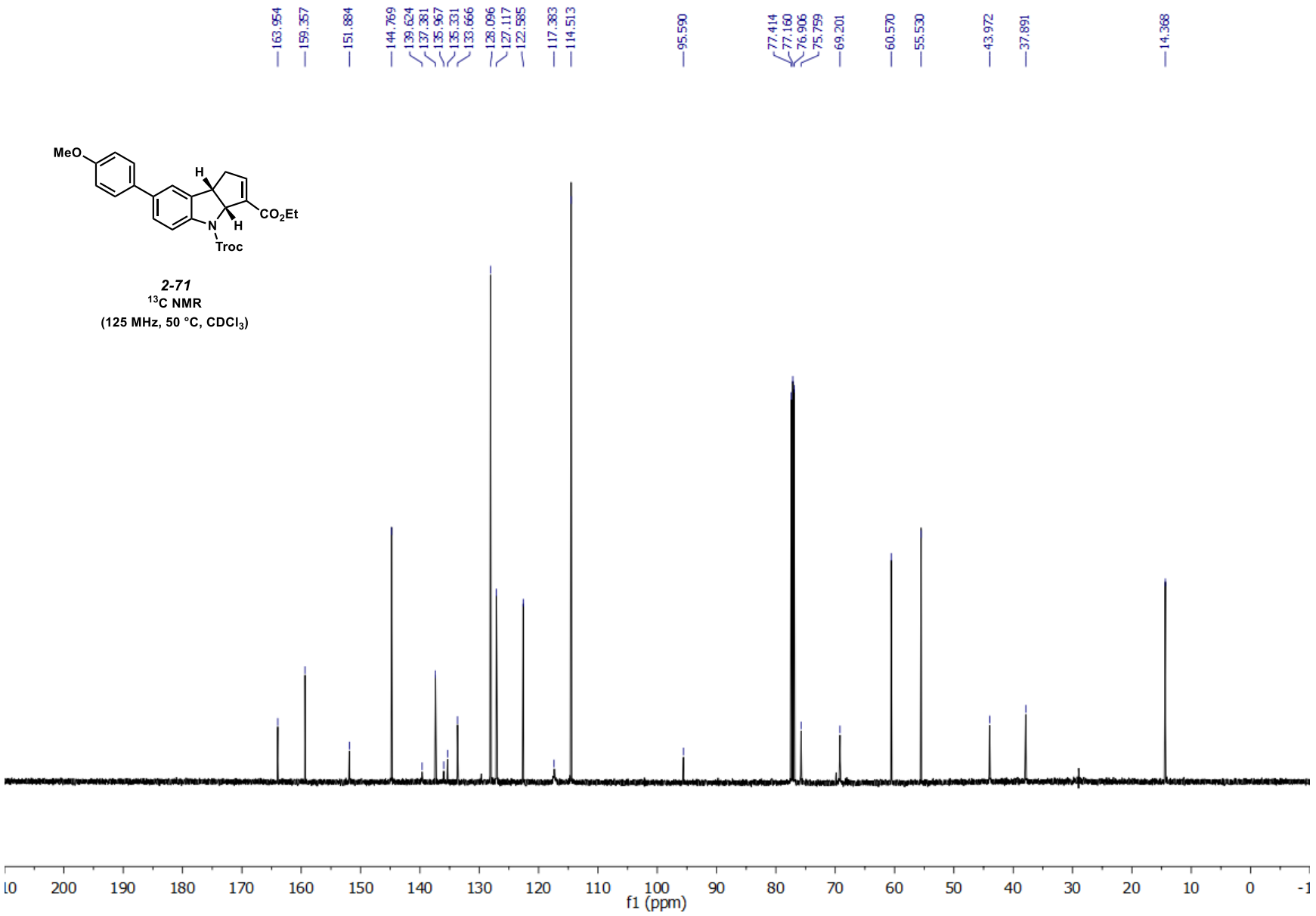
163.954
159.357
151.884
144.769
139.624
137.381
135.967
135.331
133.666
128.096
127.117
122.585
117.383
114.513
95.590
77.414
77.160
76.906
75.759
69.201
60.570
55.530
43.972
37.891
14.368
MeO
H
N
H
CO2Et
Troc
2-71
13C NMR
(125 MHz, 50 °C, CDCl3)
f1 (ppm)

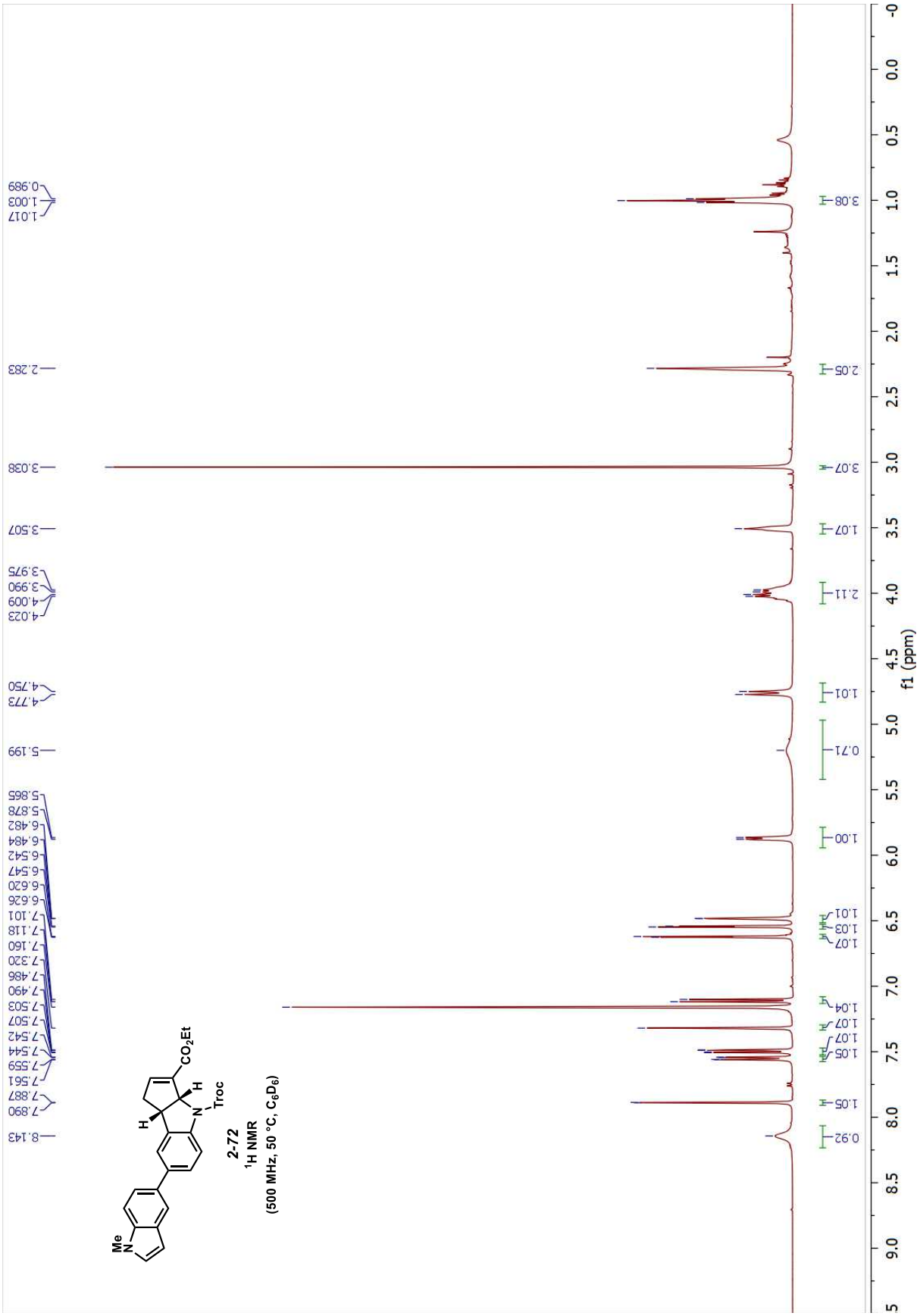
2-72
^{1}H NMR
(500 MHz, 50 °C, C_6D_6)
f1 (ppm)

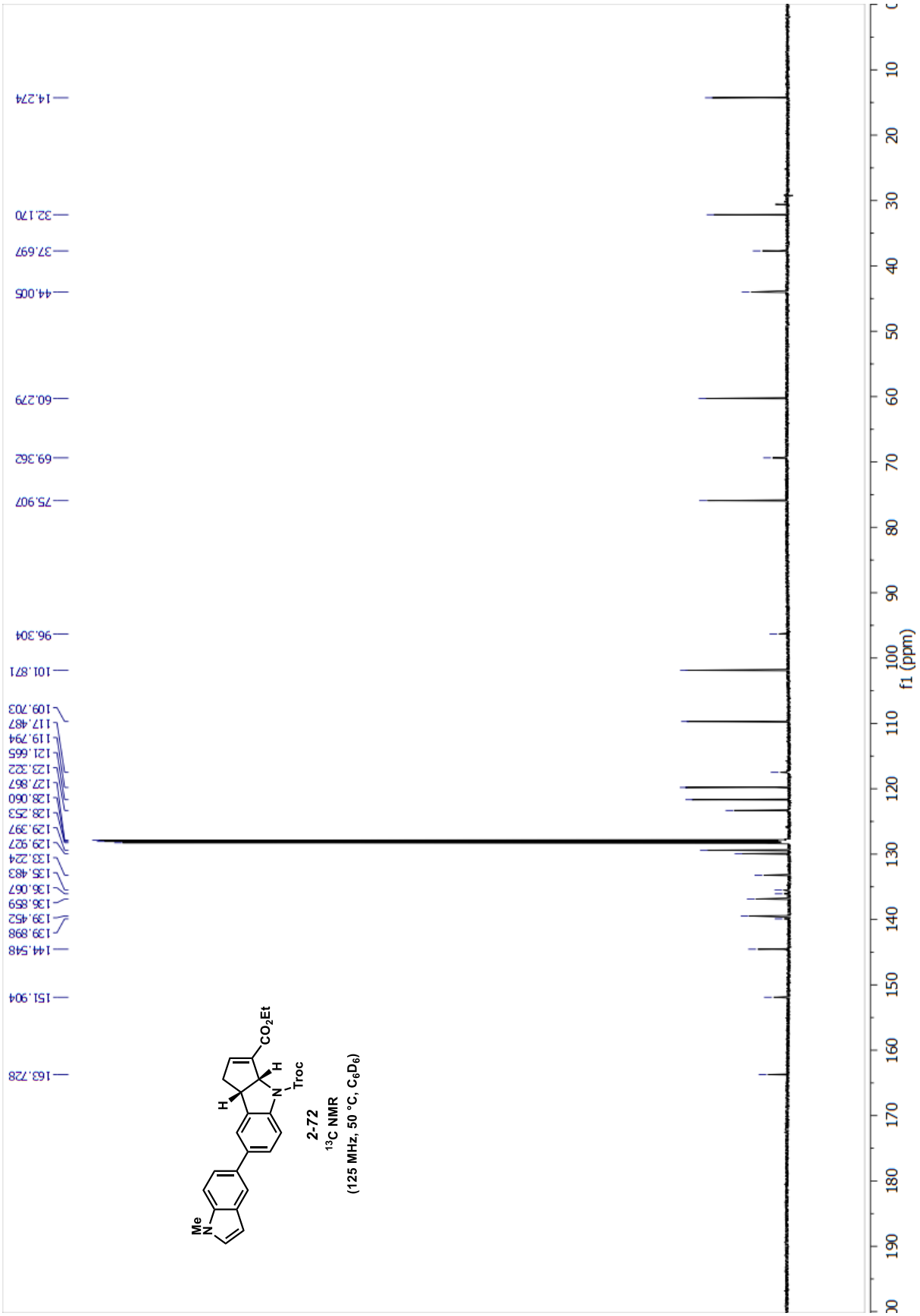
14.274
32.170
37.697
44.005
60.279
69.362
75.907
96.304
101.871
109.703
117.487
119.794
121.665
123.322
127.867
128.060
128.253
129.397
129.927
133.224
135.483
136.067
136.859
139.452
139.898
144.548
151.904
163.728
CO2Et
H
N
Troc
H
Me
N
2-72
13C NMR
(125 MHz, 50 °C, C6D6)
f1 (ppm)

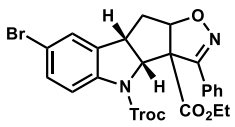

2-73
(~3 : 1 dr)
^{1}H NMR
(400 MHz, C_6D_6)

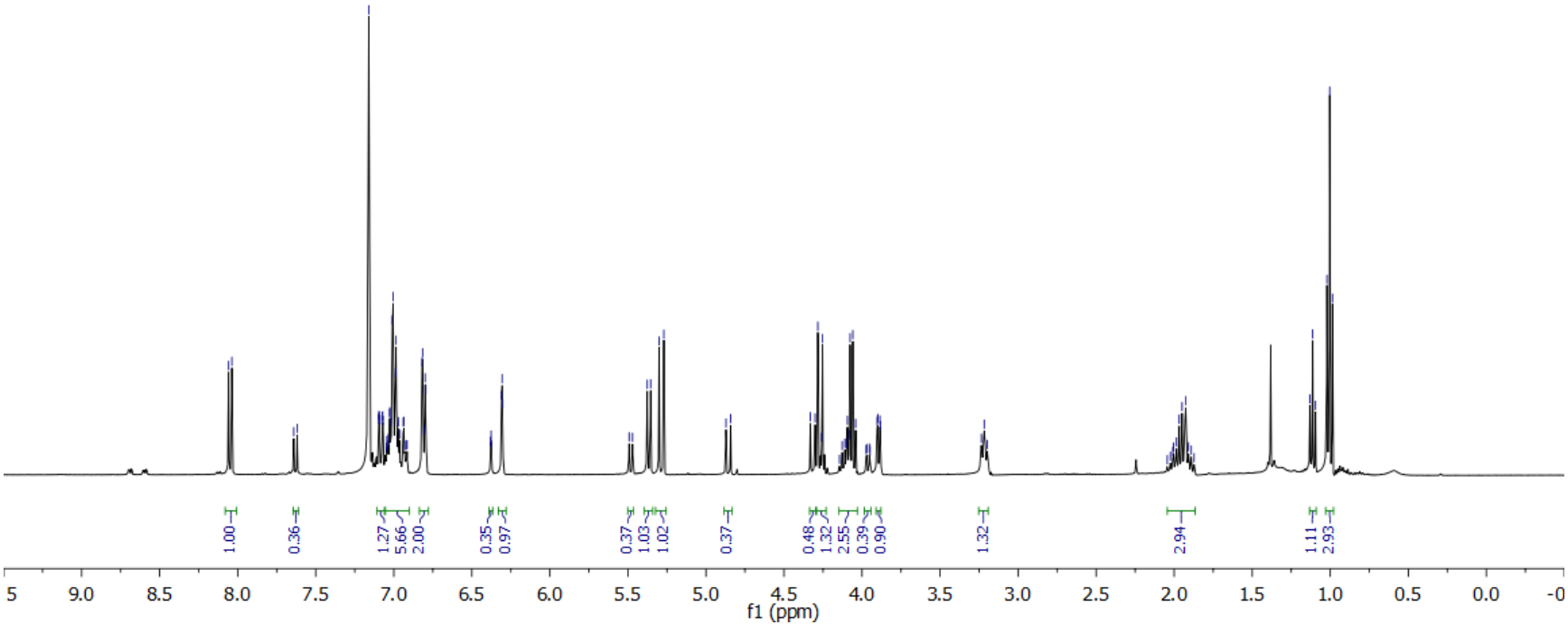

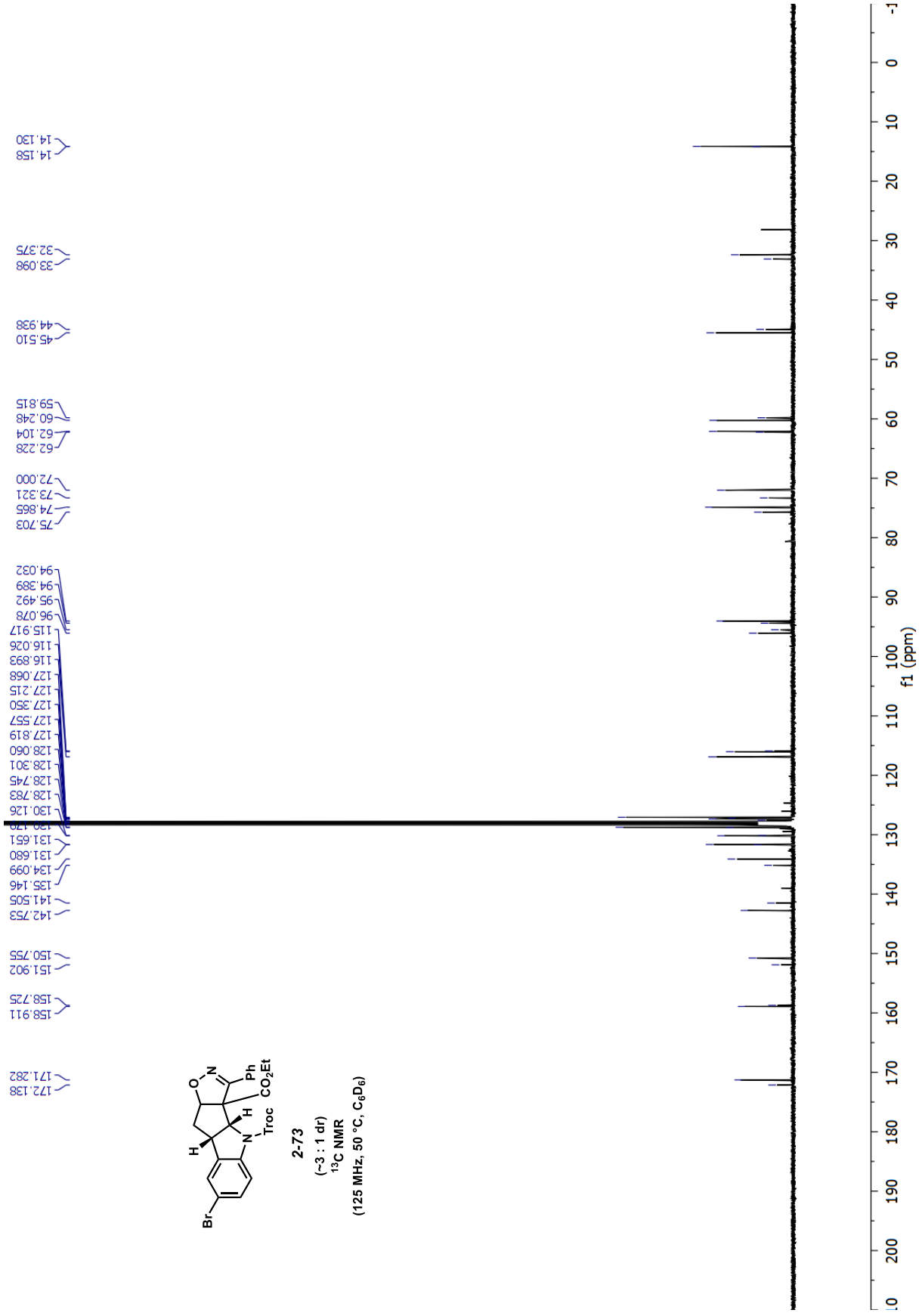
14.130
14.158
32.375
33.098
44.938
45.510
59.815
60.248
62.104
62.228
72.000
73.321
74.865
75.703
94.032
94.389
95.492
96.078
115.917
116.026
116.893
127.068
127.215
127.350
127.557
127.819
128.060
128.301
128.745
128.783
130.126
131.651
131.680
134.099
135.146
141.505
142.753
150.755
151.902
158.725
158.911
171.282
172.138
Br
H
H
N
O
N
Ph
CO2Et
Troc
2-73
(~3 : 1 dr)
13C NMR
(125 MHz, 50 °C, C6D6)
f1 (ppm)

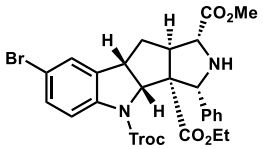

2-74

^{1}H NMR

(400 MHz, $CDCl_3$)

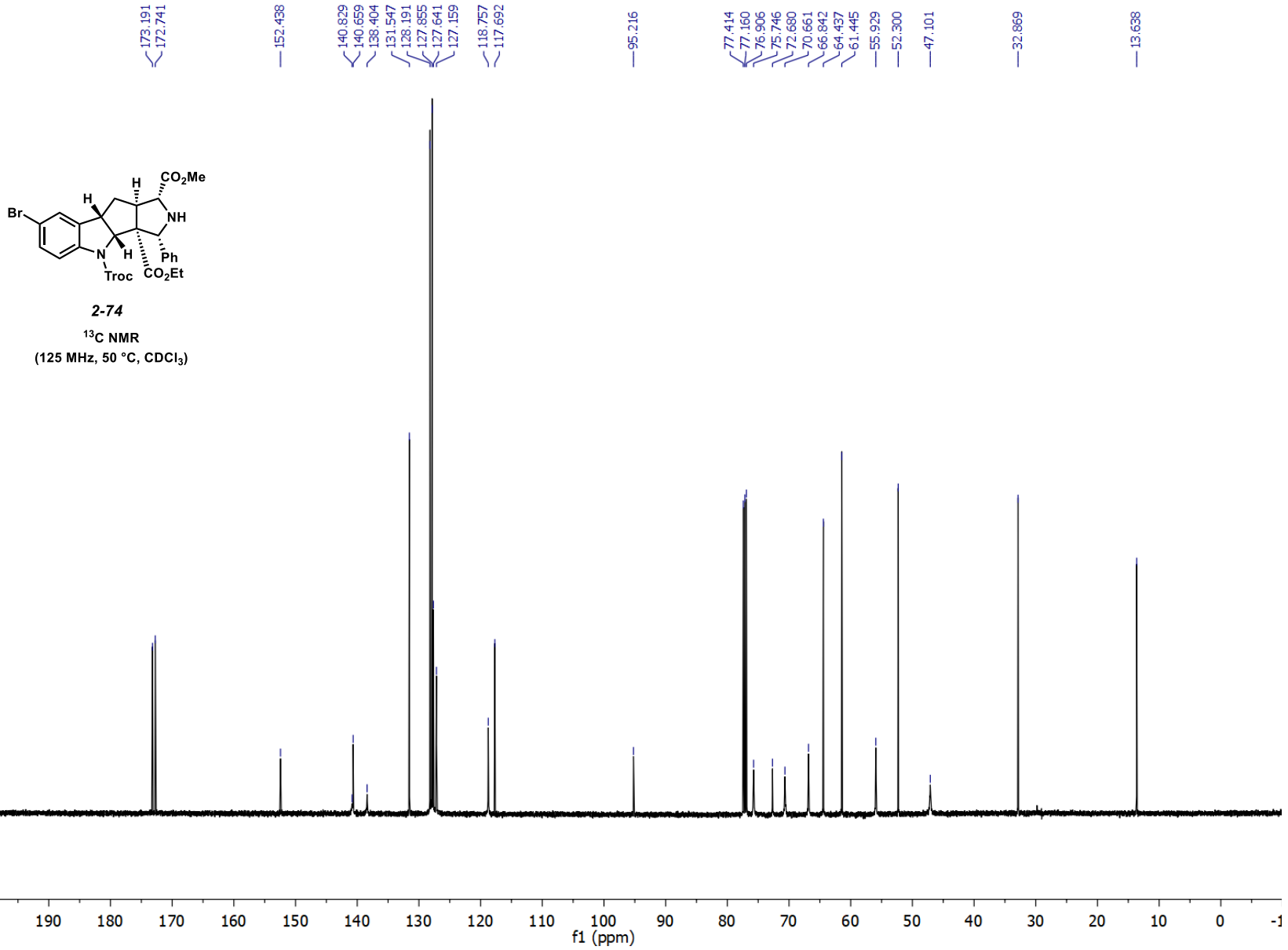
173.191
172.741
152.438
140.829
140.659
138.404
131.547
128.191
127.855
127.641
127.159
118.757
117.692
95.216
77.414
77.160
76.906
75.746
72.680
70.661
66.842
64.437
61.445
55.929
52.300
47.101
32.869
13.638
Br
H
H
CO2Me
NH
N
H
Ph
Troc
CO2Et
2-74
13C NMR
(125 MHz, 50 °C, CDCl3)
f1 (ppm)

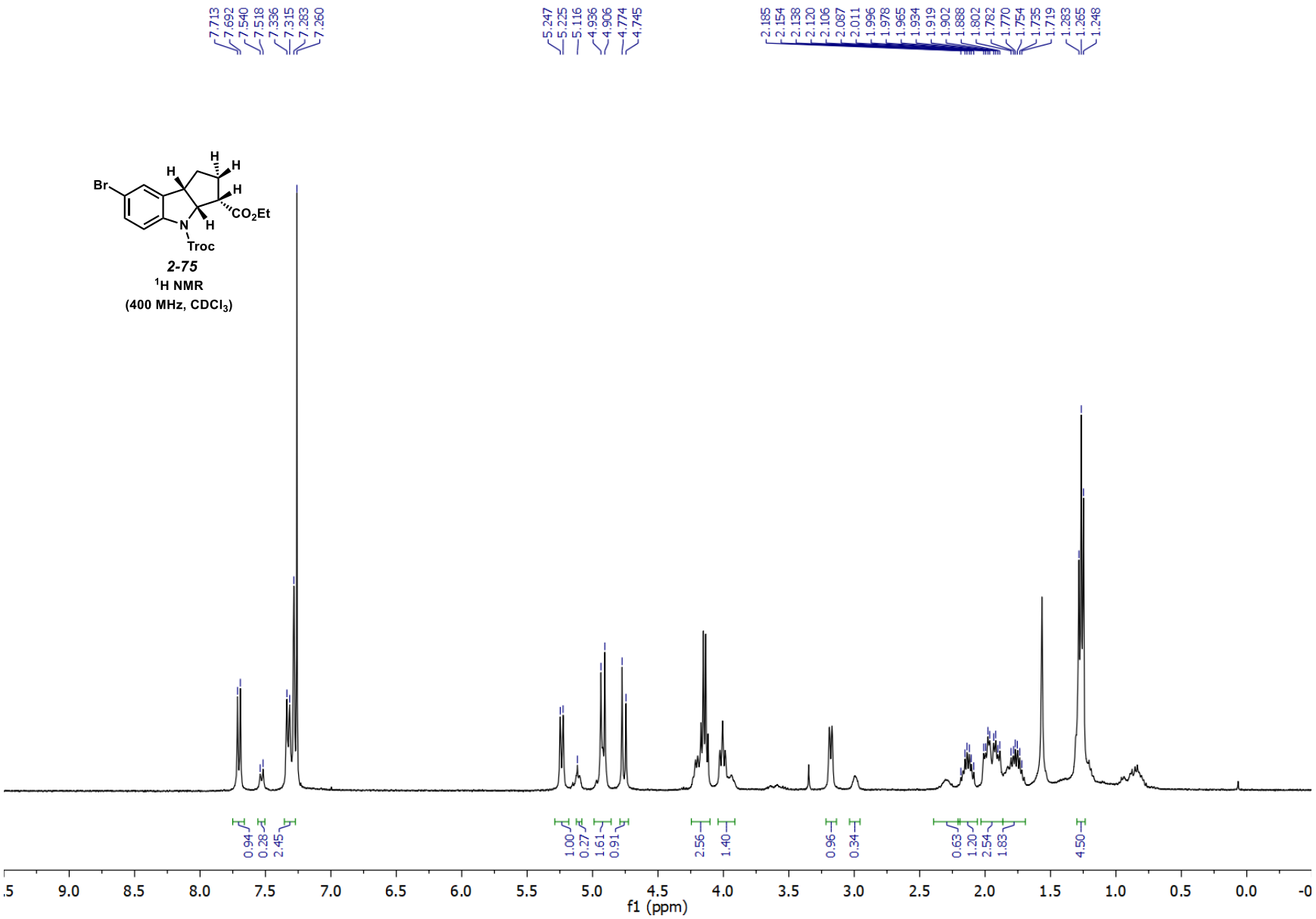
7.713
7.692
7.540
7.518
7.336
7.315
7.283
7.260
5.247
5.225
5.116
4.936
4.906
4.774
4.745
2.185
2.154
2.138
2.120
2.106
2.087
2.011
1.996
1.978
1.965
1.934
1.919
1.902
1.888
1.802
1.782
1.770
1.754
1.735
1.719
1.283
1.265
1.248
Br
H
H
H
H
H
N
H
CO2Et
Troc
2-75
1H NMR
(400 MHz, CDCl3)
0.94
0.28
2.45
1.00
0.27
1.61
0.91
2.56
1.40
0.96
0.34
0.63
1.20
2.54
1.83
4.50
f1 (ppm)

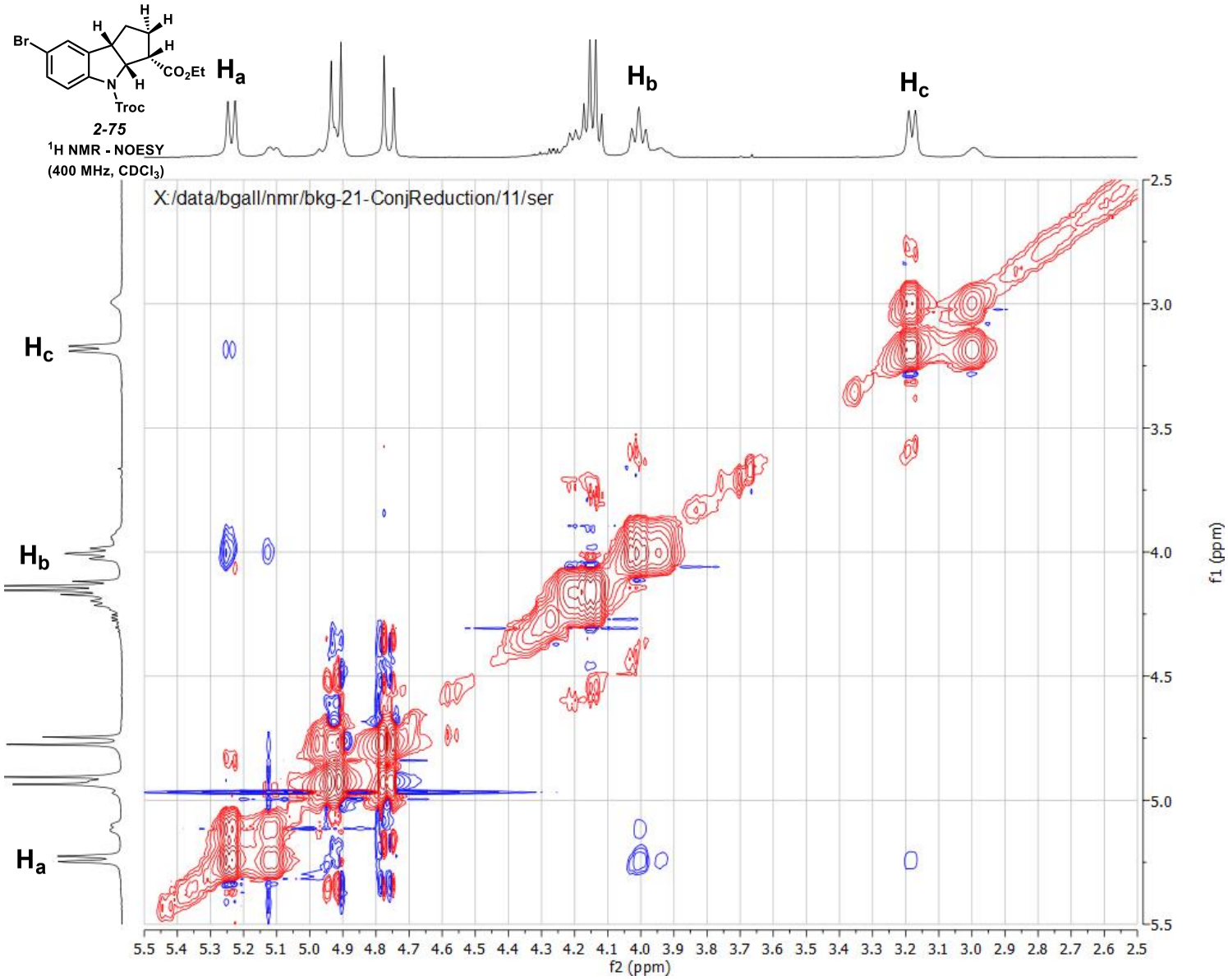
Br
H
H
H
H
CO2Et
N
H
Troc
2-75
1H NMR - NOESY
(400 MHz, CDCl3)
Ha
Hb
Hc
X:/data/bgall/nmr/bkg-21-ConjReduction/11/ser
f2 (ppm)
f1 (ppm)

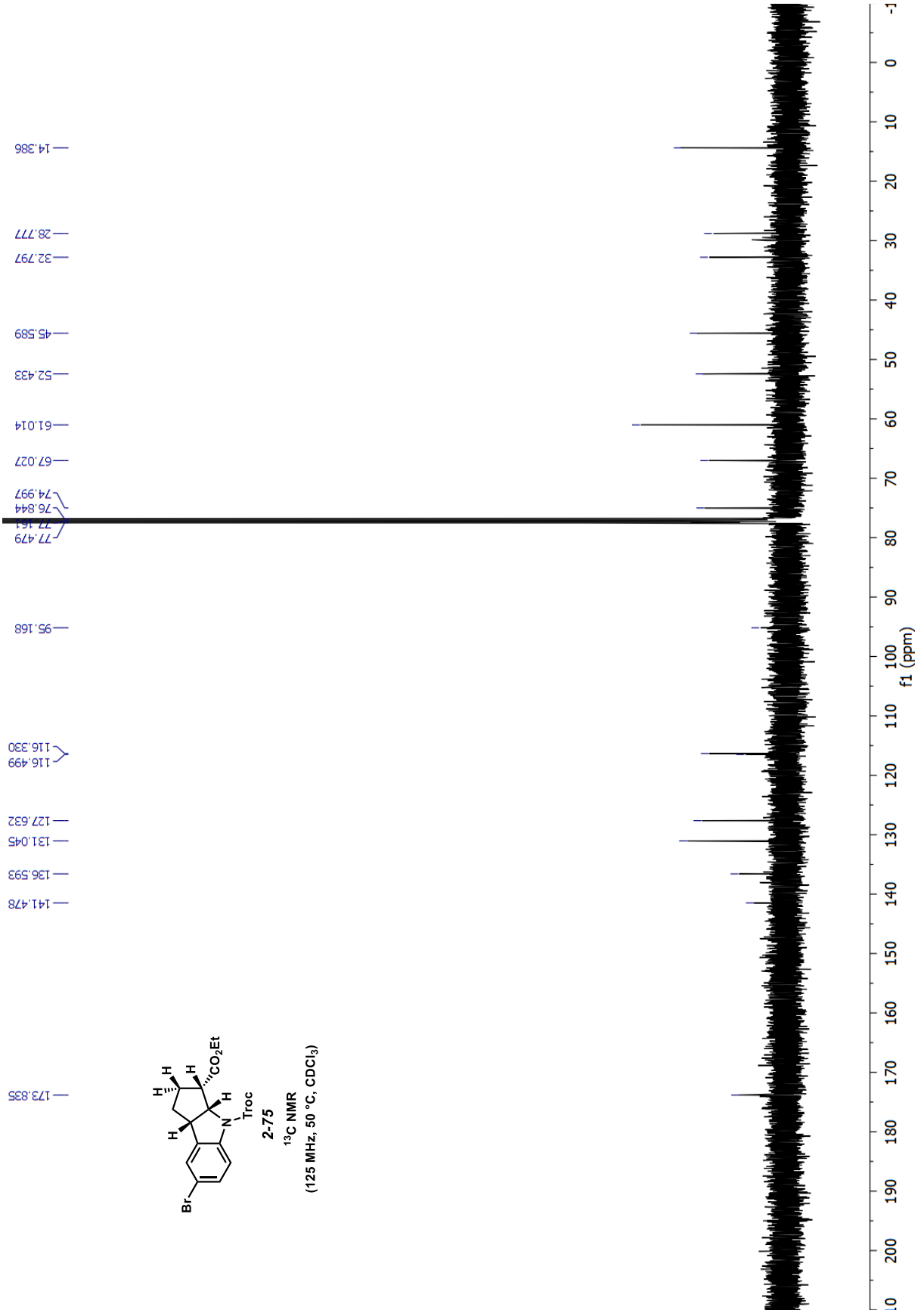
14.386
28.777
32.797
45.589
52.433
61.014
67.027
74.997
76.844
77.161
77.479
95.168
116.330
116.499
127.632
131.045
136.593
141.478
173.835
f1 (ppm)
2-75
13C NMR
(125 MHz, 50 °C, CDCl3)
CO2Et
Troc
Br

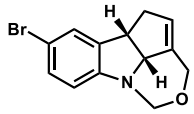

2-76

^{1}H NMR

(400 MHz, $CDCl_3$)

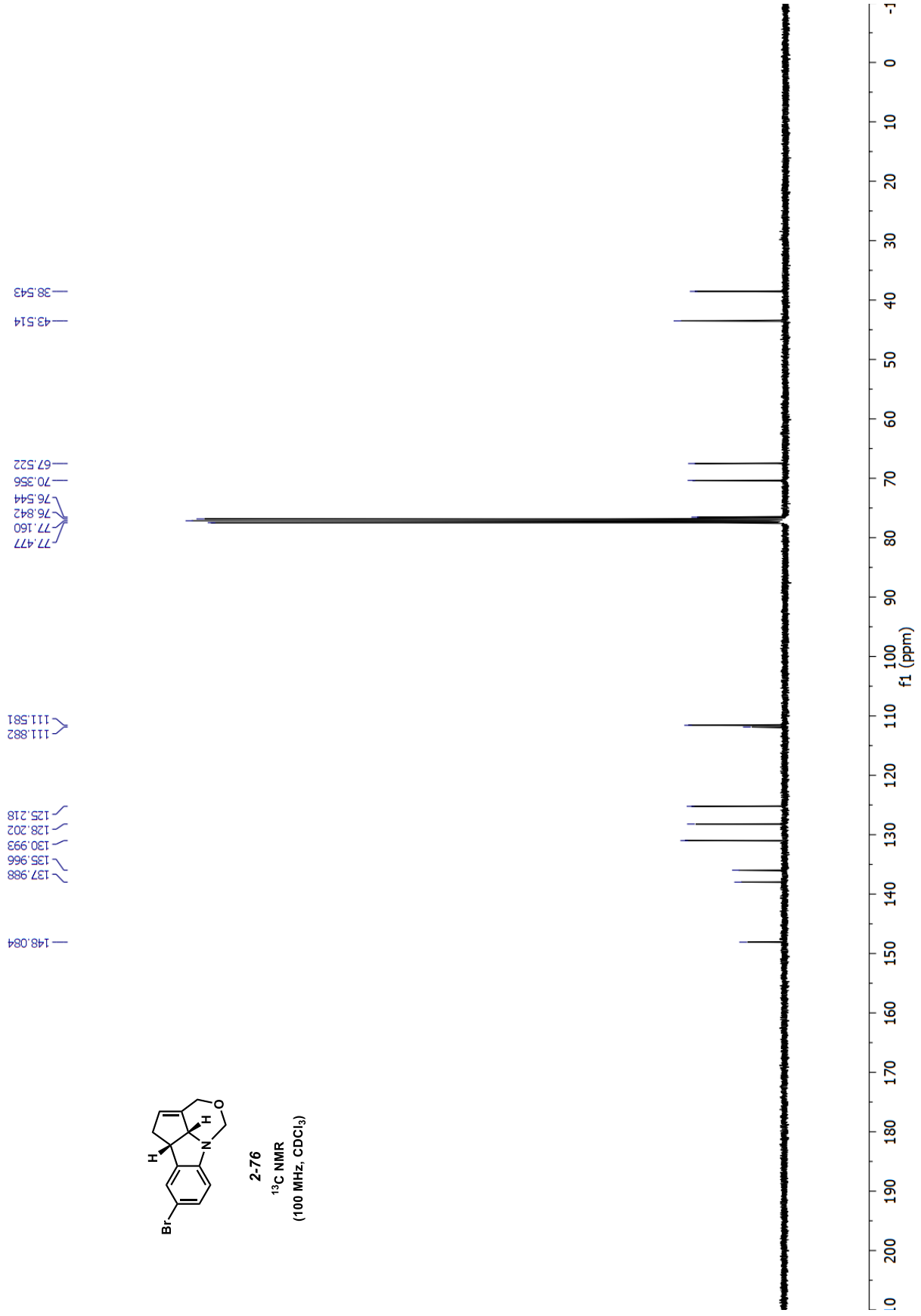
38.543
43.514
67.522
70.356
76.544
76.842
77.160
77.477
111.581
111.882
125.218
128.202
130.993
135.966
137.988
148.084
f1 (ppm)
2-76
13C NMR
(100 MHz, CDCl3)
Br
H
N
O
H

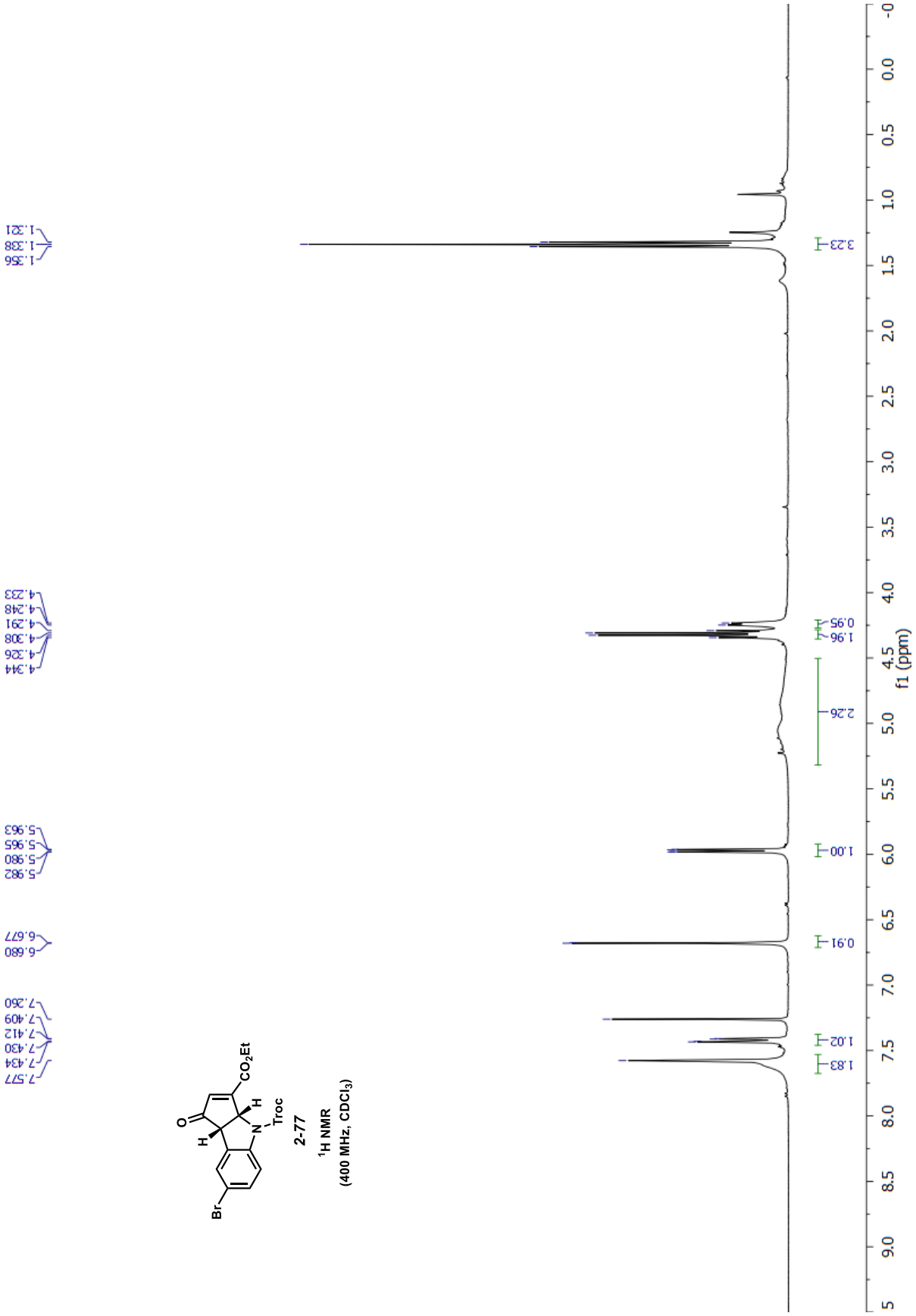
1.356
1.338
1.321
4.344
4.326
4.308
4.291
4.248
4.233
5.982
5.980
5.965
5.963
6.680
6.677
7.577
7.434
7.430
7.412
7.409
7.260
3.23
0.95
1.96
2.26
1.00
0.91
1.02
1.83
f1 (ppm)
CO2Et
Troc
N
H
O
H
Br
2-77
1H NMR
(400 MHz, CDCl3)

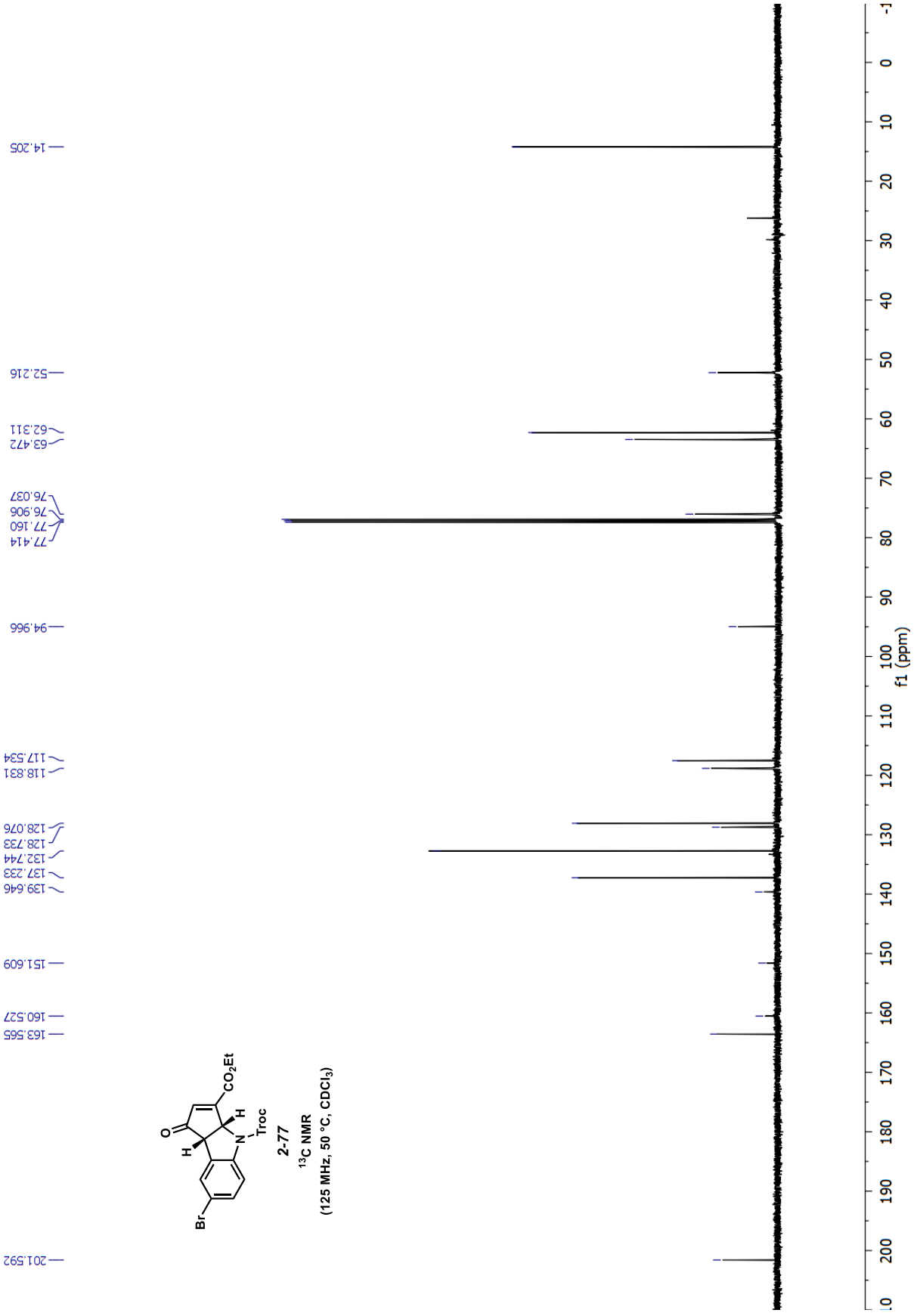
14.205
52.216
62.311
63.472
76.037
76.906
77.160
77.414
94.966
117.534
118.831
128.076
128.733
132.744
137.233
139.646
151.609
160.527
163.565
201.592
f1 (ppm)
2-77
13C NMR
(125 MHz, 50 °C, CDCl3)
CO2Et
Troc
N
O
H
H
Br

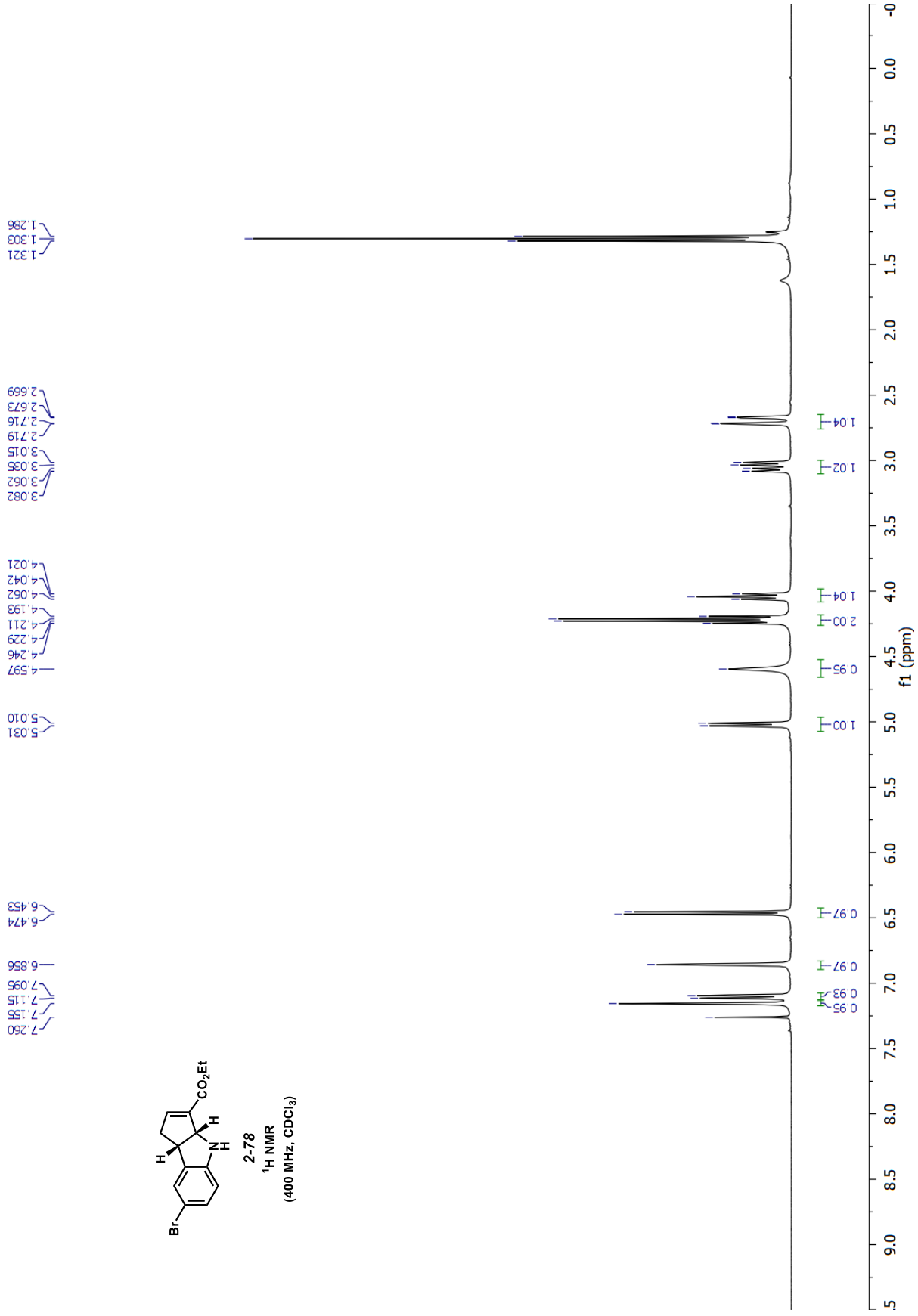
1.286
1.303
1.321
2.669
2.673
2.716
2.719
3.015
3.035
3.062
3.082
4.021
4.042
4.062
4.193
4.211
4.229
4.246
4.597
5.010
5.031
6.453
6.474
6.856
7.095
7.115
7.155
7.260
1.04
1.02
1.04
2.00
0.95
1.00
0.97
0.97
0.93
0.95
f1 (ppm)
CO2Et
H
N
H
H
Br
2-78
1H NMR
(400 MHz, CDCl3)

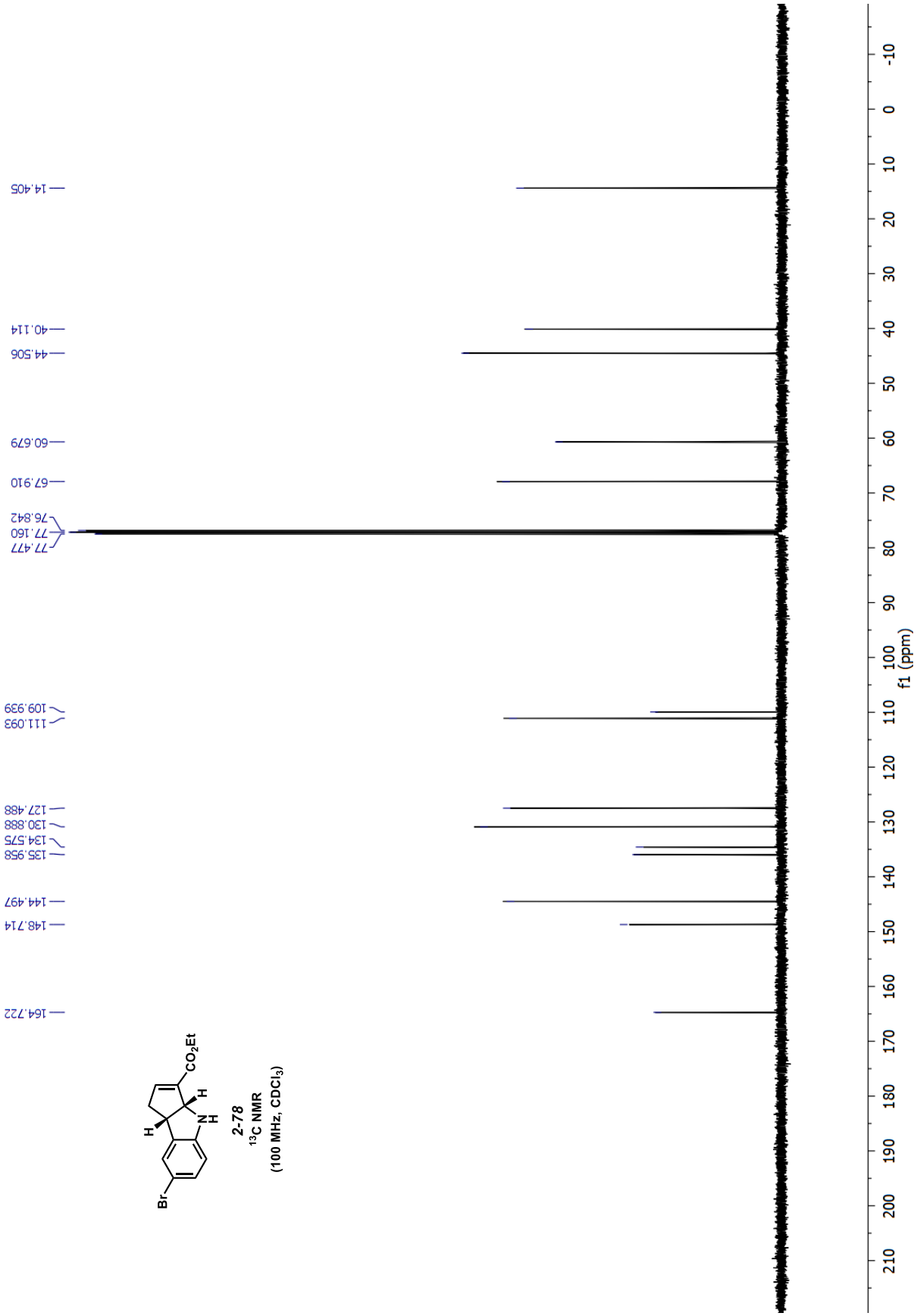
14.405
40.114
44.506
60.679
67.910
76.842
77.160
77.477
109.939
111.093
127.488
130.888
134.575
135.958
144.497
148.714
164.722
f1 (ppm)
2-78
13C NMR
(100 MHz, CDCl3)
CO2Et
H
N
H
H
Br

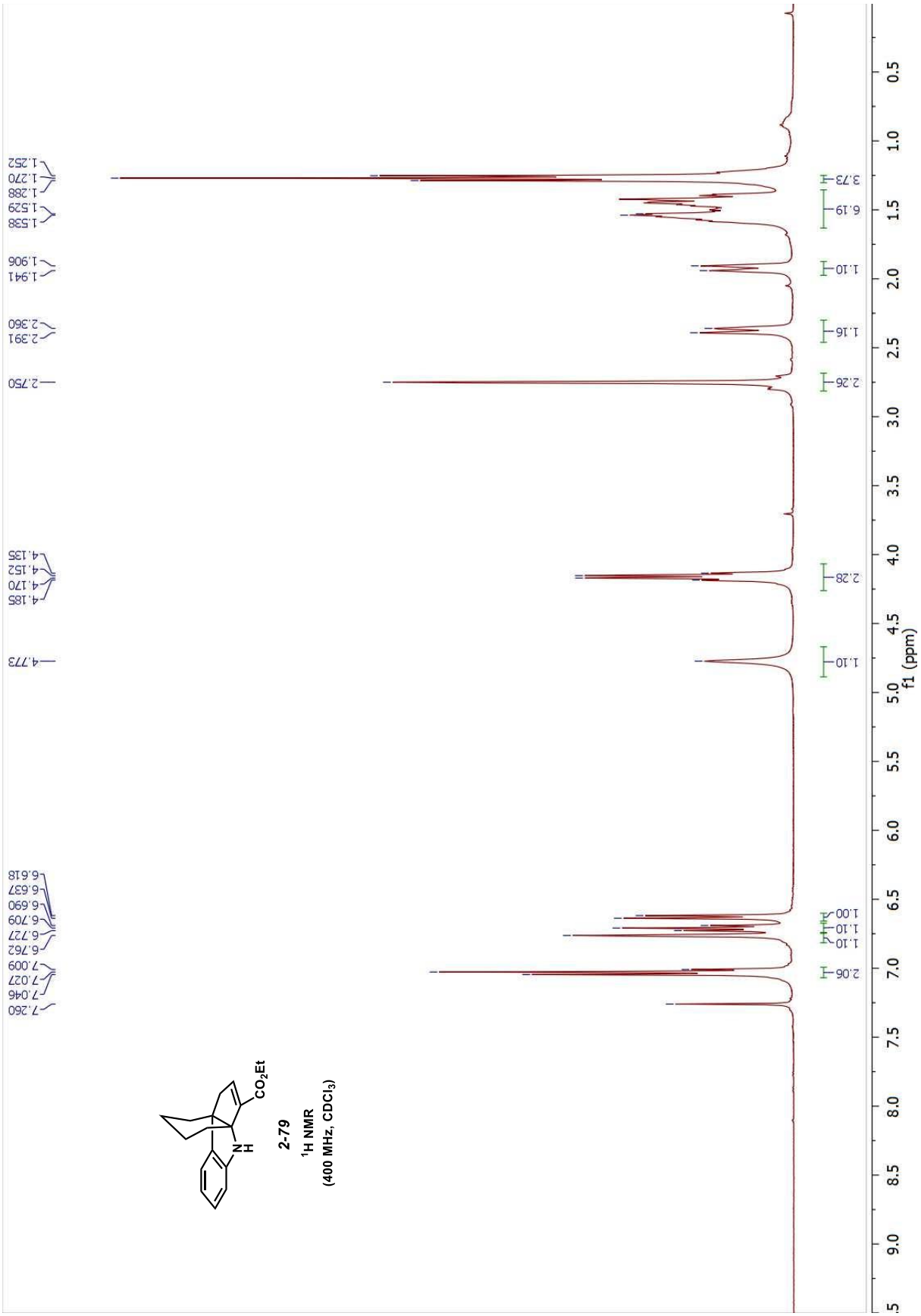
CO2Et
N
H
2-79
1H NMR
(400 MHz, CDCl3)
7.260
7.046
7.027
7.009
6.762
6.727
6.709
6.690
6.637
6.618
4.773
4.185
4.170
4.152
4.135
2.750
2.391
2.360
1.941
1.906
1.538
1.529
1.288
1.270
1.252
3.73
6.19
1.10
1.16
2.26
2.28
1.10
2.06
1.10
1.10
1.00
f1 (ppm)

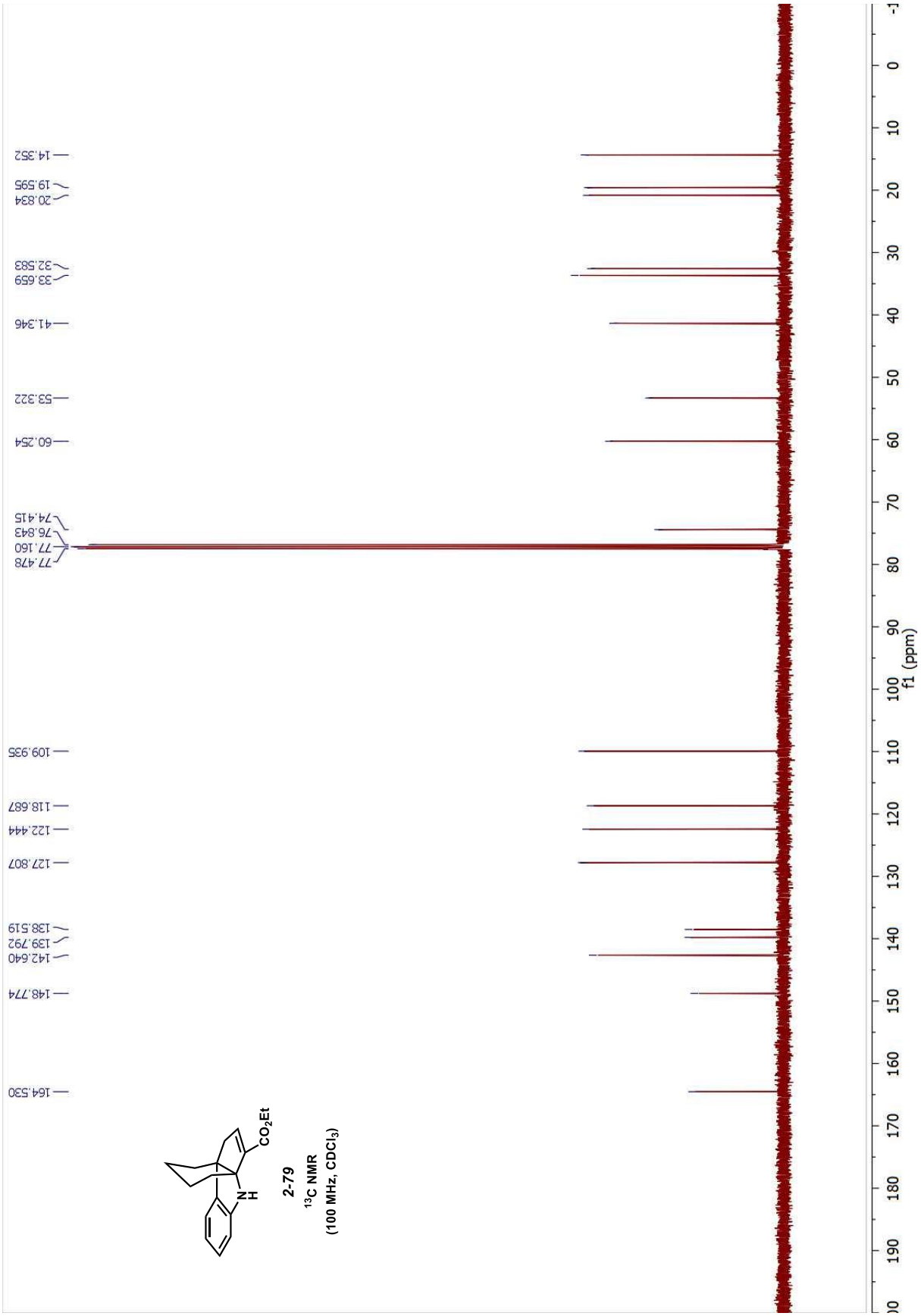
14.352
19.595
20.834
32.583
33.659
41.346
53.322
60.254
74.415
76.843
77.160
77.478
109.935
118.687
122.444
127.807
138.519
139.792
142.640
148.774
164.530
CO2Et
N
H
2-79
13C NMR
(100 MHz, CDCl3)
f1 (ppm)

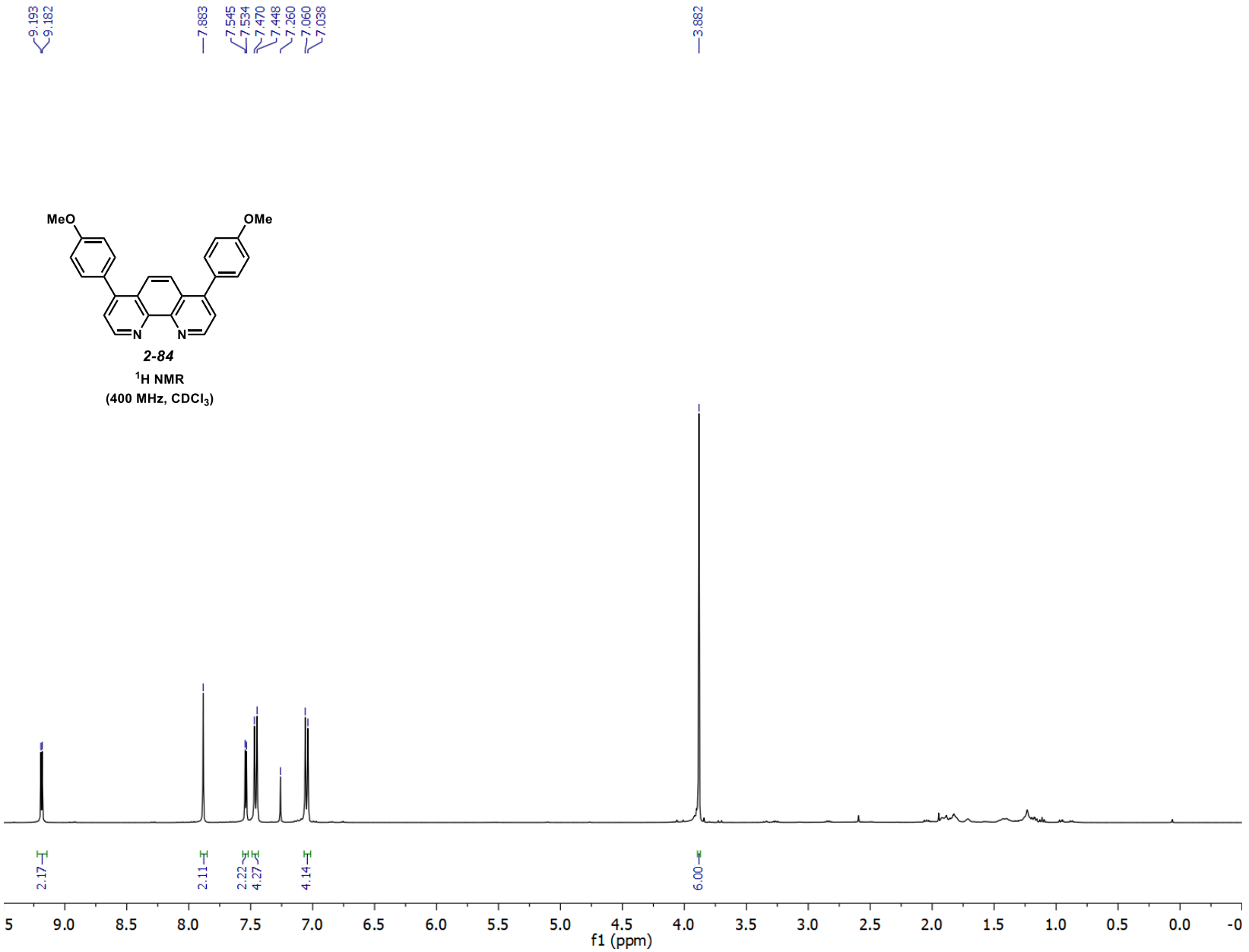
9.193
9.182
7.883
7.545
7.534
7.470
7.448
7.260
7.060
7.038
3.882
MeO
OMe
N
N
2-84
1H NMR
(400 MHz, CDCl3)
2.17
2.11
2.22
4.27
4.14
6.00
f1 (ppm)

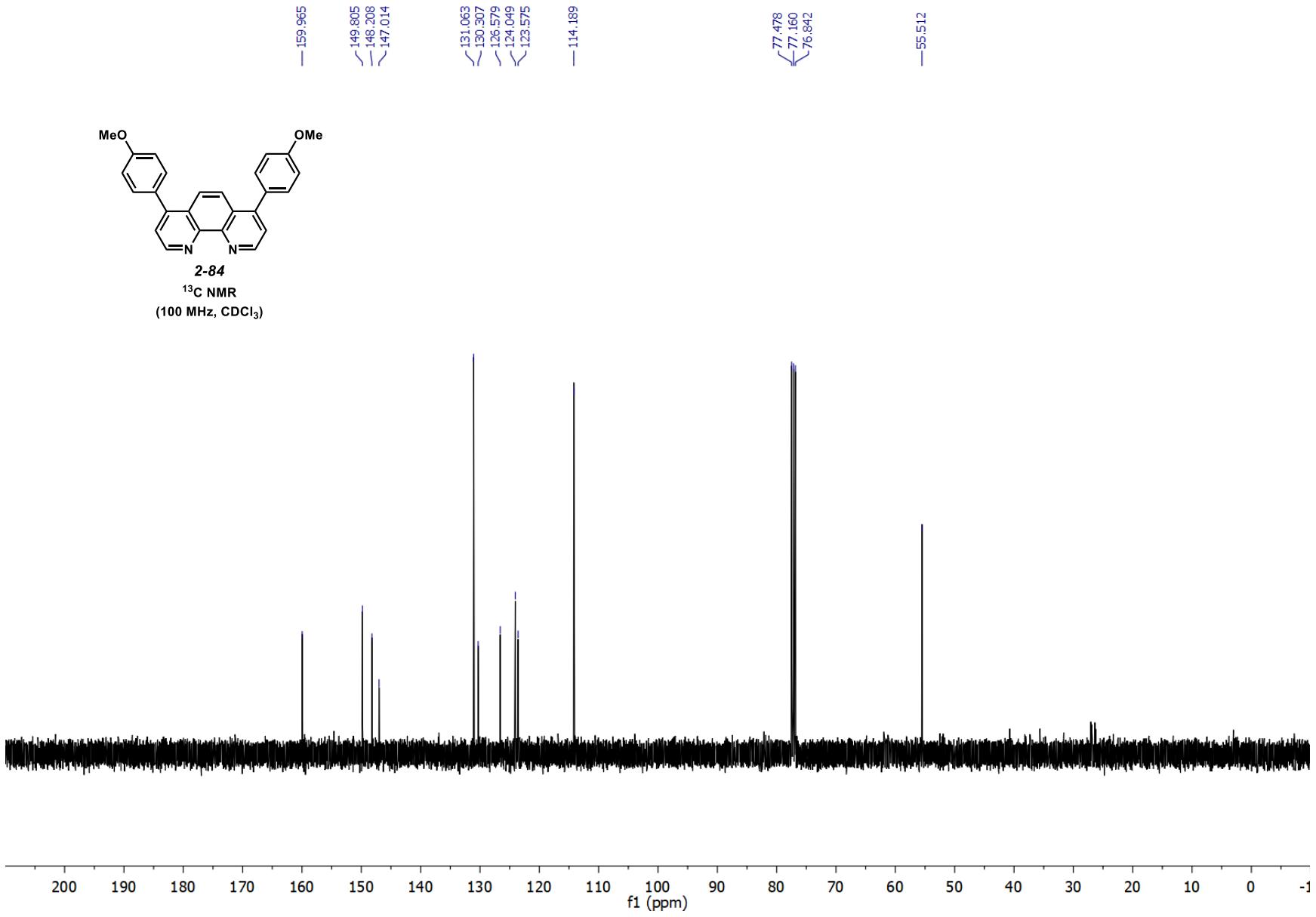
159.965
149.805
148.208
147.014
131.063
130.307
126.579
124.049
123.575
114.189
77.478
77.160
76.842
55.512
MeO
OMe
N
N
2-84
13C NMR
(100 MHz, CDCl3)
200
190
180
170
160
150
140
130
120
110
100
90
80
70
60
50
40
30
20
10
0
-1
f1 (ppm)

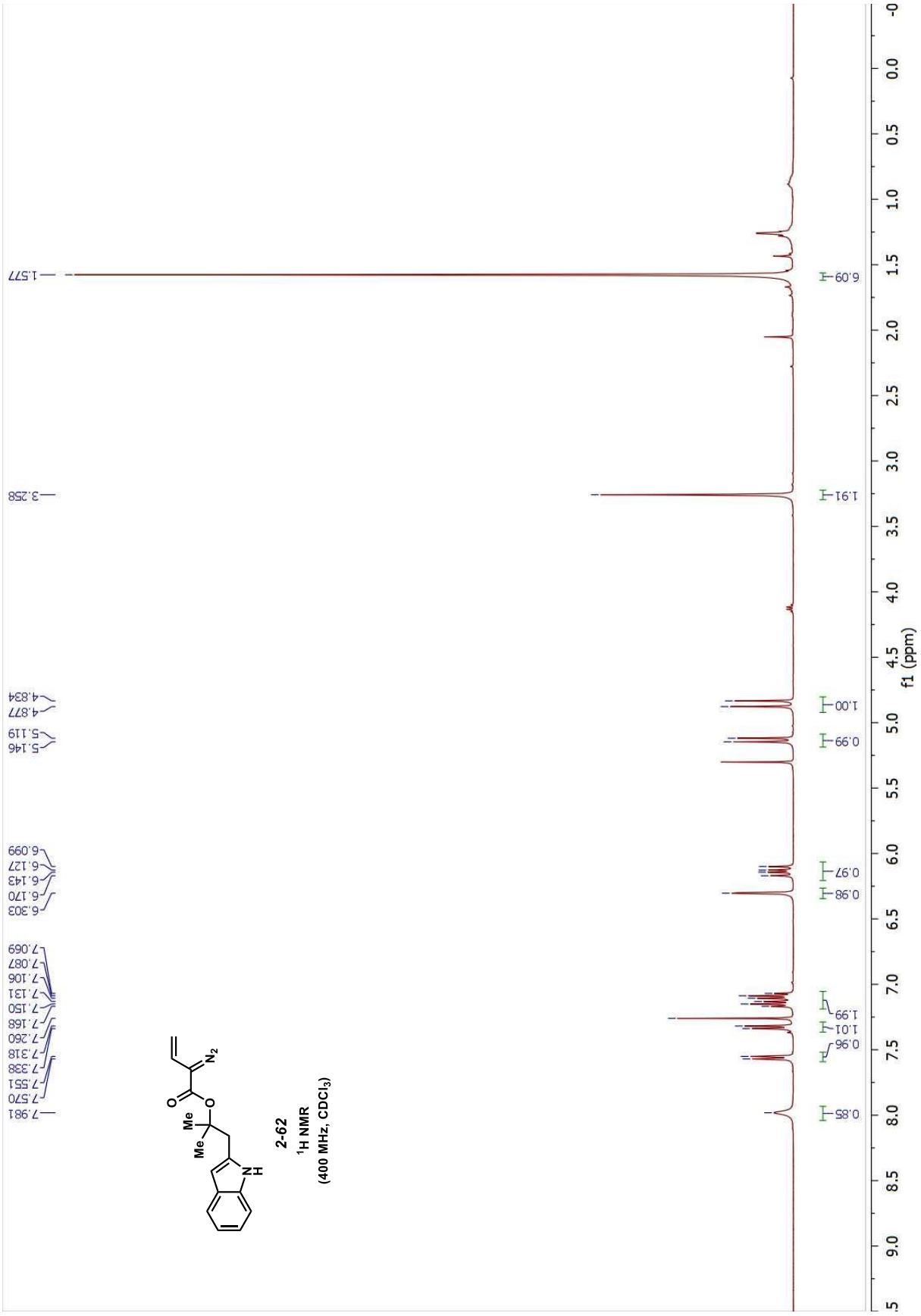
1.577
3.258
4.834
4.877
5.119
5.146
6.099
6.127
6.143
6.170
6.303
7.069
7.087
7.106
7.131
7.150
7.168
7.260
7.318
7.338
7.551
7.570
7.981
6.09
1.91
1.00
0.99
0.97
0.98
1.99
1.01
0.96
0.85
f1 (ppm)
2-62
^{1}H NMR
(400 MHz, CDCl$_3$)

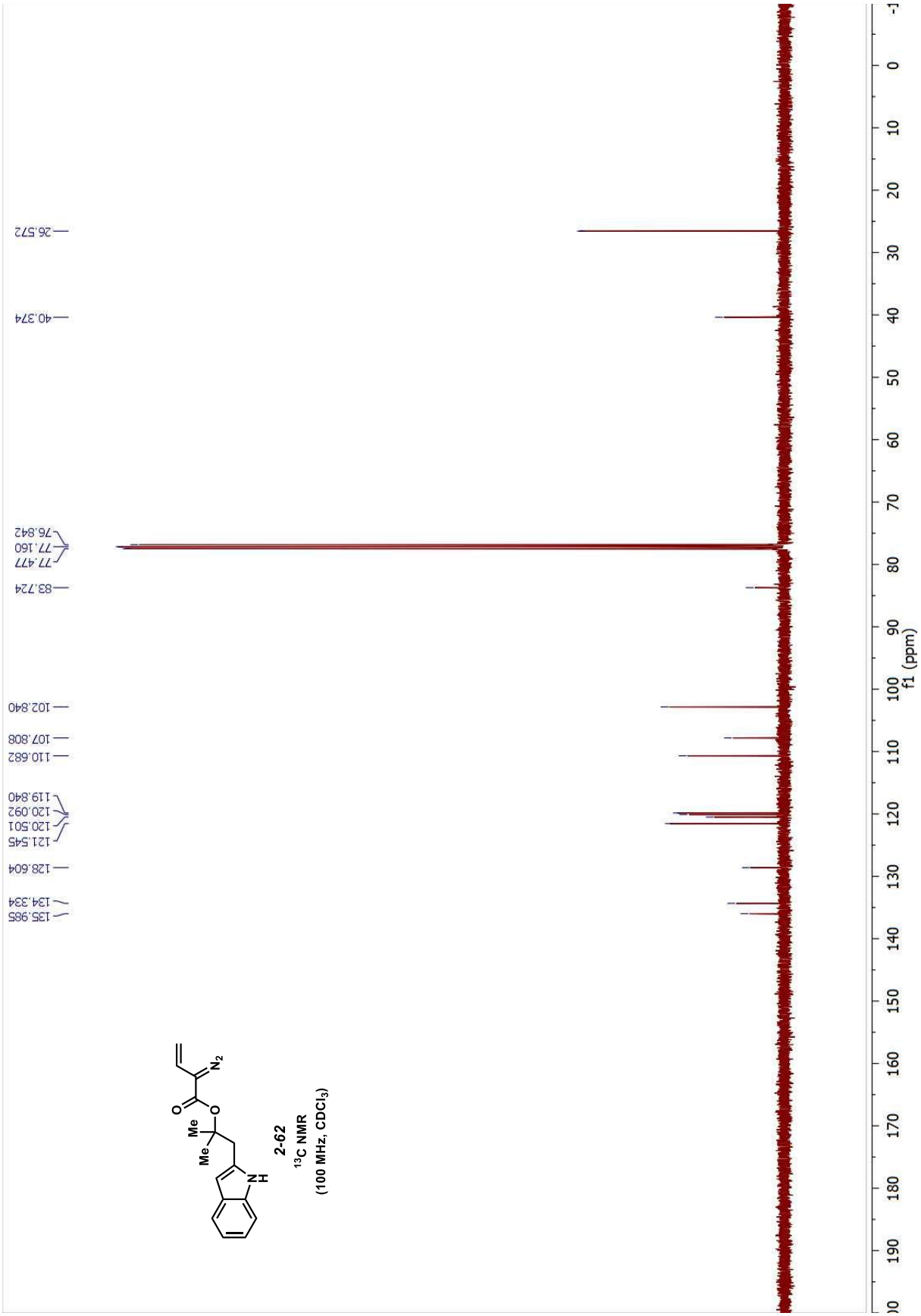
26.572
40.374
76.842
77.160
77.477
83.724
102.840
107.808
110.682
119.840
120.092
120.501
121.545
128.604
134.334
135.985
f1 (ppm)
2-62
13C NMR
(100 MHz, CDCl3)
Me
Me
O
O
N2
H
N

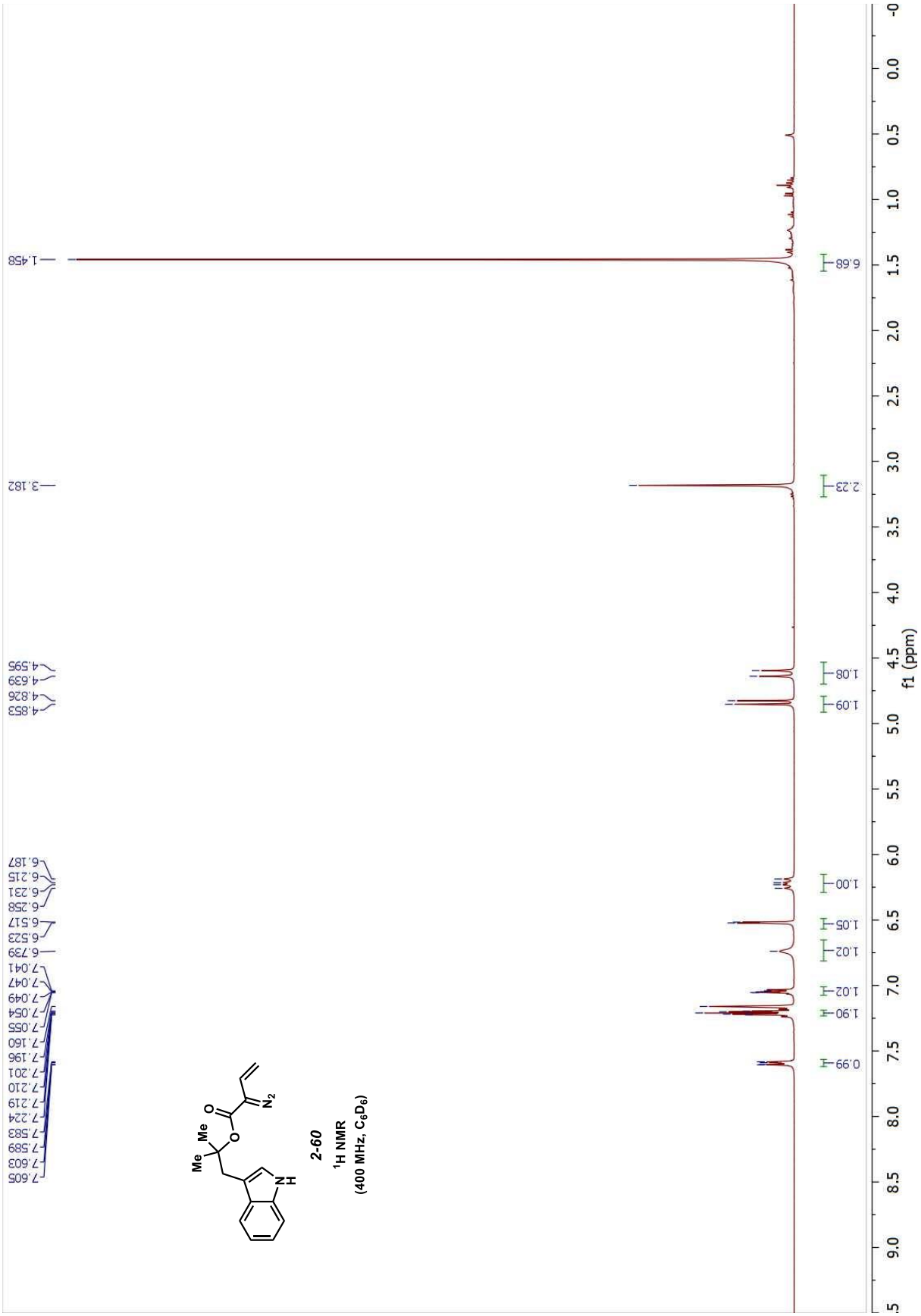
7.605
7.603
7.589
7.583
7.224
7.219
7.210
7.201
7.196
7.160
7.055
7.054
7.049
7.047
7.041
6.739
6.523
6.517
6.258
6.231
6.215
6.187
4.853
4.826
4.639
4.595
3.182
1.458
6.68
2.23
1.08
1.09
1.00
1.05
1.02
1.02
1.90
0.99
f1 (ppm)
Me
Me
O
O
N2
N
H
2-60
1H NMR
(400 MHz, C6D6)

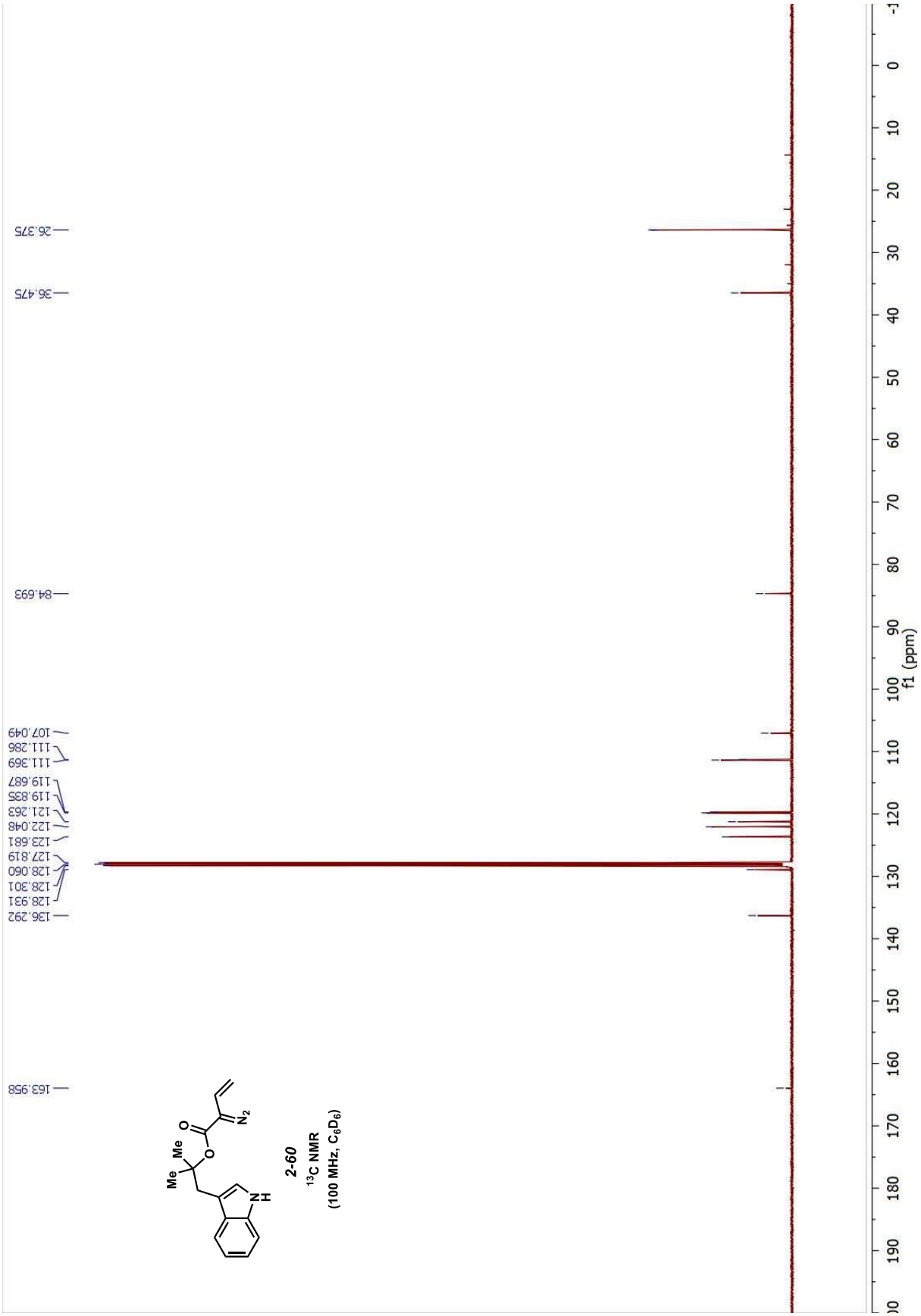
26.375
36.475
84.693
107.049
111.286
111.369
119.687
119.835
121.263
122.048
123.681
127.819
128.060
128.301
128.931
136.292
163.958
f1 (ppm)
2-60
13C NMR
(100 MHz, C6D6)

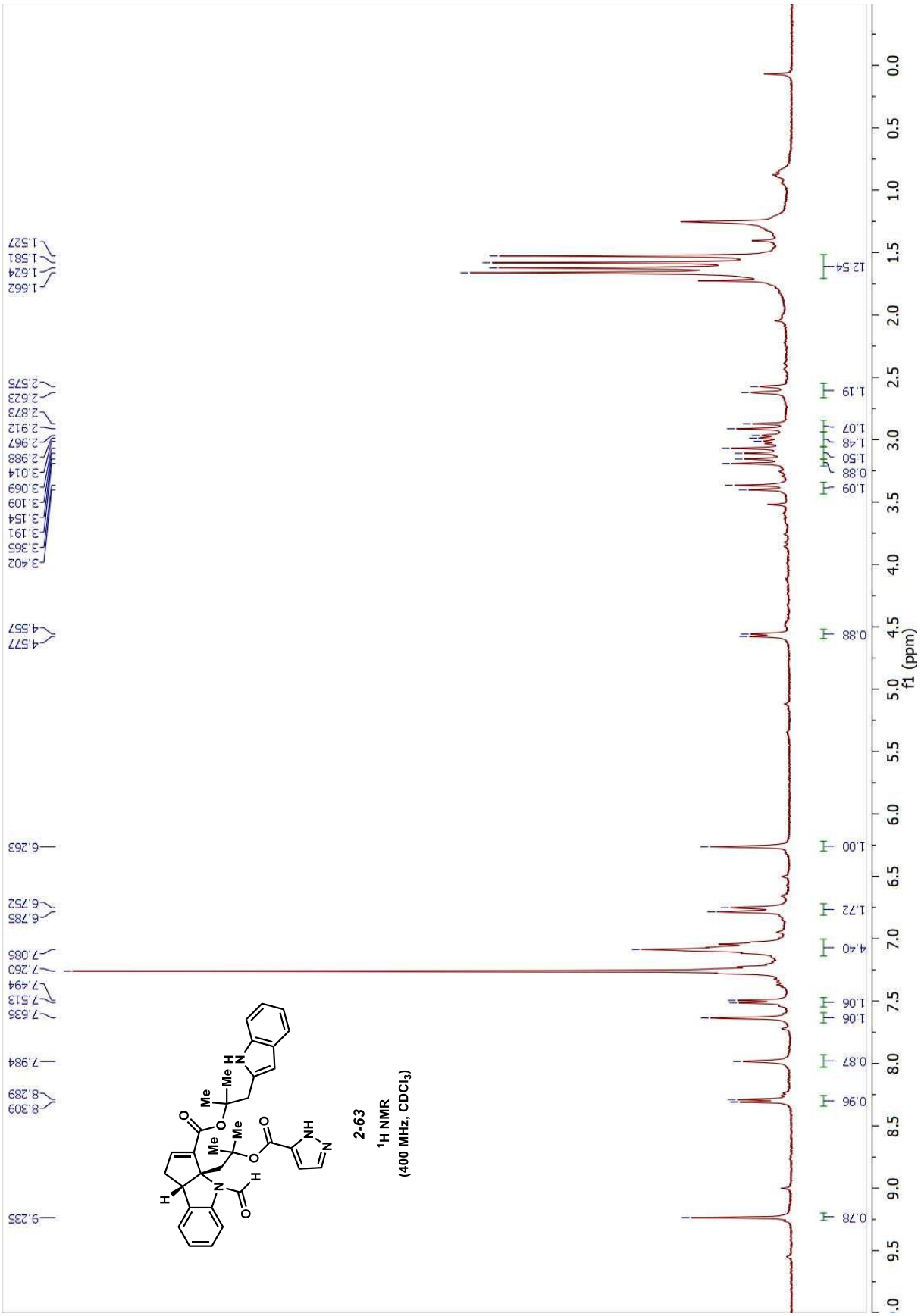
2-63
^{1}H NMR
(400 MHz, CDCl$_3$)
f1 (ppm)

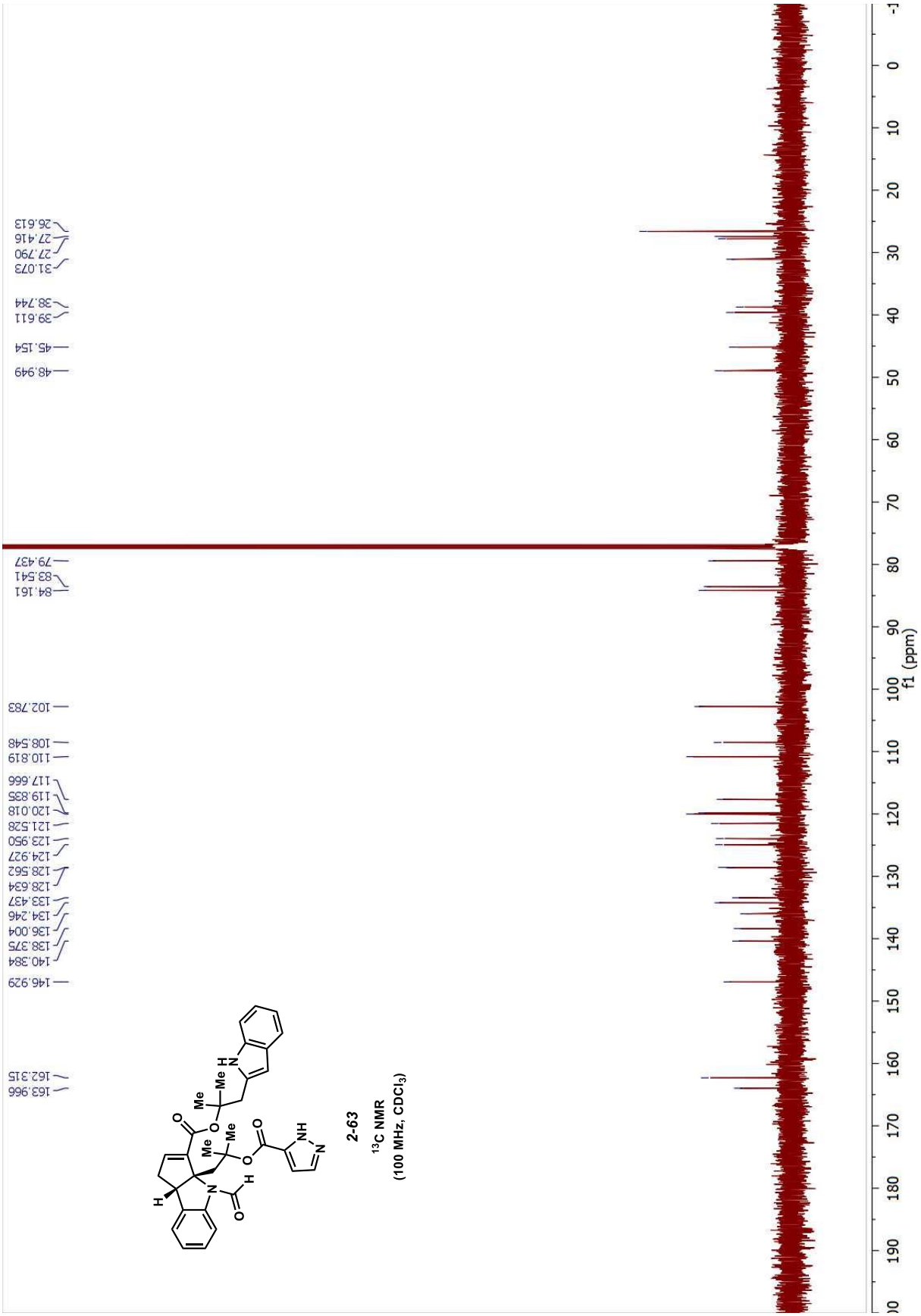
2-63
^{13}C NMR
(100 MHz, $CDCl_3$)
f1 (ppm)

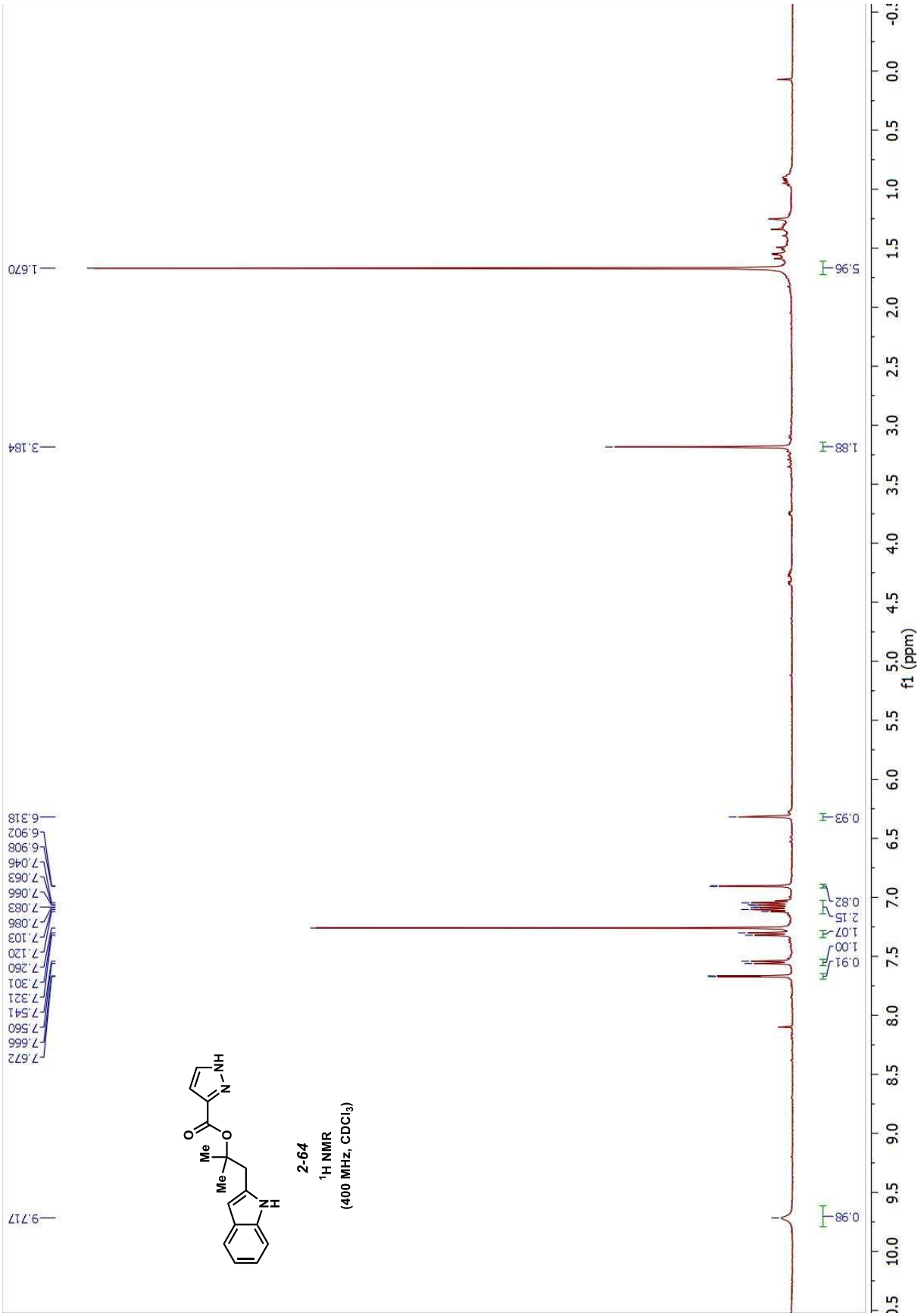
1.670
3.184
9.717
6.318
6.902
6.908
7.046
7.063
7.066
7.083
7.086
7.103
7.120
7.260
7.301
7.321
7.541
7.560
7.666
7.672
5.96
1.88
0.93
0.82
2.15
1.07
1.00
0.91
0.98
Me
Me
O
O
NH
N
H
2-64
1H NMR
(400 MHz, CDCl3)
f1 (ppm)

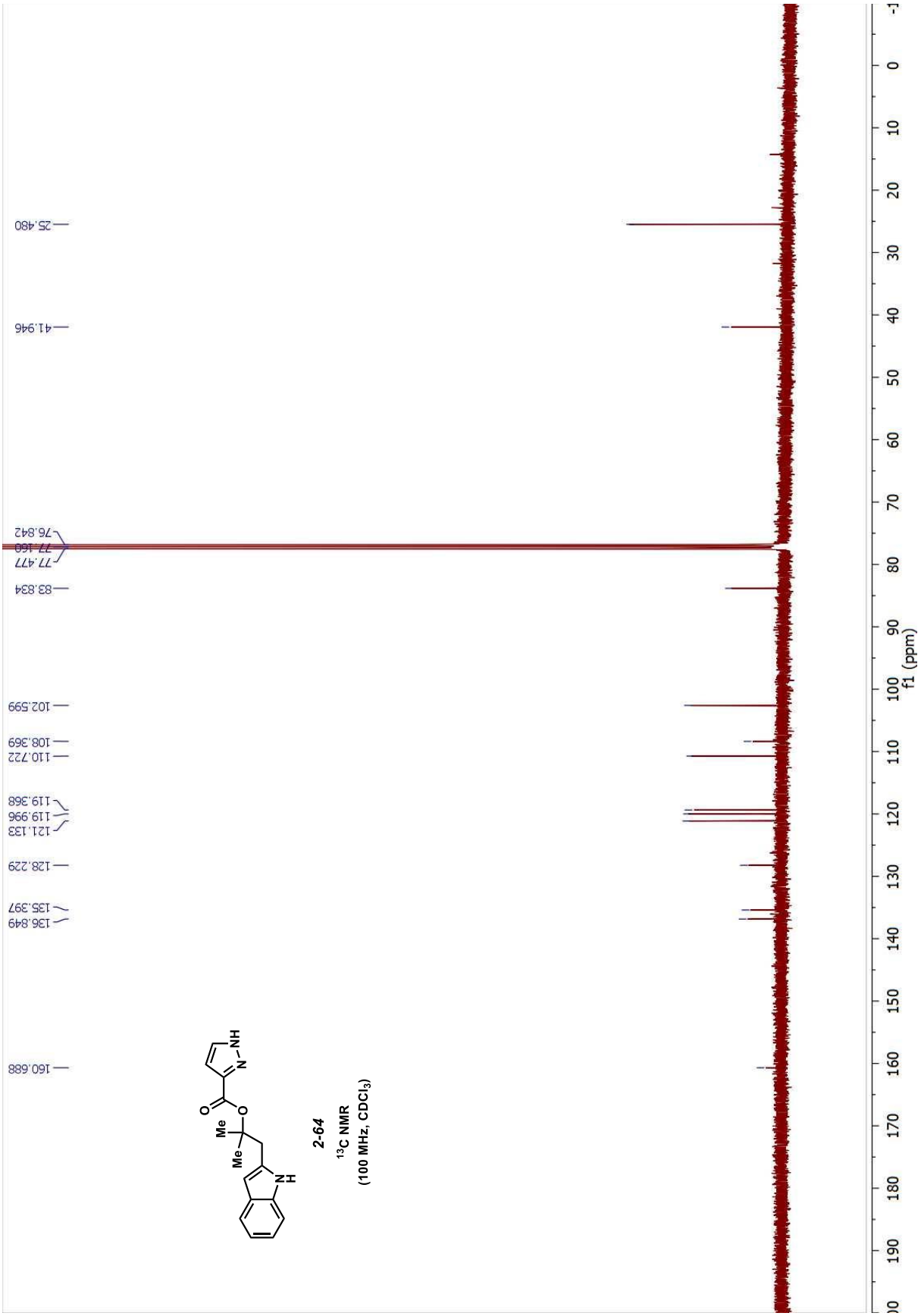
160.688
136.849
135.397
128.229
121.133
119.996
119.368
110.722
108.369
102.599
83.834
77.477
77.160
76.842
41.946
25.480
f1 (ppm)
2-64
13C NMR
(100 MHz, CDCl3)
Me
Me
O
O
NH
N
H

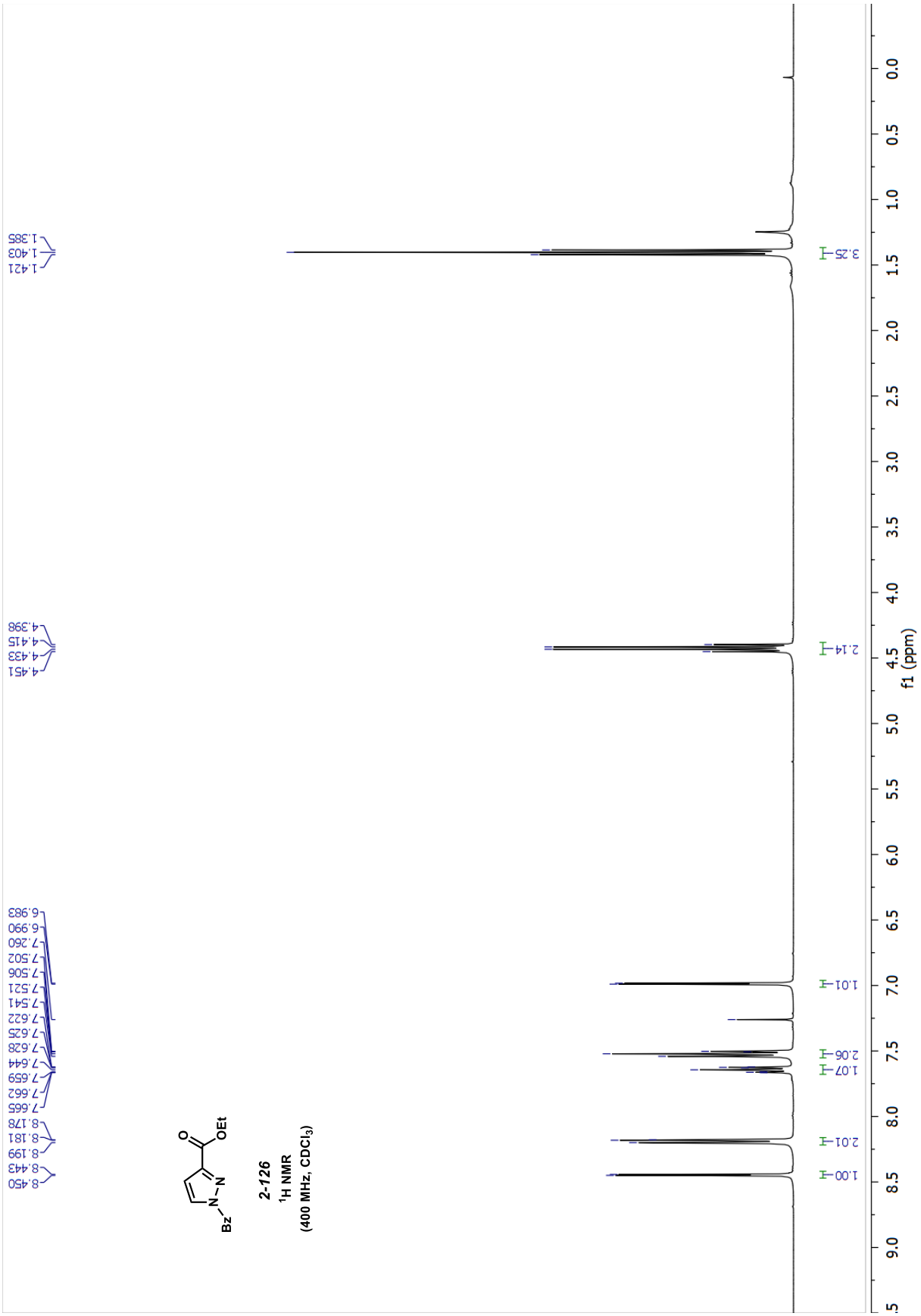
8.450
8.443
8.199
8.181
8.178
7.665
7.662
7.659
7.644
7.628
7.625
7.622
7.541
7.521
7.506
7.502
7.260
6.990
6.983
4.451
4.433
4.415
4.398
1.421
1.403
1.385
3.25
2.14
1.01
2.06
1.07
2.01
1.00
f1 (ppm)
O
OEt
N
N
Bz
2-126
1H NMR
(400 MHz, CDCl3)

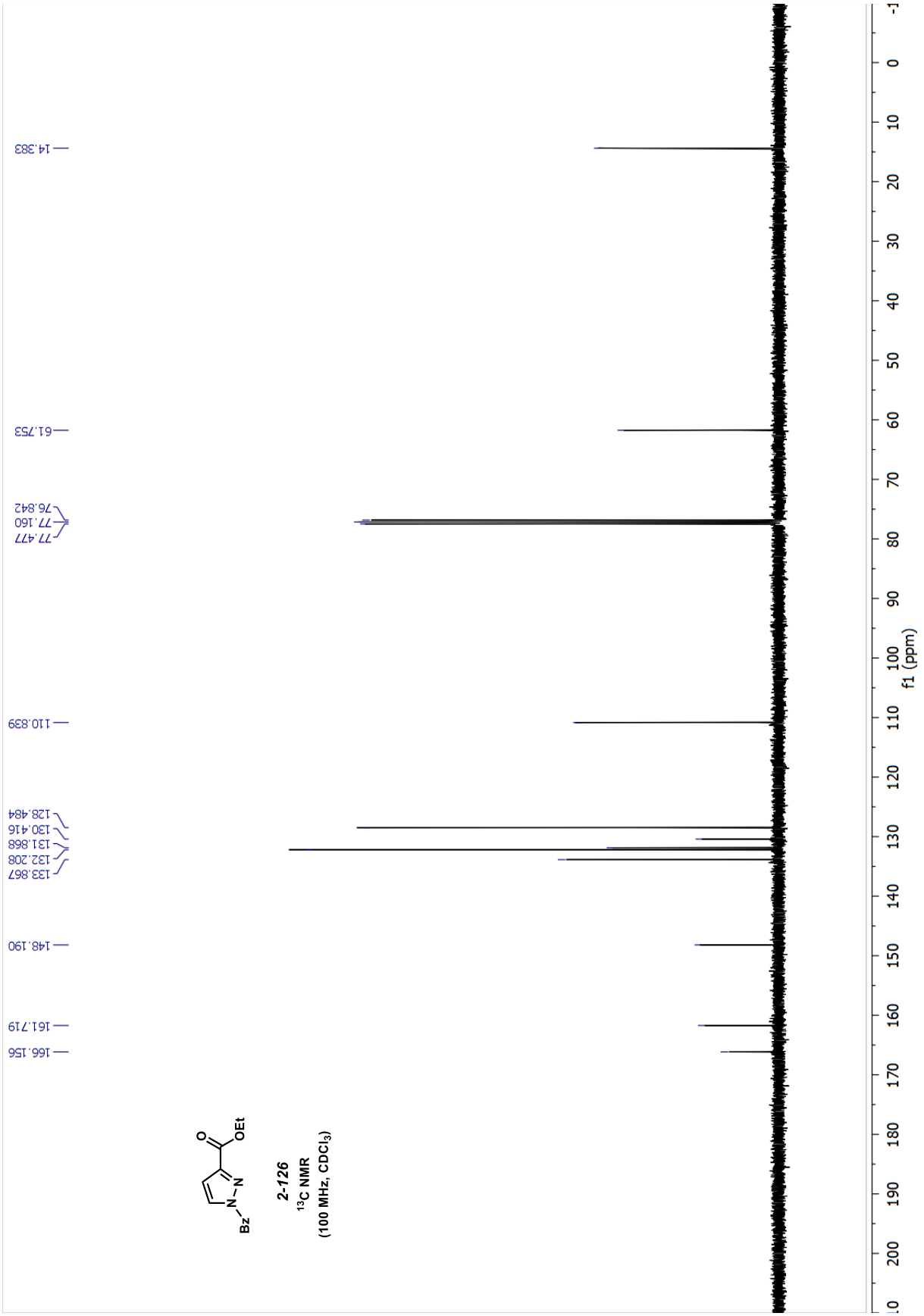
14.383
61.753
76.842
77.160
77.477
110.839
128.484
130.416
131.868
132.208
133.867
148.190
161.719
166.156
OEt
O
N
N
Bz
2-126
13C NMR
(100 MHz, CDCl3)
f1 (ppm)

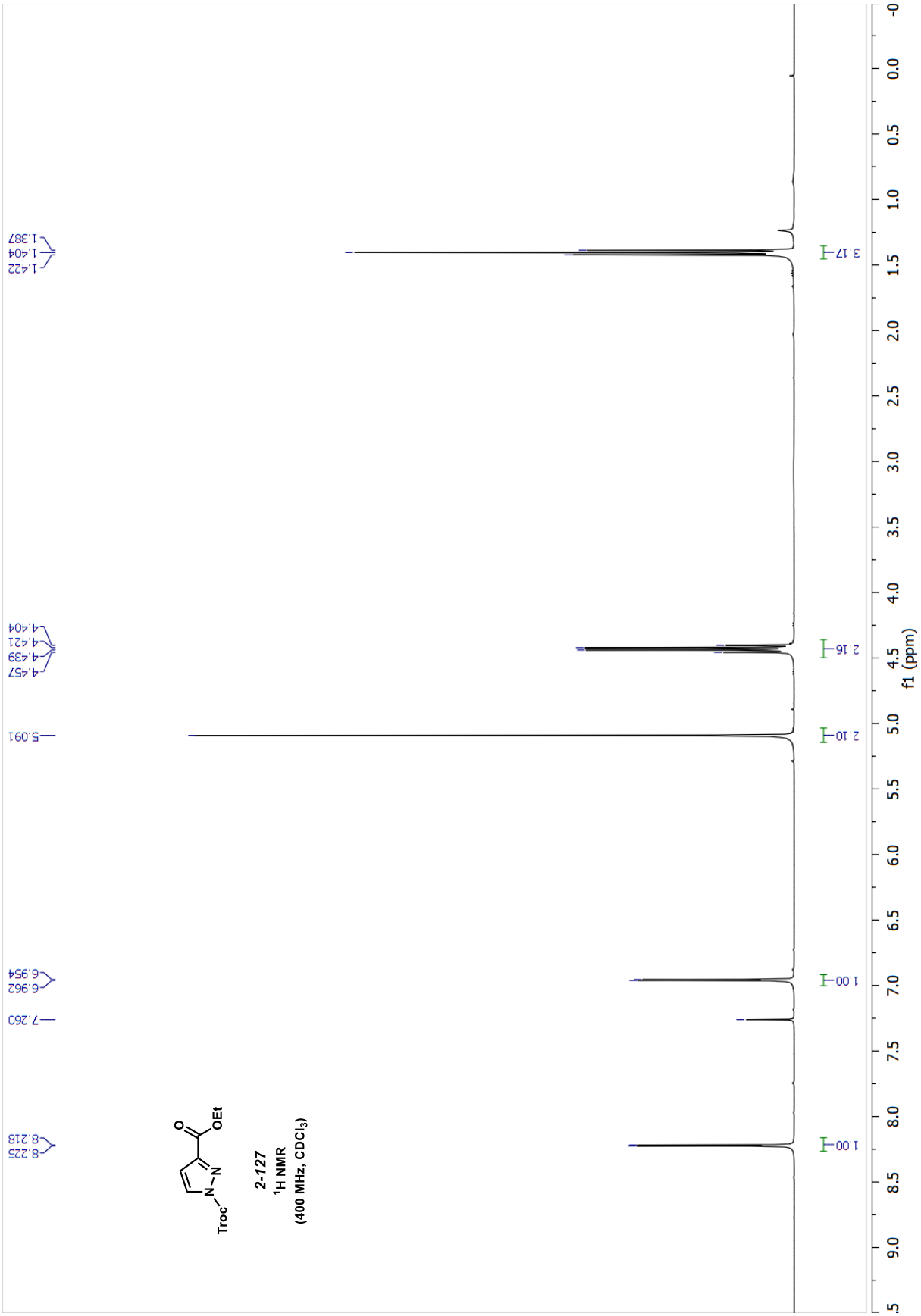
8.225
8.218
7.260
6.962
6.954
5.091
4.457
4.439
4.421
4.404
1.422
1.404
1.387
3.17
2.16
2.10
1.00
1.00
f1 (ppm)
2-127
1H NMR
(400 MHz, CDCl3)
Troc
OEt
O
N
N

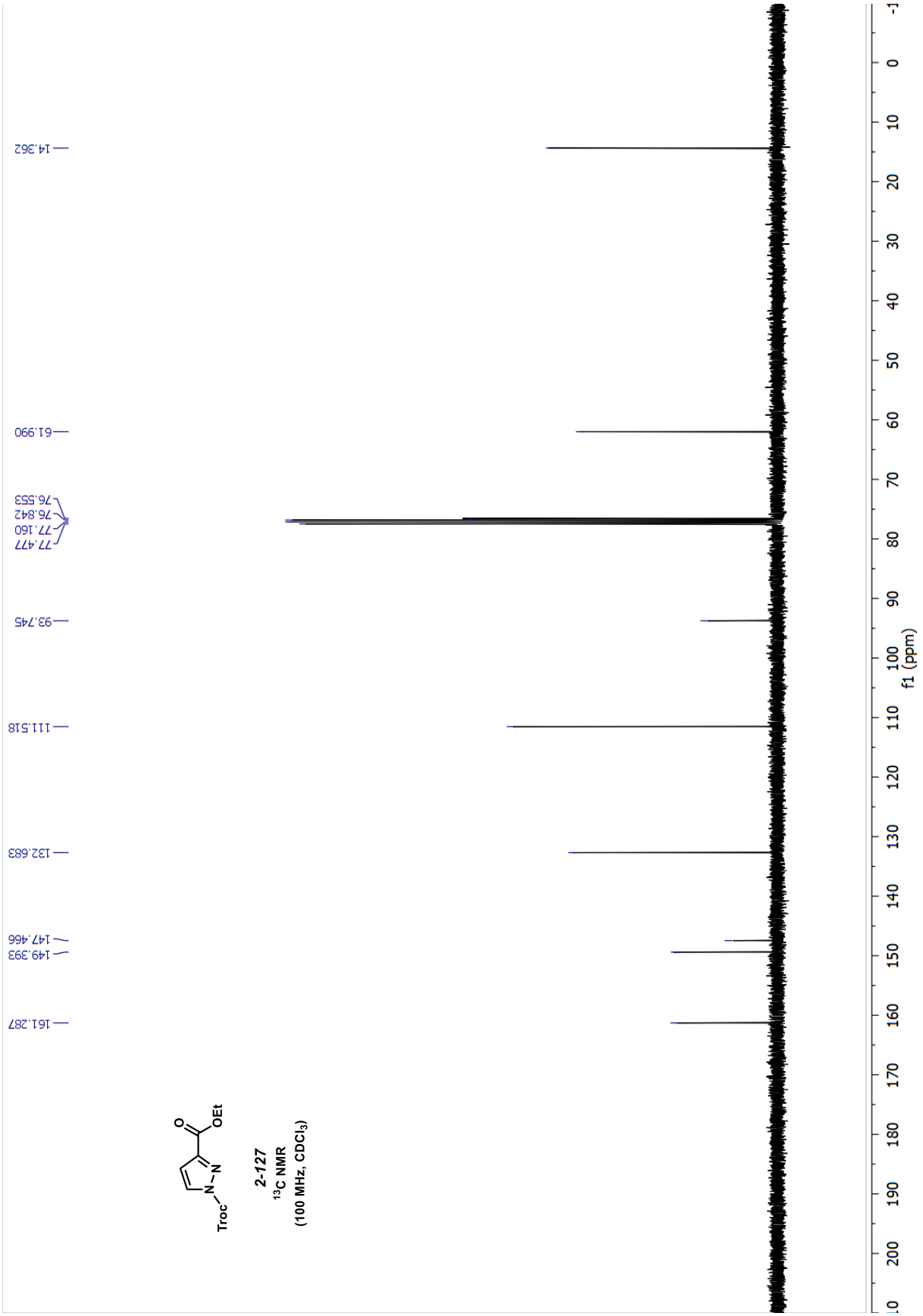
14.362
61.990
77.477
77.160
76.842
76.553
93.745
111.518
132.683
147.466
149.393
161.287
OEt
Troc
2-127
13C NMR
(100 MHz, CDCl3)
f1 (ppm)

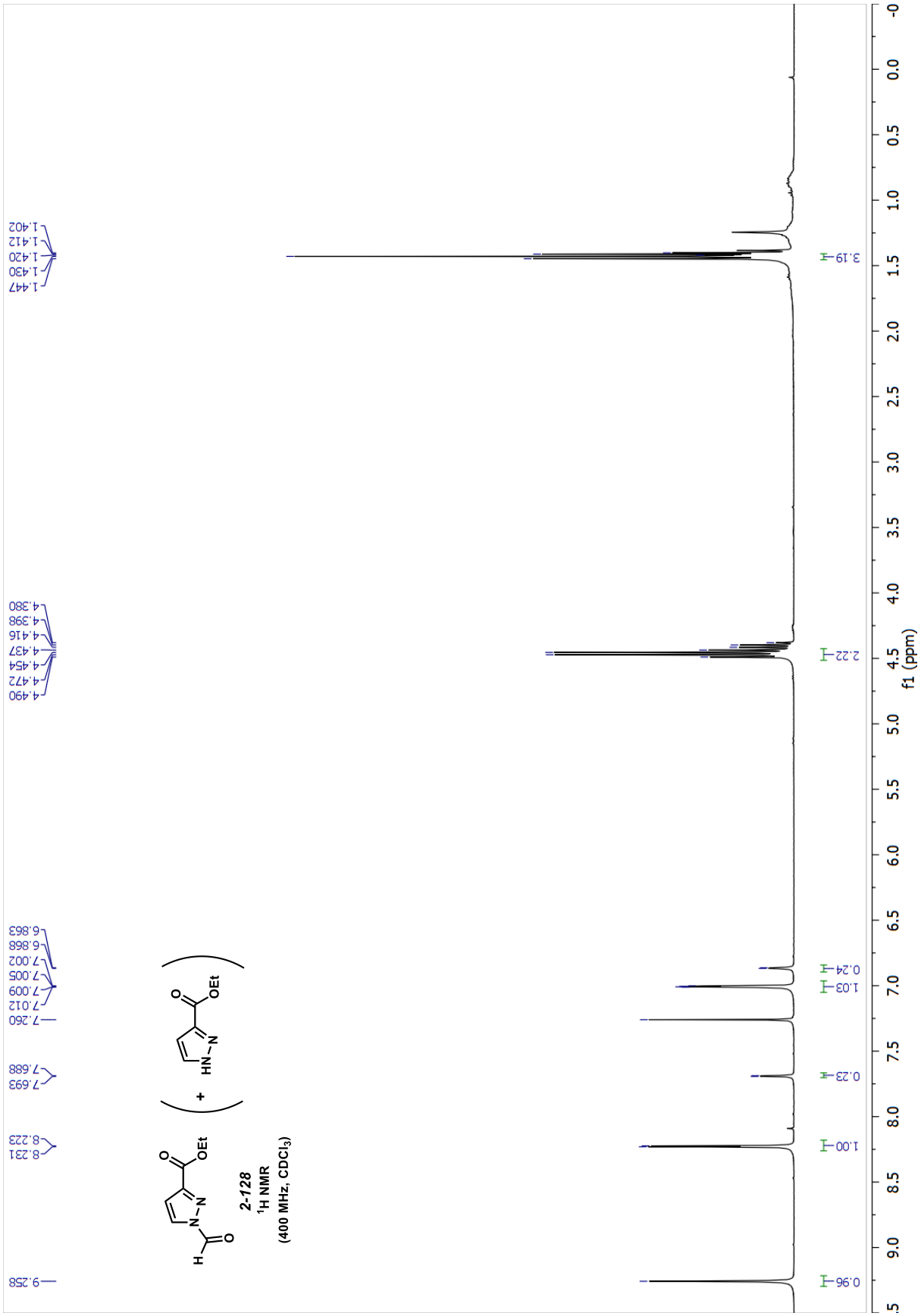
2-128
^{1}H NMR
(400 MHz, CDCl$_3$)
f1 (ppm)

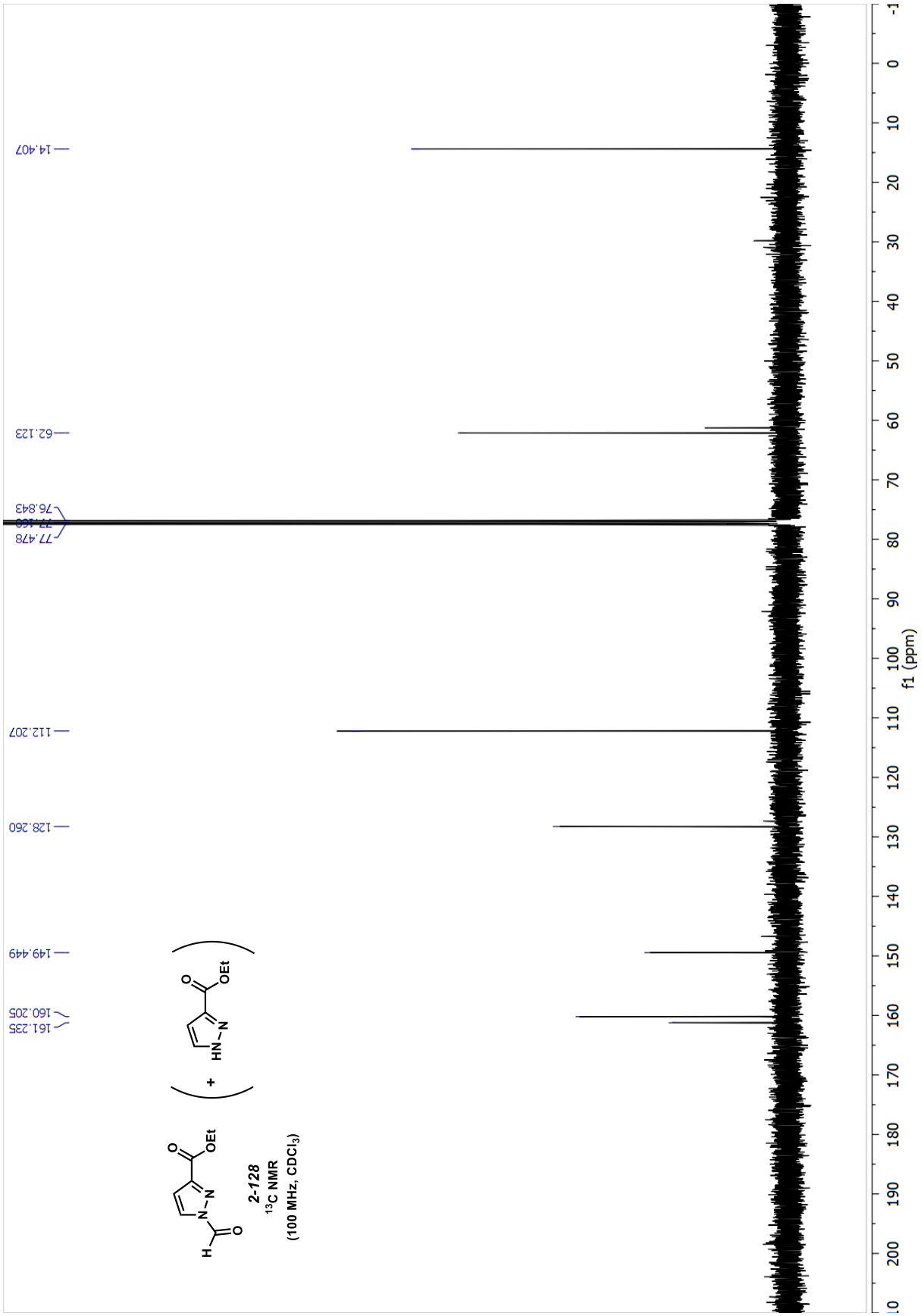
14.407
62.123
76.843
77.159
77.478
112.207
128.260
149.449
160.205
161.235
f1 (ppm)
2-128
13C NMR
(100 MHz, CDCl3)
OEt
O
N
NH
H
+

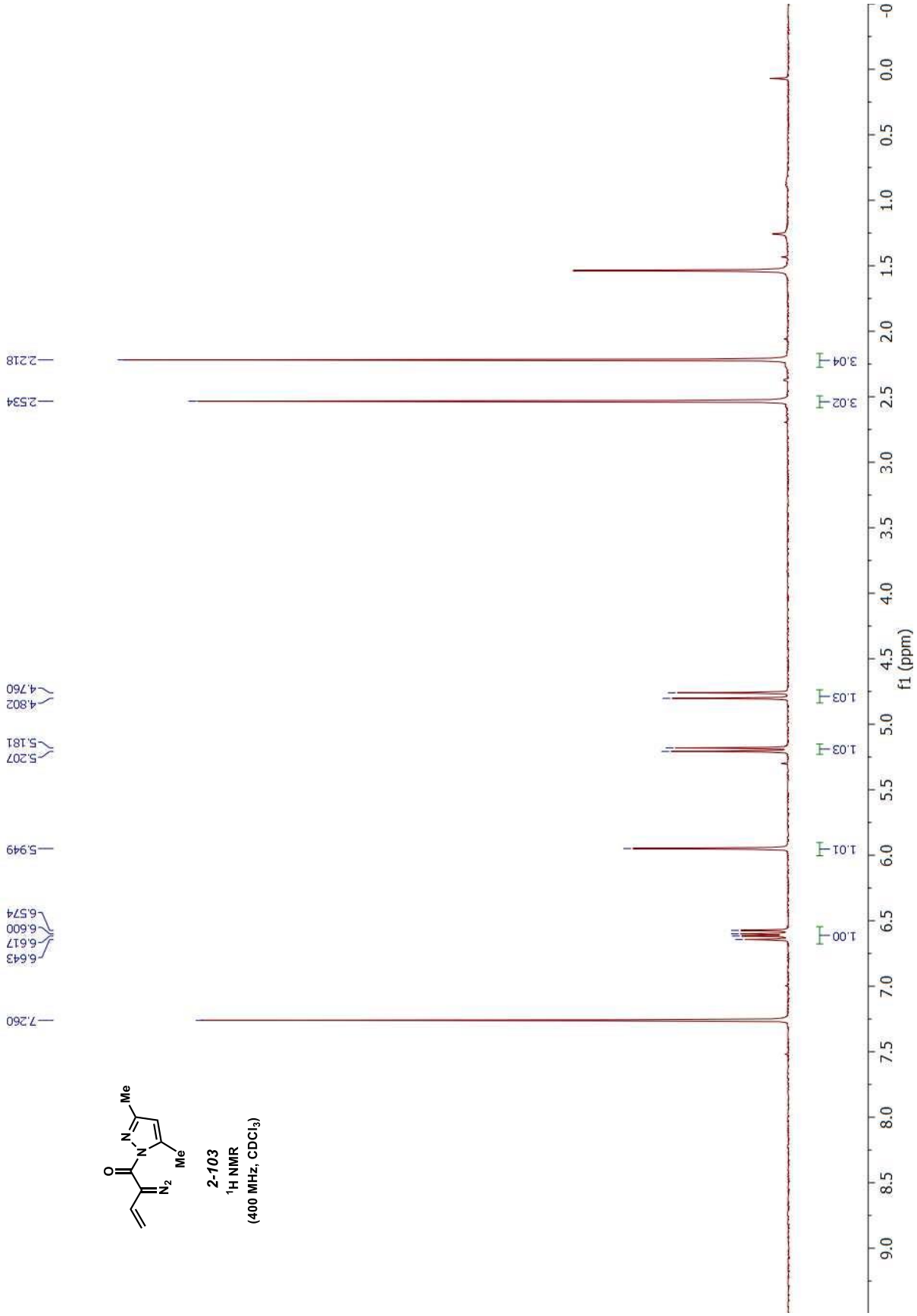
2-103
^{1}H NMR
(400 MHz, CDCl$_3$)
Me
Me
O
N$_2$
7.260
6.643
6.617
6.600
6.574
5.949
5.207
5.181
4.802
4.760
2.534
2.218
1.00
1.01
1.03
1.03
1.03
3.02
3.04
f1 (ppm)

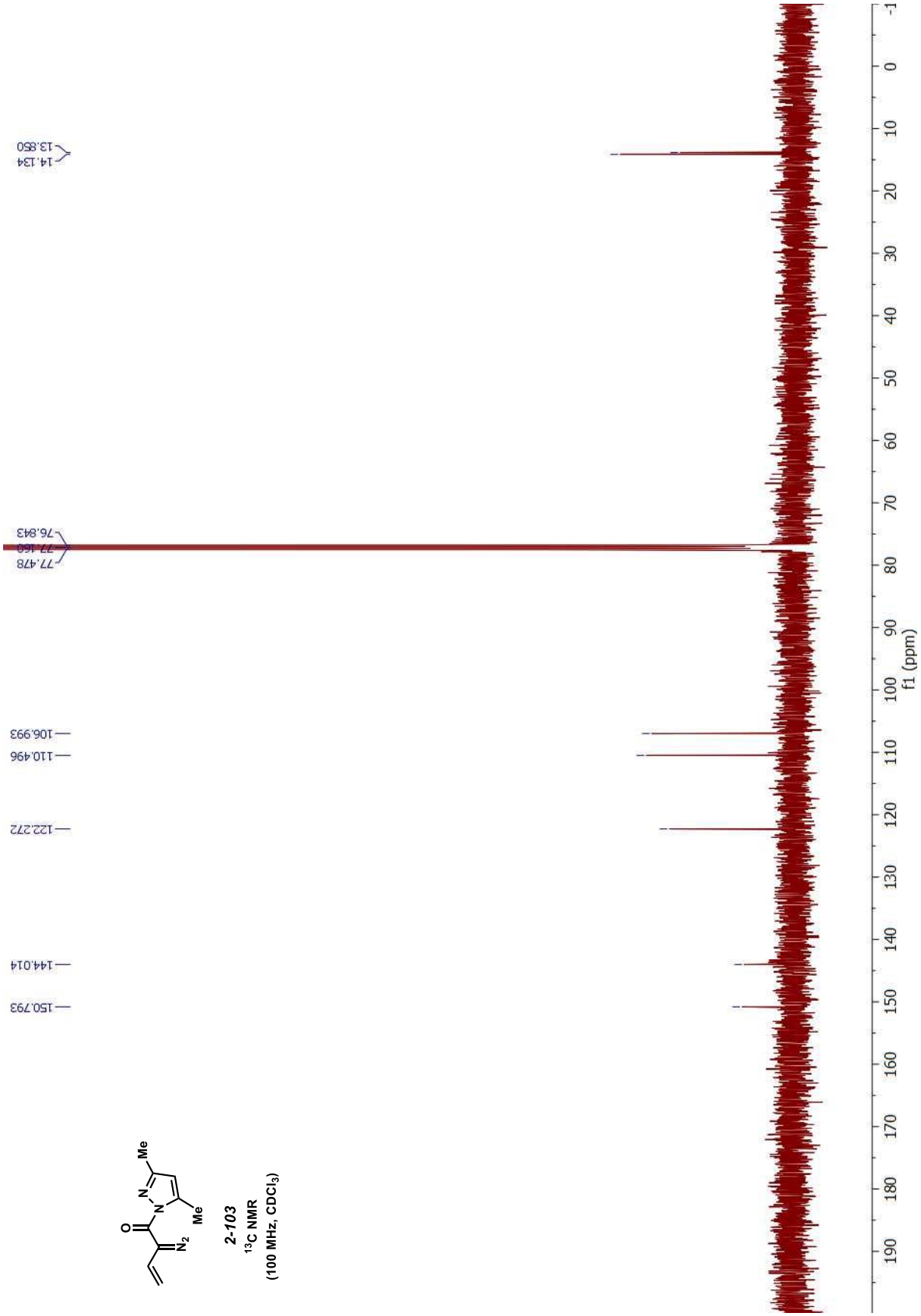
13.850
14.134
76.843
77.160
77.478
106.993
110.496
122.272
144.014
150.793
f1 (ppm)
Me
Me
O
N2
2-103
13C NMR
(100 MHz, CDCl3)

APPENDIX B

NMR SPECTRA RELEVANT TO CHAPTER 3

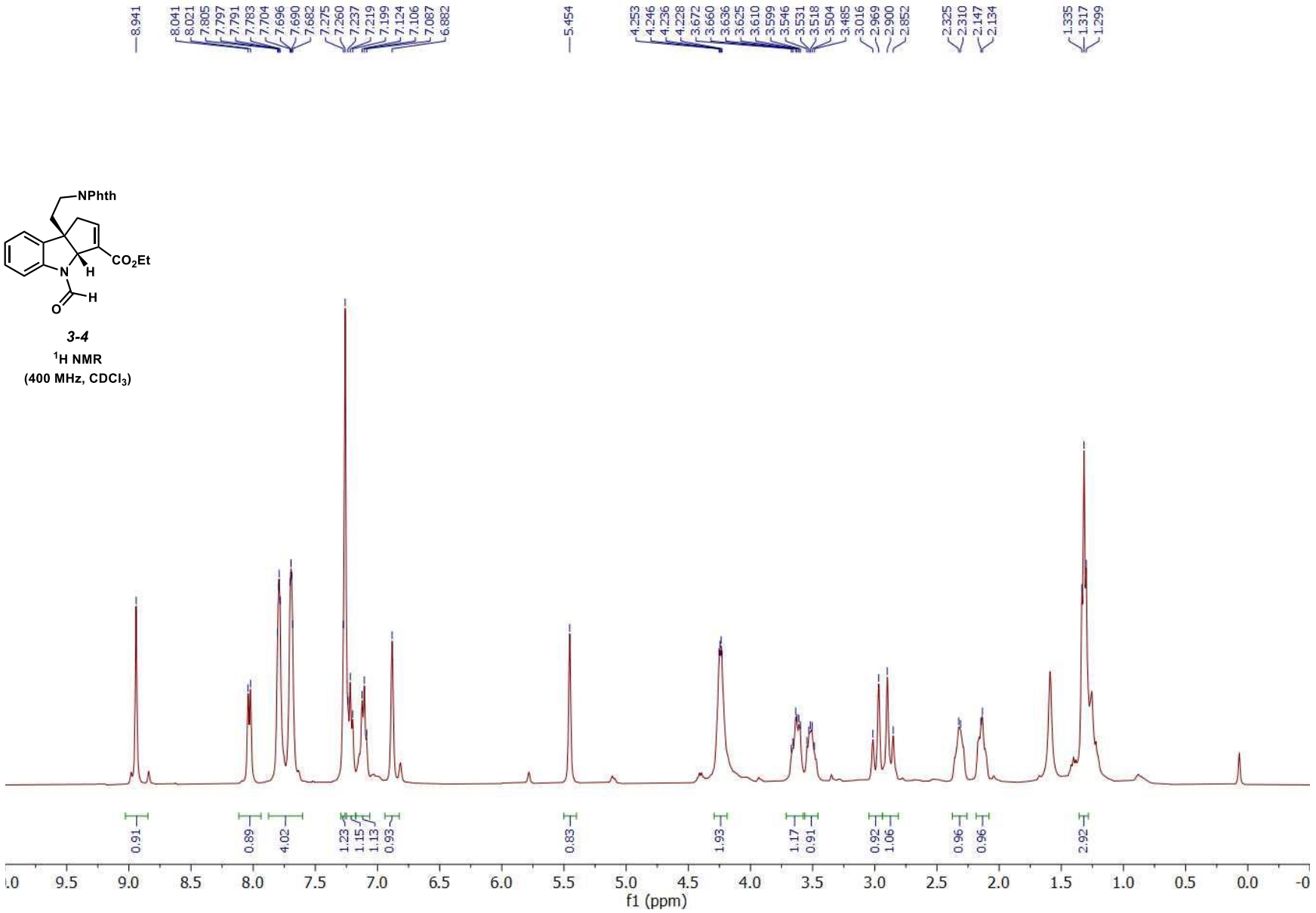
8.941
8.041
8.021
7.805
7.797
7.791
7.783
7.704
7.696
7.690
7.682
7.275
7.260
7.237
7.219
7.199
7.124
7.106
7.087
6.882
5.454
4.253
4.246
4.236
4.228
3.672
3.660
3.636
3.625
3.610
3.599
3.546
3.531
3.518
3.504
3.485
3.016
2.969
2.900
2.852
2.325
2.310
2.147
2.134
1.335
1.317
1.299
NPhth
CO2Et
N
H
O
H
3-4
1H NMR
(400 MHz, CDCl3)
0.91
0.89
4.02
1.23
1.15
1.13
0.93
0.83
1.93
1.17
0.91
0.92
1.06
0.96
0.96
2.92
f1 (ppm)

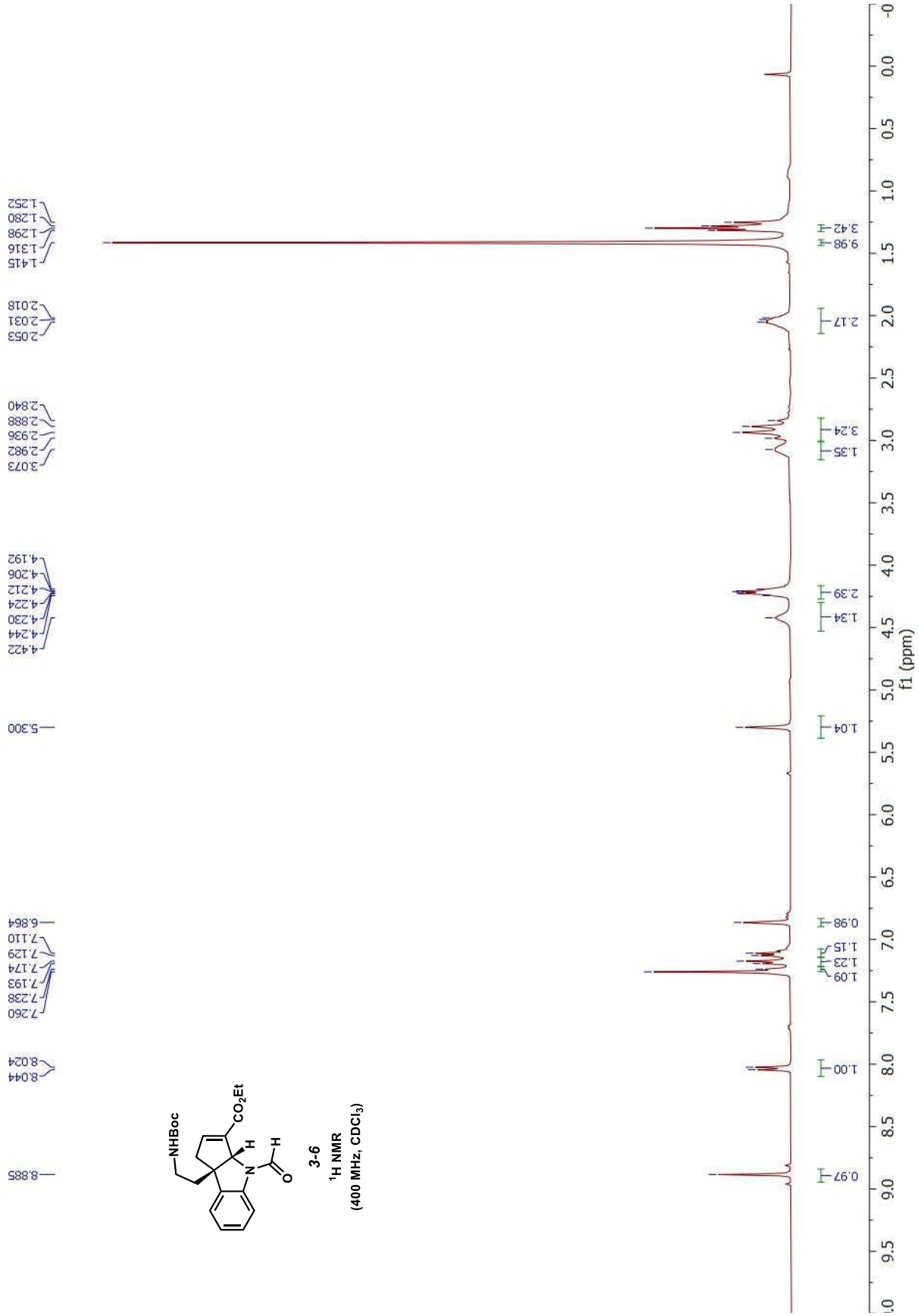
NHBoc
CO2Et
H
N
H
O
3-6
1H NMR
(400 MHz, CDCl3)
f1 (ppm)

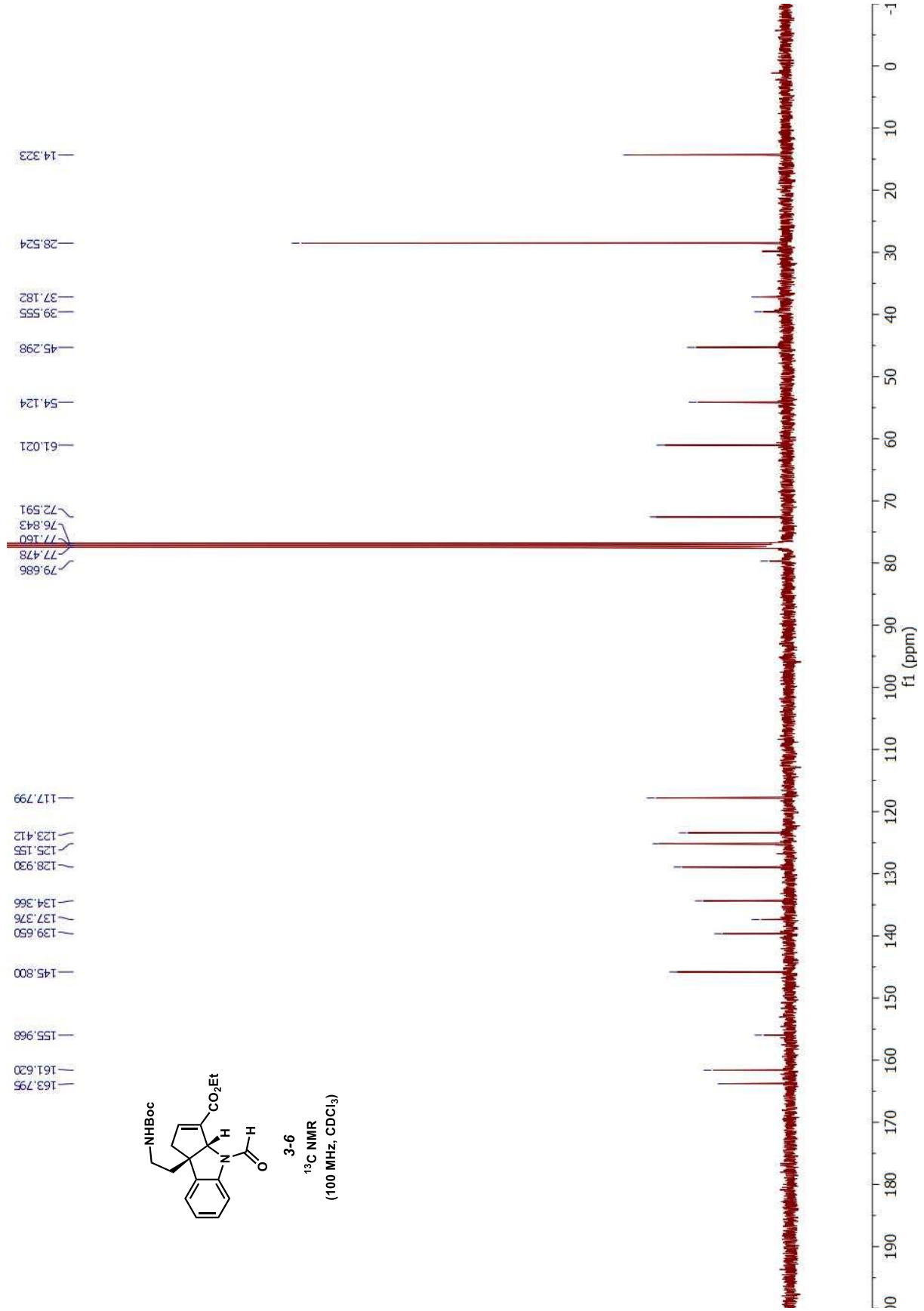
14.323
28.524
37.182
39.555
45.298
54.124
61.021
72.591
76.843
77.160
77.478
79.686
117.799
123.412
125.155
128.930
134.366
137.376
139.650
145.800
155.968
161.620
163.795
NHBoc
CO2Et
H
N
O
H
3-6
13C NMR
(100 MHz, CDCl3)
f1 (ppm)

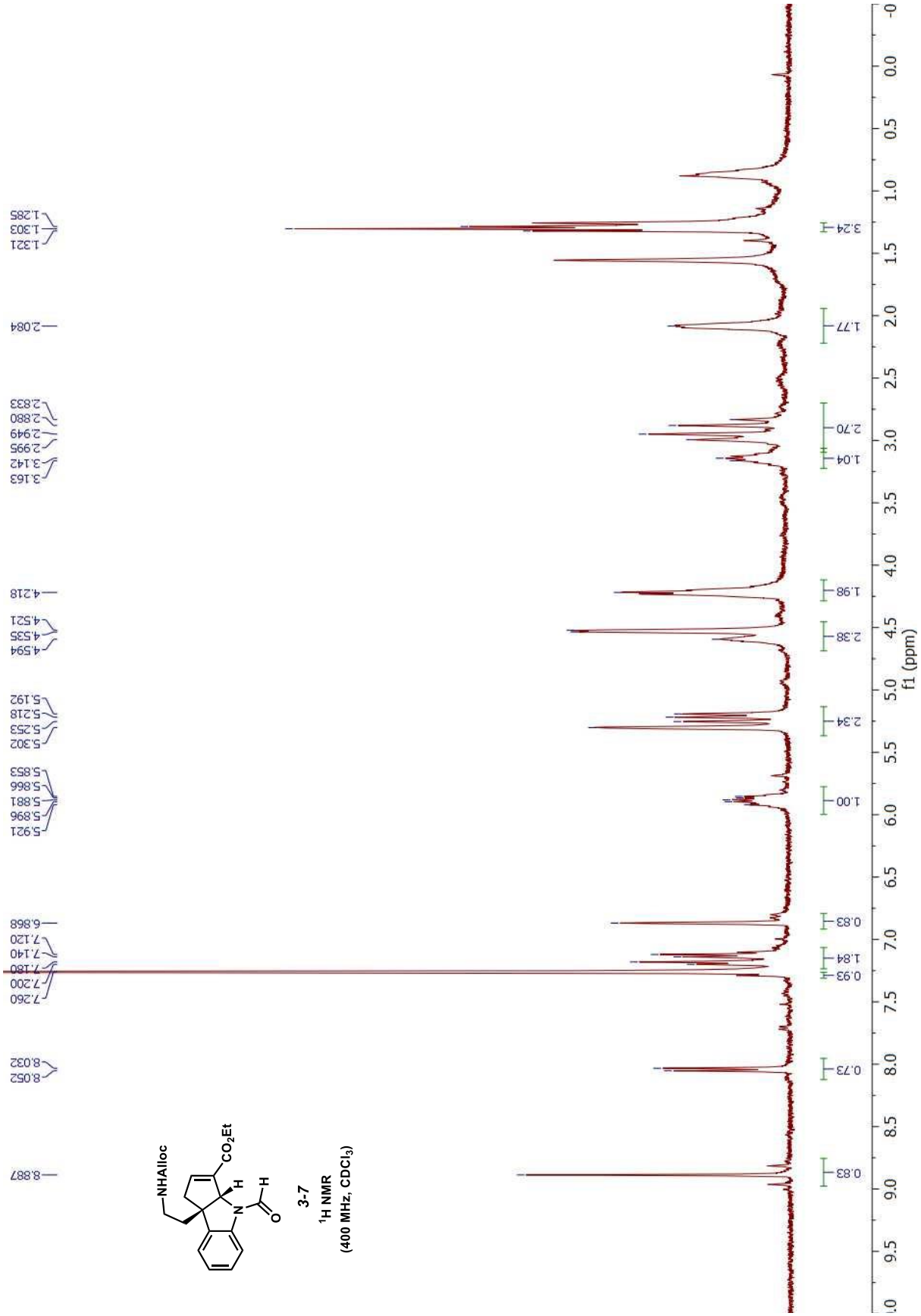
NHAlloc
CO2Et
H
N
H
O
3-7
1H NMR
(400 MHz, CDCl3)
f1 (ppm)

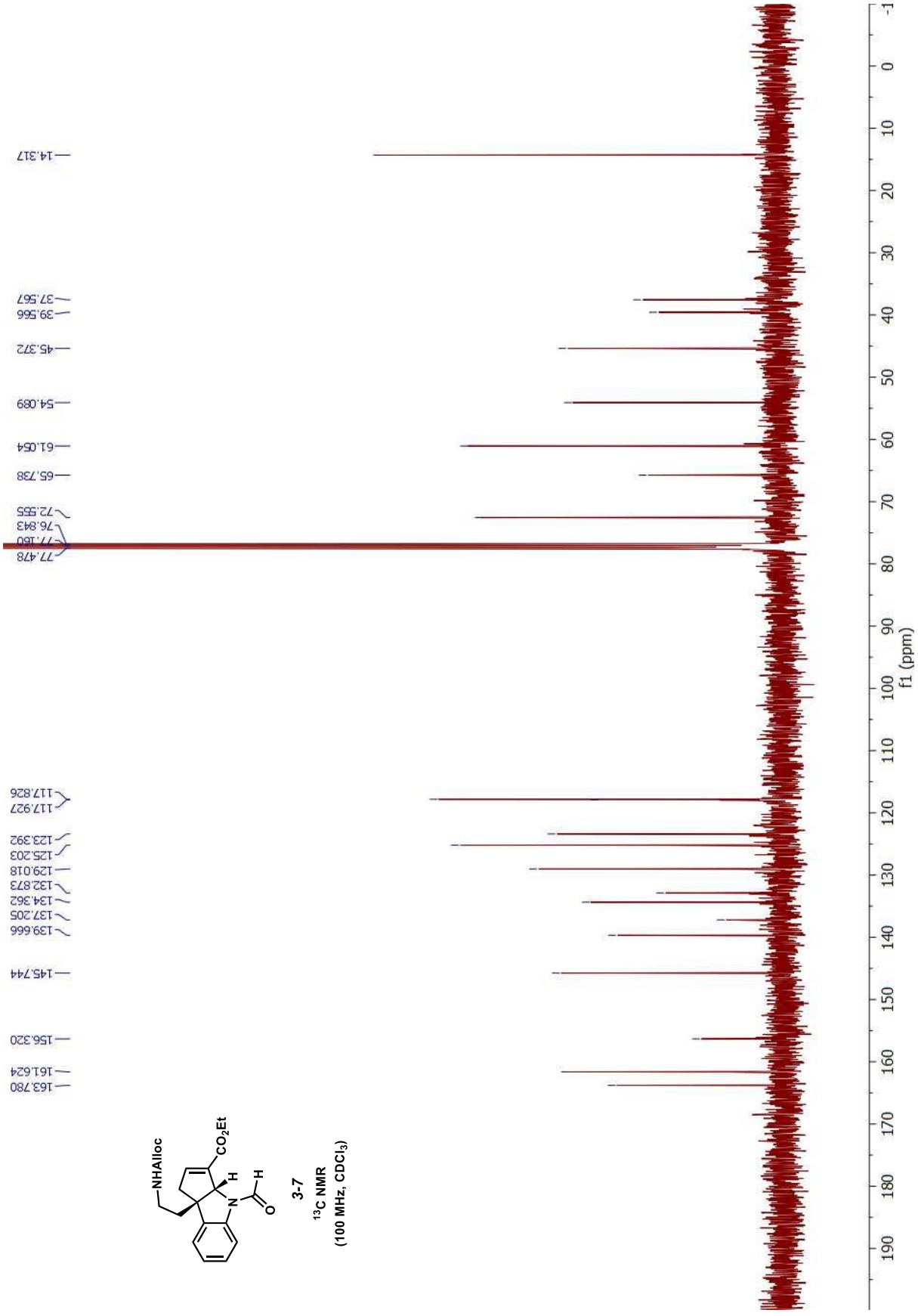
14.317
37.567
39.566
45.372
54.089
61.054
65.738
72.555
76.843
77.160
77.478
117.826
117.927
123.392
125.203
129.018
132.873
134.362
137.205
139.666
145.744
156.320
161.624
163.780
NHAlloc
CO2Et
H
N
O
H
3-7
13C NMR
(100 MHz, CDCl3)
f1 (ppm)

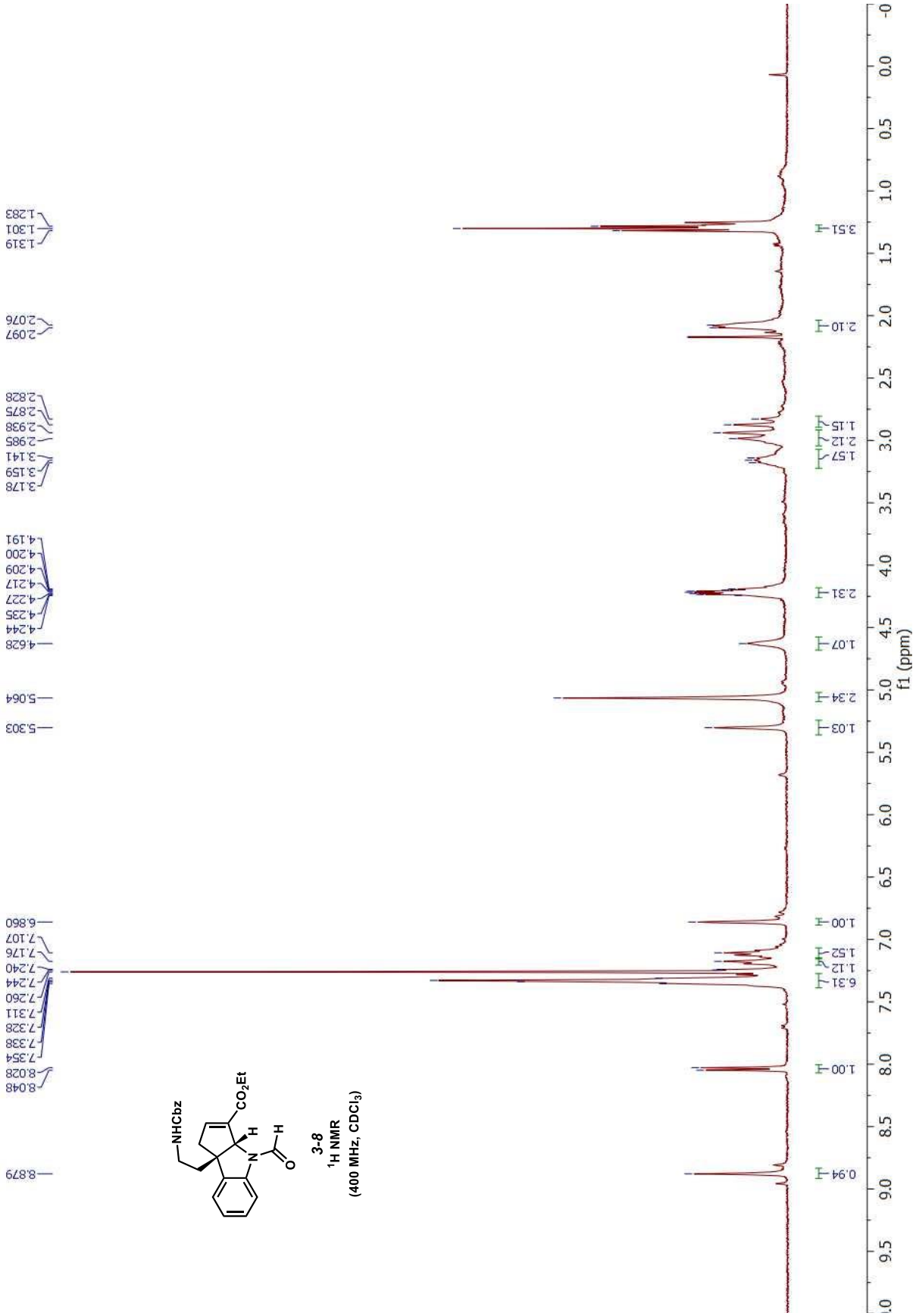
NHCbz
CO2Et
H
N
H
O
3-8
1H NMR
(400 MHz, CDCl3)
f1 (ppm)

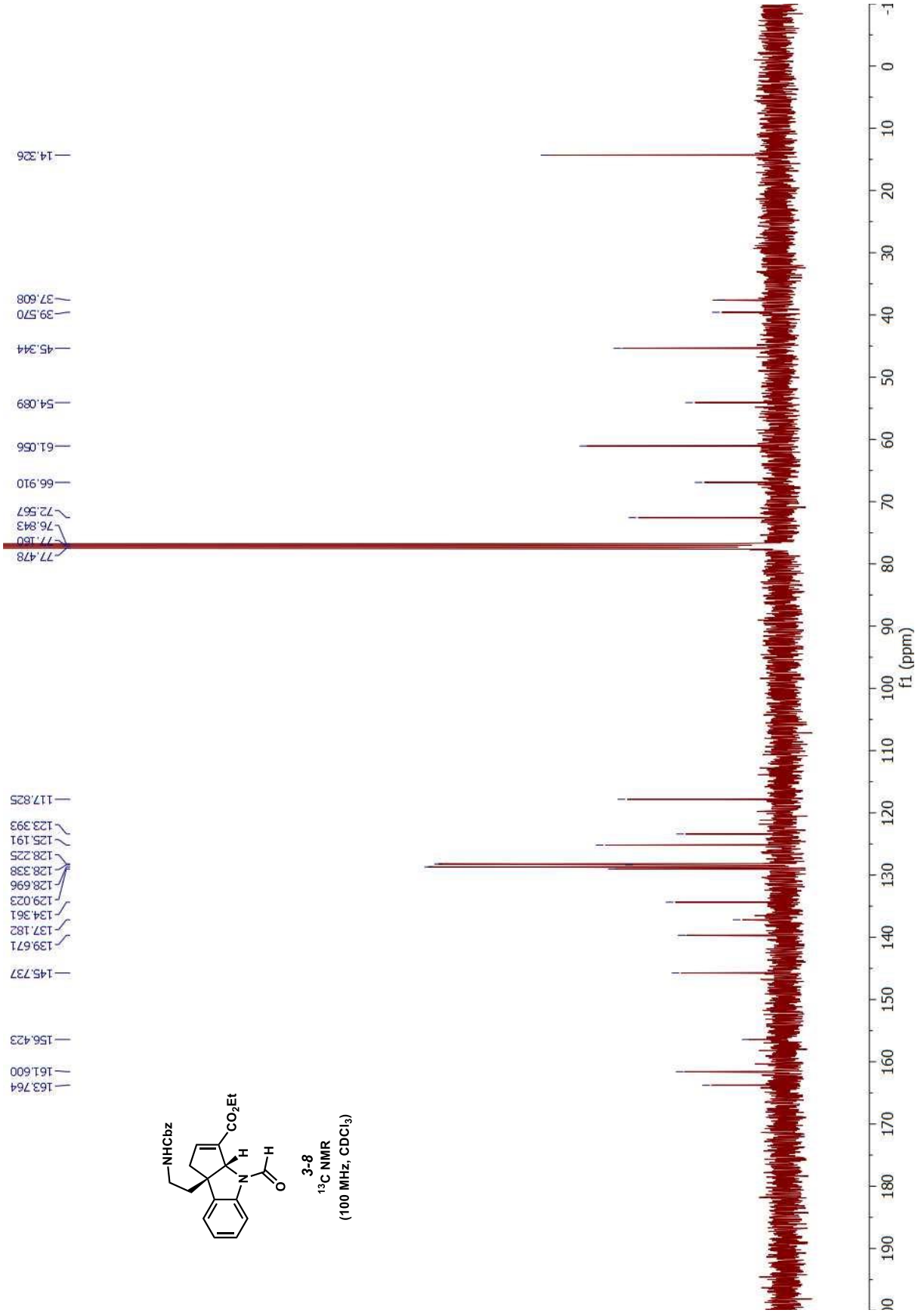
14.326
37.608
39.570
45.344
54.089
61.056
66.910
72.567
76.843
77.160
77.478
117.825
123.393
125.191
128.225
128.338
128.696
129.023
134.361
137.182
139.671
145.737
156.423
161.600
163.764
NHCbz
CO2Et
H
N
H
O
3-8
13C NMR
(100 MHz, CDCl3)
f1 (ppm)

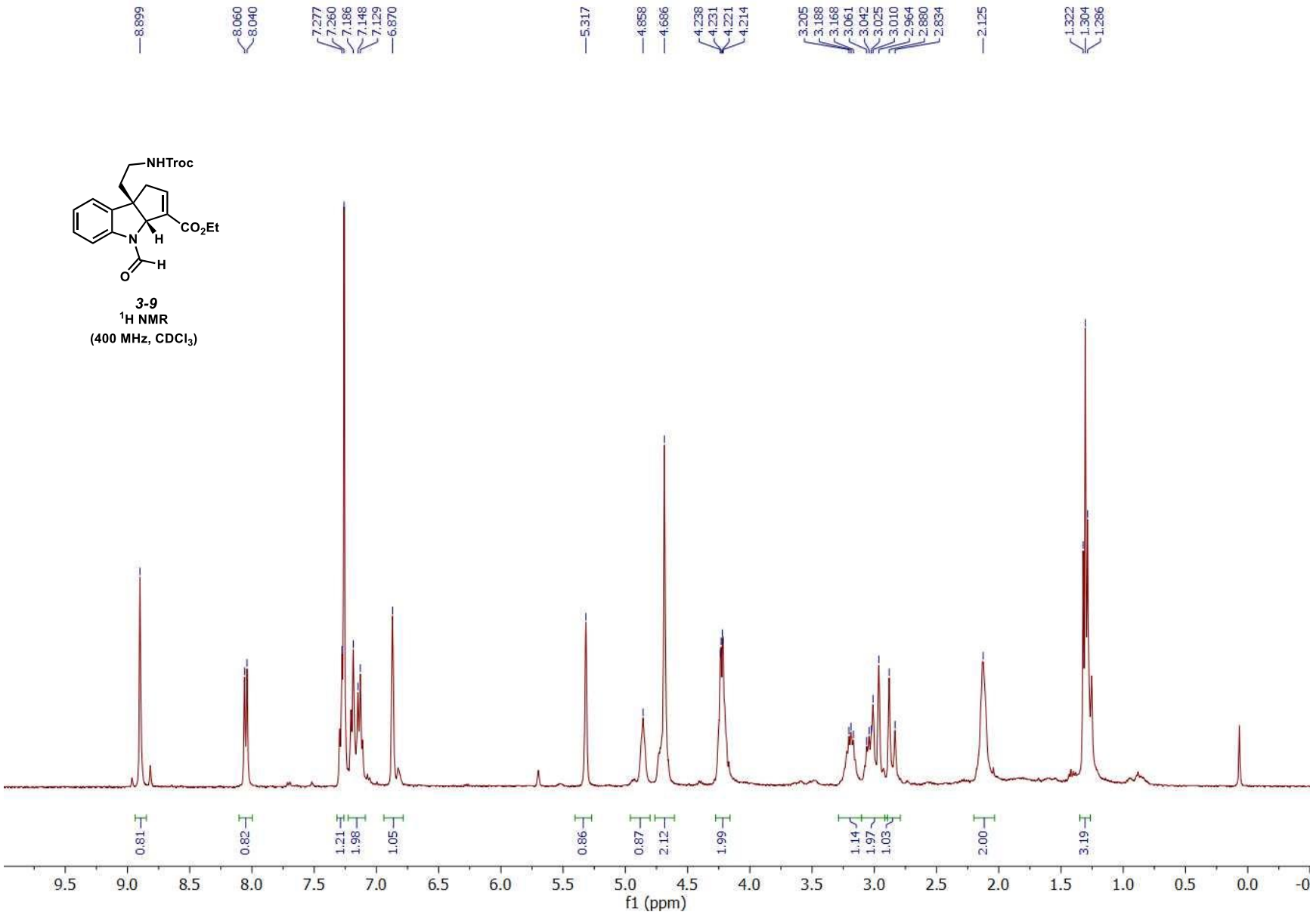
8.899
8.060
8.040
7.277
7.260
7.186
7.148
7.129
6.870
5.317
4.858
4.686
4.238
4.231
4.221
4.214
3.205
3.188
3.168
3.061
3.042
3.025
3.010
2.964
2.880
2.834
2.125
1.322
1.304
1.286
NHTroc
CO2Et
N
H
O
H
3-9
1H NMR
(400 MHz, CDCl3)
0.81
0.82
1.21
1.98
1.05
0.86
0.87
2.12
1.99
1.14
1.97
1.03
2.00
3.19
9.5
9.0
8.5
8.0
7.5
7.0
6.5
6.0
5.5
5.0
4.5
4.0
3.5
3.0
2.5
2.0
1.5
1.0
0.5
0.0
f1 (ppm)

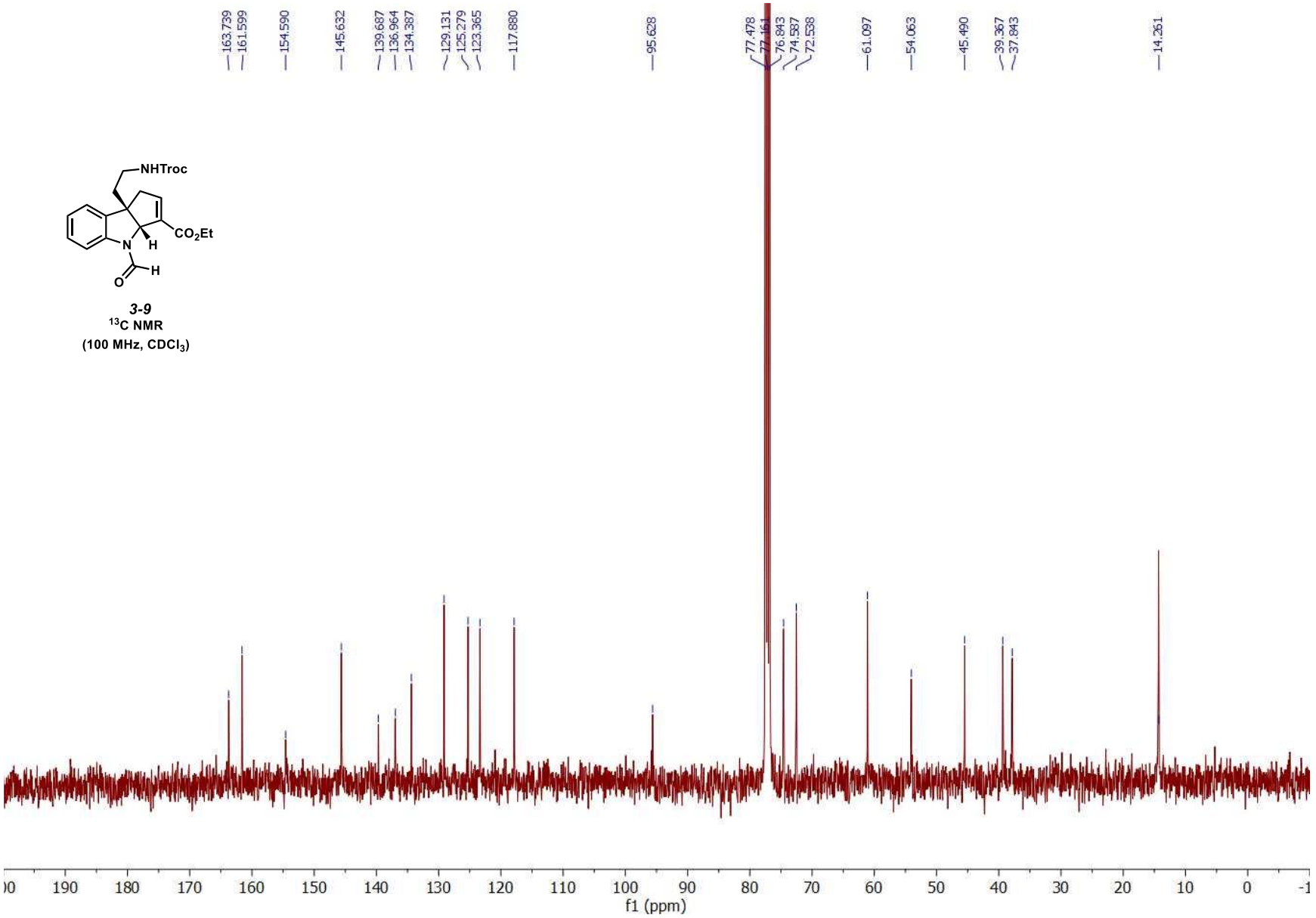
163.739
161.599
154.590
145.632
139.687
136.964
134.387
129.131
125.279
123.365
117.880
95.628
77.478
77.161
76.843
74.587
72.538
61.097
54.063
45.490
39.367
37.843
14.261
NHTroc
CO2Et
N
H
H
O
3-9
13C NMR
(100 MHz, CDCl3)
f1 (ppm)

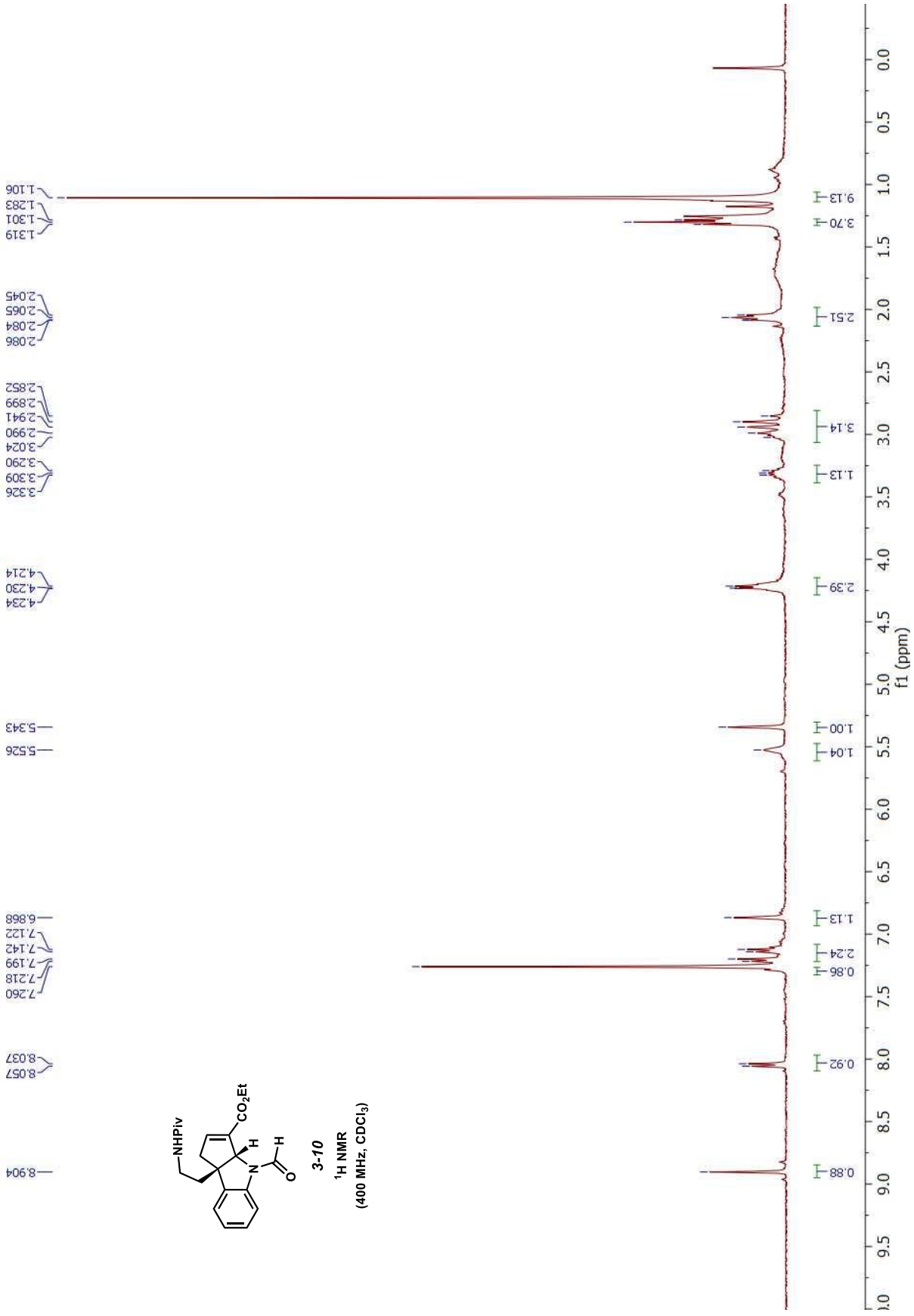

3-10

^{1}H NMR

(400 MHz, $CDCl_3$)

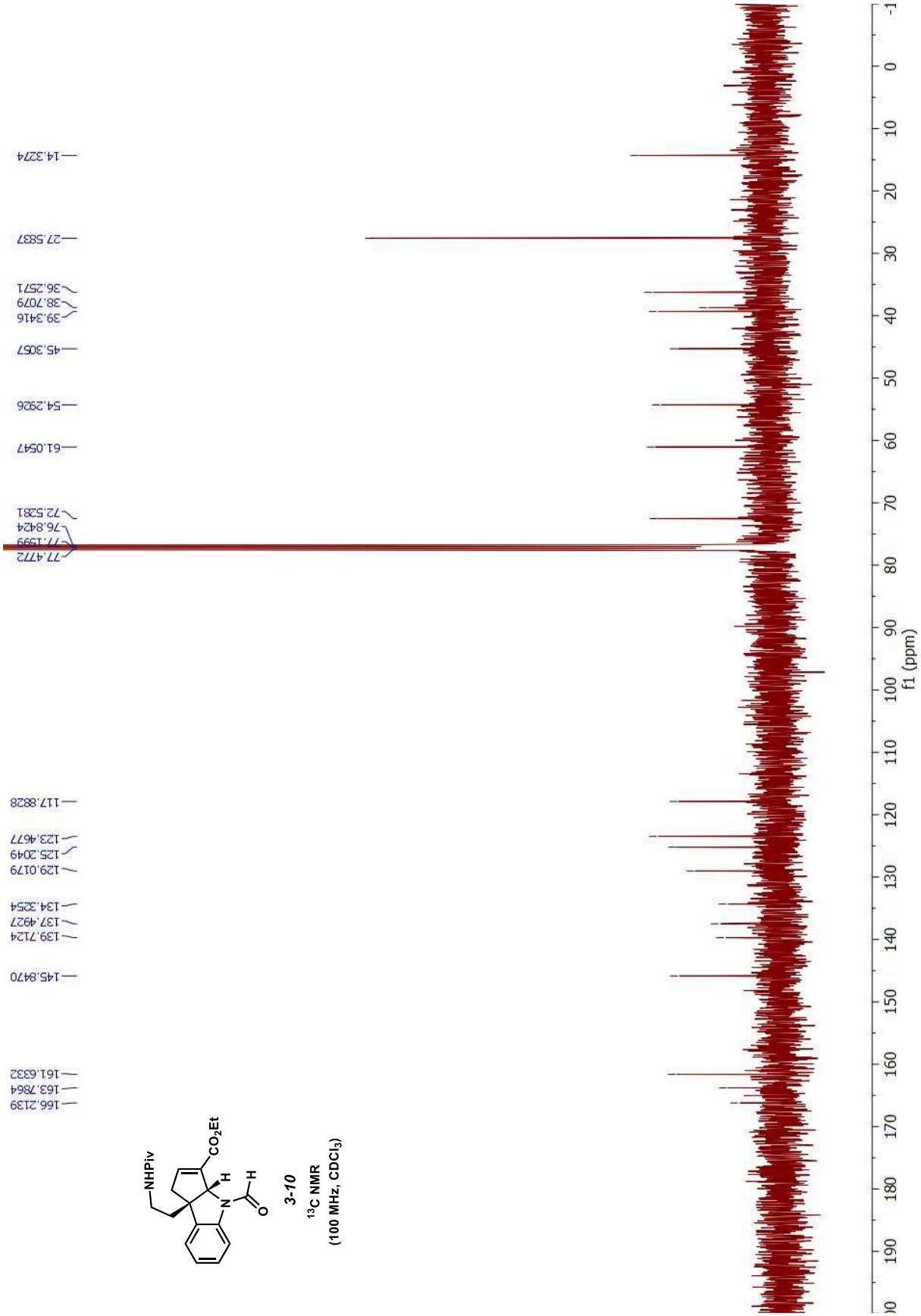
14.3274
27.5837
36.2571
38.7079
39.3416
45.3057
54.2926
61.0547
72.5281
76.8424
77.1599
77.4772
117.8828
123.4677
125.2049
129.0179
134.3254
137.4927
139.7124
145.8470
161.6332
163.7864
166.2139
NHPiv
CO2Et
H
N
H
O
3-10
13C NMR
(100 MHz, CDCl3)
f1 (ppm)

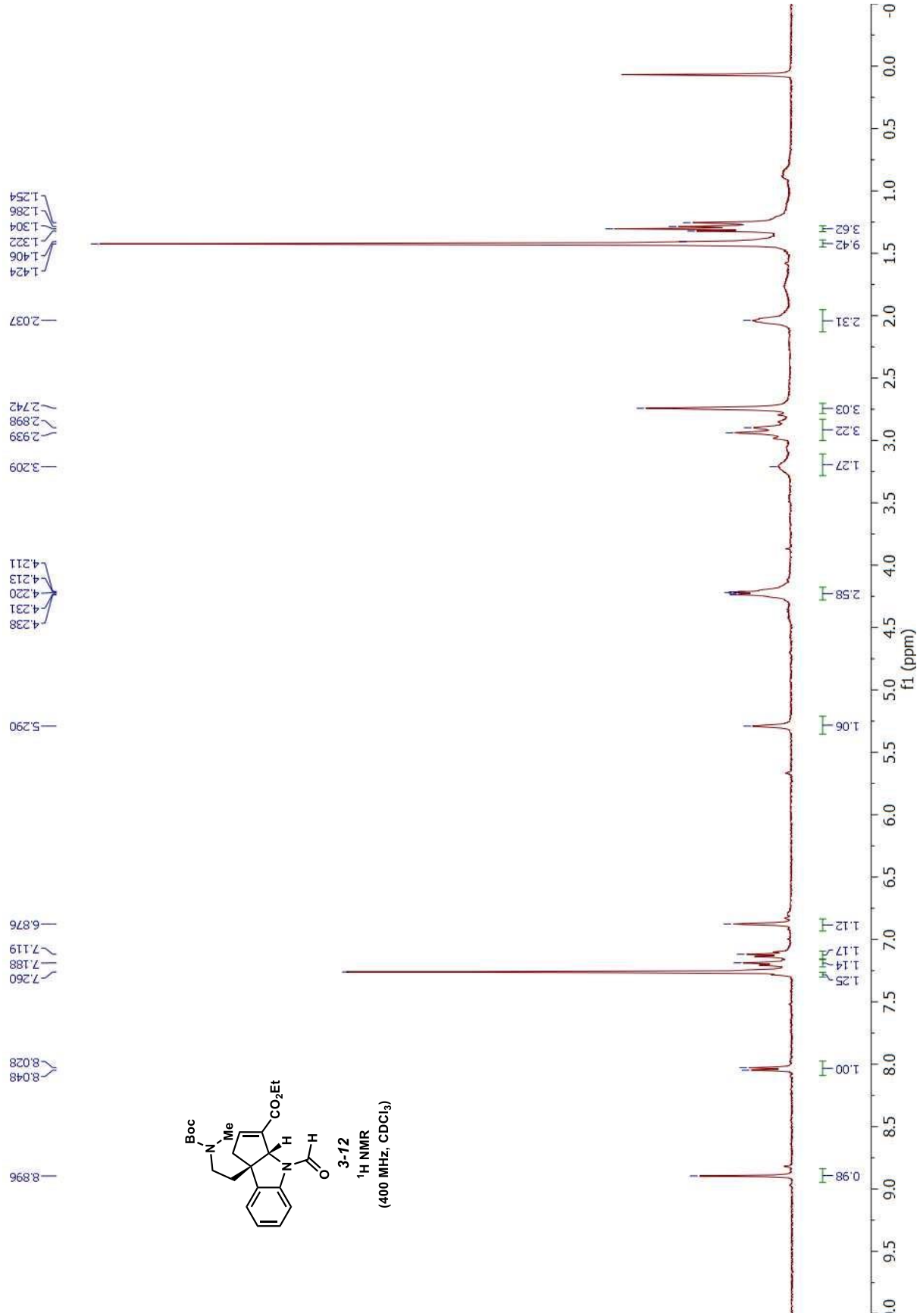
Boc
N
Me
CO2Et
H
N
H
O
3-12
1H NMR
(400 MHz, CDCl3)
f1 (ppm)

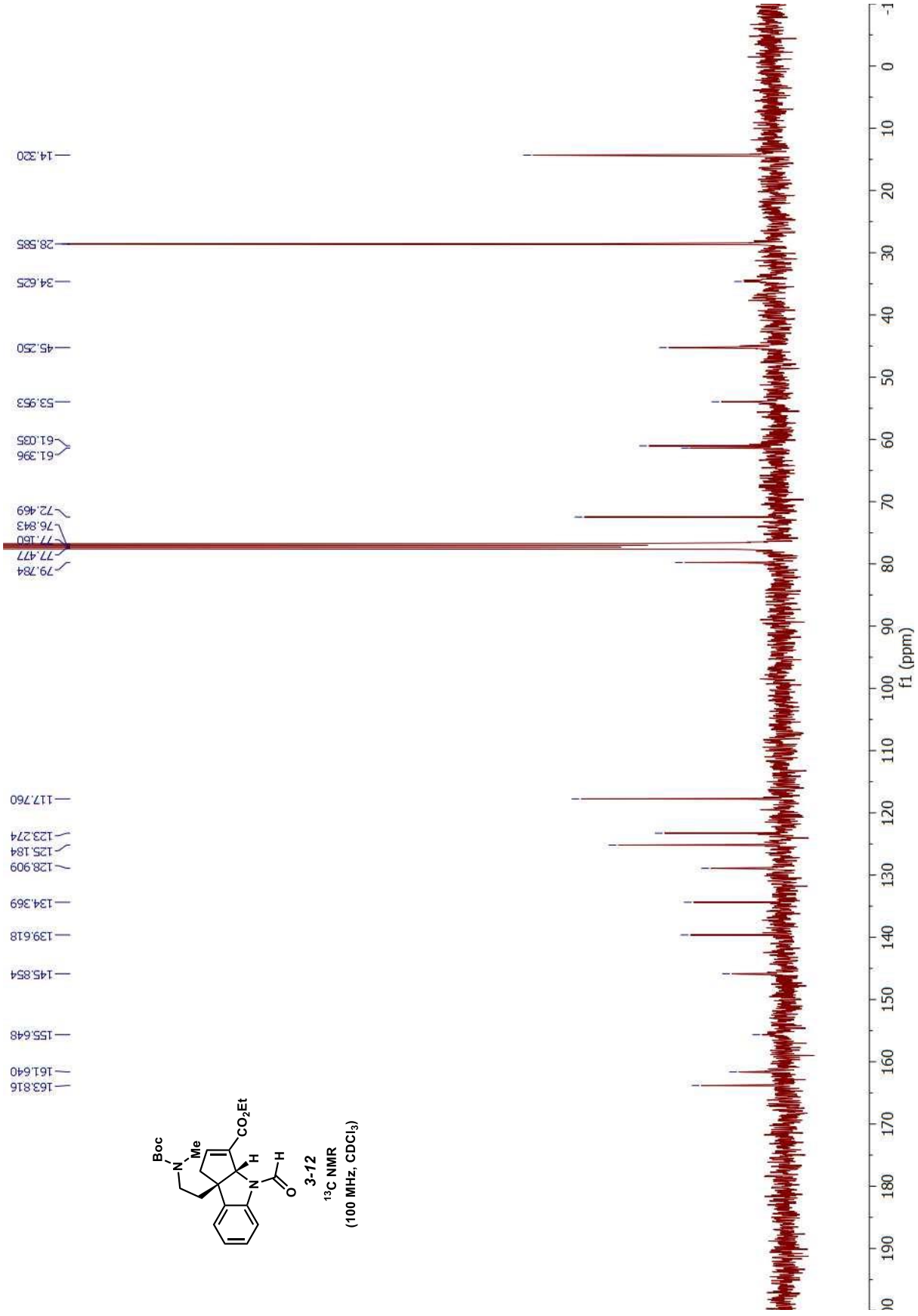
14.320
28.585
34.625
45.250
53.953
61.035
61.396
72.469
76.843
77.160
77.477
79.784
117.760
123.274
125.184
128.909
134.369
139.618
145.854
155.648
161.640
163.816
Boc
N
Me
CO2Et
H
N
H
O
3-12
13C NMR
(100 MHz, CDCl3)
f1 (ppm)

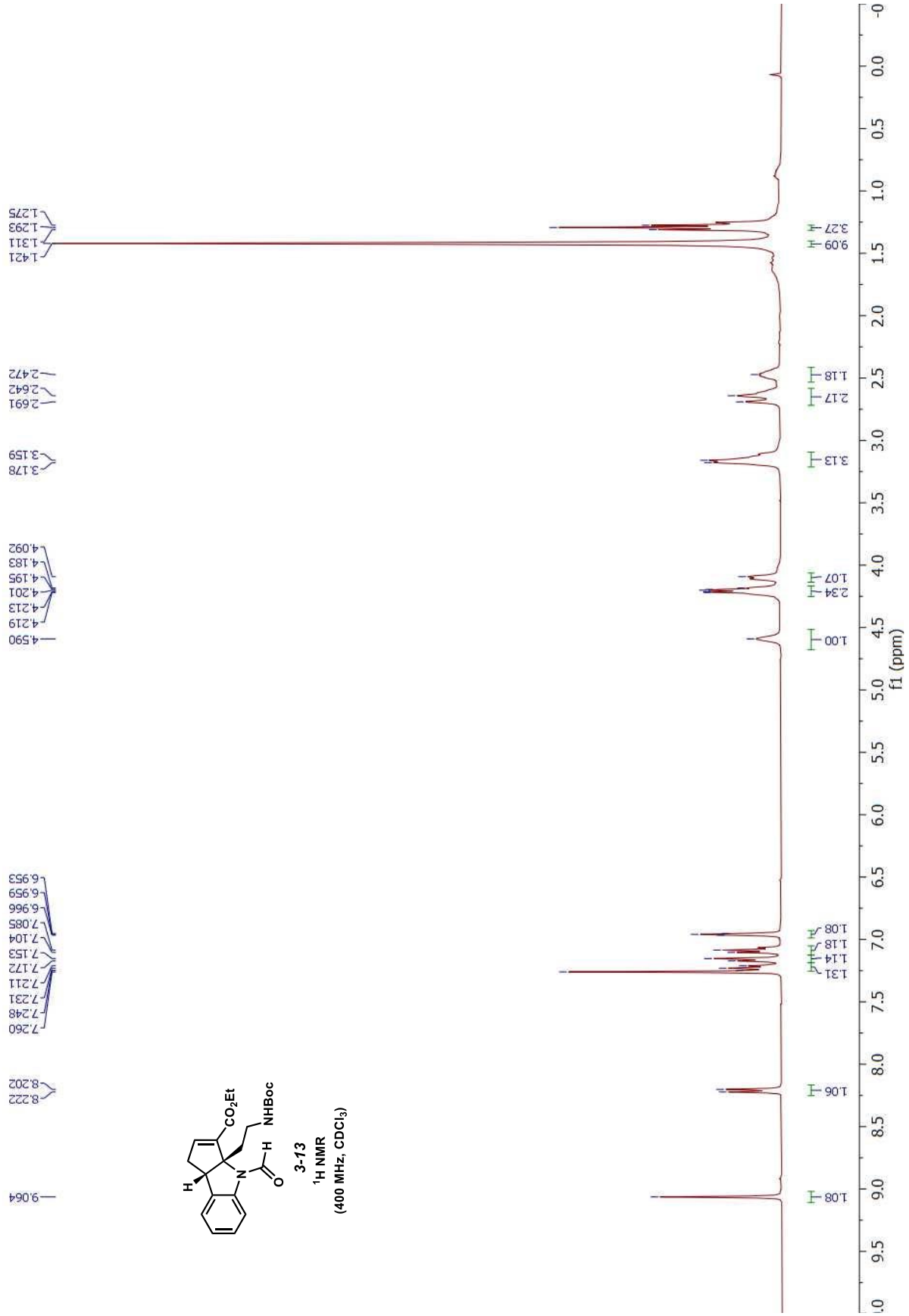
1.421
1.311
1.293
1.275
2.691
2.642
2.472
3.178
3.159
4.590
4.219
4.213
4.201
4.195
4.183
4.092
7.260
7.248
7.231
7.211
7.172
7.153
7.104
7.085
6.966
6.959
6.953
8.222
8.202
9.064
3.27
9.09
1.18
2.17
3.13
2.34
1.07
1.00
1.08
1.31
1.14
1.18
1.08
1.06
1.08
f1 (ppm)
CO2Et
NHBoc
H
N
O
H
3-13
1H NMR
(400 MHz, CDCl3)

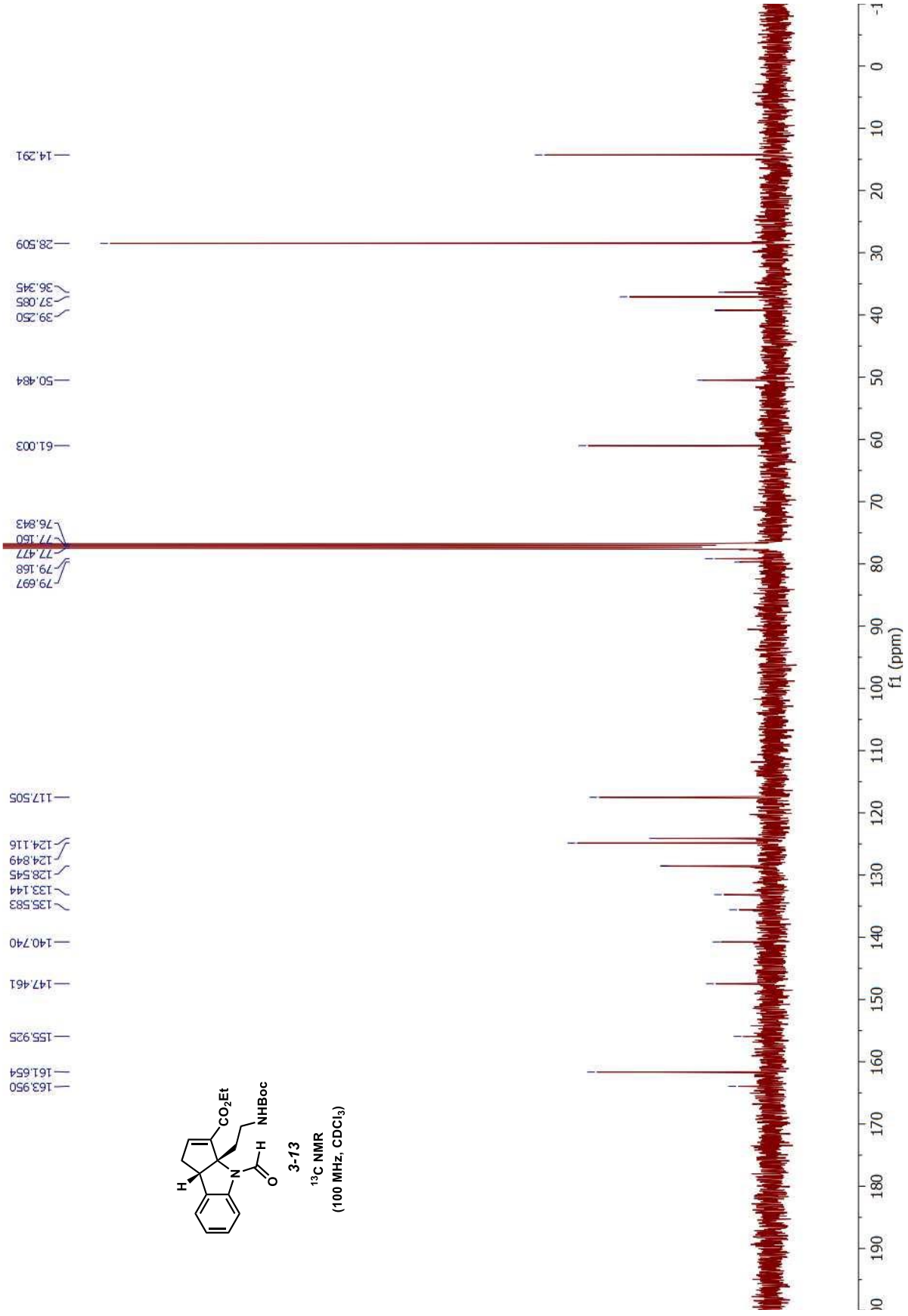
14.291
28.509
36.345
37.085
39.250
50.484
61.003
76.843
77.160
77.477
79.168
79.697
117.505
124.116
124.849
128.545
133.144
135.583
140.740
147.461
155.925
161.654
163.950
f1 (ppm)
CO2Et
NHBoc
H
N
O
H
3-13
13C NMR
(100 MHz, CDCl3)

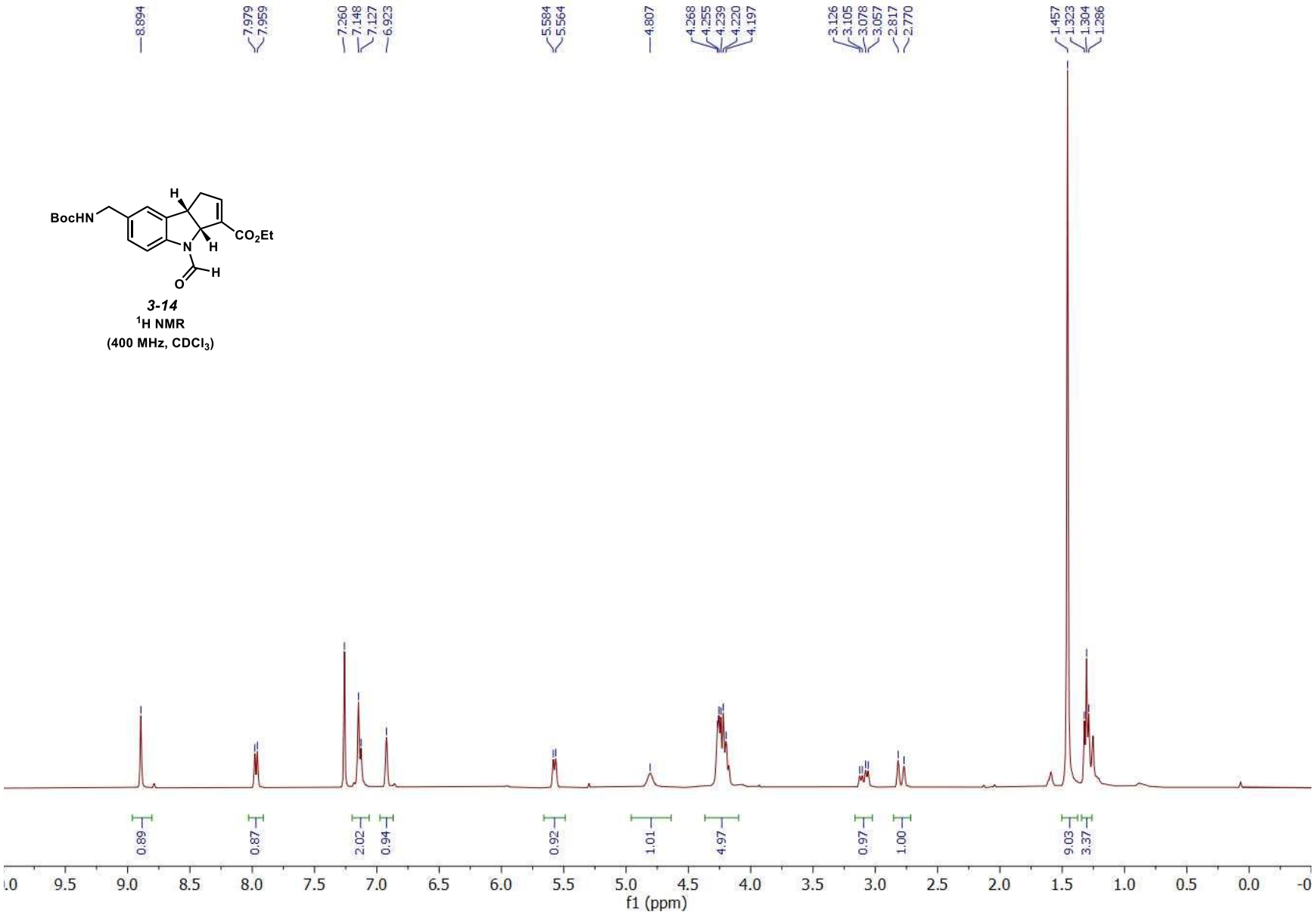

3-14

^{1}H NMR

(400 MHz, $CDCl_3$)

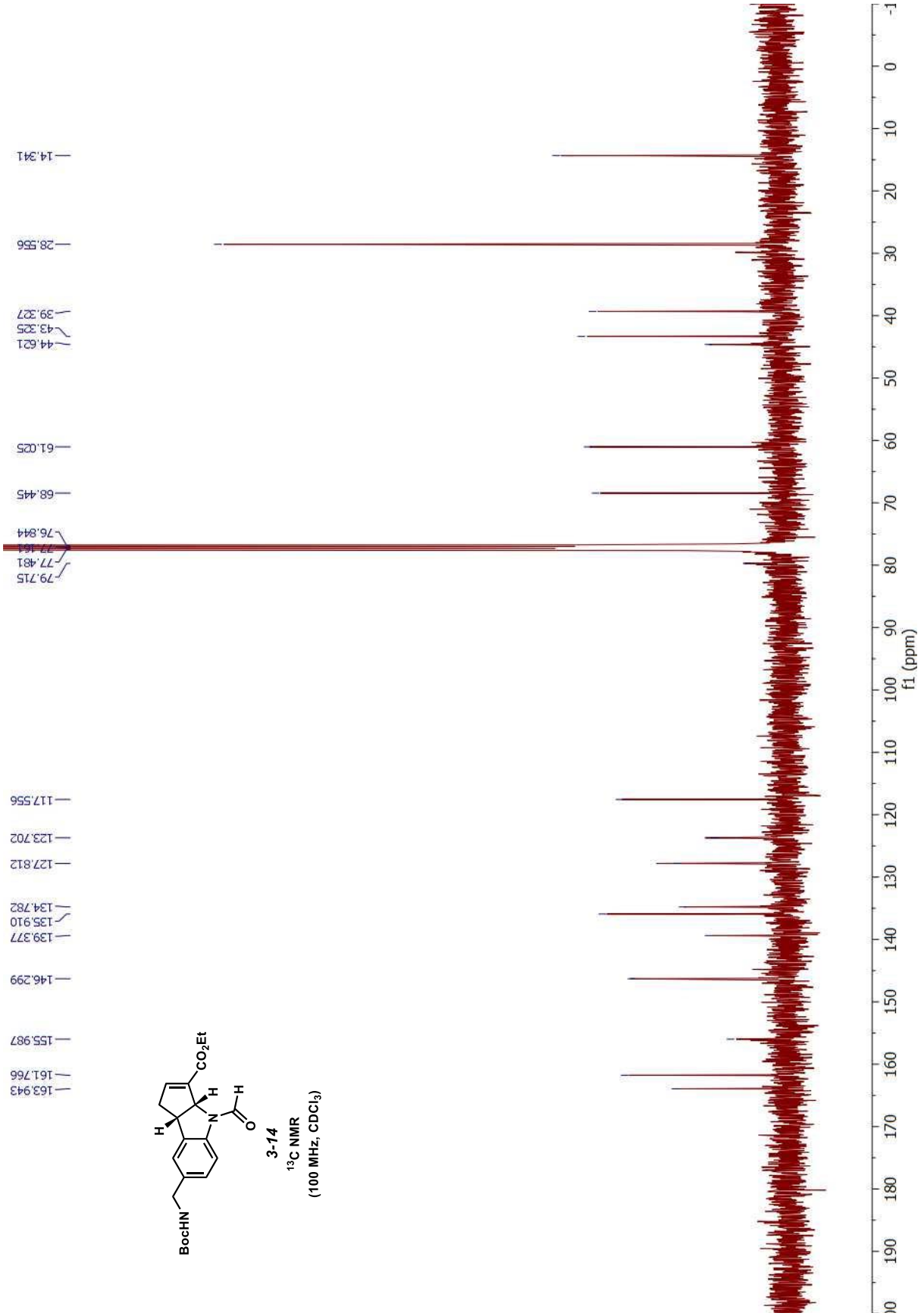
14.341
28.556
39.327
43.325
44.621
61.025
68.445
76.844
77.161
77.481
79.715
117.556
123.702
127.812
134.782
135.910
139.377
146.299
155.987
161.766
163.943
BocHN
CO2Et
3-14
13C NMR
(100 MHz, CDCl3)
f1 (ppm)

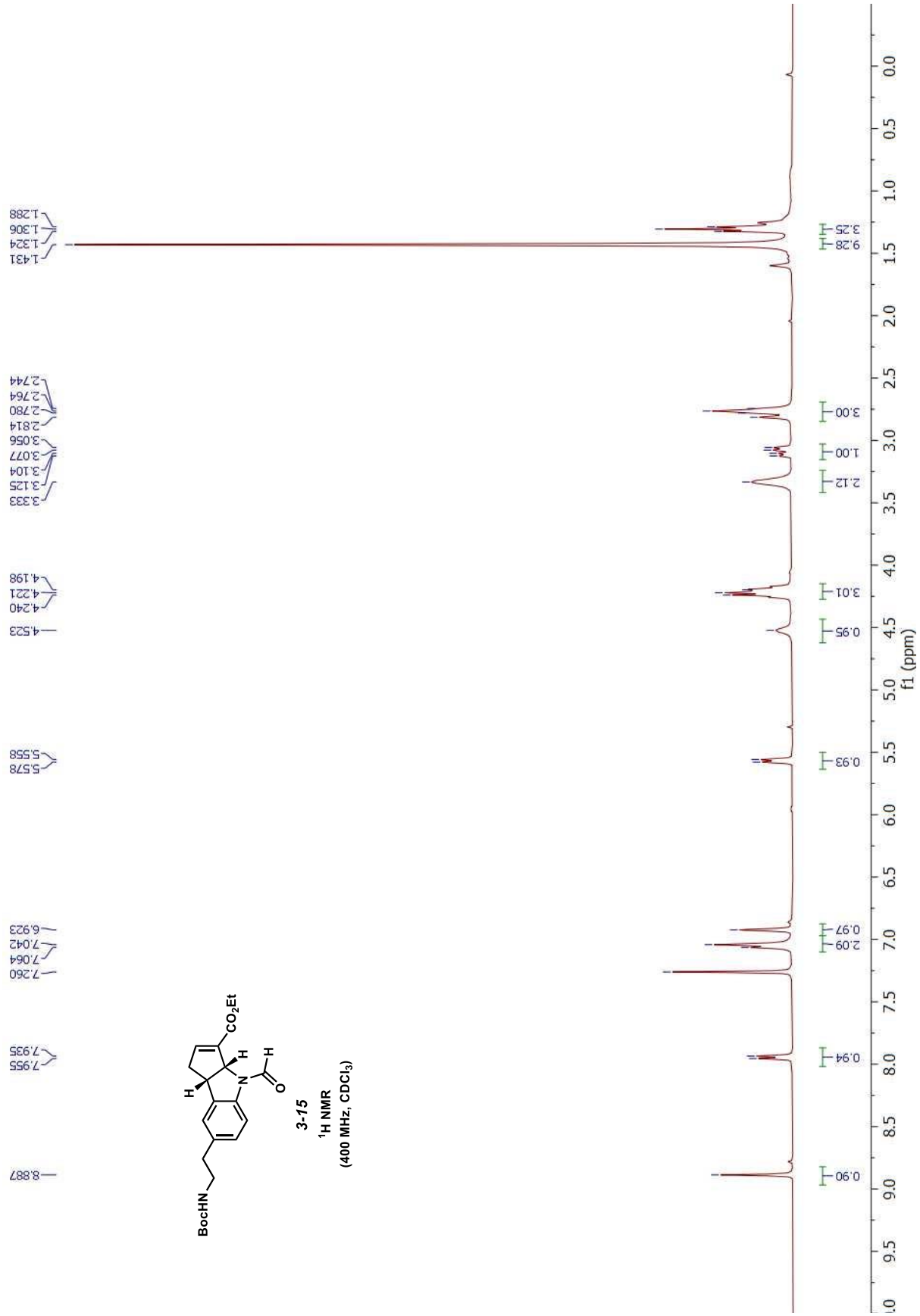
BocHN
CO2Et
H
H
N
O
H
3-15
1H NMR
(400 MHz, CDCl3)
f1 (ppm)

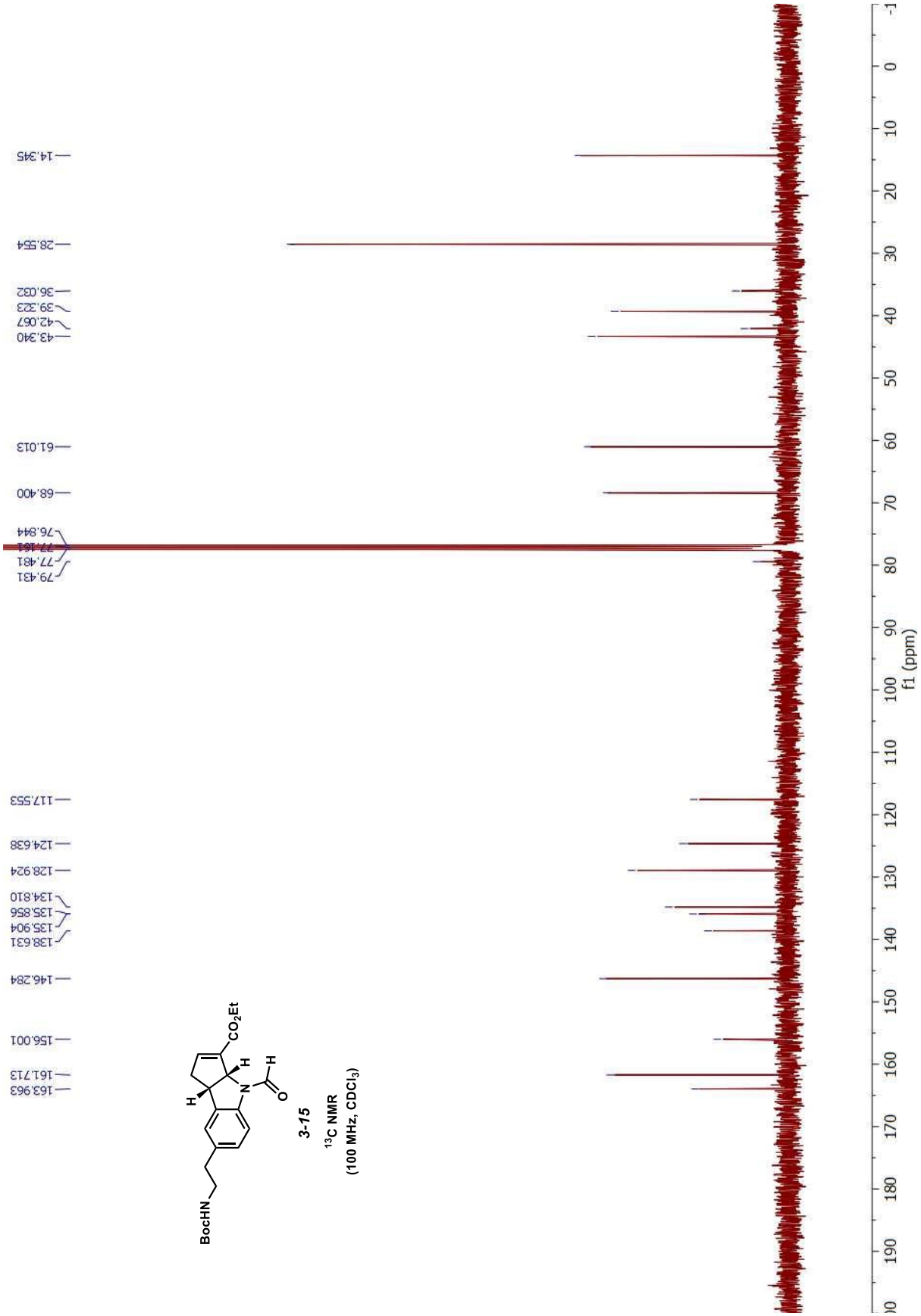
14.345
28.554
36.032
39.323
42.067
43.340
61.013
68.400
76.844
77.161
77.481
79.431
117.553
124.638
128.924
134.810
135.856
135.904
138.631
146.284
156.001
161.713
163.963
CO2Et
H
N
O
H
H
BocHN
3-15
13C NMR
(100 MHz, CDCl3)
f1 (ppm)

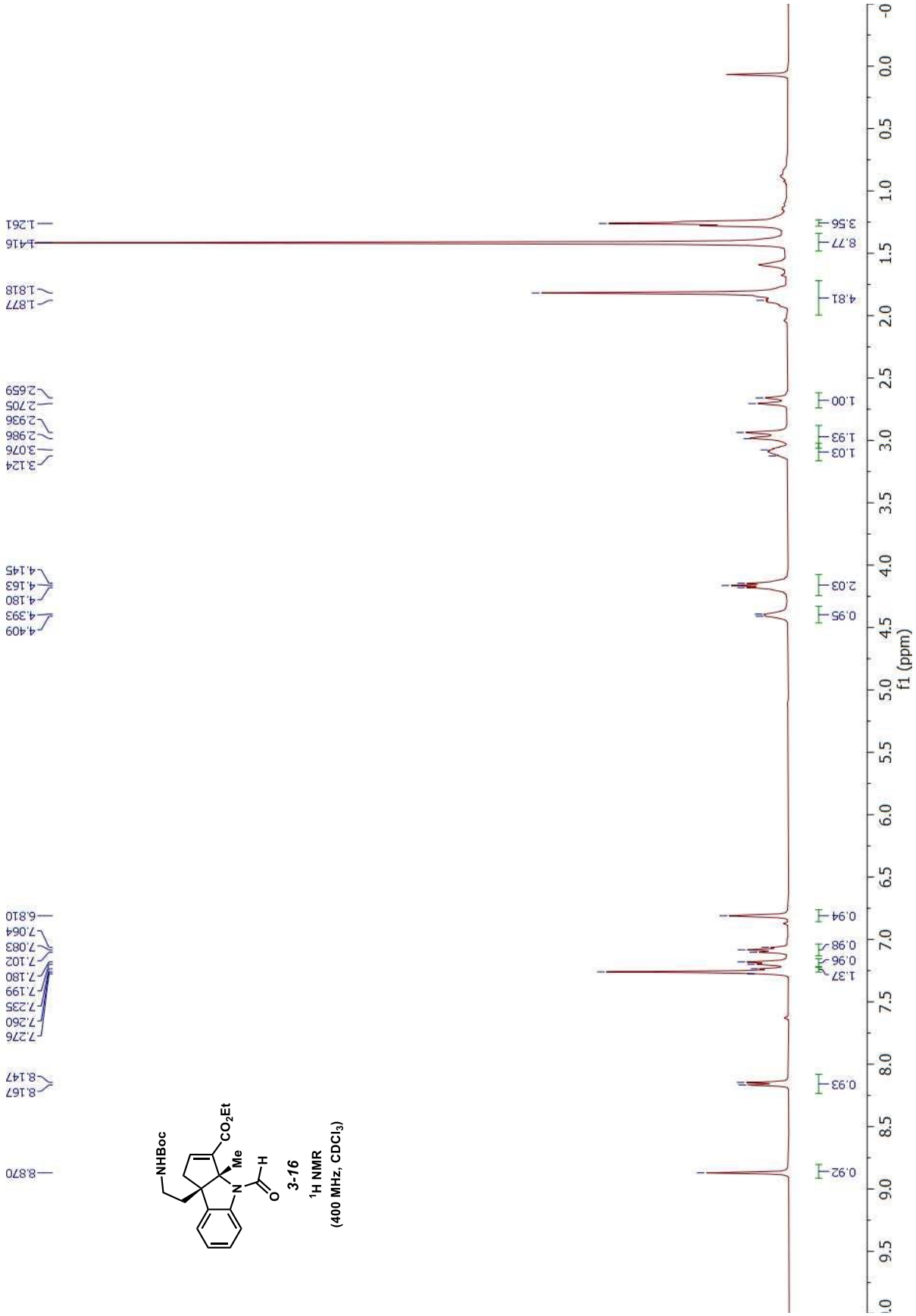
NHBoc
CO2Et
Me
N
O
H
3-16
1H NMR
(400 MHz, CDCl3)
f1 (ppm)

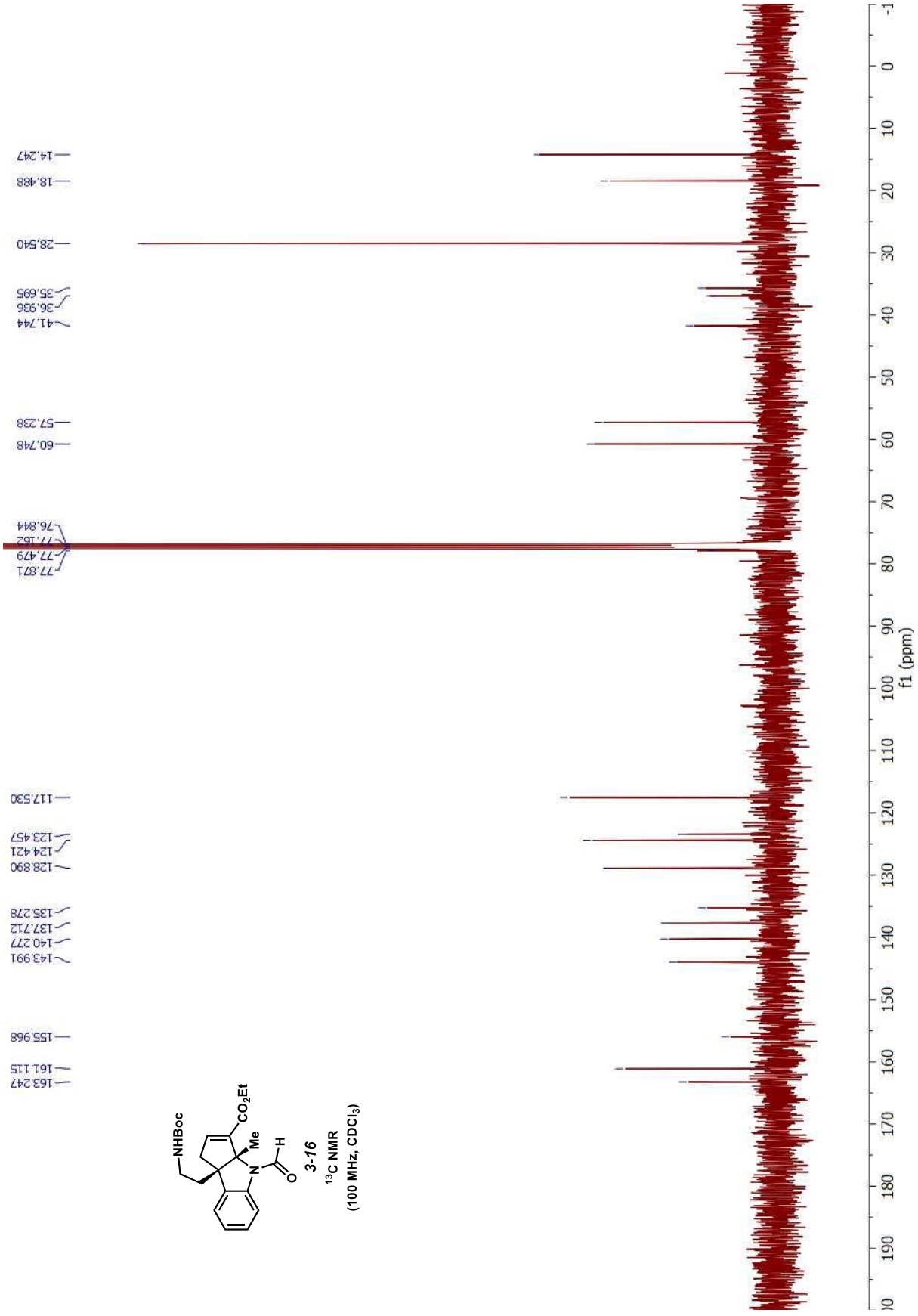
14.247
18.488
28.540
35.695
36.936
41.744
57.238
60.748
76.844
77.162
77.479
77.871
117.530
123.457
124.421
128.890
135.278
137.712
140.277
143.991
155.968
161.115
163.247
NHBoc
CO2Et
Me
N
O
H
3-16
13C NMR
(100 MHz, CDCl3)
f1 (ppm)

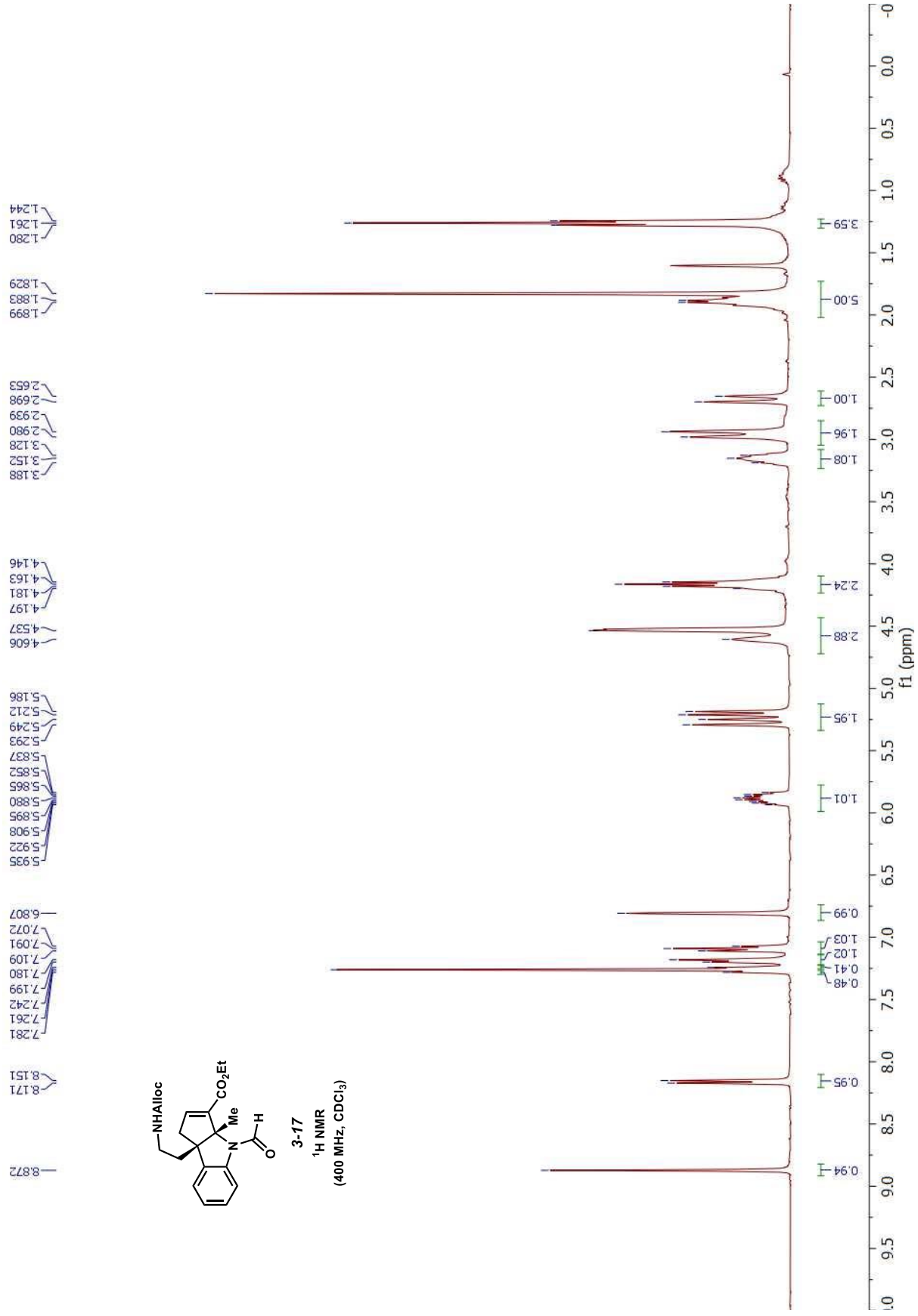
NHAlloc
CO2Et
Me
N
H
O
3-17
1H NMR
(400 MHz, CDCl3)
f1 (ppm)

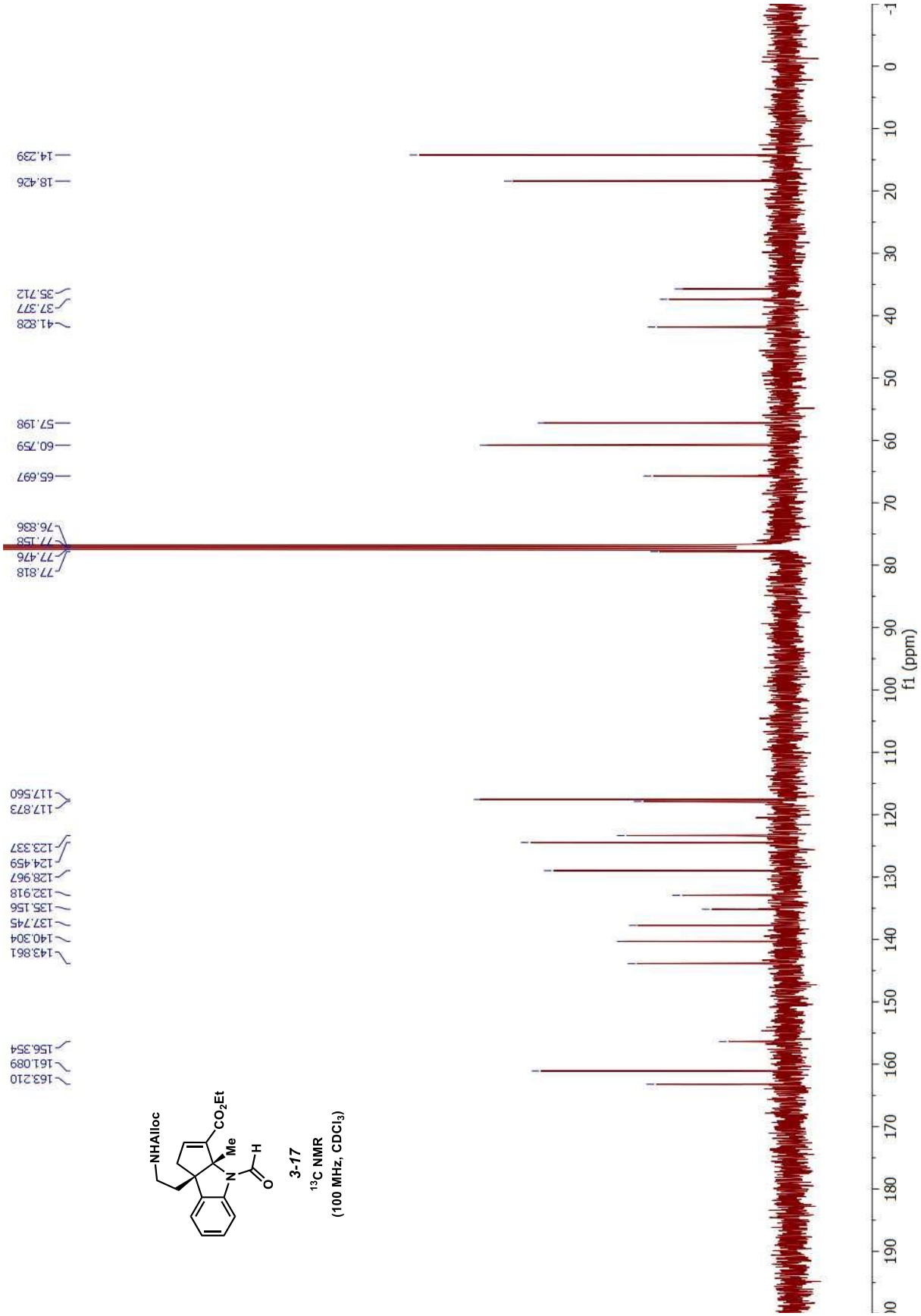
14.239
18.426
35.712
37.377
41.828
57.198
60.759
65.697
76.836
77.158
77.476
77.818
117.560
117.873
123.337
124.459
128.967
132.918
135.156
137.745
140.304
143.861
156.354
161.089
163.210
NHAlloc
CO2Et
Me
N
H
O
3-17
13C NMR
(100 MHz, CDCl3)
f1 (ppm)

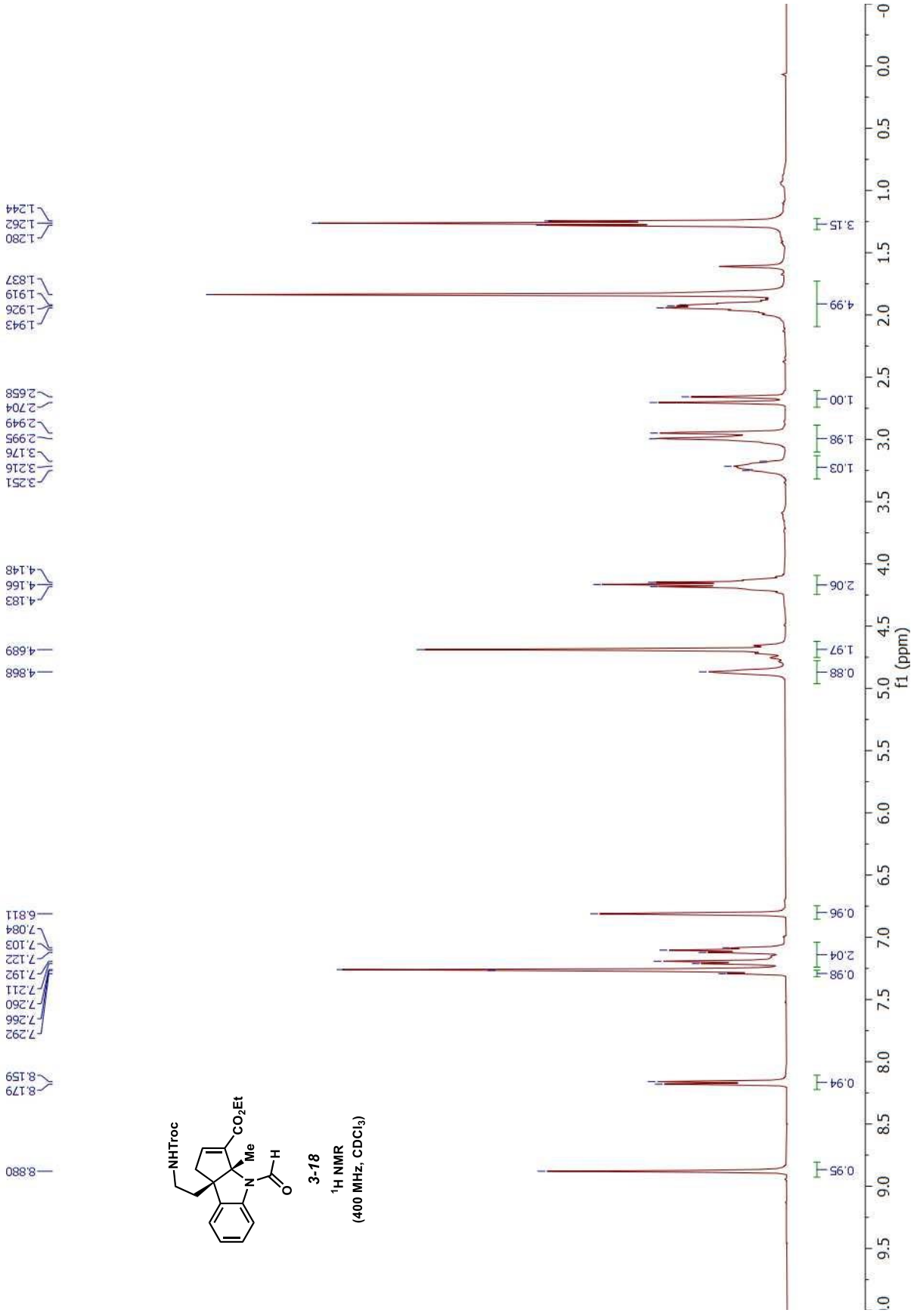
NHTroc
CO2Et
Me
N
H
O
3-18
1H NMR
(400 MHz, CDCl3)
f1 (ppm)

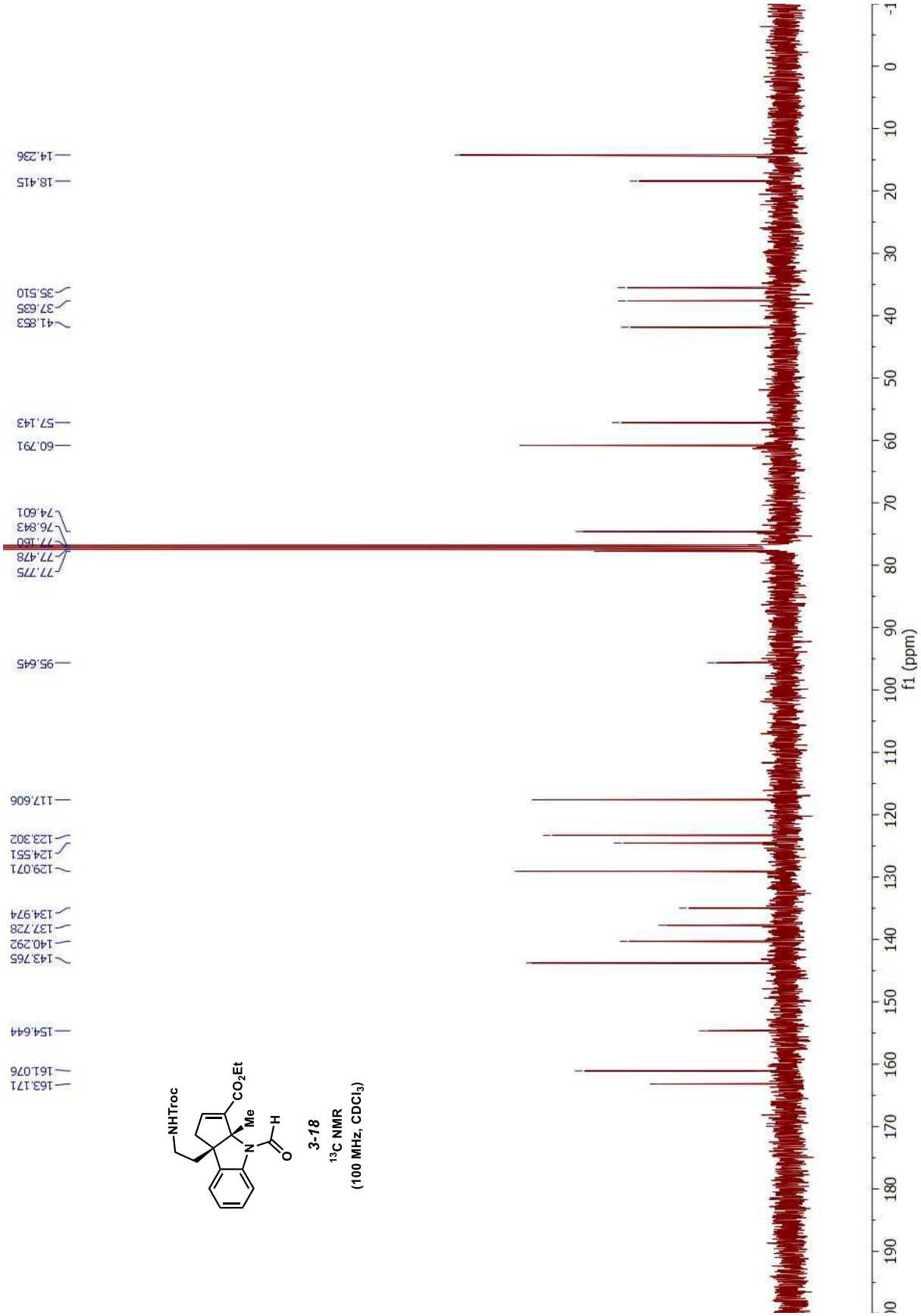
14.236
18.415
35.510
37.635
41.853
57.143
60.791
74.601
76.843
77.160
77.478
77.775
95.645
117.606
123.302
124.551
129.071
134.974
137.728
140.292
143.765
154.644
161.076
163.171
NHTroc
CO2Et
Me
N
H
O
3-18
13C NMR
(100 MHz, CDCl3)
f1 (ppm)

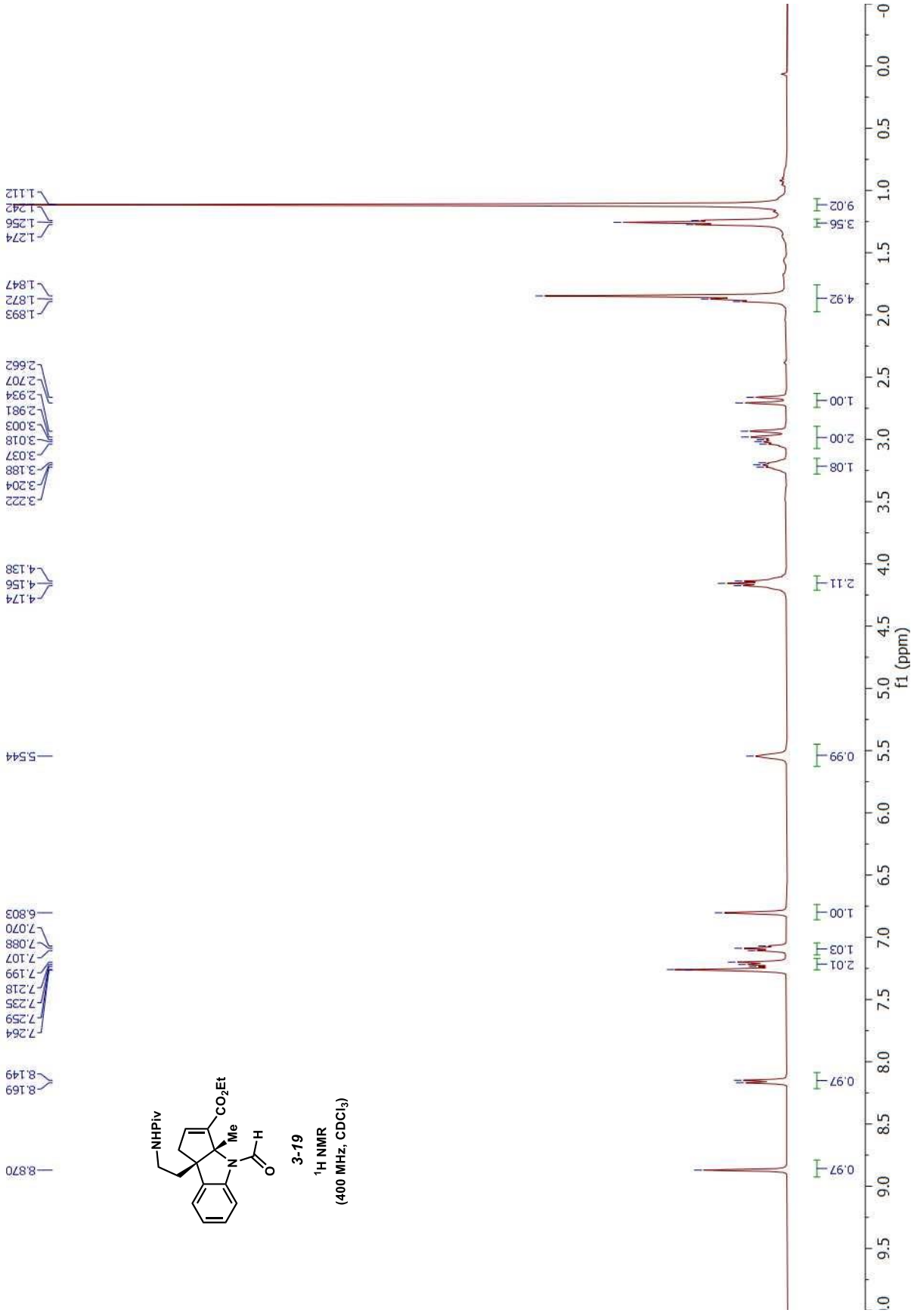
NHPiv
CO2Et
Me
N
H
O
3-19
1H NMR
(400 MHz, CDCl3)
f1 (ppm)

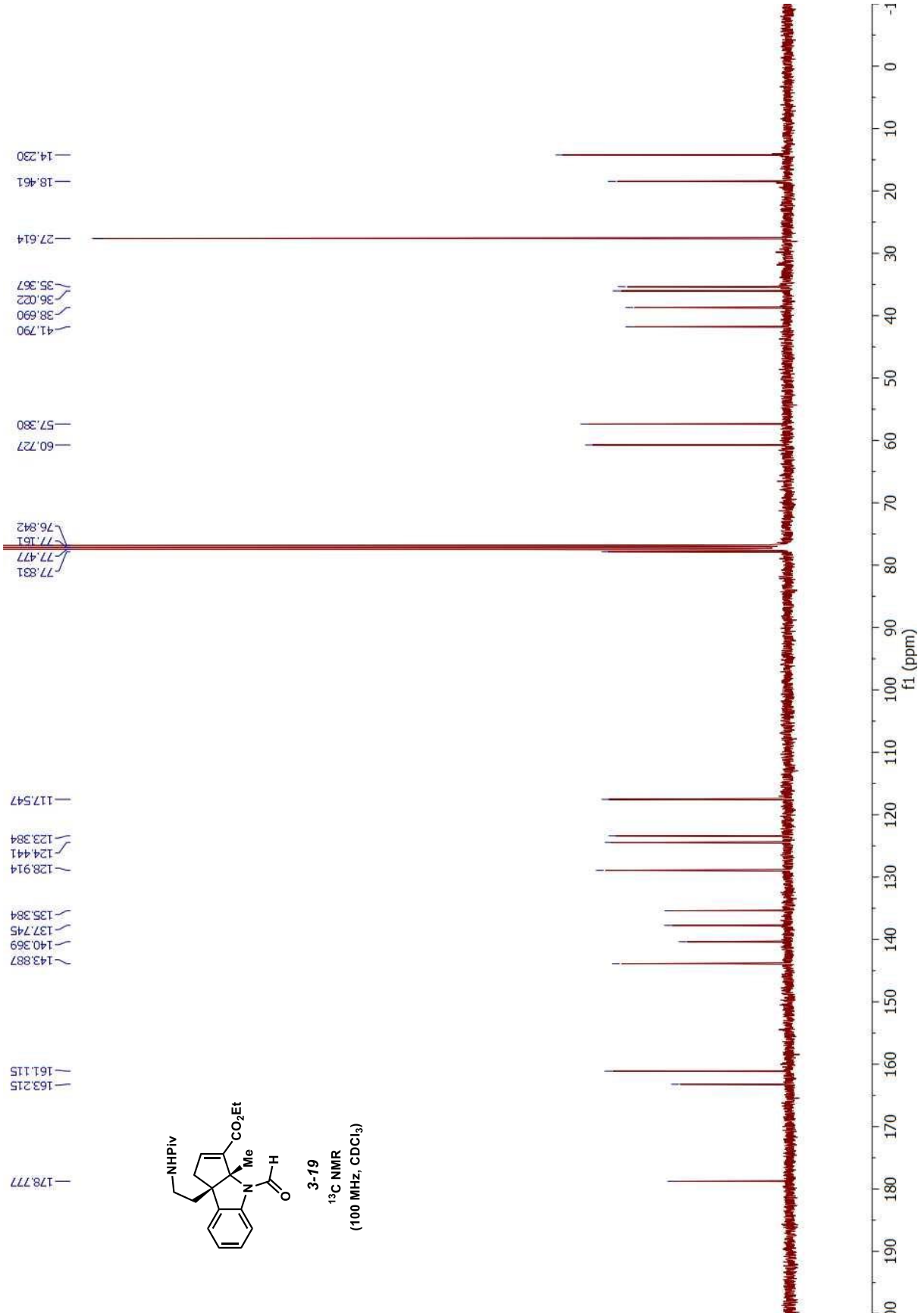
14.230
18.461
27.614
35.367
36.022
38.690
41.790
57.380
60.727
76.842
77.161
77.477
77.831
117.547
123.384
124.441
128.914
135.384
137.745
140.369
143.887
161.115
163.215
178.777
NHPiv
Me
CO2Et
H
O
N
3-19
13C NMR
(100 MHz, CDCl3)
f1 (ppm)

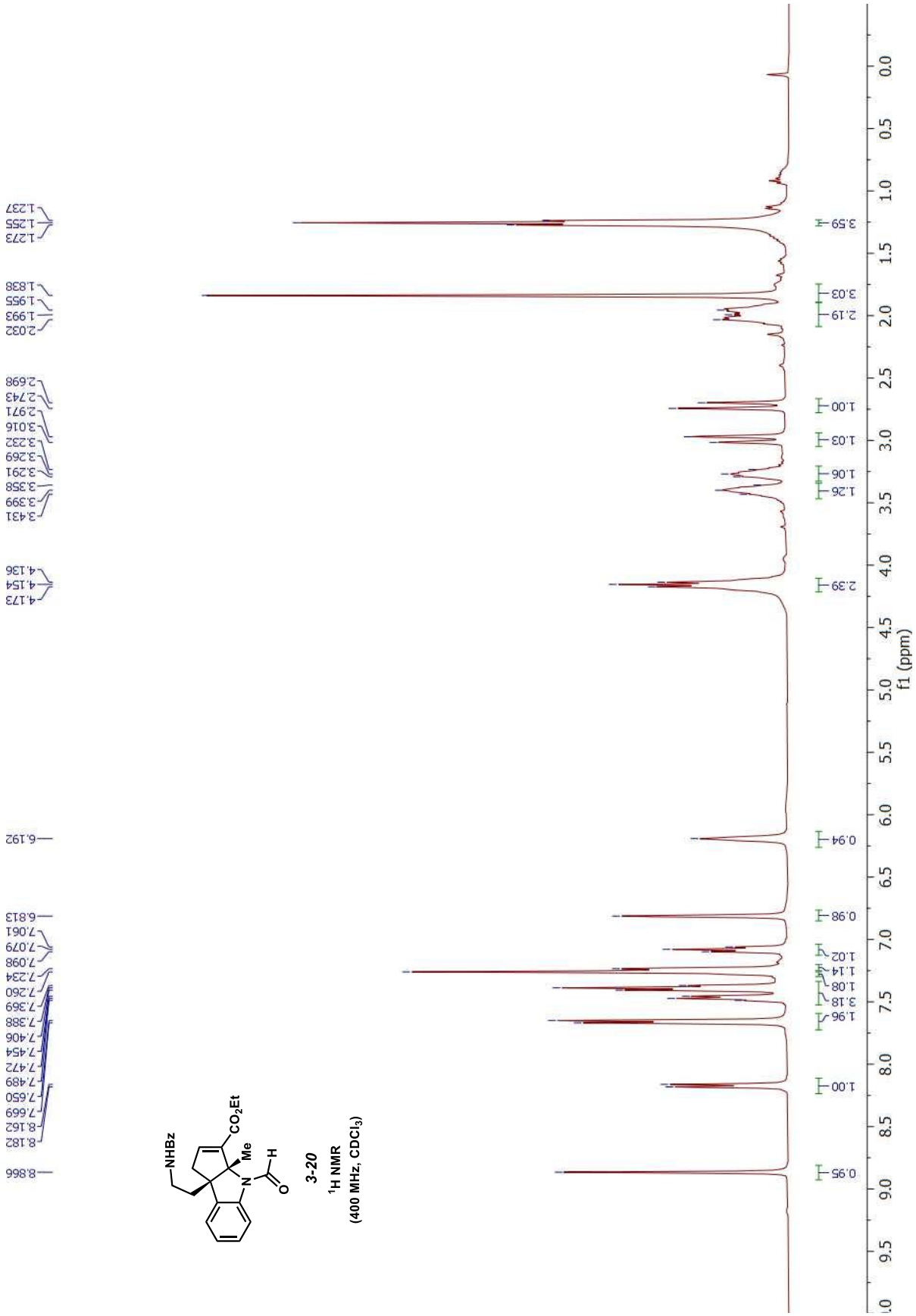
NHBz
Me
N
O
H
CO2Et
3-20
1H NMR
(400 MHz, CDCl3)
f1 (ppm)

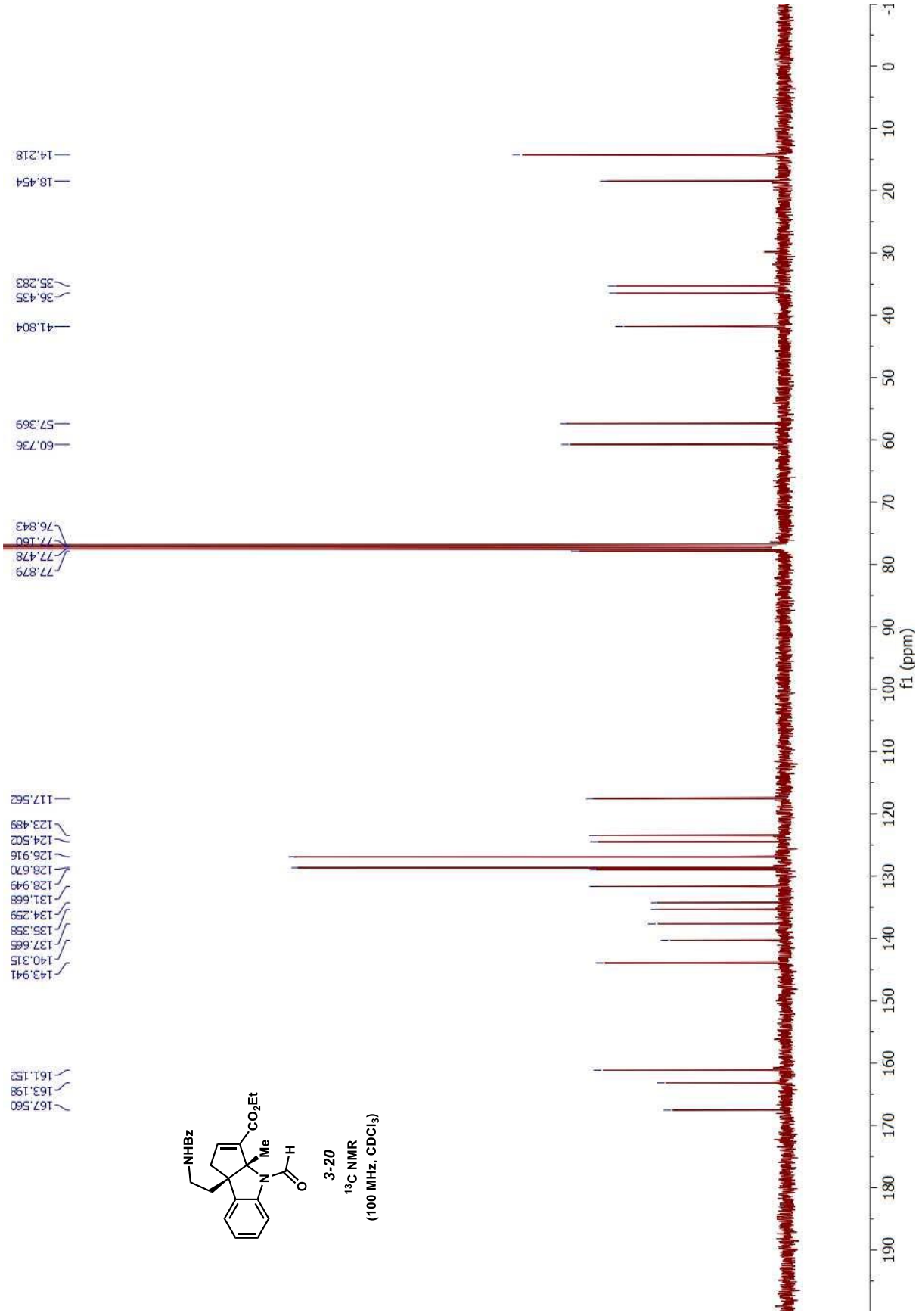
14.218
18.454
35.283
36.435
41.804
57.369
60.736
76.843
77.160
77.478
77.879
117.562
123.489
124.502
126.916
128.670
128.949
131.668
134.259
135.358
137.665
140.315
143.941
161.152
163.198
167.560
f1 (ppm)
NHBz
CO2Et
Me
N
H
O
3-20
13C NMR
(100 MHz, CDCl3)

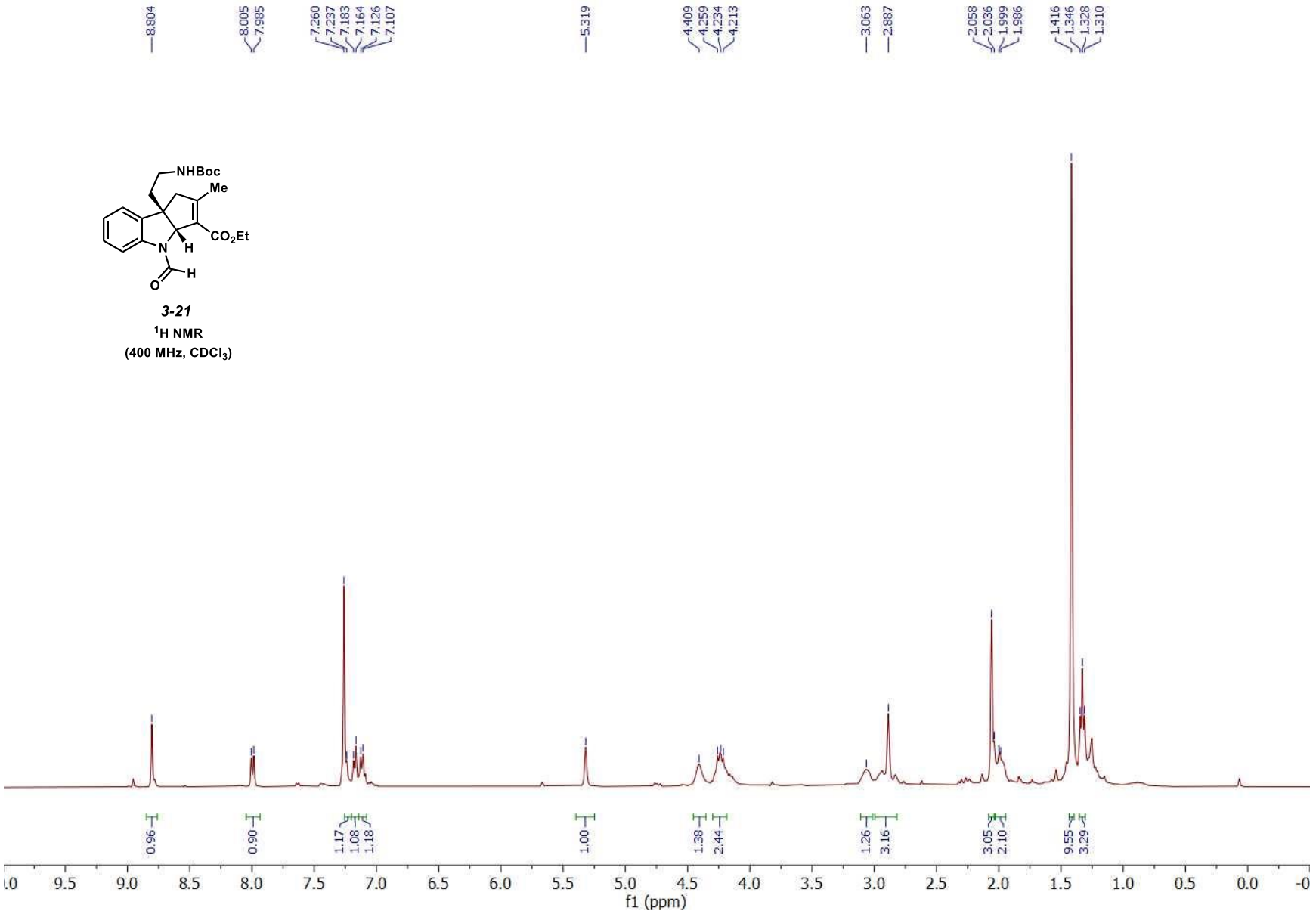
8.804
8.005
7.985
7.260
7.237
7.183
7.164
7.126
7.107
5.319
4.409
4.259
4.234
4.213
3.063
2.887
2.058
2.036
1.999
1.986
1.416
1.346
1.328
1.310
NHBoc
Me
CO2Et
N
H
O
H
3-21
1H NMR
(400 MHz, CDCl3)
0.96
0.90
1.17
1.08
1.18
1.00
1.38
2.44
1.26
3.16
3.05
2.10
9.55
3.29
f1 (ppm)

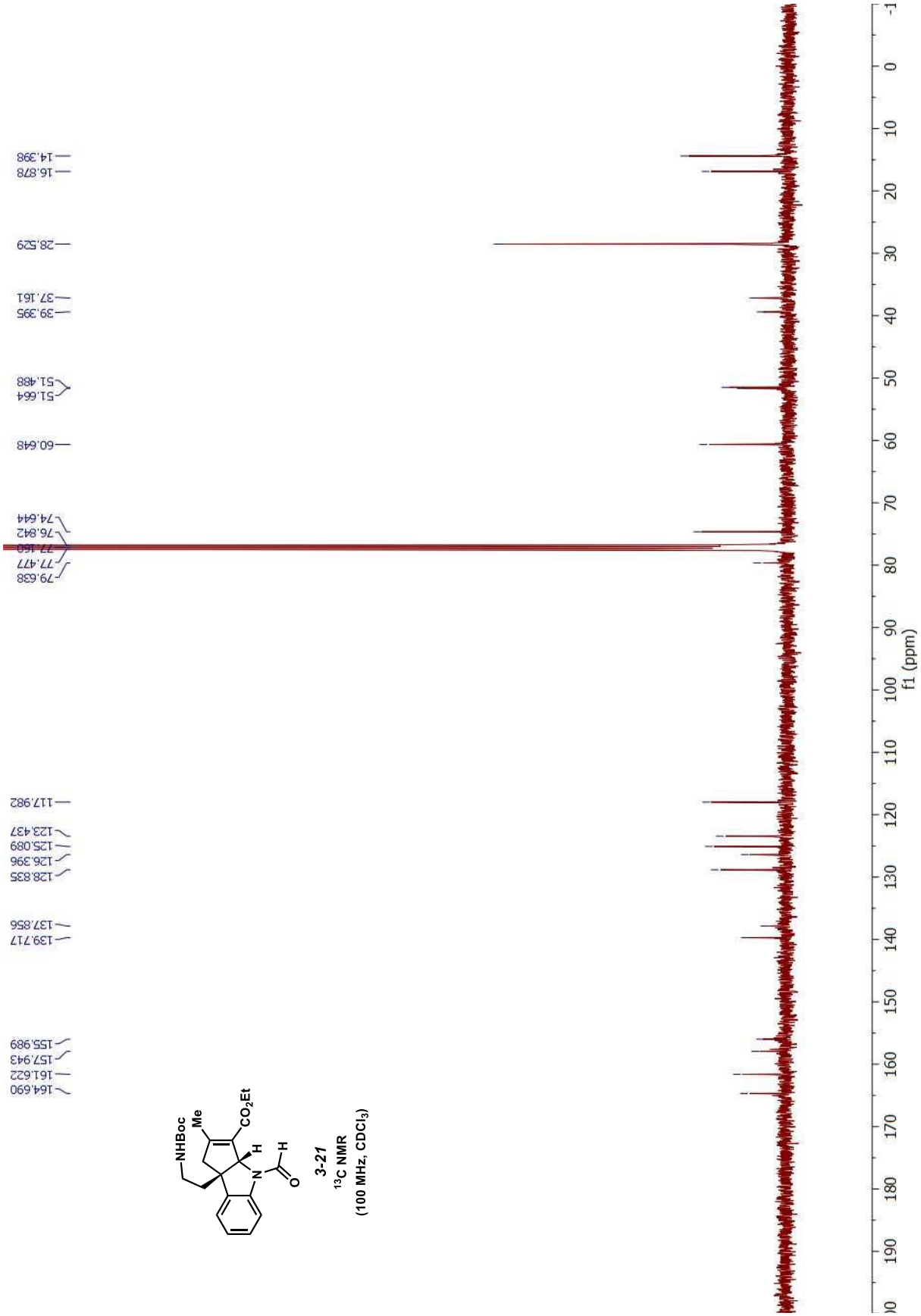
14.398
16.878
28.529
37.161
39.395
51.488
51.664
60.648
74.644
76.842
77.160
77.477
79.638
117.982
123.437
125.089
126.396
128.835
137.856
139.717
155.989
157.943
161.622
164.690
NHBoc
Me
CO2Et
H
N
O
H
3-21
13C NMR
(100 MHz, CDCl3)
f1 (ppm)

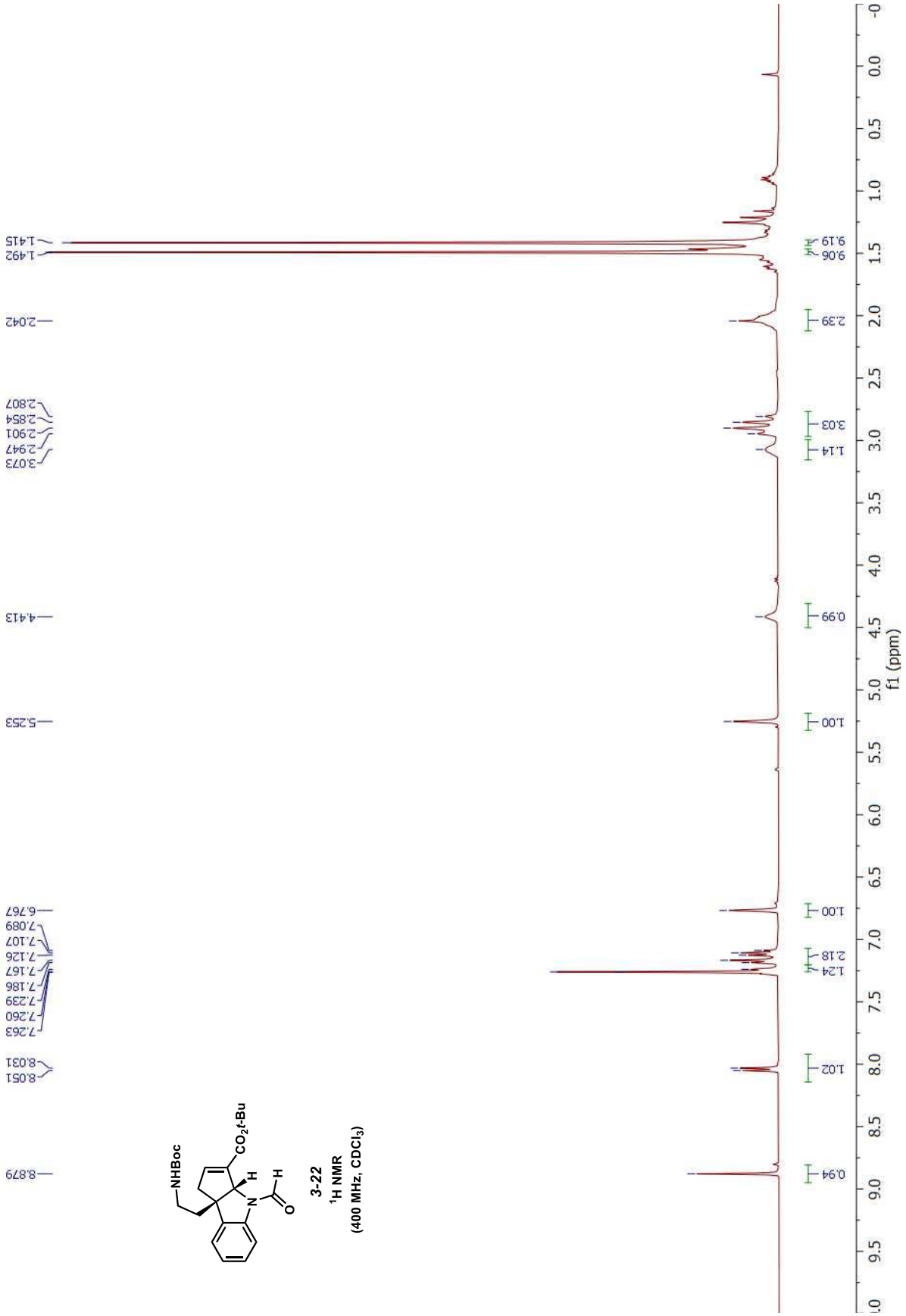
1.415
1.492
2.042
2.807
2.854
2.901
2.947
3.073
4.413
5.253
6.767
7.089
7.107
7.126
7.167
7.186
7.239
7.260
7.263
8.031
8.051
8.879
9.19
9.06
2.39
3.03
1.14
0.99
1.00
1.00
2.18
1.24
1.02
0.94
f1 (ppm)
NHBoc
CO2t-Bu
H
N
H
O
3-22
1H NMR
(400 MHz, CDCl3)

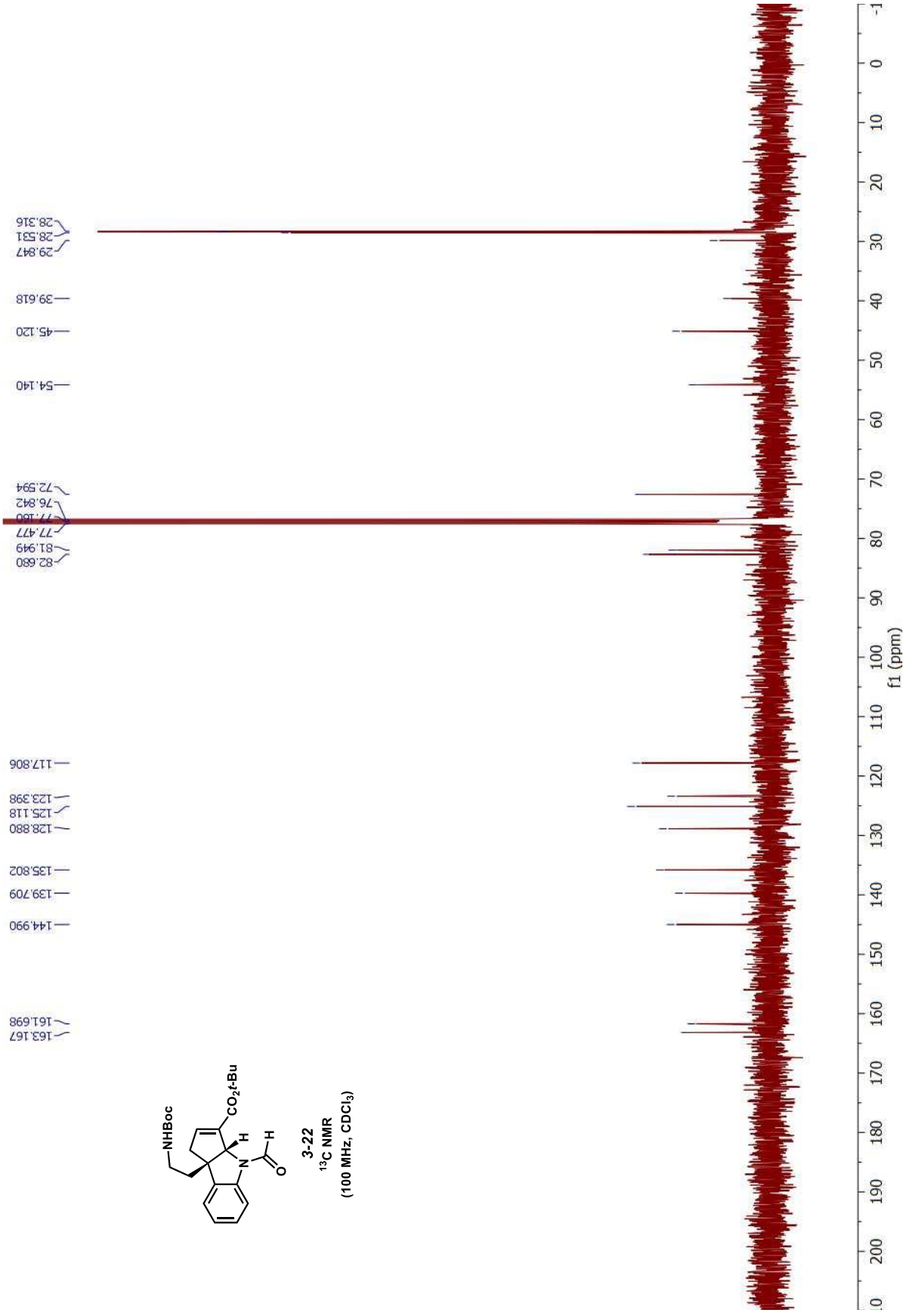
28.316
28.531
29.847
39.618
45.120
54.140
72.594
76.842
77.160
77.477
81.949
82.680
117.806
123.398
125.118
128.880
135.802
139.709
144.990
161.698
163.167
f1 (ppm)
NHBoc
CO2t-Bu
H
N
O
H
3-22
13C NMR
(100 MHz, CDCl3)

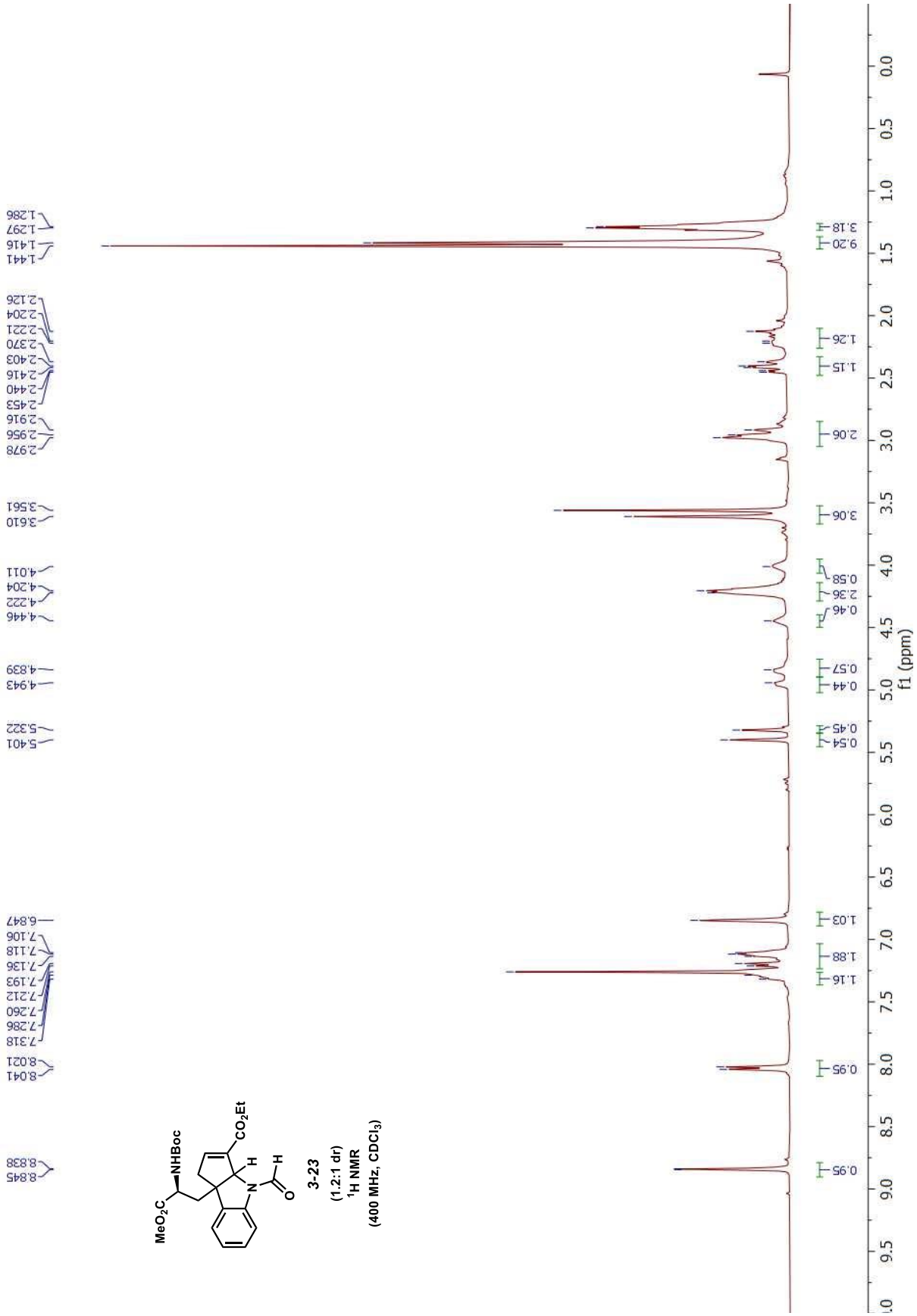
MeO2C
NHBoc
CO2Et
H
N
H
O
3-23
(1.2:1 dr)
1H NMR
(400 MHz, CDCl3)
f1 (ppm)

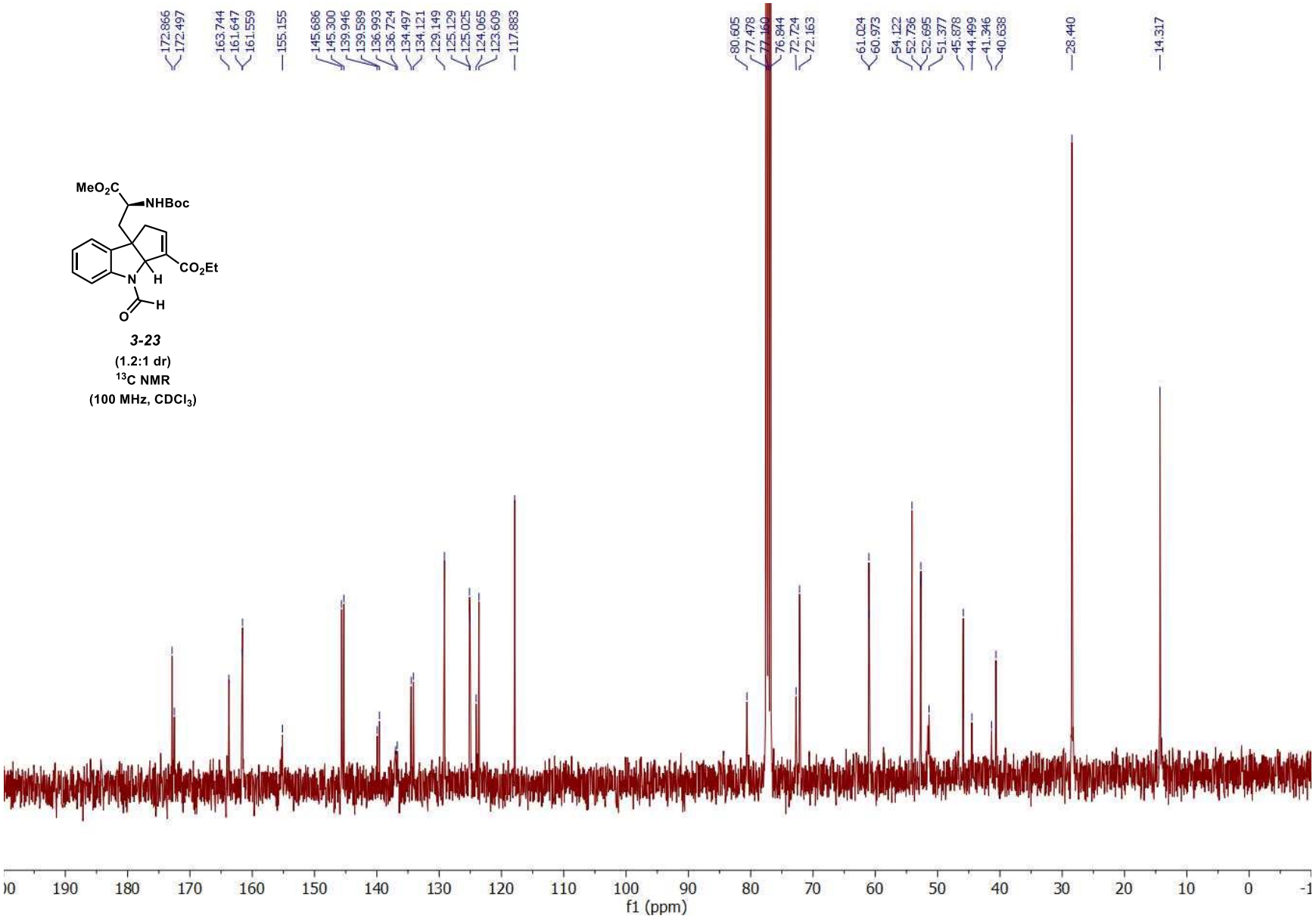
172.866
172.497
163.744
161.647
161.559
155.155
145.686
145.300
139.946
139.589
136.993
136.724
134.497
134.121
129.149
125.129
125.025
124.065
123.609
117.883
80.605
77.478
77.160
76.844
72.724
72.163
61.024
60.973
54.122
52.736
52.695
51.377
45.878
44.499
41.346
40.638
28.440
14.317
MeO2C
NHBoc
CO2Et
N
H
O
H
3-23
(1.2:1 dr)
13C NMR
(100 MHz, CDCl3)
f1 (ppm)

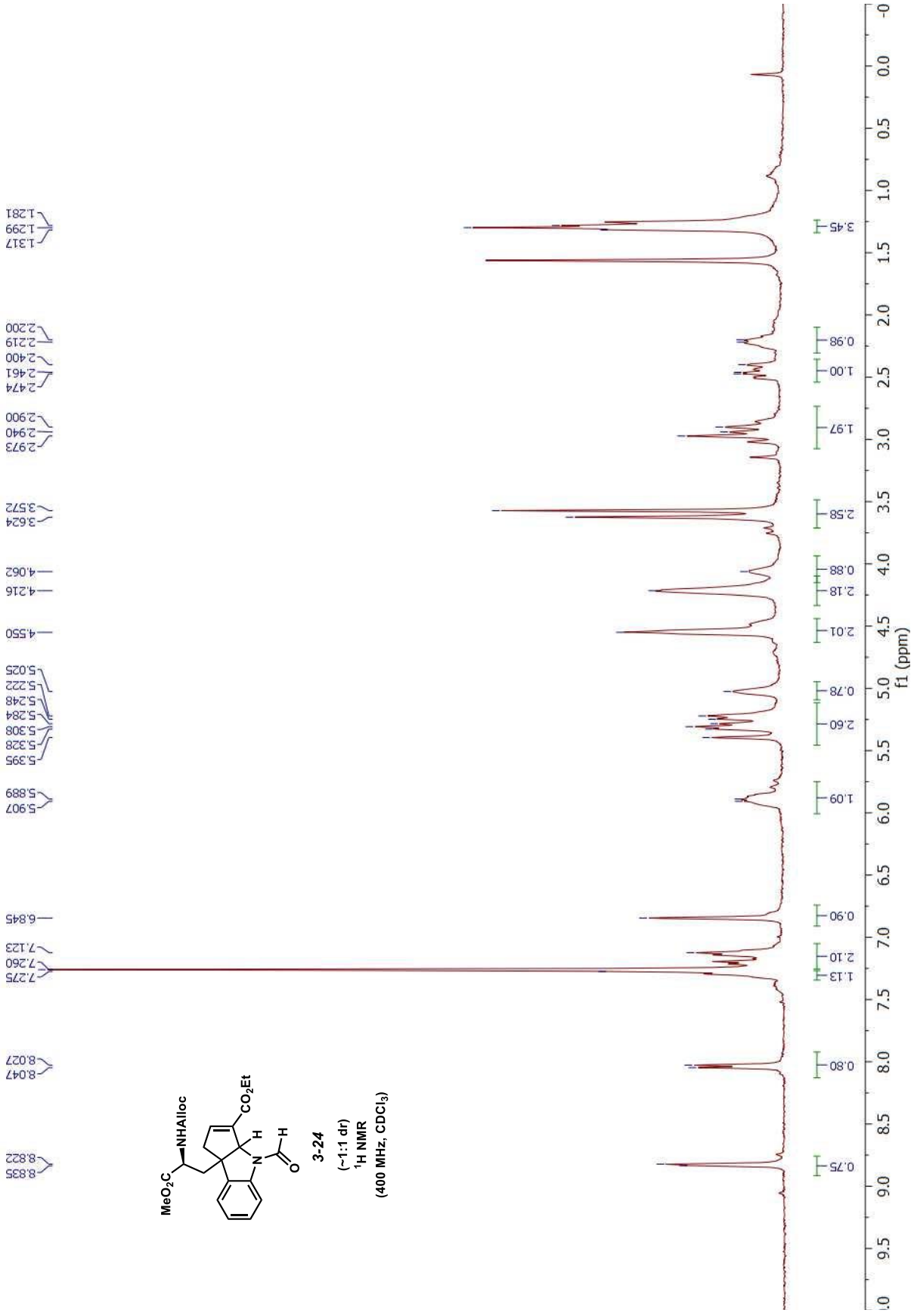
MeO2C
NHAlloc
CO2Et
H
N
H
O
3-24
(~1:1 dr)
1H NMR
(400 MHz, CDCl3)
f1 (ppm)

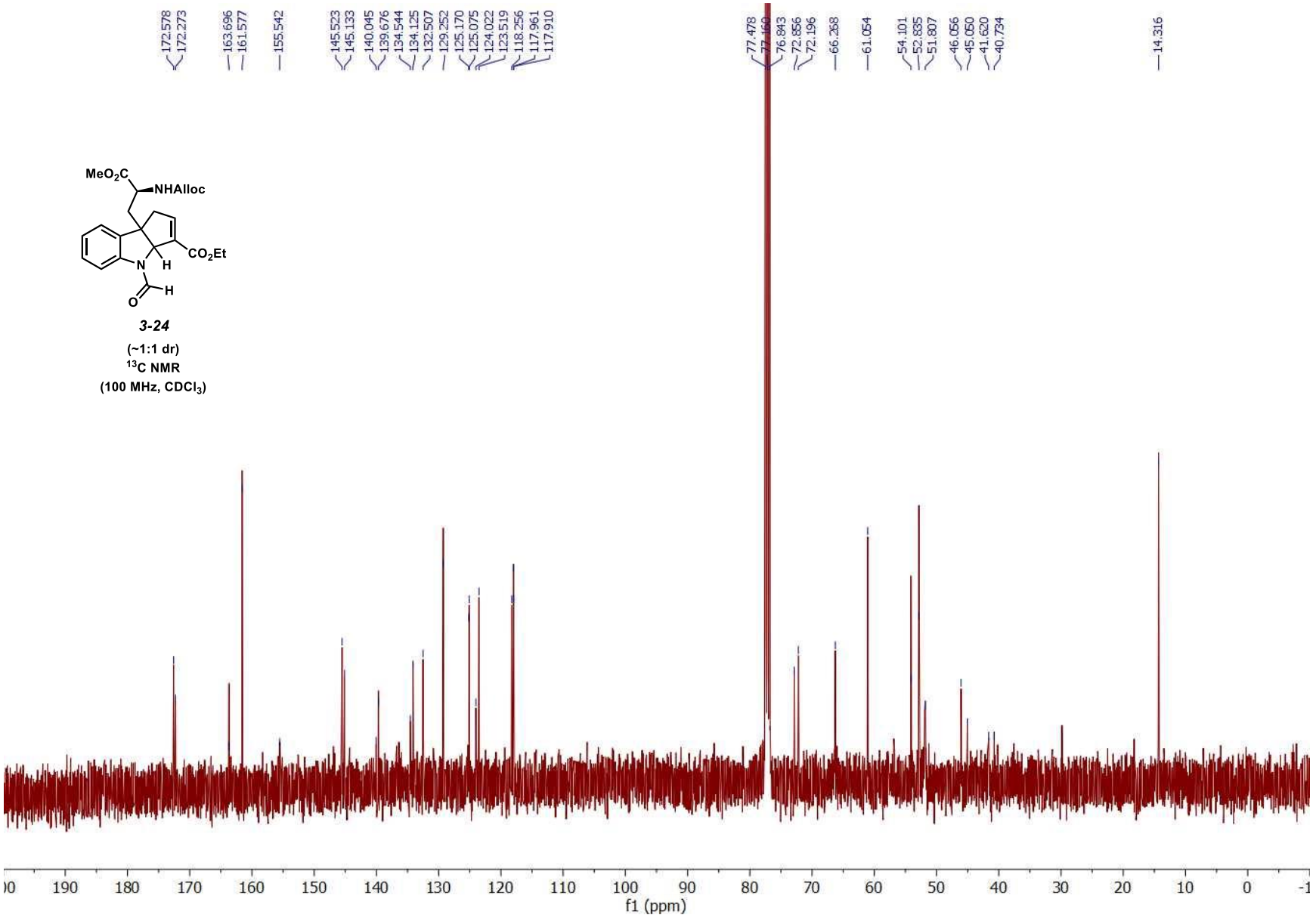
172.578
172.273
163.696
161.577
155.542
145.523
145.133
140.045
139.676
134.544
134.125
132.507
129.252
125.170
125.075
124.022
123.519
118.256
117.961
117.910
77.478
77.160
76.843
72.856
72.196
66.268
61.054
54.101
52.835
51.807
46.056
45.050
41.620
40.734
14.316
MeO2C
NHAlloc
CO2Et
N
H
O
H
3-24
(~1:1 dr)
13C NMR
(100 MHz, CDCl3)
f1 (ppm)

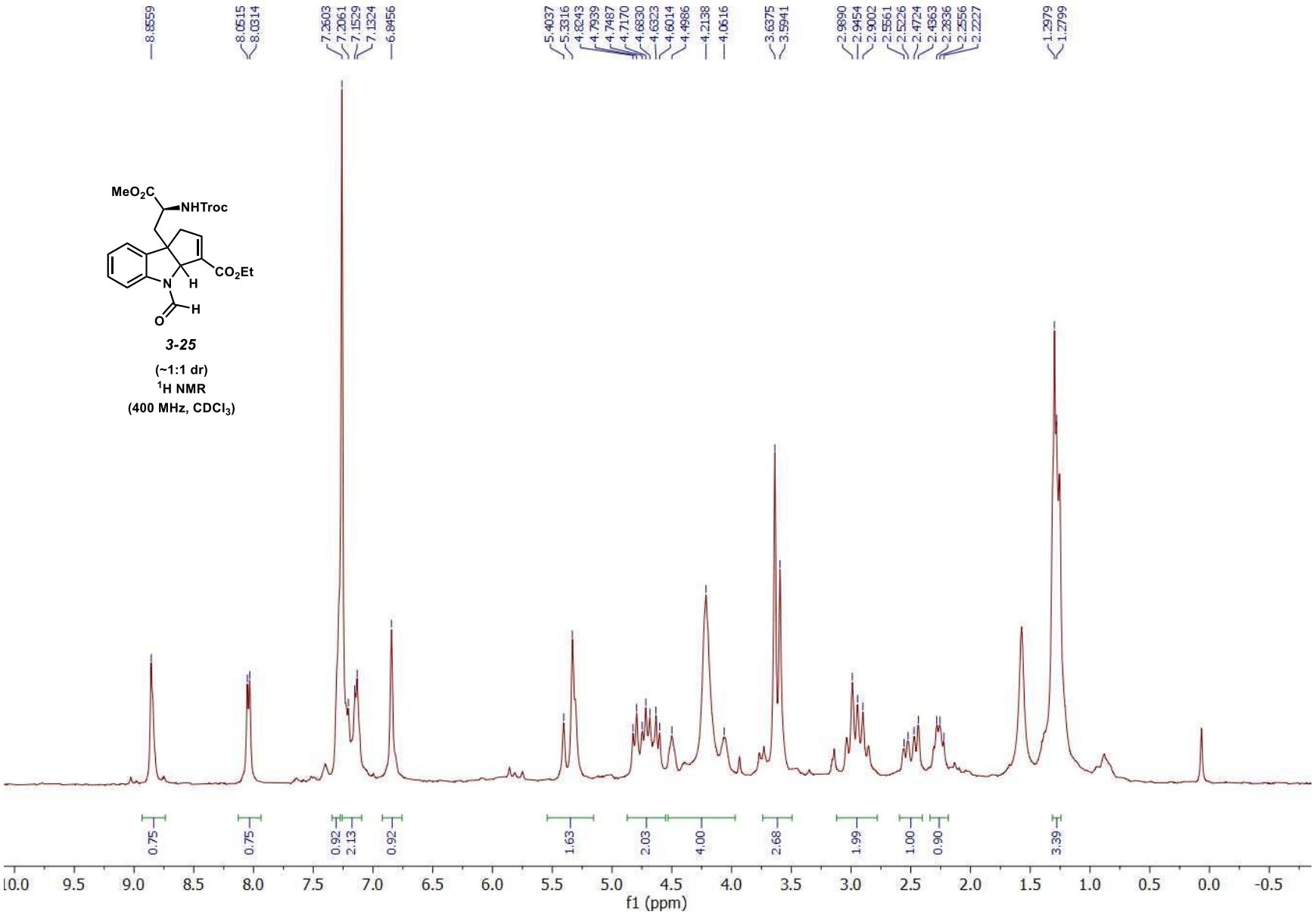
8.8559
8.0515
8.0314
7.2603
7.2061
7.1529
7.1324
6.8456
5.4037
5.3316
4.8243
4.7939
4.7487
4.7170
4.6830
4.6323
4.6014
4.4986
4.2138
4.0616
3.6375
3.5941
2.9890
2.9454
2.9002
2.5561
2.5226
2.4724
2.4363
2.2836
2.2556
2.2227
1.2979
1.2799
MeO2C
NHTroc
CO2Et
N
H
O
H
3-25
(~1:1 dr)
1H NMR
(400 MHz, CDCl3)
0.75
0.75
0.92
2.13
0.92
1.63
2.03
4.00
2.68
1.99
1.00
0.90
3.39
f1 (ppm)

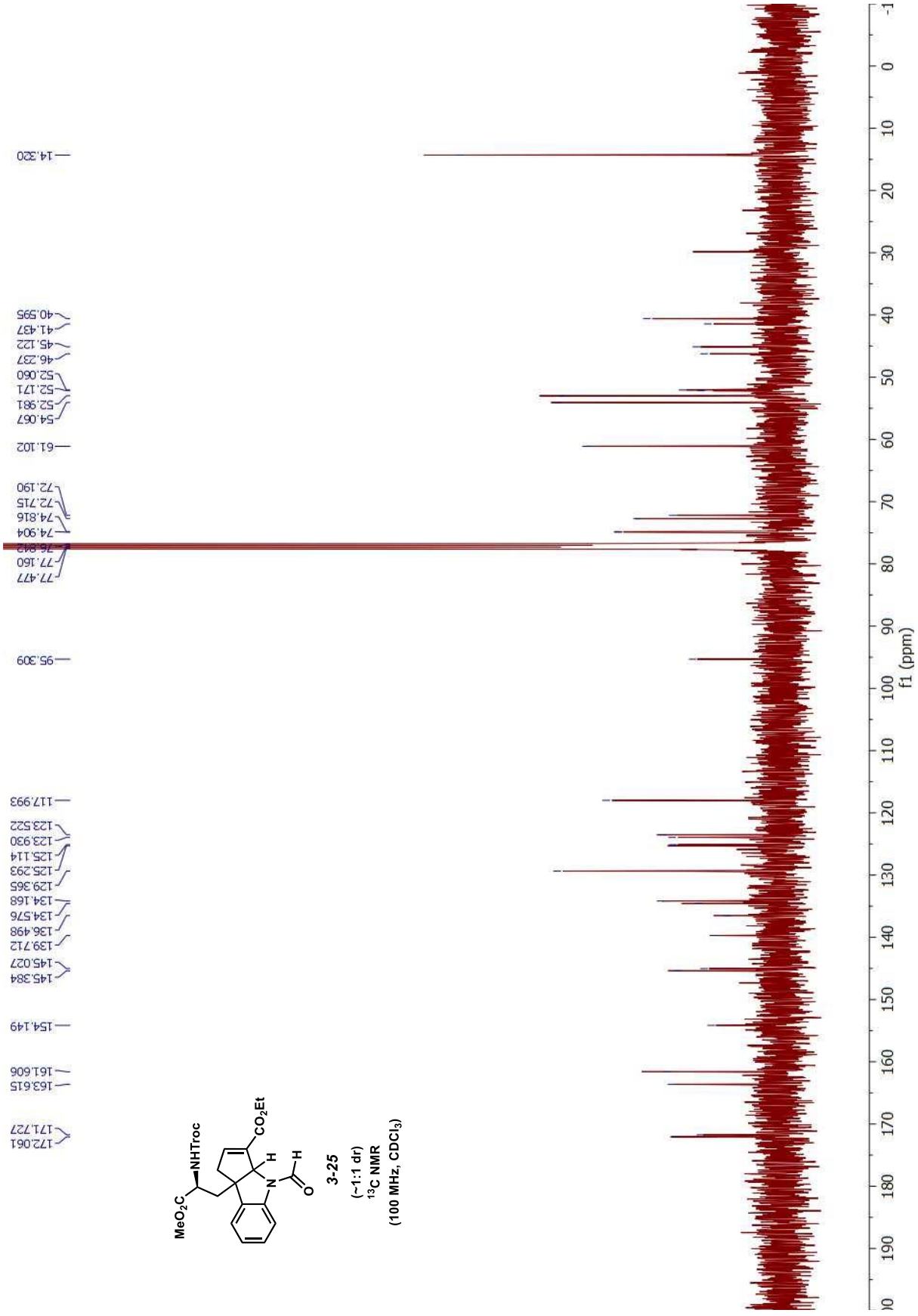
14.320
40.595
41.437
45.122
46.237
52.060
52.171
52.981
54.067
61.102
72.190
72.715
74.816
74.904
76.843
77.160
77.477
95.309
117.993
123.522
123.930
125.114
125.293
129.365
134.168
134.576
136.498
139.712
145.027
145.384
154.149
161.606
163.615
171.727
172.061
MeO2C
NHTroc
CO2Et
H
N
H
O
3-25
(~1:1 dr)
13C NMR
(100 MHz, CDCl3)
f1 (ppm)

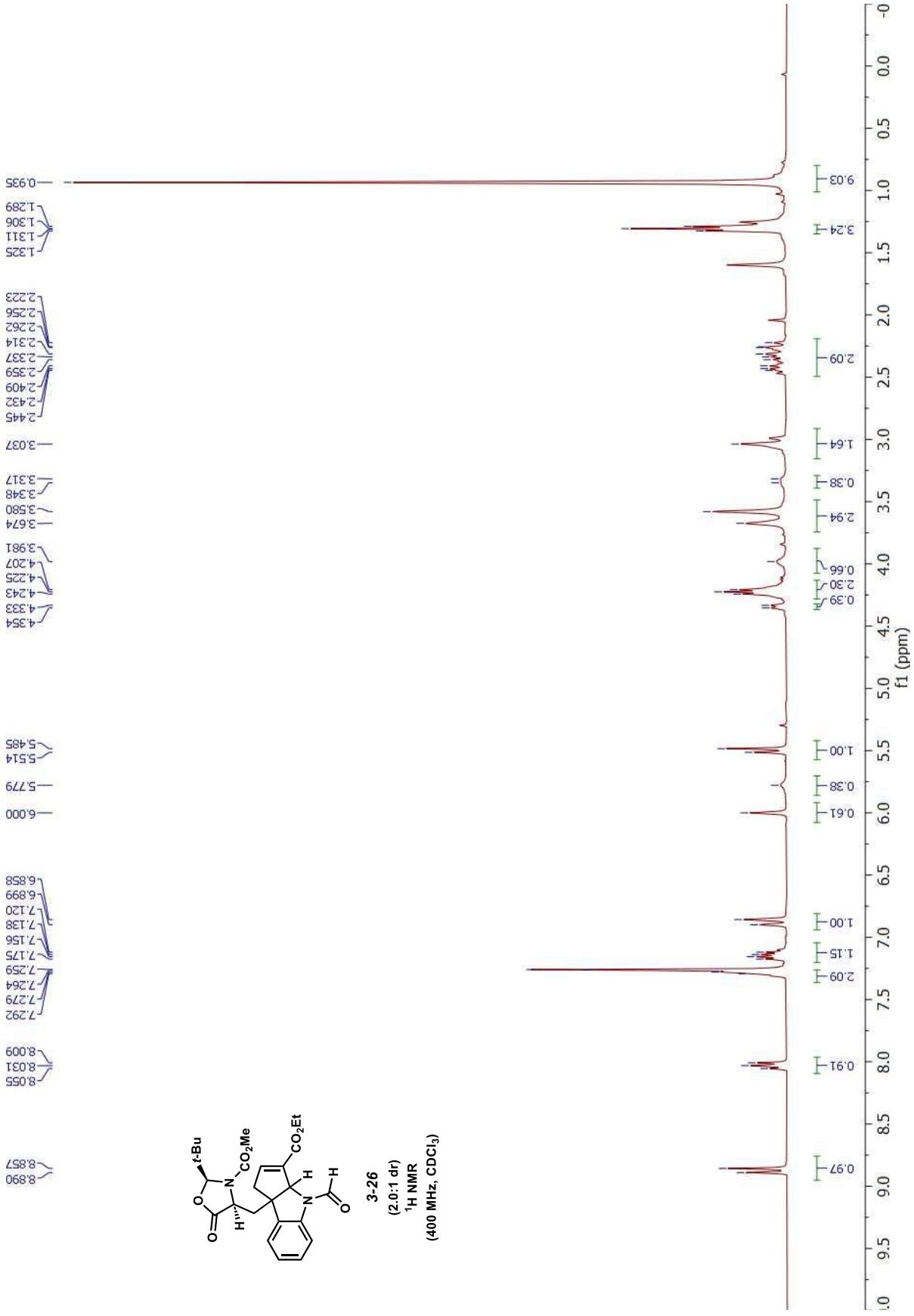
8.890
8.857
8.055
8.031
8.009
7.292
7.279
7.264
7.259
7.175
7.156
7.138
7.120
6.899
6.858
6.000
5.779
5.514
5.485
4.354
4.333
4.243
4.225
4.207
3.981
3.674
3.580
3.348
3.317
3.037
2.445
2.432
2.409
2.359
2.337
2.314
2.262
2.256
2.223
1.325
1.311
1.306
1.289
0.935
9.03
3.24
2.09
1.64
0.38
2.94
0.66
2.30
0.39
1.00
0.38
0.61
1.00
1.15
2.09
0.91
0.97
f1 (ppm)
t-Bu
CO2Me
CO2Et
H
H
O
O
O
N
N
H
3-26
(2.0:1 dr)
1H NMR
(400 MHz, CDCl3)

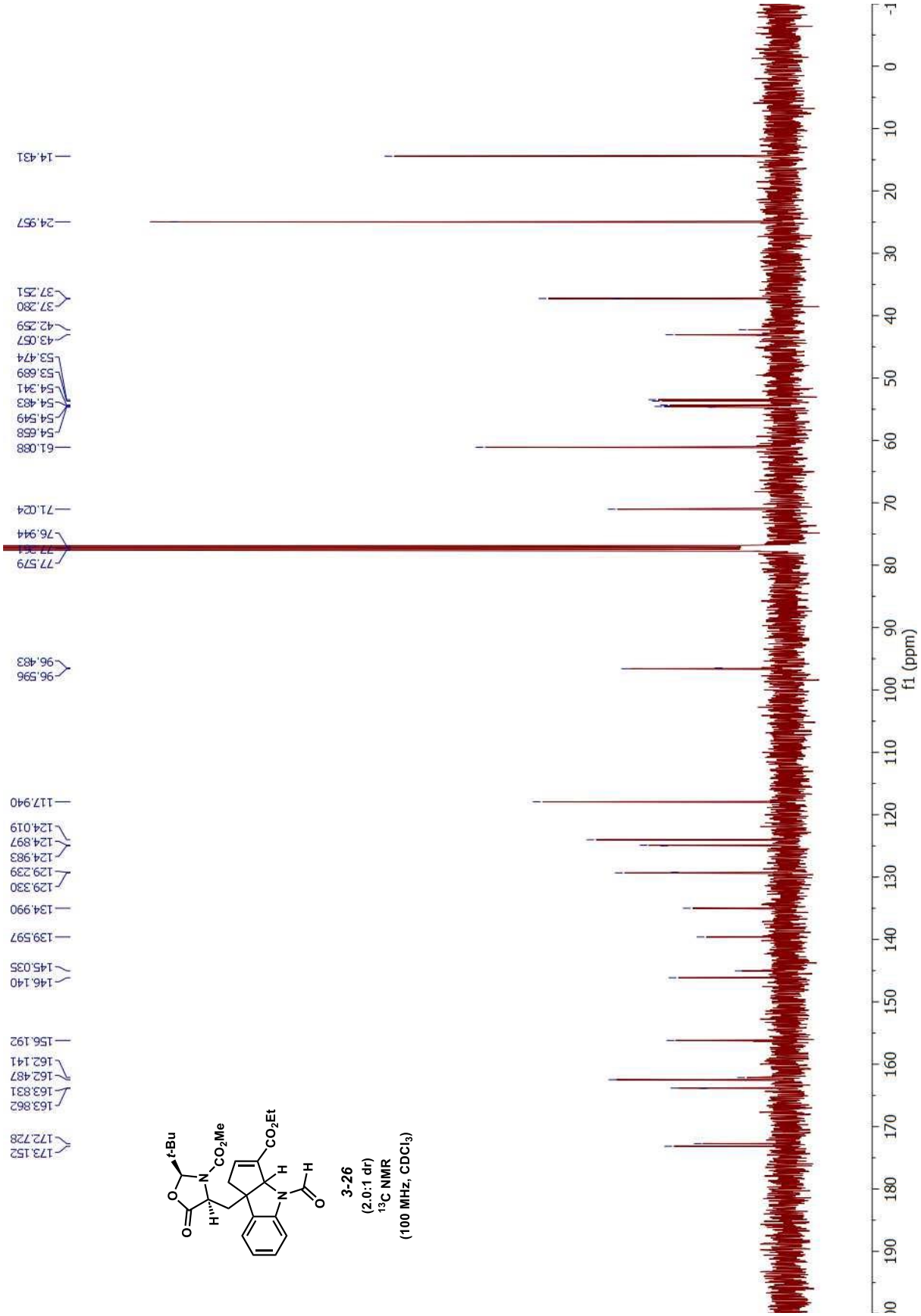
14.431
24.957
37.251
37.280
42.259
43.057
53.474
53.689
54.341
54.483
54.549
54.658
61.088
71.024
76.944
77.579
96.483
96.596
117.940
124.019
124.897
124.983
129.239
129.330
134.990
139.597
145.035
146.140
156.192
162.141
162.487
163.831
163.862
172.728
173.152
t-Bu
CO2Me
CO2Et
3-26
(2.0:1 dr)
13C NMR
(100 MHz, CDCl3)
f1 (ppm)

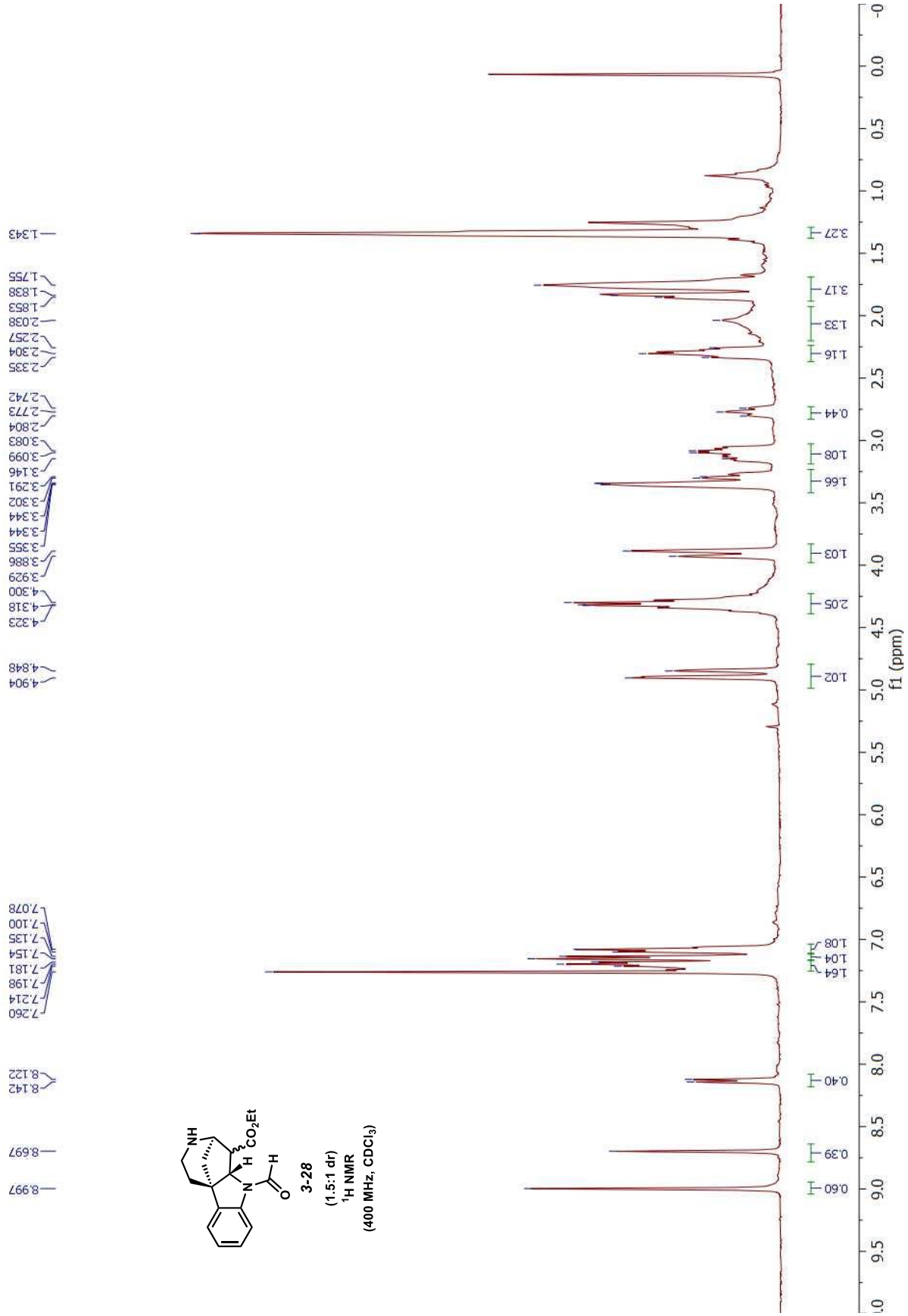
3-28
(1.5:1 dr)
^{1}H NMR
(400 MHz, $CDCl_3$)
f1 (ppm)

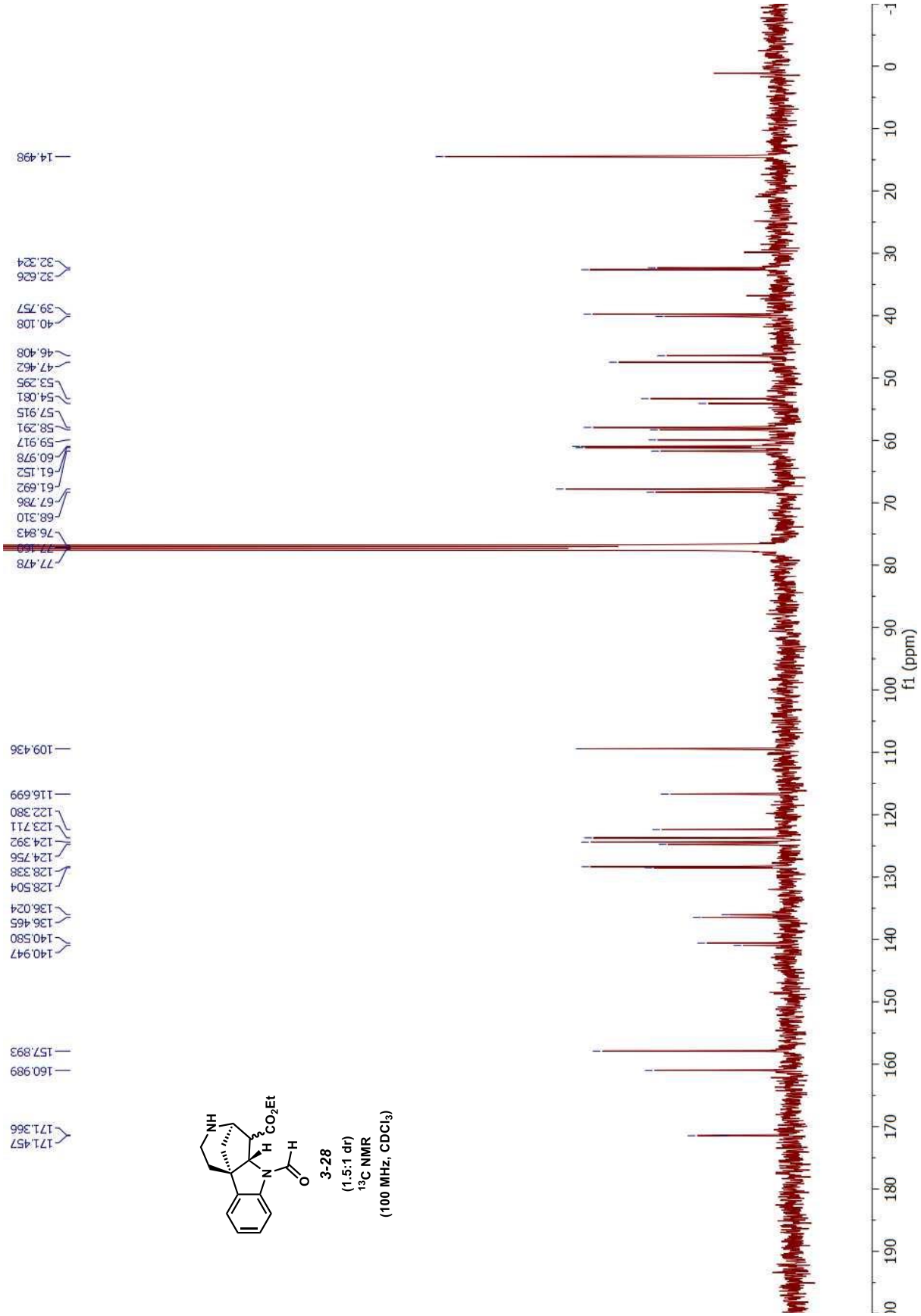
14.498
32.324
32.626
39.757
40.108
46.408
47.462
53.295
54.081
57.915
58.291
59.917
60.978
61.152
61.692
67.786
68.310
76.843
77.160
77.478
109.436
116.699
122.380
123.711
124.392
124.756
128.338
128.504
136.024
136.465
140.580
140.947
157.893
160.989
171.366
171.457
NH
H
CO2Et
N
O
H
3-28
(1.5:1 dr)
13C NMR
(100 MHz, CDCl3)
f1 (ppm)

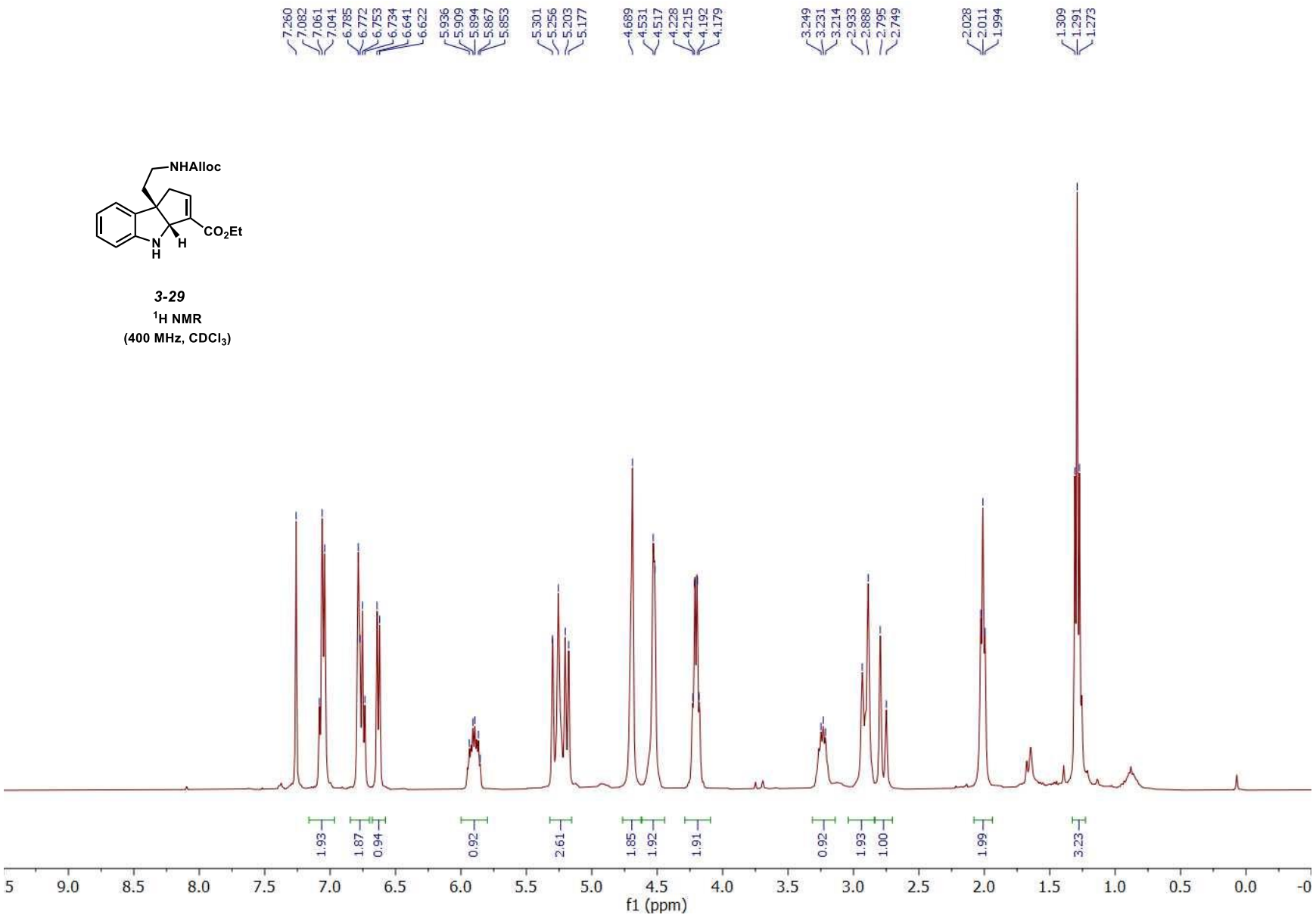
7.260
7.082
7.061
7.041
6.785
6.772
6.753
6.734
6.641
6.622
5.936
5.909
5.894
5.867
5.853
5.301
5.256
5.203
5.177
4.689
4.531
4.517
4.228
4.215
4.192
4.179
3.249
3.231
3.214
2.933
2.888
2.795
2.749
2.028
2.011
1.994
1.309
1.291
1.273
NHAlloc
CO2Et
N
H
H
3-29
1H NMR
(400 MHz, CDCl3)
1.93
1.87
0.94
0.92
2.61
1.85
1.92
1.91
0.92
1.93
1.00
1.99
3.23
f1 (ppm)

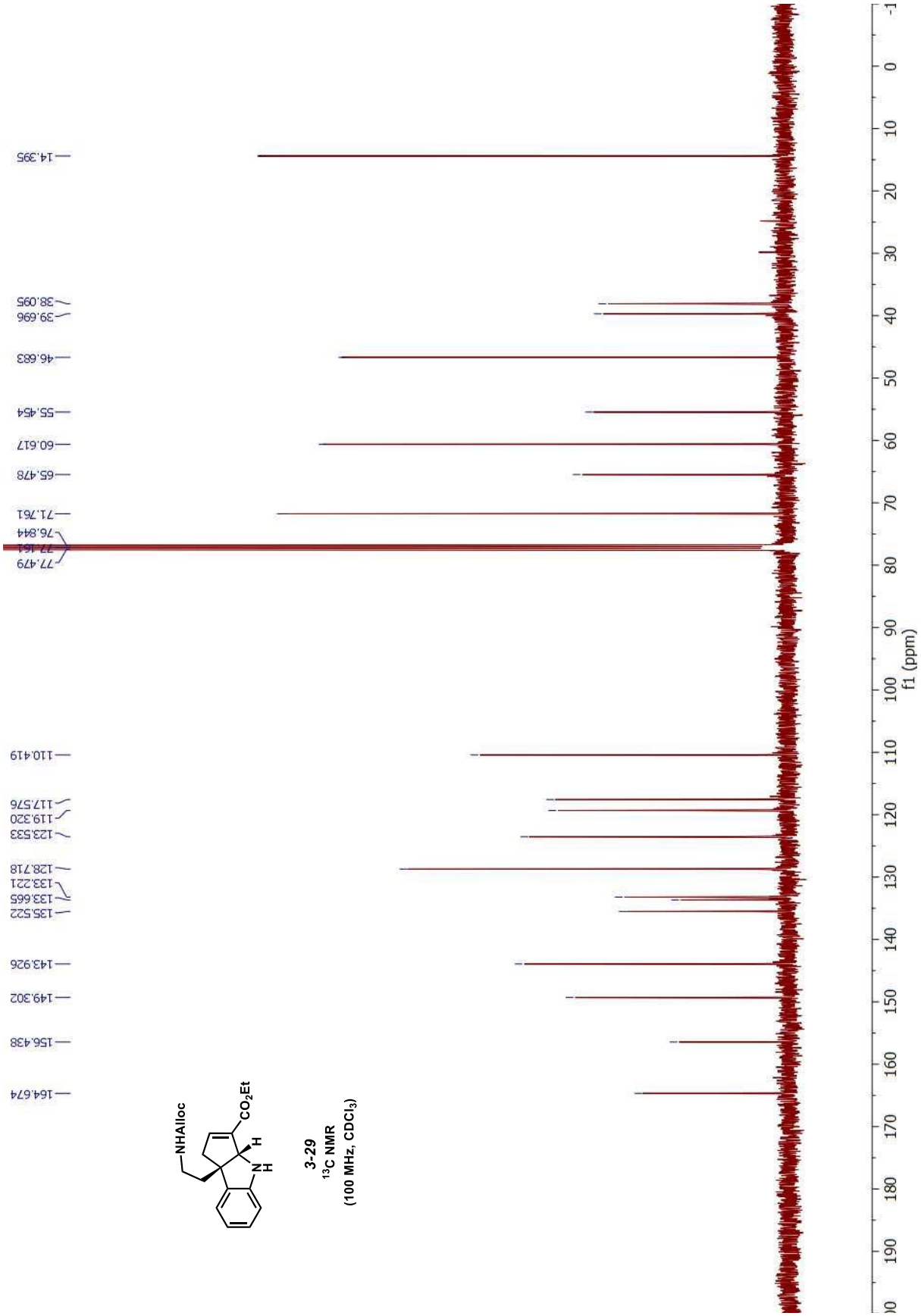
14.395
38.095
39.696
46.683
55.454
60.617
65.478
71.761
76.844
77.161
77.479
110.419
117.576
119.320
123.533
128.718
133.221
133.665
135.522
143.926
149.302
156.438
164.674
NHAlloc
CO2Et
H
N
H
3-29
13C NMR
(100 MHz, CDCl3)
f1 (ppm)

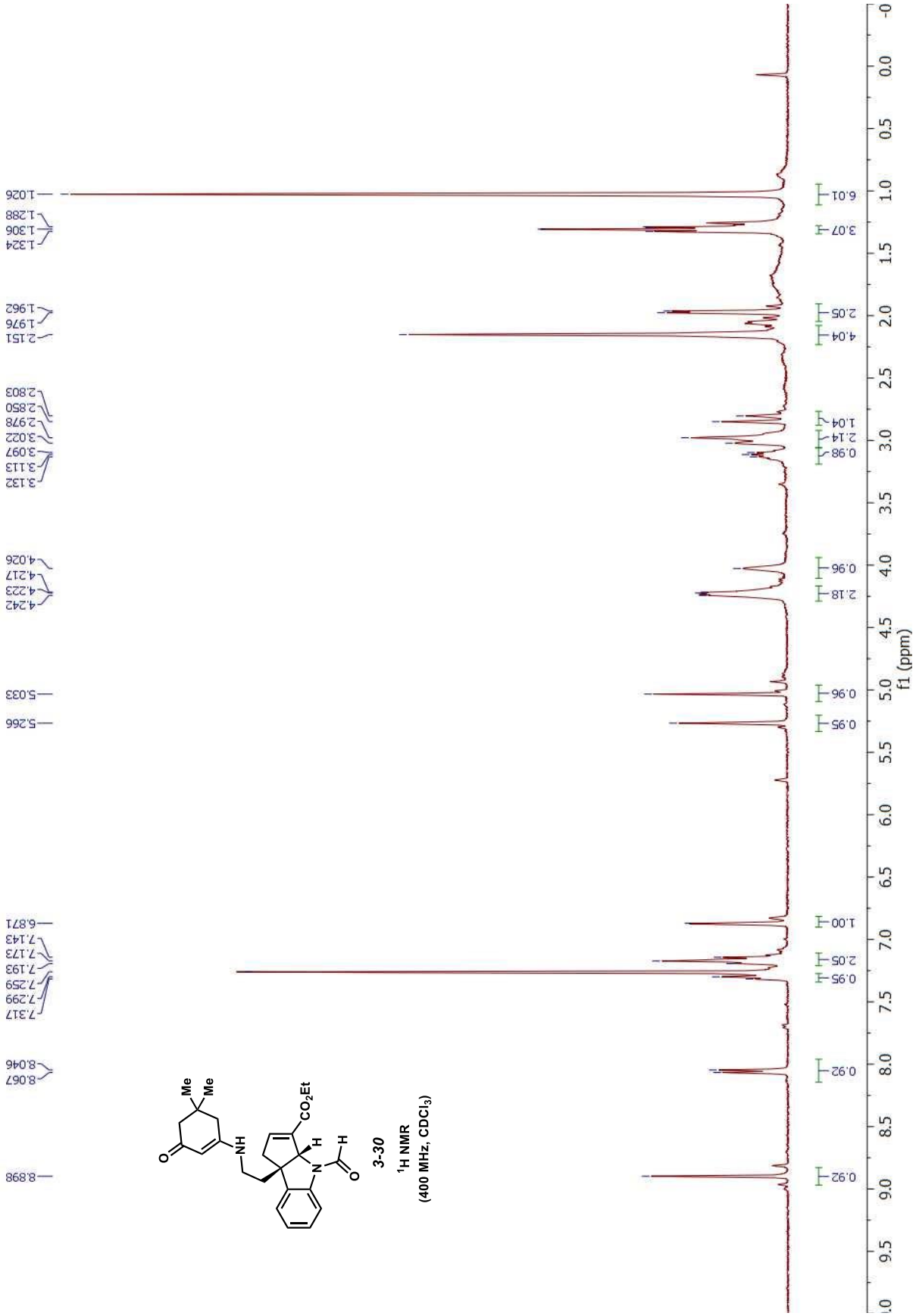
Me
Me
O
NH
CO2Et
H
N
H
O
3-30
1H NMR
(400 MHz, CDCl3)
f1 (ppm)

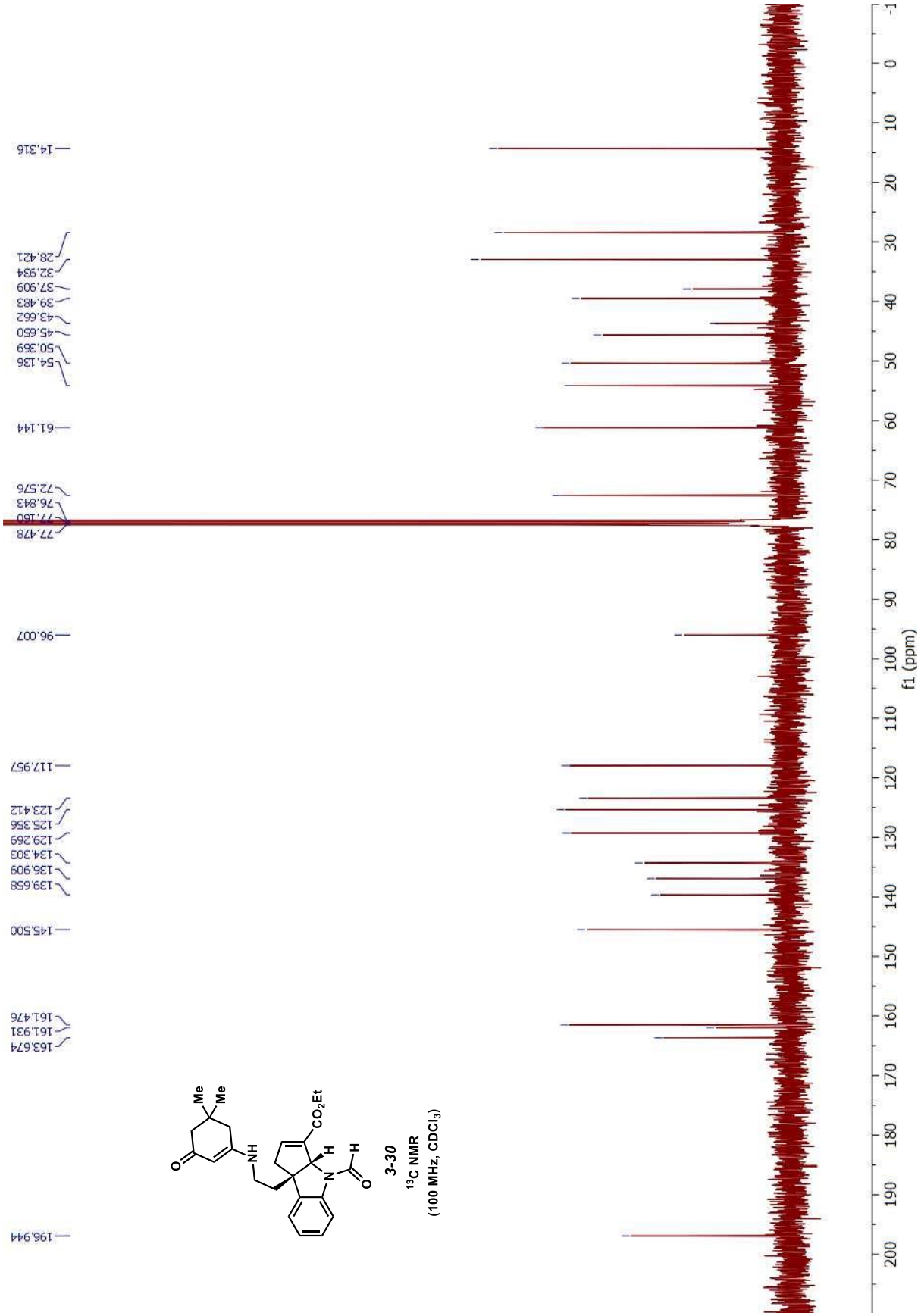
14.316
28.421
32.934
37.909
39.483
43.662
45.650
50.359
54.136
61.144
72.576
76.843
77.160
77.478
96.007
117.957
123.412
125.356
129.269
134.303
136.909
139.658
145.500
161.476
161.931
163.674
196.944
Me
Me
O
NH
CO2Et
H
N
H
O
3-30
13C NMR
(100 MHz, CDCl3)
f1 (ppm)

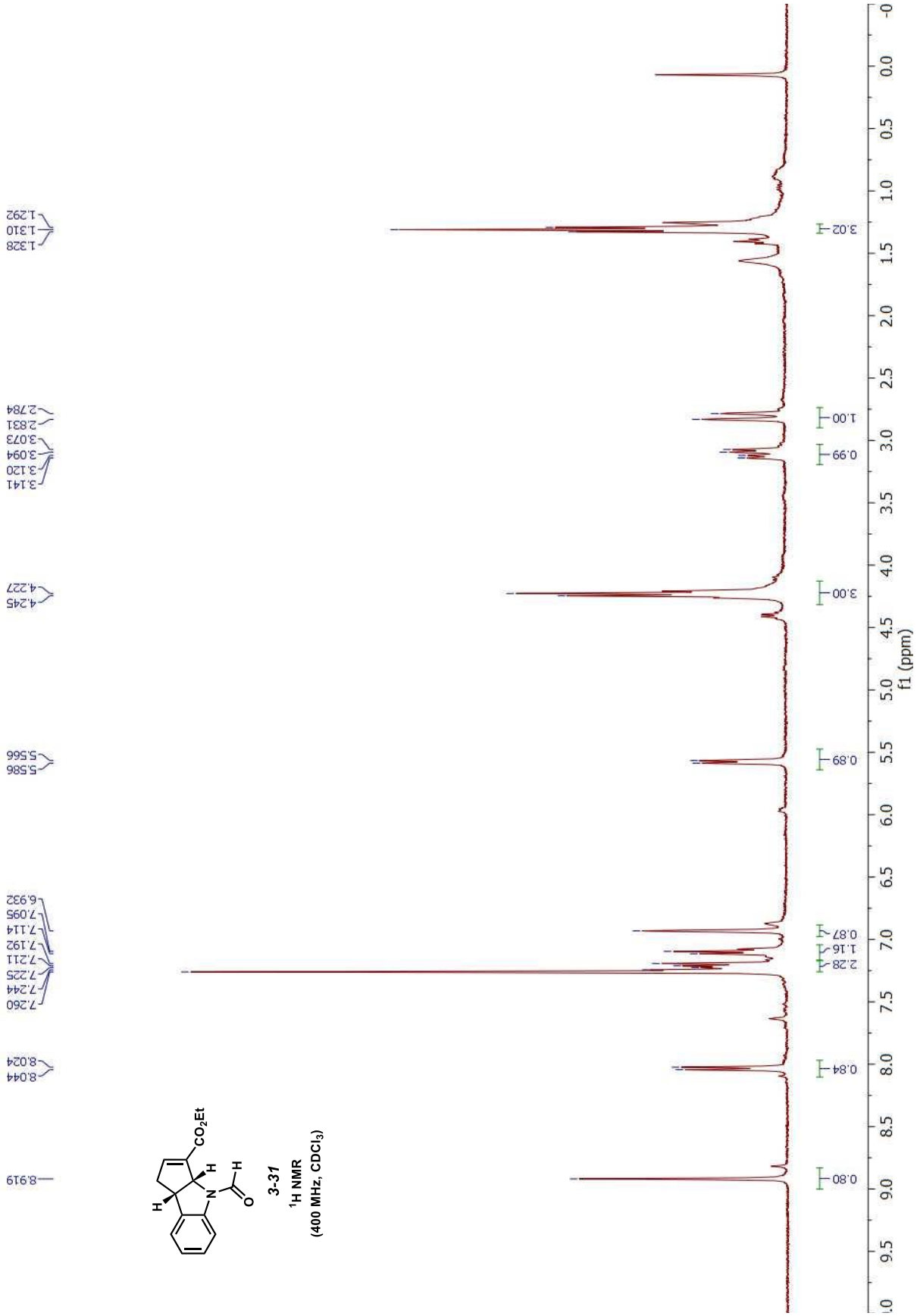
8.919
8.044
8.024
7.260
7.244
7.225
7.211
7.192
7.114
7.095
6.932
5.586
5.566
4.245
4.227
3.141
3.120
3.094
3.073
2.831
2.784
1.328
1.310
1.292
0.80
0.84
2.28
1.16
0.87
0.89
3.00
0.99
1.00
3.02
f1 (ppm)
CO2Et
H
N
O
H
3-31
1H NMR
(400 MHz, CDCl3)

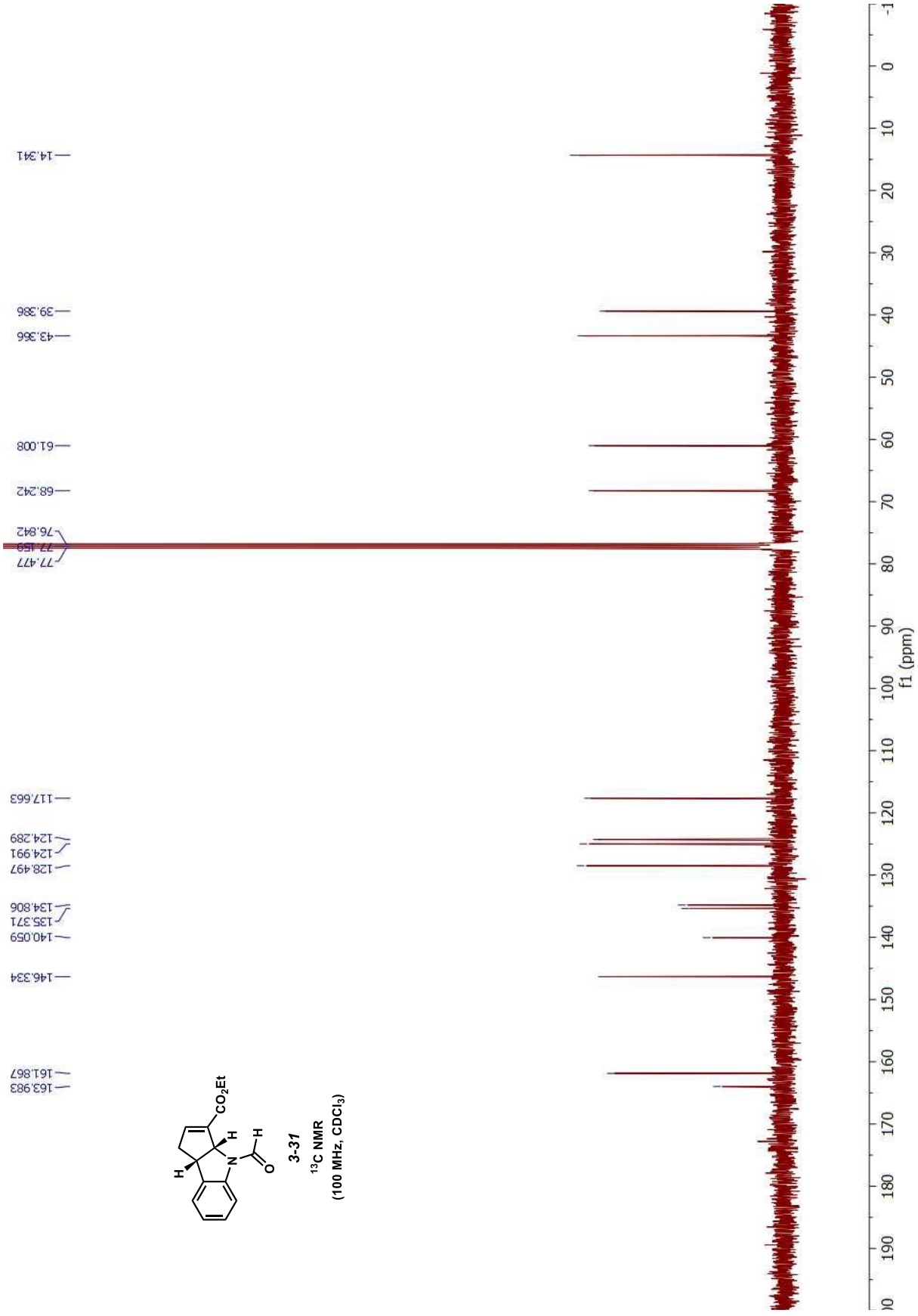
14.341
39.386
43.366
61.008
68.242
76.842
77.159
77.477
117.663
124.289
124.991
128.497
134.806
135.371
140.059
146.334
161.867
163.983
CO2Et
H
H
N
O
3-31
13C NMR
(100 MHz, CDCl3)
f1 (ppm)

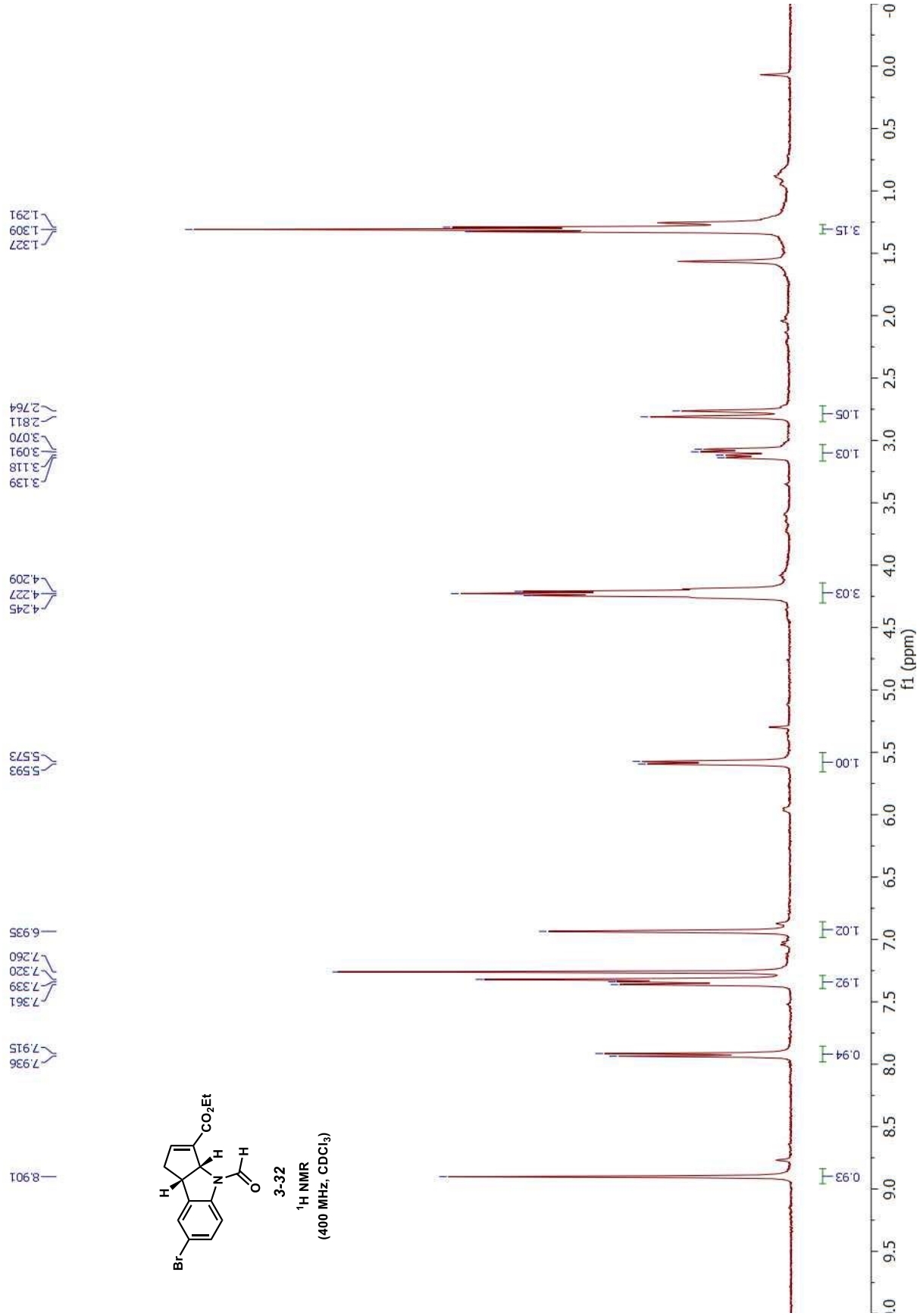
8.901
7.936
7.915
7.361
7.339
7.320
7.260
6.935
5.593
5.573
4.245
4.227
4.209
3.139
3.118
3.091
3.070
2.811
2.764
1.327
1.309
1.291
0.93
3.15
0.94
1.92
1.02
1.00
3.03
1.03
1.05
f1 (ppm)
3-32
^{1}H NMR
(400 MHz, CDCl$_3$)

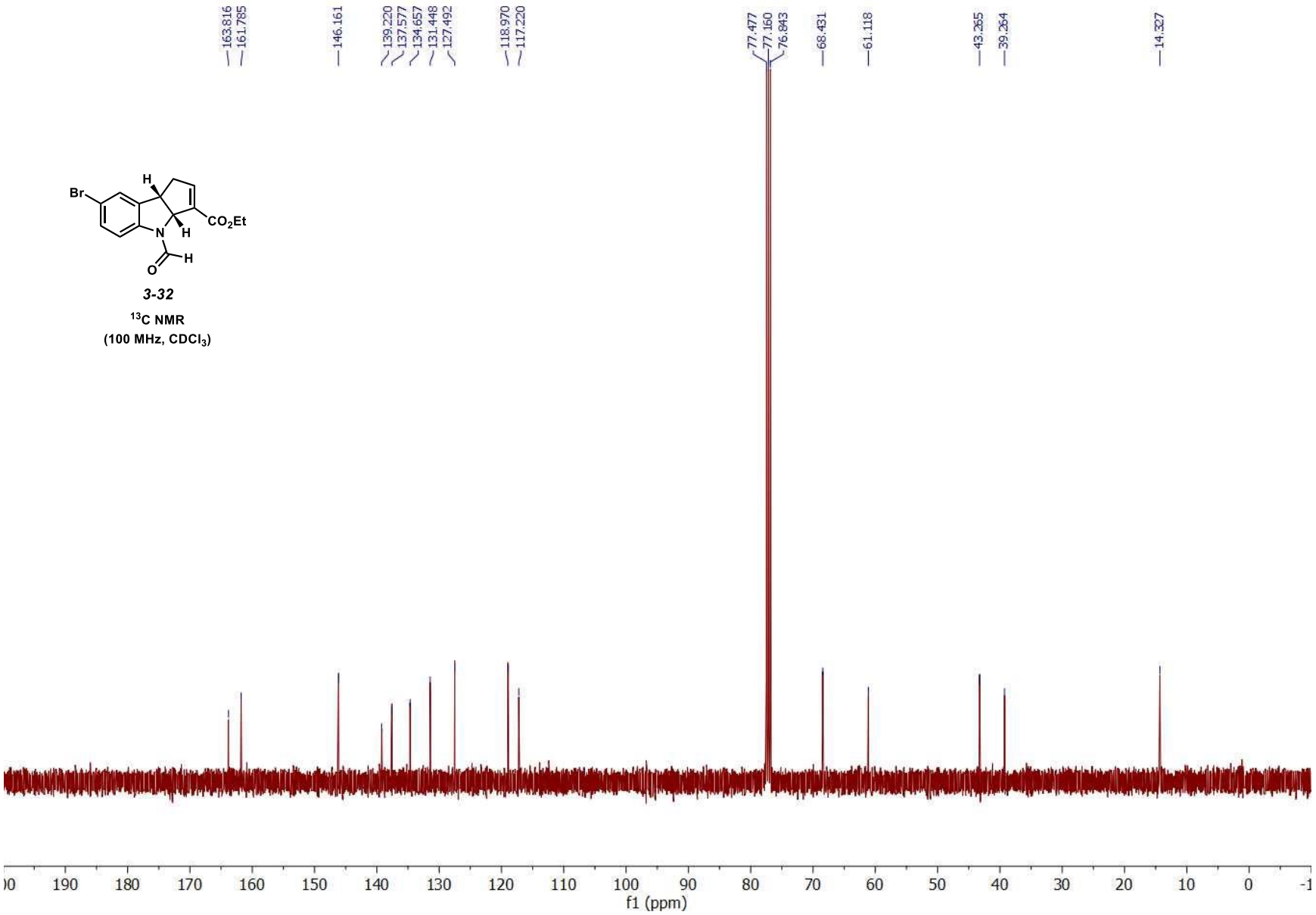
163.816
161.785
146.161
139.220
137.577
134.657
131.448
127.492
118.970
117.220
77.477
77.160
76.843
68.431
61.118
43.265
39.264
14.327
Br
H
CO2Et
N
H
O
H
3-32
13C NMR
(100 MHz, CDCl3)
f1 (ppm)

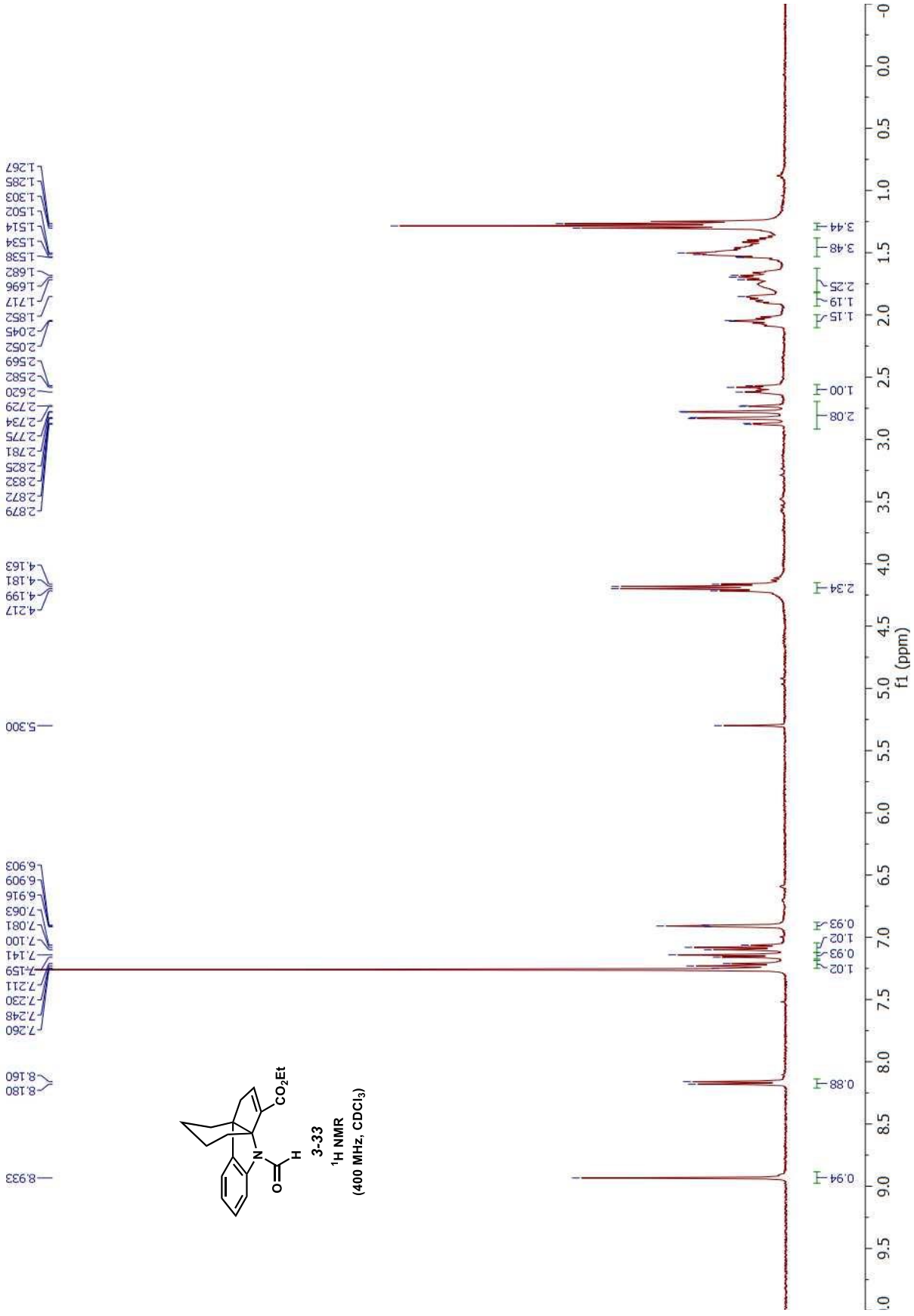
3-33
^{1}H NMR
(400 MHz, CDCl$_3$)
CO$_2$Et
N
H
O
f1 (ppm)

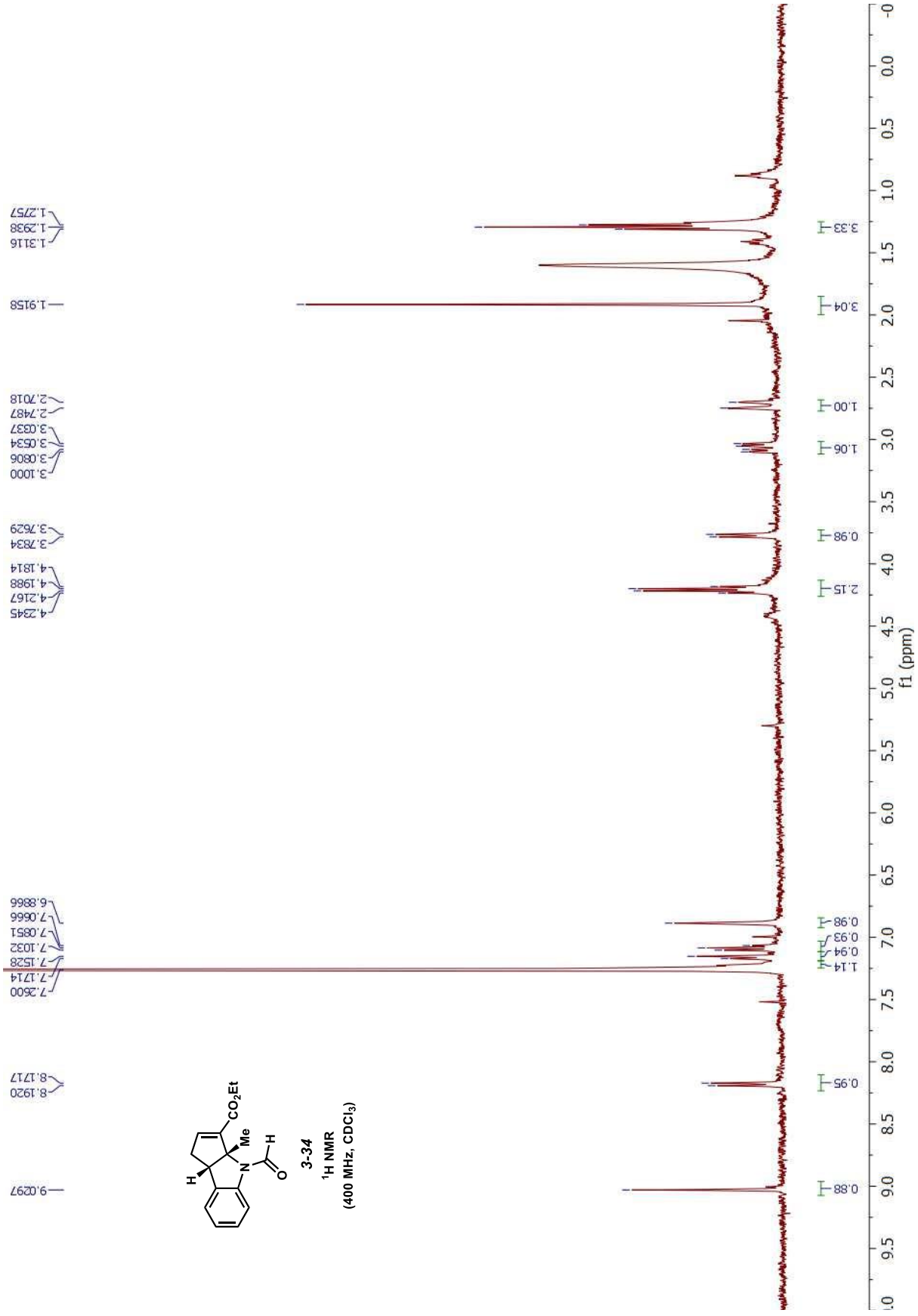
9.0297
8.1920
8.1717
7.3600
7.1714
7.1528
7.1032
7.0851
7.0666
6.8866
4.2345
4.2167
4.1988
4.1814
3.7834
3.7629
3.1000
3.0806
3.0534
3.0337
2.7487
2.7018
1.9158
1.3116
1.2938
1.2757
0.88
0.95
0.98
0.93
0.94
1.14
0.98
2.15
1.06
1.00
3.04
3.33
f1 (ppm)
CO2Et
Me
H
N
O
H
3-34
1H NMR
(400 MHz, CDCl3)

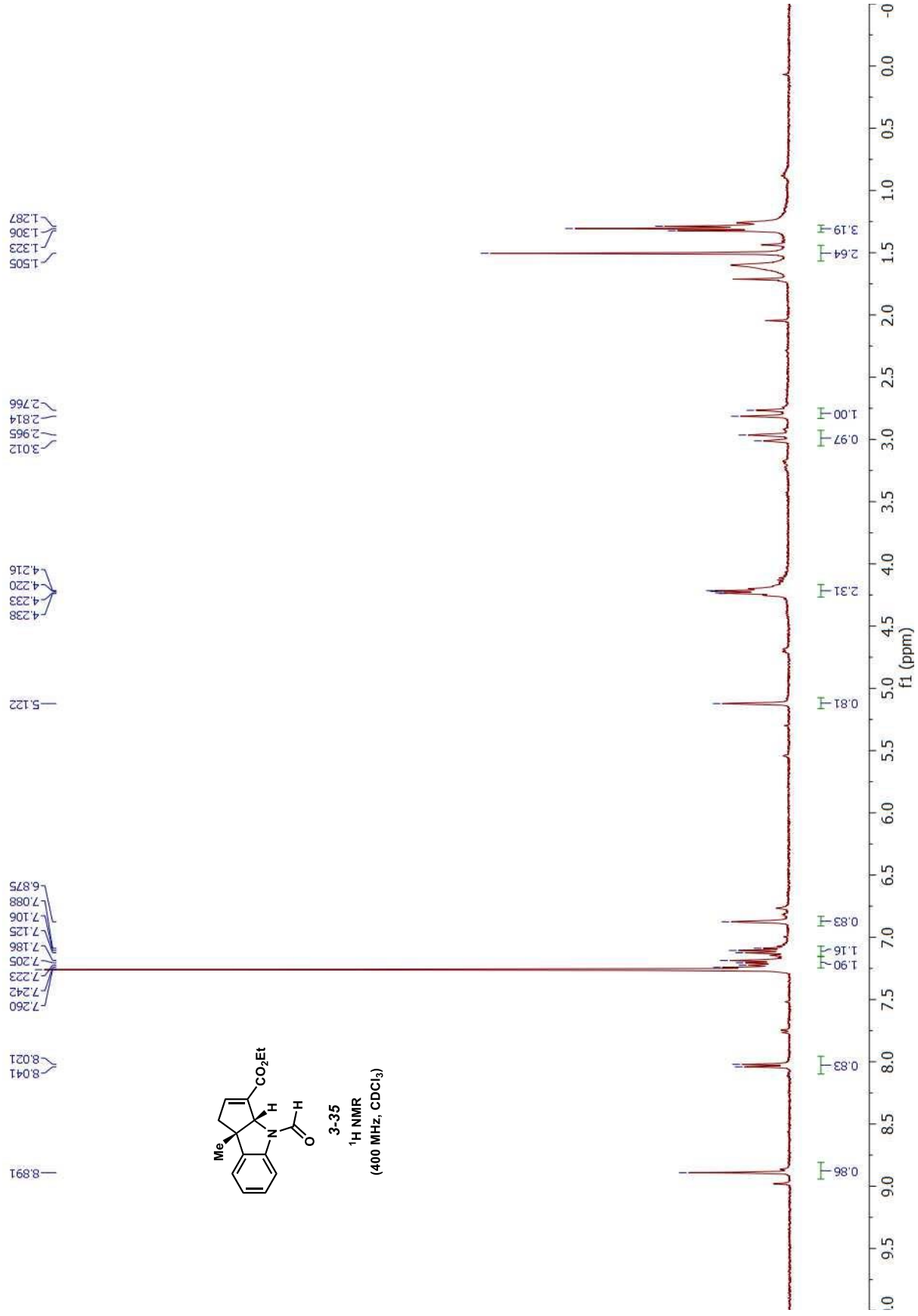
8.891
8.041
8.021
7.260
7.242
7.223
7.205
7.186
7.125
7.106
7.088
6.875
5.122
4.238
4.233
4.220
4.216
3.012
2.965
2.814
2.766
1.505
1.323
1.306
1.287
0.86
0.83
0.83
1.90
1.16
0.83
0.81
2.31
0.97
1.00
2.64
3.19
f1 (ppm)
CO2Et
H
N
H
O
Me
3-35
1H NMR
(400 MHz, CDCl3)

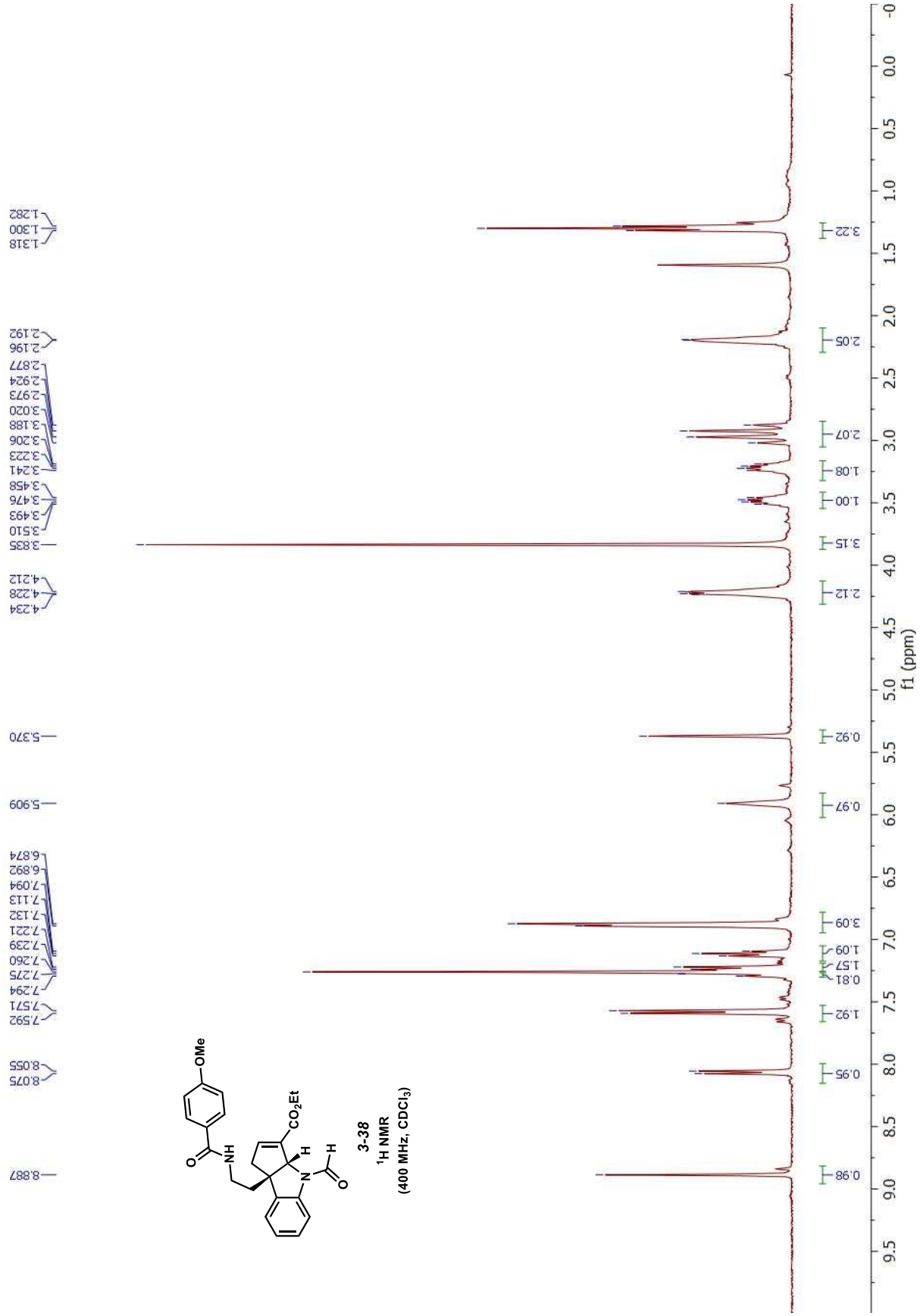
OMe
NH
O
CO2Et
H
N
H
O
3-38
1H NMR
(400 MHz, CDCl3)
f1 (ppm)

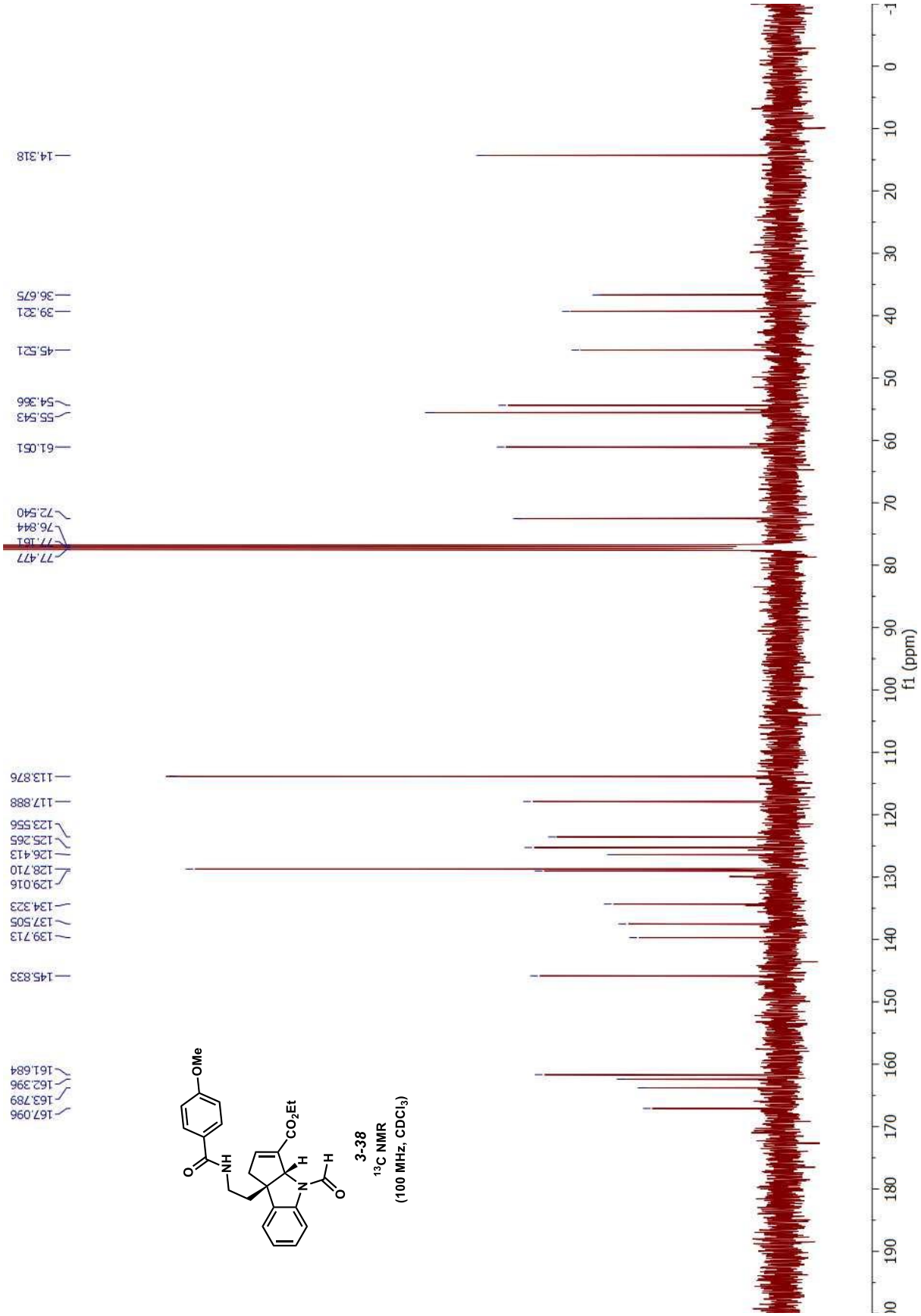
14.318
36.675
39.321
45.521
54.366
55.543
61.051
72.540
76.844
77.161
77.477
113.876
117.888
123.556
125.265
126.413
128.710
129.016
134.323
137.505
139.713
145.833
161.684
162.396
163.789
167.096
OMe
NH
O
CO2Et
H
N
H
O
3-38
13C NMR
(100 MHz, CDCl3)
f1 (ppm)

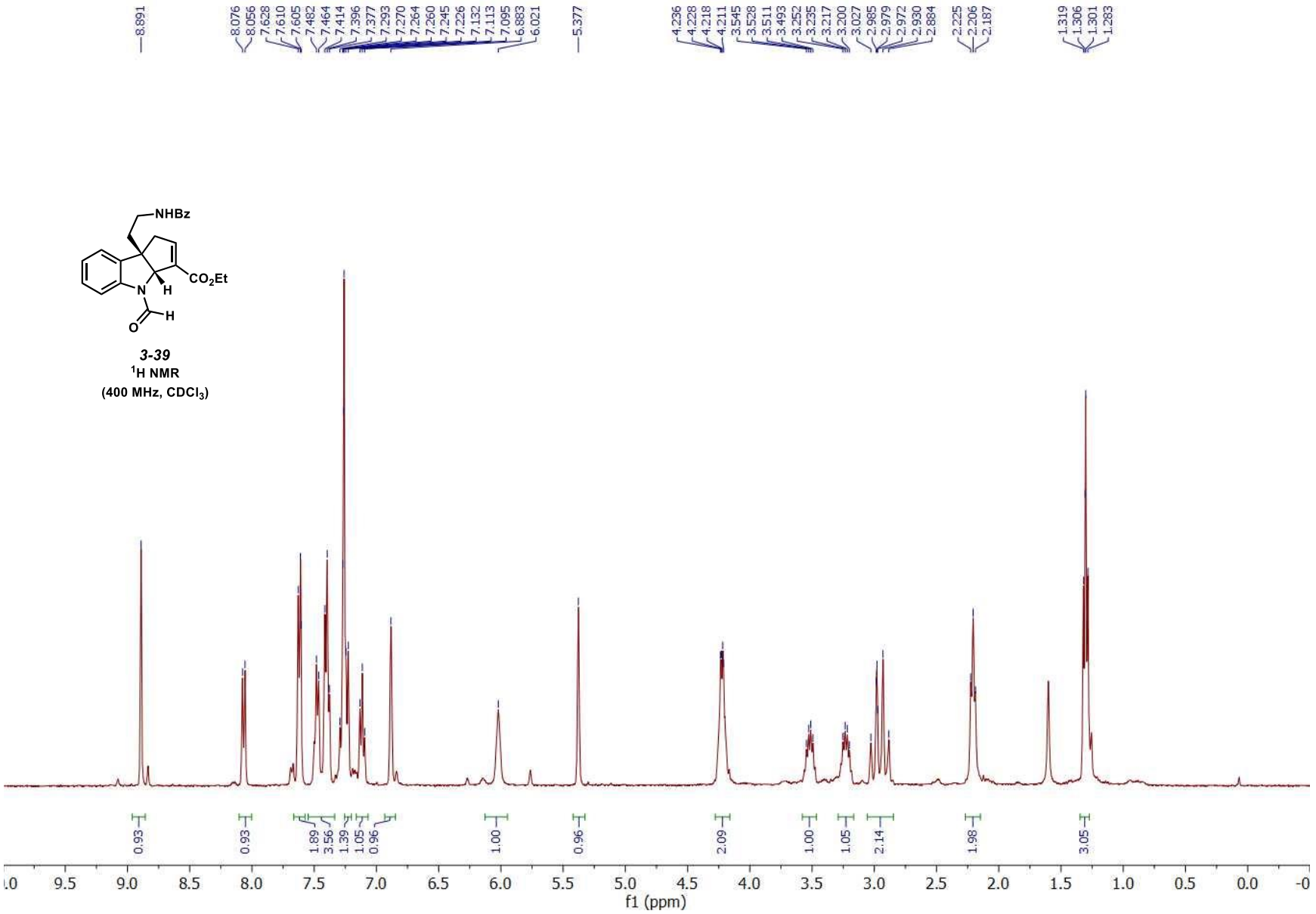
8.891
8.076
8.056
7.628
7.610
7.605
7.482
7.464
7.414
7.396
7.377
7.293
7.270
7.264
7.260
7.245
7.226
7.132
7.113
7.095
6.883
6.021
5.377
4.236
4.228
4.218
4.211
3.545
3.528
3.511
3.493
3.252
3.235
3.217
3.200
3.027
2.985
2.979
2.972
2.930
2.884
2.225
2.206
2.187
1.319
1.306
1.301
1.283
NHBz
CO2Et
N
H
O
H
3-39
1H NMR
(400 MHz, CDCl3)
0.93
0.93
1.89
3.56
1.39
1.05
0.96
1.00
0.96
2.09
1.00
1.05
2.14
1.98
3.05
f1 (ppm)

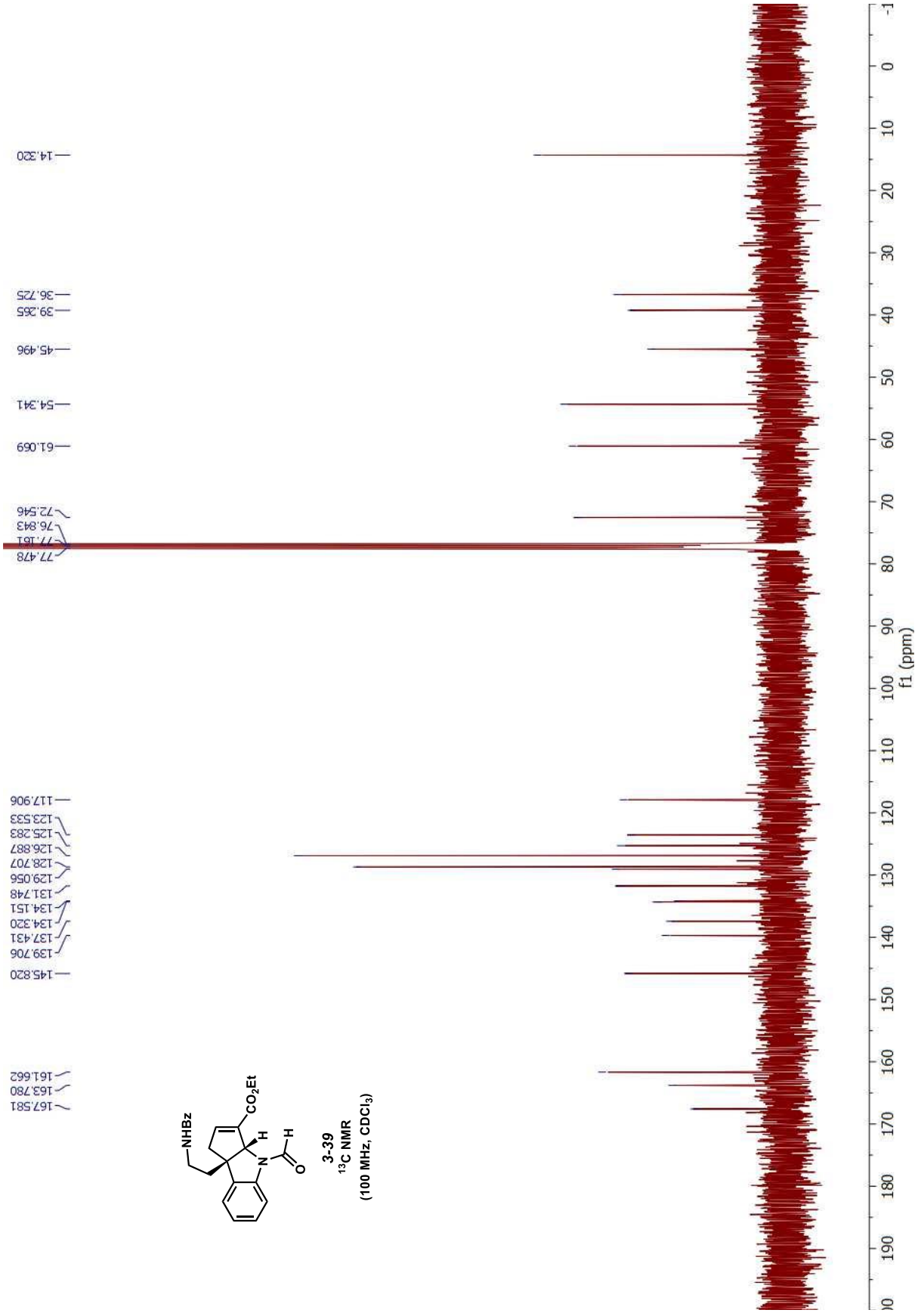
14.320
36.725
39.365
45.496
54.341
61.069
72.546
76.843
77.161
77.478
117.906
123.533
125.283
126.887
128.707
129.056
131.748
134.151
134.320
137.431
139.706
145.820
161.662
163.780
167.581
NHBz
CO2Et
H
N
H
O
3-39
13C NMR
(100 MHz, CDCl3)
f1 (ppm)

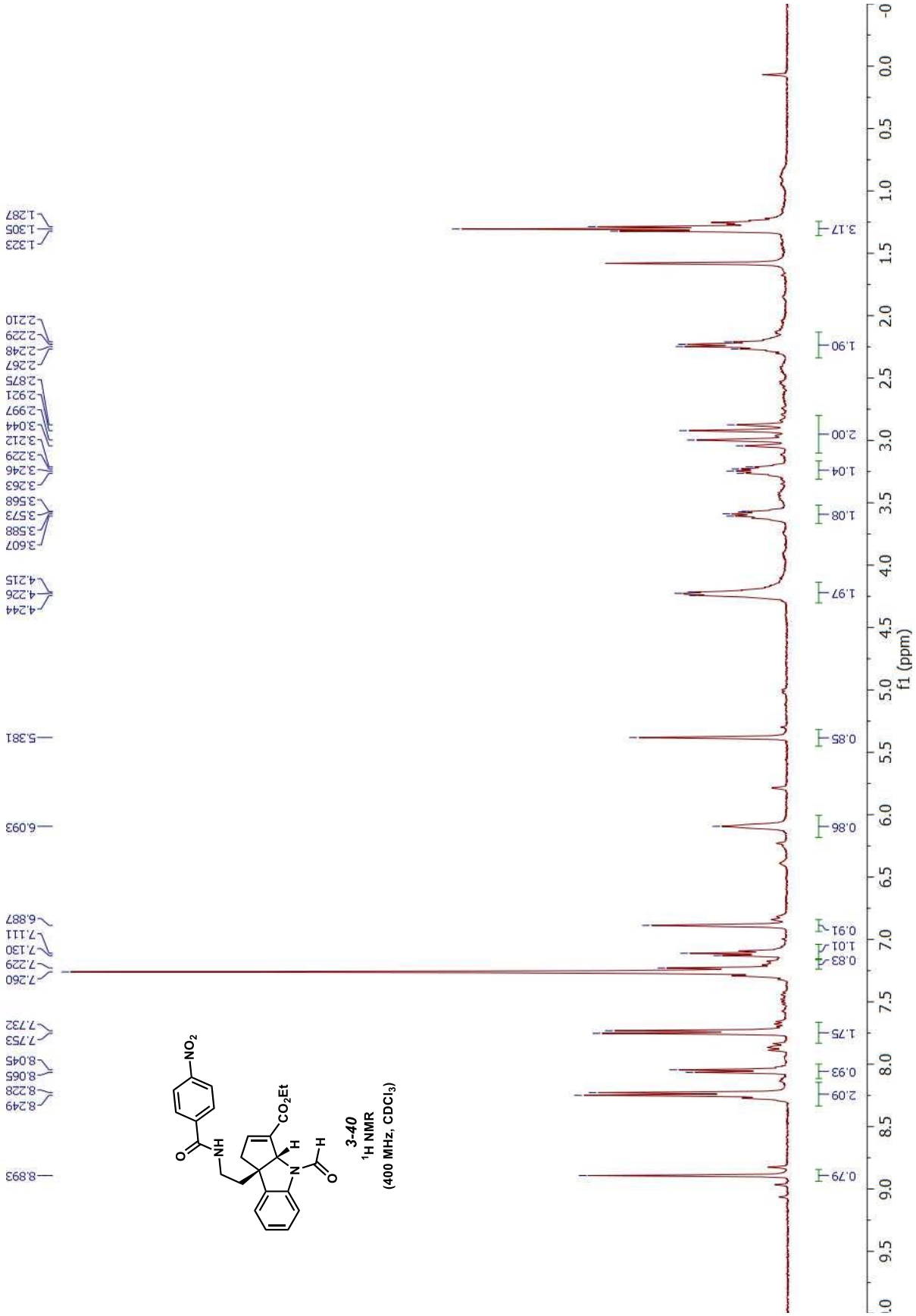
3-40
^{1}H NMR
(400 MHz, CDCl$_3$)
f1 (ppm)

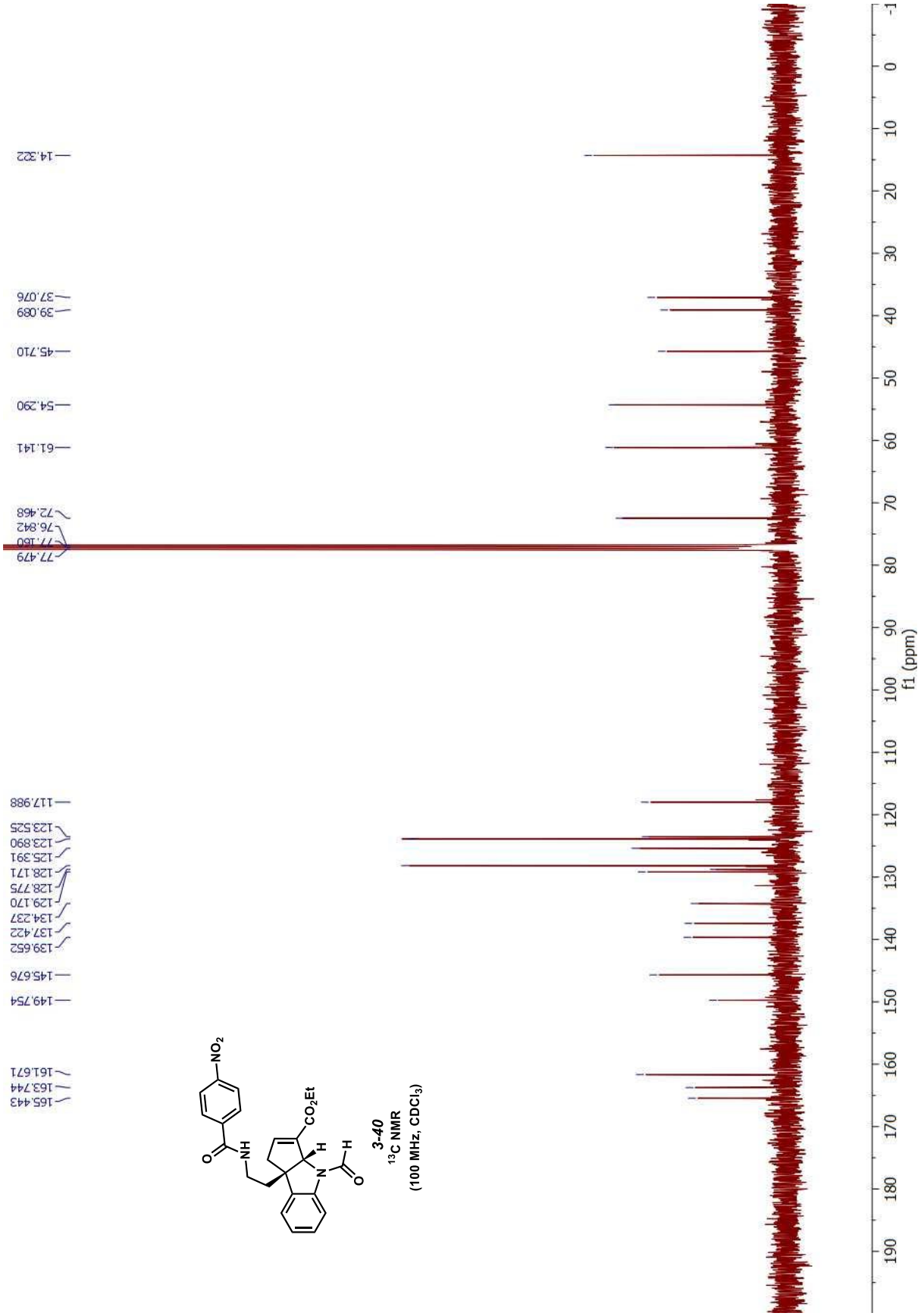
14.322
37.076
39.089
45.710
54.290
61.141
72.468
76.842
77.160
77.479
117.988
123.525
123.890
125.391
128.171
128.775
129.170
134.237
137.422
139.652
145.676
149.754
161.671
163.744
165.443
NO2
NH
O
CO2Et
H
N
H
O
3-40
13C NMR
(100 MHz, CDCl3)
f1 (ppm)

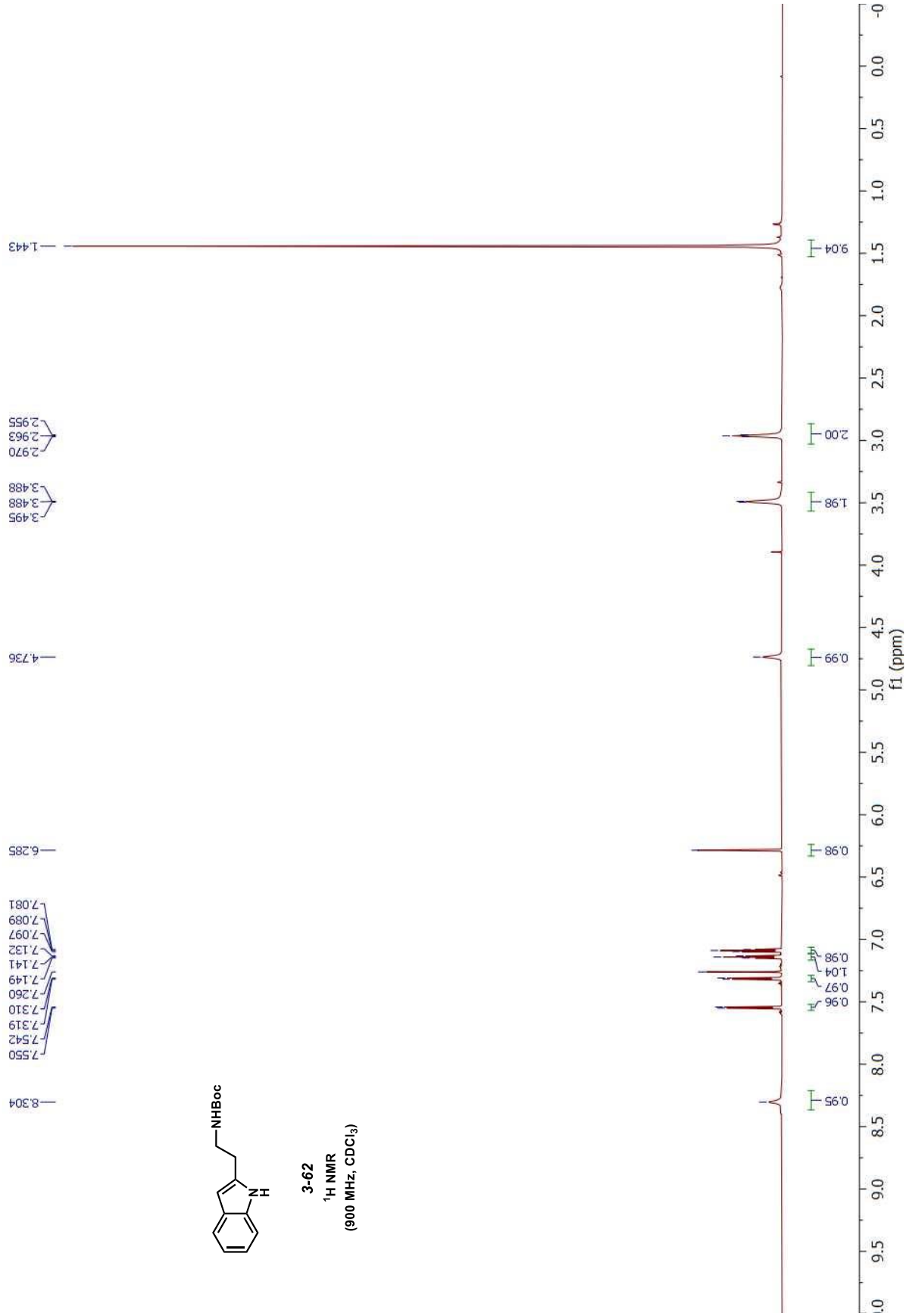
NHBoc
H
N
3-62
1H NMR
(900 MHz, CDCl3)
8.304
7.550
7.542
7.319
7.310
7.260
7.149
7.141
7.132
7.097
7.089
7.081
6.285
4.736
3.495
3.488
2.970
2.963
2.955
1.443
0.95
0.98
0.96
0.97
1.04
0.98
0.98
0.99
1.98
2.00
9.04
f1 (ppm)

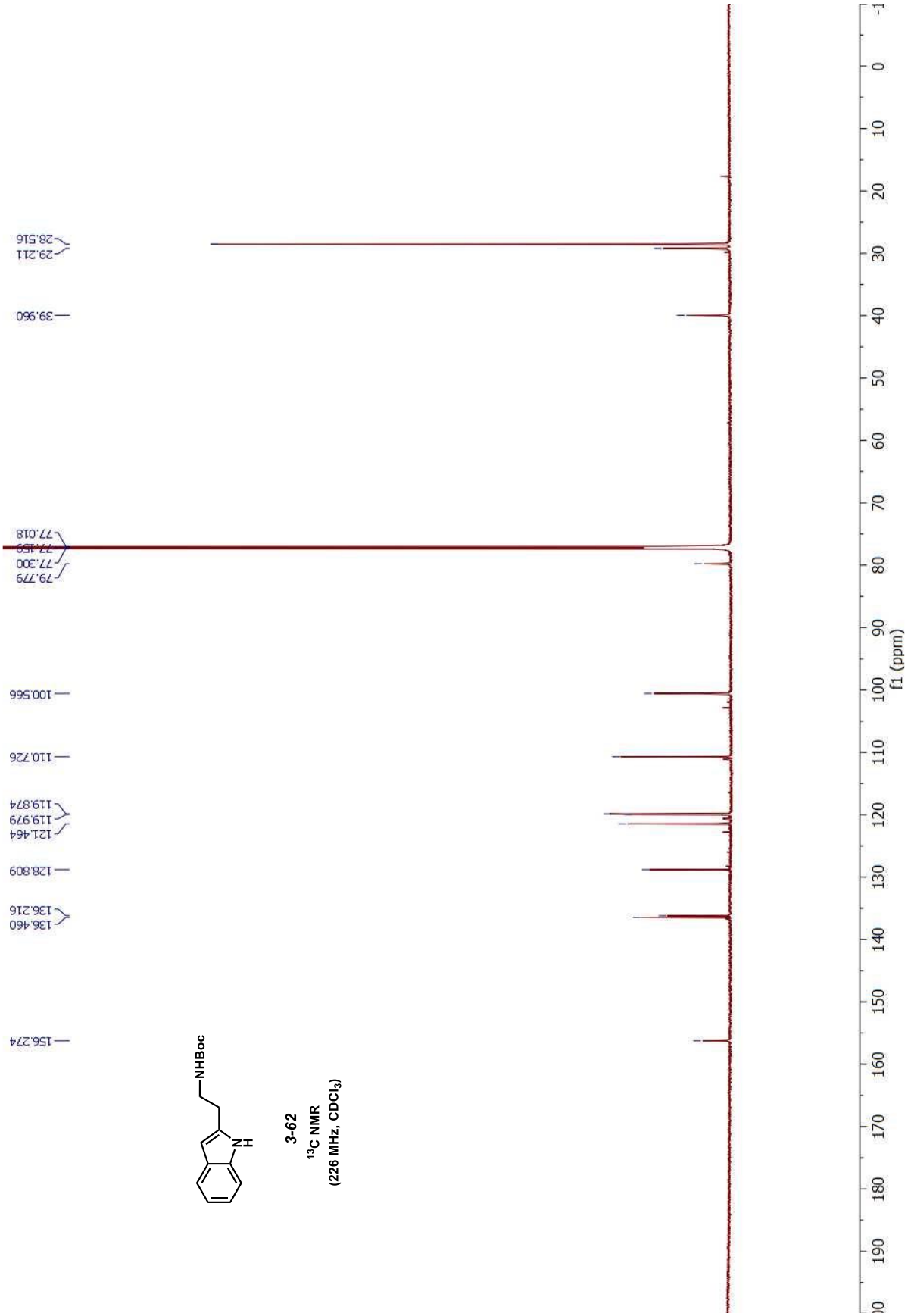
28.516
29.211
39.960
77.018
77.159
77.300
79.779
100.566
110.726
119.874
119.979
121.464
128.809
136.216
136.460
156.274
NHBoc
3-62
^{13}C NMR
(226 MHz, CDCl$_3$)
f1 (ppm)

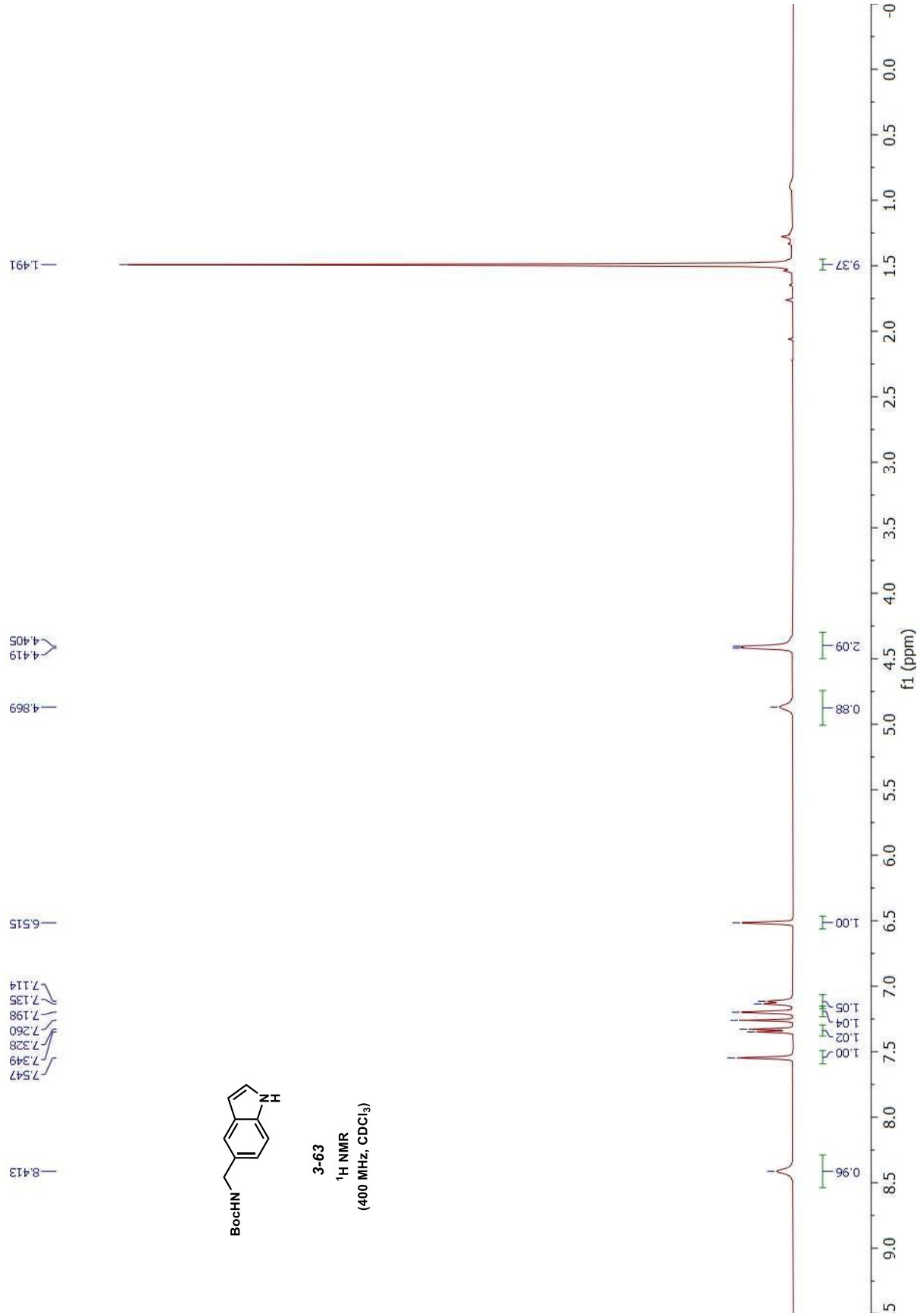
8.413
7.547
7.349
7.328
7.260
7.198
7.135
7.114
6.515
4.869
4.419
4.405
1.491
0.96
1.00
1.05
1.04
1.02
1.00
0.88
2.09
9.37
f1 (ppm)
BocHN
3-63
1H NMR
(400 MHz, CDCl3)

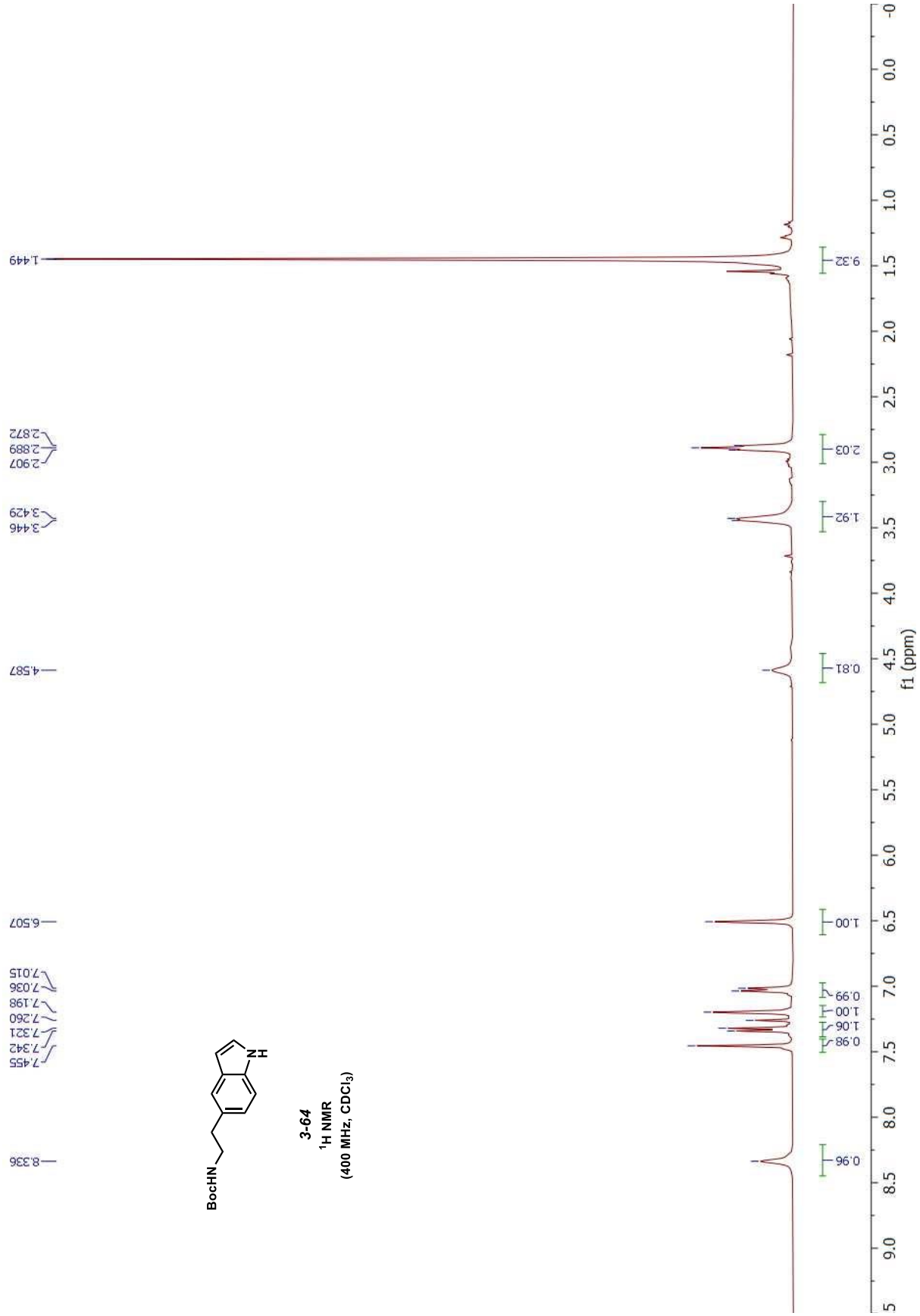
8.336
7.455
7.342
7.321
7.260
7.198
7.036
7.015
6.507
4.587
3.446
3.429
2.907
2.889
2.872
1.449
0.96
1.00
0.99
1.00
1.06
0.98
0.81
1.92
2.03
9.32
BocHN
3-64
^{1}H NMR
(400 MHz, $CDCl_3$)
f1 (ppm)

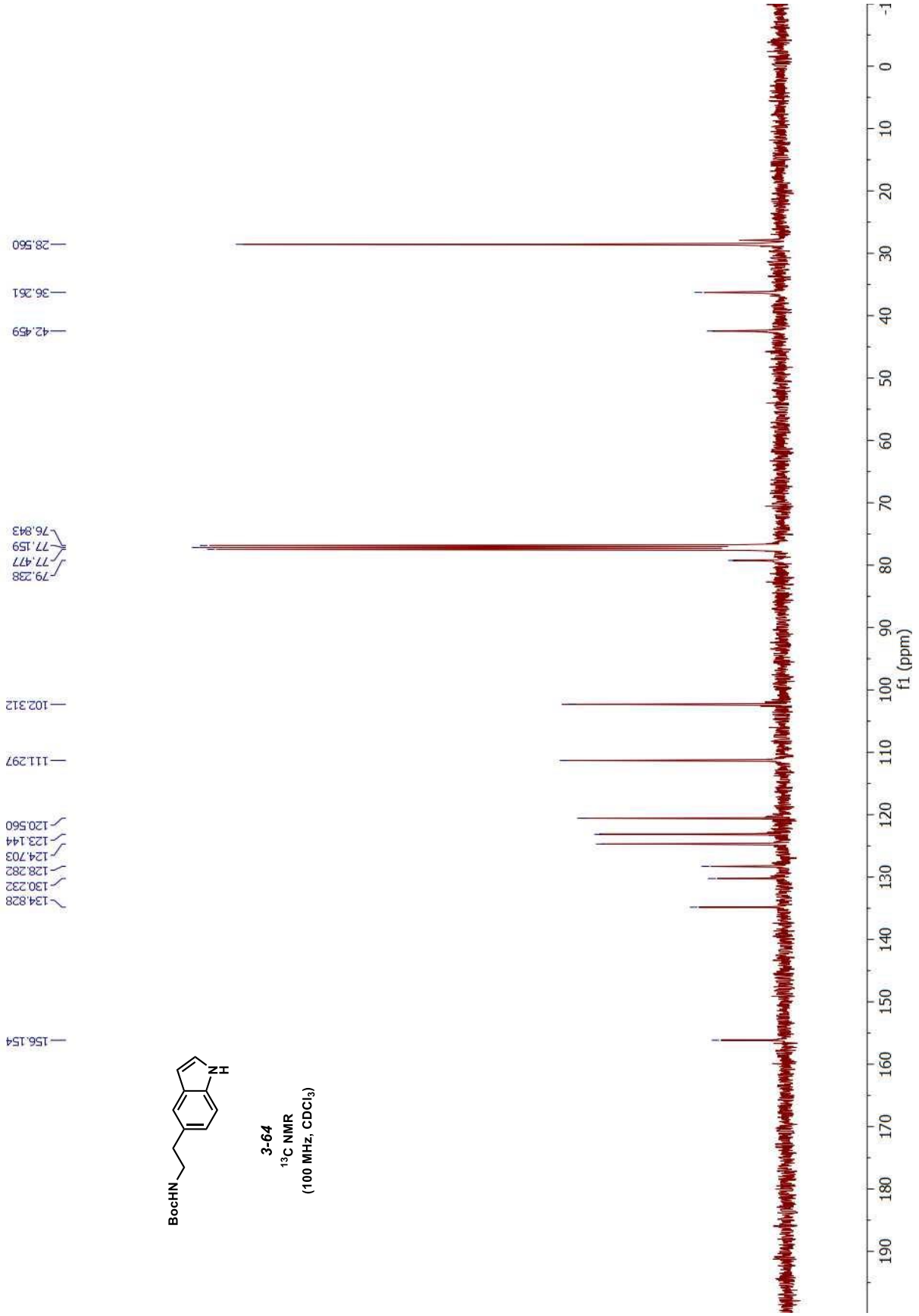
BocHN
3-64
13C NMR
(100 MHz, CDCl3)
156.154
134.828
130.232
128.282
124.703
123.144
120.560
111.297
102.312
79.238
77.477
77.159
76.843
42.459
36.261
28.560
f1 (ppm)

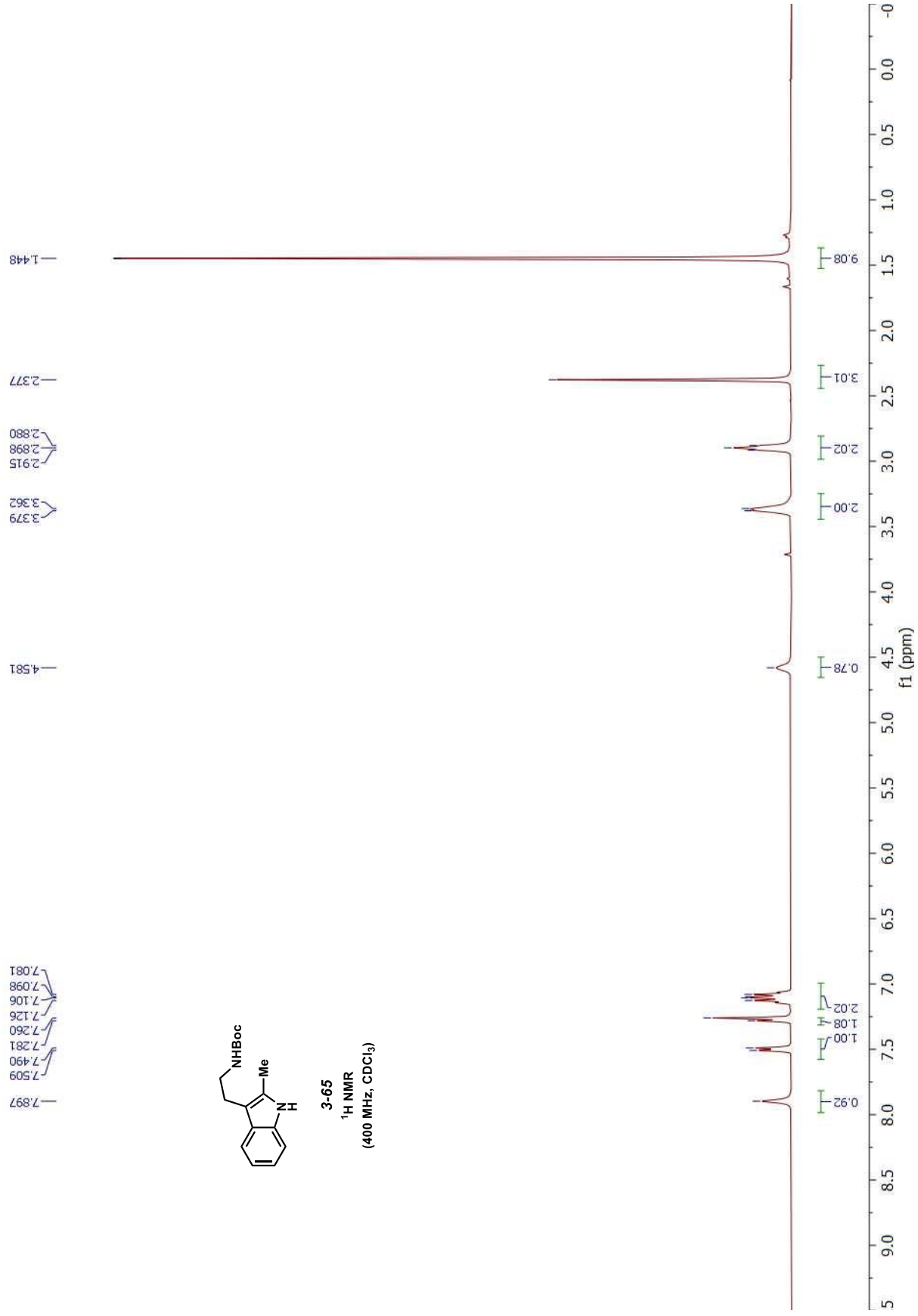
NHBoc
Me
N
H
3-65
1H NMR
(400 MHz, CDCl3)
7.897
7.509
7.490
7.281
7.260
7.126
7.106
7.098
7.081
4.581
3.379
3.362
2.915
2.898
2.880
2.377
1.448
0.92
1.00
1.08
2.02
0.78
2.00
2.02
3.01
9.08
f1 (ppm)

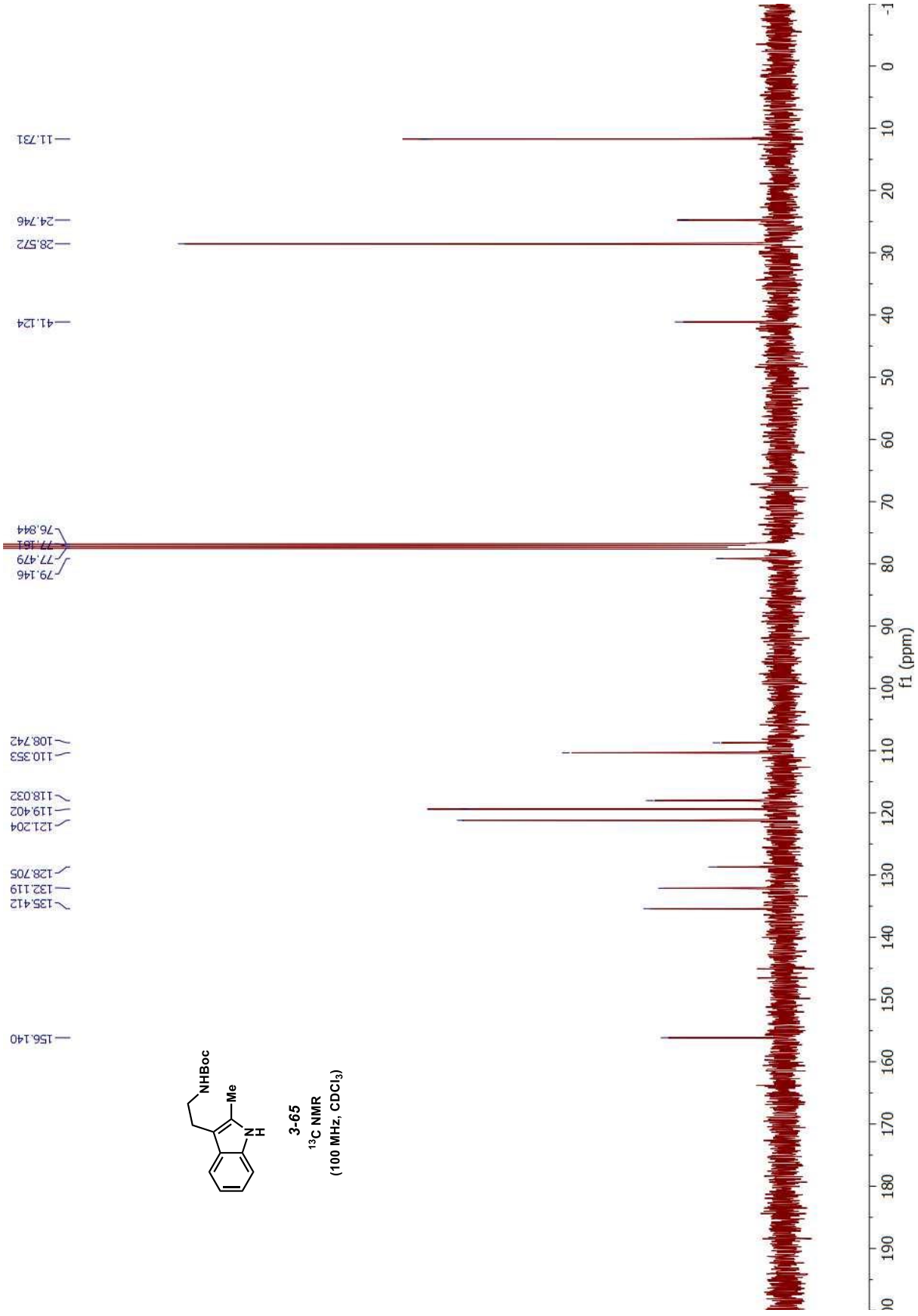
11.731
24.746
28.572
41.124
76.844
77.161
77.479
79.146
108.742
110.353
118.032
119.402
121.204
128.705
132.119
135.412
156.140
NHBoc
Me
N
H
3-65
13C NMR
(100 MHz, CDCl3)
f1 (ppm)

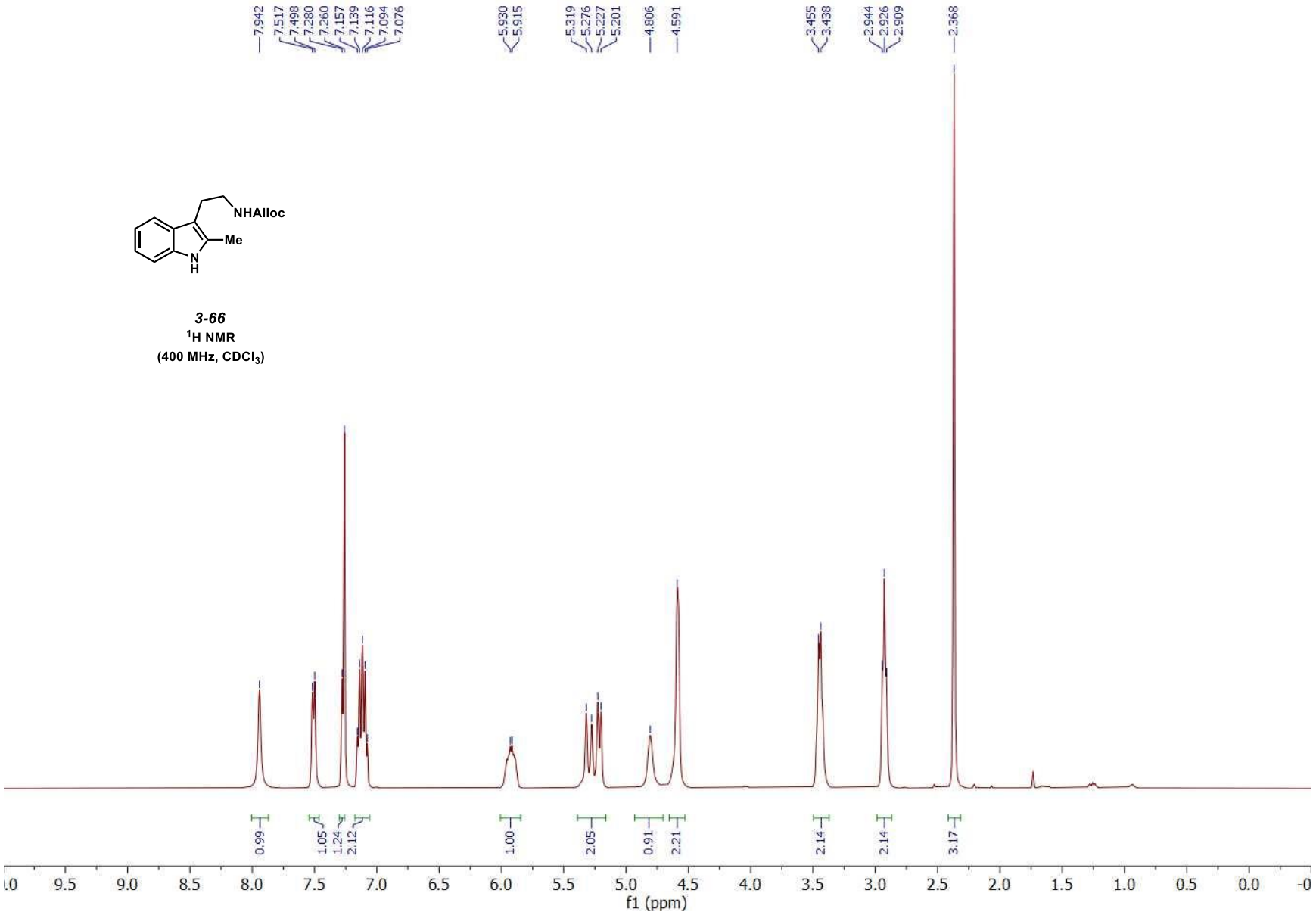

3-66

^{1}H NMR

(400 MHz, $CDCl_3$)

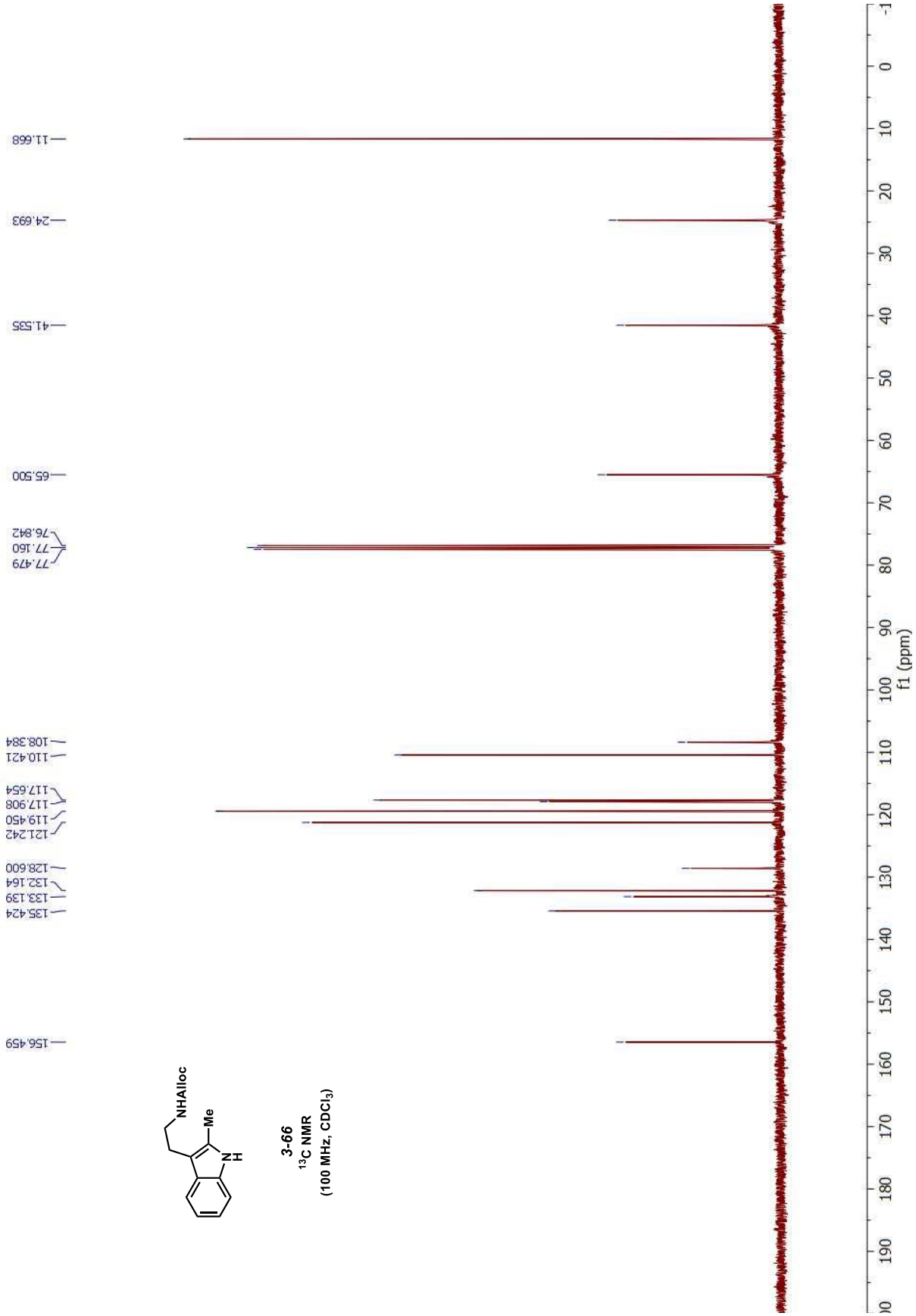
11.668
24.693
41.585
65.500
76.842
77.160
77.479
108.384
110.421
117.654
117.908
119.450
121.242
128.600
132.164
133.139
135.424
156.459
NHAlloc
Me
N
H
3-66
13C NMR
(100 MHz, CDCl3)
f1 (ppm)

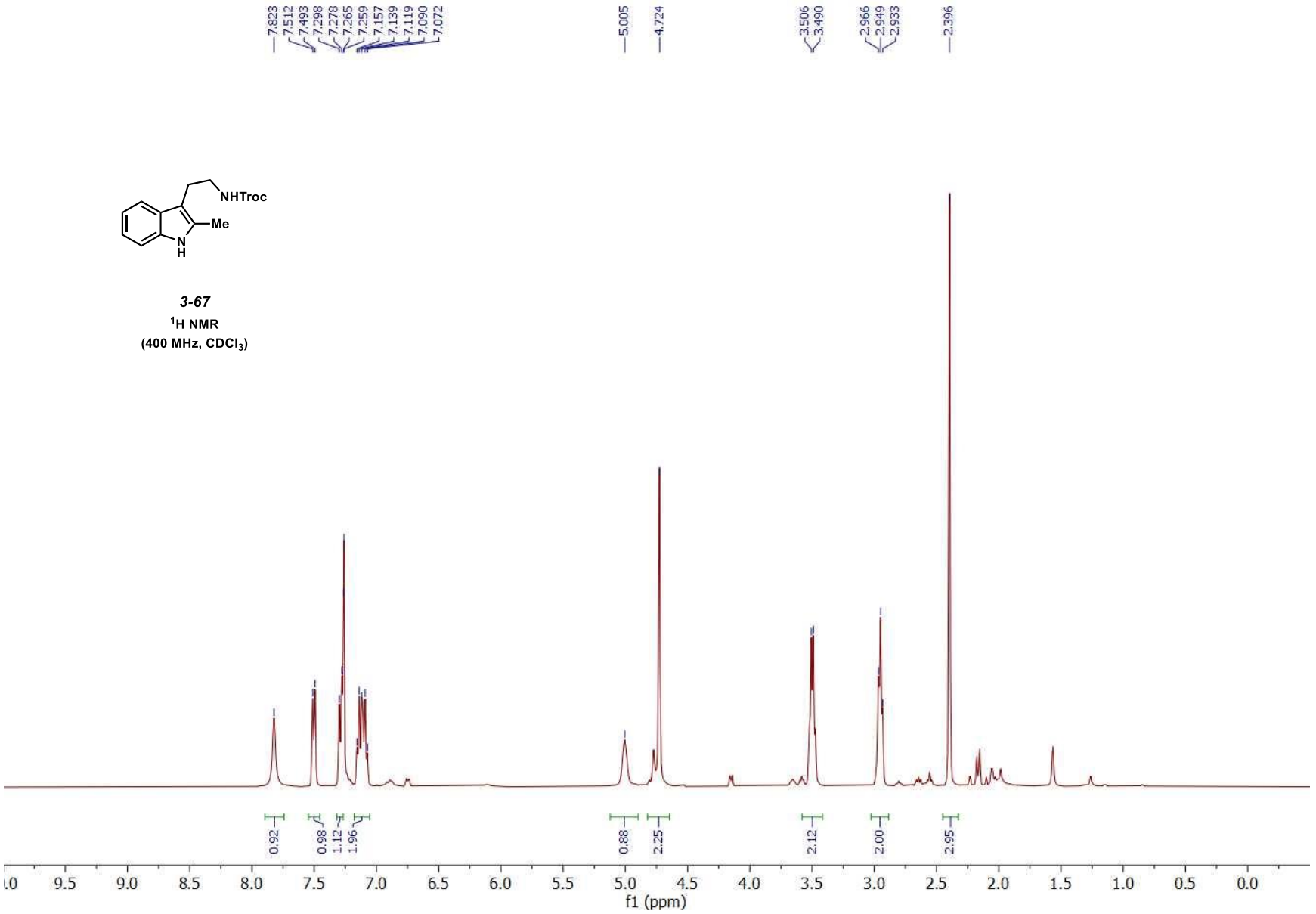
7.823
7.512
7.493
7.298
7.278
7.265
7.259
7.157
7.139
7.119
7.090
7.072
5.005
4.724
3.506
3.490
2.966
2.949
2.933
2.396
NHTroc
Me
N
H
3-67
1H NMR
(400 MHz, CDCl3)
0.92
0.98
1.12
1.96
0.88
2.25
2.12
2.00
2.95
f1 (ppm)

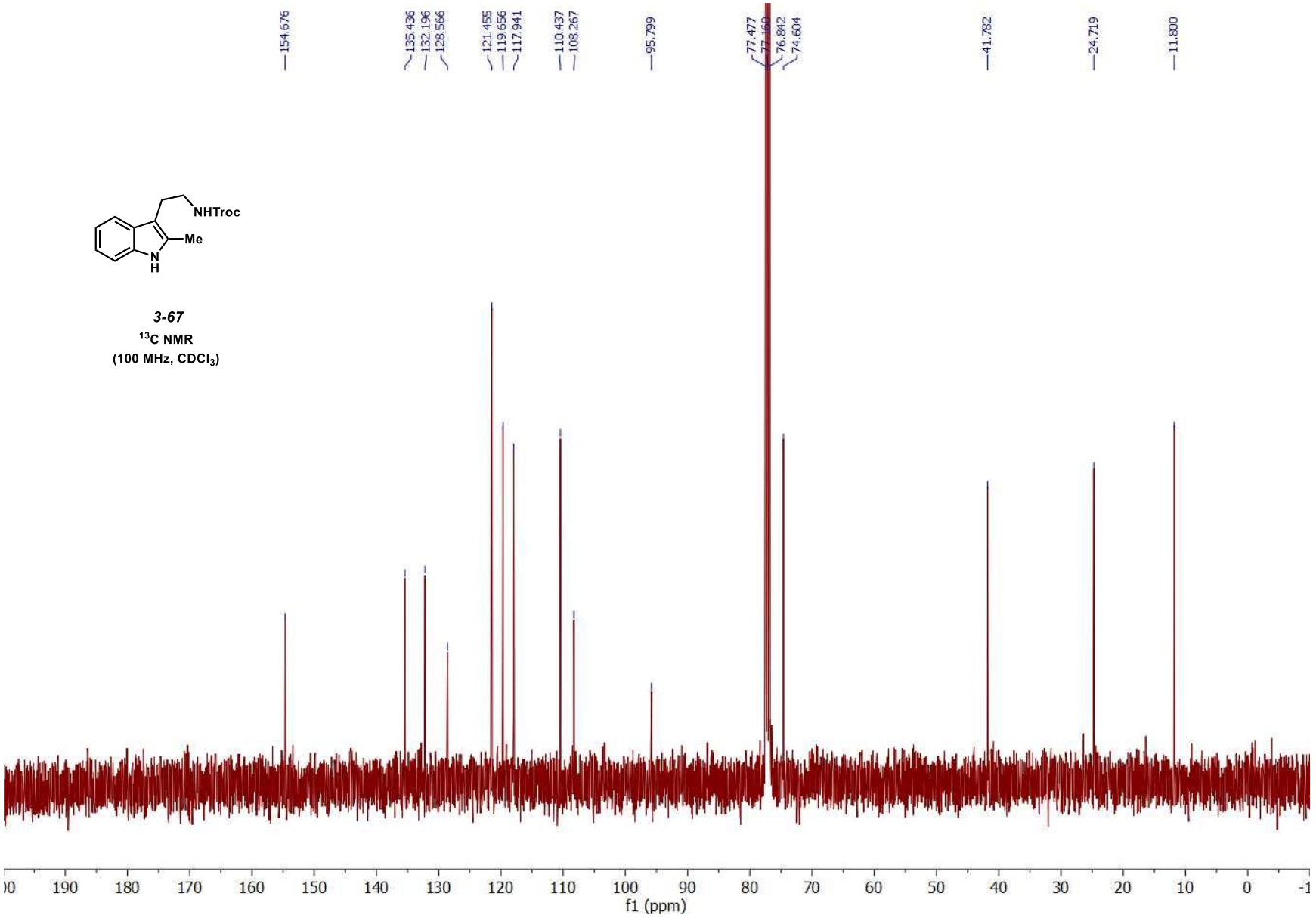
154.676
135.436
132.196
128.566
121.455
119.656
117.941
110.437
108.267
95.799
77.477
77.160
76.842
74.604
41.782
24.719
11.800
NHTroc
Me
N
H
3-67
13C NMR
(100 MHz, CDCl3)
f1 (ppm)

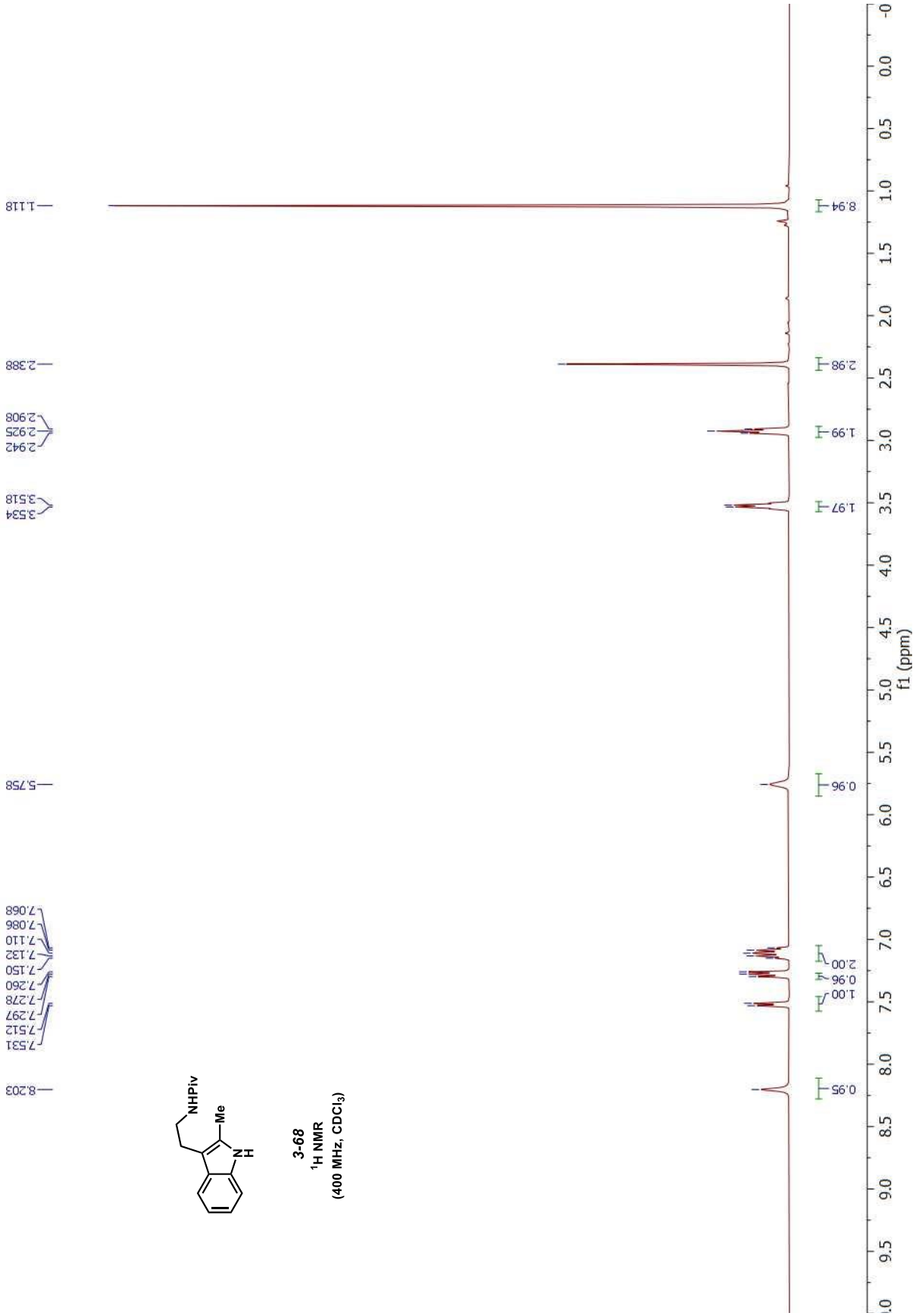
1.118
2.388
2.908
2.925
2.942
3.518
3.534
5.758
7.068
7.086
7.110
7.132
7.150
7.260
7.278
7.297
7.512
7.531
8.203
8.94
2.98
1.99
1.97
0.96
2.00
0.96
1.00
0.95
NHPiv
Me
N
H
3-68
1H NMR
(400 MHz, CDCl3)
f1 (ppm)

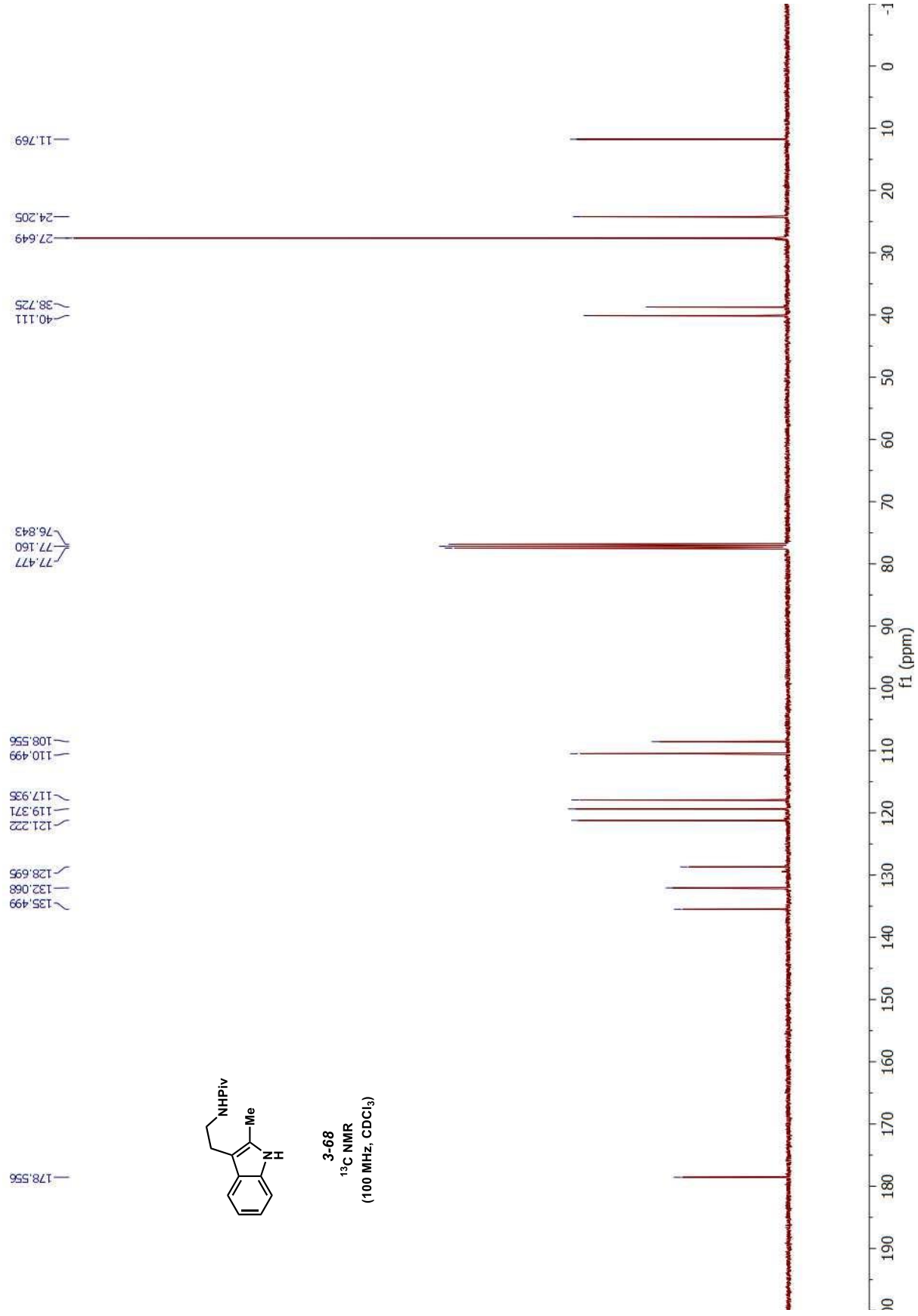
11.769
24.205
27.649
38.725
40.111
76.843
77.160
77.477
108.556
110.499
117.935
119.371
121.222
128.695
132.068
135.499
178.556
NHPiv
Me
N
H
3-68
13C NMR
(100 MHz, CDCl3)
f1 (ppm)

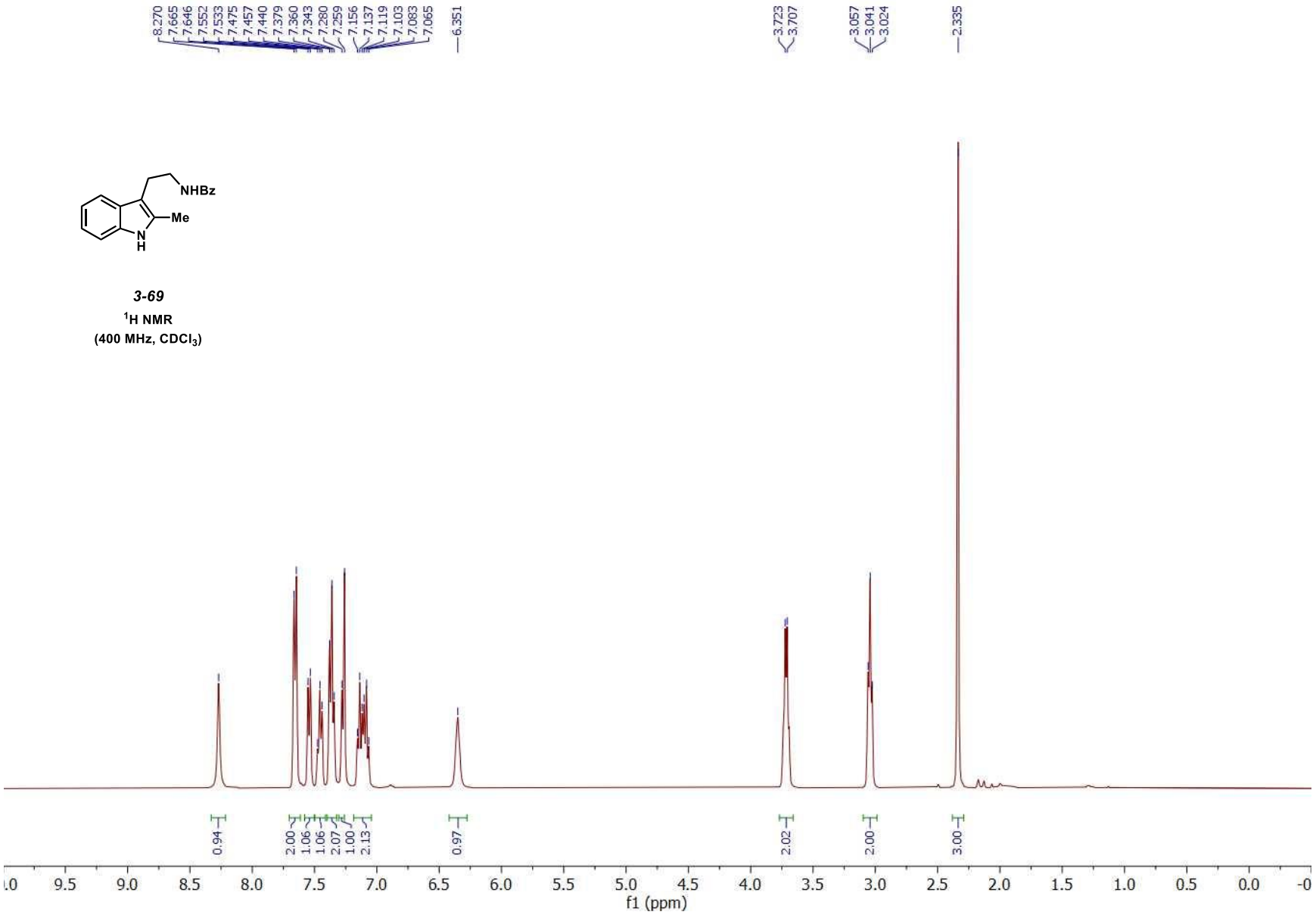

3-69

^{1}H NMR

(400 MHz, $CDCl_3$)

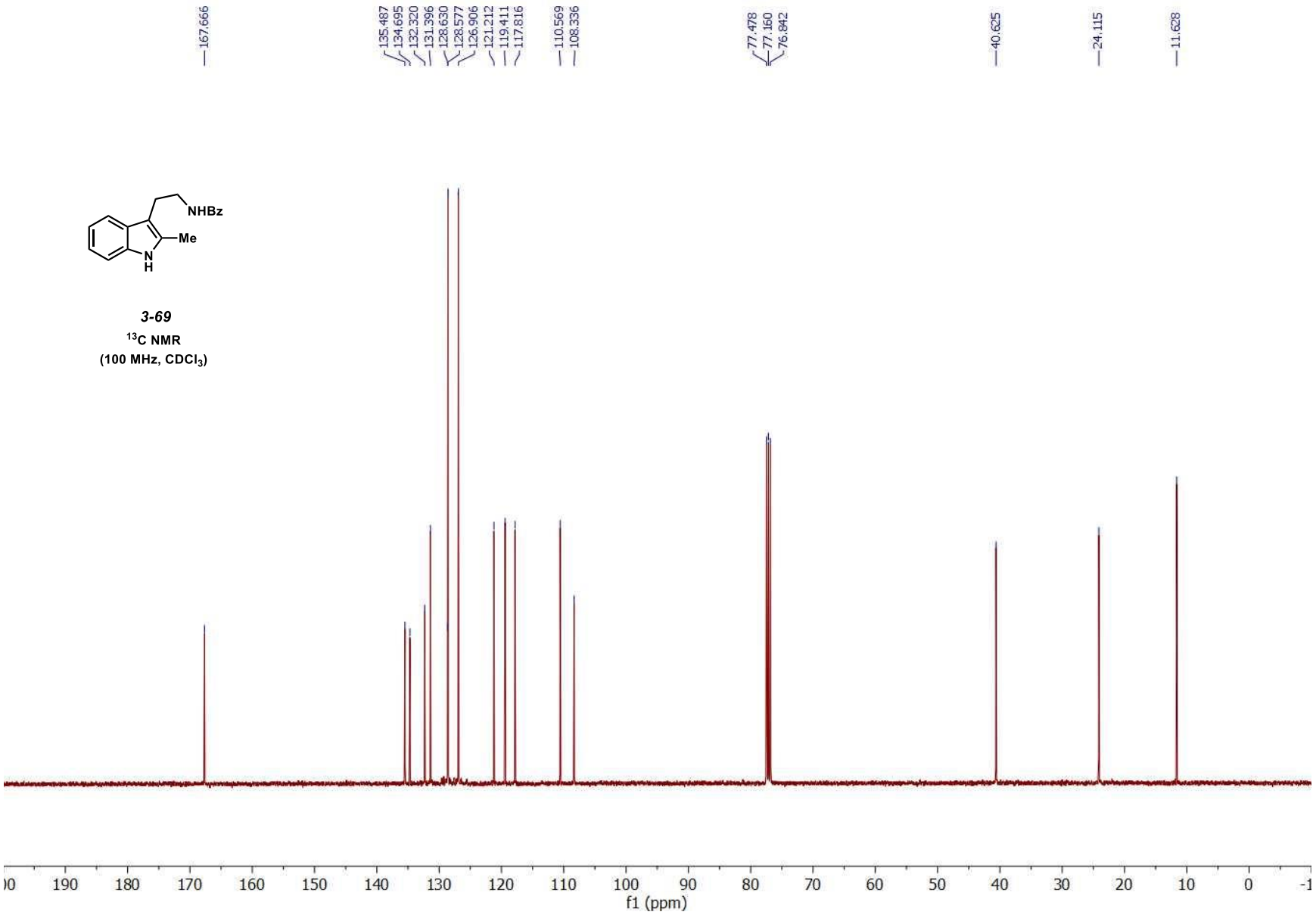
167.666
135.487
134.695
132.320
131.396
128.630
128.577
126.906
121.212
119.411
117.816
110.569
108.336
77.478
77.160
76.842
40.625
24.115
11.628
NHBz
Me
N
H
3-69
13C NMR
(100 MHz, CDCl3)
f1 (ppm)

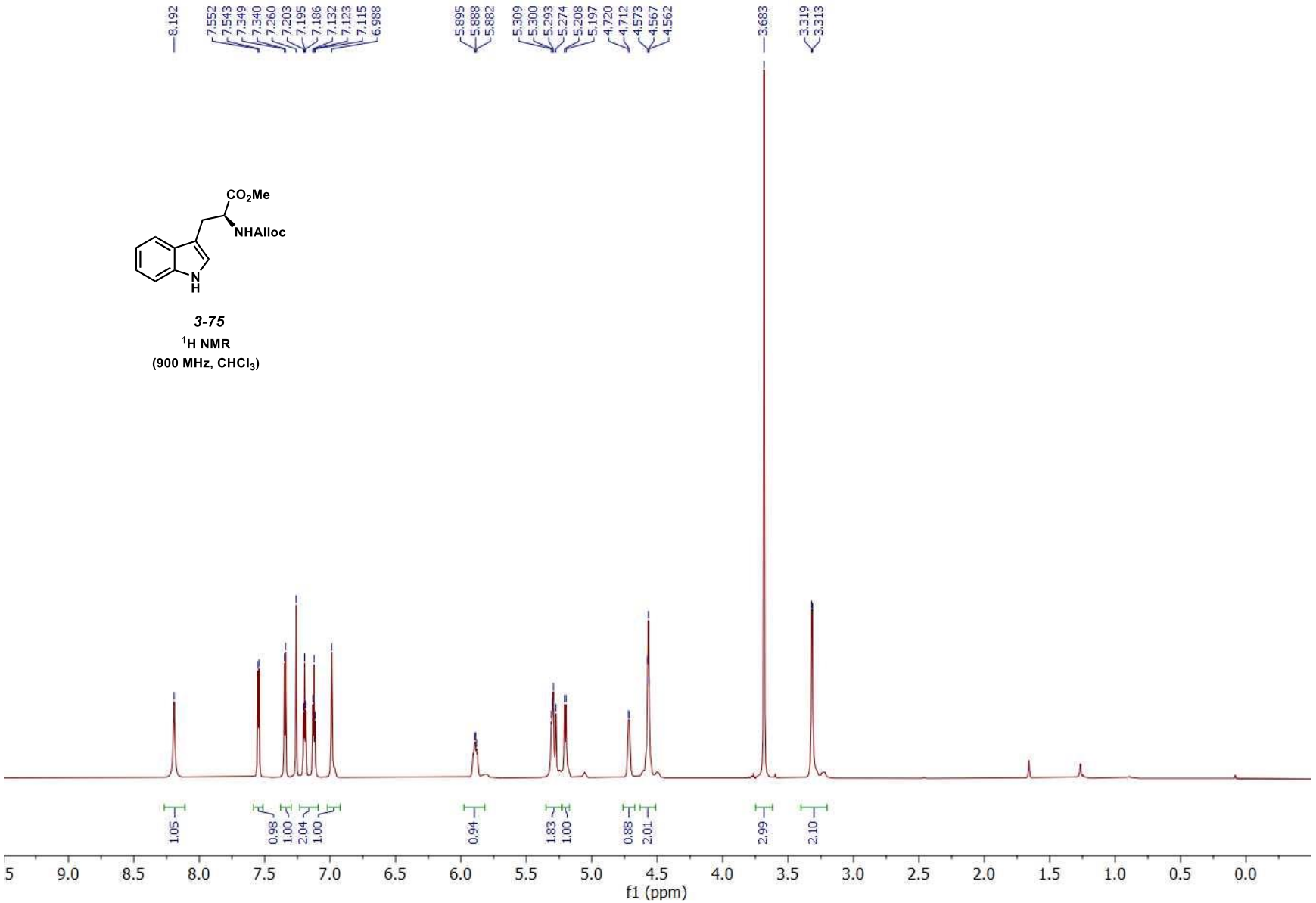
8.192
7.552
7.543
7.349
7.340
7.260
7.203
7.195
7.186
7.132
7.123
7.115
6.988
5.895
5.888
5.882
5.309
5.300
5.293
5.274
5.208
5.197
4.720
4.712
4.573
4.567
4.562
3.683
3.319
3.313
CO2Me
NHAlloc
N
H
3-75
1H NMR
(900 MHz, CHCl3)
1.05
0.98
1.00
2.04
1.00
0.94
1.83
1.00
0.88
2.01
2.99
2.10
f1 (ppm)

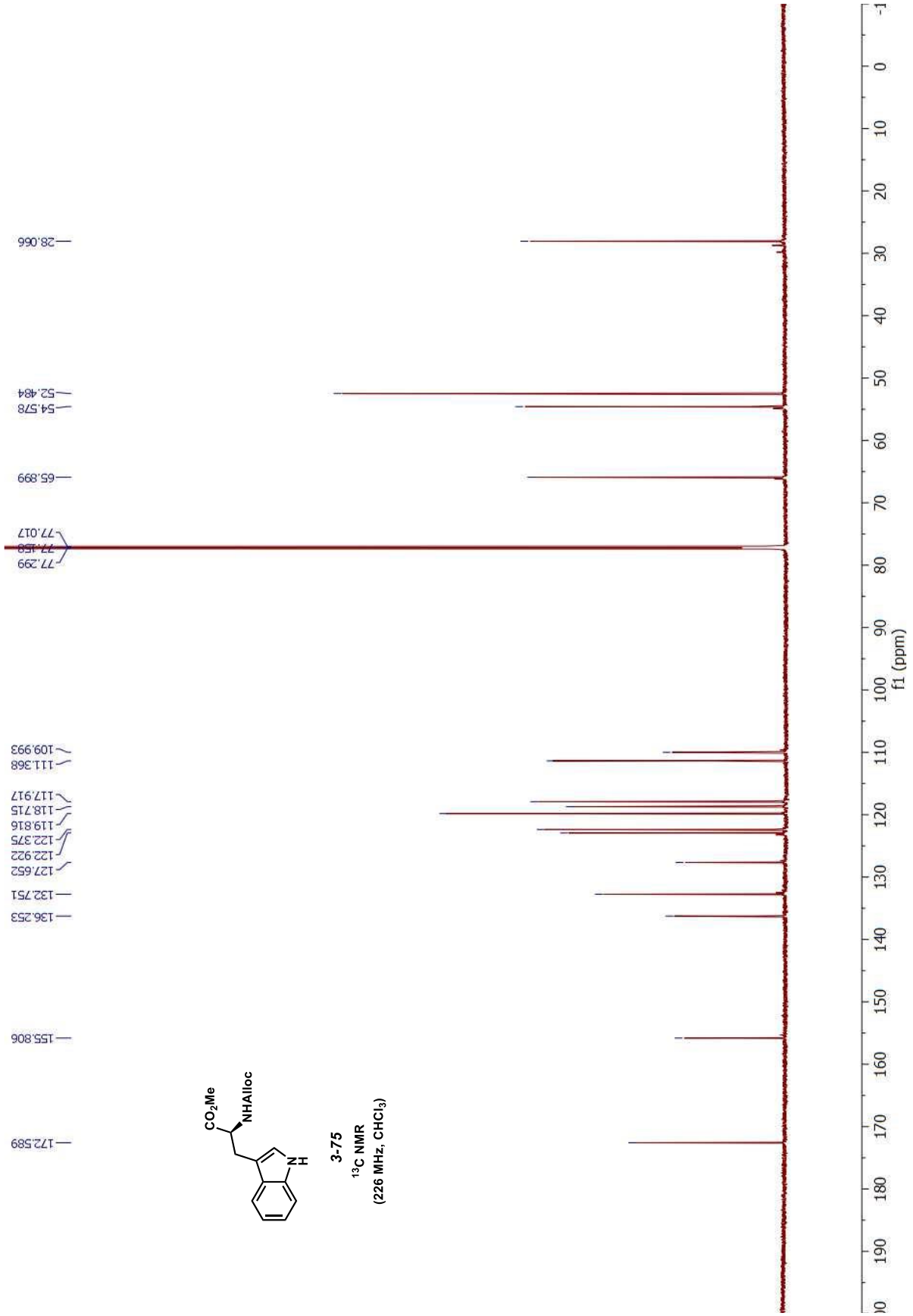
28.066
52.484
54.578
65.899
77.017
77.458
77.299
109.993
111.368
117.917
118.715
119.816
122.375
122.922
127.652
132.751
136.253
155.806
172.589
CO2Me
NHAlloc
H
N
3-75
13C NMR
(226 MHz, CHCl3)
f1 (ppm)

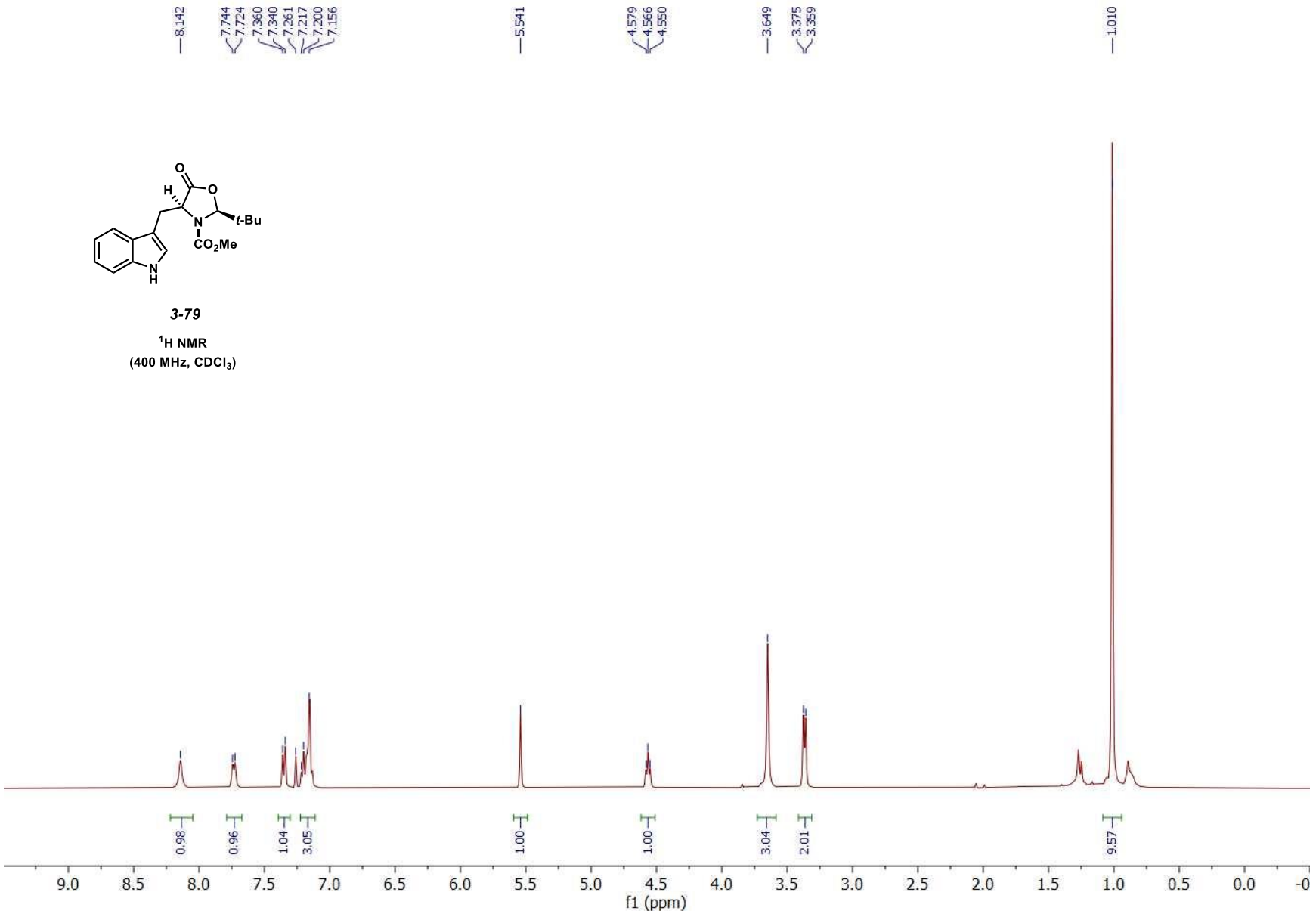

3-79

^{1}H NMR
(400 MHz, $CDCl_3$)

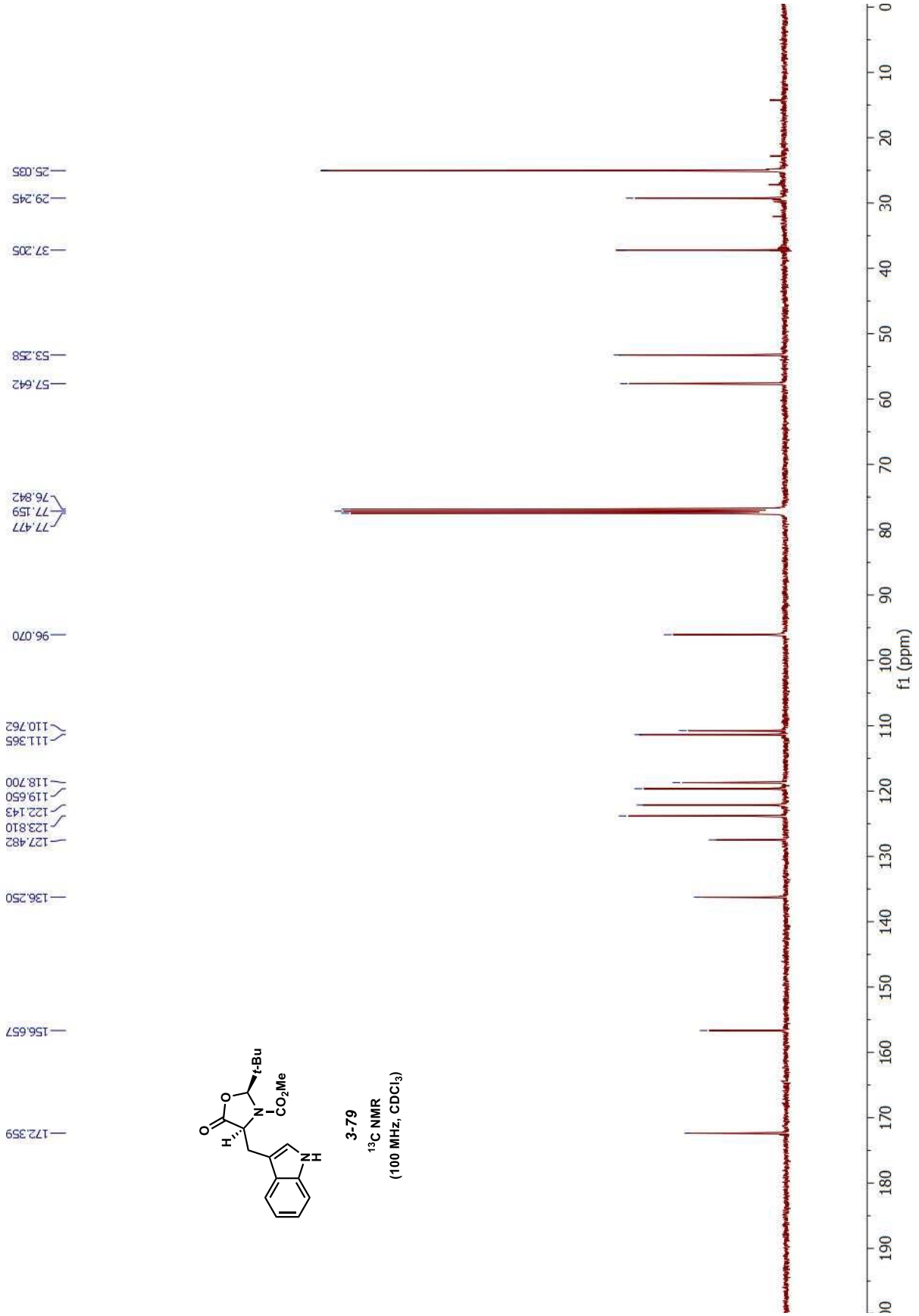
25.035
29.245
37.205
53.258
57.642
76.842
77.159
77.477
96.070
110.762
111.365
118.700
119.650
122.143
123.810
127.482
136.250
156.657
172.359
f1 (ppm)
3-79
13C NMR
(100 MHz, CDCl3)
t-Bu
CO2Me

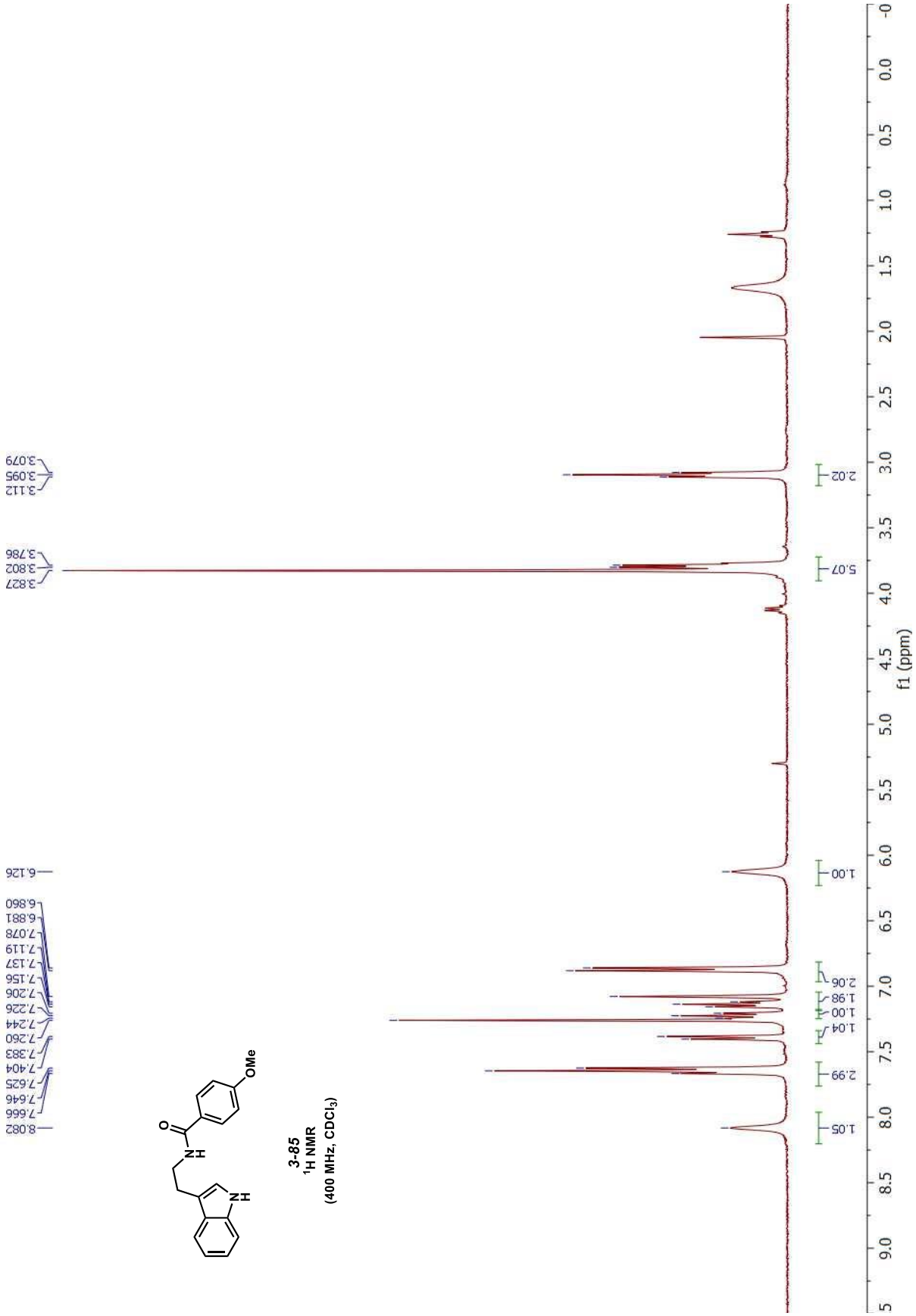
3-85
1H NMR
(400 MHz, CDCl3)
OMe
f1 (ppm)

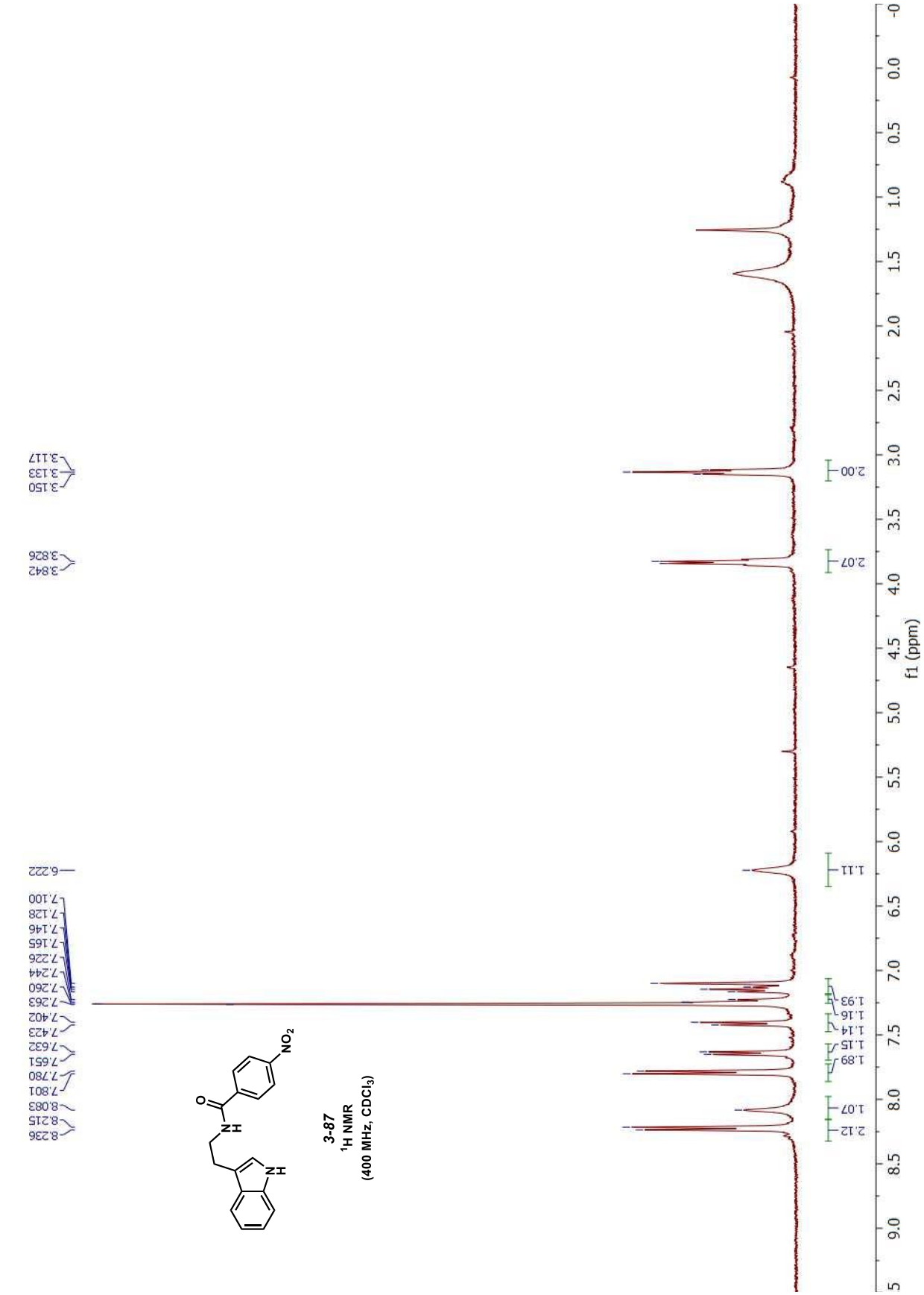
3-87
^{1}H NMR
(400 MHz, $CDCl_3$)
NO_2
f1 (ppm)

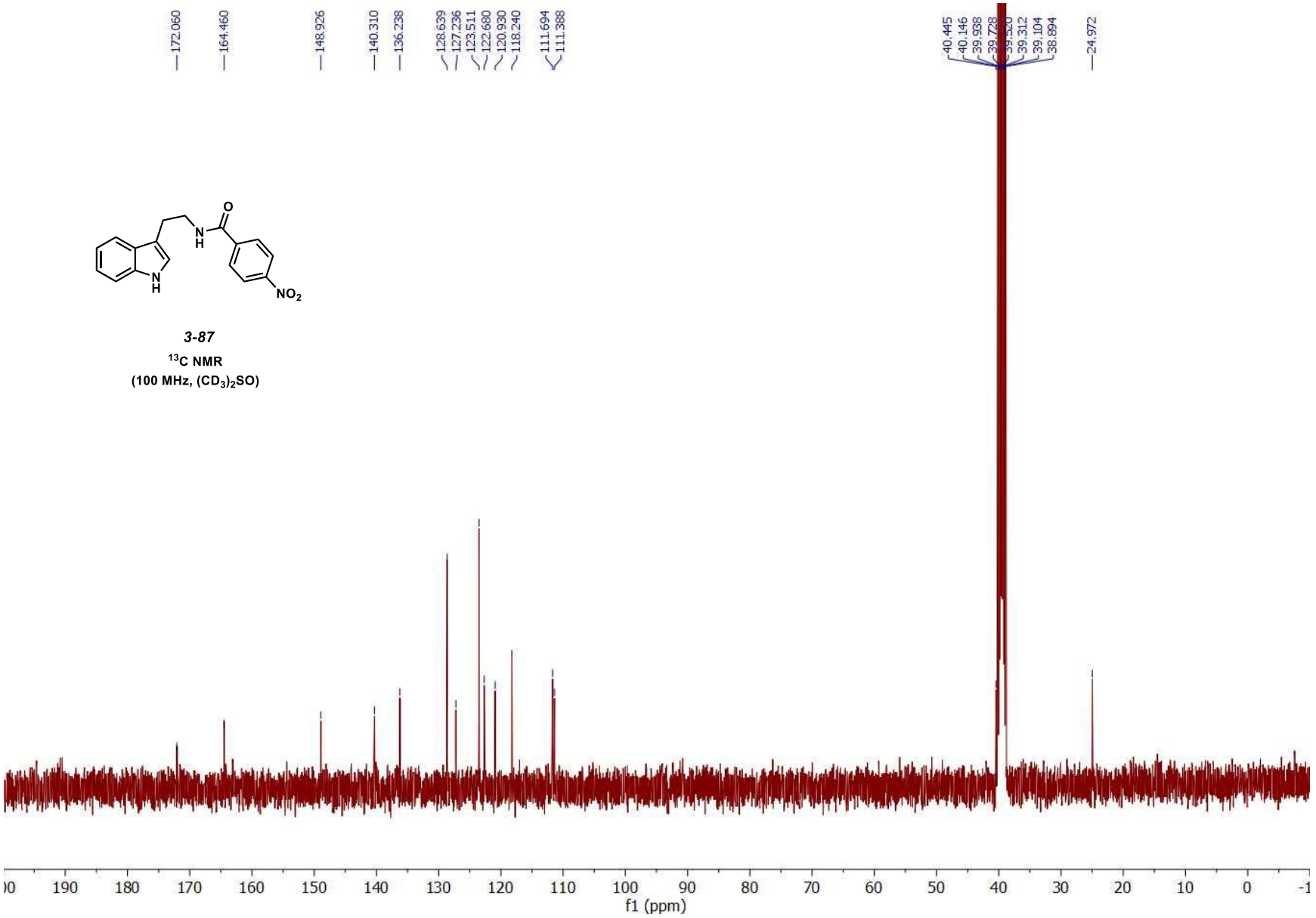
172.060
164.460
148.926
140.310
136.238
128.639
127.236
123.511
122.680
120.930
118.240
111.694
111.388
40.445
40.146
39.938
39.728
39.520
39.312
39.104
38.894
24.972
O
N
H
N
H
NO2
3-87
13C NMR
(100 MHz, (CD3)2SO)
f1 (ppm)

APPENDIX C

NMR SPECTRA RELEVANT TO CHAPTER 4

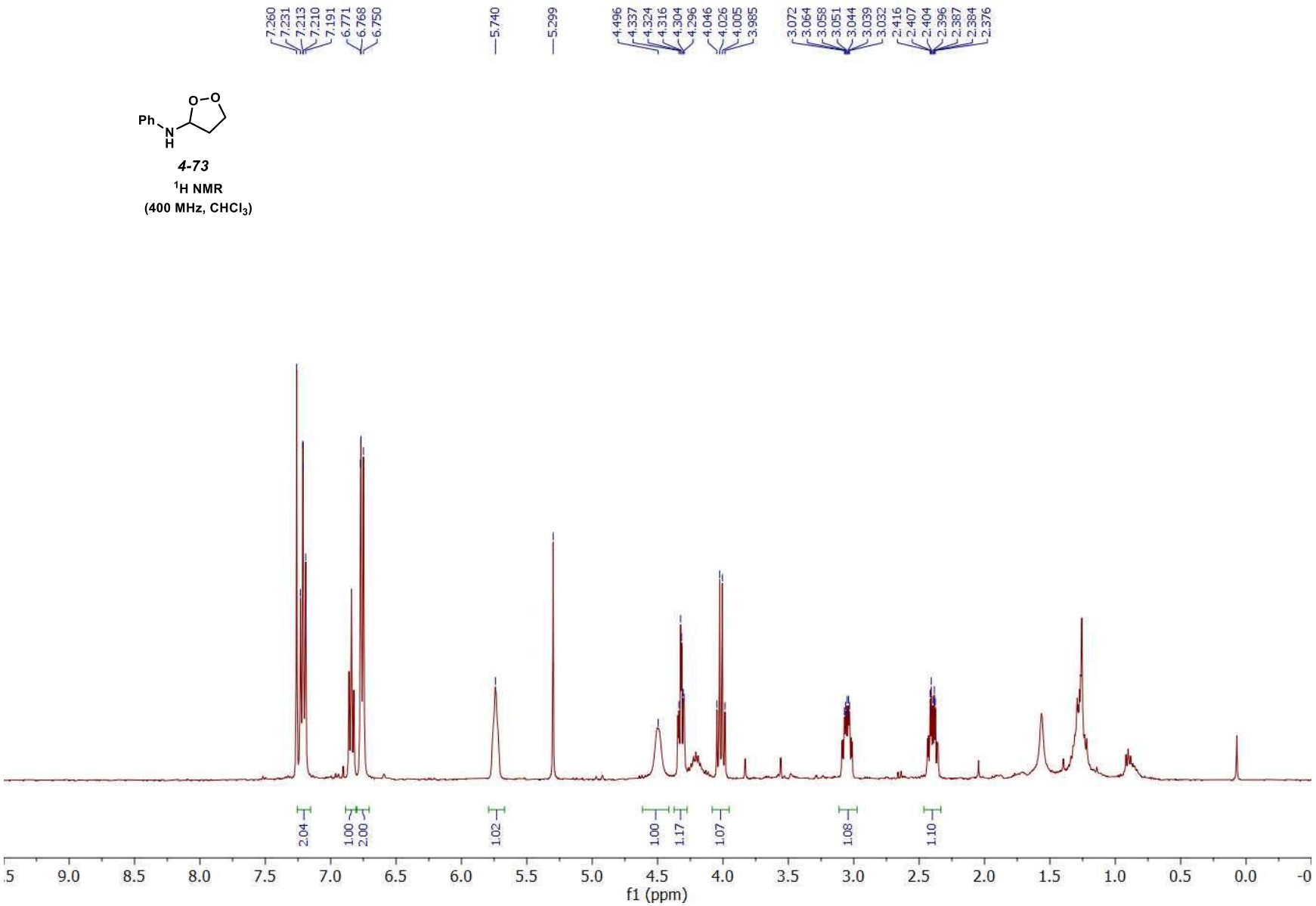
7.260
7.231
7.213
7.210
7.191
6.771
6.768
6.750
5.740
5.299
4.496
4.337
4.324
4.316
4.304
4.296
4.046
4.026
4.005
3.985
3.072
3.064
3.058
3.051
3.044
3.039
3.032
2.416
2.407
2.404
2.396
2.387
2.384
2.376
Ph
N
H
O
O
4-73
1H NMR
(400 MHz, CHCl3)
2.04
1.00
2.00
1.02
1.00
1.17
1.07
1.08
1.10
f1 (ppm)

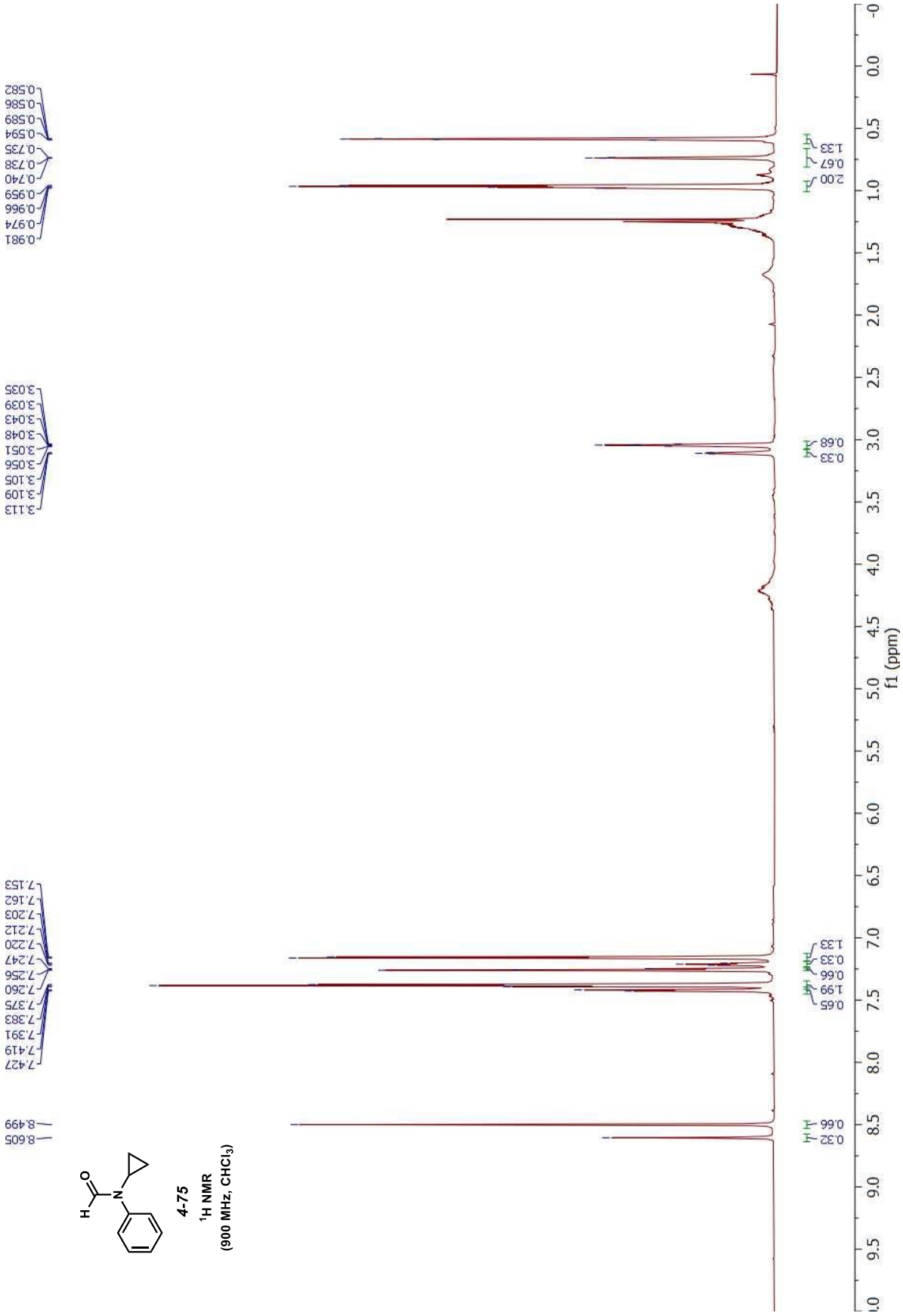
4-75
^{1}H NMR
(900 MHz, $CHCl_3$)
f1 (ppm)

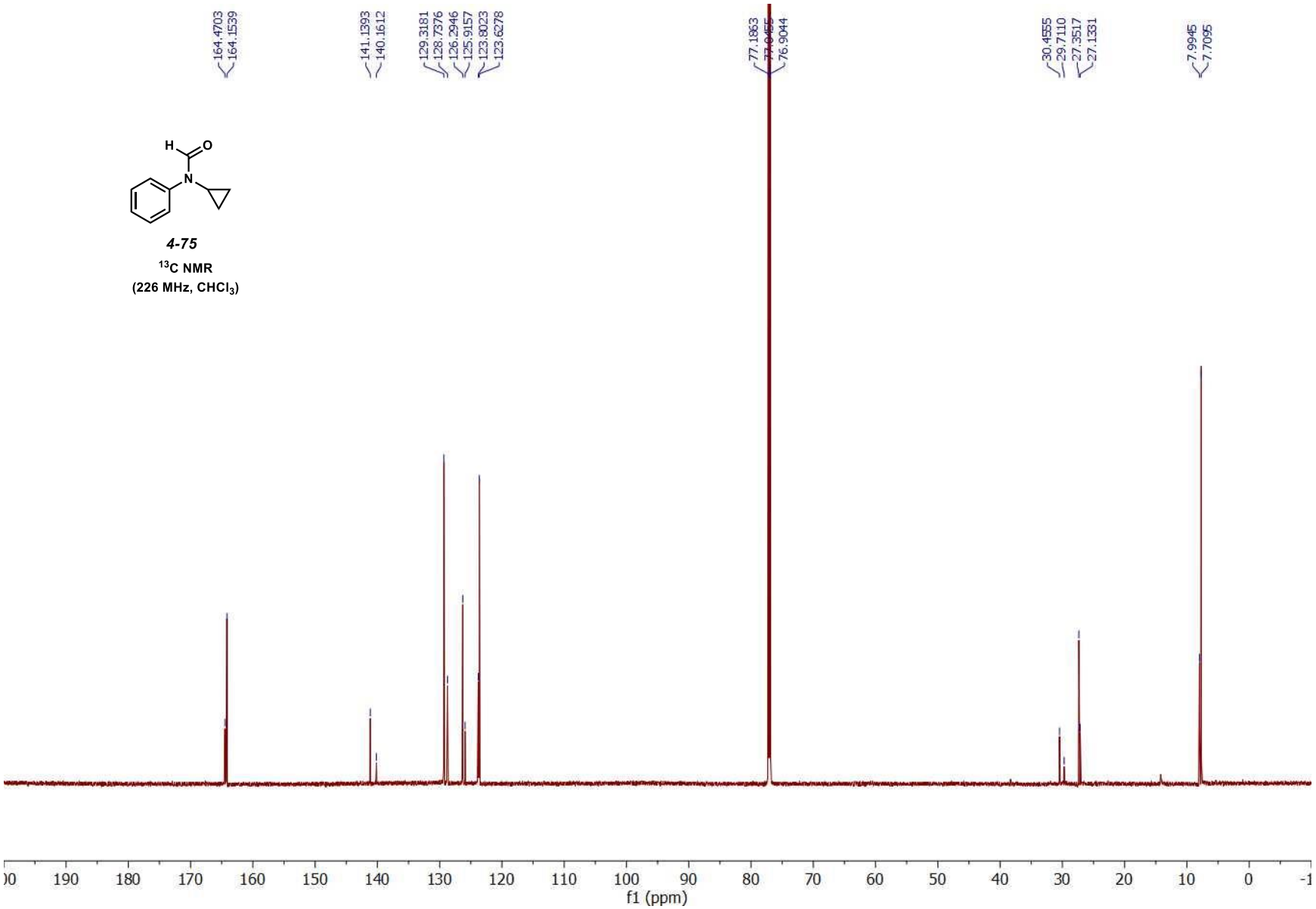
164.4703
164.1539
141.1393
140.1612
129.3181
128.7376
126.2946
125.9157
123.8023
123.6278
77.1863
76.9044
30.4555
29.7110
27.3517
27.1331
7.9945
7.7095
H
O
N
4-75
13C NMR
(226 MHz, CHCl3)
f1 (ppm)

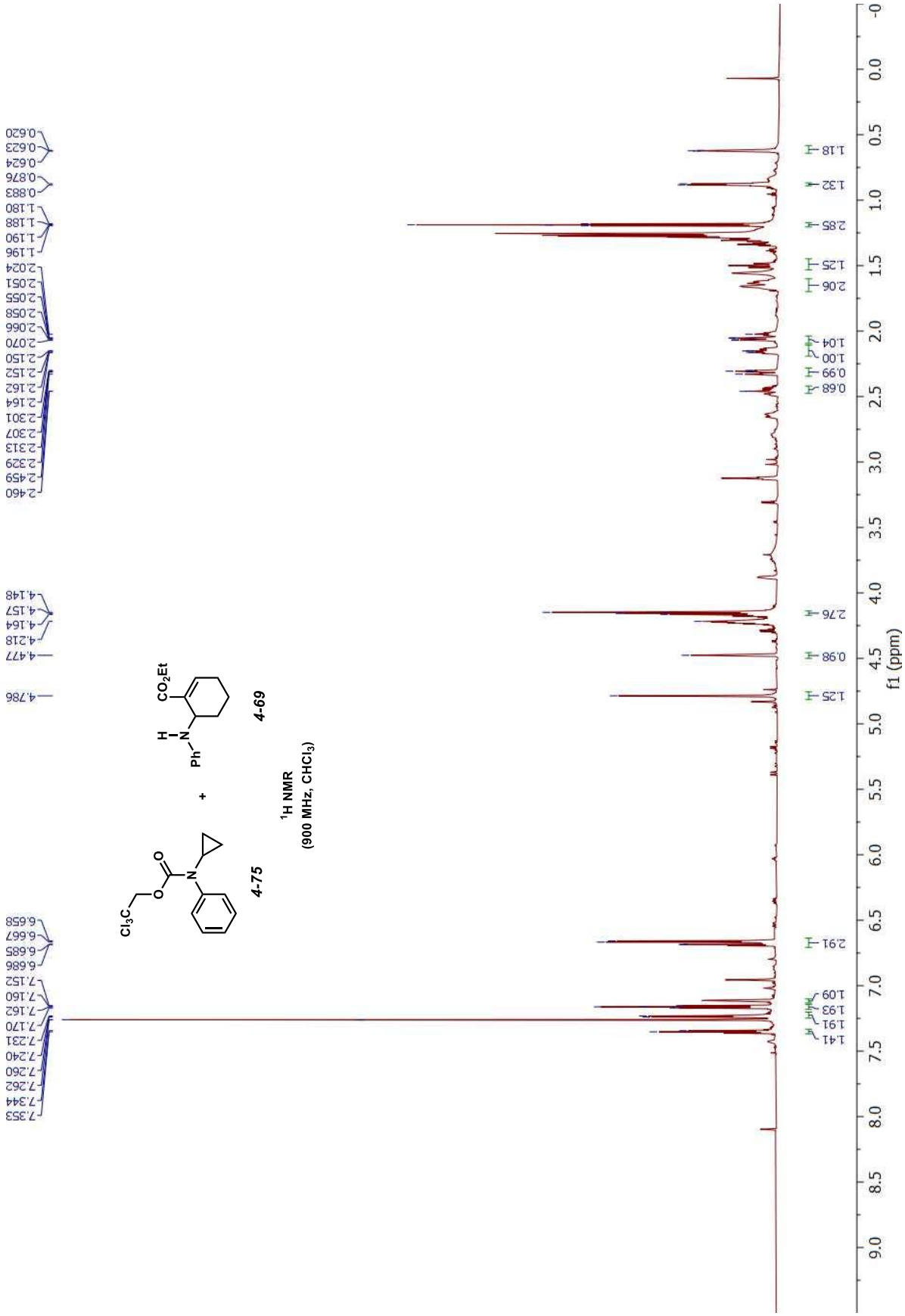
4-69
4-75
^{1}H NMR
(900 MHz, CHCl$_3$)
f1 (ppm)

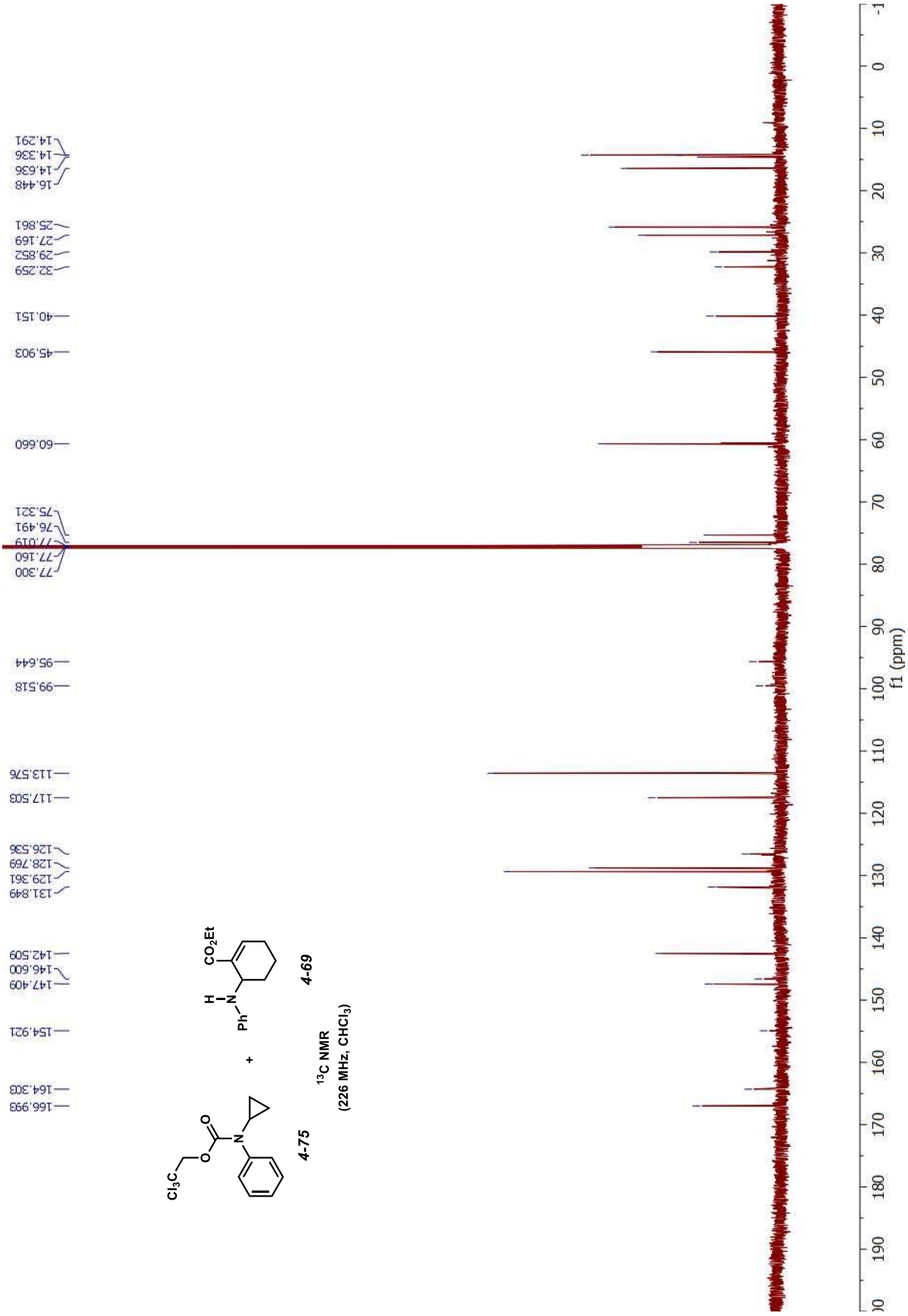
14.291
14.336
14.636
16.448
25.861
27.169
29.852
32.259
40.151
45.903
60.660
75.321
76.491
77.019
77.160
77.300
95.644
99.518
113.576
117.503
126.536
128.769
129.361
131.849
142.509
146.600
147.409
154.921
164.303
166.993
f1 (ppm)
4-69
4-75
+
^{13}C NMR
(226 MHz, CHCl$_3$)

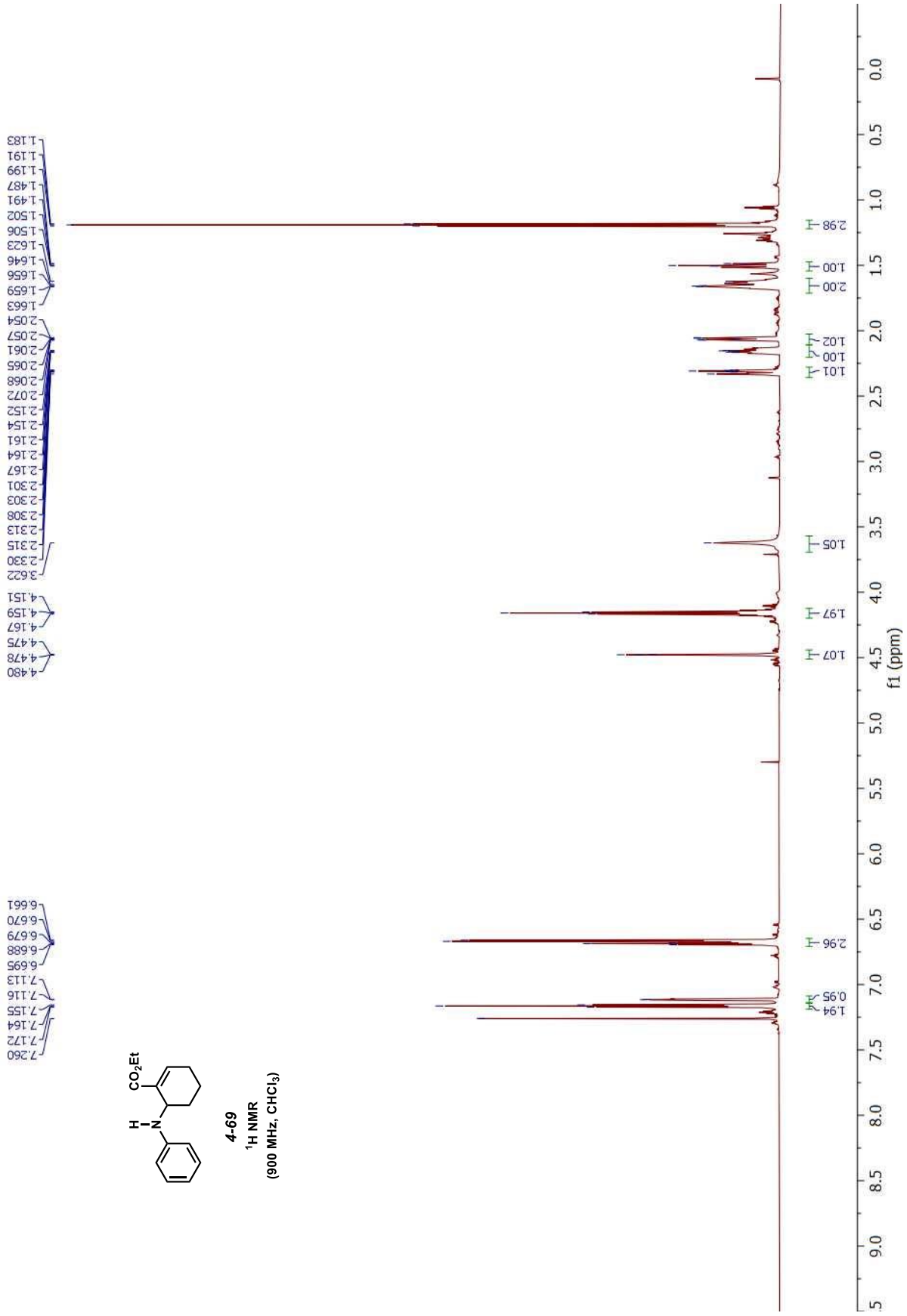
CO2Et
H
N
4-69
1H NMR
(900 MHz, CHCl3)
f1 (ppm)

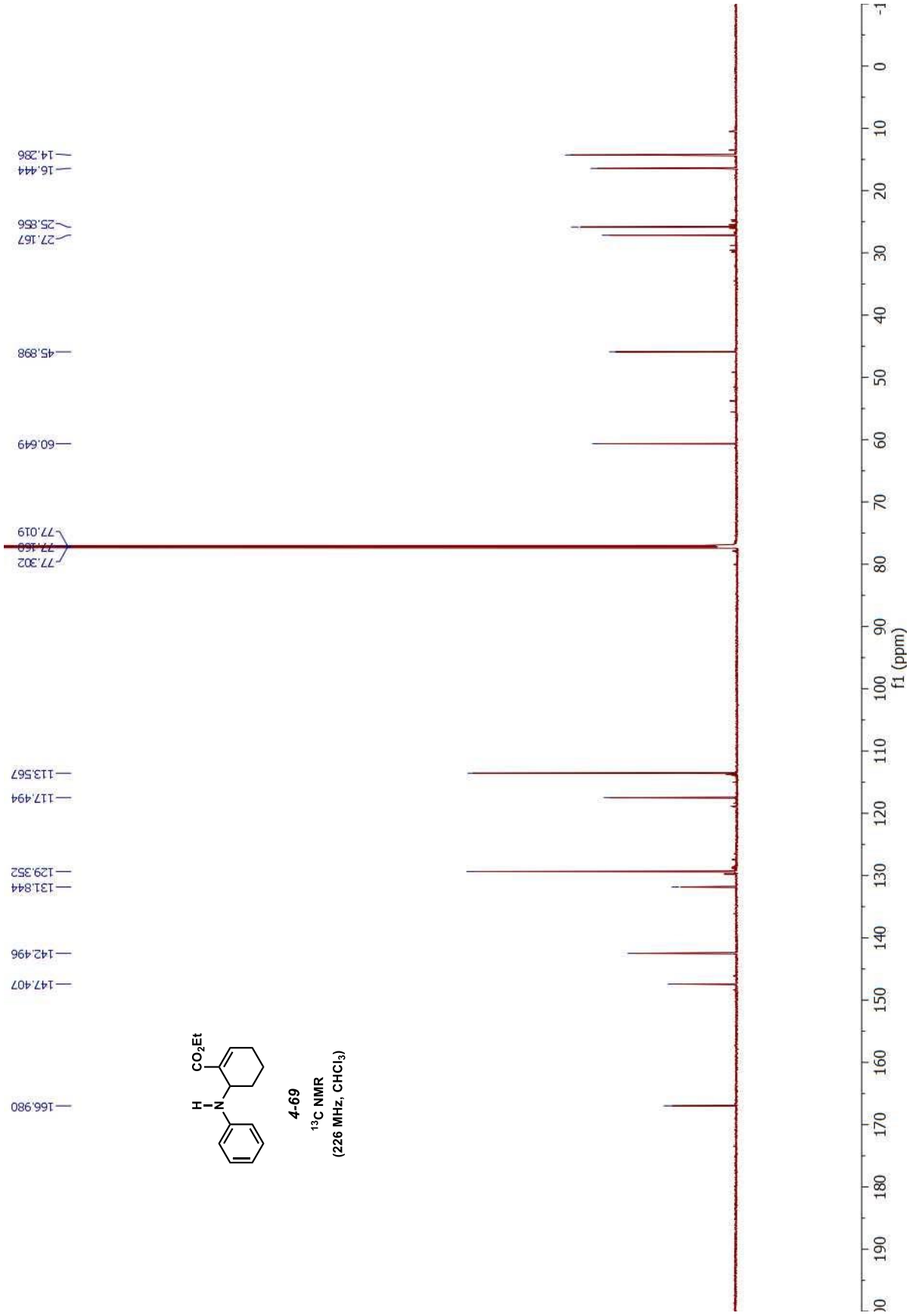
14.286
16.444
25.856
27.167
45.898
60.649
77.019
77.169
77.302
113.567
117.494
129.352
131.844
142.496
147.407
166.980
CO2Et
H
N
4-69
13C NMR
(226 MHz, CHCl3)
f1 (ppm)

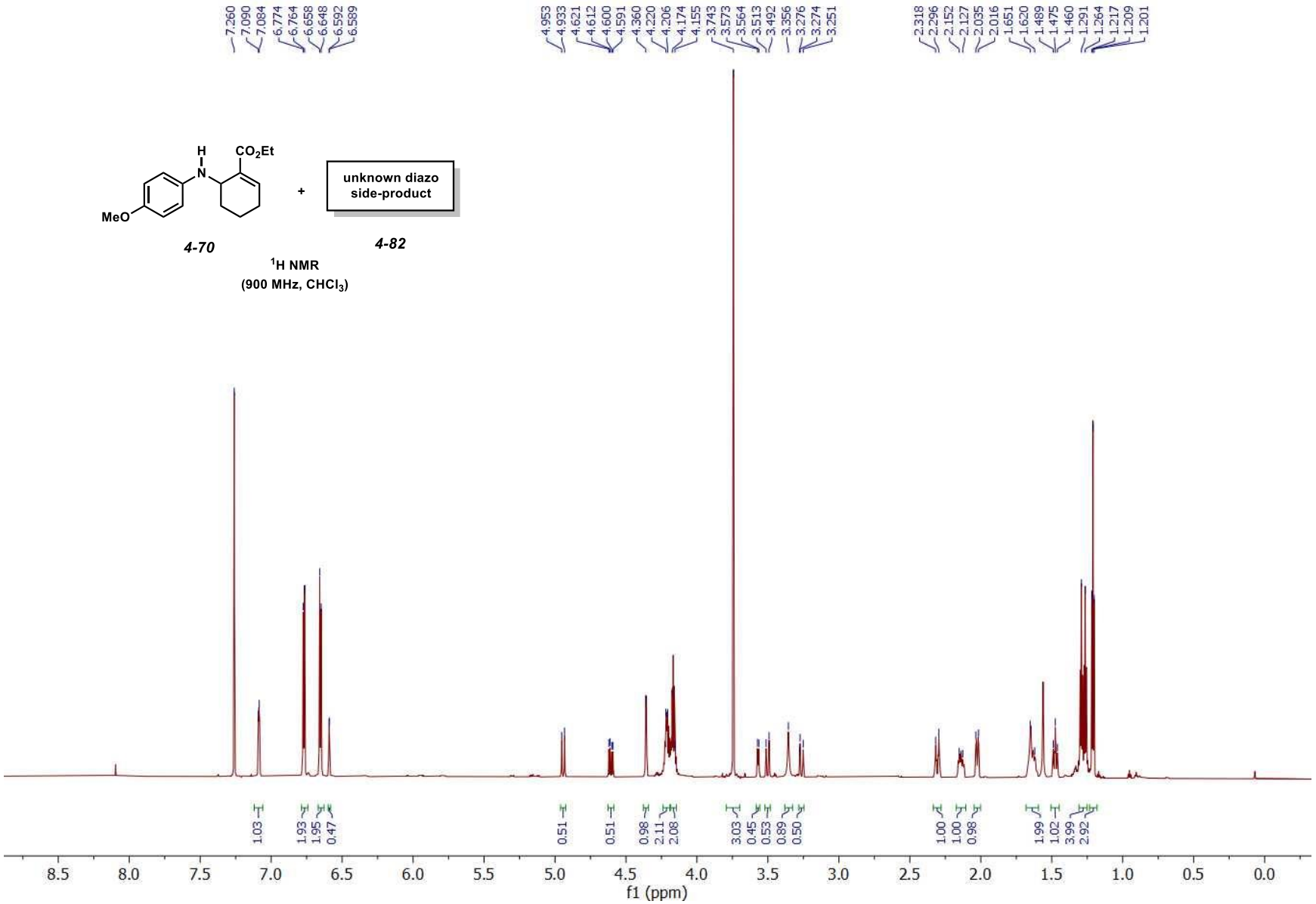
7.260
7.090
7.084
6.774
6.764
6.658
6.648
6.592
6.589
4.953
4.933
4.621
4.612
4.600
4.591
4.360
4.220
4.206
4.174
4.155
3.743
3.573
3.564
3.513
3.492
3.356
3.276
3.274
3.251
2.318
2.296
2.152
2.127
2.035
2.016
1.651
1.620
1.489
1.475
1.460
1.291
1.264
1.217
1.209
1.201
H
N
CO2Et
MeO
+
unknown diazo side-product
4-70
4-82
1H NMR
(900 MHz, CHCl3)
1.03
1.93
1.95
0.47
0.51
0.51
0.98
2.11
2.08
3.03
0.45
0.53
0.89
0.50
1.00
1.00
0.98
1.99
1.02
3.99
2.92
8.5
8.0
7.5
7.0
6.5
6.0
5.5
5.0
4.5
4.0
3.5
3.0
2.5
2.0
1.5
1.0
0.5
0.0
f1 (ppm)

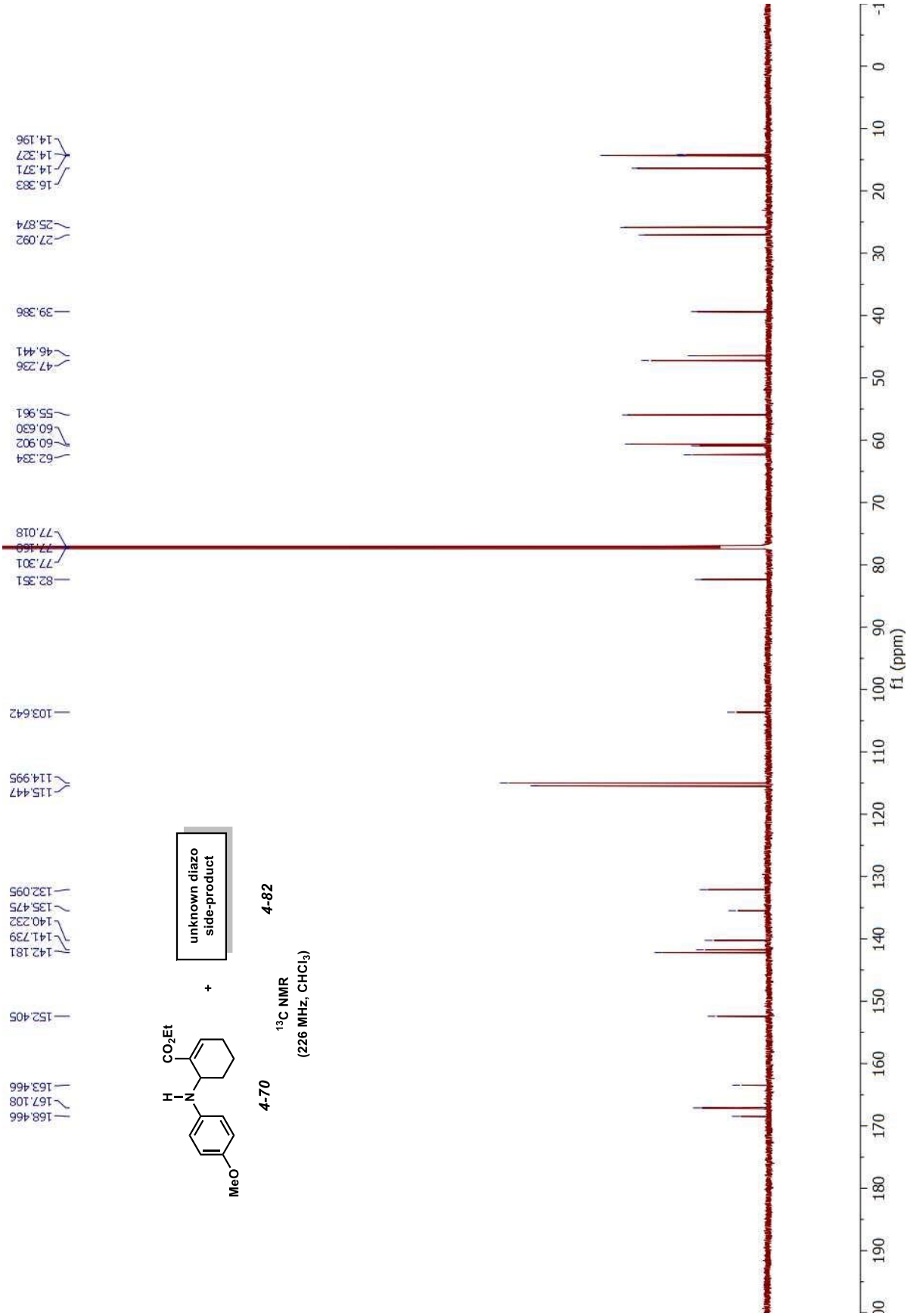
14.196
14.327
14.371
16.383
25.874
27.092
39.386
46.441
47.236
55.961
60.630
60.902
62.334
77.018
77.159
77.301
82.351
103.642
114.995
115.447
132.095
135.475
140.232
141.739
142.181
152.405
163.466
167.108
168.466
unknown diazo side-product
+
4-82
4-70
^{13}C NMR
(226 MHz, CHCl$_3$)
CO$_2$Et
H
N
MeO
f1 (ppm)

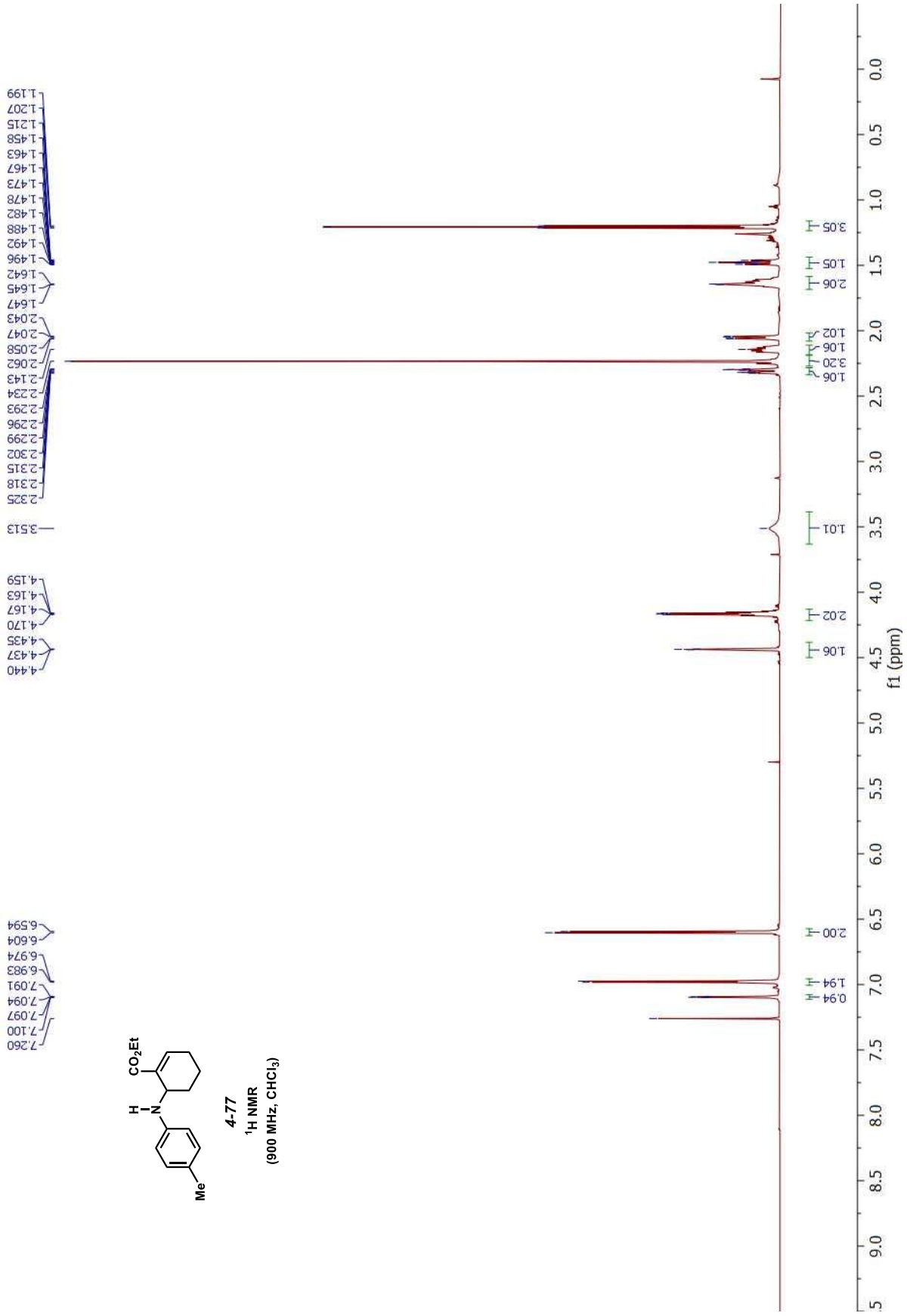
CO2Et
H
N
Me
4-77
1H NMR
(900 MHz, CHCl3)
f1 (ppm)

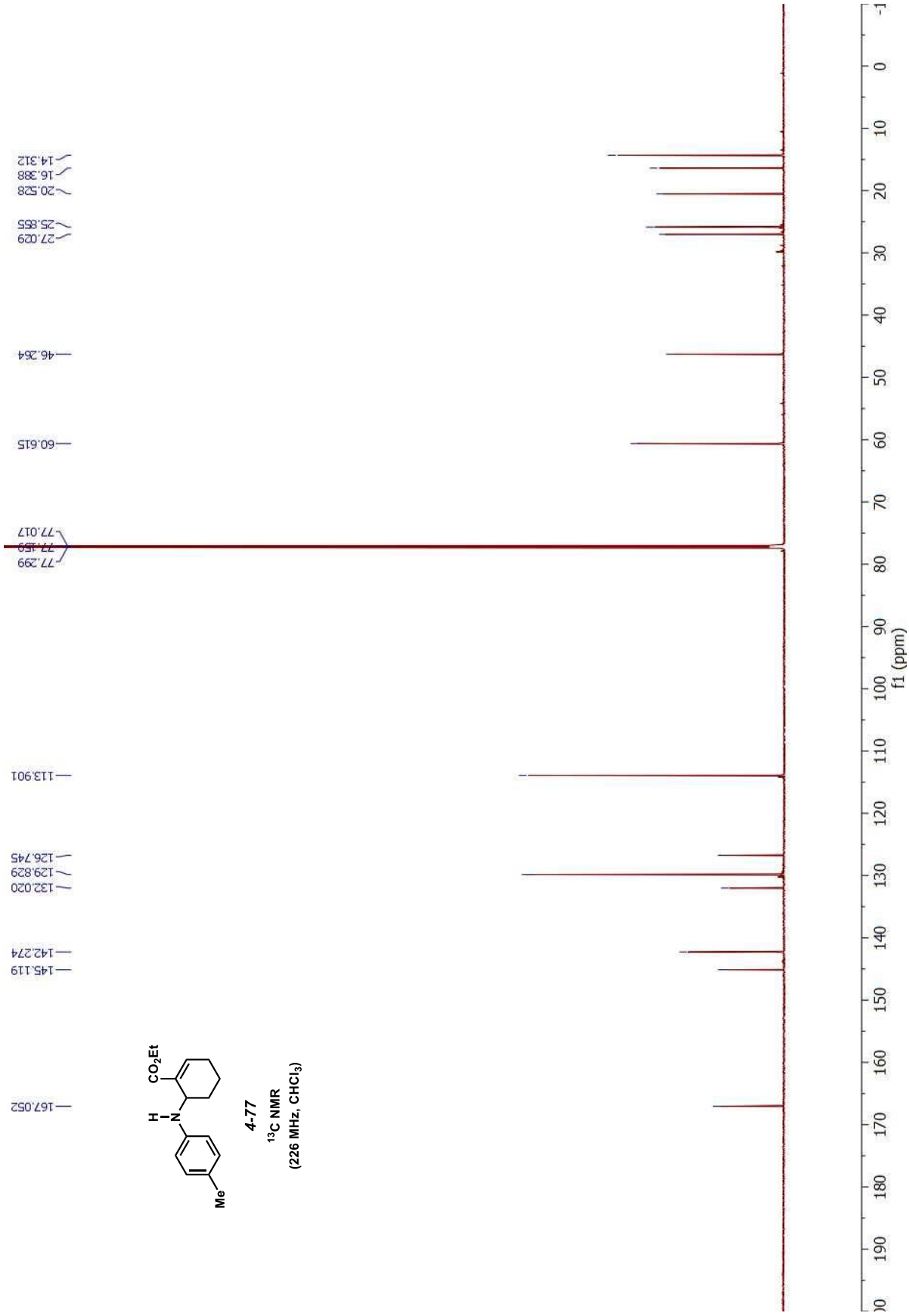
14.312
16.388
20.528
25.855
27.029
46.264
60.615
77.017
77.159
77.299
113.901
126.745
129.829
132.020
142.274
145.119
167.052
CO2Et
H
N
Me
4-77
13C NMR
(226 MHz, CHCl3)
f1 (ppm)